



A. E. Fitzgerald

Charles Kingsley, Jr.

Stephen D. Umans

Fifth Edition

ELECTRIC MACHINERY

ELECTRIC MACHINERY

McGraw-Hill Series in Electrical Engineering

Consulting Editor

Stephen W. Director, Carnegie-Mellon University

Circuits and Systems
Communications and Signal Processing
Control Theory
Electronics and Electronic Circuits
Power and Energy
Electromagnetics
Computer Engineering
Introductory
Radar and Antennas
VLSI

Previous Consulting Editors

Ronald N. Bracewell, Colin Cherry, James F. Gibbons, Willis W. Harman,
Hubert Heffner, Edward W. Herold, John G. Linvill, Simon Ramo,
Ronald A. Rohrer, Anthony E. Siegman, Charles Susskind, Frederick E.
Terman, John G. Truxal, Ernst Weber, and John R. Whinnery

Power and Energy

Consulting Editor

Stephen W. Director, Carnegie-Mellon University

Chapman: ELECTRIC MACHINERY FUNDAMENTALS
Elgerd: ELECTRIC ENERGY SYSTEMS THEORY: AN INTRODUCTION
Fitzgerald, Kingsley, and Umans: ELECTRIC MACHINERY
Gönen: ELECTRIC POWER DISTRIBUTION SYSTEM ENGINEERING
Hu and White: SOLAR CELLS: FROM BASIC TO ADVANCED SYSTEMS
Krause: ANALYSIS OF ELECTRIC MACHINERY
Krause and Wasynczuk: ELECTROMECHANICAL MOTION DEVICES
Stevenson: ELEMENTS OF POWER SYSTEM ANALYSIS

fifth edition
ELECTRIC MACHINERY

A. E. Fitzgerald

Late Vice President for Academic Affairs
and Dean of the Faculty
Northeastern University

Charles Kingsley, Jr.

Associate Professor of Electrical Engineering, Emeritus
Massachusetts Institute of Technology

Stephen D. Umans

Principal Research Engineer
Department of Electrical Engineering and Computer Science
Laboratory for Electromagnetic and Electronic Systems
Massachusetts Institute of Technology

McGraw-Hill, Inc.

New York St. Louis San Francisco Auckland Bogotá
Caracas Lisbon London Madrid Mexico Milan
Montreal New Delhi Paris San Juan Singapore
Sydney Tokyo Toronto

ELECTRIC MACHINERY

Copyright © 1990, 1983, 1971, 1961, 1952 by McGraw-Hill, Inc. All rights reserved.
Copyright renewed 1980 by Rosemary Fitzgerald and Charles Kingsley, Jr.
Printed in the United States of America. Except as permitted under the
United States Copyright Act of 1976, no part of this publication may be
reproduced or distributed in any form or by any means, or stored in a data
base or retrieval system, without the prior written permission of the publisher.

4 5 6 7 8 9 0 DOC DOC 9 5 4 3 2

ISBN 0-07-021134-5

This book was set in Century Schoolbook by Beacon Graphics Corporation.
The editors were Alar E. Elken and Jack Maisel;
the production supervisor was Leroy A. Young.
The cover was designed by Joseph Gillians.
New drawings were done by J & R Services, Inc.
R. R. Donnelley & Sons Company was printer and binder.

Library of Congress Cataloging-in-Publication Data

Fitzgerald, A. E. (Arthur Eugene), (date).

Electric machinery/A. E. Fitzgerald, Charles Kingsley, Jr.,
Stephen D. Umans. — 5th ed.

p. cm. — (McGraw-Hill series in electrical engineering.
Power and energy)

ISBN 0-07-021134-5

1. Electric machinery. I. Kingsley, Charles, (date).
II. Umans, Stephen D. III. Title. IV. Series.

TK2181.F5 1990

621.32'042 — dc20

89-49698

CONTENTS

Preface	xi
1 Magnetic Circuits and Magnetic Materials	1
1-1 INTRODUCTION TO MAGNETIC CIRCUITS	2
1-2 FLUX LINKAGE, INDUCTANCE, AND ENERGY	9
1-3 PROPERTIES OF MAGNETIC MATERIALS	16
1-4 AC EXCITATION	19
1-5 PERMANENT MAGNETS	26
1-6 APPLICATION OF PERMANENT MAGNET MATERIALS	32
1-7 SUMMARY	39
PROBLEMS	39
2 Transformers	50
2-1 INTRODUCTION TO TRANSFORMERS	51
2-2 NO-LOAD CONDITIONS	52
2-3 EFFECT OF SECONDARY CURRENT; IDEAL TRANSFORMER	57
2-4 TRANSFORMER REACTANCES AND EQUIVALENT CIRCUITS	60
2-5 ENGINEERING ASPECTS OF TRANSFORMER ANALYSIS	65
2-6 AUTOTRANSFORMERS; MULTICIRCUIT TRANSFORMERS	75
2-7 TRANSFORMERS IN THREE-PHASE CIRCUITS	78
2-8 THE PER UNIT SYSTEM	82
2-9 SUMMARY	87
PROBLEMS	89
3 Electromechanical Energy Conversion Principles	95
3-1 FORCES AND TORQUES IN MAGNETIC FIELD SYSTEMS	96
3-2 ENERGY BALANCE	101

3-3	ENERGY AND FORCE IN SINGLY EXCITED MAGNETIC FIELD SYSTEMS	102
3-4	DETERMINATIONS OF MAGNETIC FORCE: COENERGY	107
3-5	MULTIPLY EXCITED MAGNETIC FIELD SYSTEMS	114
3-6	FORCES AND TORQUES IN SYSTEMS WITH PERMANENT MAGNETS	118
3-7	DYNAMIC EQUATIONS	124
3-8	ANALYTICAL TECHNIQUES	128
3-9	SUMMARY	131
	PROBLEMS	132
4	Rotating Machines: Basic Concepts	147
4-1	ELEMENTARY CONCEPTS	147
4-2	INTRODUCTION TO AC AND DC MACHINES	150
4-3	MMF OF DISTRIBUTED WINDINGS	162
4-4	MAGNETIC FIELDS IN ROTATING MACHINERY	171
4-5	ROTATING MMF WAVES IN AC MACHINES	173
4-6	GENERATED VOLTAGE	181
4-7	TORQUE IN NON-SALIENT-POLE MACHINES	186
4-8	LINEAR MACHINES	197
4-9	MAGNETIC SATURATION	200
4-10	LEAKAGE FLUXES	203
4-11	SUMMARY	206
	PROBLEMS	207
5	Synchronous Machines: Steady State	216
5-1	INTRODUCTION TO POLYPHASE SYNCHRONOUS MACHINES	217
5-2	SYNCHRONOUS-MACHINE INDUCTANCES; EQUIVALENT CIRCUITS	219
5-3	OPEN- AND SHORT-CIRCUIT CHARACTERISTICS	225
5-4	STEADY-STATE POWER-ANGLE CHARACTERISTICS	233
5-5	STEADY-STATE OPERATING CHARACTERISTICS	240
5-6	EFFECTS OF SALIENT POLES; INTRODUCTION TO DIRECT- AND QUADRATURE-AXIS THEORY	246
5-7	POWER-ANGLE CHARACTERISTICS OF SALIENT-POLE MACHINES	252
5-8	INTERCONNECTED SYNCHRONOUS GENERATORS	256
5-9	SUMMARY	258
	PROBLEMS	260

6 Synchronous Machines: Transient Performance	266
6-1 SYNCHRONOUS-MACHINE TRANSIENTS	267
6-2 TRANSFORMATION TO DIRECT- AND QUADRATURE-AXIS VARIABLES	269
6-3 BASIC MACHINE RELATIONS IN $dq0$ VARIABLES	272
6-4 ANALYSIS OF A SUDDEN THREE-PHASE SHORT CIRCUIT	276
6-5 TRANSIENT POWER-ANGLE CHARACTERISTICS	285
6-6 EFFECTS OF ADDITIONAL ROTOR CIRCUITS	289
6-7 MODELS OF SYNCHRONOUS MACHINES FOR TRANSIENT ANALYSES	295
6-8 SYNCHRONOUS-MACHINE DYNAMICS	300
6-9 SUMMARY	309
PROBLEMS	310
 7 Polyphase Induction Machines	 321
7-1 INTRODUCTION TO POLYPHASE INDUCTION MACHINES	321
7-2 CURRENTS AND FLUXES IN INDUCTION MACHINES	325
7-3 THE INDUCTION-MOTOR EQUIVALENT CIRCUIT	328
7-4 ANALYSIS OF THE EQUIVALENT CIRCUIT	332
7-5 TORQUE AND POWER BY USE OF THEVENIN'S THEOREM	336
7-6 PERFORMANCE CALCULATIONS FROM NO-LOAD AND BLOCKED-ROTOR TESTS	342
7-7 SUMMARY	347
PROBLEMS	349
 8 Polyphase-Induction-Machine Dynamics and Control	 355
8-1 EFFECTS OF ROTOR RESISTANCE; DOUBLE-SQUIRREL-CAGE ROTORS	356
8-2 INDUCTION-MACHINE DYNAMICS	364
8-3 SPEED CONTROL OF INDUCTION MOTORS	367
8-4 ELECTRICAL TRANSIENTS IN INDUCTION MACHINES	371
8-5 APPLICATION OF ADJUSTABLE-SPEED SOLID-STATE AC MOTOR DRIVES	374
8-6 SUMMARY	381
PROBLEMS	381
 9 DC Machines: Steady State	 390
9-1 INTRODUCTION TO DC MACHINES	391
9-2 COMMUTATOR ACTION	398

9-3	EFFECT OF ARMATURE MMF	400
9-4	ANALYTICAL FUNDAMENTALS: ELECTRIC-CIRCUIT ASPECTS	404
9-5	ANALYTICAL FUNDAMENTALS: MAGNETIC-CIRCUIT ASPECTS	407
9-6	ANALYSIS OF STEADY-STATE PERFORMANCE	410
9-7	COMMUTATION AND INTERPOLES	421
9-8	COMPENSATING WINDINGS	423
9-9	DC MOTOR SPEED CONTROL	425
9-10	METADYNES AND AMPLIDYNES	430
9-11	SUMMARY: DC MACHINE APPLICATIONS PROBLEMS	433 435
10	Variable Reluctance Machines	446
10-1	BASICS OF VARIABLE RELUCTANCE MACHINE ANALYSIS	447
10-2	PRACTICAL VARIABLE RELUCTANCE MACHINE CONFIGURATIONS	455
10-3	CURRENT WAVEFORMS FOR TORQUE PRODUCTION	461
10-4	VARIABLE RELUCTANCE MACHINE MOTOR DRIVES	468
10-5	NONLINEAR ANALYSIS	478
10-6	SUMMARY PROBLEMS	483 484
11	Fractional- and Subfractional-Horsepower Motors	488
11-1	SINGLE-PHASE INDUCTION MOTORS: QUALITATIVE EXAMINATION	489
11-2	STARTING AND RUNNING PERFORMANCE OF SINGLE-PHASE INDUCTION AND SYNCHRONOUS MOTORS	492
11-3	REVOLVING-FIELD THEORY OF SINGLE-PHASE INDUCTION MOTORS	500
11-4	UNBALANCED OPERATION OF SYMMETRIC TWO-PHASE MACHINES; THE SYMMETRIC COMPONENT CONCEPT	507
11-5	SERIES UNIVERSAL MOTORS	512
11-6	STEPPING MOTORS	514
11-7	PERMANENT-MAGNET DC MOTORS	520
11-8	PERMANENT-MAGNET AC MOTORS	527
11-9	SUMMARY PROBLEMS	529 530

Appendix A	Three-Phase Circuits	536
A-1	GENERATION OF THREE-PHASE VOLTAGES	537
A-2	THREE-PHASE VOLTAGES, CURRENTS, AND POWER	539
A-3	Y- AND Δ -CONNECTED CIRCUITS	544
A-4	ANALYSIS OF BALANCED THREE-PHASE CIRCUITS; SINGLE-LINE DIAGRAMS	550
A-5	OTHER POLYPHASE SYSTEMS	552
Appendix B	Voltages, Magnetic Fields, and Inductances of Distributed AC Windings	554
B-1	GENERATED VOLTAGES	554
B-2	ARMATURE-MMF WAVES	561
B-3	AIR-GAP INDUCTANCES OF DISTRIBUTED WINDINGS	564
Appendix C	Engineering Aspects of Practical Electric- Machine Performance and Operation	569
C-1	LOSSES	569
C-2	RATING AND HEATING	573
C-3	COOLING MEANS FOR ELECTRIC MACHINES	577
C-4	EXCITATION SOURCES	579
C-5	ENERGY EFFICIENCY OF ELECTRIC MACHINERY	582
Appendix D	Table of Constants and Conversion Factors for SI Units	584
Index		585

PREFACE

The objective of *Electric Machinery* continues to be to provide an introduction to the theory of electromechanical devices, with specific emphasis on the theory of rotating electric machinery. To a great extent, the fundamental concepts have not changed over the years since Professors Fitzgerald and Kingsley wrote the first edition of this text. As a result, significant portions of the material found in the fifth edition will be familiar to readers of the previous editions.

Major advances in the application and control of electric machinery over the past few decades have occurred as a result of advances in power electronics and microprocessor-based control systems. Consequently, a much broader spectrum of electric machine types can be found in modern applications. Specifically, permanent-magnet and variable-reluctance machines can now be found in many applications and the range of such applications can be expected to continue to grow significantly. Drive systems built around these machine types are found, for example, in many applications, such as those requiring variable speed and flexibility of control, for which dc machines might have traditionally been the logical choice.

In recognition of this fact, coverage of the basics of these machine types has increased significantly in the fifth edition. An introduction to permanent-magnet materials and their application has been included in Chapter 1. In addition, an article discussing the calculation of forces and torques in systems with permanent magnets has been included in Chapter 3. Finally, Chapter 11 includes two articles which discuss permanent-magnet dc and ac motors.

Variable reluctance motors are perhaps the simplest of all electric machines in concept and construction and yet among the most complex to operate and control. As a result, they are receiving considerable attention at present and appear to be serious contenders in many applications. Study of these machines illustrates not only many fundamental issues of electromechanical energy conversion but also many of the issues which

arise when interfacing electric machines with power-electronic and control systems to form a complete motor drive. Chapter 10 of this edition is completely new material devoted to the topic of variable reluctance motors.

The philosophy of this book is to emphasize a physical understanding of the fundamental principles behind the operation of electric machines. It has been our objective to accomplish this task without requiring a level of mathematical sophistication beyond that required in basic undergraduate courses in physics and circuit theory.

As with the fourth edition, the arrangement of the material in this book is intended to follow a logical progression while providing flexibility for the instructor. The first four chapters constitute introductory material which forms the basis for the study of all machine types. Chapter 1 introduces basic analytical techniques, including the concept of magnetic circuit analysis, and also discusses important characteristics of magnetic materials.

The addition of a discussion of permanent-magnet materials to the topics previously included in Chapter 1 of the fourth edition made that chapter excessively long. A logical solution to this problem was to take out the discussion of transformers that was previously included in Chapter 1 and make it into a separate chapter. Hence Chapter 2 of this edition is devoted exclusively to a discussion of transformers. Although transformers are not electromechanical devices, they are certainly important components of energy conversion systems and their analysis employs many of the techniques which are applicable to electric machinery. Their inclusion at this point in the text serves to introduce these analytical techniques.

Chapter 3 discusses the basic principles of electromechanical energy conversion. This material is sometimes felt to be too mathematical for an introductory undergraduate course on electric machinery. Hence, following the format found in Chapter 2 of the fourth edition, the authors wrote this chapter in such a fashion that the first two articles can serve as an overview to this topic and the rest of the chapter can be omitted if desired, without a significant loss of understanding in the remainder of the book.

Chapter 4 serves as an introduction to the basic concepts of rotating machines. These concepts are common to all machine types and thus form the foundation for the material which is discussed in greater detail in the remainder of the book.

Chapters 5 through 10 are devoted to specific machine types: synchronous, induction, dc, and variable reluctance. An attempt has been made to treat each machine type separately and thus it should be possible for the instructor to change the order in which these machine

types are discussed as well as to select only those machine types on which he or she wishes to focus attention. Finally, Chapter 11 examines various examples of fractional- and subfractional-horsepower machine types.

Chapter 4 of the fourth edition included discussions of such topics as machine rating, cooling, and efficiency. Although these topics are certainly of importance to a thorough understanding of electric machinery and electromechanical energy conversion devices, they are not prerequisite to an understanding of the material covered in Chapters 5 through 11. As a result, much of the material which previously appeared in Chapter 4 has been moved to Appendix C in this edition.

Professor Kingsley, who honored me with the opportunity to participate in the fourth edition of *Electric Machinery*, has carefully followed the progress of this edition. I have very much appreciated his advice and encouragement as this work progressed. It has been a great pleasure to have started as one of Professor Kingsley's students, studying from the second edition of *Electric Machinery*, and to have seen our relationship grow to one of friends, colleagues, and coauthors.

McGraw-Hill and the authors would like to thank the following reviewers of this edition: Ali Abur, Texas A&M University; Frederick C. Brockhurst, Virginia Polytechnic Institute; W. R. Callen, Georgia Institute of Technology; Wayne E. Carr, Stevens Institute of Technology; Cyrus W. Cox, South Dakota School of Mines and Technology; Alvin L. Day, Iowa State University; Joseph Douglas, Penn State University; A. A. El-Keib, University of Alabama; G. A. Etzweiler, Penn State University; G. D. Galanos, West Virginia University; Charles Gibson, University of Alabama; C. S. Jha, Penn State University; John R. Pavlat, Iowa State University; J. R. Rankin, Rutgers University; Mahmoud Riaz, University of Minnesota; Sheppard Salon, Rensselaer Polytechnic Institute; and Paul Wildi, University of Texas, Austin.

Stephen D. Umans

ELECTRIC MACHINERY



Magnetic Circuits and Magnetic Materials

The objective of this book is to study the devices used in the interconversion of electric and mechanical energy. Emphasis is placed on electromagnetic rotating machinery, by means of which the bulk of this energy conversion takes place. Attention is also paid to the transformer, which, although not an electromechanical energy conversion device, is an important component in the overall problem of energy conversion. Moreover, in many respects its analysis uses techniques closely related to those required for rotating machinery.

Practically all transformers and electric machinery use magnetic material for shaping and directing the magnetic fields which act as the medium for transferring and converting energy. Thus the ability to analyze and describe magnetic field quantities is an essential tool for understanding these devices. Magnetic materials play a large role in determining the properties of a piece of electromagnetic equipment and affect its size and efficiency.

This chapter will develop some basic tools for the analysis of magnetic field systems and will provide a brief introduction to the properties of practical magnetic materials. These results will then be applied to the analysis of transformers. In later chapters they will be used in the analysis of rotating machinery.

In this book it is assumed that the reader has basic knowledge of magnetic and electric field theory such as given in a basic physics course for engineering students. Other readers may have had a course on electromagnetic field theory based on Maxwell's equations, but an in-depth understanding of Maxwell's equations is not a prerequisite for study of this book. The pertinent basic equations will be introduced in simplified form when required.

1-1 INTRODUCTION TO MAGNETIC CIRCUITS

The complete, detailed solution for magnetic fields in most situations of practical engineering interest involves the solution of Maxwell's equations along with various constitutive relationships which describe material properties. Although in practice exact solutions are often unattainable, various simplifying assumptions permit the attainment of useful engineering solutions.

The first assumption is that for the types of electric machines and transformers treated in this book, the frequencies and sizes involved are such that the displacement-current term in Maxwell's equations can be neglected. This term accounts for magnetic fields being produced in space by time-varying electric fields and is associated with electromagnetic radiation. Neglecting this term results in the *magneto-quasi-static* form of Maxwell's equations.

$$\oint_C \mathbf{H} \cdot d\mathbf{l} = \oint_S \mathbf{J} \cdot d\mathbf{a} \quad (1-1)$$

$$\oint_S \mathbf{B} \cdot d\mathbf{a} = 0 \quad (1-2)$$

Equation 1-1 states that the line integral of the *magnetic field intensity* \mathbf{H} around a closed contour C is equal to the total current passing through any surface S linking that contour. From Eq. 1-1 we see that the source of \mathbf{H} is the current density \mathbf{J} . Equation 1-2 states that the *magnetic flux density* \mathbf{B} is conserved, i.e., that no net flux enters or leaves a closed surface (this is equivalent to saying that there exist no monopole charge sources of magnetic fields). From these equations we see that the magnetic field quantities can be determined solely from the instantaneous values of the source currents and that the time variations of the magnetic fields follow directly from the time variations of the sources.

A second simplifying assumption involves the concept of the *magnetic circuit*. The general solution for the magnetic field intensity \mathbf{H} and the magnetic flux density \mathbf{B} in a structure of complex geometry is extremely difficult. However, a three-dimensional field problem can often be reduced to what is essentially a one-dimensional circuit equivalent, yielding solutions of acceptable engineering accuracy.

A magnetic circuit consists of a structure composed for the most part of high-permeability magnetic material. The presence of high-permeability material causes the magnetic flux to be confined to the paths defined by the structure, much as currents are confined to the conductors of an electric circuit. Use of this concept of the magnetic circuit is illustrated in this article and will be seen to apply quite well to many situations in this book.[†]

A simple example of a magnetic circuit is shown in Fig. 1-1. The core is assumed to be composed of magnetic material whose permeability is much greater than that of the surrounding air ($\mu \gg \mu_0$). The core is of uniform cross section and is excited by a winding of N turns carrying current i amperes (A). This winding produces a magnetic field in the core, as shown in the figure.

Because of the high permeability of the magnetic core, the magnetic flux is confined almost entirely to the core, the field lines follow the path defined by the core, and the flux density is essentially uniform over a cross section because the cross-sectional area is uniform. The magnetic field can be visualized in terms of flux lines which form closed loops interlinked with the winding.

As applied to the magnetic circuit of Fig. 1-1, the source of the magnetic field in the core is the ampere-turn product Ni . In magnetic circuit terminology Ni is the *magnetomotive force* (mmf) \mathcal{F} . Although Fig. 1-1 shows only a single coil, transformers and most rotating machines have at least two windings, and Ni is the algebraic sum of the ampere-turns of all the windings.

[†]For a more extensive treatment of magnetic circuits see A. E. Fitzgerald, D. E. Higgenbotham, and A. Grabel, *Basic Electrical Engineering*, 5th ed., McGraw-Hill, New York, 1981, chap. 13; also E. E. Staff, M.I.T., *Magnetic Circuits and Transformers*, M.I.T. Press, Cambridge, Mass., 1965, chaps. 1 to 3.

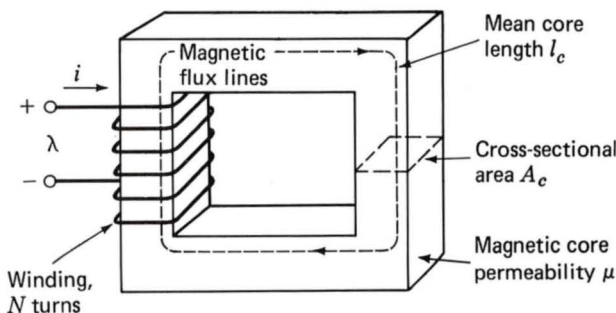


Fig. 1-1. Simple magnetic circuit.

The *magnetic flux* ϕ crossing a surface S is the surface integral of the normal component of \mathbf{B} ; thus

$$\phi = \int_S \mathbf{B} \cdot d\mathbf{a} \quad (1-3)$$

In SI units, the unit of ϕ is *webers* (Wb).

Equation 1-2 states that the net magnetic flux entering or leaving a closed surface (equal to the surface integral of \mathbf{B} over that closed surface) is zero. This is equivalent to saying that all the flux which enters the surface enclosing a volume must leave that volume over some other portion of that surface because magnetic flux lines form closed loops.

These facts can be used to justify the assumption that the magnetic flux density is uniform across the core cross section. In this case Eq. 1-3 reduces to the simple scalar equation

$$\phi_c = B_c A_c \quad (1-4)$$

where ϕ_c = flux in core

B_c = flux density in core

A_c = cross-sectional area of core

From Eq. 1-1, the relationship between the mmf and the magnetic field intensity is

$$\mathcal{F} = Ni = \oint \mathbf{H} \cdot d\mathbf{l} \quad (1-5)$$

The core dimensions are such that the path length of any flux line is close to the mean core length l_c . As a result, the line integral of Eq. 1-5 becomes simply the scalar product $H_c l_c$ of the magnitude of \mathbf{H} and the mean flux path length l_c . Thus, the relationship between the mmf and the magnetic field intensity can be written in magnetic circuit terminology as

$$\mathcal{F} = Ni = H_c l_c \quad (1-6)$$

where H_c is average magnitude of \mathbf{H} in the core.

The direction of H_c in the core can be found from the *right-hand rule*, which can be stated in two equivalent ways. (1) Imagine a current-carrying conductor held in the right hand with the thumb pointing in the direction of current flow; the fingers then point in the direction of the magnetic field created by that current. (2) Equivalently, if the coil in Fig. 1-1 is grasped in the right hand (figuratively speaking) with the fingers pointing in the direction of the current, the thumb will point in the direction of the magnetic fields.

The relationship between the magnetic field intensity \mathbf{H} and the magnetic flux density \mathbf{B} is a property of the material in which the field exists;

thus

$$\mathbf{B} = \mu \mathbf{H} \quad (1-7)$$

where μ is the *permeability*. In SI units \mathbf{B} is in *webers per square meter*, known as *teslas* (T), and μ is in *webers per ampere-turn-meter*, or equivalently *henrys per meter*. In SI units the permeability of free space is $\mu_0 = 4\pi \times 10^{-7}$. The permeability of ferromagnetic material can be expressed in terms of μ_r , its value relative to that of free space, or $\mu = \mu_r \mu_0$. Typical values of μ_r range from 2000 to 80,000 for materials used in transformers and rotating machines. The characteristics of ferromagnetic materials are described in Arts. 1-3 and 1-4. For the present we assume that μ_r is a known constant, although it actually varies appreciably with the magnitude of the magnetic flux density.

Transformers are wound on closed cores like that of Fig. 1-1. Energy conversion devices which incorporate a moving element must have air gaps in their magnetic circuits. A magnetic circuit with an air gap is shown in Fig. 1-2. When the air-gap length g is much smaller than the dimensions of the adjacent core faces, the magnetic flux ϕ is constrained essentially to reside in the core and the air gap and is continuous throughout the magnetic circuit.

Thus, the configuration of Fig. 1-2 can be analyzed as a magnetic circuit with two series components: a magnetic core of permeability μ and mean length l_c , and an air gap of permeability μ_0 , cross-sectional area A_g , and length g . In the core the flux density is uniform, and the cross-sectional area is A_c ; thus in the core

$$B_c = \frac{\phi}{A_c} \quad (1-8)$$

and in the air gap

$$B_g = \frac{\phi}{A_g} \quad (1-9)$$

where ϕ = the flux in the magnetic circuit.

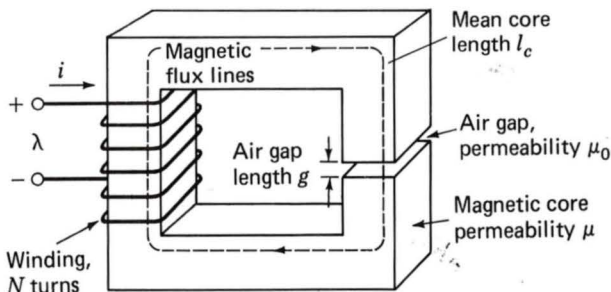


Fig. 1-2. Magnetic circuit with air gap.

The magnetic field lines bulge outward somewhat as they cross the air gap, as illustrated in Fig. 1-3. The effect of the *fringing fields* is to increase the effective cross-sectional area A_g of the air gap. Various empirical methods have been developed to account for this effect. A correction for such fringing fields in short air gaps can be made by adding the gap length to each of the two dimensions making up its cross-sectional area. In this book the effect of fringing fields is usually ignored. If fringing is neglected, $A_g = A_c$ and

$$B_g = B_c = \frac{\phi}{A_c} \quad (1-10)$$

Application of Eqs. 1-5 and 1-7 to this magnetic circuit yields

$$\mathcal{F} = Ni = H_c l_c + H_g g \quad (1-11)$$

$$\mathcal{F} = \frac{B_c}{\mu} l_c + \frac{B_g}{\mu_0} g \quad (1-12)$$

Here Ni is the total ampere-turns applied to the magnetic circuit. Thus we see that a portion of the mmf is required to excite the magnetic field in the core while the remainder excites the magnetic field in the air gap.

For practical magnetic materials (as discussed in Art. 1-3), B_c and H_c are not simply related by a known constant permeability μ . In fact, B_c is often a nonlinear, multivalued function of H_c . Thus, although Eq. 1-11 continues to hold, it does not lead directly to a simple expression relating the mmf and the flux densities, such as that of Eq. 1-12. Instead the specifics of the nonlinear B_c - H_c relation must be used, either graphically or analytically. However, in many cases, the concept of constant core permeability gives results of acceptable engineering accuracy and is frequently used.

From Eq. 1-10, Eq. 1-12 can be rewritten in terms of the total flux ϕ as

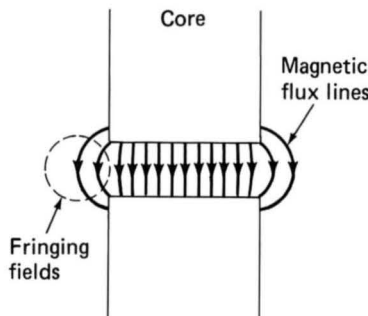


Fig. 1-3. Air-gap fringing fields.

$$\mathcal{F} = \phi \frac{l_c}{\mu A_c} + \phi \frac{g}{\mu_0 A_c} \quad (1-13)$$

in which fringing at the air gap is neglected and the flux is assumed to go straight across the gap. The terms that multiply the flux in this equation are known as the *reluctance* \mathcal{R} of the core and air gap, respectively,

$$\mathcal{R}_c = \frac{l_c}{\mu A_c} \quad (1-14)$$

$$\mathcal{R}_g = \frac{g}{\mu_0 A_c} \quad (1-15)$$

and thus

$$\mathcal{F} = \phi(\mathcal{R}_c + \mathcal{R}_g) \quad (1-16)$$

Finally, Eq. 1-16 can be inverted to solve for the flux

$$\phi = \frac{\mathcal{F}}{\mathcal{R}_c + \mathcal{R}_g} \quad (1-17)$$

Note that Eqs. 1-16 and 1-17 are analogous to the relationships between the current and voltage in an electric circuit. This analogy is illustrated in Fig. 1-4. Figure 1-4a shows an electric circuit in which a voltage V drives a current I through resistors R_1 and R_2 . Figure 1-4b shows the schematic equivalent representation of the magnetic circuit of Fig. 1-2. Here we see that the mmf \mathcal{F} (analogous to voltage in an electric circuit) drives a flux ϕ (analogous to the current in the electric circuit) through the

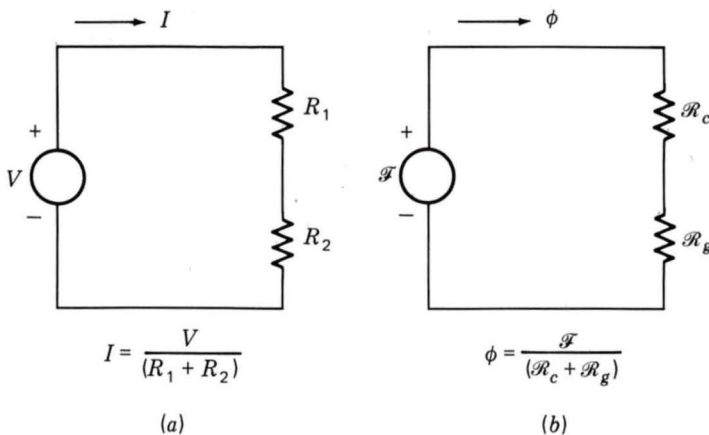


Fig. 1-4. Analog between electric and magnetic circuits. (a) Electric circuit. (b) Magnetic circuit.

series combination of the reluctances of the core \mathcal{R}_c and the air gap \mathcal{R}_g . This analogy between the solution of electric and magnetic circuits can often be exploited to produce simple solutions for the fluxes in magnetic circuits of considerable complexity.

The fraction of the total mmf required for each portion of the magnetic circuit varies inversely as its reluctance. From Eq. 1-14 we see that the core reluctance becomes small as its permeability increases and can often be made much smaller than that of the air gap; i.e., for $\mu \gg \mu_0$, $\mathcal{R}_c \ll \mathcal{R}_g$. In this case, the flux and hence B can be found from Eq. 1-17 in terms of \mathcal{F} and the air-gap properties alone:

$$\phi \approx \frac{\mathcal{F}}{\mathcal{R}_g} = \frac{\mathcal{F}\mu_0 A_c}{g} = Ni \frac{\mu_0 A_c}{g} \quad (1-18)$$

The term which multiplies the mmf is known as the *permeance* \mathcal{P} ; thus the permeance of the air gap is

$$\mathcal{P}_g = \frac{1}{\mathcal{R}_g} = \frac{\mu_0 A_c}{g} \quad (1-19)$$

As will be seen in Art. 1-3, practical magnetic materials have permeabilities which are not constant but vary with the flux level. From Eqs. 1-14 to 1-17 we see that as long as this permeability remains sufficiently large, its variation will not significantly affect the performance of the magnetic circuit.

We have now described the basic principles for reducing a magneto-quasi-static field with simple geometry to a *magnetic circuit model*. Our limited purpose in this article is to introduce some of the concepts and terminology used by engineers in solving practical design problems. We emphasize that this type of thinking depends quite heavily on engineering judgment and intuition. For example, we have tacitly assumed that the permeability of the "iron" parts of the magnetic circuit is a constant known quantity, although this is not true in general (see Art. 1-3), and that the magnetic field is confined to the core and its air gaps. As we shall see later in this book, when two or more windings are placed on a magnetic circuit, as in a transformer or rotating machine, the fields outside the core, called *leakage fields*, are extremely important in determining the coupling between the windings.

EXAMPLE 1-1

The magnetic circuit shown in Fig. 1-2 has dimensions $A_c = 9 \text{ cm}^2$, $A_g = 9 \text{ cm}^2$, $g = 0.050 \text{ cm}$, $l_c = 30 \text{ cm}$, and $N = 500$ turns. Assume the value $\mu_r = 70,000$ for iron. (a) Find the reluctances \mathcal{R}_c and \mathcal{R}_g . Assume that the

magnetic circuit is operating with $B_c = 1.0$ T, and find (b) the flux ϕ and (c) the current i .

Solution

(a) The reluctances can be found from Eqs. 1-14 and 1-15:

$$\mathcal{R}_c = \frac{l_c}{\mu_r \mu_0 A_c} = \frac{0.3}{70,000(4\pi \times 10^{-7})(9 \times 10^{-4})} = 3.79 \times 10^3 \frac{\text{A} \cdot \text{turns}}{\text{Wb}}$$

$$\mathcal{R}_g = \frac{g}{\mu_0 A_g} = \frac{5 \times 10^{-4}}{(4\pi \times 10^{-7})(9 \times 10^{-4})} = 4.42 \times 10^5 \frac{\text{A} \cdot \text{turns}}{\text{Wb}}$$

(b) From Eq. 1-4,

$$\phi = B_c A_c = 1.0(9 \times 10^{-4}) = 9 \times 10^{-4} \text{ Wb}$$

(c) From Eqs. 1-6 and 1-16,

$$i = \frac{\mathcal{F}}{N} = \frac{\phi(\mathcal{R}_c + \mathcal{R}_g)}{N} = \frac{9 \times 10^{-4}(4.46 \times 10^5)}{500} = 0.80 \text{ A}$$

EXAMPLE 1-2

The magnetic structure of a synchronous machine is shown schematically in Fig. 1-5. Assuming that rotor and stator iron have infinite permeability ($\mu \rightarrow \infty$), find the air-gap flux ϕ and flux density B_g . For this example $I = 10$ A, $N = 1000$ turns, $g = 1$ cm, and $A_g = 2000 \text{ cm}^2$.

Solution

Notice that there are two air gaps in series, of total length $2g$, and that by symmetry the flux density in each is equal. Since the iron permeability here is assumed to be infinite, its reluctance is negligible and Eq. 1-18 can be used to find the flux

$$\phi = \frac{NI\mu_0 A_g}{2g} = \frac{1000(10)(4\pi \times 10^{-7})(0.2)}{0.02} = 0.13 \text{ Wb}$$

and
$$B_g = \frac{\phi}{A_g} = \frac{0.13}{0.2} = 0.65 \text{ T}$$

1-2 FLUX LINKAGE, INDUCTANCE, AND ENERGY

When a magnetic field varies with time, an electric field is produced in space as determined by *Faraday's law*:

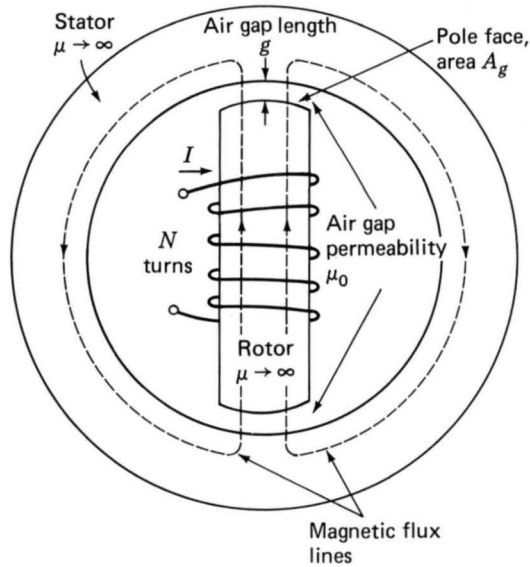


Fig. 1-5. Simple synchronous machine.

$$\oint_C \mathbf{E} \cdot d\mathbf{S} = -\frac{d}{dt} \int_S \mathbf{B} \cdot d\mathbf{a} \quad (1-20)$$

Equation 1-20 states that the line integral of the *electric field intensity* \mathbf{E} around a closed contour C is equal to the time rate of change of the magnetic flux linking that contour. In magnetic structures with windings, such as in Fig. 1-2, the \mathbf{E} field in the wire is extremely small and can be neglected, so that the left-hand side of Eq. 1-20 reduces to the negative of the *induced voltage*[†] e at the winding terminals. In addition, the flux on the right-hand side of Eq. 1-20 is dominated by the core flux ϕ . Since the winding (and hence the contour C) links the core flux N times, Eq. 1-20 reduces to

$$e = N \frac{d\phi}{dt} = \frac{d\lambda}{dt} \quad (1-21)$$

where $\lambda = N\phi$ is the *flux linkage* of the winding. The symbol ϕ is used to indicate the instantaneous value of a time-varying flux.

In general the flux linkage of a coil is equal to the surface integral of the normal component of the magnetic flux density integrated over any surface spanned by that coil. Note that the direction of the induced voltage e is defined by Eq. 1-20 so that if the winding terminals were short-circuited, a current would flow in such a direction as to oppose the change of flux linkage.

[†]The term *electromotive force* (emf) is often used instead of *induced voltage* to represent that component of voltage due to a time-varying flux linkage.

For a magnetic circuit that has a linear relationship between φ and i because of material of constant permeability or a dominating air gap, we can define the λ - i relationship by the *inductance* L as

$$L = \frac{\lambda}{i} \quad (1-22)$$

where $\lambda = N\varphi$, the flux linkage, is in weber-turns. For example, from Eq. 1-18,

$$L = \frac{NB_c A_c}{i} = \frac{N^2 \mu_0 A_c}{g} \quad (1-23)$$

for the magnetic circuit of Fig. 1-2, assuming a core of infinite permeability.

Inductance is measured in henrys or weber-turns per ampere. Equation 1-23 shows the dimensional form of expressions for inductance. Thus inductance is proportional to the square of the number of turns, to the permeability of the magnetic circuit, and to its cross-sectional area and is inversely proportional to its length.

The difficulty in applying the inductance concept in numerical calculations arises from the nonlinear dependence of the permeability μ on magnetic conditions in the core, as is explained in Arts. 1-3 and 1-4. Note that the usefulness of inductance as a parameter depends on the assumption of a linear relation between flux and mmf. This implies that the effects of the nonlinear magnetic characteristics of the core material can be approximated by some sort of empirical linear relation or that the effects of the core are of secondary importance compared with the effect of an air gap, as shown in Example 1-3.

EXAMPLE 1-3

The magnetic circuit of Fig. 1-6a consists of an N -turn winding on a magnetic core of infinite permeability with two parallel air gaps of lengths g_1 and g_2 and areas A_1 and A_2 , respectively.

Find (a) the inductance of the winding and (b) the flux density B_1 in gap 1 when the winding is carrying a current i . Neglect fringing effects at the air gap.

Solution

(a) The equivalent circuit of Fig. 1-6b shows that the total reluctance is equal to the parallel combination of the two gap reluctances. Thus

$$\phi = \frac{Ni}{\mathcal{R}_1 \mathcal{R}_2 / (\mathcal{R}_1 + \mathcal{R}_2)}$$

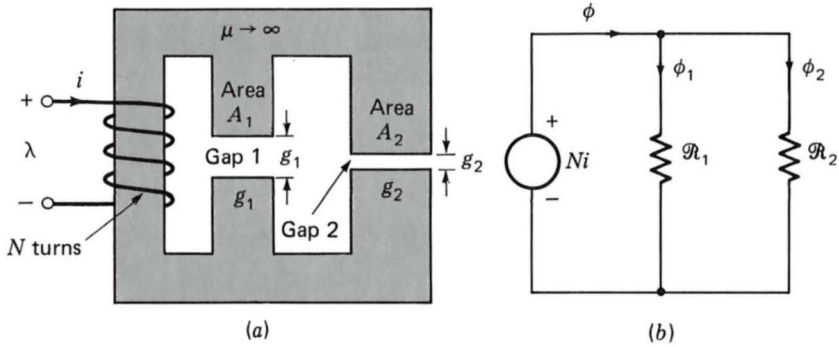


Fig. 1-6. (a) Magnetic circuit; (b) equivalent circuit.

where

$$\mathcal{R}_1 = \frac{g_1}{\mu_0 A_1} \quad \mathcal{R}_2 = \frac{g_2}{\mu_0 A_2}$$

From Eq. 1-22,

$$\begin{aligned} L &= \frac{\lambda}{i} = \frac{N\phi}{i} = \frac{N^2(\mathcal{R}_1 + \mathcal{R}_2)}{\mathcal{R}_1 \mathcal{R}_2} \\ &= \mu_0 N^2 \left(\frac{A_1}{g_1} + \frac{A_2}{g_2} \right) \end{aligned}$$

(b) From the equivalent circuit, one can see that

$$\phi_1 = \frac{Ni}{\mathcal{R}_1} = \frac{\mu_0 A_1 Ni}{g_1}$$

and thus

$$B_1 = \frac{\phi_1}{A_1} = \frac{\mu_0 Ni}{g_1}$$

Figure 1-7 shows a magnetic circuit with an air gap and two windings. Note that the reference directions for the currents have been chosen to produce flux in the same direction. The total mmf is

$$\mathcal{F} = Ni = N_1 i_1 + N_2 i_2 \quad (1-24)$$

and from Eq. 1-18 with the reluctance of the core neglected, the core flux ϕ is

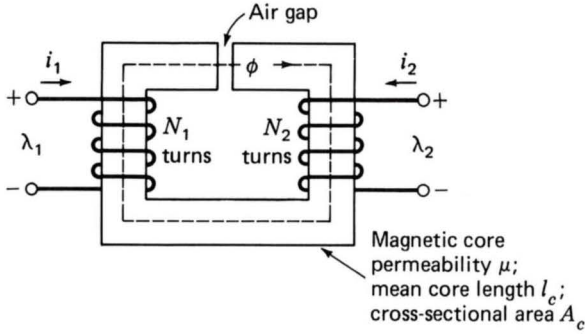


Fig. 1-7. Magnetic circuit with two windings.

$$\phi = (N_1 i_1 + N_2 i_2) \frac{\mu_0 A_c}{g} \quad (1-25)$$

In Eq. 1-25, ϕ is the *resultant core flux* produced by the *simultaneous action* of both mmf's. It is this resultant ϕ which determines the operating point of the core material.

If Eq. 1-25 is broken up into terms attributable to the individual currents, the resultant flux linkages with coil 1 can be expressed as

$$\lambda_1 = N_1 \phi = N_1^2 \frac{\mu_0 A_c}{g} i_1 + N_1 N_2 \frac{\mu_0 A_c}{g} i_2 \quad (1-26)$$

which can be written

$$\lambda_1 = L_{11} i_1 + L_{12} i_2 \quad (1-27)$$

where

$$L_{11} = N_1^2 \frac{\mu_0 A_c}{g} \quad (1-28)$$

is the *self-inductance* of coil 1 and $L_{11} i_1$ is the flux linkage with coil 1 due to its own current i_1 . The *mutual inductance* between coils 1 and 2 is

$$L_{12} = N_1 N_2 \frac{\mu_0 A_c}{g} \quad (1-29)$$

and $L_{12} i_2$ is the flux linkage with coil 1 due to current i_2 in the other coil. Similarly, the flux linkage with coil 2 is

$$\lambda_2 = N_2 \phi = N_1 N_2 \frac{\mu_0 A_c}{g} i_1 + N_2^2 \frac{\mu_0 A_c}{g} i_2 \quad (1-30)$$

or

$$\lambda_2 = L_{21} i_1 + L_{22} i_2 \quad (1-31)$$

where $L_{21} = L_{12}$ is the mutual inductance and

$$L_{22} = N_2^2 \frac{\mu_0 A_c}{g} \quad (1-32)$$

is the self-inductance of coil 2.

It is important to note that the resolution of the resultant flux linkages into the components produced by i_1 and i_2 is based on superposition of the individual effects and therefore implies a linear flux-mmfm characteristic (constant permeability).

Substitution of Eq. 1-22 in 1-21 yields

$$e = \frac{d}{dt}(Li) \quad (1-33)$$

for a magnetic circuit with a single winding. For a static magnetic circuit, the inductance is fixed (assuming that material nonlinearities do not cause the inductance to vary), and this equation reduces to the familiar circuit form

$$e = L \frac{di}{dt} \quad (1-34)$$

However, in electromechanical energy conversion devices, inductances are often time-varying, and Eq. 1-33 must be written as

$$e = L \frac{di}{dt} + i \frac{dL}{dt} \quad (1-35)$$

In situations with multiple windings, the total flux linkage of each winding must be used in Eq. 1-21 to find the winding-terminal voltage.

The power at the terminals of a winding on a magnetic circuit is a measure of the rate of energy flow into the circuit through that particular winding. The power p is determined from the product of the voltage and the current

$$p = ie = i \frac{d\lambda}{dt} \quad (1-36)$$

and its unit is *watts*, or *joules per second*. Thus the change in *magnetic stored energy* ΔW in the magnetic circuit in the time interval t_1 to t_2 is

$$\Delta W = \int_{t_1}^{t_2} p dt = \int_{\lambda_1}^{\lambda_2} i d\lambda \quad (1-37)$$

In SI units, the stored energy W is measured in joules.

For a single-winding system of constant inductance, the change in magnetic stored energy can be written as

$$\Delta W = \int_{\lambda_1}^{\lambda_2} i d\lambda = \int_{\lambda_1}^{\lambda_2} \frac{\lambda}{L} d\lambda = \frac{1}{2L} (\lambda_2^2 - \lambda_1^2) \quad (1-38)$$

The total magnetic stored energy at any given value of λ can be found from setting λ_1 equal to zero:

$$W = \frac{1}{2L} \lambda^2 = \frac{L}{2} i^2 \quad (1-39)$$

EXAMPLE 1-4

For the magnetic circuit of Example 1-1 (Fig. 1-2), find (a) the inductance L , (b) the magnetic stored energy W for $B_c = 1$ T, and (c) the induced voltage e for a 60-Hz time-varying core flux of the form $B_c = 1.0 \sin \omega t$ where $\omega = (2\pi)(60) = 377$.

Solution

(a) From Eqs. 1-17 and 1-22 and Example 1-1,

$$\begin{aligned} L &= \frac{\lambda}{i} = \frac{N\phi}{i} = \frac{N^2}{\mathcal{R}_c + \mathcal{R}_g} \\ &= \frac{500^2}{4.46 \times 10^5} = 0.56 \text{ H} \end{aligned}$$

Note that the core reluctance is much smaller than that of the gap ($\mathcal{R}_c \ll \mathcal{R}_g$). Thus to a good approximation the inductance is dominated by the gap reluctance, i.e.,

$$L \approx \frac{N^2}{\mathcal{R}_g} = 0.57 \text{ H}$$

(b) In Example 1-1 we found that when $B_c = 1.0$ T, $i = 0.80$ A. Thus from Eq. 1-39,

$$W = \frac{1}{2} Li^2 = \frac{1}{2} (0.56) (0.80)^2 = 0.18 \text{ J}$$

(c) From Eq. 1-21 and Example 1-1,

$$e = \frac{d\lambda}{dt} = N \frac{d\phi}{dt} = NA_c \frac{dB_c}{dt}$$

$$\begin{aligned}
 &= (500) (9 \times 10^{-4}) (377) (1.0 \cos 377t) \\
 &= 170 \cos 377t \quad \text{V}
 \end{aligned}$$

1-3 PROPERTIES OF MAGNETIC MATERIALS

In the context of electromechanical energy conversion devices, the importance of magnetic materials is twofold. Through their use it is possible to obtain large magnetic flux densities with relatively low levels of magnetizing force. Since magnetic forces and energy density are increased with increasing flux density, this effect plays a large role in the performance of energy conversion devices.

In addition, magnetic materials can be used to constrain and direct magnetic fields in well-defined paths. In a transformer they are used to maximize the coupling between the windings as well as to lower the excitation current required for transformer operation. In electric machinery magnetic materials are used to shape the fields to maximize the desired torque-producing characteristics. Thus a knowledgeable designer can use magnetic materials to achieve specific desirable device characteristics.

Ferromagnetic materials, composed of iron and alloys of iron with cobalt, tungsten, nickel, aluminum, and other metals, are by far the most common magnetic materials. Although these materials are characterized by a wide range of properties, the basic phenomena responsible for their properties are common to them all.

Ferromagnetic materials are composed of a large number of domains, i.e., regions in which the magnetic moments of all the atoms are parallel, giving rise to a net magnetic moment for that domain. In an unmagnetized sample of material, the domain magnetic moments are randomly oriented, and the net resulting magnetic flux in the material is zero.

When an external magnetizing force is applied to this material, the domain magnetic moments tend to align with the applied magnetic field. As a result, the dipole magnetic moments add to the applied field, resulting in a much larger value of flux density than would exist due to the magnetizing force alone. Thus the *effective permeability* μ , equal to the ratio of the total magnetic flux density to the applied magnetizing force, is large compared with the permeability of free space μ_0 . This behavior continues until all the magnetic moments are aligned with the applied field; at this point they can no longer contribute to increasing the magnetic flux density, and the material is said to be *fully saturated*.

In the absence of an externally applied magnetizing force, the domain magnetic moments naturally align along certain directions associated with the crystal structure of the domain, known as *axes of easy magnetization*. Thus if the applied magnetizing force is reduced, the domain magnetic moments relax to the direction of easy magnetism nearest to that of the

applied field. As a result, when the applied field is reduced to zero, the magnetic dipole moments will no longer be totally random in their orientation; they will retain a net magnetization component along the applied field direction. It is this effect which is responsible for the phenomenon known as *magnetic hysteresis*.

The relationship between B and H for a ferromagnetic material is both nonlinear and multivalued. In general, the characteristics of the material cannot be described analytically. They are commonly presented in graphical form as a set of empirically determined curves based on test samples of the material using methods prescribed by the American Society for Testing and Materials (ASTM).[†]

The most common curve used to describe a magnetic material is the B - H curve or *hysteresis loop*. A set of hysteresis loops is shown in Fig. 1-8

[†]Numerical data on a wide variety of magnetic materials are available from the various material manufacturers. One problem in using the references arises from the various systems of units employed. For example, magnetization may be given in oersteds or in ampere-turns per meter and the magnetic flux density in gauss, kilogauss, or teslas. A few useful conversion factors are given in Appendix C. The reader is reminded that the equations in this book are based upon SI units.

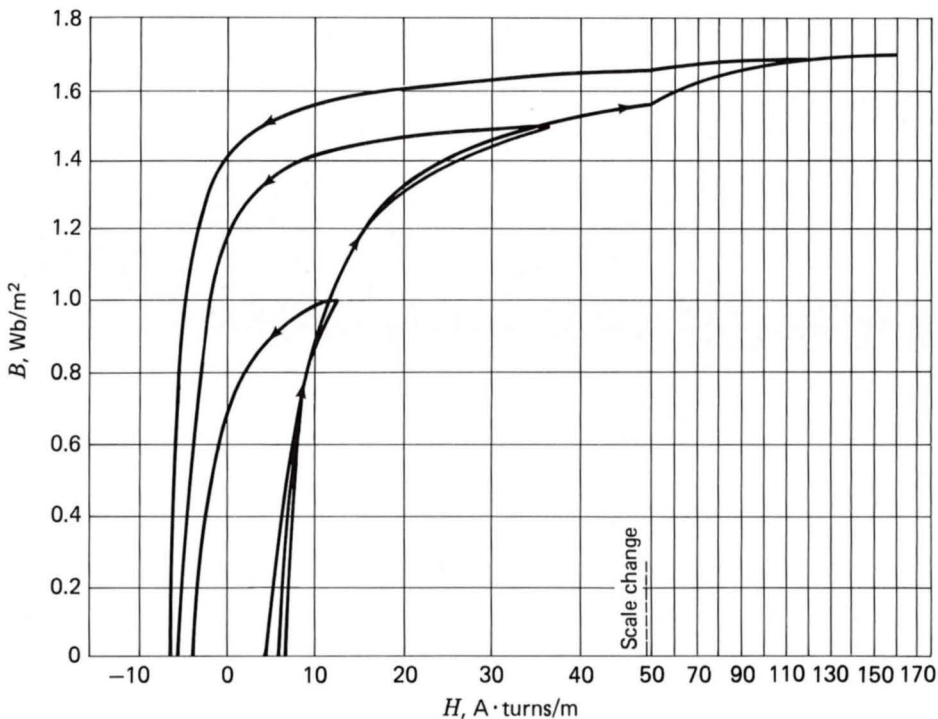


Fig. 1-8. B - H loops for M-5 grain-oriented electrical steel 0.012 in thick. Only the top halves of the loops are shown here. (Armco Inc.)

for M-5 steel, a typical grain-oriented electrical steel used in electric equipment. These loops show the relationship between the magnetic flux density B and the magnetizing force H . Each curve is obtained while cyclically varying the applied magnetizing force between equal positive and negative values of fixed magnitude. Hysteresis causes these curves to be multivalued. After several cycles the B - H curves form closed loops as shown. The arrows show the paths followed by B with increasing and decreasing H . Notice that with increasing magnitude of H the curves begin to flatten out as the material tends toward saturation. At a maximum flux density of about 1.7 T, this material is heavily saturated.

For many engineering applications it is sufficient to describe the material by the curve drawn through the maximum values of B and H at the tips of the hysteresis loops; this is known as a *dc* or *normal magnetization curve*. A dc magnetization curve for M-5 grain-oriented electrical steel is shown in Fig. 1-9. The dc magnetization curve neglects the hysteretic nature of the material but clearly displays its nonlinear characteristics.

EXAMPLE 1-5

Assume that the core material in Example 1-1 has the dc magnetization curve of Fig. 1-9. Find the current i for $B_c = 1$ T.

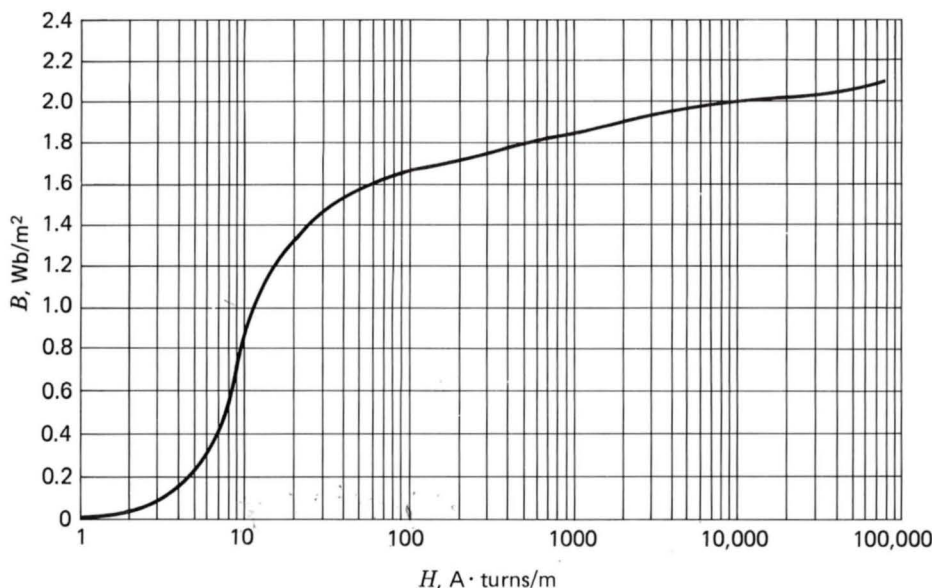


Fig. 1-9. Dc magnetization curve for M-5 grain-oriented electrical steel 0.012 in thick. (Armco Inc.)

Solution

The value of H_c for $B_c = 1$ T is read from Fig. 1-9 as

$$H_c = 12 \text{ A} \cdot \text{turns/m}$$

The mmf for the core path is

$$\mathcal{F}_c = H_c l_c = 12(0.3) = 3.6 \text{ A} \cdot \text{turns}$$

The mmf for the air gap is

$$\mathcal{F}_g = H_g g = \frac{B_g g}{\mu_0} = \frac{5 \times 10^{-4}}{4\pi \times 10^{-7}} = 396 \text{ A} \cdot \text{turns}$$

The current is

$$i = \frac{\mathcal{F}_c + \mathcal{F}_g}{N} = \frac{400}{500} = 0.80 \text{ A}$$

Note that the relative permeability agrees with the value assumed in Example 1-1:

$$\mu_r = \frac{B_c}{\mu_0 H_c} = \frac{1}{(4\pi \times 10^{-7})(12)} = 66,000$$

1-4 AC EXCITATION

In ac power systems, the waveforms of voltage and flux closely approximate sinusoidal functions of time. This article describes the excitation characteristics and losses associated with steady-state ac operation of magnetic materials. We use as our model a closed-core magnetic circuit, i.e., with no air gap, such as that shown in Fig. 1-1 or the transformer of Fig. 2-4. The magnetic path length is l_c , and the cross-sectional area is A_c throughout the length of the core.

We assume a sinusoidal variation of the core flux $\varphi(t)$; thus

$$\varphi(t) = \phi_{\max} \sin \omega t = A_c B_{\max} \sin \omega t \quad (1-40)$$

where ϕ_{\max} = amplitude of core flux φ

B_{\max} = amplitude of flux density B_c

ω = angular frequency = $2\pi f$

f = frequency, Hz

From Faraday's law, Eq. 1-21, the voltage induced in the N -turn winding is

$$e(t) = \omega N \phi_{\max} \cos \omega t = E_{\max} \cos \omega t \quad (1-41)$$

where

$$E_{\max} = \omega N \phi_{\max} = 2\pi f N A_c B_{\max} \quad (1-42)$$

In steady-state ac operation, we are usually more interested in the rms values of voltages and currents than in instantaneous or maximum values. The rms value of a sine wave is $1/\sqrt{2}$ times its peak value. Thus the rms value of the induced voltage is

$$E_{\text{rms}} = \frac{2\pi}{\sqrt{2}} f N A_c B_{\text{max}} = \sqrt{2} \pi f N A_c B_{\text{max}} \quad (1-43)$$

Because of its importance in the theory of ac machines, we return to this equation frequently.

To produce the magnetic field in the core requires current in the exciting winding known as the *exciting current* i_φ .[†] The nonlinear magnetic properties of the core mean that the waveform of the exciting current differs from the sinusoidal waveform of the flux. A curve of the exciting current as a function of time can be found graphically from the magnetic characteristics, as illustrated in Fig. 1-10*a*. Since B and H are related to φ and i_φ by known geometric constants, the ac hysteresis loop of Fig. 1-10*b*

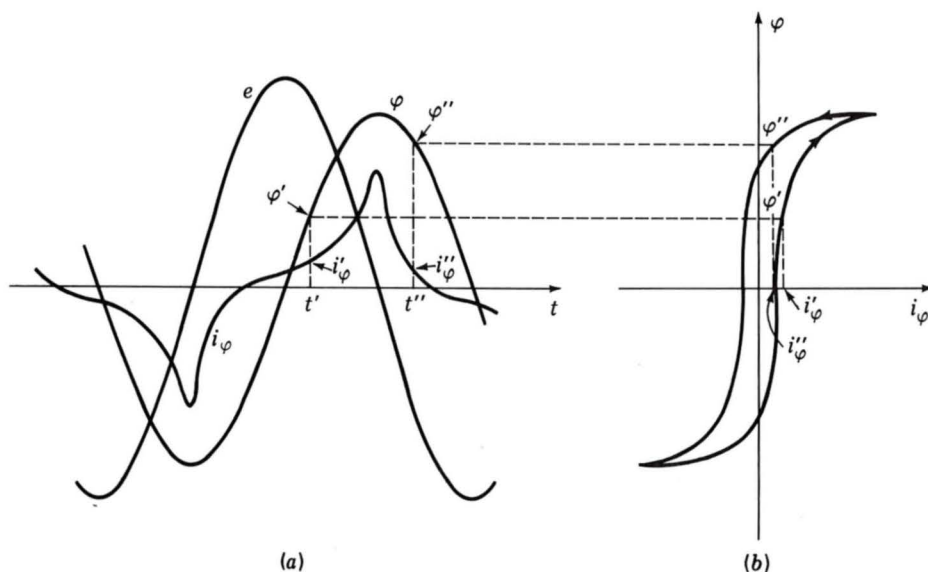


Fig. 1-10. Excitation phenomena. (a) Voltage, flux, and exciting current; (b) corresponding hysteresis loop.

*In general, the exciting current is the net ampere-turns acting on the magnetic circuit.

has been drawn in terms of $\varphi = B_c A_c$ and $i_\varphi = H_c l_c / N$. Sine waves of induced voltage e and flux φ in accordance with Eqs. 1-40 and 1-41 are shown in Fig. 1-10a.

At any given time, the value of i_φ corresponding to the given value of flux can be found directly from the hysteresis loop. For example, at time t' the flux is φ' and the current is i_φ' ; at time t'' the corresponding values are φ'' and i_φ'' . Notice that since the hysteresis loop is multivalued, it is necessary to be careful to pick the rising-flux values (φ' in the figure) from the rising-flux portion of the hysteresis loop; similarly for the falling-flux values (φ'' in the figure). Also notice that the waveform of the exciting current is sharply peaked. Its rms value $I_{\varphi, \text{rms}}$ is defined in the standard way as $\sqrt{i_\varphi^2}$ averaged over a cycle. The corresponding rms value H_{rms} of H_c is related to the rms value $I_{\varphi, \text{rms}}$ of the exciting current; thus

$$I_{\varphi, \text{rms}} = \frac{l_c H_{\text{rms}}}{N} \quad (1-44)$$

The ac excitation characteristics of core materials are usually expressed in terms of rms voltamperes rather than a magnetization curve relating B and H . The theory behind this representation can be explained by combining Eqs. 1-43 and 1-44. Thus the rms voltamperes required to excite the core to a specified flux density are

$$E_{\text{rms}} I_{\varphi, \text{rms}} = \sqrt{2} \pi f N A_c B_{\text{max}} \frac{l_c H_{\text{rms}}}{N} \quad (1-45)$$

$$= \sqrt{2} \pi f A_c l_c B_{\text{max}} H_{\text{rms}} \quad (1-46)$$

For a magnetic material of mass density ρ_c , the weight of the core is $A_c l_c \rho_c$, and the rms voltamperes P_a per unit weight are

$$P_a = \frac{\sqrt{2} \pi f}{\rho_c} B_{\text{max}} H_{\text{rms}} \quad (1-47)$$

The excitation voltamperes P_a at a given frequency f are dependent only on B_{max} because H_{rms} is a unique function of B_{max} and is independent of turns and geometry. As a result, the ac excitation requirements for a magnetic material are often given in terms of rms voltamperes per unit weight determined by laboratory tests on closed-core samples of the material. These results are illustrated in Fig. 1-11 for M-5 grain-oriented electrical steel.

The exciting current supplies the mmf required to produce the core flux and the power input associated with the energy in the magnetic field in the core. Part of this energy is dissipated as losses and appears as heat in the core. The rest appears as reactive power associated with the cyclically varying energy stored in the magnetic field. The reactive power is

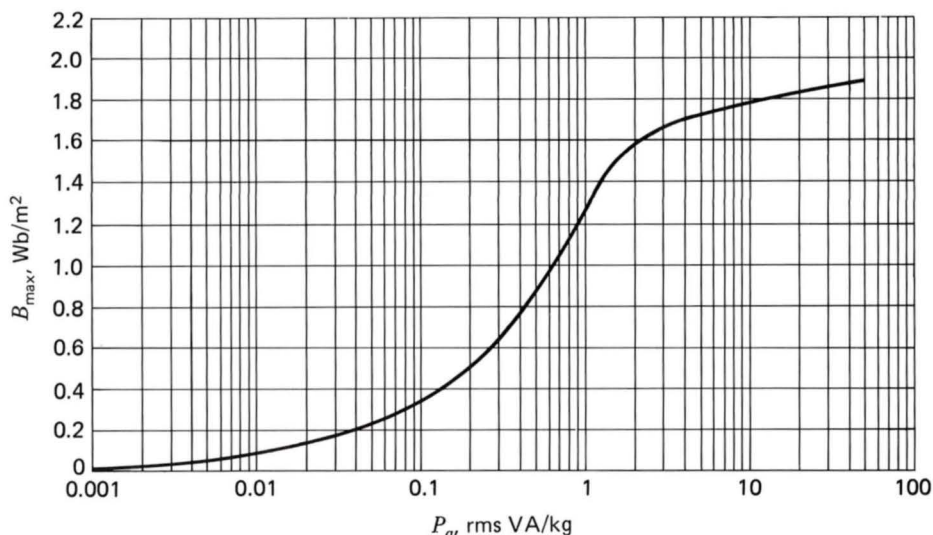


Fig. 1-11. Exciting rms voltamperes per kilogram at 60 Hz for M-5 grain-oriented electrical steel 0.012 in thick. (Armco Inc.)

not dissipated in the core; it is cyclically supplied and absorbed by the excitation source and thus contributes to the current in the source, thereby affecting I^2R losses and voltage drops in the supply system.

Two loss mechanisms are associated with time-varying fluxes in magnetic materials. The first is ohmic I^2R heating, associated with eddy currents. From Faraday's law we see that time-varying magnetic fields give rise to electric fields. In magnetic materials these electric fields result in eddy currents, which circulate in the core material and oppose the change of flux density. To counteract this demagnetizing effect, the current in the exciting winding must increase. Thus the dynamic B - H loop with ac operation is somewhat "fatter" than the hysteresis loop for slowly varying conditions. To reduce the effects of eddy currents, magnetic structures are usually built of thin sheets of laminations of the magnetic material. The laminations, which are aligned in the direction of the field lines, are insulated from each other by an oxide layer on their surfaces or by a thin coat of insulating enamel or varnish. This greatly reduces the magnitude of the eddy currents since the layers of insulation interrupt the current paths; the thinner the laminations, the lower the losses. The power loss caused by eddy currents is dissipated as heat in the core. The eddy-current loss increases as the square of the frequency of the flux variation and also as the square of the peak flux density.

The second loss mechanism is due to the hysteretic nature of magnetic material. In a magnetic circuit like that of Fig. 1-1 or the transformer of Fig. 2-4, a time-varying excitation will cause the magnetic material to undergo a cyclic variation such as the hysteresis loop shown in Fig. 1-12.

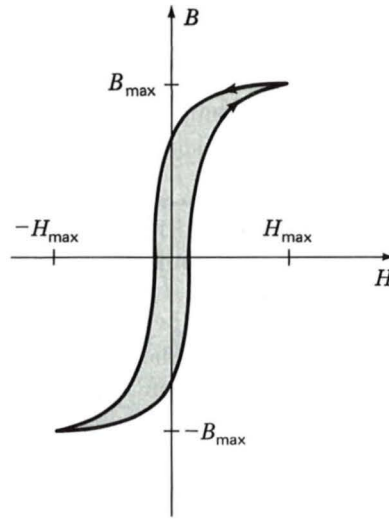


Fig. 1-12. Hysteresis loop; hysteresis loss is proportional to the loop area (shaded).

Equation 1-37 can be used to calculate the energy input to the magnetic core of Fig. 1-1 as the material undergoes a single cycle. For a single cycle

$$W = \oint i_{\phi} d\lambda = \oint \left(\frac{H_c l_c}{N} \right) (A_c N dB_c) = A_c l_c \oint H_c dB_c \quad (1-48)$$

Recognizing that $A_c l_c$ is the volume of the core and that the integral is the area of the ac hysteresis loop, we see that each time the magnetic material undergoes a cycle, there is a net energy input into the material. This energy is required to move around the magnetic dipoles in the material and is dissipated as heat. Thus for a given flux level, hysteresis losses are proportional to the area of the hysteresis loop and to the total volume of material. Since there is an energy loss per cycle, hysteresis power loss is proportional to the frequency of the applied excitation.

In general, the losses depend on the metallurgy of the material as well as the flux density and frequency. Information on core loss is typically presented in graphical form. It is plotted in terms of watts per unit weight as a function of flux density; often a family of curves for different frequencies are given. Figure 1-13 shows the core loss P_c for M-5 grain-oriented electrical steel at 60 Hz.

Nearly all transformers and certain sections of electric machines use sheet-steel material that has highly favorable directions of magnetization along which the core loss is low and the permeability is high. This material is termed *grain-oriented steel*. The reason for this property lies in the atomic structure of the simple crystal of the silicon-iron alloy, which is a body-centered cube; each cube has an atom at each corner as well as one in

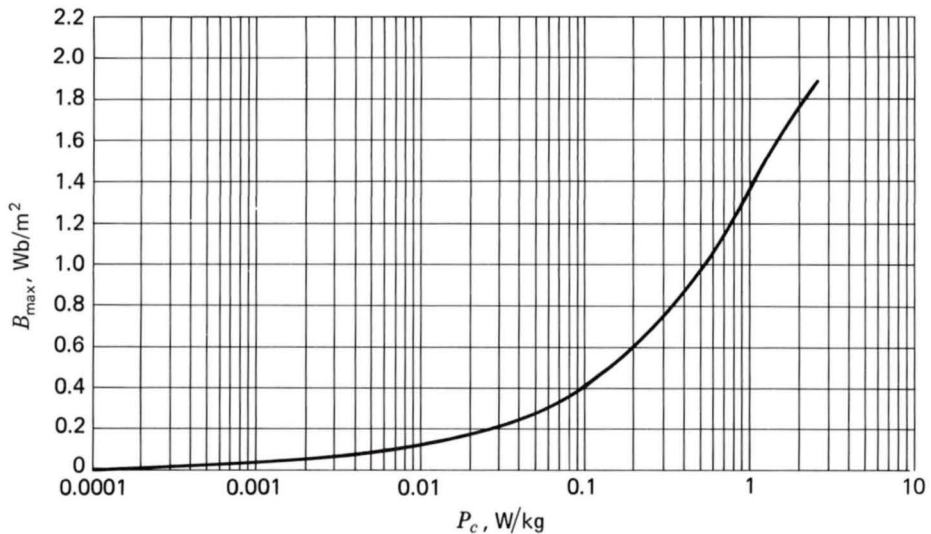


Fig. 1-13. Core loss at 60 Hz in watts per kilogram for M-5 grain-oriented electrical steel 0.012 in thick. (Armco Inc.)

the center of the cube. In the cube, the easiest axis of magnetization is the cube edge; the diagonal across the cube face is more difficult, and the diagonal through the cube is the most difficult. By suitable manufacturing techniques most of the cube edges are aligned in the rolling direction to make it the favorable direction of magnetization. The behavior in this direction is superior in core loss and permeability to nonoriented steels, so that the oriented steels can be operated at higher flux densities than the nonoriented grades. Nonoriented electrical steels are used in applications where the flux does not follow a path which can be oriented with the rolling direction or where low cost is of importance. In these steels the losses are somewhat higher and the permeability is very much lower than in grain-oriented steels.

EXAMPLE 1-6

The magnetic core in Fig. 1-14 is made from laminations of M-5 grain-oriented electrical steel. The winding is excited with a voltage to produce a flux density in the steel of $B = 1.5 \sin 377t$ T. The steel occupies 0.94 times the gross core volume. The density of the steel is 7.65 g/cm^3 . Find (a) the applied voltage, (b) the peak current, (c) the rms exciting current, and (d) the core loss.

Solution

(a) From Eq. 1-21 the voltage is

$$\begin{aligned}
 e &= N \frac{d\phi}{dt} = NA_c \frac{dB}{dt} \\
 &= 200(4 \text{ in}^2)(0.94) \frac{1 \text{ m}^2}{39.4^2 \text{ in}^2} (1.5) (377 \cos 377t) \\
 &= 275 \cos 377t \quad \text{V}
 \end{aligned}$$

(b) The magnetic intensity corresponding to $B_{\max} = 1.5 \text{ T}$ is given in Fig. 1-9 as $H = 36 \text{ A} \cdot \text{turns/m}$. Notice that the relative permeability $\mu_r = B/(\mu_0 H) = 33,000$ at the flux level of 1.5 T is significantly lower than the value of $\mu_r = 66,000$ found in Example 1-5 corresponding to a flux level of 1.0 T.

$$l_c = (6 + 6 + 8 + 8) \text{ in} \frac{1 \text{ m}}{39.4 \text{ in}} = 0.71 \text{ m}$$

The peak current is

$$I = \frac{36(0.71)}{200} = 0.13 \text{ A}$$

(c) The rms current is obtained from the value of P_a of Fig. 1-10 for $B_{\max} = 1.5 \text{ T}$.

$$P_a = 1.5 \text{ VA/kg}$$

The core volume and weight are

$$\begin{aligned}
 V_c &= (4 \text{ in}^2)(0.94)(28 \text{ in}) = 105.5 \text{ in}^3 \\
 W_c &= (105.5 \text{ in}^3) \frac{(7.65 \text{ g})(2.54^3 \text{ cm}^3)}{(1 \text{ cm}^3)(1 \text{ in}^3)} = 13.2 \text{ kg}
 \end{aligned}$$

The total rms voltamperes and current are

$$\begin{aligned}
 P_a &= (1.5 \text{ VA/kg})(13.2 \text{ kg}) = 20 \text{ VA} \\
 I_\phi &= \frac{P_a}{E_{\text{rms}}} = \frac{20}{275(0.707)} = 0.10 \text{ A}
 \end{aligned}$$

(d) The core-loss density is obtained from Fig. 1-13 as $P_c = 1.2 \text{ W/kg}$. The total core loss is

$$P_c = (1.2 \text{ W/kg})(13.2 \text{ kg}) = 16 \text{ W}$$

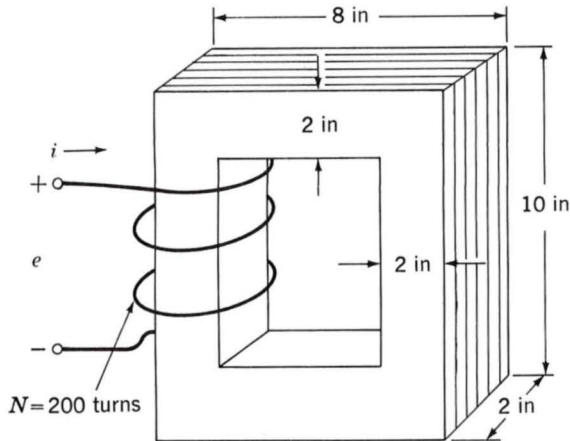


Fig. 1-14. Reactor with laminated steel core.

1-5 PERMANENT MAGNETS

Figure 1-15a shows the second quadrant of a hysteresis loop for Alnico 5, a typical permanent magnet material, while Fig. 1-15b shows the second quadrant of a hysteresis loop for M-5 steel.[†] Notice that the curves are similar in nature. However, the hysteresis loop of Alnico 5 is characterized by a large value of *residual flux density* or *remanent magnetization* B_r (approximately 1.22 Wb/m^2) as well as a large value of *coercivity* H_c (approximately -49 kA/m). The remanent magnetization B_r corresponds to the flux density which would remain in a closed magnetic structure, such as that of Fig. 1-1, made of this material if the applied mmf (and hence the magnetic field intensity H) were reduced to zero. However, although the M-5 electrical steel also has a large value of remanent magnetization (approximately 1.4 Wb/m^2), it has a much smaller value of coercivity (approximately -6 A/m , smaller by a factor of over 7500).

The significance of remanent magnetization is that it can result in the presence of magnetic flux in a magnetic circuit in the absence of external excitation in the form of currents in windings. This is a well-known phenomenon. It is commonplace in applications ranging from magnets which hold notes on refrigerator doors to small permanent magnet appliance motors and loudspeakers.

From Fig. 1-15, it would appear that both Alnico 5 and the M-5 electrical steel would be useful in producing flux in unexcited magnetic circuits since they both have large values of remanent magnetization. That this is not the case can be best illustrated by an example.

[†]To obtain the largest value of remanent magnetization, the hysteresis loops of Fig. 1-15 are those which would be obtained if the materials were excited by sufficient mmf to ensure that they were driven heavily into saturation. This is discussed further in Art. 1-6.

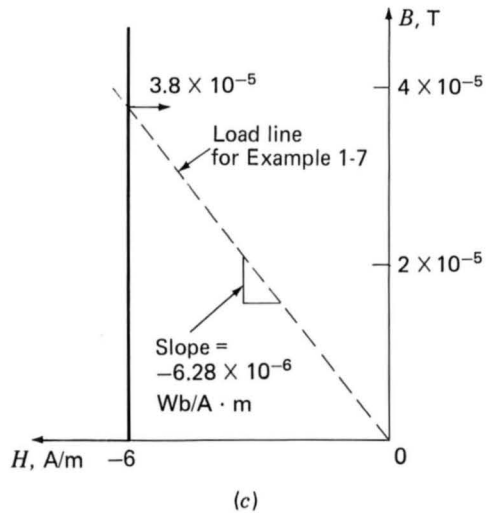
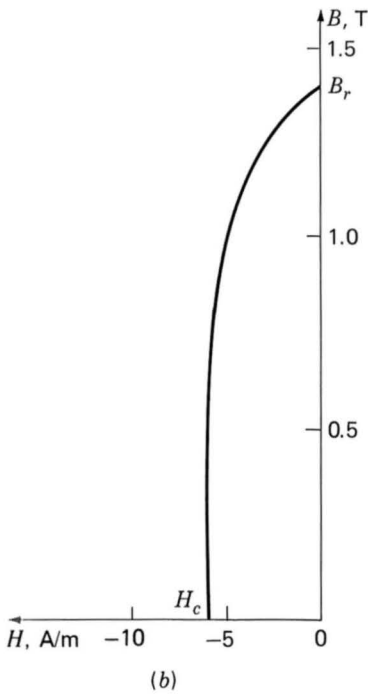
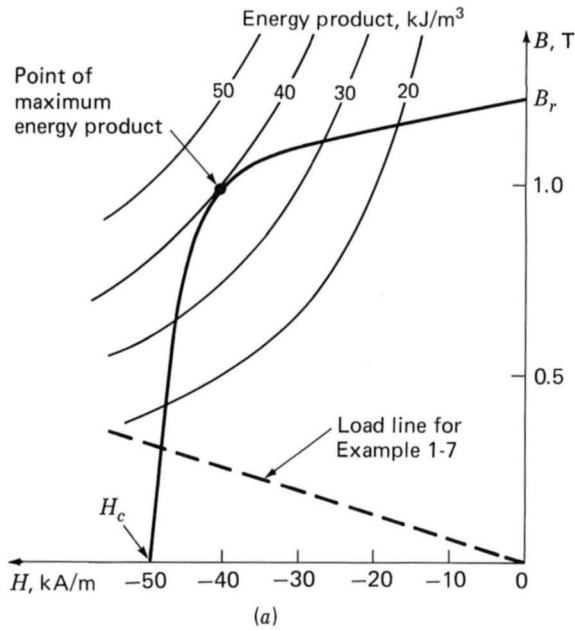


Fig. 1-15. (a) Second quadrant of hysteresis loop for Alnico 5; (b) second quadrant of hysteresis loop for M-5 electrical steel; (c) hysteresis loop for M-5 electrical steel expanded for small B . (Armco Inc.)

EXAMPLE 1-7

As shown in Fig. 1-16, a magnetic circuit consists of a core of high permeability ($\mu \rightarrow \infty$), an air gap of length g , and a section of magnetic material of length l_m . Calculate the flux density B_g in the air gap if the magnetic material is (a) Alnico 5 and (b) M-5 electrical steel.

Solution

(a) Since the core permeability is assumed infinite, we neglect H in the core as negligible. Recognizing that the mmf acting on the magnetic circuit of Fig. 1-16 is zero, we can write

$$\mathcal{F} = 0 = H_g g + H_m l_m$$

or

$$H_g = -\frac{l_m}{g} H_m$$

where H_g and H_m are the magnetic field intensities in the air gap and the magnetic material, respectively.

Since the flux must be continuous through the magnetic circuit,

$$\phi = A_g B_g = A_m B_m$$

or

$$B_g = \frac{A_m}{A_g} B_m$$

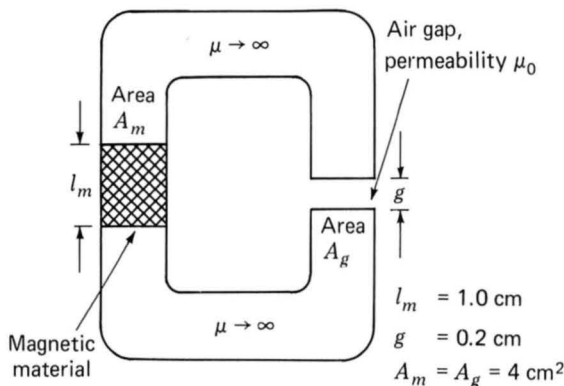


Fig. 1-16. Magnetic circuit for Example 1-7.

where B_g and B_m are the magnetic flux densities in the air gap and the magnetic material, respectively.

These equations can be solved to yield a linear relationship for B_m in terms of H_m :

$$B_m = -\mu_0 \left(\frac{A_g}{A_m} \right) \left(\frac{l_m}{g} \right) H_m = -5\mu_0 H_m = -6.28 \times 10^{-6} H_m$$

To solve for B_m , we recognize that Alnico 5, B_m , and H_m are also related by the curve of Fig. 1-15a. Thus this linear relationship, also known as the *load line*, can be plotted on Fig. 1-15a and the solution obtained graphically, resulting in

$$B_g = B_m = 0.30 \text{ T}$$

(b) The solution for M-5 electrical steel proceeds exactly as in part (a). The load line is the same as that of part (a) because it is determined only by the permeability of the air gap and the geometries of the magnet and the air gap. Hence from Fig. 1-15c

$$B_g = 3.8 \times 10^{-5} \text{ T} = 0.38 \text{ G}$$

which is much less than the value obtained with Alnico 5.

Example 1-7 shows that there is an immense difference between permanent magnet materials (often referred to as hard magnetic materials) such as Alnico 5 and soft magnetic materials such as M-5 electrical steel. This difference is characterized in large part by the immense difference in their coercivities H_c . The coercivity can be thought of as a measure of the amount of mmf required to demagnetize the material. As seen from Example 1-7, it is also a measure of the capability of the material to produce flux in a magnetic circuit which includes an air gap. Thus we see that materials which make good permanent magnets are characterized by large values of coercivity H_c (considerably in excess of 1 kA/m).

A useful measure of the capability of a permanent magnet is known as its *maximum energy product*. This corresponds to the largest B - H product $(BH)_{\max}$, which corresponds to a point on the second quadrant of the hysteresis loop. As we have seen, the product of B and H has the dimensions of energy density (joules per cubic meter). We now show that operation of a given permanent magnet material at this point will result in the smallest volume of that material required to produce a given flux density in the air gap. Similarly, choosing a material with the largest available maximum energy product will result in the smallest required magnet volume.

In Example 1-7, we found an expression for the flux density in the air gap:

$$B_g = \frac{A_m}{A_g} B_m \quad (1-49)$$

We also found that the ratio of the mmf drops across the magnet and the air gap is equal to -1 :

$$\frac{H_m l_m}{H_g g} = -1 \quad (1-50)$$

Equation 1-50 can be solved for $B_g = \mu_0 H_g$, and the result can be multiplied by Eq. 1-49 to yield

$$\begin{aligned} B_g^2 &= \mu_0 \left(\frac{l_m A_m}{g A_g} \right) (-H_m B_m) \\ &= \mu_0 \left(\frac{\text{vol}_{\text{mag}}}{\text{vol}_{\text{air gap}}} \right) (-H_m B_m) \end{aligned} \quad (1-51)$$

or

$$\text{vol}_{\text{mag}} = \frac{B_g^2 \text{vol}_{\text{air gap}}}{\mu_0 (-H_m B_m)} \quad (1-52)$$

where vol_{mag} is the volume of the magnet, $\text{vol}_{\text{air gap}}$ is the air-gap volume, and the minus sign arises because, at the operating point of the magnetic circuit, H in the magnet (H_m) is negative.

Equation 1-52 is the desired result. It indicates that to achieve a desired flux density in the air gap, the required volume of the magnet can be minimized by operating the magnet at the point of the maximum B - H product, i.e., the *point of maximum energy product*. Because the maximum energy product is a measure of the magnet volume required for a given application, it is often found as a tabulated "figure of merit" on data sheets for permanent magnet materials.

Note that Eq. 1-51 appears to indicate that one can achieve an arbitrarily large air-gap flux density simply by reducing the air-gap volume. This is not true in practice because as the flux density in the magnetic circuit increases, a point will be reached at which the magnetic core material will begin to saturate and the assumption of infinite permeability will no longer be valid, thus invalidating Eq. 1-51.

Note that a curve of constant B - H product is a hyperbola. A set of such hyperbolas for different values of the B - H product is plotted in Fig. 1-15a. From these curves, we see that the maximum energy product for Alnico 5 is 40 kJ/m^3 and that this occurs at the point $B = 1.0 \text{ Wb/m}^2$ and $H = -40 \text{ kA/m}$.

EXAMPLE 1-8

The magnetic circuit of Fig. 1-16 is modified so that the air-gap area is reduced to $A_g = 2.0 \text{ cm}^2$ as shown in Fig. 1-17. Find the minimum magnet volume required to achieve an air-gap flux density of 0.8 T.

Solution

The smallest magnet volume will be achieved with the magnet operating at its point of maximum energy product, as shown in Fig. 1-15a. At this operating point, $B_m = 1.0 \text{ T}$ and $H_m = -40 \text{ kA/m}$.

Thus from Eq. 1-49,

$$\begin{aligned} A_m &= A_g \frac{B_g}{B_m} \\ &= (2 \text{ cm}^2) \left(\frac{0.8}{1.0} \right) = 1.6 \text{ cm}^2 \end{aligned}$$

and from Eq. 1-50,

$$\begin{aligned} l_m &= -g \frac{H_g}{H_m} = -g \frac{B_g}{\mu_0 H_m} \\ &= -0.2 \text{ cm} \frac{0.8}{(4\pi \times 10^{-7}) (-40 \times 10^3)} \\ &= 3.18 \text{ cm} \end{aligned}$$

Thus the minimum magnet volume is equal to $1.6 \times 3.18 = 5.09 \text{ cm}^3$.

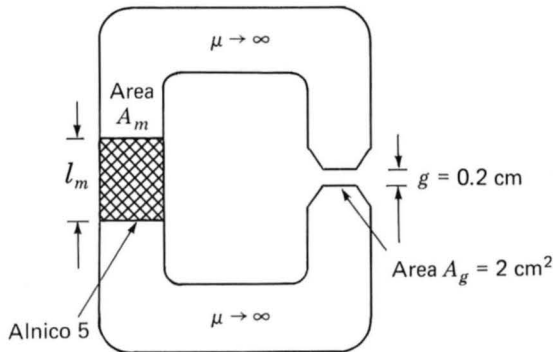


Fig. 1-17. Magnetic circuit for Example 1-8.

1-6 APPLICATION OF PERMANENT MAGNET MATERIALS

Examples 1-7 and 1-8 consider the operation of hard magnetic materials under the assumption that the operating point can be determined simply from a knowledge of the geometry of the magnetic circuit and the properties of the various magnetic materials involved. In fact, the situation is more complex.[†] This section will expand upon these issues.

Figure 1-18 shows the dc magnetization characteristics for a few common permanent magnet materials. Alnico 5 is a widely used version of an alloy of iron, nickel, aluminum, and cobalt originally discovered in 1931. It has a relatively large residual flux density. Alnico 8 has a lower residual flux density and a higher coercivity than Alnico 5. It is hence less subject to demagnetization than Alnico 5. Disadvantages of the Alnico materials are their relatively low coercivity and their mechanical brittleness.

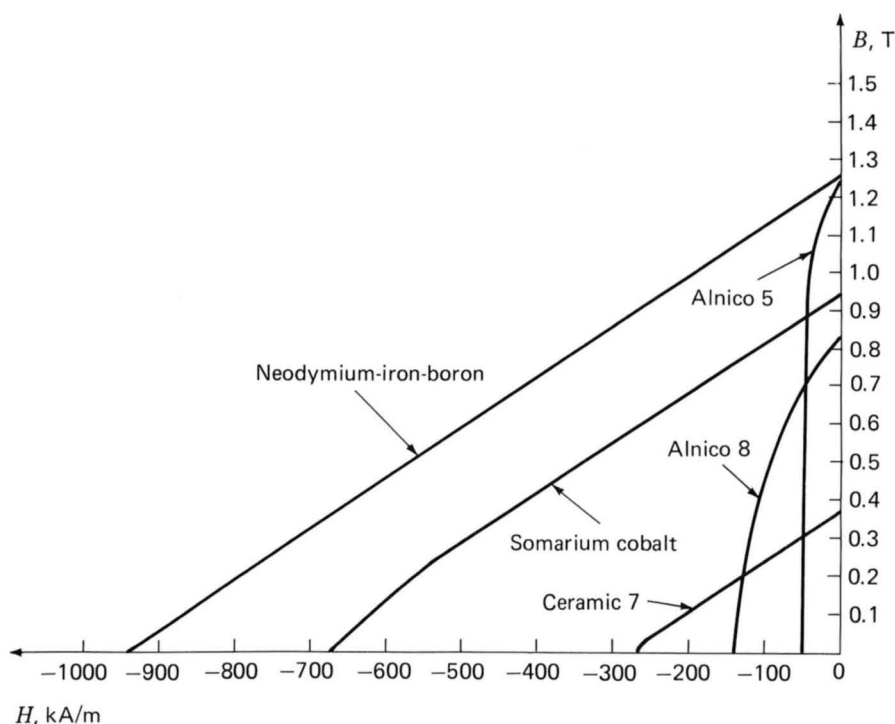


Fig. 1-18. DC magnetization curves for common permanent magnet materials.

[†]For a further discussion of permanent magnets and their applications, see F.N. Bradley, *Materials for Magnetic Functions*, Hayden Book Co., New York, 1971, chap. 4; G.R. Slemon and A. Straughen, *Electric Machines*, Addison-Wesley, Reading, Mass., 1980, secs. 1.20–1.25; and C. Heck, *Magnetic Materials and Their Applications*, Butterworth & Co., London, 1974, chap. 9.

Ceramic permanent magnet materials (also known as *ferrite magnets*) are made from iron oxide and barium or strontium carbonate powders and have lower residual flux densities than Alnico materials but significantly higher coercivities. As a result, they are much less prone to demagnetization. One such material, ceramic 7, is shown in Fig. 1-18, where its dc magnetization characteristic is almost a straight line. Ceramic magnets have good mechanical characteristics and are inexpensive to manufacture; as a result, they are the most widely used of permanent magnet materials.

Samarium cobalt represents a significant advance in permanent magnet technology which began in the 1960s with the discovery of rare-earth permanent magnet materials. From Fig. 1-18 it can be seen to have a high residual flux density such as is found with the Alnico materials, while at the same time having a much higher coercivity and maximum energy product.

The newest of the rare-earth magnetic materials is the neodymium-iron-boron material. It features even larger residual flux density, coercivity, and maximum energy product than does samarium cobalt. In addition, it has good mechanical properties and is relatively inexpensive to manufacture and thus can be expected to find increasing use in permanent magnet applications.

Consider the magnetic circuit of Fig. 1-19. This consists of a section of hard magnetic material in a core of highly permeable soft magnetic material. An N -turn excitation winding is also included. With reference to Fig. 1-20, we assume that the hard magnetic material is initially unmagnetized and consider what happens as current is applied to the excitation winding. Because the core is assumed to be of infinite permeability, the horizontal axis of Fig. 1-20 can be considered to be both a measure of the applied current $i = Hl_m/N$ as well as a measure of H in the magnetic material.

As current i is increased to its maximum value, the B - H trajectory rises from point a in Fig. 1-20 toward its maximum value at point b . To fully magnetize the material, we assume that the current has been in-

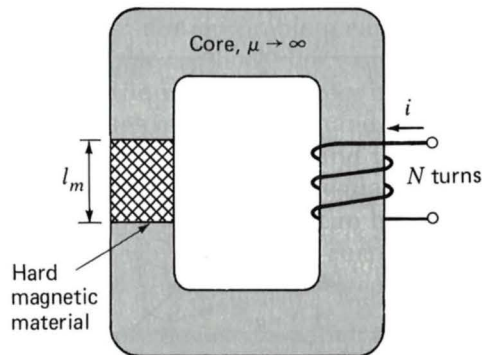


Fig. 1-19. Magnetic circuit including both a permanent magnet and an excitation winding.

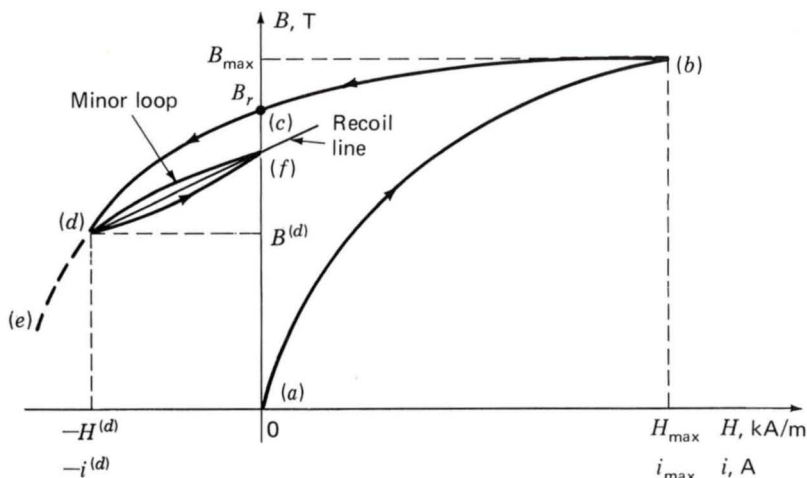


Fig. 1-20. Portion of a B - H characteristic showing a minor loop and a recoil line.

creased to a value i_{\max} sufficiently large that the material has been driven well into saturation at point b . When the current is then decreased to zero, the B - H characteristic will begin to form a hysteresis loop, arriving at point c at zero current. At point c , notice that H in the material is zero but B is at its remanent value B_r .

As the current then goes negative, the B - H characteristic continues to trace out a hysteresis loop. In Fig. 1-20, this is seen as the trajectory between points c and d . If the current is then maintained at the value $-i^{(d)}$, the operating point of the magnet will be that of point d . Note that, as in Example 1-7, this same operating point would be reached if the material were to start at point c and, with the excitation held at zero, an air gap of length $g = l_m (A_g/A_m) (-\mu_0 H^{(d)}/B^{(d)})$ were then inserted in the core.

Should the current then be made more negative, the trajectory would continue tracing out the hysteresis loop toward point e . However, if instead the current is reduced to zero, the trajectory does not in general retrace the hysteresis loop toward point c . Rather it begins to trace out a *minor hysteresis loop*, reaching point f when the current reaches zero. If the current is then varied between zero and $-i^{(d)}$, the B - H characteristic will trace out the minor loop as shown.

As can be seen from Fig. 1-20, the B - H trajectory between points d and f can be represented by a straight line, known as the *recoil line*. The slope of this line is called the *recoil permeability* μ_R . We see that once this material has been demagnetized to point d , the effective remanent magnetization of the magnetic material is that of point f which is less than the remanent magnetization B_r which would be expected based on the hysteresis loop. Note that should the demagnetization be increased past point d , for example, to point e of Fig. 1-20, a new minor loop will be created, with a new recoil line and recoil permeability.

The demagnetization effects of negative excitation which have just been discussed are equivalent to those of an air gap in the magnetic circuit. For example, clearly the magnetic circuit of Fig. 1-19 could be used as a device to magnetize hard magnetic materials. The process would simply require that a large excitation be applied to the winding and then reduced to zero, leaving the material at a remanent magnetization B_r (point c in Fig. 1-20).

Following this magnetization process, if the material were removed from the core, this would be equivalent to opening a large air gap in the magnetic circuit, demagnetizing the material in a fashion similar to that seen in Example 1-7. At this point, the magnet has been effectively weakened, since if it were again inserted in the magnetic core, it would follow a recoil line and return to a remanent magnetization somewhat less than B_r . Thus hard magnetic materials often do not operate stably in situations with varying mmf and geometry, and there is often the risk that improper operation can further demagnetize them.

At the expense of a reduction in value of the remanent magnetization, hard magnetic materials can be stabilized to operate over a specified region. This procedure, based on the recoil trajectory shown in Fig. 1-20, can best be illustrated by an example.

EXAMPLE 1-9

Figure 1-21 shows a magnetic circuit containing hard magnetic material, a core and plunger of high (assumed infinite) permeability, and a single-turn winding which will be used to magnetize the hard magnetic material. The winding will be removed after the system is magnetized. The plunger

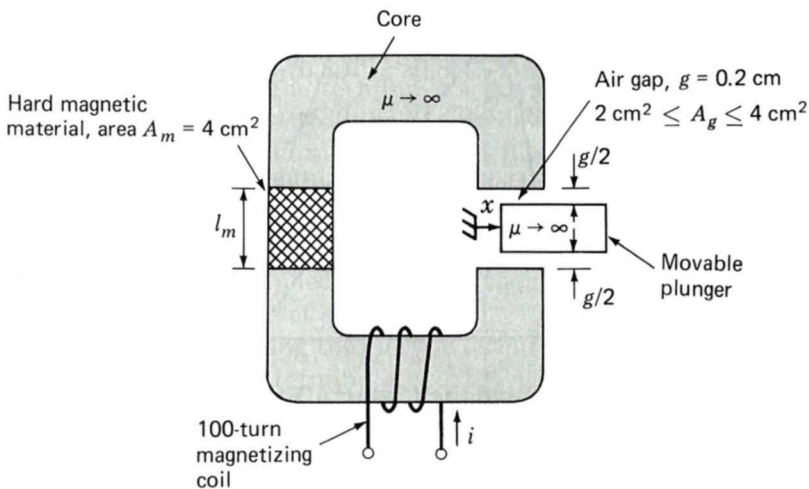


Fig. 1-21. Magnetic circuit for Example 1-9.

moves in the x direction as indicated, with the result that the air-gap area can vary ($2 \text{ cm}^2 \leq A_g \leq 4 \text{ cm}^2$). Assuming that the hard magnetic material is Alnico 5, (a) find the magnet length l_m so that the system will operate on a recoil line which intersects the maximum B - H product point on the magnetization curve for Alnico 5, (b) derive a procedure for magnetizing the magnet, and (c) calculate the flux density B_g in the air gap as the plunger moves.

Solution

(a) Figure 1-22a shows the magnetization curve for Alnico 5 and two load lines corresponding to the two extremes of the air gap, $A_g = 2 \text{ cm}^2$ and $A_g = 4 \text{ cm}^2$. We see that the system will operate on the desired recoil line if the load line for $A_g = 2 \text{ cm}^2$ intersects the B - H characteristic at the maximum energy product point (labeled point a in Fig. 1-22a), $B_m^{(a)} = 1.0 \text{ T}$ and $H_m^{(a)} = -40 \text{ kA/m}$.

From Eqs. 1-49 and 1-50, we see that the slope of the required load line is given by

$$\frac{B_m^{(a)}}{-H_m^{(a)}} = \frac{B_g}{H_g} \frac{A_g}{A_m} \frac{l_m}{g}$$

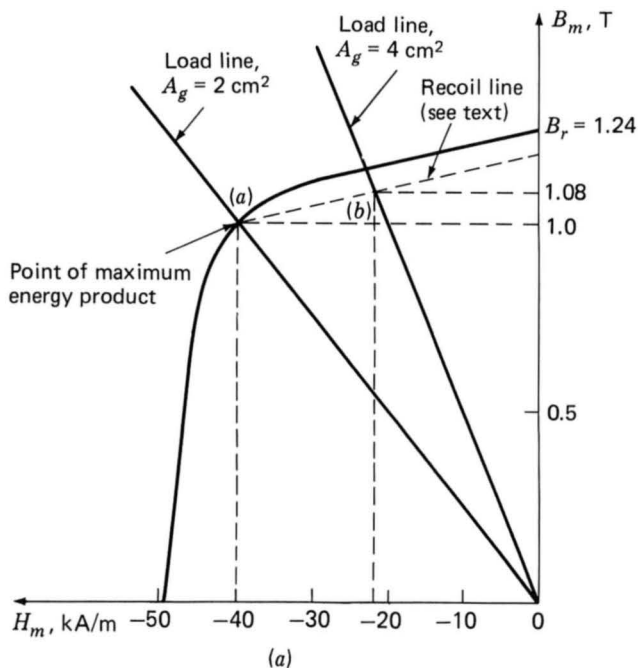


Fig. 1-22. (a) Magnetization curve for Alnico 5 for Example 1-9; (b) series of load lines for $A_g = 2 \text{ cm}^2$ and varying values of i showing the magnetization procedure for Example 1-9.

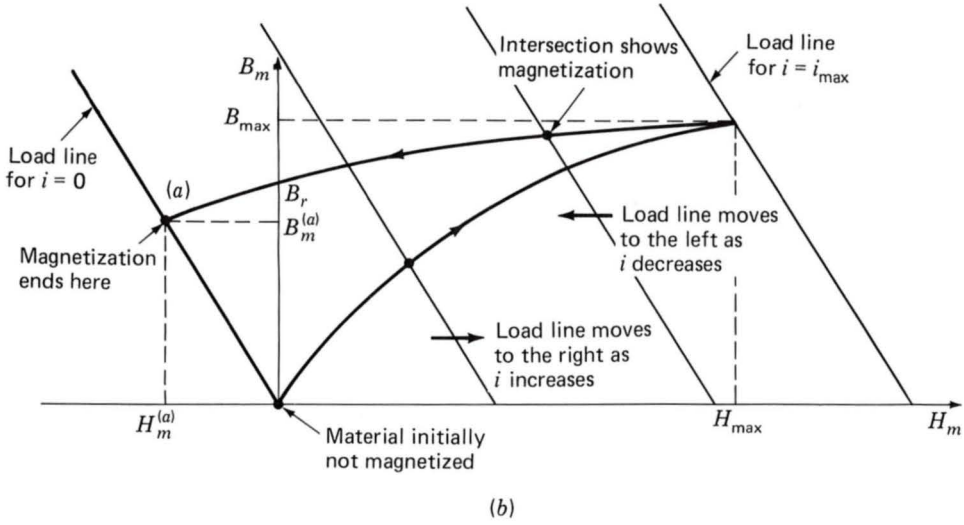


Fig. 1-22. (Continued).

and thus

$$\begin{aligned}
 l_m &= g \left(\frac{A_m}{A_g} \right) \left(\frac{B_m^{(a)}}{-\mu_0 H_m^{(a)}} \right) \\
 &= 0.2 \text{ cm} \left(\frac{4}{2} \right) \left(\frac{1.0}{4\pi \times 10^{-7} \times 4 \times 10^4} \right) \\
 &= 7.96 \text{ cm}
 \end{aligned}$$

(b) Figure 1-22b shows a series of load lines for the system with $A_g = 2 \text{ cm}^2$ and with current i applied to the excitation winding. The general equation for these load lines can be readily derived since from Eq. 1-5

$$Ni = H_m l_m + H_g g$$

and from Eqs. 1-3 and 1-7

$$B_m A_m = B_g A_g = \mu_0 H_g A_g$$

Thus

$$\begin{aligned}
 B_m &= -\mu_0 \left(\frac{A_g}{A_m} \right) \left(\frac{l_m}{g} \right) H_m + \frac{\mu_0 N}{g} \left(\frac{A_g}{A_m} \right) i \\
 &= \mu_0 \left[-\left(\frac{2}{4} \right) \left(\frac{7.96}{0.2} \right) H_m + \frac{100}{2 \times 10^{-3}} \left(\frac{2}{4} \right) i \right] \\
 &= -2.50 \times 10^{-5} H_m + 3.14 \times 10^{-2} i
 \end{aligned}$$

From Fig. 1-22*b* we see that if the plunger is set so that $A_g = 2 \text{ cm}^2$, the current in the magnetizing winding is increased to the value i_{\max} where

$$i_{\max} = \frac{B_{\max} + 2.50 \times 10^{-5} H_{\max}}{3.14 \times 10^{-2}} \quad \text{A}$$

In this case, we do not have a complete hysteresis loop for Alnico 5, and hence we will have to estimate B_{\max} and H_{\max} . Linearly extrapolating the B - H curve at $H = 0$ back to 4 times the coercivity, that is, $H_{\max} = 4 \times 50 = 200 \text{ kA/m}$, yields $B_{\max} = 2.1 \text{ T}$. This value is undoubtedly extreme and will overestimate the required current somewhat. However, using $B_{\max} = 2.1 \text{ T}$ and $H_{\max} = 200 \text{ kA/m}$ yields $i_{\max} = 22.6 \text{ A}$.

Thus with the air-gap area set to 2 cm^2 , increasing the current to 22.6 A and then reducing it to zero will achieve the desired magnetization.

(c) Because we do not have specific information about the slope of the recoil line, we assume that its slope is the same as that of the B - H characteristic at the point $H = 0$, $B = B_r$. From Fig. 1-22*a*, with the recoil line drawn with this slope, we see that as the air-gap area varies between 2 and 4 cm^2 , the magnet flux density B_m varies between 1.00 and 1.08 T. Since the air-gap flux density equals A_m/A_g times this value, the air-gap flux density will equal $4/2(1.00) = 2.0 \text{ T}$ when $A_g = 2.0 \text{ cm}^2$ and $(4/4)(1.08) = 1.08 \text{ T}$ when $A_g = 4.0 \text{ cm}^2$.

As has been seen, hard magnetic materials such as Alnico 5 can be subject to demagnetization, should their operating point be varied excessively. As shown in Example 1-9, these materials can be stabilized with some loss in effective remanent magnetization. However, this procedure does not guarantee absolute stability of operation. For example, if the material in Example 1-9 were subjected to an air-gap area smaller than 2 cm^2 or to excessive demagnetizing current, the effect of the stabilization would be erased and the material would be found to operate on a new recoil line with further reduced magnetization.

However, many materials, such as samarium cobalt, ceramic 7, and neodymium-iron-boron (see Fig. 1-18), which have large values of coercivity, tend to have very low values of recoil permeability, and the recoil line is essentially tangent to the B - H characteristic for a large portion of the useful operating region. This can be seen in Fig. 1-18, which shows the dc magnetization curve for neodymium-iron-boron, from which we see that this material has a remanent magnetization of 1.25 T and a coercivity of -940 kA/m . The portion of the curve between these points is a straight line with a slope equal to $1.06\mu_0$, which is the same as the slope of its recoil line. As long as these materials are operated on this low incremental permeability portion of their B - H characteristic, they do not require stabilization, provided they are not excessively demagnetized.

1-7 SUMMARY

Electromechanical devices which employ magnetic fields often use ferromagnetic materials for guiding and concentrating these fields. Because the magnetic permeability of ferromagnetic materials can be large (up to tens of thousands times that of the surrounding space), most of the magnetic flux is confined to fairly definite paths determined by the magnetic material. In addition, often the frequencies of interest are low enough to permit the magnetic fields to be considered quasi-static, and hence they can be determined simply from a knowledge of the net mmf acting on the magnetic structure.

As a result, the solution for the magnetic fields in these devices can be obtained in a straightforward fashion by using the techniques of magnetic circuit analysis. These techniques can be used to reduce a complex three-dimensional magnetic field solution to what is essentially a one-dimensional problem. As in all engineering solutions, a certain amount of experience and judgment is required, but the technique gives useful results in many situations of practical engineering interest.

Ferromagnetic materials are available with a wide variety of characteristics. In general, their behavior is nonlinear, and their B - H characteristics are often represented in the form of a family of hysteresis (B - H) loops. Losses, both hysteretic and eddy-current, are a function of the flux level and frequency of operation as well as the material composition and the manufacturing process used. A basic understanding of the nature of these phenomena is extremely useful in the application of these materials in practical devices. Typically, important properties are available in the form of curves supplied by the material manufacturers.

Certain magnetic materials, commonly known as hard or permanent magnet materials, are characterized by large values of remanent magnetization and coercivity. These materials produce significant magnetic flux even in magnetic circuits with air gaps. With proper design they can be made to operate stably in situations which subject them to a wide range of destabilizing forces and mmf's. Permanent magnets find application in many small devices, including loudspeakers, ac and dc motors, microphones, and analog electric meters.

PROBLEMS

1-1. A magnetic circuit with a single air gap is shown in Fig. 1-23. The core dimensions are

$$\text{Cross-sectional area } A_c = 1.5 \times 10^{-3} \text{ m}^2$$

$$\text{Mean core length } l_c = 0.7 \text{ m}$$

$$\text{Gap length } g = 2.5 \times 10^{-3} \text{ m}$$

$$N = 75 \text{ turns}$$

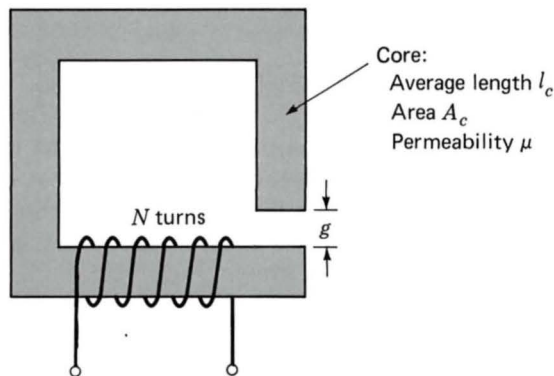


Fig. 1-23. Magnetic circuit for Prob. 1-1.

Assume that the core is of infinite permeability ($\mu \rightarrow \infty$), and neglect the effects of magnetic leakage and fringing. For a current of $i = 1$ A, calculate (a) the total flux ϕ , (b) the flux linkages λ of the coil, and (c) the coil inductance L .

1-2. Repeat Prob. 1-1 for a finite core permeability of $\mu = 1500\mu_0$.

1-3. The magnetic circuit of Fig. 1-24 consists of rings of magnetic material in a stack of height D . The rings have inner radius R_i and outer radius R_o . Assume that the iron is of infinite permeability ($\mu \rightarrow \infty$), and neglect the effects of magnetic leakage and fringing. Calculate

- (a) The mean core length l_c and the core cross-sectional area A_c
- (b) The reluctance of the core \mathcal{R}_c and that of the gap \mathcal{R}_g

For $N = 75$ turns, calculate

- (c) The inductance L

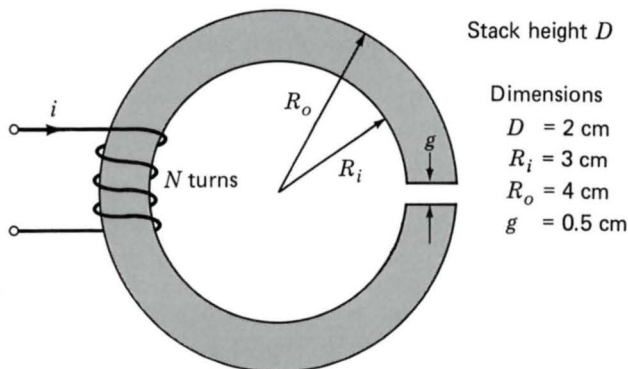


Fig. 1-24. Magnetic circuit for Prob. 1-3.

- (d) Current i required to operate at an air-gap flux density of $B_g = 1.2 \text{ T}$
 (e) The corresponding flux linkages λ of the coil

1-4. Repeat Prob. 1-3 for a finite core permeability of $\mu = 750\mu_0$.

1-5. Figure 1-25 shows the cross section of a circularly symmetric magnetic circuit with an N -turn winding. Neglect fringing and magnetic leakage, and assume the core permeability to be infinite ($\mu \rightarrow \infty$). For a current of i A in the coil, calculate the flux ϕ , the air-gap flux density B_g , the flux density λ , and the inductance L . Finally, find the values of h and R_3 in terms of R_1 and R_2 so that the magnetic flux density is uniform within the core.

1-6. Consider the magnetic circuit of Fig. 1-25. Assume the core permeability to be $\mu = 2000\mu_0$ and $N = 100$ turns. The following dimensions are specified:

$$R_1 = 1 \text{ cm} \quad R_2 = 3 \text{ cm} \quad l = 2.5 \text{ cm}$$

$$h = 1 \text{ cm} \quad g = 0.2 \text{ cm}$$

- (a) Find the values of h and R_3 so that the flux density within the core is uniform.
 (b) Find the inductance of the winding.
 (c) The core is to be operated at a peak flux density of 1.5 T at a frequency of 60 Hz. Find the corresponding peak and rms value of the voltage induced in the winding.
 (d) Repeat part (c) for a frequency of 50 Hz.

1-7. A square voltage wave having a fundamental frequency of 60 Hz and equal positive and negative half cycles of amplitude E is applied to a resistanceless winding of 1000 turns surrounding a closed iron core of $1.25 \times 10^{-3} \text{ m}^2$ cross section.

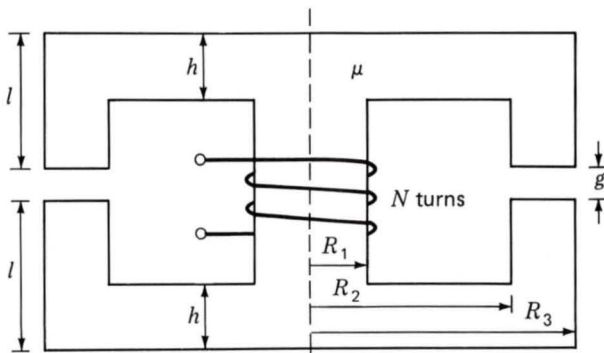


Fig. 1-25. Cross section of circularly symmetric core for Prob. 1-5.

- (a) Sketch the voltage, the winding flux linkage, and the core flux as a function of time.
- (b) Find the maximum permissible value of E if the maximum flux density is not to exceed 1.00 T.

1-8. An inductor is to be designed using the magnetic core of Fig. 1-26. The core is of uniform cross-sectional area $A_c = 0.75 \text{ in}^2$ and of mean length $l_c = 8 \text{ in}$. It has an adjustable air gap of length g and will be wound with a coil of N turns.

- (a) Calculate g and N such that the inductance is 15 mH and so that the inductor can operate at peak currents of 5 A without saturating. Assume that saturation occurs when the peak flux density in the core exceeds 1.7 T and that the core has permeability $\mu = 3000$.
- (b) For an inductor current of 5 A, use Eq. 3-20 to calculate (i) the magnetic stored energy in the air gap and (ii) the magnetic stored energy in the core. Show that the total magnetic stored energy is given by Eq. 1-39.

1-9. A proposed energy storage mechanism consists of a coil wound around the large nonmagnetic ($\mu = \mu_0$) toroidal form shown in Fig. 1-27. There are N turns, each of circular cross section of radius a . The radius of the toroid is r , measured to the center of each circular turn. The geometry of this device is such that the magnetic field can be considered to be zero everywhere outside the toroid. Under the assumption that $a \ll r$, the H field inside the torus can be considered to be directed around the torus and of uniform magnitude

$$H = \frac{Ni}{2\pi r}$$

- (a) Calculate the coil inductance L .
- (b) The coil is to be charged to a magnetic flux density of 2.0 T. Calculate the total stored magnetic energy in the torus when this flux density is achieved.

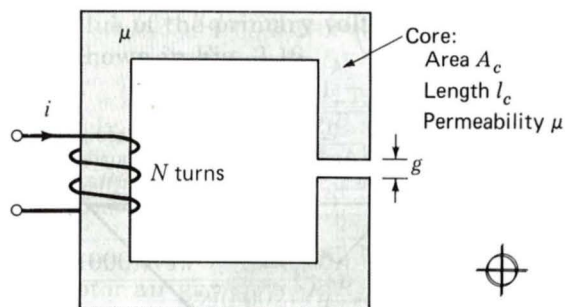


Fig. 1-26. Inductor for Prob. 1-8.

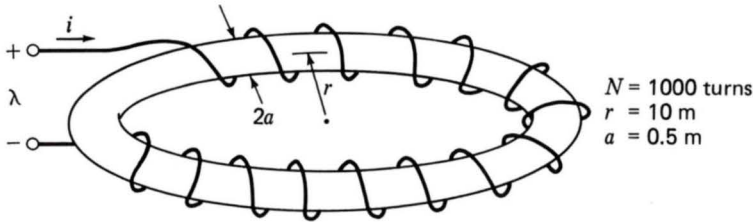


Fig. 1-27. Toroidal winding for Prob. 1-9.

- (c) If the coil is to be charged at a uniform rate, that is, $di/dt = \text{constant}$, calculate the terminal voltage required to achieve the required flux density in 25 s. Assume the coil resistance to be negligible.

1-10. Figure 1-28 shows an inductor wound on a high-permeability laminated iron core of rectangular cross section. Assume that the permeability of the iron is infinite. Neglect magnetic leakage and fringing in the air gap g . The winding is insulated copper wire whose resistivity is $\rho \, \Omega \cdot \text{m}$. Assume that the fraction f_w of the winding space is available for copper; the rest of the space being used for insulation.

- Estimate the mean length l of a turn of the winding.
- Derive an expression for the electric power dissipation in the coil for a specified steady flux density B . This expression should be in terms of B , ρ , μ_0 , l , f_w , and the given dimensions. Note that the expression is independent of the number of turns if the winding factor f_w is assumed to be independent of the turns.
- Derive an expression for the magnetic stored energy in terms of B and the given dimensions.
- From parts (b) and (c) derive an expression for the time constant L/R of the coil.

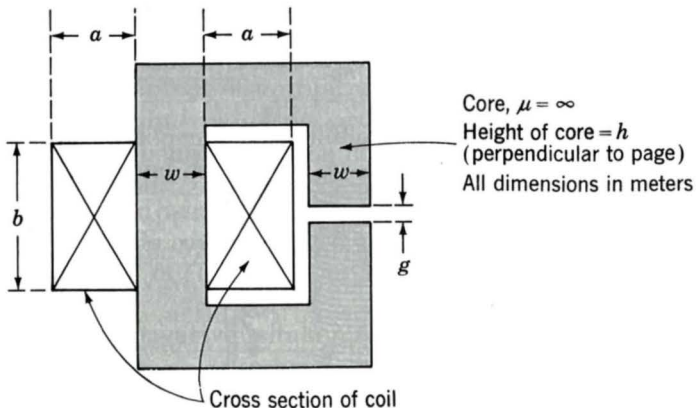


Fig. 1-28. Iron-core inductor.

1-11. The inductor of Fig. 1-28 has the following dimensions:

$$a = h = w = 1.5 \text{ cm} \quad b = 2 \text{ cm} \quad g = 0.3 \text{ cm}$$

The winding factor is $f_w = 0.7$. The resistivity of copper is $1.73 \times 10^{-6} \Omega \cdot \text{cm}$. The coil is to be operated with a constant applied voltage of 40 V, and the air-gap flux density is 1.2 T. Find the power dissipated in the coil, coil current, number of turns, coil resistance, inductance, time constant, and wire size to the nearest standard size.

1-12. The magnetic circuit of Fig. 1-29 has two windings and two air gaps. The core can be assumed to be of infinite permeability. The core dimensions are indicated in the figure.

- Assuming coil 1 to be carrying a current I_1 and the current in coil 2 to be zero, calculate (i) the magnetic flux density in each of the air gaps, (ii) the flux linkage of winding 1, and (iii) the flux linkage of winding 2.
- Repeat part (a), assuming zero current in winding 1 and a current I_2 in winding 2.
- Repeat part (a), assuming the current in winding 1 to be I_1 and the current in winding 2 to be I_2 .
- Find the self-inductances of windings 1 and 2 and the mutual inductance between the windings.

1-13. The symmetric magnetic circuit of Fig. 1-30 has three windings. Windings A and B each have N turns and are wound on the two bottom legs of the core. The core dimensions are indicated in the figure.

- Find the self-inductances of each of the windings.
- Find the mutual inductances between the three pairs of windings.
- Find the voltage induced in winding 1 by time-varying currents $i_A(t)$ and $i_B(t)$ in windings A and B. Show that this voltage can be

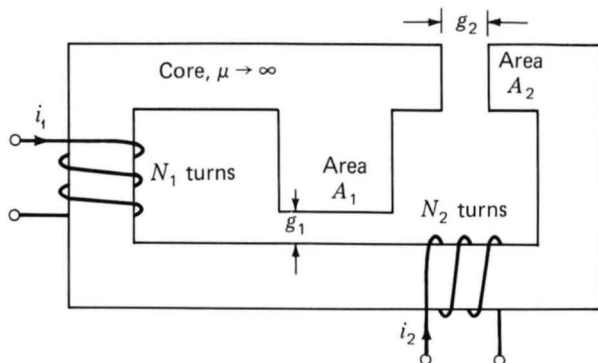


Fig. 1-29. Magnetic circuit for Prob. 1-12.

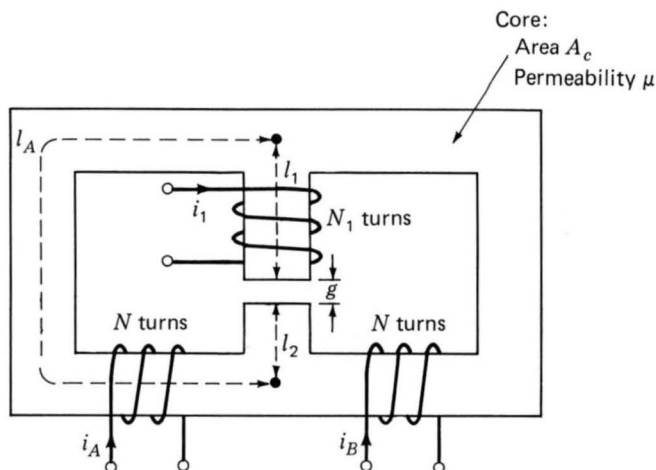


Fig. 1-30. Symmetric magnetic circuit for Prob. 1-13.

used to measure the imbalance between two sinusoidal currents of the same frequency.

1-14. The reciprocating generator of Fig. 1-31 has a movable plunger (position x) which is supported so that it can slide in and out of the magnetic yoke while maintaining a constant air gap of length g on each side adjacent to the yoke. Both the yoke and the plunger can be considered to be of infinite permeability. The motion of the plunger is constrained such that its position is limited to $0 \leq x \leq w$.

There are two windings on this magnetic circuit. The first has N_1 turns and carries a constant dc current I_0 . The second, which has N_2 turns, is open-circuited and can be connected to a load.

- Find the mutual inductance between windings 1 and 2 as a function of the plunger position x .
- The plunger is driven by an external source so that its motion is given by

$$x(t) = \frac{w(1 + \varepsilon \sin \omega t)}{2}$$

where $\varepsilon < w/2$. Show that, as a result, a sinusoidal voltage is generated in winding 2; find an expression for this voltage.

1-15. Figure 1-32 shows a configuration that can be used to measure the magnetic characteristics of electrical steel. The material to be tested is cut or punched into circular laminations which are then stacked (with interspersed insulation to avoid eddy-current formation). Two windings are wound over this stack of laminations: the first, with N_1 turns, is used to

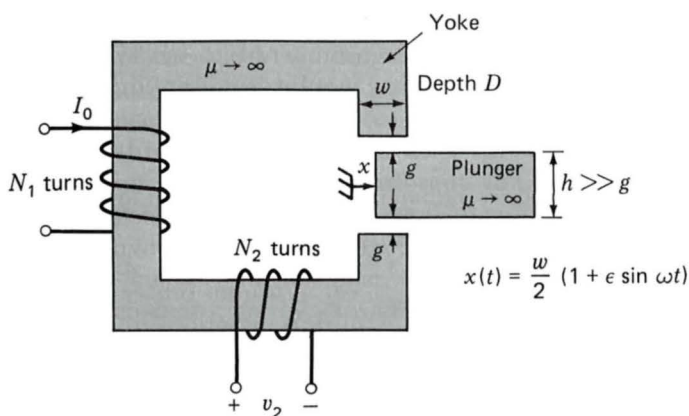


Fig. 1-31. Reciprocating generator for Prob. 1-14.

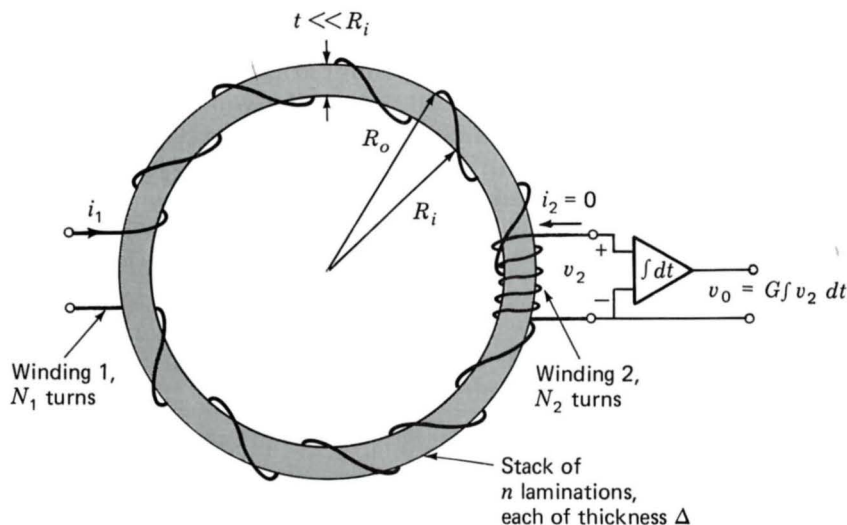


Fig. 1-32. Configuration for measurement of magnetic properties of electrical steel.

excite magnetic fields in the lamination; the second, with N_2 turns, is used to sense the resultant fields.

The accuracy of the results requires that the magnetic flux density be uniform within the laminations. This can be accomplished if the lamination width $t = R_o - R_i$ is much smaller than the lamination radius and if the excitation winding is wound uniformly around the lamination stack. For the purposes of this analysis, assume there are n laminations, each of thickness Δ . Also assume that winding 1 is excited by a current $i_1 = I_0 \sin \omega t$.

- (a) Find the relationship between the magnetic field intensity H in the laminations and current i_1 in winding 1.

- (b) Find the relationship between the voltage v_2 and the time rate of change of the flux density B in the laminations.
- (c) Find the relationship between the voltage $v_0 = G \int v_2 dt$ and the flux density.

In this problem, we have shown that the magnetic field intensity H and the magnetic flux density B in the laminations are proportional to the current i_1 and the voltage v_2 by known constants. Thus, B and H in the magnetic steel can be measured directly, and the B - H characteristics as discussed in Arts. 1-3 and 1-4 can be determined.

1-16. From the dc magnetization curve of Fig. 1-9 it is possible to calculate the relative permeability $\mu_r = B_c/(\mu_0 H_c)$ for M-5 electrical steel as a function of the flux level B_c . Assuming the core of Fig. 1-2 to be made of M-5 electrical steel with the dimensions given in Example 1-1, calculate the maximum flux density such that the reluctance of the core never exceeds 5 percent of the reluctance of the total magnetic circuit.

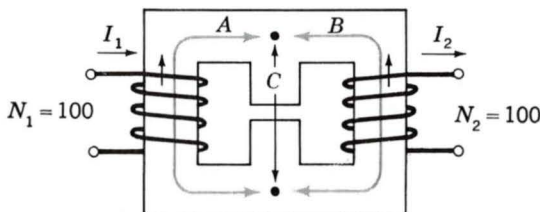
1-17. The coils of the magnetic circuit device shown in Fig. 1-33 are connected in series so that the mmf's of paths A and B both tend to set up flux in the center leg C in the same direction. The material is M-5 grade, 0.012-in steel, with a stacking factor of 0.94. Neglect fringing and leakage.

- (a) How many amperes are required to set up a flux density of 0.6 T?
- (b) How many joules of energy are stored in the magnetic field in the air gap?

1-18. Data for the top half of a symmetric hysteresis loop for the core of Prob. 1-7 are:

B, T	0	0.2	0.4	0.6	0.7	0.8	0.9	1.0	0.95	0.9	0.8	0.7	0.6	0.4	0.2	0
$H, \text{A} \cdot \text{turns/m}$	48	52	58	73	85	103	135	193	80	42	2	-18	-29	-40	-45	-48

The mean length of the flux paths in the core is 0.30 m. Find graphically the hysteresis loss in watts for a maximum flux density of 1.00 T at a frequency of 60 Hz.



Cross section area of A and B legs = 2 in^2

Cross section area of C legs = 4 in^2

Length A path = 6 in

Length B path = 6 in

Length C path = 2 in

Air gap = 0.15 in

Fig. 1-33. Magnetic circuit for Prob. 1-17.

1-19. Assume the magnetic circuit of Prob. 1-1 and Fig. 1-23 to be made up of M-5 electrical steel with the properties described in Figs. 1-9, 1-11, and 1-13. Assume the core to be operating with a 60-Hz sinusoidal flux density of the rms flux density of 1.1 T. Neglect the winding resistance and leakage inductance. Find the winding voltage, rms winding current, and core loss for this operating condition. The density of M-5 steel is 7.65 g/cm^3 .

1-20. Repeat Example 1-6 under the assumption that all the core dimensions are doubled.

1-21. Using the magnetization characteristics for samarium cobalt given in Fig. 1-18, find the point of maximum energy product and the corresponding flux density and magnetic field intensity. Using these values, repeat Example 1-8 with the Alnico 5 magnet replaced by a samarium cobalt magnet. By what factor does this reduce the magnet volume required to achieve the desired air-gap flux density?

1-22. Using the magnetization characteristics for neodymium-iron-boron given in Fig. 1-18, find the point of maximum energy product and the corresponding flux density and magnetic field intensity. Using these values, repeat Example 1-8 with the Alnico 5 magnet replaced by a neodymium-iron-boron magnet. By what factor does this reduce the magnet volume required to achieve the desired air-gap flux density?

1-23. Figure 1-34 shows the magnetic circuit for a permanent magnet loudspeaker. The voice coil (not shown) is in the form of a circular cylindrical coil which fits in the air gap. A neodymium-iron-boron magnet is used to create the air-gap dc magnetic field which interacts with the voice coil currents to produce the motion of the voice coil. The designer has determined that the air gap must have length $g = 0.2 \text{ cm}$ and height $h = 1 \text{ cm}$.

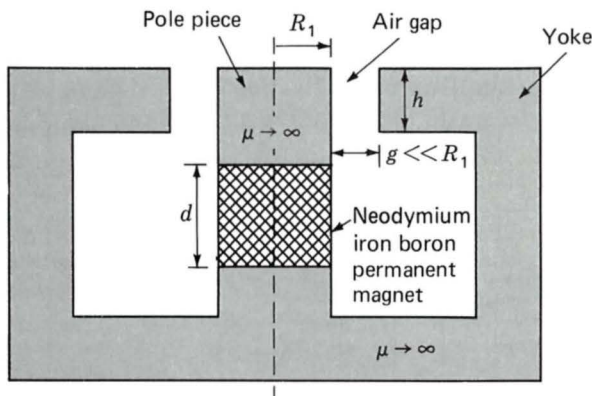


Fig. 1-34. Magnetic circuit for a loudspeaker (Prob. 1-23); voice coil not shown.

Assuming that the yolk and pole piece are of infinite magnetic permeability ($\mu \rightarrow \infty$), find the magnet height d and the magnet radius R that will result in an air-gap magnetic flux density of 1.2 T and require the smallest magnet volume.

(Hint: Refer to Example 1-8 and to Fig. 1-18 to find the point of maximum energy product for neodymium-iron-boron.)

1-24. It is desired to achieve a time-varying magnetic flux density in the air gap of the magnetic circuit of Fig. 1-35 of the form

$$B_g = B_0 + B_1 \sin \omega t$$

where $B_0 = 0.5$ T and $B_1 = 0.25$ T. The dc field B_0 is to be created by an Alnico 5 magnet, whereas the time-varying field is to be created by a time-varying current.

- For the air-gap dimensions given in Fig. 1-35, find the magnet length d and the magnet area A_m that will achieve the desired dc air-gap flux density and minimize the magnet volume.
- Find the minimum and maximum values of the time-varying current required to achieve the desired time-varying air-gap flux density. Will this current vary sinusoidally in time?

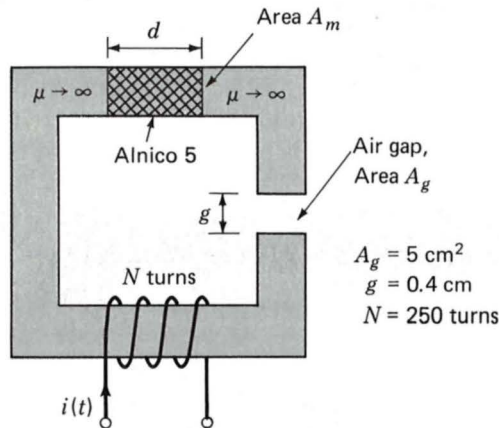


Fig. 1-35. Magnetic circuit for Prob. 1-24.

2

Transformers

Before we proceed with a study of electric machinery, it is desirable to discuss certain aspects of the theory of magnetically coupled circuits, with emphasis on transformer action. Although the static transformer is not an energy conversion device, it is an indispensable component in many energy conversion systems. As one of the principal reasons for the widespread use of ac power systems, it makes possible electric generation at the most economical generator voltage, power transfer at the most economical transmission voltage, and power utilization at the most suitable voltage for the particular utilization device. The transformer is also widely used in low-power low-current electronic and control circuits for performing such functions as matching the impedances of a source and its load for maximum power transfer, insulating one circuit from another, or isolating direct current while maintaining ac continuity between two circuits.

Moreover, the transformer is one of the simpler devices comprising two or more electric circuits coupled by a common magnetic circuit, and its analysis involves many of the principles essential to the study of electric machinery.

2-1 INTRODUCTION TO TRANSFORMERS

Essentially, a transformer consists of two or more windings interlinked by mutual magnetic flux. If one of these windings, the *primary*, is connected to an alternating-voltage source, an alternating flux will be produced whose amplitude will depend on the primary voltage and number of turns. The mutual flux will link the other winding, the *secondary*, and will induce a voltage in it whose value will depend on the number of secondary turns. By properly proportioning the numbers of primary and secondary turns, almost any desired *voltage ratio*, or *ratio of transformation*, can be obtained.

Transformer action evidently demands only the existence of time-varying mutual flux linking the two windings and is simply utilization of the mutual-inductance concept. Such action will be obtained if an air core is used, but it will be obtained much more effectively with a core of iron or other ferromagnetic material, because most of the flux is then confined to a definite path linking both windings and having a much higher permeability than air. Such a transformer is commonly called an *iron-core transformer*. Most transformers are of this type. The following discussion is concerned almost wholly with iron-core transformers.

To reduce the losses caused by eddy currents in the core, the magnetic circuit usually consists of a stack of thin laminations, two common types of construction being shown in Fig. 2-1. In the *core type* (Fig. 2-1a) the windings are wound around two legs of a rectangular magnetic core; in the *shell type* (Fig. 2-1b) the windings are wound around the center leg of a three-legged core. Silicon-steel laminations 0.014 in thick are generally used for transformers operating at frequencies below a few hundred hertz. Silicon steel has the desirable properties of low cost, low core loss, and high permeability at high flux densities (1.0 to 1.5 T). The cores of small transformers used in communication circuits at high frequencies and low energy levels are sometimes made of compressed powdered ferromagnetic alloys such as permalloy.

Most of the flux is confined to the core and therefore links both windings. Although leakage flux which links one winding without linking the other is a small fraction of the total flux, it has an important effect on the behavior of the transformer. Leakage is reduced by subdividing the windings into sections placed as close together as possible. In the core-type construction, each winding consists of two sections, one section on each of the two legs of the core, the primary and secondary windings being concentric

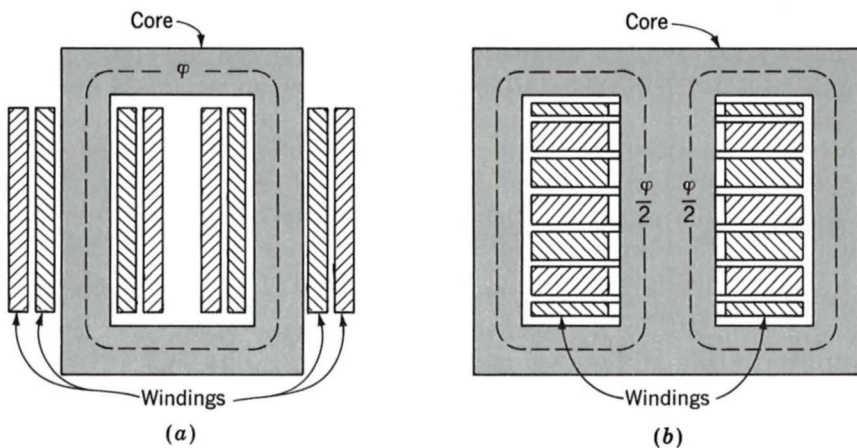


Fig. 2-1. (a) Core-type and (b) shell-type transformers.

coils. In the shell-type construction, variations of the concentric-winding arrangement may be used, or the windings may consist of a number of thin, "pancake" coils assembled in a stack with primary and secondary coils interleaved.

Figure 2-2 illustrates the internal construction of a *distribution transformer* such as is used in public utility systems to provide the appropriate voltage at the consumer's premises. A large power transformer is shown in Fig. 2-3.

2-2 NO-LOAD CONDITIONS

Figure 2-4 shows a transformer with its secondary circuit open and an alternating voltage v_1 applied to its primary terminals. To simplify the drawings, it is common on schematic diagrams of transformers to show the primary and secondary windings as if they were on separate legs of the core, as in Fig. 2-4, even though the windings are actually interleaved in practice. As discussed in Art. 1-4, a small steady-state current i_ϕ , called the *exciting current*, exists in the primary and establishes an alternating flux in the magnetic circuit.[†] This flux induces an emf in the primary equal to

$$e_1 = \frac{d\lambda_1}{dt} = N_1 \frac{d\phi}{dt} \quad (2-1)$$

where λ_1 = flux linkage with primary

ϕ = flux (here assumed all confined to core)

N_1 = number of turns in primary winding

[†]In general, the exciting current corresponds to the net ampere-turns (mmf) acting on the magnetic circuit, and it is not possible to distinguish whether it flows in the primary or secondary winding or partially in each winding.

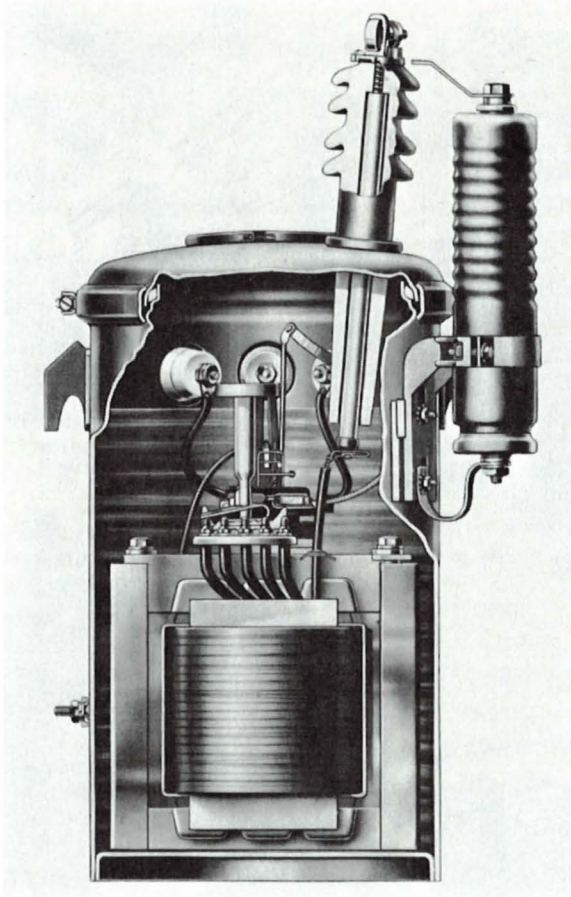


Fig. 2-2. Cutaway view of self-protected distribution transformer typical of sizes 2 to 25 kVA, 7200:240/120 V. Only one high-voltage insulator and lightning arrester is needed because one side of the 7200-V line and one side of the primary are grounded. (*General Electric Company.*)

The voltage e_1 is in volts when ϕ is in webers. This counter emf together with the voltage drop in the primary resistance R_1 must balance the applied voltage v_1 ; thus

$$v_1 = R_1 i_\phi + e_1 \quad (2-2)$$

In most power apparatus, the no-load resistance drop is very small indeed, and the induced emf e_1 very nearly equals the applied voltage v_1 . Furthermore, the waveforms of voltage and flux are very nearly sinusoidal. The analysis can then be greatly simplified, as we have shown in Art. 1-4. Thus, if the instantaneous flux is

$$\phi = \phi_{\max} \sin \omega t \quad (2-3)$$

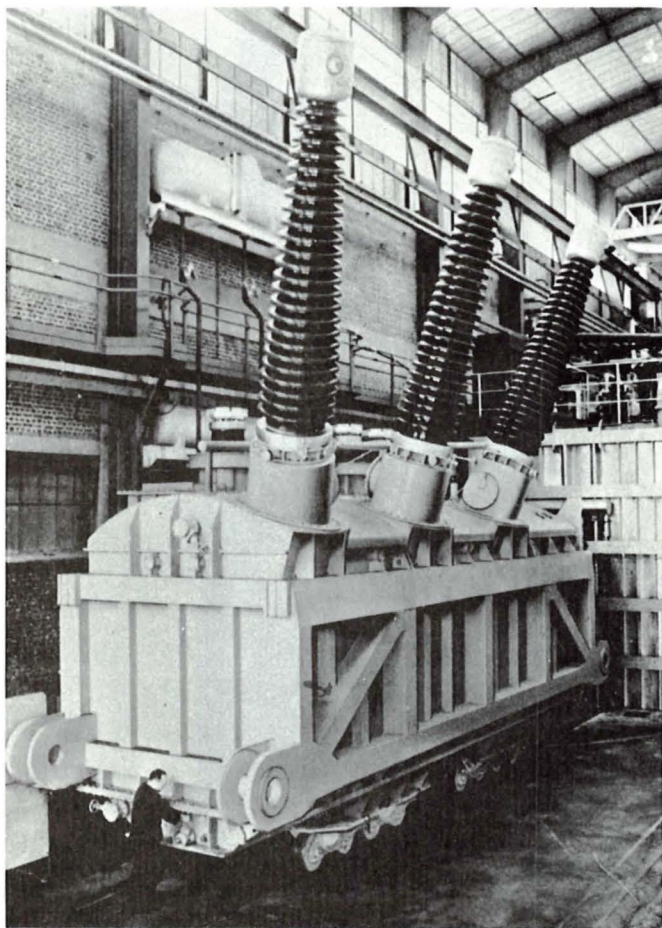


Fig. 2-3. A 660-MVA three-phase 50-Hz transformer used to step up generator voltage of 20 kV to transmission voltage of 405 kV. (CEM Le Havre, French Member of the Brown Boveri Corporation.)

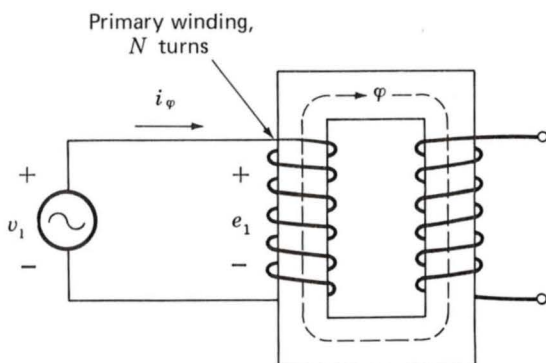


Fig. 2-4. Transformer with open secondary.

the induced voltage is

$$e_1 = N_1 \frac{d\phi}{dt} = \omega N_1 \phi_{\max} \cos \omega t \quad (2-4)$$

where ϕ_{\max} is the maximum value of the flux and $\omega = 2\pi f$, the frequency being f Hz. For the positive directions shown in Fig. 2-4, the induced emf leads the flux by 90° . The rms value of the induced emf is

$$E_1 = \frac{2\pi}{\sqrt{2}} f N_1 \phi_{\max} = \sqrt{2} \pi f N_1 \phi_{\max} \quad (2-5)$$

If the resistive voltage drop is negligible, the counter emf equals the applied voltage. Under these conditions, if a sinusoidal voltage is applied to a winding, a sinusoidally varying core flux must be established whose maximum value ϕ_{\max} satisfies the requirement that E_1 in Eq. 2-5 equal the rms value V_1 of the applied voltage; thus

$$\phi_{\max} = \frac{V_1}{\sqrt{2} \pi f N_1} \quad (2-6)$$

The flux is determined solely by the applied voltage, its frequency, and the number of turns in the winding. This important relation applies not only to transformers but also to any device operated with sinusoidal alternating impressed voltage, as long as the resistance drop is negligible. The magnetic properties of the core determine the exciting current. It must adjust itself so as to produce the mmf required to create the flux demanded by Eq. 2-6.

Because of the nonlinear magnetic properties of iron, the waveform of the exciting current differs from the waveform of the flux. A curve of the exciting current as a function of time can be found graphically from the ac hysteresis loop, as shown in Fig. 1-10.

If the exciting current is analyzed by Fourier-series methods, it is found to comprise a fundamental and a family of odd harmonics. The fundamental can, in turn, be resolved into two components, one in phase with the counter emf and the other lagging the counter emf by 90° . The fundamental in-phase component accounts for the power absorbed by hysteresis and eddy-current losses in the core. It is called the *core-loss component* of the exciting current. When the core-loss component is subtracted from the total exciting current, the remainder is called the *magnetizing current*. It comprises a fundamental component lagging the counter emf by 90° , together with all the harmonics. The principal harmonic is the third. For typical power transformers, the third harmonic usually is about 40 percent of the exciting current.

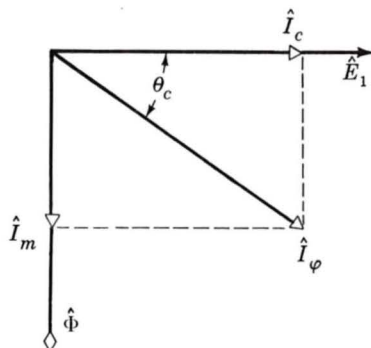


Fig. 2-5. No-load phasor diagram.

Except in problems concerned directly with the effects of harmonics, the peculiarities of the exciting-current waveform usually need not be taken into account, because the exciting current itself is small. For example, the exciting current of a typical power transformer is about 1 to 2 percent of full-load current. Consequently the effects of the harmonics usually are swamped out by the sinusoidal-current requirements of other linear elements in the circuit. The exciting current can then be represented by its *equivalent sine wave*, which has the same rms value and frequency and produces the same average power as the actual wave. Such representation is essential to the construction of a phasor diagram. In Fig. 2-5, the phasors \hat{E}_1 and $\hat{\Phi}$, respectively, represent the induced emf and the flux. The phasor \hat{I}_φ represents the equivalent sinusoidal exciting current. It lags the induced emf \hat{E}_1 by a phase angle θ_c such that

$$P_c = E_1 I_\varphi \cos \theta_c \quad (2-7)$$

where P_c is the core loss. The component \hat{I}_c in phase with \hat{E}_1 represents the core-loss current. The component \hat{I}_m in phase with the flux represents an equivalent sine wave having the same rms value as the magnetizing current. Typical core-loss and exciting volt-ampere characteristics of high-quality silicon steel used for power and distribution transformer laminations are shown in Figs. 1-11 and 1-12.

EXAMPLE 2-1

In Example 1-6 the core loss and exciting voltamperes for the core of Fig. 1-14 at $B_{\max} = 1.5$ T and 60 Hz were found to be

$$P_c = 16 \text{ W} \quad (VI)_{\text{rms}} = 20 \text{ VA}$$

and the induced voltage was $275/\sqrt{2} = 194$ V rms when the winding had 200 turns.

Find the power factor, the core-loss current I_c , and the magnetizing current I_m .

Solution

$$\text{Power factor } \cos \theta_c = \frac{16}{20} = 0.80 \quad \theta_c = 36.9^\circ \quad \sin \theta_c = 0.60$$

$$\text{Exciting current } I_\varphi = \frac{20}{194} = 0.10 \text{ A rms}$$

$$\text{Core-loss component } I_c = \frac{16}{194} = 0.082 \text{ A rms}$$

$$\text{Magnetizing component } I_m = I_\varphi \sin \theta_c = 0.060 \text{ A rms}$$

2-3 EFFECT OF SECONDARY CURRENT; IDEAL TRANSFORMER

As a first approximation to a quantitative theory, consider a transformer with a primary winding of N_1 turns and a secondary winding of N_2 turns, as shown schematically in Fig. 2-6. Notice that the secondary current is defined as positive out of the winding; thus positive secondary current creates an mmf in the opposite direction from that created by positive primary current. Let the properties of this transformer be idealized in that the winding resistances are negligible, and assume that all the flux is confined to the core and links both windings, core losses are negligible, and the permeability of the core is so high that only a negligible exciting mmf is required to establish the flux. These properties are closely approached but never actually attained in practical transformers. A hypothetical transformer having these properties is often called an *ideal transformer*.

When a time-varying voltage v_1 is impressed on the primary terminals, a core flux φ must be established such that the counter emf e_1 equals the impressed voltage when winding resistance is negligible. Thus

$$v_1 = e_1 = N_1 \frac{d\varphi}{dt} \quad (2-8)$$

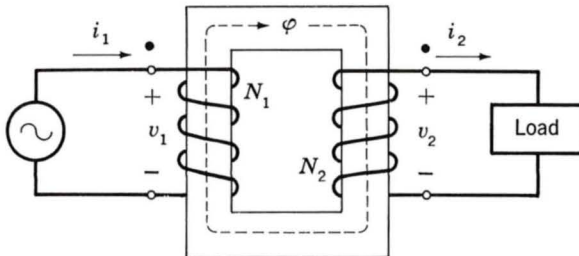


Fig. 2-6. Ideal transformer and load.

The core flux also links the secondary and produces an induced emf e_2 and an equal secondary terminal voltage v_2 , given by

$$v_2 = e_2 = N_2 \frac{d\phi}{dt} \quad (2-9)$$

From the ratio of Eqs. 2-8 and 2-9,

$$\frac{v_1}{v_2} = \frac{N_1}{N_2} \quad (2-10)$$

Thus an ideal transformer transforms voltages in the direct ratio of the turns in its windings.

Now let a load be connected to the secondary. A current i_2 and an mmf $N_2 i_2$ are then present in the secondary. Since the core permeability is assumed very large and since the impressed voltage gives rise to a finite core flux determined by Eq. 2-8, the net exciting mmf acting on the core must remain negligible. Hence, a compensating primary mmf and current i_1 must result such that

$$N_1 i_1 = N_2 i_2 \quad (2-11)$$

This is the means by which the primary "knows" of the presence of current in the secondary. Note that for the reference directions shown in Fig. 2-6 the mmf's of i_1 and i_2 are in opposite directions and therefore compensate. The net mmf acting on the core therefore is zero, in accordance with the assumption that the exciting current of an ideal transformer is zero. From Eq. 2-11

$$\frac{i_1}{i_2} = \frac{N_2}{N_1} \quad (2-12)$$

Thus an ideal transformer transforms currents in the inverse ratio of the turns in its windings. Also notice from Eqs. 2-10 and 2-12 that

$$v_1 i_1 = v_2 i_2 \quad (2-13)$$

i.e., instantaneous power input equals instantaneous power output, a necessary condition because all dissipative and energy storage mechanisms in the transformer have been neglected.

An additional property of the ideal transformer can be seen by considering the case of a sinusoidal applied voltage and an impedance load. Phasor symbolism can be used. The circuit is shown in simplified form in Fig. 2-7a, in which the dot-marked terminals of the transformer correspond to the similarly marked terminals in Fig. 2-6. The dot markings in-

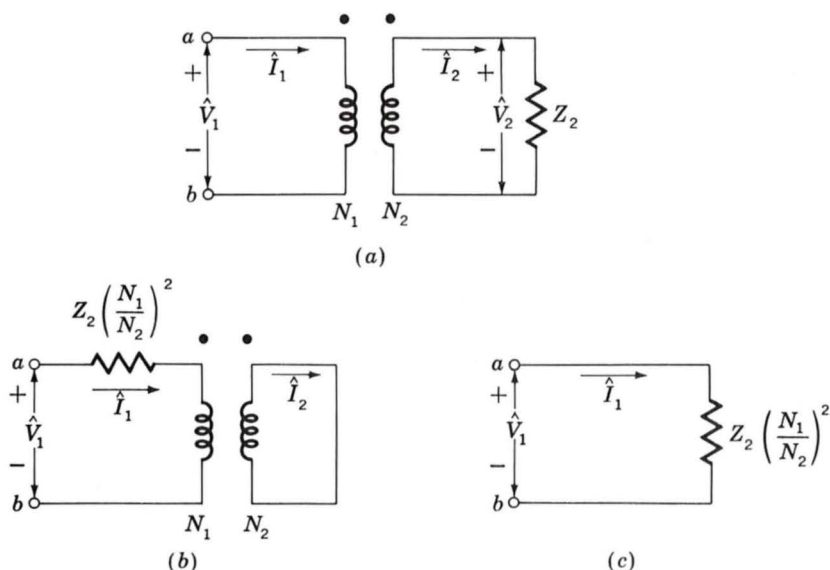


Fig. 2-7. Three circuits which are identical at terminals ab when the transformer is ideal.

dicating terminals of corresponding polarity; i.e., if one follows through the primary and secondary windings of Fig. 2-6, beginning at their dot-marked terminals, one will find that both windings encircle the core in the same direction with respect to the flux. Therefore, if one compares the voltages of the two windings, the voltages from a dot-marked to an unmarked terminal will be of the same instantaneous polarity for primary and secondary. In other words, the voltages \hat{V}_1 and \hat{V}_2 in Fig. 2-7a are in phase. Also currents \hat{I}_1 and \hat{I}_2 are in phase. The fact that their mmf's must balance is accounted for by their being in opposite directions through the windings.

In phasor form, Eqs. 2-10 and 2-12 can be expressed as

$$\hat{V}_1 = \frac{N_1}{N_2} \hat{V}_2 \quad \text{and} \quad \hat{V}_2 = \frac{N_2}{N_1} \hat{V}_1 \quad (2-14)$$

$$\hat{I}_1 = \frac{N_2}{N_1} \hat{I}_2 \quad \text{and} \quad \hat{I}_2 = \frac{N_1}{N_2} \hat{I}_1 \quad (2-15)$$

From these equations

$$\frac{\hat{V}_1}{\hat{I}_1} = \left(\frac{N_1}{N_2} \right)^2 \frac{\hat{V}_2}{\hat{I}_2} = \left(\frac{N_1}{N_2} \right)^2 Z_2 \quad (2-16)$$

where Z_2 is the complex impedance of the load. Consequently, as far as its effect is concerned, an impedance Z_2 in the secondary circuit can be replaced by an equivalent impedance Z_1 in the primary circuit, provided that

$$Z_1 = \left(\frac{N_1}{N_2}\right)^2 Z_2 \quad (2-17)$$

Thus, the three circuits of Fig. 2-7 are indistinguishable as far as their performance viewed from terminals *ab* is concerned. Transferring an impedance from one side of a transformer to the other in this fashion is called *referring the impedance* to the other side. In a similar manner, voltages and currents can be *referred* to one side or the other by using Eqs. 2-14 and 2-15 to evaluate the equivalent voltage and current on that side.

To summarize, *in an ideal transformer, voltages are transformed in the direct ratio of turns, currents in the inverse ratio, and impedances in the direct ratio squared; power and voltamperes are unchanged.*

2-4 TRANSFORMER REACTANCES AND EQUIVALENT CIRCUITS

The departures in an actual transformer from the ideal properties assumed in Art. 2-3 must be included to a greater or lesser degree in most analyses of transformer performance. A more complete theory must take into account the effects of winding resistances, magnetic leakage, fluxes, and finite exciting current. Sometimes the capacitances of the windings also have important effects, notably in problems involving transformer behavior at frequencies above the audio range or during rapidly changing transient conditions such as those encountered in pulse transformers as well as in power system transformers as a result of voltage surges caused by lightning or switching transients. The analysis of these high-frequency problems is beyond the scope of the present treatment, however, and accordingly the capacitances of the windings are neglected in the following analyses.

Two methods of analysis by which the departures from the ideal can be taken into account are (1) an equivalent-circuit technique based on physical reasoning and (2) a mathematical attack based on the classical theory of magnetically coupled circuits. Both methods are in everyday use, and both have very close parallels in the theories of rotating machines. Because it offers an excellent example of the thought process involved in translating physical concepts to a quantitative theory, the equivalent-circuit technique is presented here.

The total flux linking the primary winding can be divided into two components: the resultant mutual flux, confined essentially to the iron core and produced by the combined effect of the primary and secondary currents, and the primary leakage flux, which links only the primary. These components are identified in the elementary transformer shown in Fig. 2-8, where for simplicity the primary and secondary windings are

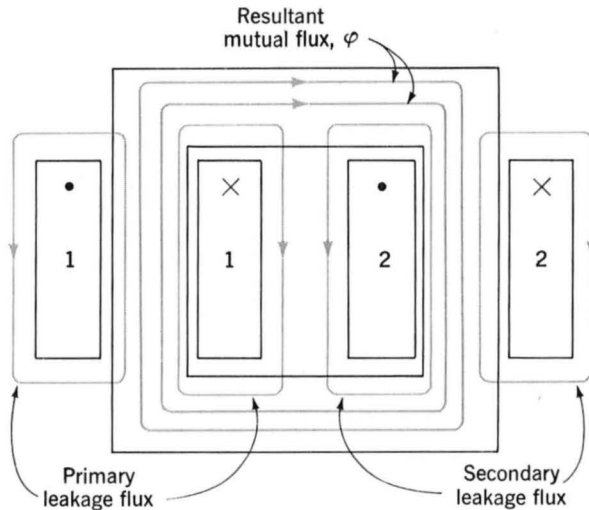


Fig. 2-8. Schematic view of mutual and leakage fluxes in a transformer.

shown on opposite legs of the core. In an actual transformer with interleaved windings, the details of the flux distribution are more complicated, but the essential features remain the same. Because the leakage path is largely in air, the leakage flux and the voltage induced by it vary linearly with primary current \hat{I}_1 . The effect on the primary circuit is the same as that of flux linkages anywhere in the circuit leading up to the transformer primary and can be simulated by assigning to the primary a *leakage inductance* (equal to the leakage-flux linkages with the primary per unit of primary current) or *leakage reactance* X_{l_1} (equal to $2\pi f$ times the leakage inductance). In addition, there will be a voltage drop in the primary effective resistance R_1 .

The impressed terminal voltage \hat{V}_1 is then opposed by three phasor voltages: the $\hat{I}_1 R_1$ drop in the primary resistance, the $\hat{I}_1 X_{l_1}$ drop arising from primary leakage flux, and the counter emf \hat{E}_1 induced in the primary by the resultant mutual flux. All these voltages are appropriately included in the equivalent circuit in Fig. 2-9a.

The resultant mutual flux links both the primary and secondary windings and is created by their combined mmf's. It is convenient to treat these mmf's by considering that the primary current must meet two requirements of the magnetic circuit: it must not only counteract the demagnetizing effect of the secondary current but also produce sufficient mmf to create the resultant mutual flux. According to this physical picture, it is convenient to resolve the primary current into two components: a load component and an exciting component. The *load component* \hat{I}'_2 is defined as the component current in the primary which would exactly counteract the mmf of secondary current \hat{I}_2 . Thus, for opposing currents

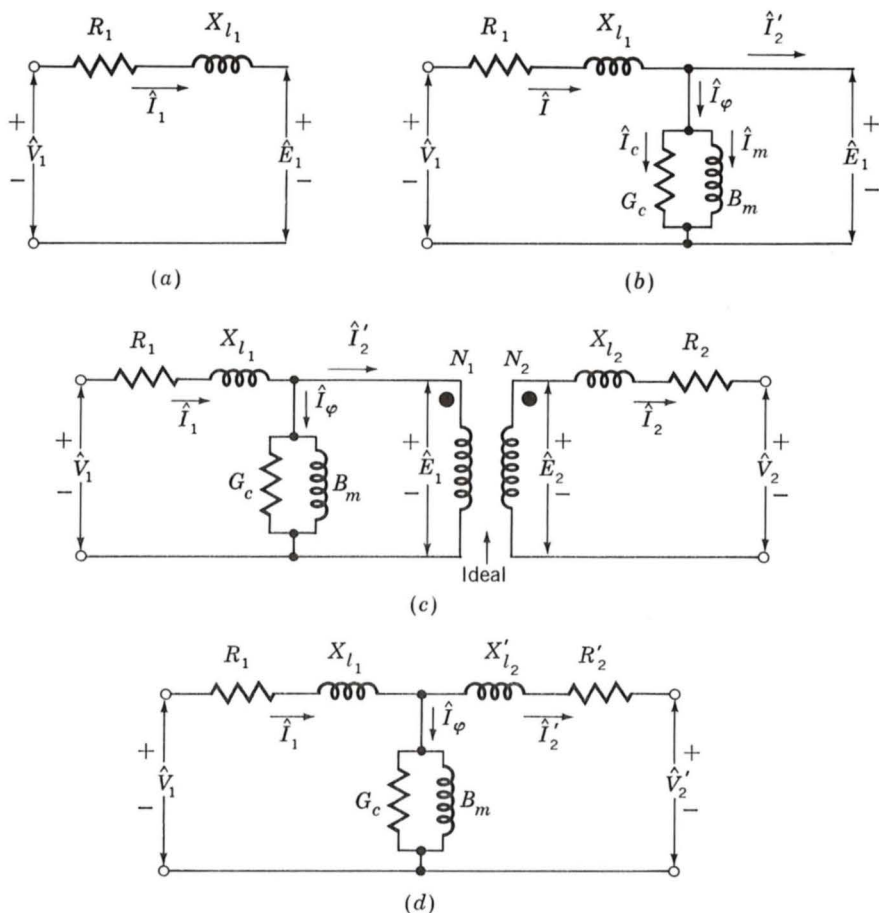


Fig. 2-9. Steps in the development of the transformer equivalent circuit.

$$\hat{I}'_2 = \frac{N_2}{N_1} \hat{I}_2 \quad (2-18)$$

It equals the secondary current referred to the primary as in an ideal transformer. The *exciting component* \hat{I}_ϕ is defined as the additional primary current required to produce the resultant mutual flux. It is a nonsinusoidal current of the nature described in Art. 2-2.[†]

The exciting current can be treated as an equivalent sinusoidal current \hat{I}_ϕ , in the manner described in Art. 2-2, and can be resolved into a core-loss component \hat{I}_c in phase with the counter emf \hat{E}_1 and a magnetizing

[†]In fact, the exciting current corresponds to the net mmf acting on the transformer core and cannot, in general, be considered to flow in the primary alone. However, for the purposes of this discussion, this distinction is not significant.

component \hat{I}_m lagging \hat{E}_1 by 90° . In the equivalent circuit (Fig. 2-9b) the equivalent sinusoidal exciting current is accounted for by means of a shunt branch connected across \hat{E}_1 , comprising a noninductive resistance whose conductance is G_c in parallel with a lossless inductance whose susceptance is B_m . Alternatively, a series combination of resistance and reactance can be connected across \hat{E}_1 . In the parallel combination (Fig. 2-9b) the power $E_1^2 G_c$ accounts for the core loss due to the resultant mutual flux. When G_c is assumed constant, the core loss is thereby assumed to vary as E_1^2 or (for sine waves) as $\phi_{\max}^2 f^2$, where ϕ_{\max} is the maximum value of the resultant mutual flux. The *magnetizing susceptance* B_m varies with the saturation of the iron. When the inductance corresponding to B_m is assumed constant, the magnetizing current is thereby assumed to be independent of frequency and directly proportional to the resultant mutual flux. Both G_c and B_m are usually determined at rated voltage and frequency; they are then assumed to remain constant for the small departures from rated values associated with normal operation.

The resultant mutual flux $\hat{\Phi}$ induces an emf \hat{E}_2 in the secondary, and since this flux links both windings, the induced-voltage ratio is

$$\frac{\hat{E}_1}{\hat{E}_2} = \frac{N_1}{N_2} \quad (2-19)$$

just as in an ideal transformer. This voltage transformation and the current transformation of Eq. 2-18 can be accounted for by introducing an ideal transformer in the equivalent circuit, as in Fig. 2-9c. The emf \hat{E}_2 is not the secondary terminal voltage, however, because of the secondary resistance and because the secondary current \hat{I}_2 creates *secondary leakage flux* (see Fig. 2-8). The secondary terminal voltage \hat{V}_2 differs from the induced voltage \hat{E}_2 by the voltage drops due to secondary resistance R_2 and *secondary leakage reactance* X_{l2} , as in the portion of the equivalent circuit (Fig. 2-9c) to the right of \hat{E}_2 .

The actual transformer therefore is equivalent to an ideal transformer plus external impedances. By referring all quantities to the primary or secondary, the ideal transformer in Fig. 2-9c can be moved out to the right or left, respectively, of the equivalent circuit. This is almost invariably done, and the equivalent circuit is usually drawn as in Fig. 2-9d, with the ideal transformer not shown and all voltages, currents, and impedances referred to the same side.

In Fig. 2-9d the referred values are indicated with primes, for example, X'_{l2} and R'_2 , to distinguish them from the actual values of Fig. 2-9c. In what follows we almost always deal with referred values, and the primes are omitted. One must simply keep in mind the side of the transformers to which all quantities have been referred. The circuit of Fig. 2-9d is called the *equivalent T circuit* for a transformer.

EXAMPLE 2-2

A 50-kVA 2400:240-V 60-Hz distribution transformer has a leakage impedance of $0.72 + j0.92 \, \Omega$ in the high-voltage winding and $0.0070 + j0.0090 \, \Omega$ in the low-voltage winding. At rated voltage and frequency, the admittance Y_ϕ of the shunt branch accounting for the exciting current is $(0.324 - j2.24) \times 10^{-2}$ mho when viewed from the low-voltage side. Draw the equivalent circuit referred to (a) the high-voltage side and (b) the low-voltage side, and label the impedances numerically.

Solution

The circuits are given in Fig. 2-10a and b, respectively, with the high-voltage side numbered 1 and the low-voltage side numbered 2. The voltages given on the nameplate of a power system transformer are based on the turns ratio and neglect the small leakage-impedance voltage drops under load. Since this is a 10-to-1 transformer, impedances are referred by multiplying or dividing by 100. The value of an impedance referred to the high-voltage side is greater than its value referred to the low-voltage side. Since admittance is the reciprocal of impedance, an admittance is referred from one side to the other by use of the reciprocal of the referring factor for impedance. The value of an admittance referred to the high-voltage side is smaller than its value referred to the low-voltage side.

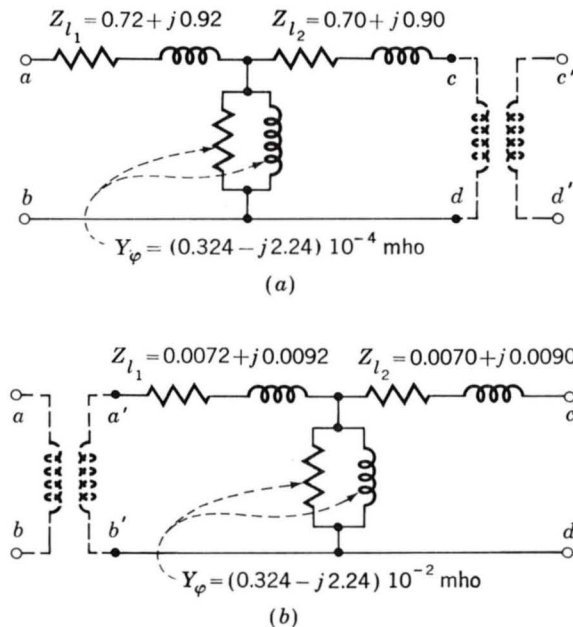


Fig. 2-10. Equivalent circuits for transformer of Example 2-2.

The ideal transformer may be explicitly drawn, as shown dotted in Fig. 2-10, or it may be omitted in the diagram and remembered mentally, making the unprimed letters the terminals.

2-5 ENGINEERING ASPECTS OF TRANSFORMER ANALYSIS

In engineering analyses involving the transformer as a circuit element, it is customary to adopt one of several approximate forms of the equivalent circuit of Fig. 2-9 rather than the full circuit. The approximations chosen in a particular case depend largely on physical reasoning based on orders of magnitude of the neglected quantities. The more common approximations are presented in this article. In addition, test methods are given for determining the transformer constants.

a. Approximate Equivalent Circuits; Power Transformers

The approximate equivalent circuits commonly used for constant-frequency power transformer analyses are summarized for comparison in Fig. 2-11. All quantities in these circuits are referred to either the primary or the secondary, and the ideal transformer is not shown.

The computational labor involved often can be appreciably reduced by moving the shunt branch representing the exciting current out from the middle of the T circuit to either the primary or the secondary terminals, as in Fig. 2-11a and b. These are *cantilever circuits*. The series branch is the

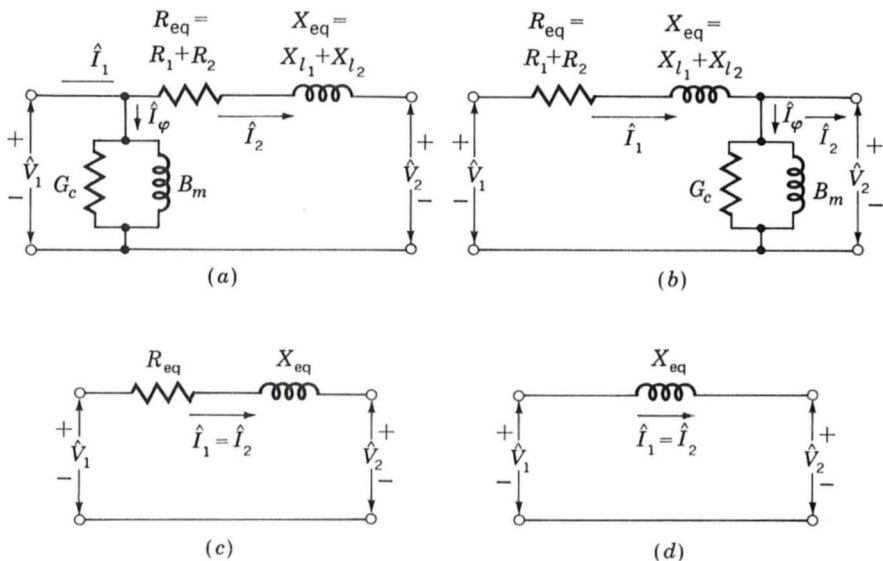


Fig. 2-11. Approximate transformer equivalent circuits.

combined resistance and leakage reactance referred to the same side. This impedance is sometimes called the *equivalent impedance* and its components the *equivalent resistance* R_{eq} and *equivalent reactance* X_{eq} , as shown in Fig. 2-11a and b. Error is introduced by neglect of the voltage drop in the primary or secondary leakage impedance caused by the exciting current, but this error is insignificant in most problems involving power system transformers.

Further simplification results from neglecting the exciting current entirely, as in Fig. 2-11c, in which the transformer is represented as an equivalent series impedance. If the transformer is large (several hundred kilovoltamperes or more), the equivalent resistance R_{eq} is small compared with the equivalent reactance X_{eq} and can frequently be neglected, giving Fig. 2-11d. The circuits of Fig. 2-11c and d are sufficiently accurate for most ordinary power system problems. Finally, in situations where the currents and voltages are determined almost wholly by the circuits external to the transformer or when a high degree of accuracy is not required, the entire transformer impedance can be neglected and the transformer considered to be ideal, as in Art. 2-3.

The circuits of Fig. 2-11 have the additional advantage that the total equivalent resistance R_{eq} and equivalent reactance X_{eq} can be found from a very simple test, whereas measurement of the values of the component leakage reactances X_{l1} and X_{l2} is a difficult experimental task.

EXAMPLE 2-3

The 50-kVA 2400:240-V transformer whose constants are given in Example 2-2 is used to step down the voltage at the load end of a feeder whose impedance is $0.30 + j1.60 \Omega$. The voltage V_s at the sending end of the feeder is 2400 V.

Find the voltage at the secondary terminals of the transformer when the load connected to its secondary draws rated current from the transformer and the power factor of the load is 0.80 lagging. Neglect the voltage drops in the transformer and feeder caused by the exciting current.

Solution

The circuit with all quantities referred to the high-voltage (primary) side of the transformer is shown in Fig. 2-12a, where the transformer is represented by its equivalent impedance, as in Fig. 2-11c. From Fig. 2-10a, the value of the equivalent impedance is $Z_{eq} = 1.42 + j1.82 \Omega$, and the combined impedance of the feeder and transformer in series is $Z = 1.72 + j3.42 \Omega$. From the transformer rating, the load current referred to the high-voltage side is $I = 50,000/2400 = 20.8 \text{ A}$.

This solution is most easily obtained with the aid of the phasor diagram referred to the high-voltage side as shown in Fig. 2-12b, from which

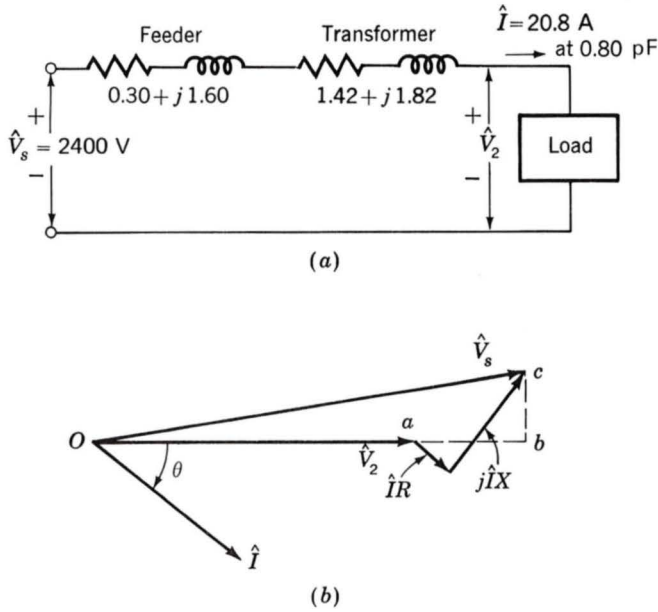


Fig. 2-12. Equivalent circuit and phasor diagram for Example 2-3.

$$Ob = \sqrt{V_s^2 - (bc)^2} \quad \text{and} \quad V_2 = Ob - ab$$

Note that

$$bc = IX \cos \theta - IR \sin \theta \quad ab = IR \cos \theta + IX \sin \theta$$

where R and X are the combined resistance and reactance, respectively. Thus

$$bc = 20.8(3.42)(0.80) - 20.8(1.72)(0.60) = 35.5 \text{ V}$$

$$ab = 20.8(1.72)(0.80) + 20.8(3.42)(0.60) = 71.4 \text{ V}$$

Substitution of numerical values shows that Ob very nearly equals V_s , or 2400 V. Then $V_2 = 2329$ V is referred to the high-voltage side. The actual voltage at the secondary terminals is $2329/10$, or

$$V_2 = 233 \text{ V}$$

b. Approximate Equivalent Circuits; Variable-Frequency Transformers

Small iron-core transformers operating in the audio-frequency range (hence called *audio-frequency transformers*) are often used as coupling devices in electronic circuits for communication, measurement, and control. Their

principal functions are either to step up voltage, thereby contributing to the overall voltage gain in amplifiers, or to act as impedance-transforming devices, bringing about the optimum relation between the apparent impedance of a load and the impedance of a source. They may also serve other auxiliary functions, such as providing a path for direct current through the primary while keeping it out of the secondary circuit.

Application of transformers for impedance matching makes direct use of the impedance-transforming property shown in Eq. 2-17. Oscillators and amplifiers, for example, give optimum performance when working into a definite order of magnitude of load impedance, and transformer coupling can be used to change the apparent impedance of the actual load to this optimum. A transformer so used is called an *output transformer*.

When the frequency varies over a wide range, it is important that the output voltage be as closely instantaneously proportional to the input voltage as possible. Ideally, this means that voltages should be amplified equally and the phase shift should be zero for all frequencies. The *amplitude-frequency characteristic* (often abbreviated to *frequency characteristic*) is a curve of the ratio of the load voltage on the secondary side to the internal source voltage on the primary side plotted as a function of frequency, with a flat characteristic being the most desirable. The *phase characteristic* is a curve of the phase angle of the load voltage relative to the source voltage plotted as a function of frequency, with a small phase angle being desirable. These characteristics depend not only on the transformer but also on the constants of the entire primary and secondary circuits.

As an example of the use of engineering approximations, consider an amplifier coupled to its load through an output transformer. The amplifier is considered equivalent to a source of voltage E_G in series with an internal resistance R_G , and the load is considered as a resistance R_L . This is shown in Fig. 2-13a, where the transformer is represented by the equivalent circuit of Fig. 2-9c, with core loss neglected. Sometimes the stray capacitances of the windings must be taken into account at high audio frequencies, especially when the source impedance is sufficiently large.

The analysis of a properly designed circuit breaks down into three frequency ranges.

Intermediate. At intermediate frequencies, none of the inductances are important, and the equivalent circuit reduces to a network of resistances, as shown in Fig. 2-13b, where all quantities have been referred to the primary, as indicated by the prime superscripts. Analysis of this circuit shows that the ratio of load voltage V_L to source voltage E_G is

$$\frac{V_L}{E_G} = \frac{N_2}{N_1} \frac{R'_L}{R'_{se}} \quad (2-20)$$

where

$$R'_{se} = R_G + R_1 + R'_2 + R'_L \quad (2-21)$$

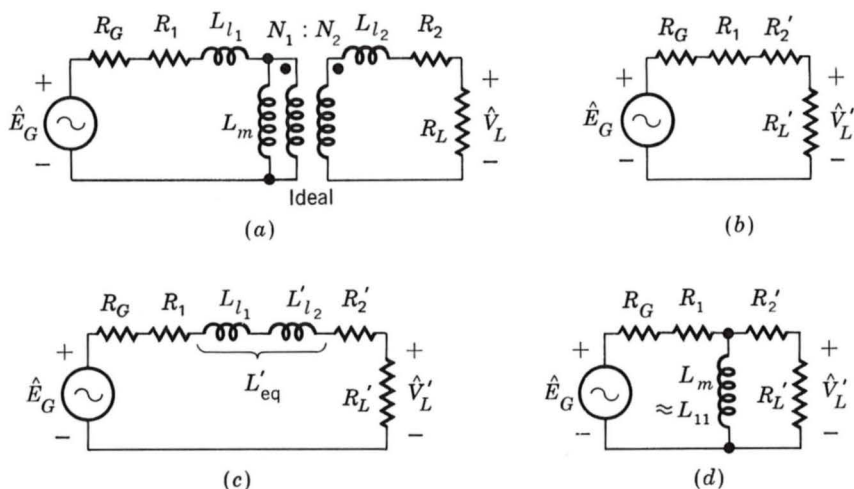


Fig. 2-13. Equivalent circuits of an output transformer: (a) complete equivalent circuit; (b) approximate equivalent in the middle range of audio frequencies; (c) high-frequency equivalent; (d) low-frequency equivalent.

In this middle range (which usually extends over several octaves) the voltage ratio is very nearly constant; i.e., the amplitude characteristic is flat, and the phase shift is zero.

High. As the frequency is increased, the leakage reactances of the transformer become increasingly important. The equivalent circuit in the high audio range is shown in Fig. 2-13c. Analysis of this circuit shows that at high frequencies

$$\frac{V_L}{E_G} = \frac{N_2}{N_1} \frac{R'_L}{R'_{se}} \frac{1}{\sqrt{1 + (\omega L'_{eq}/R'_{se})^2}} \quad (2-22)$$

where L'_{eq} is the equivalent leakage inductance. The voltage ratio relative to its midrange value is

$$\text{Relative voltage ratio} = \frac{1}{\sqrt{1 + (\omega L'_{eq}/R'_{se})^2}} \quad (2-23)$$

The phase angle by which the load voltage lags the source voltage is

$$\theta = \tan^{-1} \frac{\omega L'_{eq}}{R'_{se}} \quad (2-24)$$

Curves of the relative voltage ratio and phase angle as functions of the reactance-to-resistance ratio $\omega L'_{eq}/R'_{se}$ are shown in Fig. 2-14.

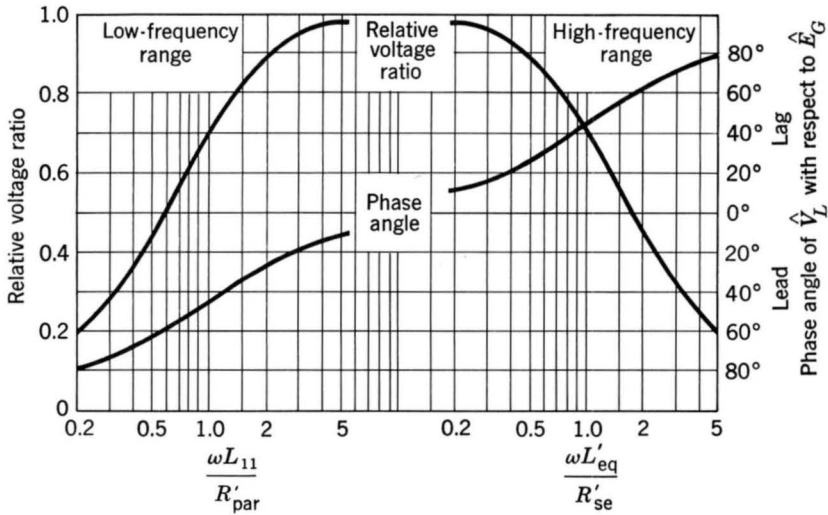


Fig. 2-14. Normalized frequency characteristic of output transformers.

Low. At low frequencies, the leakage reactances are negligible, but the shunting effect of the magnetizing branch becomes increasingly important as its reactance decreases. The inductance of the magnetizing branch very nearly equals the self-inductance L_{11} of the primary. The equivalent circuit at low frequencies is shown in Fig. 2-13d, from which

$$\frac{V_L}{E_G} = \frac{N_2}{N_1} \frac{R'_L}{R'_{se}} \frac{1}{\sqrt{1 + [R'_{par}/(\omega L_{11})]^2}} \quad (2-25)$$

where

$$R'_{par} = \frac{(R_G + R_1)(R'_2 + R'_L)}{R_G + R_1 + R'_2 + R'_L} \quad (2-26)$$

The voltage ratio relative to its midrange value is

$$\text{Relative voltage ratio} = \frac{1}{\sqrt{1 + [R'_{par}/(\omega L_{11})]^2}} \quad (2-27)$$

and the phase angle by which the load voltage leads the source voltage is

$$\theta = \tan^{-1} \frac{R'_{par}}{\omega L_{11}} \quad (2-28)$$

Curves of the relative voltage ratio and phase angle as functions of the reactance-to-resistance ratio $\omega L_{11}/R'_{par}$ are shown in Fig. 2-14.

The points at which the relative voltage ratio is 0.707 are called the *half-power points*. From Eq. 2-23 the upper half-power point occurs at a frequency f_h for which the equivalent leakage reactance $\omega_h L'_{eq}$ equals the series resistance R'_{se} , or

$$f_h = \frac{R'_{se}}{2\pi L'_{eq}} \quad (2-29)$$

and from Eq. 2-27 the lower half-power point occurs at a frequency f_l for which the self-reactance ωL_{11} equals the parallel resistance R'_{par} , or

$$f_l = \frac{R'_{par}}{2\pi L_{11}} \quad (2-30)$$

The bandwidth is describable in terms of the ratio

$$\frac{f_h}{f_l} = \frac{R'_{se}}{R'_{par}} \frac{L_{11}}{L'_{eq}} \quad (2-31)$$

A broad bandwidth requires a high ratio of self-inductance to leakage inductance or a coefficient of coupling as close as possible to unity.

Stray capacitances of the windings may have a significant effect on the frequency characteristics at high audio frequencies. This effect tends to produce a peak in the voltage ratio in the high-frequency range at the frequency where the capacitances are in resonance with the leakage inductances. The height of the peak depends on the circuit impedances as well as the transformer inductances and stray capacitances. These capacitances are difficult to calculate accurately. The frequency-response characteristics of a specific circuit can usually best be determined by tests. The foregoing analysis should be regarded more as an explanation of the effects of the transformer inductances than as an accurate analysis.

c. Short-Circuit and Open-Circuit Tests

Two very simple tests serve to determine the constants of the equivalent circuits of Fig. 2-11 and the power losses in a transformer. These consist of measuring the input voltage, current, and power to the primary, first with the secondary short-circuited and then with the secondary open-circuited.

With the secondary short-circuited, typically a primary voltage of only 2 to 12 percent of the rated value need be impressed to obtain the rated current. For convenience, the high-voltage side is usually taken as the primary in this test. The equivalent circuit with the secondary terminals short-circuited is shown in Fig. 2-15. The voltage induced in the secondary by the resultant core flux equals the secondary leakage-impedance voltage

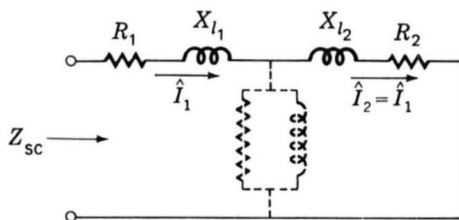


Fig. 2-15. Equivalent circuit with short-circuited secondary.

drop; at rated current this voltage is typically only about 1 to 6 percent of the rated voltage. At the correspondingly low value of core flux, the exciting current and core losses are negligible. The exciting admittance, shown dashed in Fig. 2-15, can then be omitted, and the primary and secondary currents are very nearly equal when referred to the same side. The power input very nearly equals the total I^2R loss in the primary and secondary windings, and the impressed voltage equals the drop in the combined primary and secondary leakage impedance $Z_{eq} = R_{eq} + jX_{eq}$. The equivalent resistance and reactance referred to the primary very nearly equal the short-circuit resistance and reactance, $Z_{sc} = Z_{eq}$.

If \hat{V}_{sc} , \hat{I}_{sc} , and P_{sc} are the impressed voltage, primary current, and power input, respectively, then the short-circuit impedance $Z_{sc} = R_{sc} + jX_{sc}$ and its resistance and reactance components R_{sc} and X_{sc} referred to the primary are

$$Z_{eq} = Z_{sc} = \frac{\hat{V}_{sc}}{\hat{I}_{sc}} \quad (2-32)$$

$$R_{eq} = R_{sc} = \frac{P_{sc}}{I_{sc}^2} \quad (2-33)$$

$$X_{eq} = X_{sc} = \sqrt{|Z_{sc}|^2 - R_{sc}^2} \quad (2-34)$$

The equivalent impedance can, of course, be referred from one side to the other in the usual manner. On the rare occasions when the equivalent T circuit in Fig. 2-9d must be resorted to, approximate values of the individual primary and secondary resistances and leakage reactances can be obtained by assuming that $R_1 = R_2 = 0.5R_{eq}$ and $X_{l1} = X_{l2} = 0.5X_{eq}$ when all impedances are referred to the same side.

The open-circuit test is performed with the secondary open-circuited and the rated voltage impressed on the primary. Under this condition an exciting current of a few percent of full-load current (less on large transformers and more on smaller ones) is obtained. If the transformer is to be used at other than its rated voltage, the test should be done at that voltage. For convenience, the low-voltage side is usually taken as the primary

in this test. The voltage drop in the primary leakage impedance caused by the small exciting current is negligible, and the primary impressed voltage \hat{V}_1 very nearly equals the emf \hat{E}_1 induced by the resultant core flux. Also, the primary I^2R loss caused by the exciting current is negligible, so that the power input P_1 very nearly equals the core loss P_c . Thus the exciting admittance $Y_\varphi = G_c - jB_m$ in Fig. 2-9d very nearly equals the open-circuit admittance $Y_{oc} = G_{oc} - jB_{oc}$ determined from the impressed voltage \hat{V}_1 , exciting current \hat{I}_φ , and power input P_1 measured in the primary with the secondary open-circuited. Thus the exciting admittance and its conductance and susceptance components are very nearly

$$Y_\varphi = Y_{oc} = \frac{\hat{I}_\varphi}{\hat{V}_1} \quad (2-35)$$

$$G_c = G_{oc} = \frac{P_1}{V_1^2} \quad (2-36)$$

$$B_m = B_{oc} = \sqrt{|Y_{oc}|^2 - G_{oc}^2} \quad (2-37)$$

The values obtained are, of course, referred to the side used as the primary in this test. With the approximate equivalent circuits of Fig. 2-11c and d, the open-circuit test is used only to obtain the core loss for efficiency computations and to check the magnitude of the exciting current. Sometimes the voltage at the terminals of the open-circuited secondary is measured as a check on the turns ratio.

EXAMPLE 2-4

With the instruments located in the high-voltage side and the low-voltage side short-circuited, the short-circuit test readings for the 50-kVA 2400:240-V transformer of Example 2-2 are 48 V, 20.8 A, and 617 W. An open-circuit test with the low-voltage side energized gives instrument readings on that side of 240 V, 5.41 A, and 186 W. Determine the efficiency and the voltage regulation at full load, 0.80 power factor lagging.

Solution

From the short-circuit test, the equivalent impedance, resistance, and reactance of the transformer (referred to the high-voltage side as denoted by the subscript H) are

$$|Z_{eq,H}| = \frac{48}{20.8} = 2.31 \, \Omega \quad R_{eq,H} = \frac{617}{20.8^2} = 1.42 \, \Omega$$

$$X_{eq,H} = \sqrt{2.31^2 - 1.42^2} = 1.82 \, \Omega$$

Full-load high-tension current is

$$I_H = \frac{50,000}{2400} = 20.8 \text{ A}$$

$$\text{Loss} = I_H^2 R_{\text{eq}, H} = 20.8^2 (1.42) = 617 \text{ W}$$

$$\text{Core loss} = 186$$

$$\text{Total losses at full load} = 803$$

$$\text{Output} = 50,000(0.80) = 40,000$$

$$\text{Input} = 40,803 \text{ W}$$

$$\frac{\text{Losses}}{\text{Input}} = \frac{803}{40,803} = 0.0197$$

The *efficiency* of any power-transmitting device is

$$\text{Efficiency} = \frac{\text{power output}}{\text{power input}}$$

which can also be expressed as

$$\text{Efficiency} = \frac{\text{input} - \text{losses}}{\text{input}} = 1 - \frac{\text{losses}}{\text{input}}$$

For the specific load, the efficiency of this transformer is

$$\text{Efficiency} = 1 - 0.0197 = 0.980$$

The *voltage regulation* of a transformer is the change in secondary terminal voltage from no load to full load and is usually expressed as a percentage of the full-load value. The equivalent circuit of Fig. 2-11c will be used with everything still referred to the high-voltage side. The primary voltage is assumed to be adjusted so that the secondary terminal voltage has its rated value at full load, or $V_{2H} = 2400 \text{ V}$ referred to the high-voltage side. The required value of the primary voltage \hat{V}_{1H} can be computed from the phasor diagram shown in Fig. 2-16.

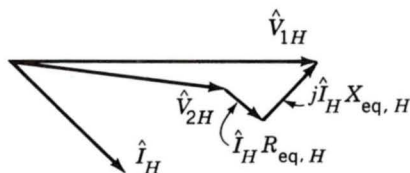


Fig. 2-16. Phasor diagram for Example 2-4.

$$\begin{aligned}
 \hat{V}_{1H} &= \hat{V}_{2H} + \hat{I}_H(R_{eq,H} + jX_{eq,H}) \\
 &= 2400 + 20.8(0.80 - j0.60)(1.42 + j1.82) \\
 &= 2446 + j13
 \end{aligned}$$

The magnitude of \hat{V}_{1H} is 2446 V. If this voltage were held constant and the load removed, the secondary voltage on open circuit would rise to 2446 V referred to the high-voltage side. Then

$$\text{Regulation} = \frac{2446 - 2400}{2400}(100) = 1.92\%$$

2-6 AUTOTRANSFORMERS; MULTICIRCUIT TRANSFORMERS

The principles discussed in previous articles have been developed with specific reference to two-winding transformers. They are also generally applicable to transformers with other than two separate windings. Aspects relating to autotransformers and multiwinding transformers are considered in this article.

a. Autotransformers

As viewed from the terminals, substantially the same transformation effect on voltages, currents, and impedances can be obtained with the connections of Fig. 2-17a, as in the normal transformer with two separate windings shown in Fig. 2-17b. In Fig. 2-17a, winding bc is common to both primary and secondary circuits. This type of transformer is called an *autotransformer*. It is really little more than a normal transformer connected in a special way. The only difference structurally is that winding ab must be provided with extra insulation.

The performance of an autotransformer is governed by the fundamental considerations already discussed for transformers having two separate

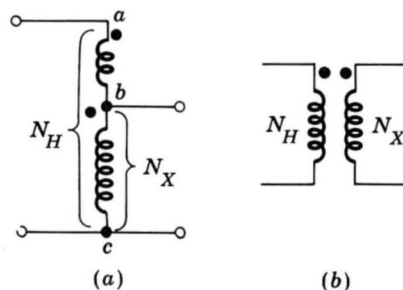


Fig. 2-17. (a) Autotransformer; (b) two-winding transformer.

windings. Autotransformers have lower leakage reactances, lower losses, and smaller exciting current and cost less than two-winding transformers when the voltage ratio does not differ too greatly from 1:1. A disadvantage is the direct electric connection between the high- and low-voltage sides. Their performance can best be illustrated by way of an example.

EXAMPLE 2-5

The 2400:240-V 50-kVA transformer of Example 2-4 is connected as an autotransformer, as shown in Fig. 2-18, in which ab is the 240-V winding and bc is the 2400-V winding. (It is assumed that the 240-V winding has enough insulation to withstand a voltage of 2640 V to ground.)

(a) Compute the voltage ratings V_H and V_X of the high- and low-tension sides, respectively, when the transformer is connected as an autotransformer.

(b) Compute the kVA rating as an autotransformer.

(c) Data with respect to the losses are given in Example 2-4. Compute the full-load efficiency as an autotransformer at 0.80 power factor.

Solution

(a) Since the 2400-V winding bc is connected to the low-tension circuit, $V_X = 2400$ V. When $V_{bc} = 2400$ V, a voltage $V_{ab} = 240$ V in phase with V_{bc} will be induced in winding ab (leakage-impedance voltage drops being neglected). The voltage of the high-tension side therefore is

$$V_H = V_{ab} + V_{bc} = 2640 \text{ V}$$

(b) From the rating of 50 kVA as a normal two-winding transformer, the rated current of the 240-V winding is $50,000/240 = 208$ A. Since the 240-V winding is in series with the high-tension circuit, the rated current of this winding is the rated current I_H on the high-tension side as an autotransformer. The kVA rating as an autotransformer therefore is

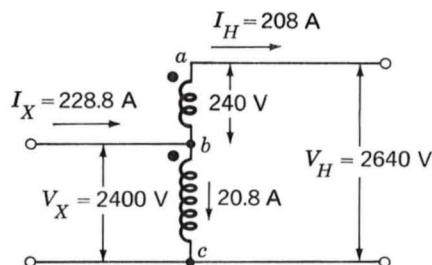


Fig. 2-18. Autotransformer for Example 2-5.

$$\frac{V_H I_H}{1000} = \frac{2640(208)}{1000} = 550 \text{ kVA}$$

The rating can also be computed on the low-tension side in a manner which highlights the current-transforming properties. Thus, if the current in the 240-V winding has its rated value of 208 A, the current in the 2400-V winding must produce an equal and opposite mmf (exciting current being neglected) and therefore must be 20.8 A in the arrow direction (Fig. 2-18). The current I_X on the low-tension side as an autotransformer therefore is

$$I_X = 208 + 20.8 = 228.8 \text{ A}$$

and the kVA rating is

$$\frac{V_X I_X}{1000} = \frac{2400(228.8)}{1000} = 550 \text{ kVA}$$

Note that this transformer, whose rating as a normal two-winding transformer is 50 kVA, is capable of handling 550 kVA as an autotransformer. The higher rating as an autotransformer is a consequence of the fact that not all the 550 kVA has to be transformed by electromagnetic induction. In fact, all that the transformer has to do is to boost a current of 208 A through a potential rise of 240 V, corresponding to a power transformation capacity of 50 kVA.

(c) When it is connected as an autotransformer with the currents and voltages shown in Fig. 2-18, the losses are the same as in Example 2-4, namely, 803 W. But the output as an autotransformer at 0.80 power factor is $0.80(550,000) = 440,000 \text{ W}$. The efficiency therefore is

$$1 - \frac{803}{440,803} = 0.9982$$

The efficiency is so high because the losses are those corresponding to transforming only 50 kVA.

b. Multicircuit Transformers

Transformers having three or more windings, known as *multicircuit*, or *multiwinding*, *transformers*, are often used to interconnect three or more circuits which may have different voltages. For these purposes a multicircuit transformer costs less and is more efficient than an equivalent number of two-circuit transformers. A transformer having a primary and two secondaries is generally used to supply power to electronic units. The distribution transformers used to supply power for domestic purposes usually

have two 120-V secondaries connected in series. Lighting circuits are connected across each of the 120-V windings, while electric ranges, domestic hot-water heaters, and other similar loads are supplied with 240-V power from the series-connected secondaries. A large distribution system may be supplied through a three-phase bank of multicircuit transformers from two or more transmission systems having different voltages. The three-phase transformer banks used to interconnect two transmission systems of different voltages often have a third, or tertiary, set of windings to provide voltage for auxiliary power purposes in the substation or to supply a local distribution system. Static capacitors or synchronous condensers may be connected to the tertiary windings for power factor correction or voltage regulation. Sometimes Δ -connected tertiary windings are put on three-phase banks to provide a circuit for the third harmonics of the exciting current.

Some of the problems arising in the use of multicircuit transformers concern the effects of leakage impedances on voltage regulation, short-circuit currents, and division of load among circuits. These problems can be solved by an equivalent-circuit technique similar to that used in dealing with two-circuit transformers.

The equivalent circuits of multiwinding transformers are more complicated than in the two-winding case because they must take into account the leakage impedances associated with each pair of windings. In these equivalent circuits, all quantities are referred to a common base, either by use of the appropriate turns ratios as referring factors or by expressing all quantities in per unit. The exciting current usually is neglected.

2-7 TRANSFORMERS IN THREE-PHASE CIRCUITS[†]

Three single-phase transformers can be connected to form a three-phase bank in any of the four ways shown in Fig. 2-19. In all four parts of this figure, the windings at the left are the primaries, those at the right are the secondaries, and any primary winding in one transformer corresponds to the secondary winding drawn parallel to it. Also shown are the voltages and currents resulting from balanced impressed primary line-to-line voltages V and line currents I when the ratio of primary-to-secondary turns N_1/N_2 is a and ideal transformers are assumed. Note that, for fixed line-to-line voltages and total kVA, the kVA rating of each transformer is one-third the kVA rating of the bank, regardless of the connections used, but the voltage and current ratings of the individual transformers depend on the connections.

The Y- Δ connection is commonly used in stepping down from a high voltage to a medium or low voltage. One reason is that a neutral is thereby provided for grounding on the high-voltage side, a procedure which can be

[†]The relationship between three-phase and single-phase quantities is discussed in Appendix A.

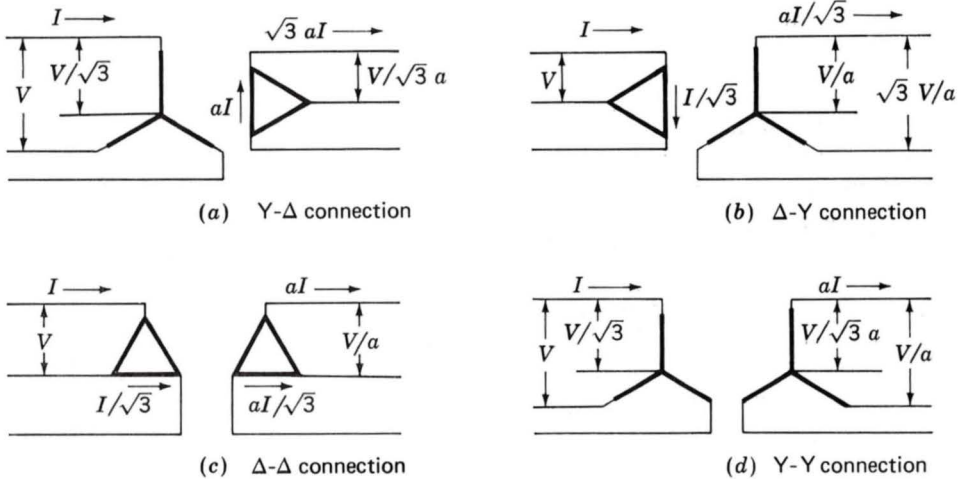


Fig. 2-19. Common three-phase transformer connections; the transformer windings are indicated by the heavy lines.

shown to be desirable in most cases. Conversely, the Δ -Y connection is commonly used for stepping up to a high voltage. The Δ - Δ connection has the advantage that one transformer can be removed for repair or maintenance while the remaining two continue to function as a three-phase bank with the rating reduced to 58 percent of that of the original bank; this is known as the *open-delta*, or *V*, connection. The Y-Y connection is seldom used because of difficulties with exciting-current phenomena.

Instead of three single-phase transformers, a three-phase bank may consist of one three-phase transformer having all six windings on a common multilegged core and contained in a single tank. Advantages of three-phase transformers are that they cost less, weigh less, require less floor space, and have somewhat higher efficiency. A photograph of the internal parts of a large three-phase transformer is shown in Fig. 2-20.

Circuit computations involving three-phase transformer banks under balanced conditions can be made by dealing with only one of the transformers or phases and recognizing that conditions are the same in the other two phases except for the phase displacements associated with a three-phase system. It is usually convenient to carry out the computations on a per-phase-Y line-to-neutral basis, since transformer impedances can then be added directly in series with transmission line impedances. The impedances of transmission lines can be referred from one side of the transformer bank to the other by use of the square of the ideal line-to-line voltage ratio of the bank. In dealing with Y- Δ or Δ -Y banks, all quantities can be referred to the Y-connected side. In dealing with Δ - Δ banks in series with transmission lines, it is convenient to replace the Δ -connected impedances of the transformers by equivalent Y-connected impedances. It can be shown that a balanced Δ -connected circuit of $Z_{\Delta}\Omega/\text{phase}$ is equivalent to

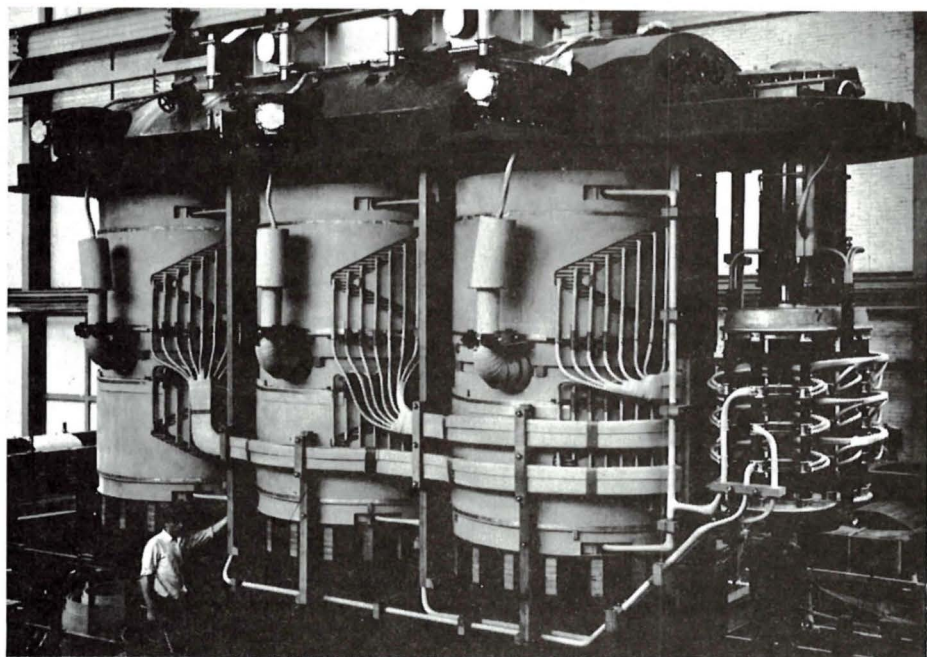


Fig. 2-20. A 200-MVA three-phase 50-Hz three-winding 210/80/10.2-kV transformer removed from its tank. The 210-kV winding has an on-load tap changer for adjustment of the voltage. (Brown Boveri Corporation.)

a balanced Y-connected circuit of $Z_Y \Omega/\text{phase}$ if

$$Z_Y = \frac{1}{3}Z_{\Delta} \quad (2-38)$$

EXAMPLE 2-6

Three single-phase 50-kVA 2400:240-V transformers, each identical with that of Example 2-4, are connected Y- Δ in a three-phase 150-kVA bank to step down the voltage at the load end of a feeder whose impedance is $0.15 + j1.00 \Omega/\text{phase}$. The voltage at the sending end of the feeder is 4160 V line to line. On their secondary sides, the transformers supply a balanced three-phase load through a feeder whose impedance is $0.0005 + j0.0020 \Omega/\text{phase}$. Find the line-to-line voltage at the load when the load draws the rated current from the transformers at a power factor of 0.80 lagging.

Solution

The computations can be made on a per-phase-Y basis by referring everything to the high-voltage Y-connected side of the transformer bank. The

voltage at the sending end of the feeder is equivalent to a source voltage V_s of

$$V_s = \frac{4160}{\sqrt{3}} = 2400 \text{ V to neutral}$$

From the transformer rating, the rated current on the high-voltage side is 20.8 A/phase Y. The low-voltage feeder impedance referred to the high-voltage side by means of the square of the ideal line-to-line voltage ratio of the bank is

$$\left(\frac{4160}{240}\right)^2 (0.0005 + j0.0020) = 0.15 + j0.60 \Omega$$

and the combined series impedance of the high- and low-voltage feeders referred to the high-voltage side is

$$Z_{\text{feeder}} = 0.30 + j1.60 \Omega/\text{phase Y}$$

From Example 2-4 the equivalent impedance of the transformer bank referred to its high-voltage Y-connected side is

$$Z_{\text{eq},H} = 1.42 + j1.82 \Omega/\text{phase Y}$$

The equivalent circuit for one phase referred to the Y-connected primary side then is exactly the same as Fig. 2-12a, and the solution on a per phase basis is exactly the same as the solution of Example 2-3, whence the load voltage referred to the high-voltage side is 2329 V to neutral. The actual load voltage is

$$V_{\text{load}} = 233 \text{ V line to line}$$

This is the line-to-line voltage because the secondaries are Δ -connected.

EXAMPLE 2-7

The three transformers of Example 2-6 are connected Δ - Δ and supplied with power through a 2400-V (line-to-line) three-phase feeder whose reactance is $0.80 \Omega/\text{phase}$. The equivalent reactance of each transformer referred to its high-voltage side is 1.82Ω . All circuit resistances are neglected. At its sending end, the feeder is connected to the secondary terminals of a three-phase Y- Δ -connected transformer whose three-phase rating is 500 kVA, 24,000:2400 V (line-to-line voltages). The equivalent reactance of the sending-end transformers is $2.76 \Omega/\text{phase } \Delta$ referred to the

2400-V side. The voltage applied to the primary terminals is 24,000 V line to line.

A three-phase short circuit occurs at the 240-V terminals of the receiving-end transformers. Compute the steady-state short-circuit current in the 2400-V feeder wires, in the primary and secondary windings of the receiving-end transformers, and at the 240-V terminals.

Solution

The computations will be made on an equivalent line-to-neutral basis with everything referred to the 2400-V feeder. The source voltage then is

$$\frac{2400}{\sqrt{3}} = 1385 \text{ V to neutral}$$

In sending-end transformers (from Eq. 2-38),

$$X_{\text{eq}} = \frac{2.76}{3} = 0.92 \text{ equivalent } \Omega/\text{phase Y}$$

In receiving-end transformers,

$$X_{\text{eq}} = \frac{1.82}{3} = 0.61 \text{ equivalent } \Omega/\text{phase Y}$$

$$\text{Feeder } X = 0.80 \text{ } \Omega/\text{phase Y}$$

$$\text{Total reactance} = 0.92 + 0.61 + 0.80 = 2.33 \text{ } \Omega$$

$$\text{Current in 2400-V feeder} = \frac{1385}{2.33} = 594 \text{ A}$$

$$\text{Current in 2400-V windings} = \frac{594}{\sqrt{3}} = 342 \text{ A}$$

$$\text{Current in 240-V windings} = 3420 \text{ A}$$

$$\text{Current at the 240-V terminals} = 5940 \text{ A}$$

2-8 THE PER UNIT SYSTEM

Computations relating to machines, transformers, and systems of machines are often carried out in per unit form, i.e., with all pertinent quantities expressed as decimal fractions of appropriately chosen *base values*. All the usual computations are then carried out in these per unit values instead of the familiar volts, amperes, ohms, etc.

There are two advantages to the system. One is that the constants of machines and transformers lie in a reasonably narrow numerical range

when expressed in a per unit system related to their rating. The correctness of their values is thus subject to a rapid approximate check. The other advantage is that the analyst is relieved of the worry of referring circuit quantities to one side or the other of transformers. For complicated systems involving many transformers of different turns ratios, this advantage is a significant one in that a possible cause of serious mistakes is removed. The per unit system is also very useful in simulating machine systems on analog and digital computers for transient and dynamic analyses.

Quantities such as voltage V , current I , power P , reactive power Q , voltamperes VA , resistance R , reactance X , impedance Z , conductance G , susceptance B , and admittance Y can be translated to and from per unit form as follows:

$$\text{Quantity in per unit} = \frac{\text{actual quantity}}{\text{base value of quantity}} \quad (2-39)$$

where "actual quantity" refers to the value in volts, amperes, ohms, etc. To a certain extent, base values can be chosen arbitrarily, but certain relations between them must be observed for the normal electrical laws to hold in the per unit system. Thus, for a single-phase system,

$$P_{\text{base}}, Q_{\text{base}}, VA_{\text{base}} = V_{\text{base}} I_{\text{base}} \quad (2-40)$$

$$R_{\text{base}}, X_{\text{base}}, Z_{\text{base}} = \frac{V_{\text{base}}}{I_{\text{base}}} \quad (2-41)$$

In normal usage, values of VA_{base} and V_{base} are chosen first; values of I_{base} and all other quantities in Eqs. 2-40 and 2-41 being thereby established.

The value of VA_{base} must be the same over the entire system concerned. When a transformer is encountered, the values of V_{base} are different on each side and must be in the same ratio as the turns on the transformer. Usually the rated or nominal voltages of the respective sides are chosen. The process of referring quantities to one side of the transformer is then taken care of automatically by using Eqs. 2-40 and 2-41 in finding and interpreting per unit values.

This can be seen with reference to the equivalent circuit of Fig. 2-9c. If the base voltages of the primary and secondary are chosen to be in the ratio of the turns of the ideal transformer, the per unit ideal transformer will have a unity turns ratio and hence can be eliminated. The procedure thus becomes one of translating all quantities to per unit values, using these values in all the customary circuit analysis techniques, and translating the end results back to the more usual forms.

When only one electric device, such as a transformer, is involved, the device's own rating is generally used for the volt-ampere base. When expressed in per unit form on the rating as a base, the characteristics of power and distribution transformers do not vary much over a wide range of ratings. For example, the exciting current usually is between 0.02 and

0.06 per unit, the equivalent resistance usually is between 0.005 and 0.02 per unit (the smaller values applying to large transformers), and the equivalent reactance usually is between 0.015 and 0.10 per unit (the larger values applying to large high-voltage transformers). Similarly, the per unit values of synchronous and induction machine constants fall within a relatively narrow range. When several devices are involved, however, an arbitrary choice of volt-ampere base must usually be made so that the same base will be used for the overall system. Per unit (pu) values can be changed from one base to another by the following relations:

$$(P, Q, VA)_{\text{pu on base 2}} = (P, Q, VA)_{\text{pu on base 1}} \frac{VA_{\text{base 1}}}{VA_{\text{base 2}}} \quad (2-42)$$

$$(R, X, Z)_{\text{pu on base 2}} = (R, X, Z)_{\text{pu on base 1}} \frac{(V_{\text{base 1}})^2 VA_{\text{base 2}}}{(V_{\text{base 2}})^2 VA_{\text{base 1}}} \quad (2-43)$$

$$V_{\text{pu on base 2}} = V_{\text{pu on base 1}} \frac{V_{\text{base 1}}}{V_{\text{base 2}}} \quad (2-44)$$

$$I_{\text{pu on base 2}} = I_{\text{pu on base 1}} \frac{V_{\text{base 2}} VA_{\text{base 1}}}{V_{\text{base 1}} VA_{\text{base 2}}} \quad (2-45)$$

EXAMPLE 2-8

The exciting current measured on the low-voltage side of a 50-kVA 2400:240-V transformer is 5.41 A. Its equivalent impedance referred to the high-voltage side is $1.42 + j1.82 \Omega$. Taking the transformer rating as a base, express in per unit on the low- and high-voltage sides (a) the exciting current and (b) the equivalent impedance.

Solution

The base values of voltages and currents are

$$V_{\text{base},H} = 2400 \text{ V} \quad V_{\text{base},X} = 240 \text{ V} \quad I_{\text{base},H} = 20.8 \text{ A} \quad I_{\text{base},X} = 208 \text{ A}$$

where subscripts H and X indicate the high- and low-voltage sides, respectively.

From Eq. 2-41

$$Z_{\text{base},H} = \frac{2400}{20.8} = 115.2 \Omega \quad Z_{\text{base},X} = \frac{240}{208} = 1.152 \Omega$$

(a) From Eq. 2-39

$$I_{\varphi X} = \frac{5.41}{208} = 0.0260 \text{ per unit}$$

The exciting current referred to the high-voltage side is 0.541 A. Its per unit value is

$$I_{\phi H} = \frac{0.541}{20.8} = 0.0260 \text{ per unit}$$

The per unit values are the same referred to either side. The turns ratios required to refer currents in amperes from one side of the transformer to the other are taken care of in the per unit system by the base values for currents on the two sides when the volt-ampere base is the same on both sides and the voltage bases are in the ratio of the turns.

(b) From Eq. 2-39 and the value for $Z_{\text{base},H}$

$$Z_{\text{eq},H} = \frac{1.42 + j1.82}{115.2} = 0.0123 + j0.0158 \text{ per unit}$$

The equivalent impedance referred to the low-voltage side is $0.0142 + j0.0182 \Omega$. Its per unit value is

$$Z_{\text{eq},X} = \frac{0.0142 + j0.0182}{1.152} = 0.0123 + j0.0158 \text{ per unit}$$

The per unit values referred to the high- and low-voltage sides are the same, the referring factors being taken care of in per unit by the base values.

When they are applied to three-phase problems, the base values for the per unit system are chosen so that the relations for a balanced three-phase system hold between them:

$$(P_{\text{base}}, Q_{\text{base}}, VA_{\text{base}})_{3\text{-phase}} = 3VA_{\text{base per phase}} \quad (2-46)$$

$$V_{\text{base, line to line}} = \sqrt{3} V_{\text{base, line to neutral}} \quad (2-47)$$

$$I_{\text{base, per phase } \Delta} = \frac{1}{\sqrt{3}} I_{\text{base, per phase Y}} \quad (2-48)$$

In dealing with three-phase systems, the three-phase VA base and the line-to-line voltage base are usually chosen first. The base values for phase voltages and currents then follow from Eqs. 2-46 to 2-48. Equations 2-42 to 2-45 still apply to the base values per phase. For example, the base value for Y-connected impedances is given by Eq. 2-43 with V_{base} taken as the base voltage to neutral and I_{base} taken as the base current per phase Y; the base value for Δ -connected impedances is also given by Eq. 2-43, but with V_{base} taken as the base line-to-line voltage and I_{base} taken as the base current per phase Δ . Division of Eq. 2-47 by Eq. 2-48 shows that

$$Z_{\text{base, per phase } \Delta} = 3Z_{\text{base, per phase Y}} \quad (2-49)$$

The factors of $\sqrt{3}$ and 3 relating Δ and Y quantities in volts, amperes, and ohms in a balanced three-phase system are thus automatically taken care of in per unit by the base values. Such three-phase problems can be solved in per unit as if they were single-phase problems without paying any attention to the details of the transformer connections except in translating volt-ampere-ohm values into and out of the per unit system.

EXAMPLE 2-9

Solve Example 2-7 in per unit on a three-phase 150-kVA rated-voltage base. The reactance of the three-phase 500-kVA sending-end transformer is 0.08 per unit on its rating as a base. The reactance of the 2400-V feeder is 0.80 Ω /phase. The reactance of the receiving-end transformers is 0.0158 per unit, as computed in Example 2-8.

Solution

Convert reactance of the sending-end transformer to the 150-kVA base by using Eq. 2-43:

$$X_{\text{sending end}} = 0.08 \left(\frac{150}{500} \right) = 0.024 \text{ per unit}$$

For the 2400-V feeder,

$$V_{\text{base}} = \frac{2400}{\sqrt{3}} = 1385 \text{ V line to neutral}$$

$$I_{\text{base}} = \frac{50,000}{1385} = 36.1 \text{ A/phase Y}$$

$$Z_{\text{base}} = \frac{1385}{36.1} = 38.3 \text{ } \Omega/\text{phase Y}$$

Therefore
$$X_{\text{feeder}} = \frac{0.80}{38.3} = 0.021 \text{ per unit}$$

For the receiving-end transformers,

$$X_{\text{receiving end}} = 0.0158 \text{ per unit}$$

$$\text{Total reactance} = \text{sum} = 0.0608 \text{ per unit}$$

$$\text{Short-circuit current} = \frac{1.00}{0.0608} = 16.4 \text{ per unit}$$

The currents in various parts of the circuit can now be computed. For example, the current in the 2400-V feeder wires is $16.4(36.1) = 594$ A. Compare with the result in Example 2-7.

Note: It can readily be shown that the reactance of 0.08 per unit for the sending-end transformers is consistent with the value of $2.76 \Omega/\text{phase}$ given in Example 2-7.

2-9 SUMMARY

Although not an electromechanical device, the transformer is a common and indispensable component of ac systems where it is used to transform voltages, currents, and impedances to appropriate levels for optimal use. For the purposes of our study of electromechanical systems, transformers serve as valuable examples of the analysis techniques which must be employed. Thus they offer us opportunities to investigate the properties of magnetic circuits, including the concepts of mutual flux and inductance, magnetizing flux, mmf and current, and the issues of leakage inductance.

In both transformers and rotating machines, a magnetic field is created by the combined action of the currents in the windings. In an iron-core transformer, most of this flux is confined to the core and links all the windings. This resultant mutual flux induces voltages in the windings proportional to their number of turns and provides the voltage-changing property. In rotating machines, most of the flux crosses the air gap, like the core flux in a transformer, and links all the windings on both stator and rotor. The voltages induced in the windings by this resultant mutual air-gap flux are similar to those induced by the resultant core flux in a transformer. The difference is that mechanical motion together with electromechanical energy conversion is involved in rotating machines. The torque associated with this energy conversion process is created by the interaction of the air-gap flux with the magnetic field of the rotor currents.

In addition to the useful mutual fluxes, in both transformers and rotating machines there are leakage fluxes which link one winding without linking the other. Although the detailed picture of the leakage fluxes in rotating machines is more complicated than that in transformers, their effects are essentially the same. In both, the leakage fluxes induce voltages in ac windings which are accounted for as leakage-reactance voltage drops. In both, the leakage-flux paths are mostly in air, and the leakage fluxes are nearly linearly proportional to the currents producing them. The leakage reactances therefore are often assumed to be constant, independent of the degree of saturation of the main magnetic circuit.

From the viewpoint of the winding, the induced-voltage phenomena in transformers and rotating machines are essentially the same, although the internal phenomena causing the time variations in flux linkages are dif-

ferent. In a rotating machine, the time variation in flux linkages is caused by relative motion of the field and the winding, and the induced voltage is sometimes referred to as a *speed voltage*. Speed voltages accompanied by mechanical motion are a necessary counterpart of the electromechanical energy conversion. In a static transformer, however, the time variation of flux linkages is caused by the growth and decay of a stationary magnetic field; no mechanical motion is involved, and no electromechanical energy conversion takes place.

The resultant core flux in a transformer induces a counter emf in the primary which, together with the primary resistance and leakage-reactance voltage drops, must balance the applied voltage. Since the resistance and leakage-reactance voltage drops usually are small, the counter emf must approximately equal the applied voltage and the core flux must adjust itself accordingly. Exactly similar phenomena must take place in the armature windings of an ac motor; the resultant air-gap flux wave must adjust itself to generate a counter emf approximately equal to the applied voltage. In both transformers and rotating machines, the net mmf of all the currents must accordingly adjust itself to create the resultant flux required by this voltage balance. In any ac electromagnetic device in which the resistance and leakage-reactance voltage drops are small, the resultant flux is very nearly determined by the applied voltage and frequency, and the currents must adjust themselves accordingly to produce the mmf required to create this flux.

In a transformer, the secondary current is determined by the voltage induced in the secondary, the secondary leakage impedance, and the electric load. In an induction motor, the secondary (rotor) current is determined by the voltage induced in the secondary, the secondary leakage impedance, and the mechanical load on its shaft. Essentially the same phenomena take place in the primary winding of the transformer and in the armature (stator) windings of induction and synchronous motors. In all three, the primary, or armature, current must adjust itself so that the combined mmf of all currents creates the flux required by the applied voltage.

Further examples of these basic similarities can be cited. Except for friction and windage, the losses in transformers and rotating machines are essentially the same. Tests for determining the losses and equivalent-circuit constants are essentially the same: an open-circuit, or no-load, test gives information regarding the excitation requirements and core losses (and friction and windage in rotating machines), while a short-circuit test together with dc resistance measurements gives information regarding leakage reactances and winding resistances. The handling of the effects of magnetic saturation is another example: in both transformers and ac rotating machines, the leakage reactances are usually assumed to be unaffected by saturation, and the saturation of the main magnetic circuit is assumed to be determined by the resultant mutual or air-gap flux.

PROBLEMS

2-1. A potential transformer is made up of a 1000-turn primary coil and an open-circuited 80-turn secondary coil wound around a closed core of cross-sectional area 32 cm^2 . The core material can be considered to saturate when the rms applied flux density reaches 1.4 T . What maximum 60-Hz rms primary voltage is possible without reaching this saturation level? What is the corresponding secondary voltage? How are these values modified if the applied frequency is lowered to 50 Hz ?

2-2. A transformer is to be used to transform the impedance of a $2\text{-}\Omega$ resistor to an impedance of $75 \text{ }\Omega$. Calculate the required turns ratio, assuming the transformer to be ideal.

2-3. A source which can be represented by a voltage source of 5 V rms in series with an internal resistance of $3000 \text{ }\Omega$ is connected to a $150\text{-}\Omega$ load resistance through an ideal transformer. Calculate the power in milliwatts supplied to the load as a function of the transformer ratio, covering ratios from 1.0 to 10.0 . For what turns ratio is the maximum power transferred to the load?

2-4. Repeat Prob. 2-3 with the source resistance replaced by a $3000\text{-}\Omega$ reactance.

2-5. A single-phase 60-Hz transformer has a nameplate voltage rating of $7.97 \text{ kV}:266 \text{ V}$, which is based on its winding turns ratio. The manufacturer calculates that the primary (7.97-kV) leakage inductance is 172 mH and the primary magnetizing inductance is 110 H . For an applied primary voltage of 7970 V at 60 Hz , calculate the resultant open-circuit secondary voltage.

2-6. The manufacturer calculates that the transformer of Prob. 2-5 has a secondary leakage inductance of 0.21 mH .

- (a) Calculate the magnetizing inductance as referred to the secondary side.
- (b) A voltage of 266 V , 60 Hz is applied to the secondary. Calculate
 - (i) the resultant open-circuit primary voltage and
 - (ii) the secondary current which would result if the primary were short-circuited.

2-7. A $3.46\text{-kV}:2400\text{-V}$ transformer has a series leakage reactance of $38.3 \text{ }\Omega$ as referred to the high-voltage side. A 20-kW load (unity power factor) is connected to the low-voltage side, and the voltage is measured to be 2380 V . Calculate the corresponding voltage and power factor as measured at the high-voltage terminals.

2-8. The resistances and leakage reactances in ohms of a 25-kVA 60-Hz 2400:240-V distribution transformer are

$$\begin{aligned} R_1 &= 0.650 & R_2 &= 0.00650 \\ X_{l_1} &= 8.40 & X_{l_2} &= 0.0840 \end{aligned}$$

where subscript 1 denotes the 2400-V winding and subscript 2 denotes the 240-V winding. Each quantity is referred to its own side of the transformer.

- (a) Draw the equivalent circuit referred to (i) the high- and (ii) the low-voltage sides. Label the impedances numerically.
- (b) Consider the transformer to deliver its rated kilovoltamperes at 0.80 power factor lagging to a load on the low-voltage side with 240 V across the load. Find the high-tension terminal voltage.

2-9. Repeat Prob. 2-8. In part (b), assume the load to be operating at 0.8 power factor leading.

2-10. A single-phase load is supplied through a 35-kV feeder whose impedance is $115 + j380 \, \Omega$ and a 35-kV:2400-V transformer whose equivalent impedance is $0.26 + j1.21 \, \Omega$ referred to its low-voltage side. The load is 180 kW at 0.87 leading power factor and 2320 V.

- (a) Compute the voltage at the high-voltage terminals of the transformer.
- (b) Compute the voltage at the sending end of the feeder.
- (c) Compute the power and reactive power input at the sending end of the feeder.

2-11. An audio-frequency output transformer has a primary-to-secondary turns ratio of 31.6. Its primary inductance measured with the secondary open is 19.6 H and measured with the secondary short-circuited is 0.207 H. The winding resistances are negligible. This transformer is used to connect an $8\text{-}\Omega$ resistive load to a source which can be represented by a variable-frequency internal emf in series with a resistance of $5000 \, \Omega$. Compute the following that relate to the frequency characteristics of the circuit: (a) the upper half-power frequency, (b) lower half-power frequency, (c) geometric mean of these frequencies, and (d) ratio of load voltage to source voltage at the frequency of part (c).

2-12. Repeat Example 2-4 with the transformer operating at full load and a power factor of unity.

2-13. The nameplate on a 50-MVA, 60-Hz single-phase transformer indicates that it has a voltage rating of 8.0 kV:78 kV. An open-circuit test is conducted from the low-voltage side, and the corresponding instrument

readings are 8.0 kV, 61.9 A, and 136 kW. Similarly, a short-circuit test from the low-voltage side gives readings of 650 V, 6.25 kA, and 103 kW.

- Calculate the equivalent series impedance, resistance, and reactance of the transformer as referred to the low-voltage terminals.
- Calculate the equivalent series impedance of the transformer as referred to the high-voltage terminals.
- Making appropriate approximations, draw a T equivalent circuit for the transformer.
- Determine the efficiency and voltage regulation if the transformer is operating at the rated voltage and load (unity power factor).
- Repeat part (d), assuming the load to be at 0.9 power factor leading.

2-14. A 550-kVA 60-Hz transformer with a 13.8-kV primary winding draws 4.55 A and 3250 W at no load, rated voltage and frequency. Another transformer has a core with all its linear dimensions $\sqrt{2}$ times as large as the corresponding dimensions of the first transformer. The core material and lamination thickness are the same in both transformers. If the primary windings of both transformers have the same number of turns, what no-load current and power will the second transformer draw with 27.6 kV at 60 Hz impressed on its primary?

2-15. The following data were obtained for a 20-kVA, 60-Hz, 2400:240-V distribution transformer tested at 60 Hz:

	Voltage, V	Current, A	Power, W
With high-voltage winding open-circuited	240	1.066	126.6
With low-voltage terminals short-circuited	57.5	8.34	284

- Compute the efficiency at full-load current and the rated terminal voltage at 0.8 power factor.
- Assume that the load power factor is varied while the load current and secondary terminal voltage are held constant. Use a phasor diagram to determine the load power factor for which the regulation is greatest. What is this regulation?

2-16. A 120:480-V, 10-kVA transformer is to be used as an autotransformer to supply a 480-V circuit from a 600-V source. When it is tested as a two-winding transformer at rated load, unity power factor, its efficiency is 0.975.

- Make a diagram of connections as an autotransformer.
- Determine its kVA rating as an autotransformer.
- Find its efficiency as an autotransformer at full load, with 0.85 power factor lagging.

2-17. The transformer of Prob. 2-8 is to be connected as an autotransformer. Determine (a) the voltage ratings of the high- and low-voltage windings for this connection and (b) the kVA rating of the autotransformer connection.

2-18. Consider the 8-kV:78-kV, 50-MVA transformer of Prob. 2-13 connected as an autotransformer.

- (a) Determine the voltage ratings of the high- and low-voltage windings for this connection and the kVA rating of the autotransformer connection.
- (b) Calculate the efficiency of the transformer in this connection when it is supplying its rated load at unity power factor.

2-19. The high-voltage terminals of a three-phase bank of three single-phase transformers are connected to a three-wire three-phase 13,800-V (line-to-line) system. The low-voltage terminals are connected to a three-wire three-phase substation load rated at 1500 kVA and 2300 V line to line. Specify the voltage, current, and kVA ratings of each transformer (both high- and low-voltage windings) for the following connections:

	High-voltage windings	Low-voltage windings
(a)	Y	Δ
(b)	Δ	Y
(c)	Y	Y
(d)	Δ	Δ

2-20. Three 100-MVA single-phase transformers, rated at 13.8 kV:66.4 kV, are to be connected in a three-phase bank. Each transformer has a series impedance of $0.004 + j0.18 \Omega$ referred to its 13.8-kV winding.

- (a) If the transformers are connected Y-Y, calculate (i) the voltage and power rating of the three-phase connection, (ii) the equivalent impedance as referred to its low-voltage terminals, and (iii) the equivalent impedance as referred to its high-voltage terminals.
- (b) Repeat part (a) if the transformer is connected Y on its low-voltage side and Δ on its high-voltage side.

2-21. Repeat Example 2-6 for a load drawing rated current from the transformers at unity power factor.

2-22. A three-phase Y- Δ transformer is rated 225 kV:24 kV, 400 MVA and has a series reactance of 13.3Ω as referred to its high-voltage terminals. The transformer is supplying a load of 325 MVA, with 0.9 power factor lag-

ging at a voltage of 24 kV (line to line) on its low-voltage side. It is supplied from a feeder whose impedance is $0.15 + j1.9 \Omega$ connected to its high-voltage terminals. For these conditions, calculate (a) the voltage at the high-voltage terminals of the transformer and (b) the voltage at the sending end of the feeder.

2-23. A Δ -Y-connected bank of three identical 100-kVA 2400:120-V 60-Hz transformers is supplied with power through a feeder whose impedance is $0.30 + j0.80 \Omega$ per phase. The voltage at the sending end of the feeder is held constant at 2400 V line to line. The results of a single-phase short-circuit test on one of the transformers with its low-voltage terminals short-circuited are

$$V_H = 57.5 \text{ V} \quad f = 60 \text{ Hz} \quad I_H = 41.6 \text{ A} \quad P = 875 \text{ W}$$

- (a) Determine the secondary line-to-line voltage when the bank delivers rated current to a balanced three-phase unity power factor load.
- (b) Compute the currents in the transformer primary and secondary windings and in the feeder wires if a solid three-phase short circuit occurs at the secondary line terminals.

2-24. A 15-kV:175-kV 125-MVA transformer has primary and secondary impedances of $0.012 + j0.06$ per unit each. The magnetizing impedance is $j135$ per unit. All quantities are in per unit on the transformer base. Calculate the primary and secondary resistances and inductances and the magnetizing inductance (referred to the low-voltage side) in ohms and henrys.

2-25. The nameplate on a 7.97-kV:480-V, 100-kVA single-phase transformer indicates that it has a series reactance of 14 percent (0.14 per unit).

- (a) Calculate the series reactance in ohms as referred to (i) the low-voltage terminal and (ii) the high-voltage terminal.
- (b) If three of these transformers are connected in a three-phase Y-Y connection, calculate (i) the transformer voltage and power rating, (ii) the per unit impedance of the transformer, and (iii) the series reactance in ohms as referred to the low-voltage terminal.

2-26. Consider the Y-Y connection of three single-phase transformers as described in Prob. 2-20.

- (a) Calculate the per unit impedance for this connection.
- (b) If the rated voltage is applied to the high-voltage terminals and the three low-voltage terminals are short-circuited, calculate the magnitude of the phase current in per unit and in amperes on (i) the high-voltage side and (ii) the low-voltage side.

2-27. A three-phase generator step-up transformer is rated 26 kV:345 kV, 1000 MVA and has a series impedance of $0.004 + j0.085$ per unit on this base. It is connected to a 26-kV 800-MVA generator, which can be represented as a voltage source in series with a reactance of $j1.65$ per unit on the generator base.

- (a) Convert the per unit generator reactance to the step-up transformer base.
- (b) The unit is supplying 500 MW, unity power factor, at 345 kV, to the system at the transformer terminals. Draw a phasor diagram for this condition, using the transformer high-side voltage as the reference phasor.
- (c) Calculate the transformer low-side voltage and the generator internal voltage behind its reactance in kilovolts for the conditions of part (b). Find the generator output power in megawatts and the power factor.

3

Electromechanical Energy Conversion Principles

We are concerned here with the electromechanical energy conversion process, which takes place through the medium of the electric or magnetic field of the conversion device. Although the various conversion devices operate on similar principles, their structures depend on their function. Devices for measurement and control are frequently referred to as *transducers*; they generally operate under linear input-output conditions and with relatively small signals. The many examples include microphones, pickups, and loudspeakers. A second category of devices encompasses force-producing devices and includes solenoids, relays, and electromagnets. The third category includes continuous energy conversion equipment such as motors and generators.

This chapter is devoted to the principles of electromechanical energy conversion and the analysis of the devices which accomplish this function. Emphasis is placed on the analysis of systems which use magnetic fields as

the conversion medium since the remaining chapters of the book deal with such devices. However, the analytical techniques for electric field systems are quite similar.

The purpose of this analysis is threefold: (1) to assist us in understanding how energy conversion takes place, (2) to provide us with the techniques for designing and optimizing the devices for specific requirements, and (3) to show how to develop models of electromechanical energy conversion devices that can be used in analyzing their performance as components in engineering systems. Transducers and force-producing devices are treated in this chapter; continuous energy conversion devices are treated in the rest of the book.

The concepts and techniques presented in this chapter are quite powerful and can be applied to a wide range of engineering situations involving electromechanical energy conversion. However, they are somewhat mathematical in nature, perhaps more so than the reader may find comfortable in an introduction to electric machinery. With this in mind, Arts. 3-1 and 3-2 present a quantitative discussion of the forces in electromechanical systems; the analytical details are developed in the remaining articles. Based on the techniques developed in this chapter, torque expressions are developed as needed throughout the book. Thus the reader may elect to omit the later sections of this chapter at the expense of accepting these expressions on faith when they are presented.

3-1 FORCES AND TORQUES IN MAGNETIC FIELD SYSTEMS

The Lorentz force law

$$\mathbf{F} = q(\mathbf{E} + \mathbf{v} \times \mathbf{B}) \quad (3-1)$$

gives the force \mathbf{F} on a particle of charge q in the presence of electric and magnetic fields. In SI units, \mathbf{F} is given in newtons, q in coulombs, \mathbf{E} in volts per meter, \mathbf{B} in teslas, and \mathbf{v} , which is the velocity of the particle relative to the magnetic field, in meters per second.

Thus in a pure electric field system, the force is determined simply by the charge on the particle and the electric field

$$\mathbf{F} = q\mathbf{E} \quad (3-2)$$

The force acts in the direction of the electric field and is independent of the particle motion.

In magnetic field systems, the situation is somewhat more complex. Here the force

$$\mathbf{F} = q(\mathbf{v} \times \mathbf{B}) \quad (3-3)$$

is determined by the magnitude of the charge on the particle and the magnitude of the \mathbf{B} field as well as the velocity of the particle. In fact, the direction of the force is always perpendicular to both the direction of particle motion and the magnetic field direction. Mathematically, this is given by the vector cross product $\mathbf{v} \times \mathbf{B}$ in Eq. 3-3. The magnitude of this cross product is equal to the product of the magnitudes of \mathbf{v} and \mathbf{B} and the sine of the angle between them; its direction can be found from the right-hand rule, which states that when the thumb of the right hand points in the direction of \mathbf{v} and the index finger points in the direction of \mathbf{B} , the force points in the direction normal to the palm of the hand, as shown in Fig. 3-1.

For situations where large numbers of charged particles are in motion, it is convenient to rewrite Eq. 3-3 in terms of the current density \mathbf{J} , in which case the force is a force density

$$\mathbf{F} = \mathbf{J} \times \mathbf{B} \quad \text{N/m}^3 \quad (3-4)$$

For currents flowing in conducting media, Eq. 3-4 can be used to find the force density acting on the material itself. A considerable amount of physics is hidden in this result since the mechanism by which the force is transferred from the moving charges to the conducting medium is a complex one.

EXAMPLE 3-1

A nonmagnetic rotor containing a single-turn coil is placed in a uniform magnetic field of magnitude B_0 , as shown in Fig. 3-2. The coil sides are at radius R , and the wire carries current I as indicated. Find the θ -directed torque as a function of rotor position α when $I = 10$ A, $B_0 = 0.5$ T, and $R = 0.1$ m. Assume that the rotor is 0.6 m long.

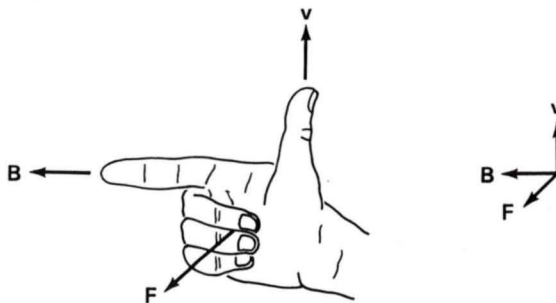


Fig. 3-1. Right-hand rule for determining the direction of the Lorentz force $\mathbf{F} = q\mathbf{v} \times \mathbf{B}$.

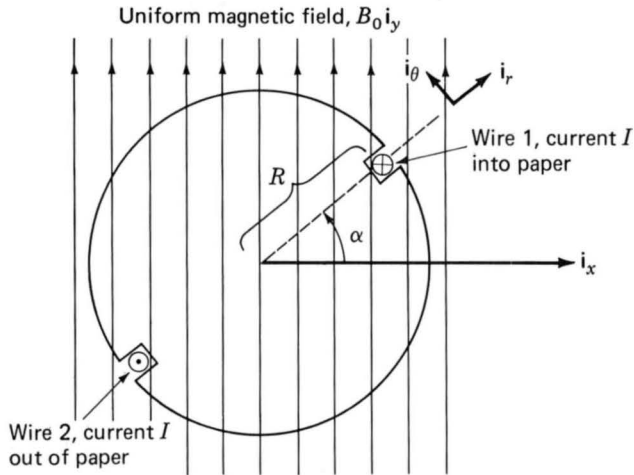


Fig. 3-2. Single-coil rotor for Example 3-1.

Solution

The force per unit length on a wire carrying current I can be found by multiplying Eq. 3-4 by the cross-sectional area of the wire. When we recognize that the product of the cross-sectional area and the current density is simply the current I , the force per unit length acting on the wire is given by

$$\mathbf{F} = \mathbf{I} \times \mathbf{B}$$

Thus, for wire 1 carrying current I into the paper, the θ -directed force is given by

$$F_{1\theta} = -IB_0 l \sin \alpha$$

and for wire 2 (which carries current in the opposite direction and is located 180° away from wire 1)

$$F_{2\theta} = -IB_0 l \sin \alpha$$

where l is the length of the rotor. The torque T acting on the rotor is given by the sum of the force–moment–arm products for each wire

$$T = 2IB_0 R l \sin \alpha = 2(10)(0.5)(0.1)(0.6)(\sin \alpha) = 0.6 \sin \alpha \quad \text{N} \cdot \text{m}$$

For situations in which the forces act only on current-carrying elements and which are of simple geometry, Eq. 3-4 is generally the simplest

and easiest way to calculate the forces acting on the system. Very few practical situations fall into this class, however. In fact, as discussed in Chap. 1, most electromechanical energy conversion devices contain magnetic material; in these systems, forces act directly on the magnetic material and clearly cannot be calculated from Eq. 3-4.

Techniques for calculating the detailed, localized forces acting on magnetic materials are extremely complex and require detailed knowledge of the field distribution throughout the structure. Fortunately, most electromechanical energy conversion devices are constructed of rigid, nondeforming structures. In these devices, it is the net force or torque that is of importance, and the details of the localized force distribution are of secondary interest. For example, in a properly designed motor, the net accelerating torque acting on the rotor determines the motor's characteristics; accompanying forces, which act to squash or make the solid rotor oval, play no significant role and generally are not even calculated.

To understand the behavior of rotating machinery, a simple physical picture is quite useful. Associated with the rotor structure is a magnetic field, and similarly with the stator; one can picture them as a set of north and south magnetic poles associated with each structure. Just as a compass needle tries to align with the earth's magnetic field, these two sets of fields attempt to align, and torque is associated with their displacement from alignment. Thus in a motor, the stator magnetic field rotates ahead of that of the rotor, pulling on it and performing work. The opposite is true for a generator; here the rotor does the work on the stator.

Various techniques have evolved to calculate the net forces of concern in electromechanical energy conversion. The technique developed in this chapter and used throughout the book is known as the *energy method* and is based on the principle of *conservation of energy*. The basis for this method can be understood with reference to Fig. 3-3a, where a magnetic field-based electromechanical energy conversion device is indicated schematically as a lossless magnetic energy storage system with two terminals. The electric terminal has the terminal variables voltage e and current i , and the mechanical terminal has the terminal variables force f_{fld} and position x . This sort of representation is valid in situations where the loss mechanism can be separated from the energy storage mechanism. In these cases the electrical losses, such as ohmic losses, can be included as external elements connected to the electric terminals, and the mechanical losses, such as friction, can be included external to the mechanical terminals. Figure 3-3b shows an example of such a system; a simple force-producing device with a single coil forming the electric terminal, and a movable plunger serving as the mechanical terminal.

The interaction between the electric and mechanical terminals, i.e., the electromechanical energy conversion, occurs through the medium of the magnetic stored energy. Since the energy storage system is lossless, it is a simple matter to write that the time rate of change of W_{fld} , the stored

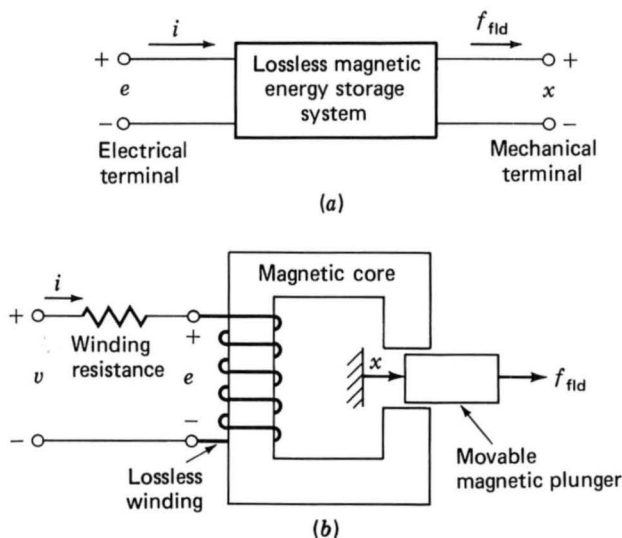


Fig. 3-3. (a) Schematic magnetic-field electromechanical energy conversion device; (b) simple force-producing device.

energy in the magnetic field, is equal to the electric power input less the mechanical power output of the energy storage system:

$$\frac{dW_{fld}}{dt} = ei - f_{fld} \frac{dx}{dt} \quad (3-5)$$

Using Eq. 1-21 and multiplying Eq. 3-5 by dt , we get

$$dW_{fld} = i d\lambda - f_{fld} dx \quad (3-6)$$

As shown in Art. 3-4, Eq. 3-6 permits us to solve for the force simply as a function of the flux λ and the mechanical terminal position x . This result comes about as a consequence of our ability to separate the losses out of the physical problem, resulting in a lossless energy storage system, as in Fig. 3-3a.

Equations 3-5 and 3-6 form the basis for the energy method. This technique is quite powerful in its ability to calculate forces and torques in complex situations of electromechanical energy conversion systems. The reader should recognize that this power comes at the expense of a detailed picture of the force-producing mechanism. The forces themselves are produced by such well-known physical phenomena as the Lorentz force on current-carrying elements, described by Eq. 3-4, or the interaction of the magnetic fields with the dipoles in the magnetic material.

3-2 ENERGY BALANCE

The principle of conservation of energy states that energy is neither created nor destroyed; it is merely changed in form. For example, a golf ball leaves the tee with a certain amount of kinetic energy; this energy is eventually dissipated as heat due to air friction or rolling friction by the time the ball comes to rest on the fairway. Similarly, the kinetic energy of a hammer is eventually dissipated as heat as a nail is driven into a piece of wood. For isolated systems with clearly identifiable boundaries, this fact permits us to keep track of energy in a simple fashion: the net flow of energy into the system across its boundary is equal to the time rate of change of energy stored in the system.

Although this result, which is a statement of the first law of thermodynamics, is quite general, we apply it in this chapter to electromechanical systems whose predominant energy storage mechanism is in magnetic fields. In such systems, one can account for energy transfer as

$$\left(\begin{array}{c} \text{Energy input} \\ \text{from electric} \\ \text{sources} \end{array} \right) = \left(\begin{array}{c} \text{mechanical} \\ \text{energy} \\ \text{output} \end{array} \right) + \left(\begin{array}{c} \text{increase in energy} \\ \text{stored in} \\ \text{magnetic field} \end{array} \right) + \left(\begin{array}{c} \text{energy} \\ \text{converted} \\ \text{into heat} \end{array} \right) \quad (3-7)$$

Equation 3-7 is written so that the electric and mechanical energy terms have positive values for motor action. The equation applies equally well to generator action: these terms then simply have negative values.

In these systems the conversion of energy into heat occurs by such mechanisms as ohmic heating due to current flow in the windings of the electric terminals and mechanical friction due to the motion of the system components forming the mechanical terminals. As discussed in Art. 3-1, it is generally possible to mathematically separate these loss mechanisms from the energy storage mechanism. In this case, the device can be represented as a lossless magnetic energy storage system with electric and mechanical terminals, as shown in Fig. 3-4. The loss mechanisms can then be represented by external elements connected to these terminals, resistances to the electric terminals, and mechanical dashpots to the mechanical ter-

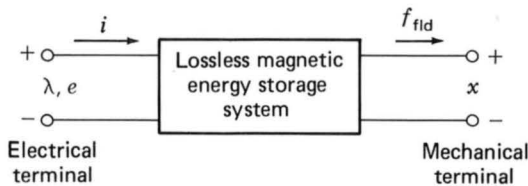


Fig. 3-4. Lossless magnetic energy storage system with electric and mechanical terminals.

minals. Figure 3-4 is quite general in the sense that there is no limit to the number of electric or mechanical terminals. For this type of system, the magnetic field serves as the coupling medium between the electric and mechanical terminals.

The ability to identify a lossless energy storage system is the essence of the energy method. It is important to recognize that this is done mathematically as part of the modeling process. It is not possible, of course, to take the resistance out of windings or the friction out of bearings. Instead we are making use of the fact that a model in which this is done is a valid representation of the physical system.

For the lossless magnetic energy storage system of Fig. 3-4, Eq. 3-7 becomes

$$dW_{\text{elec}} = dW_{\text{mech}} + dW_{\text{fld}} \quad (3-8)$$

where dW_{elec} = differential electric energy input

dW_{mech} = differential mechanical energy output

dW_{fld} = differential change in magnetic stored energy

In time dt , from Eq. 1-36,

$$dW_{\text{elec}} = ei dt \quad (3-9)$$

Here e is the voltage induced in the electric terminals by the changing magnetic stored energy. It is through this reaction voltage that the external electric circuit supplies power to the coupling magnetic field and hence to the mechanical output terminals. Thus the basic energy conversion process is one involving the coupling field and its action and reaction on the electric and mechanical systems.

Combining Eqs. 3-8 and 3-9 results in

$$dW_{\text{elec}} = ei dt = dW_{\text{mech}} + dW_{\text{fld}} \quad (3-10)$$

Equation 3-10, together with Faraday's law for induced voltage, Eq. 1-21, forms the basis for the energy method; the following sections illustrate its use in the analysis of electromagnetic energy conversion devices.

3-3 ENERGY AND FORCE IN SINGLY EXCITED MAGNETIC FIELD SYSTEMS

In Chaps. 1 and 2 we were concerned primarily with the closed-core magnetic circuits used for transformers. Energy in those devices is stored in the leakage fields and to some extent in the core itself; the stored energy does not enter directly into the transformation process. In this chapter we are dealing with energy conversion; the magnetic circuits have air gaps be-

tween the stationary and moving members in which considerable energy is stored in the magnetic field. This field acts as the energy conversion medium, and its energy is the reservoir between the electric and mechanical systems.

Consider the electromagnetic relay shown schematically in Fig. 3-5. The resistance of the excitation coil is shown as an external resistance R , and the mechanical terminal variables are shown as a force f_{fld} produced by the magnetic field directed from the relay to the external mechanical system and a displacement x ; mechanical losses can be included as external elements connected to the mechanical terminal. Similarly, the moving armature is shown as being massless; its mass represents mechanical energy storage and can be included as an external mass connected to the mechanical terminal. As a result, the magnetic core and armature constitute a lossless magnetic energy system, as in Fig. 3-4.

This relay structure is essentially the same as the magnetic structures analyzed in Chap. 1. From Faraday's law (Eq. 1-21) we can solve for the induced voltage e in terms of the flux linkages λ

$$e = \frac{d\lambda}{dt} \quad (3-11)$$

and thus from Eq. 3-9

$$dW_{elec} = i d\lambda \quad (3-12)$$

In Chap. 1 we saw that the magnetic circuit of Fig. 3-5 can be described by an inductance L , which is a function of the geometry of the magnetic structure and the permeability of the magnetic material. Electromagnetic energy conversion devices contain air gaps in their magnetic circuits to separate the moving parts. As discussed in Art. 1-1, in most such cases the

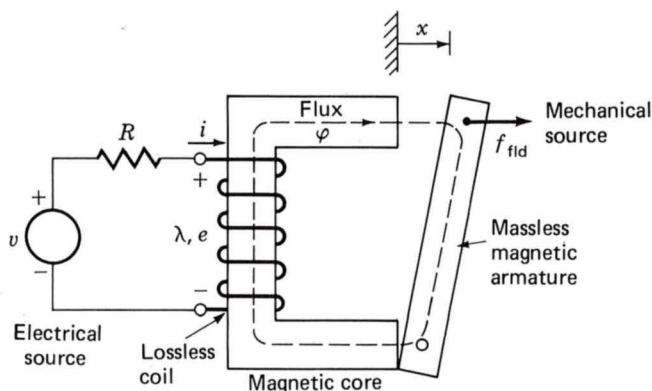


Fig. 3-5. Schematic of an electromagnetic relay.

reluctance of the air gap is much larger than that of the magnetic material. Thus the predominant energy storage occurs in the air gap, and the properties of the magnetic circuit are determined by the dimensions of the air gap.

Because of the simplicity of the resulting relations, magnetic nonlinearity and core losses are often neglected in the analysis of practical devices. The final results of such approximate analyses can, if necessary, be corrected for the effects of these neglected factors by semiempirical methods. Consequently, analyses are carried out under the assumption that the flux and mmf are directly proportional, as in air, for the entire magnetic circuit. Thus the flux linkages λ and current i are considered to be linearly related by a factor which depends solely on the geometry and hence on the armature position x

$$\lambda = L(x)i \quad (3-13)$$

where the explicit dependence of L on x has been indicated.

Since the magnetic force f_{fld} has been defined as acting from the relay upon the external mechanical system and dW_{mech} is defined as the mechanical energy output of the relay, we can write

$$dW_{mech} = f_{fld} dx \quad (3-14)$$

Thus, using Eqs. 3-12 and 3-14, we can write Eq. 3-8 as

$$dW_{fld} = i d\lambda - f_{fld} dx \quad (3-15)$$

Since our magnetic energy storage system is lossless, it is a *conservative system* and the value of W_{fld} is uniquely specified by the values of λ and x . Thus, W_{fld} is the same regardless of how λ and x are brought to their final values. Consider Fig. 3-6, in which two separate paths are shown over

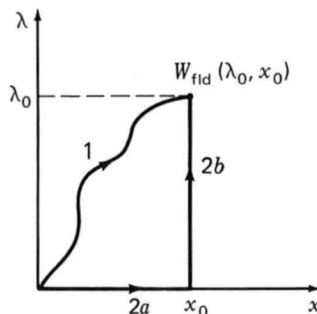


Fig. 3-6. Integration paths for W_{fld} .

which Eq. 3-15 can be integrated to find W_{fld} at the point (λ_0, x_0) . Path 1 is the general case and is difficult to integrate unless both i and f_{fld} are known explicitly as a function of λ and x . However, path 2 gives the same result and is much easier to integrate. From Eq. 3-15

$$W_{fld}(\lambda_0, x_0) = \int_{\text{path } 2a} dW_{fld} + \int_{\text{path } 2b} dW_{fld} \quad (3-16)$$

Notice that on path 2a, $d\lambda = 0$ and $f_{fld} = 0$ since $\lambda = 0$, i.e., there can be no magnetic force in the absence of magnetic fields. Thus from Eq. 3-15, $dW_{fld} = 0$ on path 2a. On path 2b, $dx = 0$, and thus, from Eq. 3-15, Eq. 3-16 reduces to

$$W_{fld}(\lambda_0, x_0) = \int_0^{\lambda_0} i(\lambda, x_0) d\lambda \quad (3-17)$$

For a linear system in which λ is proportional to i , as in Eq. 3-13, Eq. 3-17 gives

$$W_{fld}(\lambda_0, x_0) = \int_0^{\lambda_0} i(\lambda, x_0) d\lambda = \int_0^{\lambda_0} \frac{\lambda}{L(x_0)} d\lambda = \frac{1}{2} \frac{\lambda_0^2}{L(x_0)} \quad (3-18)$$

The energy can also be expressed in terms of the energy density of the magnetic field integrated over the volume V of the magnetic field. In this case

$$W_{fld} = \int_V \left(\int_0^{B_0} \mathbf{H} \cdot d\mathbf{B} \right) dV \quad (3-19)$$

For a magnetic medium with constant permeability ($\mathbf{B} = \mu\mathbf{H}$), this reduces to

$$W_{fld} = \int_V \left(\frac{1}{2} \frac{B^2}{\mu} \right) dV \quad (3-20)$$

EXAMPLE 3-2

The relay shown in Fig. 3-7a is made from infinitely permeable magnetic material with a movable plunger, also of infinitely permeable material. The height of the plunger is much greater than the air-gap length ($h \gg g$). Calculate the magnetic stored energy W_{fld} as a function of plunger position ($0 < x < d$) for $N = 1000$ turns, $g = 0.002$ m, $d = 0.15$ m, $l = 0.1$ m, and $i = 10$ A.

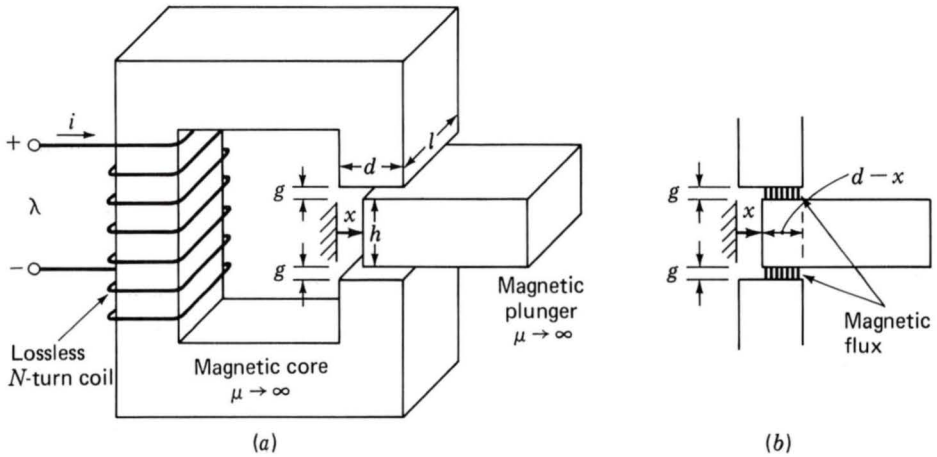


Fig. 3-7. (a) Relay with movable plunger; (b) detail showing air-gap configuration with the plunger partially removed.

Solution

Equation 3-18 can be used to solve for W_{fld} when λ is known. For this situation, i is held constant, and thus it would be useful to have an expression for W_{fld} as a function of i and x . This can be obtained quite simply by substituting Eq. 3-13 into Eq. 3-18

$$W_{fld} = \frac{1}{2} L(x) i^2$$

The inductance is given by (see Example 1-3)

$$L(x) = \frac{N^2 \mu_0 A_{gap}}{2g}$$

where A_{gap} is the gap cross-sectional area. From Fig. 3-7b it can be seen to be

$$A_{gap} = l(d - x) = ld \left(1 - \frac{x}{d} \right)$$

Thus

$$L(x) = \frac{N^2 \mu_0 ld (1 - x/d)}{2g}$$

and

$$\begin{aligned} W_{fld} &= \frac{1}{2} \frac{N^2 \mu_0 ld (1 - x/d)}{2g} i^2 \\ &= \frac{1}{2} \frac{(1000^2) (4\pi \times 10^{-7}) (0.15) (0.1)}{2(0.002)} \times 10^2 \left(1 - \frac{x}{d} \right) \\ &= 236 \left(1 - \frac{x}{d} \right) \quad \text{J} \end{aligned}$$

In this article we have seen the relationship between the magnetic stored energy and the electric and mechanical terminal variables for a system which can be represented in terms of a lossless magnetic energy storage element. If we had chosen for our example a device with a rotating mechanical terminal instead of a linearly displacing one, the results would have been identical except that force should be replaced by torque and linear displacement by angular displacement. In the next article we see how knowledge of the magnetic stored energy permits us to solve for the mechanical force.

3-4 DETERMINATION OF MAGNETIC FORCE; COENERGY

As discussed in the previous article, the magnetic stored energy W_{fld} is determined uniquely by λ and x . The lossless magnetic energy storage system is a conservative system, and W_{fld} is a *state function*, determined uniquely by the values of the independent *state variables* λ and x . This can be shown explicitly by writing Eq. 3-15 in the form

$$dW_{fld}(\lambda, x) = i d\lambda - f_{fld} dx \quad (3-21)$$

For any function $F(x_1, x_2)$, the total differential of F with respect to the two independent state variables x_1 and x_2 can be written

$$dF(x_1, x_2) = \frac{\partial F}{\partial x_1} dx_1 + \frac{\partial F}{\partial x_2} dx_2 \quad (3-22)$$

It is extremely important to recognize that the partial derivatives in Eq. 3-22 are each taken by holding the opposite state variable constant.

Since Eq. 3-22 is valid for any state function F , it is certainly valid for W_{fld} ; thus

$$dW_{fld}(\lambda, x) = \frac{\partial W_{fld}}{\partial \lambda} d\lambda + \frac{\partial W_{fld}}{\partial x} dx \quad (3-23)$$

Since λ and x are independent variables, Eqs. 3-21 and 3-23 must be equal for all values of $d\lambda$ and dx , and so

$$i = \frac{\partial W_{fld}(\lambda, x)}{\partial \lambda} \quad (3-24)$$

where the partial derivative is taken while holding x constant and

$$f_{fld} = - \frac{\partial W_{fld}(\lambda, x)}{\partial x} \quad (3-25)$$

in this case holding λ constant while taking the partial derivative.

This is the result we have been seeking. Once we know W_{fld} as a function of λ and x , Eq. 3-24 can be used to solve for $i(\lambda, x)$. More importantly, Eq. 3-25 can be used to solve for the mechanical force $f_{\text{fld}}(\lambda, x)$. It cannot be overemphasized that the partial derivative of Eq. 3-25 is taken while holding the flux linkages λ constant. This is easily done provided W_{fld} is known as a function of λ and x . This is purely a mathematical requirement and has nothing to do with whether λ is held fixed in the actual device.

The force f_{fld} is determined from Eq. 3-25 directly in terms of the electrical state variable λ . If we then want to express the force as a function of i , we can do so by substituting the appropriate expression for λ as a function of i into the expression for f_{fld} that is obtained by using Eq. 3-25. Alternatively, one can use a state function other than energy, namely, the coenergy, to obtain the force directly as a function of the current. The selection of the state function is purely a matter of convenience; they both give the same result, but one or the other may be simpler analytically, depending on the desired result and the initial description of the system being analyzed.

The *coenergy* W'_{fld} is defined as a function of i and x such that

$$W'_{\text{fld}}(i, x) = i\lambda - W_{\text{fld}}(\lambda, x) \quad (3-26)$$

and the desired result can be obtained from the energy expression of Eq. 3-21. The transformation is carried out by using the differential of $i\lambda$

$$d(i\lambda) = i d\lambda + \lambda di \quad (3-27)$$

and the differential of $dW_{\text{fld}}(\lambda, x)$ from Eq. 3-21. From Eq. 3-26

$$dW'_{\text{fld}}(i, x) = d(i\lambda) - dW_{\text{fld}}(\lambda, x) \quad (3-28)$$

Substitution of Eqs. 3-21 and 3-27 into Eq. 3-28 results in

$$dW'_{\text{fld}}(i, x) = \lambda di + f_{\text{fld}} dx \quad (3-29)$$

Coenergy $W'_{\text{fld}}(i, x)$ is a state function of the two independent variables i and x . Thus, its differential can be expressed as

$$dW'(i, x) = \frac{\partial W'_{\text{fld}}}{\partial i} di + \frac{\partial W'_{\text{fld}}}{\partial x} dx \quad (3-30)$$

Equations 3-29 and 3-30 must be equal for all values of di and dx ; thus

$$\lambda = \frac{\partial W'_{\text{fld}}(i, x)}{\partial i} \quad (3-31)$$

$$f_{\text{fld}} = \frac{\partial W'_{\text{fld}}(i, x)}{\partial x} \quad (3-32)$$

Equation 3-32 gives the mechanical force directly in terms of i and x . The reader is cautioned that the partial derivative in Eq. 3-32 is taken while holding i constant; thus W'_{fld} must be known as a function of i and x . Equations 3-25 and 3-32 are equivalent and can both be used to calculate the force for a given system; user preference and convenience often dictate the choice. For a system with a rotating mechanical terminal, similar expressions for the mechanical torque are derived, and the partial derivatives are taken with respect to the angular displacement.

By arguments directly analogous to those leading to Eq. 3-17, the coenergy for any given values of i and x can be found

$$W'_{\text{fld}}(i_0, x_0) = \int_0^{i_0} \lambda(i, x_0) di \quad (3-33)$$

For a linear system in which λ and i are proportional and which can be described by a position-dependent inductance, as in Eq. 3-13, the coenergy is

$$W'_{\text{fld}}(i, x) = \int_0^i L(x)i' di' = \frac{1}{2}L(x)i^2 \quad (3-34)$$

By analogy with Eq. 3-19, the coenergy can be expressed in field terms as

$$W'_{\text{fld}} = \int_V \left(\int_0^{H_0} \mathbf{B} \cdot d\mathbf{H} \right) dV \quad (3-35)$$

For a medium with constant permeability μ , this reduces to

$$W'_{\text{fld}} = \int_V \frac{1}{2} \mu H^2 dV \quad (3-36)$$

In some cases, magnetic circuit representations may be difficult to realize or may not yield solutions of the desired accuracy. Often such situations are characterized by complex geometries and/or magnetic materials driven deeply into saturation. In such situations, numerical techniques can be used to evaluate the coenergy of Eq. 3-35.

One such technique, known as the *finite-element method*,[†] has become widely accepted. By using this method, the force expression of Eq. 3-32 can be evaluated by numerically calculating the coenergy of Eq. 3-35 at constant current for differing values of the displacement x . The derivative of Eq. 3-32 can then be calculated numerically.

[†]See, for example, P. P. Sylvester and R. L. Ferrari, *Finite Elements for Electrical Engineers*, Cambridge University Press, New York, 1983.

EXAMPLE 3-3

For the relay of Example 3-2, find the force on the plunger as a function of x when the coil current is held constant at 10 A. Use both the energy and coenergy expressions.

Solution

From Example 3-2

$$L(x) = \frac{N^2 \mu_0 l d (1 - x/d)}{2g}$$

The energy, expressed as a function of λ and x , is, from Eq. 3-18,

$$W_{\text{fld}} = \frac{1}{2} \frac{\lambda^2}{L(x)} = \frac{g \lambda^2}{N^2 \mu_0 l d (1 - x/d)}$$

and from Eq. 3-25

$$f_{\text{fld}} = -\frac{\partial W_{\text{fld}}}{\partial x} = -\frac{g \lambda^2}{N^2 \mu_0 l d^2 (1 - x/d)^2}$$

This can now be expressed in terms of i by using Eq. 3-13

$$f_{\text{fld}} = -\frac{g L^2(x) i^2}{N^2 \mu_0 l d^2 (1 - x/d)^2} = -\frac{N^2 \mu_0 l}{4g} i^2$$

and we see that for constant current the force is independent of the plunger position and acts to pull the plunger back into the relay.

Alternately, the force can be found from the coenergy. From Eq. 3-34

$$W'_{\text{fld}} = \frac{1}{2} L(x) i^2 = \frac{N^2 \mu_0 l d (1 - x/d)}{4g} i^2$$

and from Eq. 3-32

$$f_{\text{fld}} = \frac{\partial W'_{\text{fld}}}{\partial x} = -\frac{N^2 \mu_0 l}{4g} i^2$$

Notice that this gives the same answer, but because of the form of the inductance expression and specifically because we want a solution in terms of current, the choice of coenergy yielded a much simpler solution. Notice also that if one attempts to substitute $\lambda = L(x)i$ in the expression for W'_{fld} before the derivative is taken, one gets the wrong answer (by a minus

sign). This is because it is λ and not i that must be held constant when the partial derivative of Eq. 3-25 is taken.

Finally, for $i = 10$ A

$$f_{fld} = -\frac{N^2 \mu_0 l}{4g} i^2 = -\frac{(1000^2)(4\pi \times 10^{-7})(0.1)(10^2)}{4(0.002)} = -1570 \text{ N}$$

For a linear system, the energy and coenergy are numerically equal; for example, $\frac{1}{2} Li^2 = \frac{1}{2} \lambda^2 / L$ or $\frac{1}{2} \mu H^2 = \frac{1}{2} B^2 / \mu$. For a nonlinear system in which λ and i or B and H are not linearly proportional, the two functions are not even numerically equal. A graphical interpretation of the energy and coenergy for a nonlinear system is shown in Fig. 3-8. The area between the λ - i curve and the vertical axis given by the integral of $i d\lambda$ is the energy. The area to the horizontal axis given by the integral of λdi is the coenergy. The sum for the singly excited system is, by definition,

$$W_{fld} + W'_{fld} = \lambda i \quad (3-37)$$

The force of the field in the device of Fig. 3-5 for some particular value of x and i or λ must be independent of whether it is calculated from the energy or coenergy. A graphical illustration will demonstrate this point. Assume that the armature is at position x so that the device is operating at point a in Fig. 3-9a. The partial derivative of Eq. 3-25 can be interpreted as the limit of $-\Delta W_{fld} / \Delta x$ with λ constant as $\Delta x \rightarrow 0$. If we allow a change Δx , the change $-\Delta W_{fld}$ is shown by the shaded area in Fig. 3-9a. Hence, the force $f_{fld} = (\text{shaded area}) / \Delta x$ as $\Delta x \rightarrow 0$. On the other hand, the partial derivative of Eq. 3-32 can be interpreted as the limit of $\Delta W'_{fld} / \Delta x$ with i constant as $\Delta x \rightarrow 0$. This perturbation of the device is shown in Fig. 3-9b; the force $f_{fld} = (\text{shaded area}) / \Delta x$ as $\Delta x \rightarrow 0$. The shaded areas differ only by the small triangle abc of sides Δi and $\Delta \lambda$, so that in the limit the shaded

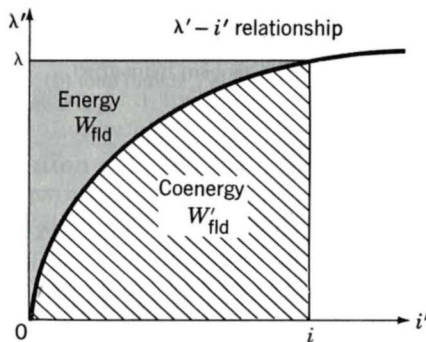


Fig. 3-8. Graphical interpretation of energy and coenergy in a singly excited system.

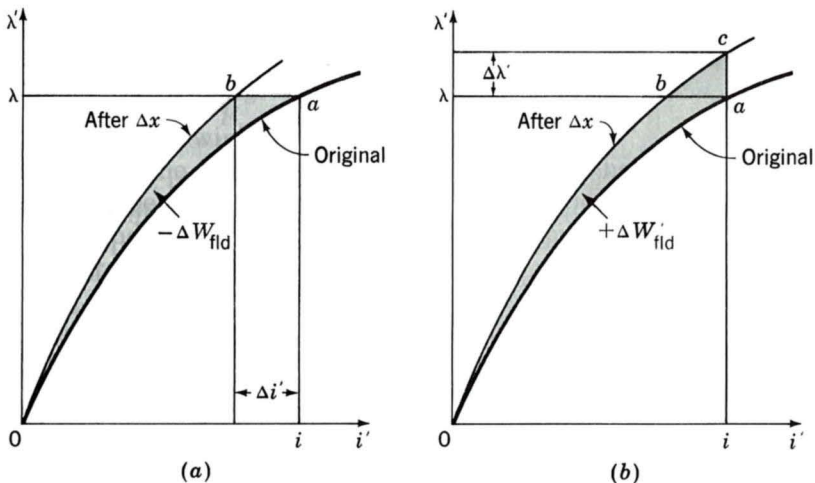


Fig. 3-9. Effect of Δx on the energy and coenergy of a singly excited device: (a) change of energy with λ held constant; (b) change of coenergy with i held constant.

areas resulting from Δx at constant λ or at constant i are equal. Thus the force of the field is independent of whether the determination is made with energy or coenergy.

Equations 3-25 and 3-32 express the mechanical force of electrical origin in terms of partial derivatives of the energy and coenergy functions $W_{fld}(\lambda, x)$ and $W'_{fld}(i, x)$. It is important to note two things about them: the variables in terms of which they must be expressed and their algebraic signs. Physically, of course, the force depends on the dimension x and the magnetic field. The field can be specified in terms of flux linkage λ , or current i , or related variables. As seen in Example 3-3, the selection of the energy or coenergy function as a basis for analysis is a matter of convenience; the choice depends on the initial description of the system and the desired variables in the result.

The algebraic signs in Eqs. 3-25 and 3-32 show that the force acts in a direction to decrease the magnetic field stored energy at constant flux or to increase the coenergy at constant current. In a singly excited device, the force acts to increase the inductance by pulling on members so as to reduce the reluctance of the magnetic path linking the winding.

EXAMPLE 3-4

The magnetic circuit shown in Fig. 3-10 is made of cast steel. The rotor is free to turn about a vertical axis. The dimensions are shown in the figure.

(a) Derive an expression in SI units for the torque acting on the rotor in terms of the dimensions and the magnetic field in the two air gaps. Neglect the effects of fringing.

(b) The maximum flux density in the overlapping portions of the air gaps is limited to approximately 130 kilolines/in², because of saturation in the steel. Compute the maximum torque in inch-pounds for $r_1 = 1.00$ in, $h = 1.00$ in, and $g = 0.10$ in.

Solution

The torque T can be obtained from the derivative of the coenergy with respect to angle θ , as discussed following Eq. 3-32.

(a) The air-gap field intensity H_{ag} will be used as the independent variable because it is related to the terminal variable i by a constant; that is, $Ni = 2gH_{ag}$. The coenergy density is $\mu_0 H_{ag}^2/2$ (Eq. 3-36), and the volume of the two overlapping air gaps is $2gh(r_1 + 0.5g)\theta$. Consequently, the coenergy is

$$W'_{ag} = \mu_0 H_{ag}^2 gh(r_1 + 0.5g)\theta$$

and

$$T_{fld} = \frac{\partial W'_{ag}(H_{ag}, \theta)}{\partial \theta} = \mu_0 H_{ag}^2 gh(r_1 + 0.5g) = \frac{B_{ag}^2 gh(r_1 + 0.5g)}{\mu_0}$$

The torque acts in a direction to align the rotor with the stator pole faces.

(b) Convert the flux density and dimensions to SI units.

$$B_{ag} = \frac{130,000}{6.45} \times 10^4 \times 10^{-8} = 2.02 \text{ T}$$

$$g = 0.1(2.54 \times 10^{-2}) = 0.00254 \text{ m}$$

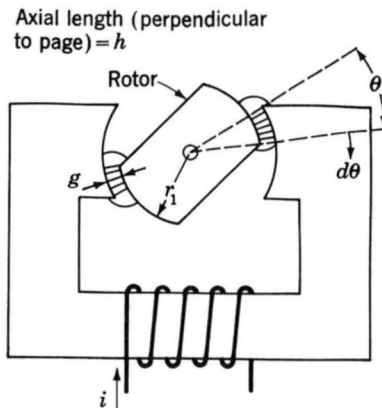


Fig. 3-10. Magnetic system of Example 3-4.

$$h = r_1 = 1.00(2.54 \times 10^{-2}) = 0.0254 \text{ m}$$

$$\mu_0 = 4\pi \times 10^{-7}$$

Substitution of these numerical values gives

$$T = 5.56 \text{ N} \cdot \text{m}$$

$$= 5.56(0.738)(12) = 49.3 \text{ in} \cdot \text{lb}$$

Moving-iron devices are used in a wide variety of applications for producing mechanical force or torque. Some of them, such as lifting magnets and magnetic chucks, are required merely to hold a piece of ferromagnetic material. Others, such as iron-core solenoids, relays, and contactors, are required to exert a force through a specified distance. Still others, such as iron-vane instruments, are required to produce a rotational torque against a restraining spring so that the deflection of a pointer is indicative of the steady-state value of the current or voltage of the circuit to which they are connected. With others, such as moving-iron telephone receivers and the electromagnets used for controlling the operation of hydraulic motors in servomechanisms, the force or torque should be very nearly proportional to an electric signal, and the dynamic response should be as rapid as possible. The dynamics of electromagnetically coupled systems are discussed in Art. 3-6.

3-5 MULTIPLY EXCITED MAGNETIC FIELD SYSTEMS

Many electromechanical devices have multiple sets of electric terminals. In measurement systems it is often desirable to obtain torques proportional to two electric signals; power as the product of voltage and current is a common example. Similarly, most electromechanical energy conversion devices consist of multiply excited magnetic field systems.

Analysis of these systems follows directly from the techniques discussed in previous articles. This article illustrates these techniques based on a system with two electric terminals. The model of a simple system with two sets of electric terminals and one mechanical terminal is shown in Fig. 3-11; in this case there is a rotating mechanical terminal with terminal variables of torque T_{fld} and angular displacement θ . Since there are three terminals, the system must be described in terms of three independent variables; these can be the mechanical angle θ along with the flux linkages λ_1 and λ_2 , currents i_1 and i_2 , or a hybrid set including one current and one flux.[†]

[†]See, for example, H. H. Woodson and J. R. Melcher, *Electromechanical Dynamics*, Wiley, New York, 1968, pt. I, chap. 3.

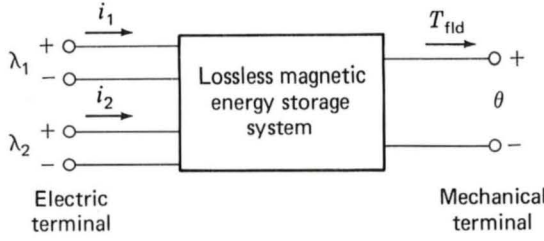


Fig. 3-11. Multiply excited magnetic energy storage system.

When the fluxes are used, the differential energy function $dW_{\text{fld}}(\lambda_1, \lambda_2, \theta)$ corresponding to Eq. 3-21 is

$$dW_{\text{fld}}(\lambda_1, \lambda_2, \theta) = i_1 d\lambda_1 + i_2 d\lambda_2 - T_{\text{fld}} d\theta \quad (3-38)$$

and in direct analog to Eqs. 3-24 and 3-25

$$i_1 = \frac{\partial W_{\text{fld}}(\lambda_1, \lambda_2, \theta)}{\partial \lambda_1} \quad (3-39)$$

$$i_2 = \frac{\partial W_{\text{fld}}(\lambda_1, \lambda_2, \theta)}{\partial \lambda_2} \quad (3-40)$$

and

$$T_{\text{fld}} = - \frac{\partial W_{\text{fld}}(\lambda_1, \lambda_2, \theta)}{\partial \theta} \quad (3-41)$$

The energy W_{fld} can be found by integrating Eq. 3-38. As in the singly excited case, this is most conveniently done by holding λ_1 and λ_2 fixed at zero and integrating first over θ ; T_{fld} is zero, and thus this integral is zero. One can then integrate over λ_2 (while holding λ_1 zero) and finally over λ_1 . Thus

$$\begin{aligned} W_{\text{fld}}(\lambda_{10}, \lambda_{20}, \theta_0) &= \int_0^{\lambda_{20}} i_2(\lambda_1 = 0, \lambda_2 = \lambda_2, \theta = \theta_0) d\lambda_2 \\ &\quad + \int_0^{\lambda_{10}} i_1(\lambda_1 = \lambda_1, \lambda_2 = \lambda_{20}, \theta = \theta_0) d\lambda_1 \end{aligned} \quad (3-42)$$

The path of integration is illustrated in Fig. 3-12 and is directly analogous to that of Fig. 3-6. One could, of course, interchange the order of integration for λ_2 and λ_1 . It is extremely important to recognize, however, that the state variables are integrated over a specific path and that, for example, λ_1 is maintained at zero while integrating over λ_2 in Eq. 3-42. This is explicitly indicated in Eq. 3-42 and can also be seen from Fig. 3-12. Failure to observe this fact is one of the most common errors made in analyzing these systems.

In a linear system, the relationships between λ and i are specified in terms of inductances

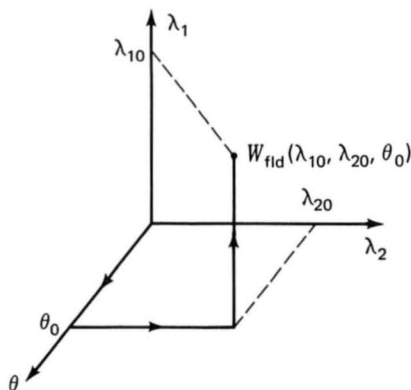


Fig. 3-12. Integration path to obtain $W_{fld}(\lambda_{10}, \lambda_{20}, \theta_0)$.

$$\lambda_1 = L_{11}i_1 + L_{12}i_2 \quad (3-43)$$

$$\lambda_2 = L_{21}i_1 + L_{22}i_2 \quad (3-44)$$

where

$$L_{12} = L_{21} \quad (3-45)$$

Here the inductances are, in general, functions of angular position θ . These equations can be inverted to obtain expressions for the i 's as a function of the θ 's:

$$i_1 = \frac{L_{22}\lambda_1 - L_{12}\lambda_2}{D} \quad (3-46)$$

$$i_2 = \frac{-L_{21}\lambda_1 + L_{11}\lambda_2}{D} \quad (3-47)$$

where

$$D = L_{11}L_{22} - L_{12}L_{21} \quad (3-48)$$

The energy can be found from Eq. 3-42:

$$\begin{aligned} W_{fld}(\lambda_{10}, \lambda_{20}, \theta_0) &= \int_0^{\lambda_{20}} \frac{L_{11}\lambda_2}{D} d\lambda_2 + \int_0^{\lambda_{10}} \frac{L_{22}\lambda_1 - L_{12}\lambda_{20}}{D} d\lambda_1 \\ &= \frac{1}{2D} L_{11}\lambda_{20}^2 + \frac{1}{2D} L_{22}\lambda_{10}^2 - \frac{L_{12}}{D} \lambda_{10}\lambda_{20} \end{aligned} \quad (3-49)$$

Similarly, when the currents are used to describe the system, the differential of the coenergy is

$$dW'_{fld}(i_1, i_2, \theta) = \lambda_1 di_1 + \lambda_2 di_2 + T_{fld} d\theta \quad (3-50)$$

and

$$\lambda_1 = \frac{\partial W'_{fld}(i_1, i_2, \theta)}{\partial i_1} \quad (3-51)$$

$$\lambda_2 = \frac{\partial W'_{\text{fld}}(i_1, i_2, \theta)}{\partial i_2} \quad (3-52)$$

$$T_{\text{fld}} = + \frac{\partial W'_{\text{fld}}(i_1, i_2, \theta)}{\partial \theta} \quad (3-53)$$

Analogous to Eq. 3-41, the coenergy can be found

$$W'_{\text{fld}}(i_{10}, i_{20}, \theta_0) = \int_0^{i_{20}} \lambda_2(i_1 = 0, i_2, \theta_0) di_2 + \int_0^{i_{10}} \lambda_1(i_1, i_2 = i_{20}, \theta_0) di_1 \quad (3-54)$$

For the linear system of Eqs. 3-43 to 3-45

$$W'_{\text{fld}}(i_1, i_2, \theta) = \frac{1}{2} L_{11} i_1^2 + \frac{1}{2} L_{22} i_2^2 + L_{12} i_1 i_2 \quad (3-55)$$

Systems with more than two pairs of electric terminals are handled in analogous fashion; one independent variable is chosen for each terminal pair.

EXAMPLE 3-5

In the system shown in Fig. 3-13, the inductances in henrys are given as $L_{11} = (3 + \cos 2\theta) \times 10^{-3}$; $L_{12} = 0.1 \cos \theta$; $L_{22} = 30 + 10 \cos 2\theta$. Find the torque $T_{\text{fld}}(\theta)$ for current $i_1 = 1$ A and $i_2 = 0.01$ A.

Solution

Since the expression for torque is needed as a function of currents i_1 and i_2 rather than the flux linkages, we use the coenergy of the system as the

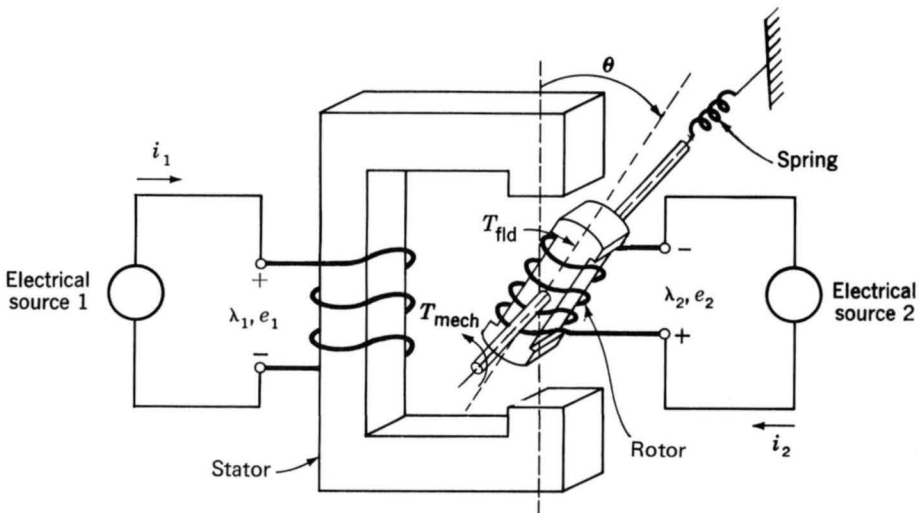


Fig. 3-13. Multiply excited magnetic system of Example 3-5.

state function. When the inductances are given, the coenergy of the system from Eq. 3-55 is

$$W'_{\text{fld}} = \frac{1}{2}L_{11}i_1^2 + L_{12}i_1i_2 + \frac{1}{2}L_{22}i_2^2$$

The torque is given by Eq. 3-53 as

$$T_{\text{fld}} = + \frac{\partial W'_{\text{fld}}}{\partial \theta} = -1 \times 10^{-3} i_1^2 \sin 2\theta - 0.1 i_1 i_2 \sin \theta - 10 i_2^2 \sin 2\theta$$

At $i_1 = 1$ A and $i_2 = 0.01$ A, the torque is

$$T_{\text{fld}} = -2 \times 10^{-3} \sin 2\theta - 10^{-3} \sin \theta \quad \text{N} \cdot \text{m}$$

Notice that the torque expression consists of terms of two types. One term is proportional to the product of the two currents and to the sine of the angular displacement. This torque is due to the mutual interaction between the rotor and stator currents; it acts in a direction to align the rotor and stator so as to maximize the coenergy. Alternately, it can be thought of as being due to the tendency of two magnetic fields (in this case those of the rotor and stator) to align.

The torque expression also has two terms each proportional to the sine of twice the angle and to the square of one of the coil currents. These terms correspond to the torques one sees in singly excited systems. Here the torque is due to the fact that the coenergy is a function of rotor position (corresponding to the position of the movable plunger in Art. 3-4), and the torque acts in a direction to align the rotor so as to maximize the coenergy. The 2θ variation is due to the corresponding variation in the self-inductances, which in turn is due to the variation of the air-gap reluctance; notice that rotating the rotor by 180° from any given position gives the same air-gap reluctance (hence the twice-angle variation). This torque component is known as the *reluctance torque*. The two torque components (mutual and reluctance) are plotted in Fig. 3-14.

3-6 FORCES AND TORQUES IN SYSTEMS WITH PERMANENT MAGNETS

The derivations of the force and torque expressions of Arts. 3-3 through 3-5 assume that the magnetic fields in the magnetic energy storage system arise only due to the electrical excitation of specific windings in the system. This assumption comes specifically into play in the derivation of the equations for the magnetic stored energy W_{fld} . For example, the derivation of Eq. 3-17 depends on the fact that in Eq. 3-16 the force f_{fld} is zero when there is no electrical excitation in the system. A similar argument applies in the derivation of the coenergy expressions of Eqs. 3-33 and 3-54.

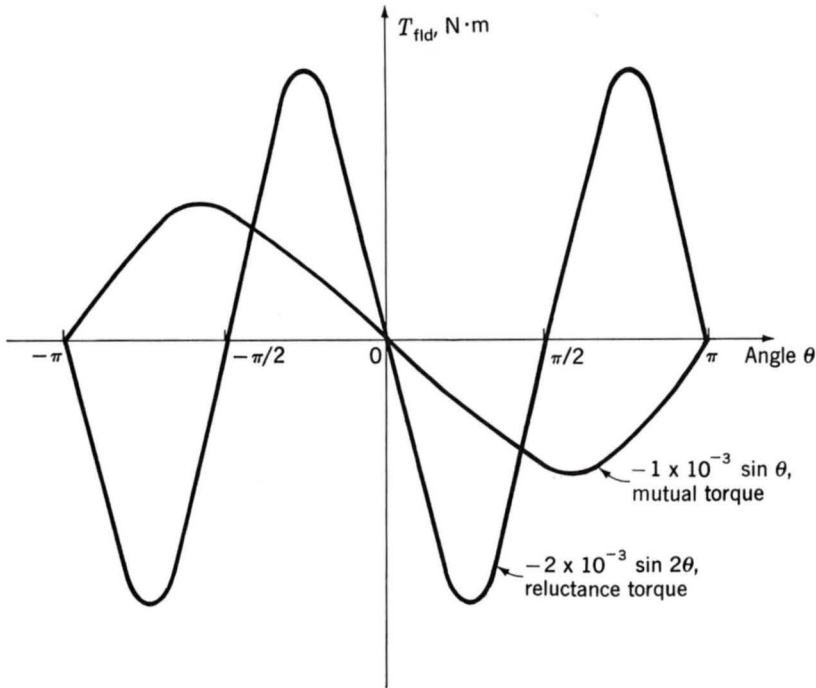


Fig. 3-14. Plot of torque components for multiply excited system of Example 3-5.

In systems with permanent magnets, this condition must be carefully investigated. In some cases these systems have no windings at all, their magnetic fields are due solely to the presence of permanent magnet material, and it is not possible to talk about winding fluxes and currents. In other cases, magnetic fields may be produced by a combination of permanent magnets and windings.

A modification of the techniques presented in the previous articles can be used in systems with permanent magnets. The essence of this technique is to consider the system as having an additional fictitious winding acting upon the same portion of the magnetic circuit as does the permanent magnet. Under normal operating conditions, the fictitious winding carries zero current. Its function is simply that of a mathematical "crutch" which can be used to accomplish the required analysis. The current in this winding can be adjusted to zero-out the magnetic fields produced by the permanent magnet, in order to achieve the "zero-force" starting point for the analyses such as that leading from Eq. 3-16 to 3-17.

For the purpose of calculating the energy and coenergy of the system, this winding is treated as any other winding, with its own set of current and flux linkages. As a result, energy and coenergy expressions can be obtained as a function of all the winding flux linkages or currents, including those of the fictitious winding. However, since under normal operating conditions the current in this winding will be set equal to zero, it is useful to

derive the expression for the force from the system coenergy since the winding currents are explicitly expressed in this representation.

Figure 3-15a shows a magnetic circuit with a permanent magnet and a movable plunger. To find the force on the plunger as a function of the plunger position, we assume that there is a fictitious winding of N_f turns carrying a current I_f wound in series with the permanent magnet, as shown in Fig. 3-15b.

For this single-winding system, from Eq. 3-29 we can write the expression for the differential in coenergy as

$$dW'_{\text{fld}}(i_f, x) = \lambda_f di_f + f_{\text{fld}} dx \quad (3-56)$$

where the subscript f indicates the fictitious winding. Corresponding to Eq. 3-32, the force in this system can be written as

$$f_{\text{fld}} = \frac{dW'_{\text{fld}}(i_f = 0, x)}{dx} \quad (3-57)$$

where the partial derivative is taken while holding i_f constant and the result is evaluated for $i_f = 0$.

To calculate the coenergy $W'_{\text{fld}}(i_f = 0, x)$ in this system, it is necessary to integrate Eq. 3-56. Since $W'_{\text{fld}}(i_f, x)$ is a state function, we are free to choose any integration path we wish. Figure 3-16 illustrates a path over which this integration is particularly simple. For this path we can write the expression for coenergy in this system as

$$\begin{aligned} W'_{\text{fld}}(i_f = 0, x) &= \int_{\text{path 1a}} dW'_{\text{fld}} + \int_{\text{path 1b}} dW'_{\text{fld}} \\ &= \int_0^x f_{\text{fld}}(i_f = I_{f0}, x') dx' + \int_{I_{f0}}^0 \lambda_f(i_f, x) di_f \end{aligned} \quad (3-58)$$

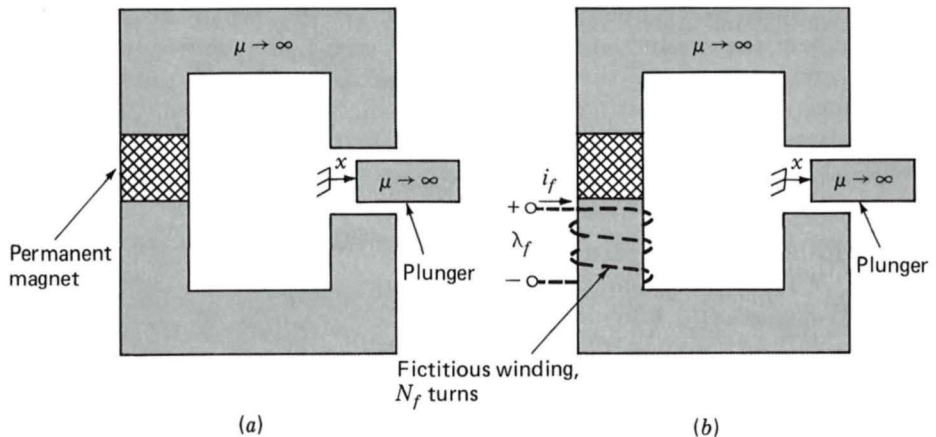


Fig. 3-15. (a) Magnetic circuit with permanent magnet and movable plunger; (b) fictitious winding added.

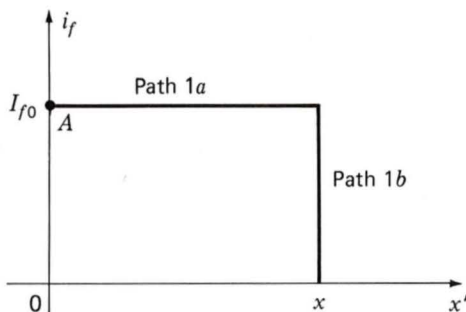


Fig. 3-16. Integration path for calculating $W'_{\text{fld}}(i_f = 0, x)$ in the permanent magnet system of Fig. 3-15.

which corresponds directly to the analogous expression for energy found in Eq. 3-16.

We begin our integration at point A in the figure. This is a very specific point in that it corresponds to a current I_{f0} in the fictitious winding for which the stored energy in the system is zero and for which both the flux linkage λ_f of the winding and the force f_{fld} acting on the plunger are zero. In other words, the current I_{f0} is that current in the fictitious winding which totally counteracts the magnetic field produced by the permanent magnet. Because there is zero force in the system when $i_f = I_{f0}$, the integral over path 1a in Eq. 3-58 is zero, and Eq. 3-58 reduces to

$$W'_{\text{fld}}(i_f = 0, x) = \int_{I_{f0}}^0 \lambda_f(i_f, x) di_f \quad (3-59)$$

Note that Eq. 3-59 is perfectly general and does not require either the permanent magnet or the magnetic material in the magnetic circuit to be linear. Once Eq. 3-59 has been evaluated, the force at a given plunger position x can be readily found from Eq. 3-57. Note also that due to the presence of the permanent magnet, neither the coenergy nor the force is zero when i_f is zero, which is to be expected due to the presence of the permanent magnet.

EXAMPLE 3-6

The magnetic circuit of Fig. 3-17 is excited by a samarium cobalt permanent magnet and includes a movable plunger. The system dimensions are included in the figure. Also shown is the fictitious winding of N_f turns carrying a current i_f which does not exist in the actual system but which is included for the purposes of analysis.

Find (a) an expression for the coenergy of the system as a function of plunger position x and (b) an expression for the force on the plunger as a function of x . Finally, (c) calculate the force at $x = 0$ and $x = 0.5$ cm. Neglect fringing in this calculation.

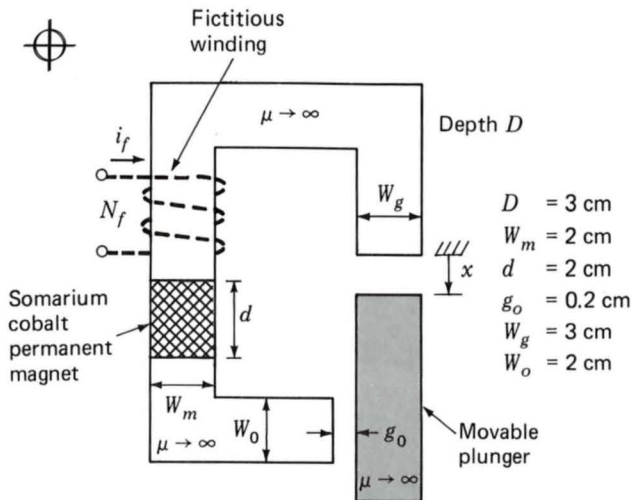


Fig. 3-17. Magnetic circuit for Example 3-6.

Solution

(a) As seen in Fig. 1-18, over the operating range of interest in this example, the dc magnetization curve for somarium cobalt can be represented as a straight line of the form

$$B_m = \mu_R(H_m - H'_c) = \mu_R H_m + B_r$$

where

$$\mu_R = 1.05\mu_0 \text{ is the recoil permeability}$$

$$H'_c = 712 \text{ kA/m}$$

$$B_r = 0.94 \text{ T}$$

The subscript m indicates that we are referring to quantities within the magnetic material.

From Eq. 1-5 we can write

$$N_f i_f = H_m d + H_g x + H_0 g_0$$

where the subscript g refers to the variable gap and the subscript 0 refers to the fixed gap. Similarly from the continuity of flux condition, Eq. 1-3, we can write

$$B_m W_m D = B_g W_g D = B_0 W_0 D$$

Recognizing that in the air gaps $B_g = \mu_0 H_g$ and $B_0 = \mu_0 H_0$, we can solve the above equations for B_m :

$$B_m = \frac{\mu_R(N_f i_f - H'_c d)}{d + W_m \left(\frac{\mu_R}{\mu_0} \right) \left(\frac{x}{W_g} + \frac{g_0}{W_0} \right)}$$

Finally we can solve for the flux linkages λ_f of the fictitious winding as

$$\lambda_f = N_f W_m D B_m = \frac{N_f W_m D \mu_R (N_f i_f - H'_c d)}{d + W_m \left(\frac{\mu_R}{\mu_0} \right) \left(\frac{x}{W_g} + \frac{g_0}{W_0} \right)}$$

Thus we see that the flux linkages λ_f will be zero when $i_f = I_{f0} = H'_c d / N_f$, and from Eq. 3-59 we can find the coenergy as

$$W'_{fld}(x) = \int_{H'_c d / N_f}^0 \frac{N_f W_m D \mu_R (N_f i_f - H'_c d)}{d + W_m \left(\frac{\mu_R}{\mu_0} \right) \left(\frac{x}{W_g} + \frac{g_0}{W_0} \right)} di_f = \frac{W_m D \mu_R H'^2_c d^2}{2 \left[d + W_m \left(\frac{\mu_R}{\mu_0} \right) \left(\frac{x}{W_g} + \frac{g_0}{W_0} \right) \right]}$$

Note that the answer does not depend upon N_f or I_{f0} , which is as we would expect since the winding does not actually exist in this system.

(b) Once the coenergy has been found, the force can be found from Eq. 3-57 as

$$f_{fld} = - \frac{W_m^2 D B_r^2}{2 \mu_0 W_g \left[1 + \left(\frac{W_m}{d} \right) \left(\frac{\mu_R}{\mu_0} \right) \left(\frac{x}{W_g} + \frac{g_0}{W_0} \right) \right]^2}$$

where we have used the fact that $B_r = -\mu_R H'_c$. Notice that the force is negative, indicating that the force is acting in the direction to decrease x , that is, to pull the plunger in the direction which decreases the gap.

(c) Finally, substitution into the force expression yields

$$f_{fld} = \begin{cases} -122 \text{ N} & \text{at } x = 0 \text{ cm} \\ -90.7 \text{ N} & \text{at } x = 0.5 \text{ cm} \end{cases}$$

Clearly the method described above can be readily extended to handle situations in which there are both permanent magnets and current-carrying windings. It should be emphasized that an alternate procedure applicable

to any situation with permanent magnets (with or without additional windings) is to employ the finite-element method discussed in conjunction with Eq. 3-35. Using this method, the coenergy of Eq. 3-35 can be evaluated numerically at constant winding current and for varying values of displacement. In situations where magnetic circuit analysis is not applicable, use of the finite-element method or an equivalent numerical procedure is often the only way to obtain a useful result.

3-7 DYNAMIC EQUATIONS

We have derived expressions for the forces produced in electromechanical energy conversion devices as functions of the electrical variables and the mechanical displacement. These expressions were derived for conservative energy conversion systems; any losses were assigned to the electric and mechanical sources. These conversion devices always operate as a coupling means between an electric system and a mechanical system. Hence, we should be interested not only in how the conversion device itself operates but in how the complete electromechanical system operates with the conversion device contained within it.

The model of a simple conversion system in Fig. 3-18 shows the basic system components, the details of which may vary from system to system. The system shown consists of three parts: an external electric system, the energy conversion means, and the external mechanical system. The electric system is merely represented by a voltage source v_0 and resistance R ; the source could alternatively be represented by a current source and a parallel conductance G . The electric equation is thus

$$v_0 = iR + \frac{d\lambda}{dt} \quad (3-60)$$

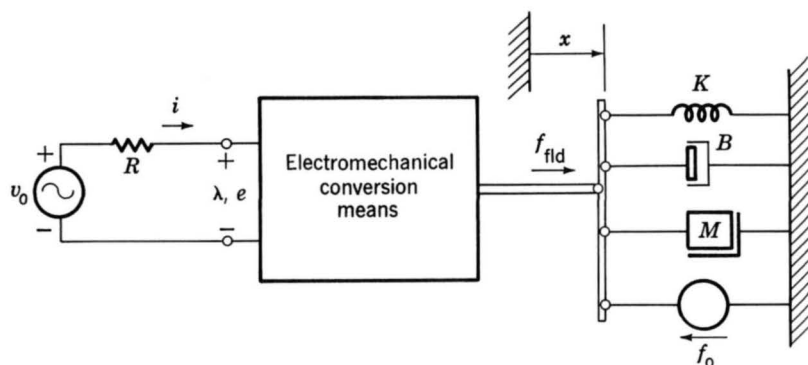


Fig. 3-18. Model of a singly excited electromechanical system.

If the flux linkage λ can be expressed as $\lambda = L(x)i$, the external equation becomes

$$v_0 = iR + L(x)\frac{di}{dt} + i\frac{dL(x)}{dx}\frac{dx}{dt} \quad (3-61)$$

The term $L(di/dt)$ is the self-inductance voltage term, and the term $i(dL/dx)(dx/dt)$ is the speed-dependent voltage term (often called simply the *speed voltage*). The speed voltage term is common to all electromechanical energy conversion systems and is responsible for energy transfer to and from the mechanical system by the electrical system. For a multiply excited system, electric equations corresponding to Eq. 3-60 are written for each input pair. If the expressions for the λ 's are to be expanded in terms of inductances, as in Eq. 3-61, both self- and mutual-inductance terms will be required.

The mechanical system of Fig. 3-18 shows symbols for a spring (spring constant K), a damper (damping constant B), a mass M , and an external mechanical excitation force f_0 . The forces and displacement x are related as follows:

$$\text{Spring:} \quad f_K = K(x - x_0) \quad (3-62)$$

$$\text{Damper:} \quad f_D = B\frac{dx}{dt} \quad (3-63)$$

$$\text{Mass:} \quad f_M = M\frac{d^2x}{dt^2} \quad (3-64)$$

where x_0 is the value of x with the spring unstretched and the applied mechanical force $f_0 = 0$. Force equilibrium thus requires that

$$f_{\text{nd}} = f_K + f_D + f_M + f_0 = K(x - x_0) + B\frac{dx}{dt} + M\frac{d^2x}{dt^2} + f_0 \quad (3-65)$$

The differential equations for the overall system of Fig. 3-18 for arbitrary inputs $v_0(t)$ and $f_0(t)$ are

$$v_0(t) = iR + L(x)\frac{di}{dt} + i\frac{dL(x)}{dx}\frac{dx}{dt} \quad (3-66)$$

$$f_0(t) = -M\frac{d^2x}{dt^2} - B\frac{dx}{dt} - K(x - x_0) + f_{\text{nd}}(x, i) \quad (3-67)$$

The functions $L(x)$ and $f_{\text{nd}}(x, i)$ depend on the properties of the energy conversion device and are calculated as previously discussed.

EXAMPLE 3-7

Figure 3-19 shows in cross section a cylindrical solenoid magnet in which the cylindrical plunger of mass M moves vertically in brass guide rings of thickness g and mean diameter d . The permeability of brass is the same as that of free space and is $\mu_0 = 4\pi \times 10^{-7}$ H/m in SI units. The plunger is supported by a spring whose spring constant is K . Its unstretched length is l_0 . A mechanical load force f_t is applied to the plunger from the mechanical system connected to it, as shown in Fig. 3-19. Assume that frictional force is linearly proportional to the velocity and that the coefficient of friction is B . The coil has N turns and resistance R . Its terminal voltage is v_t , and its current is i . The effects of magnetic leakage and reluctance of the steel are negligible.

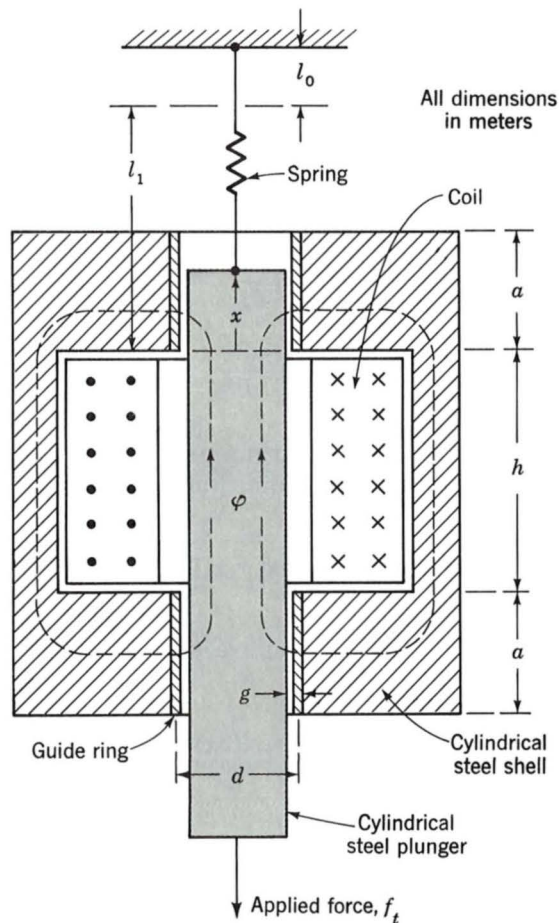


Fig. 3-19. Solenoid magnet for Example 3-7.

Derive the dynamic equations of motion of the electromechanical system, i.e., the differential equations expressing the dependent variables i and x in terms of v_t , f_t , and the given constants and dimensions.

Solution

We begin by expressing the inductance as a function of x . The coupling terms, i.e., magnetic force f_{fld} and induced emf e , can then be expressed in terms of x and i , and these relations substituted in the equations for the mechanical and electric systems.

The reluctance of the magnetic circuit is that of the two guide rings in series, with the flux directed radially through them, as shown by the dashed flux lines φ in Fig. 3-19. Because $g \ll d$, the flux density in the guide rings is very nearly constant with respect to the radial distance. In a region where the flux density is constant, the reluctance is

$$\frac{\text{Length of flux path in direction of field}}{\mu(\text{area perpendicular to field})}$$

The reluctance of the upper gap is

$$\mathcal{R}_1 = \frac{g}{\mu_0 \pi x d}$$

in which it is assumed that the field is concentrated in the area between the upper end of the plunger and the lower end of the upper guide ring. Similarly, the reluctance of the lower gap is

$$\mathcal{R}_2 = \frac{g}{\mu_0 \pi a d}$$

The total reluctance is

$$\mathcal{R} = \mathcal{R}_1 + \mathcal{R}_2 = \frac{g}{\mu_0 \pi d} \left(\frac{1}{a} + \frac{1}{x} \right) = \frac{g}{\mu_0 \pi a d} \frac{a + x}{x}$$

Hence, the inductance is

$$L = \frac{N^2}{\mathcal{R}} = \frac{\mu_0 \pi a d N^2}{g} \frac{x}{a + x} = L' \frac{x}{a + x}$$

where

$$L' = \frac{\mu_0 \pi a d N^2}{g}$$

The magnetic force acting upward on the plunger in the positive direction

of x is

$$f_{\text{fld}} = \frac{+\partial W'_{\text{fld}}(i, x)}{\partial x} = +\frac{1}{2}i^2 \frac{dL}{dx} = +\frac{1}{2}L' \frac{ai^2}{(a+x)^2}$$

The induced emf in the coil is

$$e = \frac{d}{dt}(Li) = L \frac{di}{dt} + i \frac{dL}{dx} \frac{dx}{dt}$$

or

$$e = L' \frac{x}{a+x} \frac{di}{dt} + L' \frac{ai}{(a+x)^2} \frac{dx}{dt}$$

Substitution of the magnetic force in the differential equation of motion of the mechanical system (Eq. 3-67) gives

$$f_t = -M \frac{d^2x}{dt^2} - B \frac{dx}{dt} - K(x - l_0) + \frac{1}{2}L' \frac{ai^2}{(a+x)^2}$$

The voltage equation for the electric system is (from Eq. 3-66)

$$v_t = iR + L' \frac{x}{a+x} \frac{di}{dt} + iL' \frac{a}{(a+x)^2} \frac{dx}{dt}$$

These last two equations are the desired results. They are valid only as long as the upper end of the plunger is well within the upper guide ring, say, between the limits $0.1a < x < 0.9a$. This is the normal working range of the solenoid.

3-8 ANALYTICAL TECHNIQUES

We have described relatively simple devices in this chapter. The devices have one or two pairs of electric terminals and one mechanical terminal, which is usually constrained to incremental motion. More complicated devices capable of continuous energy conversion are treated in the following chapters. The analytical techniques discussed here apply to the simple devices, but the principles are applicable to the more complicated devices as well.

a. Reasons for Analysis

Some of the devices described in this chapter are used with gross motion, such as in relays and solenoids, where the devices operate under essentially "on" and "off" conditions. Analysis of these devices is carried out to determine force as a function of displacement and reaction on the electric

source. Such calculations have already been made in this chapter. If the details of the motion are required, such as the displacement as a function of time after the device is energized, nonlinear differential equations of the form of Eqs. 3-66 and 3-67 must be solved.

Compared with gross-motion devices, other devices are used with small motion, as in loudspeakers, pickups, and transducers of various kinds, for converting electric signals to mechanical signals and vice versa. The relationship between the electrical and mechanical variables is made linear either by the design of the device or by restricting the excursion of the signals to a linear range. In such case the differential equations are linear and can be solved for transient response, frequency response, or equivalent-circuit representation, as required.

b. Gross Motion

The differential equations for a singly excited device as derived in Example 3-7 are of the form

$$\frac{1}{2}L' \frac{ai^2}{(a+x)^2} = M \frac{d^2x}{dt^2} + B \frac{dx}{dt} + K(x - l_0) + f_t \quad (3-68)$$

$$v_t = iR + L' \frac{x}{a+x} \frac{di}{dt} + \frac{L'ai}{(a+x)^2} \frac{dx}{dt} \quad (3-69)$$

A typical problem using these differential equations is to find the excursion $x(t)$ when a prescribed voltage $v_t = V$ is applied at $t = 0$. An even simpler problem is to find the time required for the armature to move from its position $x(0)$ at $t = 0$ to a given displacement $x = X$ when a voltage $v_t = V$ is applied at $t = 0$. There is no general solution for these differential equations; they involve products of variables x and i and their derivatives and are termed nonlinear. They can be solved by using numerical step-by-step techniques on a digital computer. Either a program can be prepared for the solution of the equations, or a standard library program can be called on and the coefficients for the particular problem inserted into that program.

In many cases the gross-motion problem can be simplified and a solution found by relatively simple methods. For example, when the winding of the device is connected to the voltage source with a relatively large resistance, the iR term dominates on the right-hand side of Eq. 3-69 compared with the di/dt transformer voltage term and the dx/dt velocity voltage term. The current i can then be assumed equal to V/R and inserted directly into Eq. 3-68. The same assumption can be made when the winding is driven from a transistor which acts as a current source to the winding. With the assumption that $i = V/R$, two cases can be solved easily.

Case 1. We can handle those devices in which the dynamic motion is governed by damping rather than inertia, e.g., devices purposely having low inertia or relays having dashpots or dampers to slow down the motion. In

such case, the differential equation 3-68 reduces to

$$f(x) = \frac{1}{2}L' \frac{a}{(a+x)^2} \left(\frac{V}{R} \right)^2 - K(x - l_0) = B \frac{dx}{dt} \quad (3-70)$$

where $f(x)$ is the difference between the force of electrical origin and the spring force in the device of Fig. 3-19. The velocity at any value of x is merely $dx/dt = f(x)/B$; the time t to reach $x = X$ is given by

$$t = \int_0^X \frac{B}{f(x)} dx \quad (3-71)$$

The integration of Eq. 3-71 can be carried out analytically or graphically.

Case 2. The dynamic motion is governed by the inertia rather than the damping. Where additional damping is not introduced, the inertia usually governs the motion. In such a case, the differential equation 3-68 reduces to

$$f(x) = M \frac{d^2x}{dt^2} \quad (3-72)$$

Equation 3-72 can be written in the form

$$f(x) = \frac{M}{2} \frac{d}{dx} \left(\frac{dx}{dt} \right)^2 \quad (3-73)$$

and the velocity $v(x)$ at any value x is then given by

$$v(x) = \frac{dx}{dt} = \left[\frac{2}{M} \int_0^X f(x) dx \right]^{1/2} \quad (3-74)$$

The integration of Eq. 3-74 can be carried out analytically or graphically to find $v(x)$ and to find the time t to reach any value of x .

c. Linearization

Devices characterized by nonlinear differential equations such as Eqs. 3-68 and 3-69 will yield nonlinear responses to input signals when used as transducers. To obtain linear behavior, such devices must be restricted to small excursions of displacement and electrical quantities about an equilibrium position. The equilibrium position is determined either by a bias mmf produced by current or a permanent magnet acting against a spring or by a pair of windings producing mmf's whose forces cancel at the equilibrium point. The equilibrium point must be stable; the transducer following a small disturbance should return to the equilibrium position. The equilibrium condition is determined with the time derivatives set to zero

in Eqs. 3-68 and 3-69; this occurs for

$$\frac{1}{2}L' \frac{aI_0^2}{(a + X_0)^2} = K(X_0 - l_0) + f_{i0} \quad (3-75)$$

$$V_0 = I_0 R \quad (3-76)$$

where $i = I_0$ and $x = X_0$ at equilibrium.

The incremental operation can be described by expressing the variables as $i = I_0 + i_1$, $f_i = f_{i0} + f_1$, $v_i = V_0 + v_1$, and $x = X_0 + x_1$ and canceling the products of increments as being of second order. Equations 3-68 and 3-69 thus become

$$\frac{1}{2} \frac{L' a (I_0 + i_1)^2}{(a + X_0 + x_1)^2} = M \frac{d^2 x_1}{dt^2} + B \frac{dx_1}{dt} + K(X_0 + x_1 - l_0) + f_{i0} + f_1 \quad (3-77)$$

and

$$V_0 + v_1 = (I_0 + i_1)R + \frac{L'(X_0 + x_1)}{a + X_0 + x_1} \frac{di_1}{dt} + \frac{L'a(I_0 + i_1)}{(a + X_0 + x_1)^2} \frac{dx_1}{dt} \quad (3-78)$$

The equilibrium terms cancel, and retaining only first-order incremental terms yields a set of linear differential equations in terms of just the incremental variables of first order as

$$\frac{L'aI_0 i_1}{(a + X_0)^2} = M \frac{d^2 x_1}{dt^2} + B \frac{dx_1}{dt} + \left[K + \frac{L'aI_0^2}{(a + X_0)^3} \right] x_1 + f_1 \quad (3-79)$$

$$v_1 = i_1 R + \frac{L'(X_0)}{a + X_0} \frac{di_1}{dt} + \frac{L'aI_0}{(a + X_0)^2} \frac{dx_1}{dt} \quad (3-80)$$

These equations can be written in more compact form in terms of the self-inductance L_0 at the equilibrium point and a coefficient K_0 of energy conversion as

$$K_0 i_1 = M \frac{d^2 x_1}{dt^2} + B \frac{dx_1}{dt} + \left[K + \frac{L'aI_0^2}{(a + x_0)^3} \right] x_1 + f_1 \quad (3-81)$$

$$v_1 = i_1 R + L_0 \frac{di_1}{dt} + K_0 \frac{dx_1}{dt} \quad (3-82)$$

3-9 SUMMARY

Magnetic and electric fields are seats of energy storage. Whenever the energy in the field is influenced by the configuration of the mechanical parts

constituting the boundaries of the field, mechanical forces are created which tend to move the mechanical elements so that energy is transmitted from the field to the mechanical system.

The singly excited magnetic system is considered first in Art. 3-3. When the electric and mechanical loss elements are removed from the electromechanical conversion device and combined with the external electric and mechanical systems, the device can be considered as a conservative system. Its energy is thus a state function and is described by its independent variables λ and x . The energy can be specified in terms of field quantities, electric circuit quantities, and magnetic circuit quantities.

In Art. 3-4 the state function is enlarged in concept to include the coenergy as a function of i and x . The force of field origin acting on the movable members is derived as the partial derivative of the energy or coenergy expressed in the suitable independent variables, and the values of force are independent of the method of analysis. Article 3-6 discusses systems in which permanent magnets are included among the sources of the magnetic energy storage.

Most rotating machinery and signal-handling transducers are built with multiple windings or excitation sources. The analysis is extended in Art. 3-5 for such magnetic field systems in terms of energy and coenergy. The use of self- and mutual inductances for expressing the state functions is introduced.

Energy conversion devices operate between electric and mechanical systems. The behavior is described in Art. 3-7 by the differential equations which include the coupling terms between the systems. The equations are usually nonlinear and can be solved by computer or numerical methods if necessary. Usually, the solution is required for special conditions which can be handled as discussed in Art. 3-8. A useful condition is that for small signal amplitudes, where the resulting equations are linear.

This chapter has been concerned with basic principles applying broadly to the electromechanical energy conversion process, with emphasis on magnetic field coupling. Basically, rotating machines and linear motion transducers work in the same way. The remainder of this text is devoted almost entirely to the rotating-machine aspects of electromechanical energy conversion, both the dynamic characteristics of the machines as system components and their behavior under steady-state conditions. The rotating machine is a fairly complicated assembly of electric and magnetic circuits with a number of variations of machine types. For all of them, the electromechanical coupling terms (torque and induced voltage) can be found by the principles developed in this chapter.

PROBLEMS

3-1. The rotor of Fig. 3-20 is similar to that of Fig. 3-2 (Example 3-1) except that it has two coils instead of one. The rotor is nonmagnetic and is

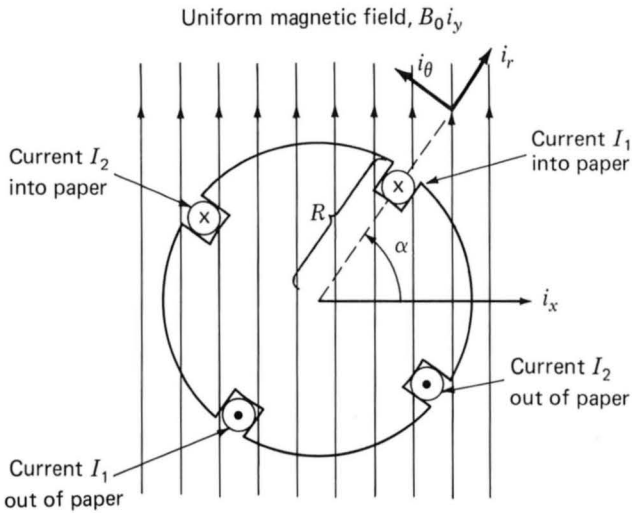


Fig. 3-20. Two-coil rotor for Prob. 3-1.

placed in a uniform magnetic field of magnitude B_0 . The coil sides are of radius R and are uniformly spaced around the rotor surface. The first coil is carrying a current I_1 , and the second coil is carrying a current I_2 .

Assuming that the rotor is 0.35 m long, $R = 0.15$ m, and $B_0 = 0.8$ T, find the θ -directed torque as a function of rotor position α for (a) $I_1 = 0$ A and $I_2 = 5$ A, (b) $I_1 = 5$ A and $I_2 = 0$ A, and (c) $I_1 = 5$ A and $I_2 = 5$ A.

3-2. Calculate the magnetic stored energy in the magnetic circuit of Example 1-2.

3-3. An inductor has an inductance which is found experimentally to be of the form

$$L = \frac{2L_0}{1 + x/x_0}$$

where $L_0 = 10$ mH, $x_0 = 0.015$ in, and x is the displacement of a movable element. Its winding resistance is measured and found to equal 125 m Ω .

- (a) The displacement x is held constant at 0.025 in, and the current is increased from 0 to 2.5 A. Find the resultant magnetic stored energy in the inductor.
- (b) The current is then held constant at 2.5 A, and the displacement is increased to 0.05 in. Find the corresponding change in magnetic stored energy.

3-4. Repeat Prob. 3-3, assuming that the inductor is connected to a voltage source which increases from 0 to 0.4 V [part (a)] and then is held constant

at 0.4 V [part (b)]. For both calculations, assume that all electric transients have decayed.

3-5. The inductor of Prob. 3-3 is driven by a sinusoidal current source of the form

$$i(t) = I_0 \sin \omega t$$

where $I_0 = 2$ A and $\omega = 120\pi$. With the displacement held fixed at $x = x_0$, calculate (a) the time-averaged magnetic stored energy $\langle W_{fld} \rangle$ in the inductor and (b) the time-averaged power dissipated in the winding resistance.

3-6. An inductor is made from a magnetic core with two air gaps of equal length g_0 , as shown in Fig. 3-21.

- (a) Find the inductance in terms of the core dimensions and the number of turns.

The applied voltage $v(t)$ is varied linearly from 0 to V_0 in 2 s, after which it is held constant.

- (b) Calculate the magnetic stored energy in the inductor after all electric transients have ended.
- (c) With the voltage held constant at V_0 , the air-gap lengths are decreased from g_0 to g_1 . Again assuming that all electric transients have ended, calculate the resultant change in the magnetic stored energy.

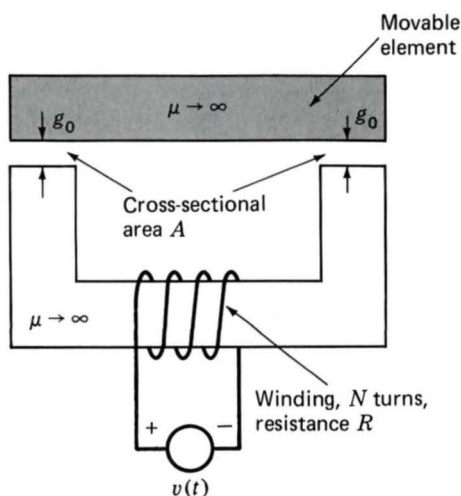


Fig. 3-21. Inductor for Prob. 3-6.

3-7. The voltage source of Fig. 3-21 is made to vary sinusoidally in time as

$$v(t) = V_0 \cos \omega t$$

With the air-gap lengths held fixed at g_0 , calculate the time-averaged magnetic stored energy $\langle W_{\text{fld}} \rangle$ in the inductor and the instantaneous and time-averaged output of the voltage source as a function of the winding resistance R . Compare with the time-averaged power dissipated in the resistor.

3-8. An RC circuit is connected to a battery, as shown in Fig. 3-22. Switch S_1 is initially closed and is opened at time $t = 0$.

- Find the capacitor voltage $v_c(t)$ for $t \geq 0$.
- What are the initial and final ($t = \infty$) values of the stored energy in the capacitor? [Hint: $W_{\text{fld}} = \frac{1}{2}(q^2/C)$, where $q = Cv_c$.] What is the energy stored in the capacitor as a function of time?
- What is the power dissipated in the resistor as a function of time? What is the total energy dissipated in the resistor?

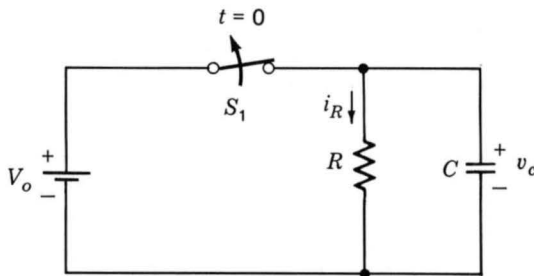


Fig. 3-22. An RC circuit for Prob. 3-8.

3-9. An RL circuit is connected to a battery, as shown in Fig. 3-23. Switch S_1 is initially closed and is opened at time $t = 0$.

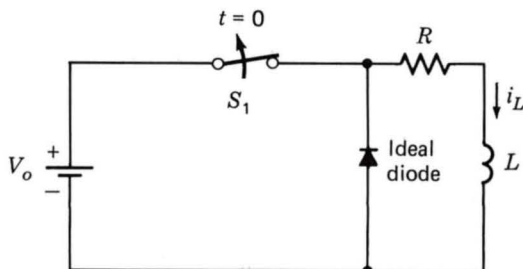


Fig. 3-23. An RL circuit for Prob. 3-9.

- (a) Find the inductor current $i_L(t)$ for $t \geq 0$. *Hint:* Note that while the switch is closed, the diode is reverse-biased and can be assumed to be an open circuit. Immediately after the switch is opened, the diode becomes forward-biased and can be assumed to be a short circuit.
- (b) What are the initial and final ($t = \infty$) values of the stored energy in the inductor? What is the energy stored in the inductor as a function of time?
- (c) What is the power dissipated in the resistor as a function of time? What is the total energy dissipated in the resistor?

3-10. The time constant L/R of the field winding of an 850-MVA synchronous generator is 5.5 s. At normal operating conditions, the field winding is known to be dissipating 2.5 MW. Calculate the corresponding magnetic stored energy.

3-11. The movable element in the inductor of Fig. 3-21 is constrained to move such that the two air gaps must remain of equal length.

- (a) A constant current I_0 is applied to the winding.
 - (i) Calculate the magnetic stored energy in the inductor.
 - (ii) Calculate the corresponding coenergy.
 - (iii) Calculate the force on the movable element. Does this force act in a direction to increase or decrease the air-gap length?
- (b) Repeat part (a) if the inductor voltage is held constant at V_0 (assuming that the voltage has been applied for sufficient time that all electric transients have decayed).

3-12. The inductance of a phase winding of a three-phase salient-pole motor is measured to be of the form

$$L(\theta) = L_0 + L_2 \cos 2\theta$$

where θ is the angular position of the rotor.

- (a) How many poles are on the rotor of this motor?
- (b) Assuming that all other winding currents are zero and that this phase is excited by a constant current I_a , find the torque $T_{\text{nd}}(\theta)$ acting on the rotor.

3-13. The cylindrical iron-clad solenoid magnet shown in Fig. 3-24 is used for tripping circuit breakers, for operating valves, and in other applications in which a relatively large force is applied to a member which moves a relatively short distance. When the coil current is zero, the plunger drops against a stop such that the gap g is 2.5 cm. When the coil is energized by a direct current of sufficient magnitude, the plunger is raised until it hits another stop set so that g is 0.5 cm. The plunger is supported so that it can

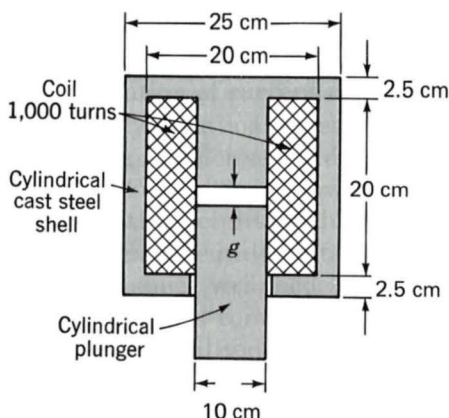


Fig. 3-24. Plunger magnet.

move freely in the vertical direction. The radial air gap between the shell and the plunger can be assumed to be uniform and 0.05 cm long. For this problem neglect the magnetic leakage and fringing in the air gaps. The exciting coil has 1000 turns and carries a constant current of 3.0 A. If the mmf in the iron is neglected, compute (a) the flux densities in teslas between the working faces of the center core and plunger for gap g of 0.50, 1.0, and 2.5 cm; (b) the corresponding values of the energy stored in the magnetic field in joules; and (c) the corresponding values of the coil inductance in henrys.

3-14. Consider the plunger magnet of Fig. 3-24. The air gap between the shell and the plunger can be assumed to be uniform and 0.02 cm long. Magnetic leakage and fringing may be neglected. The coil has 1000 turns and carries a constant current of 2.5 A.

- (a) If the plunger is allowed to move slowly, reducing the gap g from 1.00 to 0.20 cm, how much mechanical work in joules will be done by the plunger?
- (b) For the conditions of part (a), how much energy will be supplied by the electric source (in excess of the power dissipated in the coil)?

3-15. As shown in Fig. 3-25, an electromagnet is to be used to lift a 130-kg slab of iron. The surface roughness of the iron is such that when the iron and the electromagnet are in contact, there is a minimum air gap of 0.015 cm in each leg. The coil resistance is 3 Ω . Calculate the minimum coil voltage which must be used to lift the slab against the force of gravity. Neglect the reluctance of the iron.

3-16. Data for the magnetization curve of the iron portion of the magnetic circuit of the plunger magnet of Prob. 3-13 are given below:

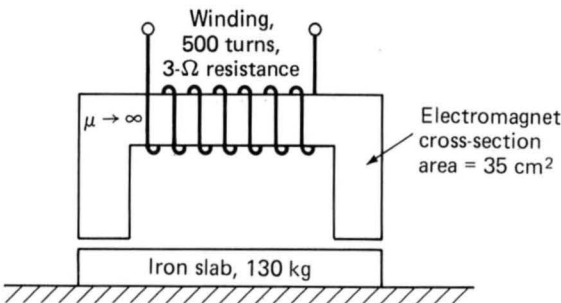


Fig. 3-25. Electromagnet lifting an iron slab (Prob. 3-15).

Flux, kilolines	300	450	600	720	750	780	810	825
mmf, A · turns	60	95	150	250	305	425	600	725

Plot magnetization curves for the complete magnetic circuit (flux in webers versus total mmf in ampere-turns) for (a) gap $g = 2.5$ cm and (b) gap $g = 0.5$ cm. (c) From these curves find graphically the magnetic field energy and coenergy for each of the gaps in parts (a) and (b) with a 3.0-A coil current.

3-17. An inductor is made up of a 600-turn coil on a core of 12-cm² cross-sectional area and gap length 0.025 cm. The coil is connected directly to a 120-V 60-Hz voltage source. Neglect the coil resistance and leakage inductance. Assuming the coil reluctance to be negligible, calculate the time-averaged force acting on the core tending to close the air gap. How would this force vary if the air-gap length were doubled?

3-18. Figure 3-26 shows the general nature of the slot-leakage flux produced by current i in a rectangular conductor embedded in a rectangular slot in iron. Assume that the iron reluctance is negligible and that the slot-

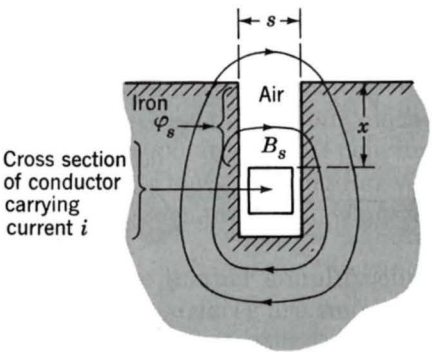


Fig. 3-26. Conductor in a slot (Prob. 3-18).

leakage flux φ_s goes straight across the slot in the region between the top of the conductor and the top of the slot.

- Derive an expression for the flux density B_s in the region between the top of the conductor and the top of the slot.
- Derive an expression for the slot-leakage flux φ_s crossing the slot above the conductor, in terms of the height x of the slot above the conductor, the slot width s , and the embedded length l perpendicular to the paper.
- Derive an expression for the force f created by this magnetic field on a conductor of length l . Use SI units. In what direction does this force act on the conductor?
- Compute the force in pounds on a conductor 1.0 ft long in a slot 1.0 in wide when the current in the conductor is 1000 A.

3-19. A long, thin solenoid of radius r_0 and height h is shown in Fig. 3-27. The magnetic field inside such a solenoid is axially directed and essentially uniform and equal to $H = Ni/h$. The magnetic field outside the solenoid is negligible. Calculate the radial pressure in newtons per square meter acting on the sides of the solenoid for constant coil current $i = I_0$.

3-20. An electromechanical system in which electric energy storage is in electric fields can be analyzed by techniques directly analogous to those derived in this chapter for magnetic field systems. Consider such a system in which it is possible to separate the loss mechanism mathematically from those of energy storage in electric fields. Then the system can be represented as in Fig. 3-28. For a single electric terminal, Eq. 3-8 applies, where

$$dW_{\text{elec}} = v i dt = v dq$$

where v is the electric terminal voltage and q is the net charge associated with electric energy storage. Thus, by analogy to Eq. 3-15,

$$dW_{\text{fld}} = v dq - f_{\text{fld}} dx$$

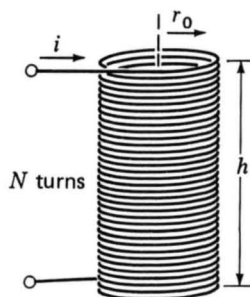


Fig. 3-27. Solenoid coil (Prob. 3-19).

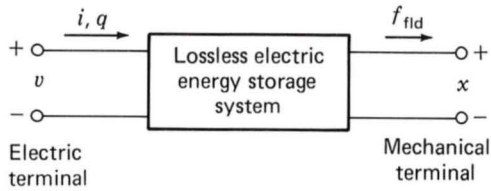


Fig. 3-28. Lossless electric energy storage system.

- Derive an expression for the electric stored energy $W_{\text{fld}}(q, x)$ analogous to that for the magnetic stored energy in Eq. 3-17.
- Derive an expression for the force of electric origin f_{fld} analogous to that of Eq. 3-25. State clearly which variable must be held constant when the derivative is taken.
- By analogy to the derivation of Eqs. 3-26 to 3-33, derive an expression for the coenergy $W'_{\text{fld}}(v, x)$ and the corresponding force of electric origin.

3-21. A capacitor (Fig. 3-29) is made of two conducting plates of area A separated in air by a spacing x . The terminal voltage is v , and the charge on the plates is q . The capacitance C , defined as the ratio of charge to voltage, is

$$C = \frac{q}{v} = \frac{\epsilon_0 A}{x}$$

where ϵ_0 is the dielectric constant of free space (in SI units $\epsilon_0 = 8.85 \times 10^{-12}$ F/m).

- Using the results of Prob. 3-20, calculate the energy $W_{\text{fld}}(q, x)$ and the coenergy $W'_{\text{fld}}(v, x)$.
- The terminals of the capacitor are connected to a source of constant voltage V_0 . Calculate the force required to maintain the plates separated by a constant spacing $x = \delta$.

3-22. The magnetic circuit of Fig. 3-30 is similar to that of Fig. 3-21 (Prob. 3-6) with the addition of a second winding on the movable element. The movable element is constrained to motion such that the lengths of both air gaps remain equal.

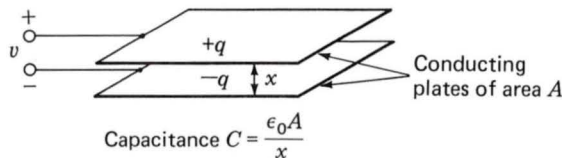


Fig. 3-29. Capacitor plates (Prob. 3-21).

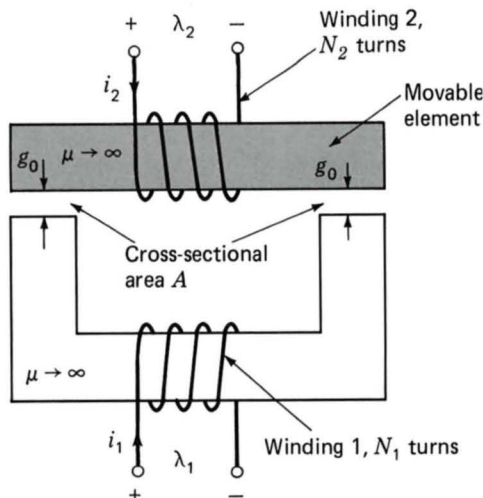


Fig. 3-30. Two-winding magnetic circuit for Prob. 3-22.

- Find the self-inductances of windings 1 and 2 in terms of the core dimensions and the number of turns.
- Find the mutual inductance between the two windings.
- Calculate the coenergy $W'_{\text{fld}}(i_1, i_2)$.
- Find an expression for the force acting on the movable element as a function of the winding currents.

3-23. Two coils, one mounted on a stator and the other on a rotor, have self- and mutual inductances of

$$L_{11} = 0.25 \text{ mH} \quad L_{22} = 0.15 \text{ mH} \quad L_{12} = 0.10 \cos \theta \quad \text{mH}$$

where θ is the angle between the axes of the coils. The coils are connected in series and carry a current

$$i = \sqrt{2}I \sin \omega t$$

- Derive an expression for the instantaneous torque T on the rotor as a function of the angular position θ .
- Give an expression for the time-averaged torque T_{av} as a function of θ .
- Compute the numerical value of T_{av} for $I = 10 \text{ A}$ and $\theta = 0^\circ$ and 90° .
- Sketch three curves of T_{av} versus θ for currents $I = 5, 7.07$, and 10 A .
- A helical restraining spring which tends to hold the rotor at $\theta = 90^\circ$ is now attached to the rotor. The restraining torque of the spring is proportional to the angular deflection from $\theta = 90^\circ$ and is

0.08 N · m when the rotor is turned to $\theta = 0$. Show on the curves of part (d) how you could find the angular position of the rotor-plus-spring combination for coil currents $I = 5, 7.07$, and 10 A. Sketch a curve showing θ versus I . A reasonable-looking sketch with estimated numerical values is all that is required.

Note: This problem illustrates the principles of the dynamometer-type ac ammeter.

3-24. Two windings, one mounted on a stator and the other on a rotor, have self- and mutual inductances of

$$L_{11} = 2.20 \text{ H} \quad L_{22} = 1.00 \text{ H} \quad L_{12} = 1.414 \cos \theta_0 \quad \text{H}$$

where θ_0 is the angle between the axes of the windings. The resistances of the windings may be neglected. Winding 2 is short-circuited, and the current in winding 1 as a function of time is $i_1 = 14.14 \sin \omega t$.

- If the rotor is stationary, derive an expression for the numerical value in newton-meters of the instantaneous torque on the rotor in terms of the angle θ_0 .
- Compute the average torque in newton-meters when $\theta_0 = 45^\circ$.
- If the rotor is allowed to move, will it rotate continuously or will it tend to come to rest? If the latter, at what value of θ_0 ?

3-25. A loudspeaker is made of a magnetic core of infinite permeability and circular symmetry, as shown in Fig. 3-31a and b. The air-gap length g is much less than the radius r_0 of the central core. The voice coil is constrained to move only in the x direction and is attached to the speaker cone, which is not shown in the figure. A constant radial magnetic field is produced in the air gap by a direct current in coil 1, $i_1 = I_1$. An audio-

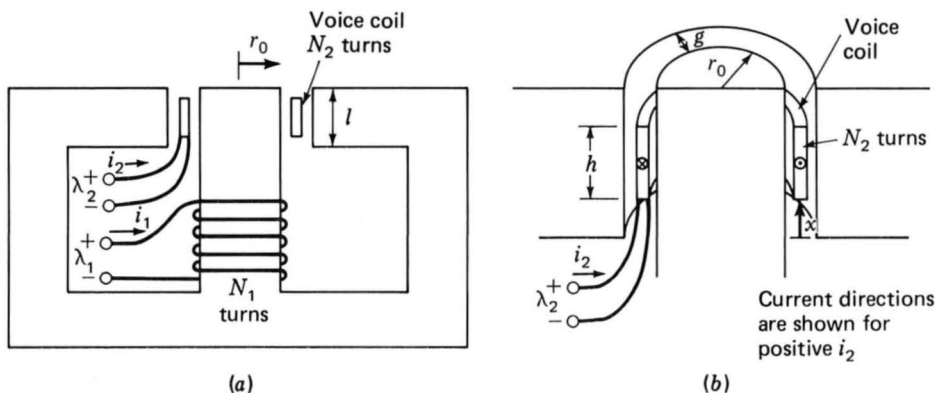


Fig. 3-31. Loudspeaker for Prob. 3-25.

frequency signal $i_2 = I_2 \cos \omega t$ is then applied to the voice coil. Assume the voice coil to be of negligible thickness and composed of N_2 turns uniformly distributed over its height h . Also assume that its displacement is such that it remains in the air gap ($0 \leq x \leq l - h$).

- Calculate the force on the voice coil, using the Lorentz law as in Example 3-1.
- Calculate the self-inductance of each coil.
- Calculate the mutual inductance between the coils. *Hint:* Assume that current is applied to the voice coil, and calculate the flux linkages of coil 1. Note that these flux linkages vary with the displacement x .
- Calculate the force on the voice coil from the coenergy W'_{fld} .

3-26. Repeat Example 3-6 with the samarium cobalt magnet replaced by neodymium-iron-boron.

3-27. The magnetic structure of Fig. 3-32 is a schematic view of a system designed to support a block of magnetic material ($\mu \rightarrow \infty$) of mass M against the force of gravity. The system includes a permanent magnet and a winding. Under normal conditions, the force is supplied by the permanent magnet alone. The function of the winding is to counteract the field produced by the permanent magnet so that the mass can be removed from the device. The system is designed such that the air gaps at each side of the mass remain constant at length $g_0/2$.

Assume that the permanent magnet can be represented by a linear characteristic of the form

$$B_m = \mu_R(H_m - H_c)$$

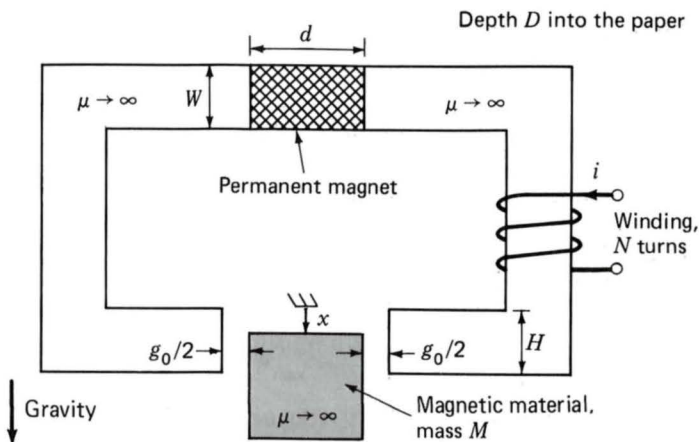


Fig. 3-32. Magnetic support system for Prob. 3-27.

and that the winding direction is such that positive winding current reduces the air-gap flux produced by the permanent magnet. Neglect the effects of magnetic fringing.

- (a) Assume the winding current to be zero.
 - (i) Find the force f_{fld} acting on the mass in the x direction due to the permanent magnet alone as a function of x ($0 \leq x \leq H$).
 - (ii) Find the maximum mass M_{max} that can be supported against gravity for $0 \leq x \leq H$.
- (b) For $M = M_{max}/2$, find the minimum current required to ensure that the mass will fall out of the system when the current is applied.

3-28. Winding 1 in the loudspeaker of Prob. 3-25 (Fig. 3-31) is replaced by a permanent magnet as shown in Fig. 3-33. The magnet can be represented by the linear characteristic $B_m = \mu_R(H_m - H_c)$.

- (a) Assuming the voice coil current to be zero, ($i_2 = 0$), calculate the magnetic flux density in the air gap.
- (b) Calculate the flux linkage of the voice coil due to the permanent magnet as a function of the displacement x .
- (c) Calculate the coenergy $W'_{fld}(i_2, x)$ assuming that the voice coil current is sufficiently small so that the component of W'_{fld} due to the voice coil self inductance can be ignored.
- (d) Calculate the force on the voice coil.

3-29. The plunger of a solenoid is connected to a spring. The spring force is given by $f = -K_0(x - 2a)$, where x is the air-gap length. The inductance of the solenoid is of the form $L = L_0(a - x)$, and its winding resistance is R .

The plunger is initially at position $x = a/2$ when a dc voltage of magnitude V_0 is applied to the solenoid.

- (a) Find an expression for the force as a function of time required to hold the plunger at position $a/2$.

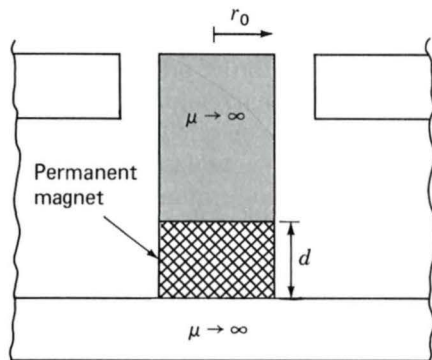


Fig. 3-33. Central core of loudspeaker of Fig. 3-31 with winding 1 replaced by a permanent magnet (Prob. 3-28).

- (b) If the plunger is then released and allowed to come to equilibrium, find the equilibrium position X_0 . You may assume that this position falls in the range $0 \leq X_0 \leq a$.

3-30. Consider the solenoid system of Prob. 3-29. Assume the following parameter values:

$$L_0 = 0.5 \text{ mH/cm} \quad a = 2 \text{ cm} \quad R = 1 \, \Omega \quad K_0 = 0.25 \text{ N/cm}$$

The plunger has mass $M = 0.1 \text{ kg}$. Assume the coil to be connected to a dc source of magnitude 5 A. Neglect any effects of gravity.

- (a) Find the equilibrium displacement X_0 .
- (b) Write the dynamic equations of motion for the system.
- (c) Linearize these dynamic equations for incremental motion of the system around its equilibrium position.
- (d) If the plunger is displaced by an incremental distance ε from its equilibrium position X_0 and released at time $t = 0$, find
 - (i) the resultant motion of the plunger as a function of time
 - (ii) the corresponding time-varying component of current induced across the coil terminals

3-31. The solenoid of Prob. 3-30 is now connected to a dc voltage source of magnitude 5 V.

- (a) Find the equilibrium displacement X_0 .
- (b) Write the dynamic equations of motion for the system.
- (c) Linearize these dynamic equations for incremental motion of the system around its equilibrium position.

3-32. Consider the single-coil rotor of Example 3-1. Assume the rotor winding to be carrying a constant current of $I = 10 \text{ A}$ and the rotor to have a moment of inertia $J = 0.25 \text{ kg} \cdot \text{m}^2$.

- (a) Find the equilibrium position of the rotor. Is it stable?
- (b) Write the dynamic equations for the system.
- (c) Find the natural frequency in hertz for incremental rotor motion around this equilibrium position.

3-33. Consider a solenoid magnet similar to that of Example 3-7 (Fig. 3-18) except that the length of the cylindrical plunger is reduced to $a + h$. Derive the dynamic equations of motion of the system.

3-34. The following dimensions and data apply to the solenoid magnet of Prob. 3-33:

$$a = 2 \text{ cm} \quad h = 6 \text{ cm} \quad d = 2.2 \text{ cm} \quad g = 0.06 \text{ cm}$$

$$\text{Turns } N = 1200 \quad \text{Coil resistance } R = 100 \, \Omega$$

$$\text{Mass of plunger } M = 0.25 \, \text{kg} \quad \text{Spring constant } K = 6.25 \, \text{N/cm}$$

With $i = 0$, the plunger is at rest at $x = 0.25 \, \text{cm}$. The external applied force is zero, and friction is negligible. A voltage with a quiescent value of $10 \, \text{V}$ is applied to the coil.

- (a) Find the quiescent operating point. Is it stable?
- (b) Linearize the dynamic equations of motion for small incremental changes in the applied voltage. Give numerical values for the parameters in SI units.

4

Rotating Machines: Basic Concepts

The object of this chapter is to discuss the techniques and approximations involved in reducing a physical machine to a simple mathematical model and to give some simple concepts relating to the basic machine types. The models developed in this chapter are sufficient to illustrate the basic principles involved. Later chapters will refine these models into various forms applicable to the analysis of practical engineering situations.

4-1 ELEMENTARY CONCEPTS

Faraday's law (Eq. 1-21), $e = d\lambda/dt$, describes quantitatively the induction of voltages by a time-varying magnetic field. Electromagnetic energy conversion takes place when the change in flux is associated with mechanical motion. In rotating machines, voltages are generated in windings or

groups of coils by rotating these windings mechanically through a magnetic field, by mechanically rotating a magnetic field past the winding, or by designing the magnetic circuit so that the reluctance varies with rotation of the rotor. By any of these methods the flux linking a specific coil is changed cyclically, and a time-varying voltage is generated. A group of such coils interconnected so that their generated voltages all make a positive contribution to the desired result is called an *armature winding*. The armature of a dc machine is shown in Fig. 4-1; the armature is the rotating member, or *rotor*. Figure 4-2 shows the armature of an ac machine, in this case a synchronous generator. Here the armature is the stationary member, or *stator*.

In general, these coils are wound on iron cores. This is done to maximize the coupling between the coils, to increase the magnetic energy density associated with the electromechanical interaction, and to shape and distribute the magnetic fields according to the requirements of each particular machine design. Because the armature iron is subjected to a time-varying magnetic flux, eddy currents will be induced in it. To minimize this eddy-current loss, the armature iron is built up of thin laminations, as illustrated in Fig. 4-3 for the armature of an ac machine. The magnetic cir-

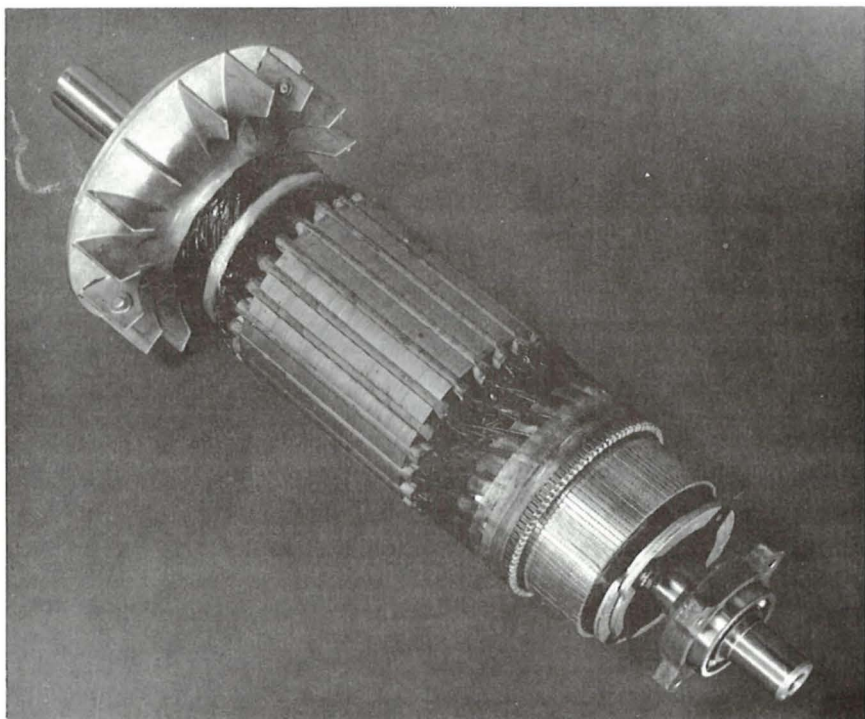


Fig. 4-1. Armature of a dc motor. (General Electric Company.)

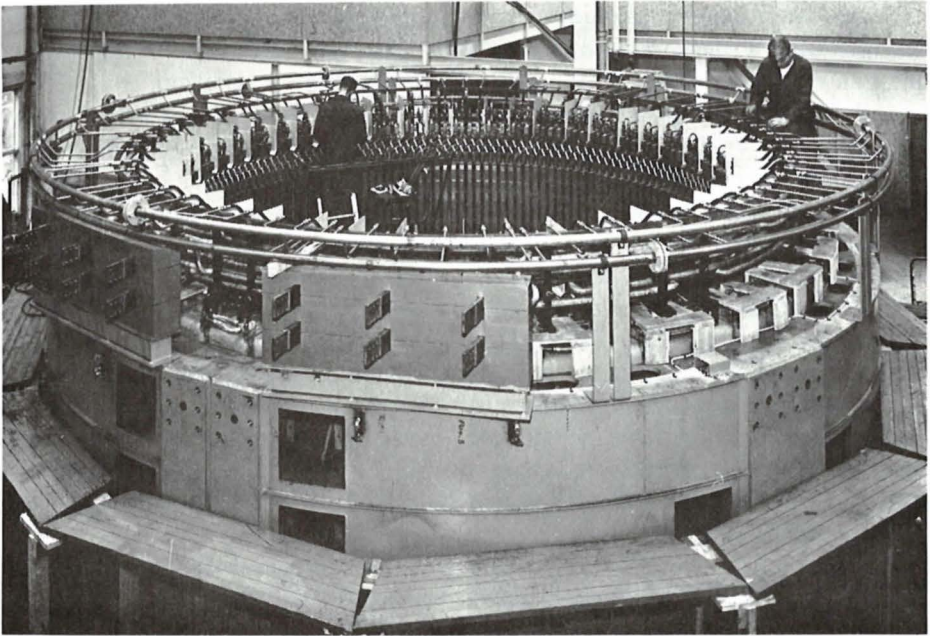


Fig. 4-2. Stator of a 190-MVA three-phase 12-kV 375-r/min hydroelectric generator. The conductors have hollow passages through which cooling water is circulated. (Brown Boveri Corporation.)

cuit is completed through the iron of the other machine member, and excitation coils, or *field windings*, may be placed on that member to act as the primary source of flux. Permanent magnets may be used in small machines, and developments in permanent magnet technology are resulting

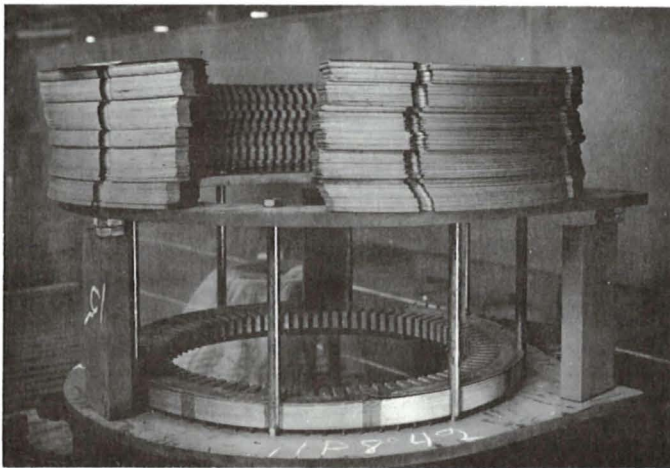


Fig. 4-3. Partially completed stator core for an ac motor. (Westinghouse Electric Corporation.)

in their use in larger machines. In variable reluctance machines, there are no windings on the rotor, and operation depends on the nonuniformity of air-gap reluctance associated with variations in rotor position.

Rotating electric machines take many forms and are known by many names—dc, synchronous, permanent magnet, induction, variable reluctance, hysteresis, etc. Although these machines appear to be quite dissimilar and require a variety of analytical techniques, the physical principles governing their behavior are quite similar, and in fact these machines can often be explained from the same physical picture. For example, analysis of a dc machine shows that associated with both the rotor and the stator are magnetic flux distributions which are fixed in space and that the torque-producing characteristic of the dc machine stems from the tendency of these flux distributions to align. An induction machine, in spite of many fundamental differences, works on exactly the same principle; one can identify flux distributions associated with the rotor and stator, which rotate in synchronism and which are separated by some torque-producing angular displacement.

Although mathematical analytical techniques and models are essential to the analysis of electric machines, physical insight is a very useful engineering tool for the analysis and application of these devices. One object of this and subsequent chapters is to guide the reader in the development of such insight.

4-2 INTRODUCTION TO AC AND DC MACHINES

a. Elementary Synchronous Machines

Preliminary ideas of generator action can be gained by discussing the armature-induced voltage in the very much simplified ac synchronous generator shown in Fig. 4-4. With rare exceptions, the armature winding of a synchronous machine is on the stator, and the field winding is on the rotor, as in Fig. 4-4. The field winding is excited by direct current conducted to it by means of carbon *brushes* bearing on *slip rings* or *collector rings*. Constructional factors usually dictate this orientation of the two windings: it is advantageous to have the low-power field winding on the rotor. The armature winding, consisting here of a single coil of N turns, is indicated in cross section by the two coil sides a and $-a$ placed in diametrically opposite narrow slots on the inner periphery of the stator of Fig. 4-4. The conductors forming these coil sides are parallel to the shaft of the machine and are connected in series by end connections (not shown in the figure). The rotor is turned at a constant speed by a source of mechanical power connected to its shaft. Flux paths are shown schematically by dashed lines in Fig. 4-4.

An idealized radial distribution of the air-gap flux density B is shown in Fig. 4-5a as a function of the space angle θ around the air-gap periphery. The flux-density wave of practical machines can be made to approximate a

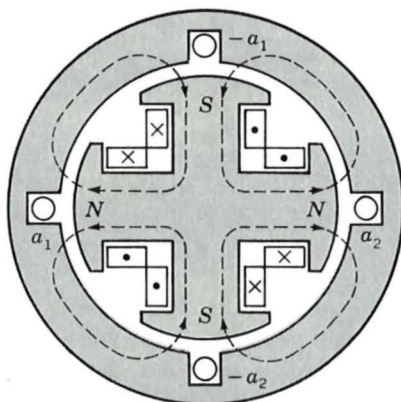


Fig. 4-6. Elementary four-pole synchronous generator.

When a machine has more than two poles, it is convenient to concentrate on a single pair of poles and to recognize that the electric, magnetic, and mechanical conditions associated with every other pole pair are repetitions of those for the pair under consideration. For this reason it is convenient to express angles in *electrical degrees* or *electrical radians* rather than in mechanical units. One pair of poles in a P -pole machine or one cycle of flux distribution equals 360 electrical degrees or 2π electrical radians. Since there are $P/2$ complete wavelengths or cycles in one complete revolution, it follows that

$$\theta = \frac{P}{2} \theta_m \quad (4-1)$$

where θ is the angle in electrical units and θ_m is the mechanical angle. The coil voltage of a P -pole machine passes through a complete cycle every time a pair of poles sweeps by, or $P/2$ times each revolution. The frequency of the voltage wave is therefore

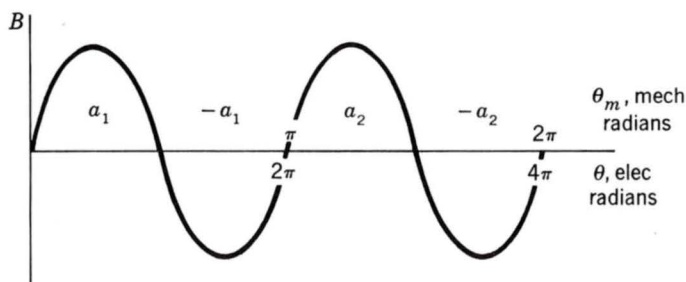


Fig. 4-7. Space distribution of flux density in a four-pole synchronous generator.

$$f = \frac{P}{2} \frac{n}{60} \quad \text{Hz} \quad (4-2)$$

where n is the mechanical speed in revolutions per minute and $n/60$ is the speed in revolutions per second. The frequency ω of the voltage wave in radians per second is

$$\omega = \frac{P}{2} \omega_m \quad (4-3)$$

where ω_m is the mechanical speed in radians per second.

The rotors shown in Figs. 4-4 and 4-6 have *salient*, or projecting, *poles* with *concentrated windings*. Figure 4-8 shows diagrammatically a *non-salient-pole*, or *cylindrical*, rotor. The field winding is a *distributed winding* placed in slots and arranged to produce an approximately sinusoidal two-pole field. The reason that some synchronous generators have salient-pole rotor structures and others have cylindrical rotors can be appreciated with the help of Eq. 4-2. Most power systems in the United States operate at a frequency of 60 Hz. A salient-pole construction is characteristic of hydroelectric generators because hydraulic turbines operate at relatively low speeds and a relatively large number of poles are required to produce the desired frequency; the salient-pole construction is better adapted mechanically to this situation. The rotor of a large hydroelectric generator is shown in Fig. 4-9. Steam turbines and gas turbines, however, operate best at relatively high speeds, and turbine-driven alternators or turbine generators are commonly two- or four-pole cylindrical-rotor machines. The rotors are made from a single steel forging or from several forgings, as shown in Figs. 4-10 and 4-11.

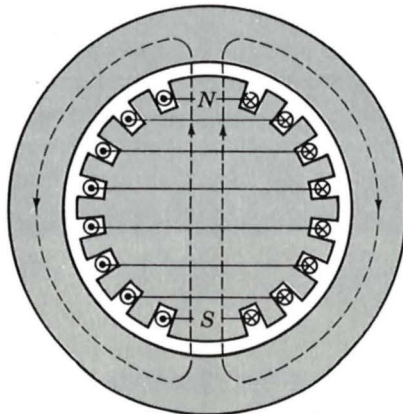


Fig. 4-8. Elementary two-pole cylindrical-rotor field winding.

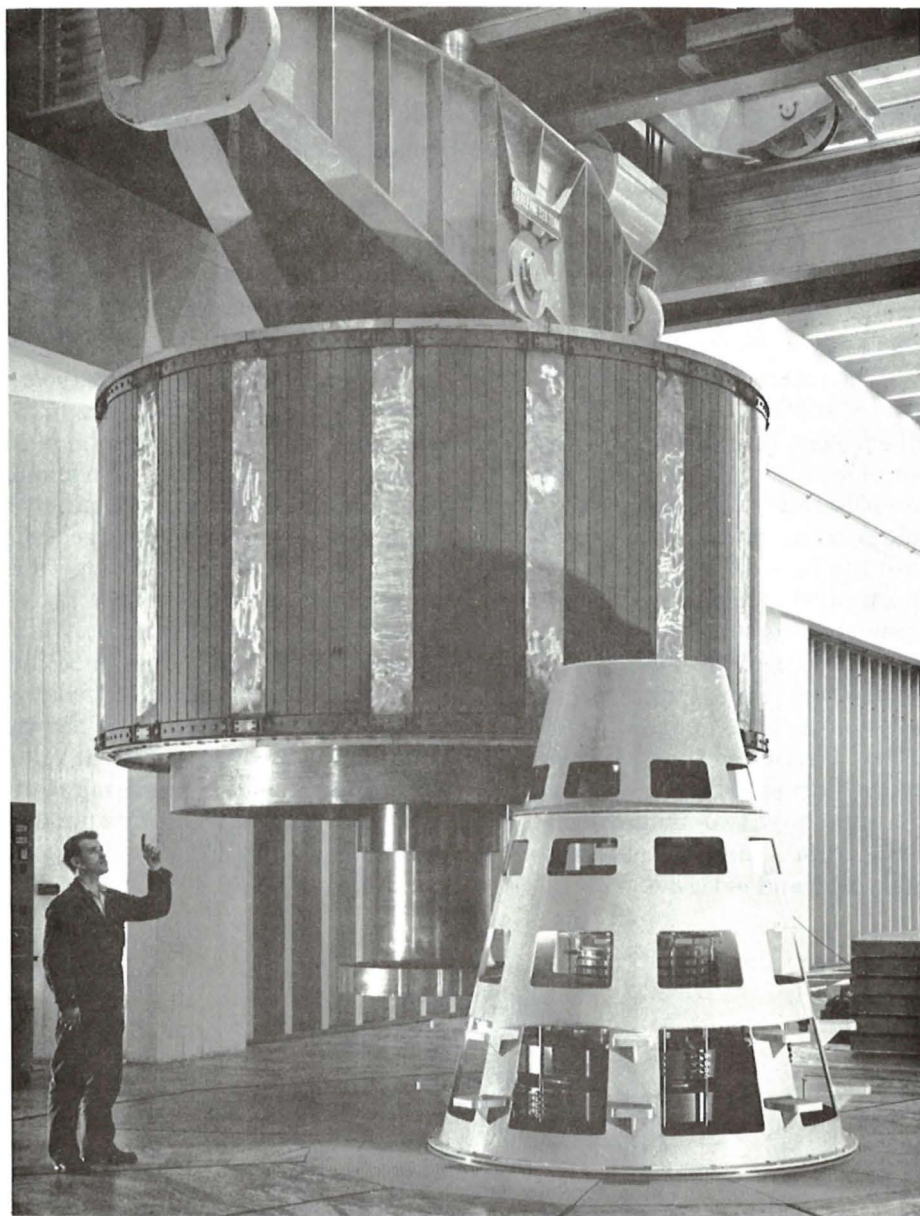


Fig. 4-9. Water-cooled rotor of the 190-MVA hydroelectric generator whose stator is shown in Fig. 4-2. (*Brown Boveri Corporation.*)

With very few exceptions, synchronous generators are three-phase machines because of advantages of three-phase systems for generation, transmission, and heavy-power utilization. For the production of a set of three

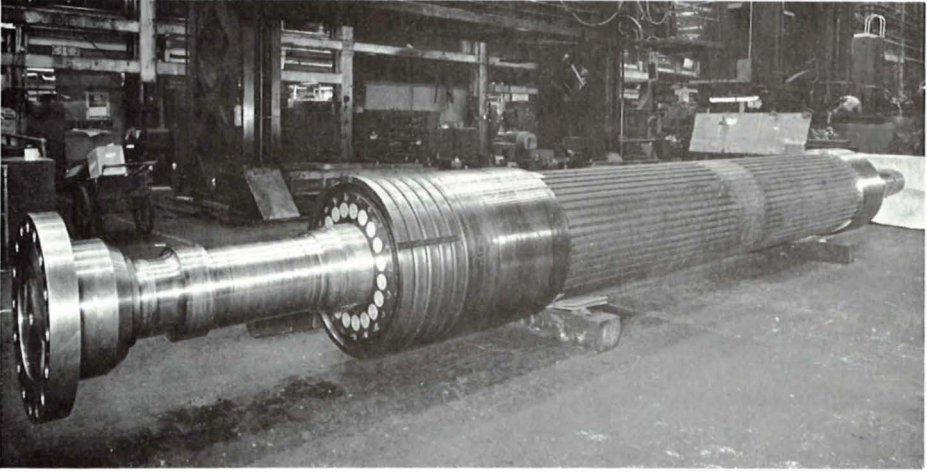


Fig. 4-10. Rotor of a two-pole 3600 r/min turbine generator. (*Westinghouse Electric Corporation.*)

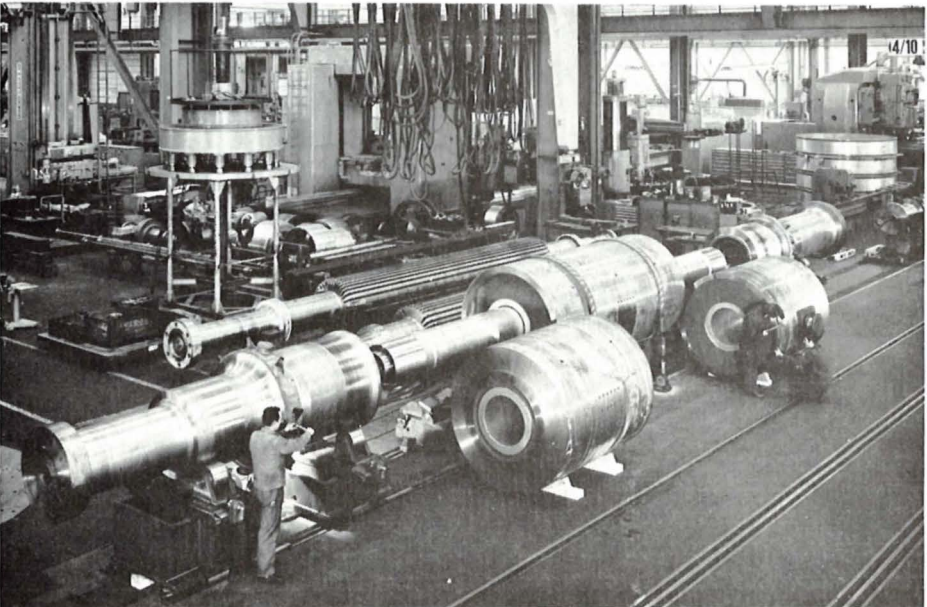


Fig. 4-11. Parts of multipiece rotor for a 1333-MVA three-phase 1800 r/min turbine generator. The separate forgings will be shrunk on the shaft before final machining and milling slots for the windings. The total weight of the rotor is 435,000 lb. (*Brown Boveri Corporation.*)

voltages phase-displaced by 120 electrical degrees in time, it follows that a minimum of three coils phase-displaced 120 electrical degrees in space must be used. An elementary three-phase two-pole machine with one coil

per phase is shown in Fig. 4-12a. The three phases are designated by the letters a , b , and c . In an elementary four-pole machine, a minimum of two such sets of coils must be used, as illustrated in Fig. 4-12b; in an elementary P -pole machine, $P/2$ such sets must be used. The two coils in each phase of Fig. 4-12b are connected in series so that their voltages add, and the three phases may then be either Y- or Δ -connected. Figure 4-12c shows how the coils may be interconnected to form a Y connection.

When a synchronous generator supplies electric power to a load, the armature current creates a magnetic flux wave in the air gap which rotates at synchronous speed, as shown in Art. 4-5. This flux reacts with the flux created by the field current, and electromagnetic torque results from the tendency of these two magnetic fields to align. In a generator this torque opposes rotation, and mechanical torque must be applied from the prime mover to sustain rotation. This electromagnetic torque is the mechanism through which the synchronous generator converts mechanical to electric energy.

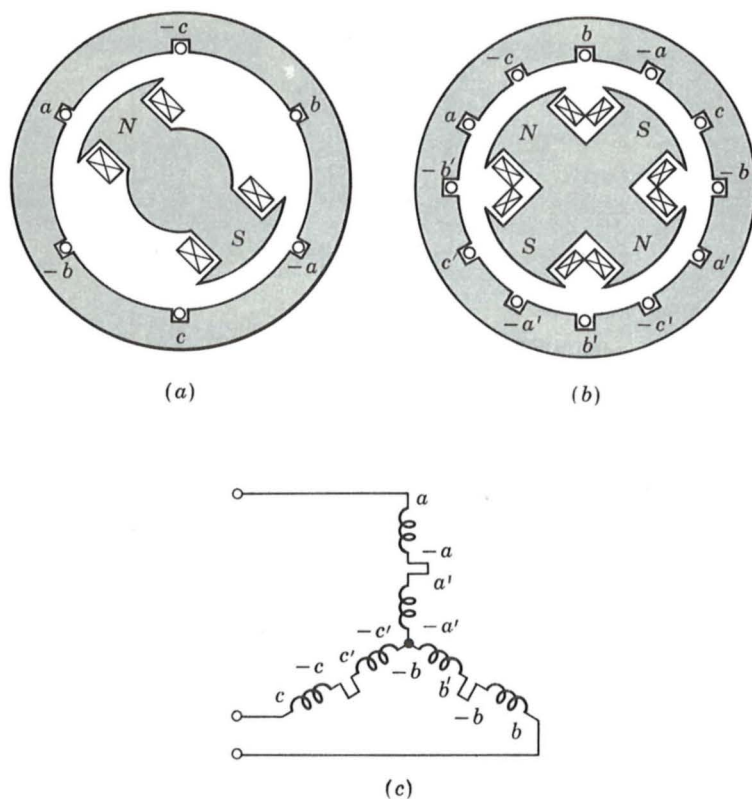


Fig. 4-12. Elementary three-phase generators: (a) two-pole, (b) four-pole, and (c) Y connection of the windings.

The counterpart of the synchronous generator is the *synchronous motor*. A cutaway view of a three-phase 60-Hz synchronous motor is shown in Fig. 4-13. Alternating current is supplied to the armature winding (usually the stator), and dc excitation is supplied to the field winding (usually the rotor). The magnetic field of the armature currents rotates at synchronous speed. To produce a steady electromagnetic torque, the magnetic fields of the stator and rotor must be constant in amplitude and stationary with respect to each other. In a synchronous motor, the steady-state speed is determined by the number of poles and the frequency of the armature current, exactly as in Eq. 4-2 or 4-3 for a synchronous generator. Thus a synchronous motor operated from a constant-frequency ac source must run at a constant steady-state speed.

In a motor the electromagnetic torque is in the direction of rotation and balances the opposing torque required to drive the mechanical load. The flux produced by currents in the armature of a synchronous motor rotates ahead of that produced by the field, thus pulling on the field and doing work. This is the opposite of the situation in a synchronous genera-

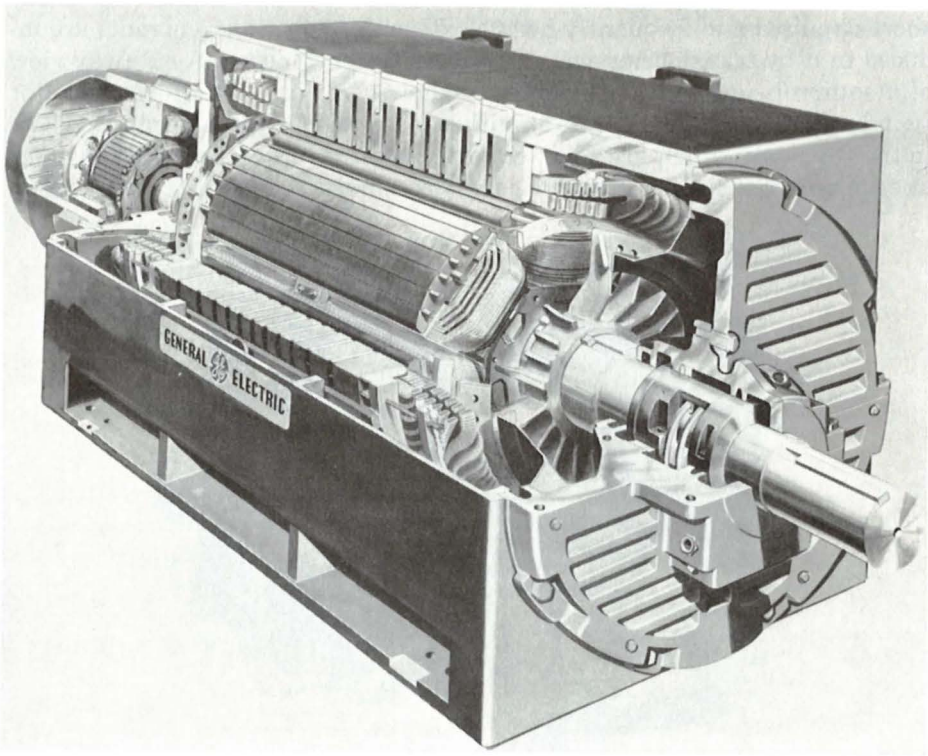


Fig. 4-13. Cutaway view of a high-speed synchronous motor. The excitor shown on the left end of the rotor is a small ac generator with a rotating semiconductor rectifier assembly. (General Electric Company.)

tor, where the field does work as its flux pulls on that of the armature, which is lagging behind. In both generators and motors, an electromagnetic torque and a rotational voltage are produced. These are the essential phenomena for electromechanical energy conversion.

b. Elementary Induction Machines

A second type of ac machine is the *induction machine*, in which there are alternating currents in both the stator and rotor windings. The most common example is the induction motor, in which alternating current is supplied directly to the stator and by induction, i.e., transformer action, to the rotor. The induction machine may be regarded as a generalized transformer in which electric power is transformed between rotor and stator together with a change of frequency and a flow of mechanical power. Although the induction motor is the most common of all motors, it is seldom used as a generator; its performance characteristics as a generator are unsatisfactory for most applications. The induction machine may also be used as a frequency changer.

In the induction motor, the stator winding is essentially the same as that of a synchronous machine. However, the rotor winding is electrically short-circuited and frequently has no external connections; currents are induced in it by transformer action from the stator winding. A cutaway view of a squirrel-cage induction motor is shown in Fig. 4-14. Here the rotor "windings" are actually solid aluminum bars which are cast into the slots in the rotor and which are short-circuited together by cast aluminum rings at each end of the rotor. This type of rotor construction results in induction

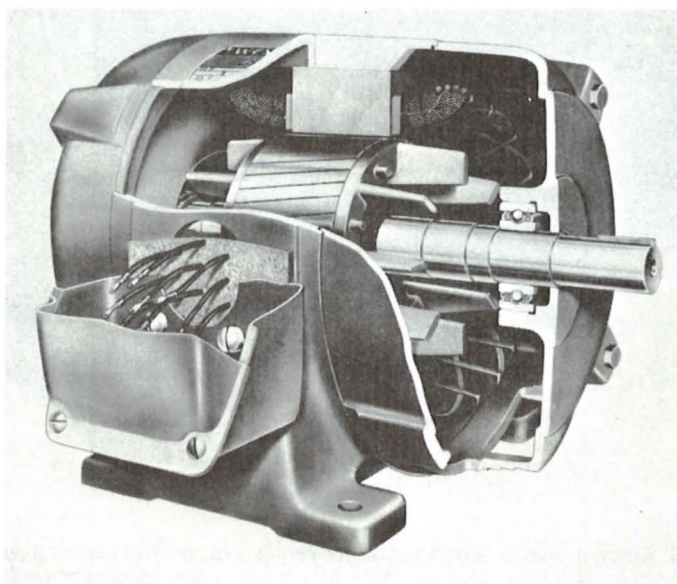


Fig. 4-14. Cutaway view of a squirrel-cage induction motor. (Westinghouse Electric Corporation.)

motors which are relatively inexpensive and highly reliable, factors contributing to their immense popularity and widespread application.

As in a synchronous motor, the armature flux in the induction motor leads that of the rotor and produces an electromagnetic torque. It is essential to recognize that the rotor and stator fluxes rotate in synchronism with each other and that this torque is related to the relative displacement between them. However, unlike a synchronous machine, the rotor does not itself rotate synchronously; it is the slipping of the rotor through the synchronous armature flux that gives rise to the induced rotor currents and hence the torque. An induction motor operates at some speed less than the synchronous mechanical speed of Eq. 4-3. A typical speed-torque characteristic for an induction motor is shown in Fig. 4-15.

c. Elementary DC Machines

The armature winding of a dc generator is on the rotor with current conducted from it by means of carbon brushes. The field winding is on the stator and is excited by direct current. A cutaway view of a dc motor is shown in Fig. 4-16.

A very elementary two-pole dc generator is shown in Fig. 4-17. The armature winding, consisting of a single coil of N turns, is indicated by the two coil sides a and $-a$ placed at diametrically opposite points on the rotor with the conductors parallel to the shaft. The rotor is normally turned at a constant speed by a source of mechanical power connected to the shaft. The air-gap flux distribution usually approximates a flat-topped wave, rather than the sine wave found in ac machines, and is shown in Fig. 4-18a. Rotation of the coil generates a coil voltage which is a time function having the same waveform as the spatial flux-density distribution.

Although the ultimate purpose is the generation of a direct voltage, the voltage induced in an individual armature coil is an alternating voltage, which must therefore be rectified. Rectification is sometimes provided externally, e.g., by semiconductor rectifiers. The machine then is an ac generator plus external rectifiers. In the conventional dc machine, rectifi-

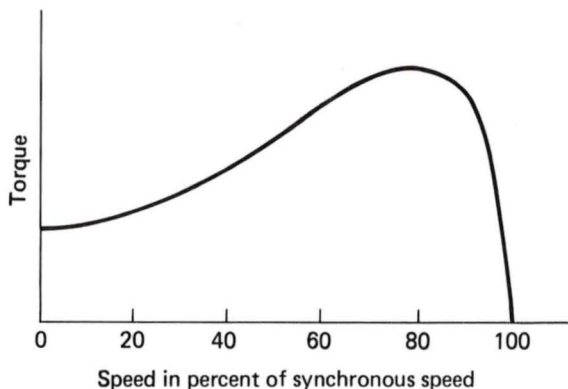


Fig. 4-15. Typical induction-motor speed-torque characteristic.

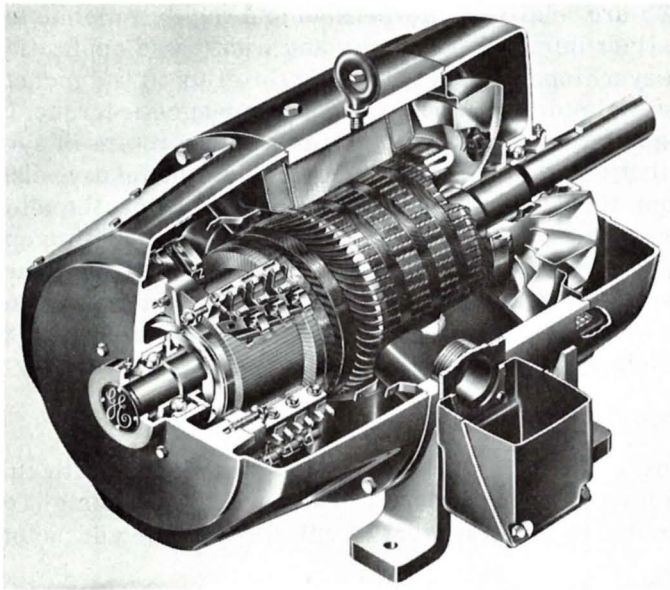


Fig. 4-16. Cutaway view of a typical integral-horsepower dc motor. (General Electric Company.)

cation is provided mechanically by means of a *commutator*, which is a cylinder formed of copper segments insulated from each other by mica and mounted on, but insulated from, the rotor shaft. Stationary carbon brushes held against the commutator surface connect the winding to the external armature terminals. The commutator and brushes can readily be seen in Fig. 4-16. The need for commutation is the reason why the armature windings of dc machines are placed on the rotor.

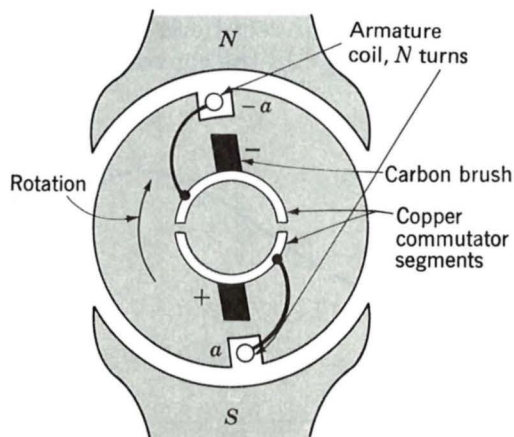


Fig. 4-17. Elementary dc machine with commutator.

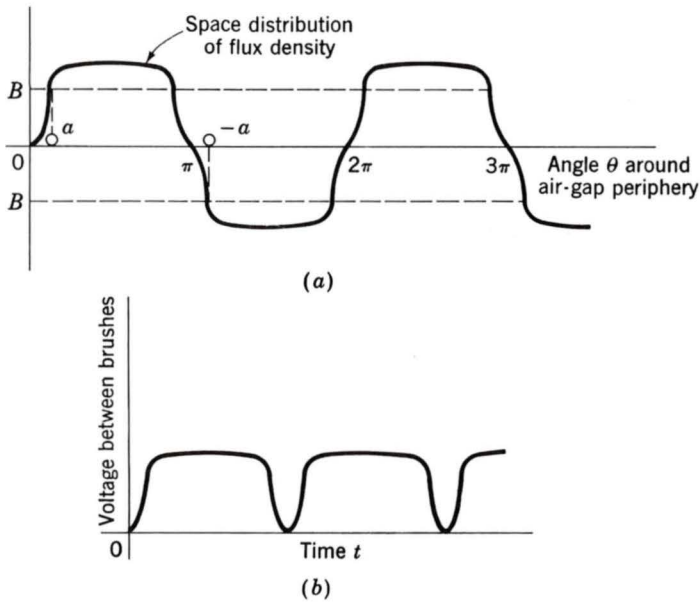


Fig. 4-18. (a) Space distribution of air-gap flux density in an elementary dc machine; (b) waveform of voltage between brushes.

For the elementary dc generator, the commutator takes the form shown in Fig. 4-17. For the direction of rotation shown, the commutator at all times connects the coil side which is under the south pole to the positive brush and that under the north pole to the negative brush. The commutator provides full-wave rectification, transforming the voltage waveform between brushes to that of Fig. 4-18b and making available a unidirectional voltage to the external circuit. The dc machine of Fig. 4-17 is, of course, simplified to the point of being unrealistic in the practical sense, and later it will be essential to examine the action of more realistic commutators.

The effect of direct current in the field winding of a dc machine is to create a magnetic flux distribution which is stationary with respect to the stator. Similarly, the effect of the commutator is such that when direct current flows through the brushes, the armature creates a magnetic flux distribution which is also fixed in space and whose axis, determined by the design of the machine and the position of the brushes, is typically perpendicular to the axis of the field flux. Just as in the ac machines discussed previously, it is the interaction of these two flux distributions that creates the torque of the dc machine. If the machine is acting as a generator, this torque opposes rotation. If it is acting as a motor, the electromagnetic torque acts in the direction of the rotation. Remarks similar to those already made concerning the roles played by the generated voltage and electromagnetic torque in the energy conversion process in synchronous machines apply equally well to dc machines.

4-3 MMF OF DISTRIBUTED WINDINGS

Most armatures have distributed windings, i.e., windings which are spread over a number of slots around the air-gap periphery, as in Figs. 4-1 and 4-2. The individual coils are interconnected so that the result is a magnetic field having the same number of poles as the field winding.

The study of the magnetic fields of distributed windings can be approached by study of the magnetic field of the single N -turn coil which spans 180 electrical degrees and is defined as a *full-pitch coil*, as shown in Fig. 4-19a. The dots and crosses indicate current toward and away from the reader, respectively. For simplicity, a concentric cylindrical rotor is shown. The general nature of the magnetic field produced by the current in the coil is shown by the dashed lines in Fig. 4-19a. Since the permeability of the armature and field iron is much greater than that of air, it is sufficiently accurate for our present purposes to assume that all the reluctance of the magnetic circuit is in the two air gaps. From symmetry of the structure it is evident that the magnetic field intensity H in the air gap at angle θ under one pole is the same in magnitude as that at $\theta + \pi$ under the opposite pole, but the fields are in the opposite direction.

As discussed in Art. 1-1, the mmf \mathcal{F} of any closed path in a magnetic circuit is defined by Eq. 1-5 as the net ampere-turns Ni enclosed by that path. The usefulness of the concept of mmf stems from the fact that in

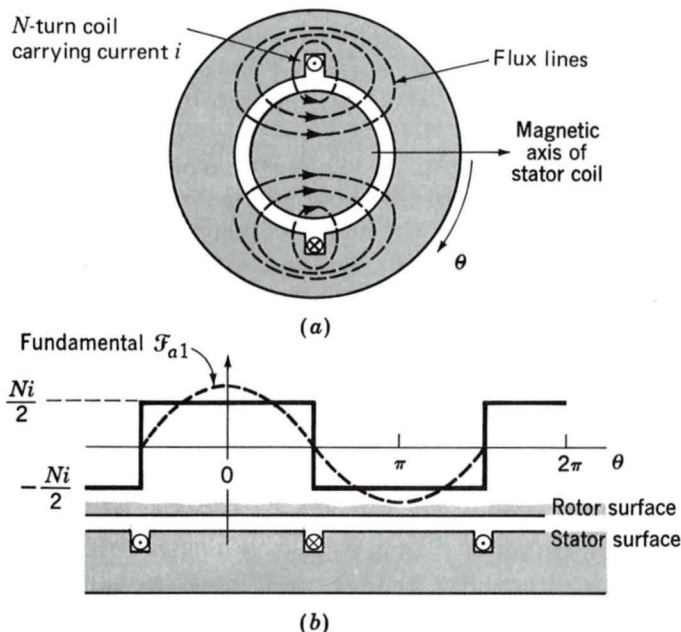


Fig. 4-19. The mmf of a concentrated full-pitch coil.

well-defined magnetic circuits mmf can be associated with various portions of a path in such a fashion that it is related by some simple geometric coefficient to the magnetic field intensity which exists over that portion of the path.

Around any of the closed paths shown by the flux lines in Fig. 4-19a the mmf is Ni . The assumption that all the reluctance of this magnetic circuit is in the air gap leads to the result that the line integral of \mathbf{H} inside the iron is negligibly small, and thus it is reasonable to neglect the mmf drops associated with portions of the magnetic circuit inside the iron. Symmetry has shown that the air-gap \mathbf{H} fields on opposite sides of the rotor are equal in magnitude but opposite in direction. It follows that the air-gap mmf should be similarly distributed.

Figure 4-19b shows the air gap and winding in developed form, i.e., laid out flat. The air-gap mmf distribution is shown by the steplike distribution of amplitude $\pm Ni/2$. On the assumption of narrow slot openings, the mmf jumps abruptly by Ni in crossing from one side to the other of a coil. This mmf distribution is discussed again in Art. 4-4, where the resultant magnetic fields are evaluated.

a. AC Machines

In the design of ac machines, serious efforts are made to distribute the winding so as to produce a close approximation to a sinusoidal space distribution of mmf. We focus attention on the fundamental component.

The rectangular mmf wave of the concentrated full-pitch coil of Fig. 4-19b can be resolved into a Fourier series comprising a fundamental component and a series of odd harmonics. The fundamental component \mathcal{F}_{a1} is

$$\mathcal{F}_{a1} = \frac{4}{\pi} \frac{Ni}{2} \cos \theta \quad (4-4)$$

where θ is measured from the magnetic axis of the stator coil, as shown by the dashed sinusoid in Fig. 4-19b. It is a sinusoidal space wave of amplitude

$$F_{1,\text{peak}} = \frac{4}{\pi} \frac{Ni}{2} \quad (4-5)$$

with its peak aligned with the magnetic axis of the coil.

Now consider the effect of distributing a winding in several slots. For example, Fig. 4-20a shows phase a of the armature winding of a somewhat simplified two-pole three-phase ac machine. Phases b and c occupy the empty slots. The windings of the three phases are identical and are located with their magnetic axes 120 electrical degrees apart. We direct attention to the mmf of phase a alone, postponing the discussion of the effects of all three phases until Art. 4-5. The winding is arranged in two layers, each

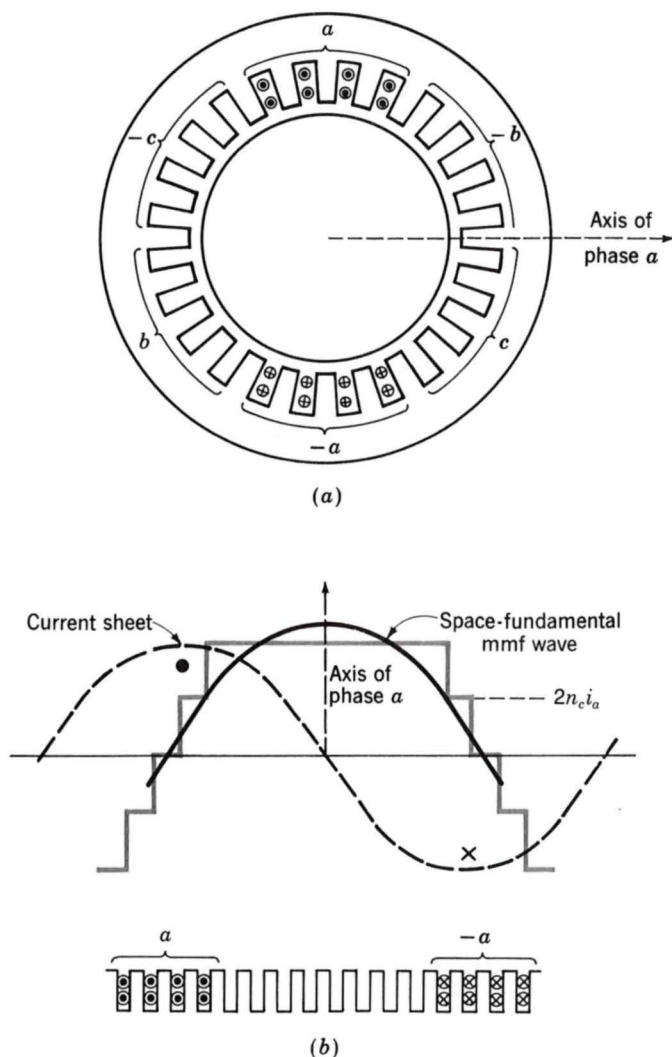


Fig. 4-20. The mmf of one phase of a distributed two-pole three-phase winding with full-pitch coils.

coil of n_c turns having one side in the top of a slot and the other coil side in the bottom of a slot a pole pitch away. The two-layer arrangement simplifies the geometric problem of getting the end turns of the individual coils past each other.

Figure 4-20b shows one pole of this winding laid out flat. The mmf wave is a series of steps each of height $2n_c i_a$ equal to the ampere-conductors in the slot, where i_a is the winding current. Its space-fundamental component is shown by the sinusoid. It can be seen that the distributed winding pro-

duces a closer approximation to a sinusoidal mmf wave than the concentrated coil of Fig. 4-19.

The resultant fundamental mmf wave of a distributed winding is less than the sum of the fundamental components of the individual coils because the magnetic axes of the individual coils are not aligned with the resultant. The modified form of Eq. 4-4 for a distributed P -pole winding having N_{ph} series turns per phase is

$$\mathcal{F}_{a1} = \frac{4}{\pi} k_w \frac{N_{ph}}{P} i_a \cos \theta \quad (4-6)$$

in which the factor $4/\pi$ arises from the Fourier-series analysis of the sawtooth mmf wave of a concentrated full-pitch coil, as in Eq. 4-4, and the *winding factor* k_w takes into account the distribution of the winding. The factor $k_w N_{ph}$ is the effective series turns per phase for the fundamental mmf. (See Appendix B for details.) Through the use of fractional-pitch coils and other artifices the effects of space harmonics in ac machines can be made small.

Equation 4-6 describes the space-fundamental component of the mmf wave produced by current in phase a . It is equal to the mmf wave produced by a finely divided sinusoidally distributed current sheet placed on the inner periphery of the stator, as shown by the sine wave labeled "Current sheet" in Fig. 4-20*b*. This component of the mmf is a standing wave whose *spatial* distribution around the periphery is described by $\cos \theta$. Its peak is along the magnetic axis of phase a , and its peak amplitude is proportional to the instantaneous current i_a . Accordingly, if the current $i_a = I_m \cos \omega t$, the *time* maximum of the peak is

$$F_{\max} = \frac{4}{\pi} k_w \frac{N_{ph}}{P} I_m \quad (4-7)$$

In Art. 4-5 we study the effect of currents in all three phases.

In a directly analogous fashion, rotor windings are often distributed in slots to reduce the effects of space harmonics. Figure 4-21*a* shows the rotor of a typical two-pole round-rotor generator. Although the winding is symmetric with respect to the rotor axis, the number of turns per slot can be varied to control the various harmonics. In Fig. 4-21*b* there are fewer turns in the slots nearest the pole face. In addition, the designer can vary the spacing of the slots. As for distributed armature windings, the fundamental mmf wave of a P -pole rotor winding \mathcal{F}_{r1} can be expressed in terms of the total number of turns N_r , the winding current I_r , and a winding factor k_r , as

$$\mathcal{F}_{r1} = \frac{4}{\pi} k_r \frac{N_r}{P} I_r \cos \theta \quad (4-8)$$

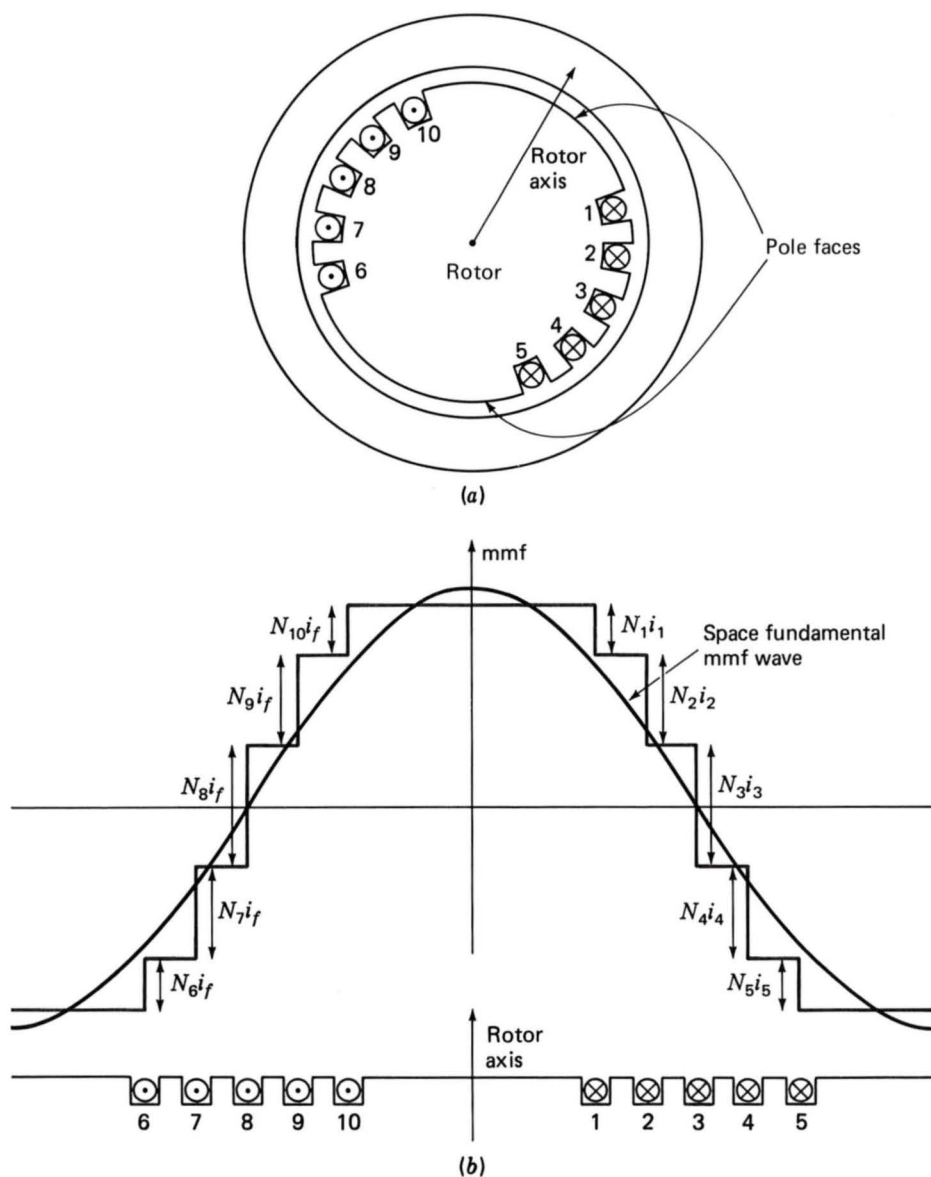


Fig. 4-21. The mmf of a distributed winding on the rotor of a round-rotor generator.

Its peak amplitude is

$$F_{1,\text{peak}} = \frac{4}{\pi} k_r \frac{N_r}{P} I_r \quad (4-9)$$

b. DC Machines

Because of the restrictions imposed on the winding arrangement by the commutator, the mmf wave of a dc machine armature approximates a sawtooth waveform more nearly than the sine wave of ac machines. For example, Fig. 4-22 shows diagrammatically in cross section the armature of a two-pole dc machine. (In practice a larger number of slots would probably be used.) The current directions are shown by dots and crosses. The armature winding is equivalent to a coil wrapped around the armature and producing a magnetic field whose axis is vertical. As the armature rotates, the coil connections to the external circuit are changed through commutator action, so that the magnetic field of the armature is always perpendicular to that of the field winding and a continuous unidirectional torque results. Commutator action is described in Art. 9-2.

Figure 4-23a shows this winding laid out flat. The mmf wave is shown in Fig. 4-23b. On the assumption of narrow slots, it consists of a series of steps. The height of each step equals the number of ampere-conductors $2n_c i_c$ in a slot, where n_c is the number of turns in each coil and i_c is the coil current, with a two-layer winding and full-pitch coils being assumed. The

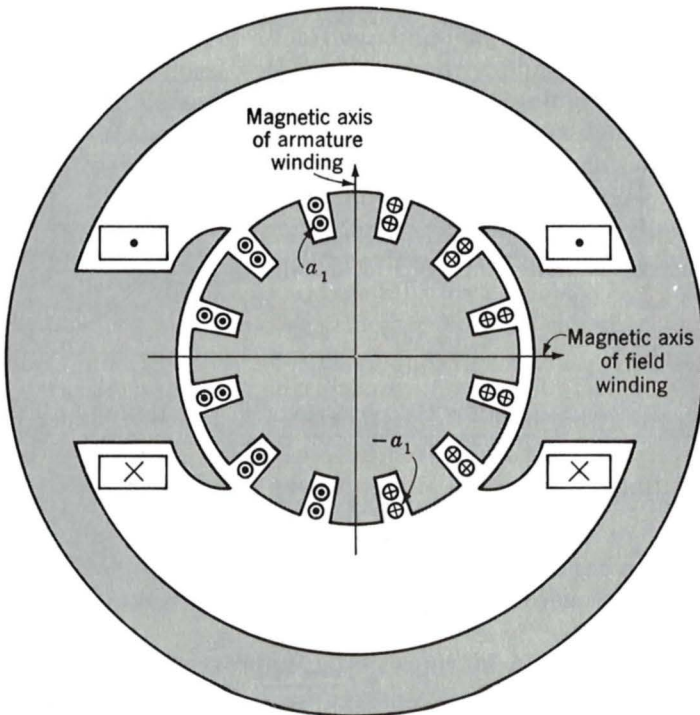


Fig. 4-22. Cross section of a two-pole dc machine.

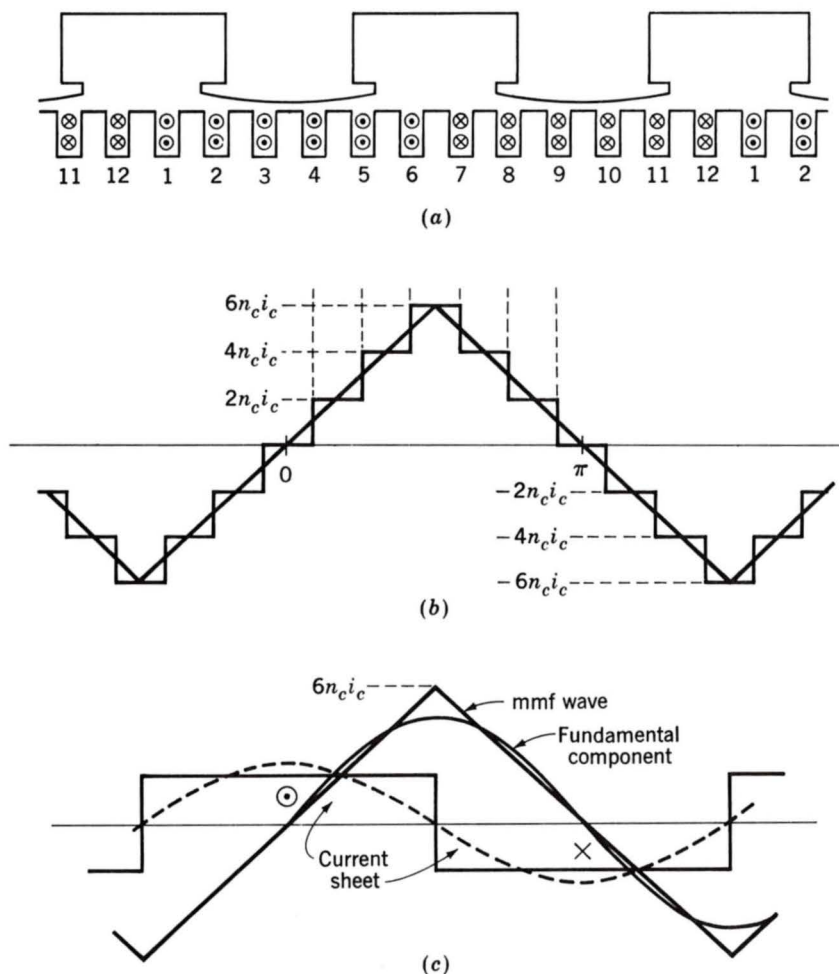


Fig. 4-23. (a) Developed sketch of the dc machine of Fig. 4-22; (b) mmf wave; (c) equivalent sawtooth mmf wave, its fundamental component, and equivalent rectangular current sheet.

peak value of the mmf wave is along the magnetic axis of the armature, midway between the field poles. This winding is equivalent to a coil of $12n_c i_c$ A · turns distributed around the armature. On the assumption of symmetry at each pole, the peak value of the mmf wave at each armature pole is $6n_c i_c$ A · turns.

This mmf wave can be represented approximately by the sawtooth wave drawn in Fig. 4-23b and repeated in Fig. 4-23c. For a more realistic winding with a larger number of armature slots per pole, the triangular distribution becomes a close approximation. It is the exact equivalent of

the mmf wave of a uniformly distributed current sheet wrapped around the armature and carrying current in the dot and cross directions, as shown by the rectangular space distribution of current density in Fig. 4-23c.

For our preliminary study, it is convenient to resolve the mmf waves of distributed windings into a Fourier series. The fundamental component of the sawtooth mmf wave of Fig. 4-23c is shown by the sine wave. Its peak value is $8/\pi^2 = 0.81$ times the height of the sawtooth wave. The fundamental mmf wave is the exact equivalent of the mmf wave of a sinusoidally distributed current sheet wrapped around the armature whose peak value equals the fundamental component of the rectangular current sheet of Fig. 4-23c. This sinusoidally distributed current sheet is shown dashed in Fig. 4-23c.

Note that the mmf wave depends on only the winding arrangement and symmetry of the magnetic structure at each pole. The flux-density wave, however, depends not only on the mmf but also on the magnetic boundary conditions, primarily the length of the air gap, the effect of the slot openings, and the shape of the pole face. The designer takes these effects into account by means of detailed analyses, but these details need not concern us here.

Machines often have a magnetic structure with more than two poles. For example, Fig. 4-24a shows schematically a four-pole dc machine. The field winding produces alternate north-south-north-south polarity, and the armature conductors are distributed in four belts of slots carrying currents alternately toward and away from the reader, as symbolized by the cross-hatched areas. This machine is shown in laid-out form in Fig. 4-24b. The corresponding sawtooth armature-mmf wave is also shown. On the assumption of symmetry of the winding and field poles, each successive pair of poles is like every other pair of poles. Magnetic conditions in the air gap can then be determined by examining any pair of adjacent poles, that is, 360 electrical degrees.

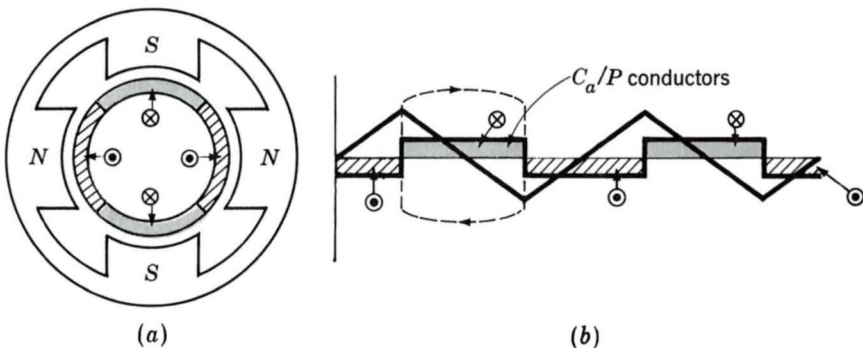


Fig. 4-24. (a) Cross section of a four-pole dc machine; (b) development of current sheet and mmf wave.

The peak value of the sawtooth armature-mmF wave is

$$F_a = \frac{1}{2} \frac{C_a}{P} \frac{i_a}{m} \quad \text{A} \cdot \text{turns/pole} \quad (4-10)$$

where C_a = total number of conductors in armature winding

P = number of poles

i_a = armature current

m = number of parallel paths through armature winding

Thus i_a/m is the current in each conductor. This equation comes directly from the line integral around the dotted closed path in Fig. 4-24*b* which crosses the air gap twice and encloses C_a/P conductors, each carrying current i_a/m in the same direction. In more compact form,

$$F_a = \frac{N_a}{P} i_a \quad (4-11)$$

where $N_a = C_a/(2m)$ is the number of series armature turns. From the Fourier series for the sawtooth mmF wave of Fig. 4-24*b*, the peak value of the space fundamental is

$$F_{a1, \text{peak}} = \frac{8}{\pi^2} \frac{N_a}{P} i_a \quad (4-12)$$

We base our preliminary investigations of both ac and dc machines on the assumption of sinusoidal space distributions of mmF. This model will be found to give very satisfactory results for most problems involving ac machines because their windings can be distributed so as to minimize the effects of harmonics. Because of the restrictions placed on the winding arrangement by the commutator, the mmF waves of dc machines inherently approach more nearly a sawtooth waveform. Nevertheless, the theory based on a sinusoidal model brings out the essential features of dc machine theory. The results can readily be modified whenever necessary to account for any significant discrepancies.

We shall also use a two-pole machine as our mathematical model. The results can immediately be extrapolated to a P -pole machine when it is recalled that electrical angles θ and electrical angular velocities ω are related to mechanical angles θ_m and mechanical angular velocities ω_m through Eqs. 4-1 and 4-3.

For a preliminary study we further simplify our model by assuming that the stator and rotor air-gap surfaces are smooth, concentric cylinders.

4-4 MAGNETIC FIELDS IN ROTATING MACHINERY

The behavior of electric machinery is determined by the magnetic fields created by currents in the various windings of the machine. This section discusses how these magnetic fields and currents are related.

a. Machines with Uniform Air Gaps

Figure 4-25a shows a single full-pitch N -turn coil in a magnetic structure with a concentric cylindrical rotor. The mmf of this configuration is shown in Fig. 4-25b. For such a structure, with a uniform air gap of length g at radius r_r (very much larger than g), it is quite accurate to assume that the magnetic field \mathbf{H} in the air gap is directed only radially and has constant magnitude across the air gap.

As discussed in Art. 4-3, the mmf distribution of Fig. 4-25b is equal to the line integral of \mathbf{H} across the air gap. For this case of constant radial H , this integral is simply equal to the product of the radial magnetic field H times the air-gap length g , and thus H can be found simply by dividing the mmf by the air-gap length:

$$H = \frac{\mathcal{F}}{g} \quad (4-13)$$

In Fig. 4-25c the radial H field and mmf are identical in form, simply related by a factor of $1/g$.

The fundamental space-harmonic component of H can be found directly from the fundamental component \mathcal{F}_{a1} , given by Eq. 4-4,

$$H_{a1} = \frac{\mathcal{F}_{a1}}{g} = \frac{4}{\pi} \frac{Ni}{2g} \cos \theta \quad (4-14)$$

It is a sinusoidal space wave of amplitude

$$H_{1,\text{peak}} = \frac{4}{\pi} \frac{Ni}{2g} \quad (4-15)$$

For a distributed winding such as that of Fig. 4-20, the air-gap magnetic field intensity is easily found once the mmf is known. Thus the fundamental component of H can be found from Eq. 4-6

$$H_{a1} = \frac{4}{\pi} k_w \frac{N_{ph}}{Pg} i_a \cos \theta \quad (4-16)$$

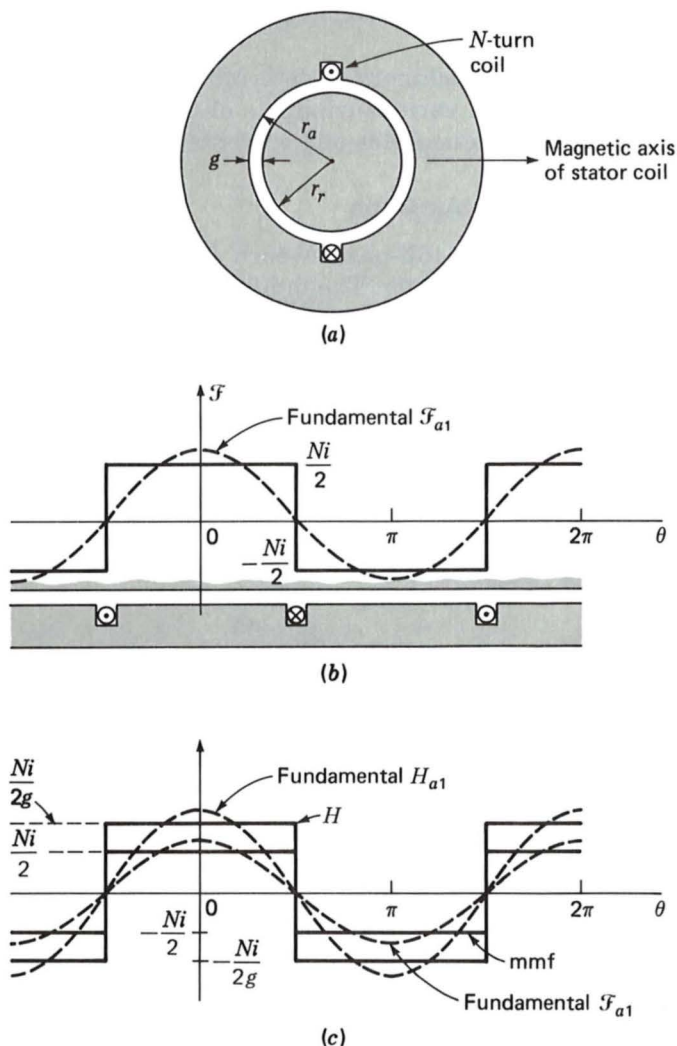


Fig. 4-25. The mmf and H field of a concentrated full-pitch winding.

where N_{ph} = number of series turns per phase

θ = electrical angle measured with respect to magnetic axis of the winding

k_w = winding factor

and the equation has been written for the general case of a P -pole machine. It is useful to notice that the space-fundamental mmf and H produced by a distributed winding of winding factor k_w and N_{ph}/P series turns per pole produce the same fundamental mmf and H as a single full-pitch winding

of $k_w N_{ph}/P$ turns per pole. In the analysis of machines with distributed windings, this result is useful since in considering space-fundamental quantities it permits the distributed solution to be obtained from the single N -turn full-pitch coil solution simply by replacing N by the effective number of turns of the distributed winding.

b. Machines with Nonuniform Air Gaps

Figure 4-26a shows the structure of a typical dc machine, and Fig. 4-26b shows the structure of a typical salient-pole synchronous machine. Both machines consist of magnetic structures with extremely nonuniform air gaps. In such cases the magnetic fields are somewhat more complex than for a uniform air gap. In fact, the effect of slots, which clearly violate the assumption of an absolutely uniform air gap, may be significant enough in some cases to require modification of the uniform-air-gap results.

Detailed analysis of the magnetic field distributions in such complex situations requires complete solutions of the field problem. For example, Fig. 4-27 shows the magnetic field distribution in a salient-pole dc generator (obtained by a digital-computer-based finite-element solution). However, experience has shown that through various simplifying assumptions, analytical techniques which yield reasonably accurate results can be developed. These techniques are illustrated in later chapters, where the effects of saliency on both dc and ac machines are discussed.

4-5 ROTATING MMF WAVES IN AC MACHINES

To understand the theory and operation of polyphase ac machines, it is necessary to study the nature of the mmf wave produced by a polyphase

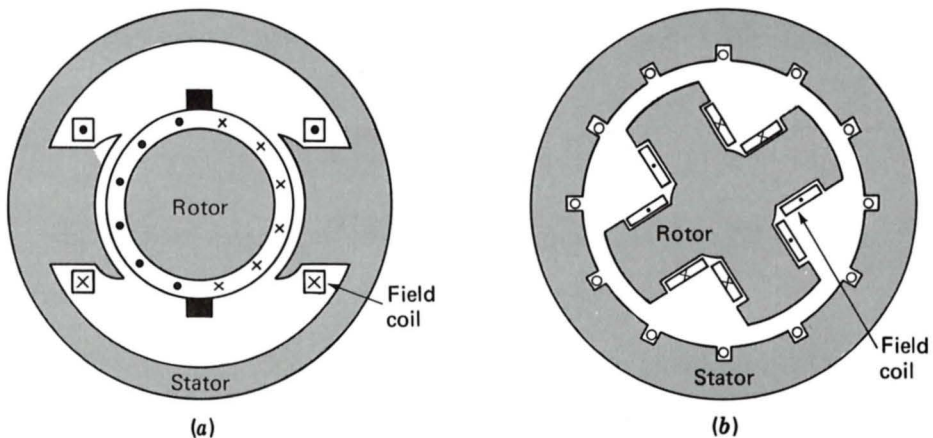


Fig. 4-26. Structure of typical salient-pole machines: (a) dc machine and (b) salient-pole synchronous machine.

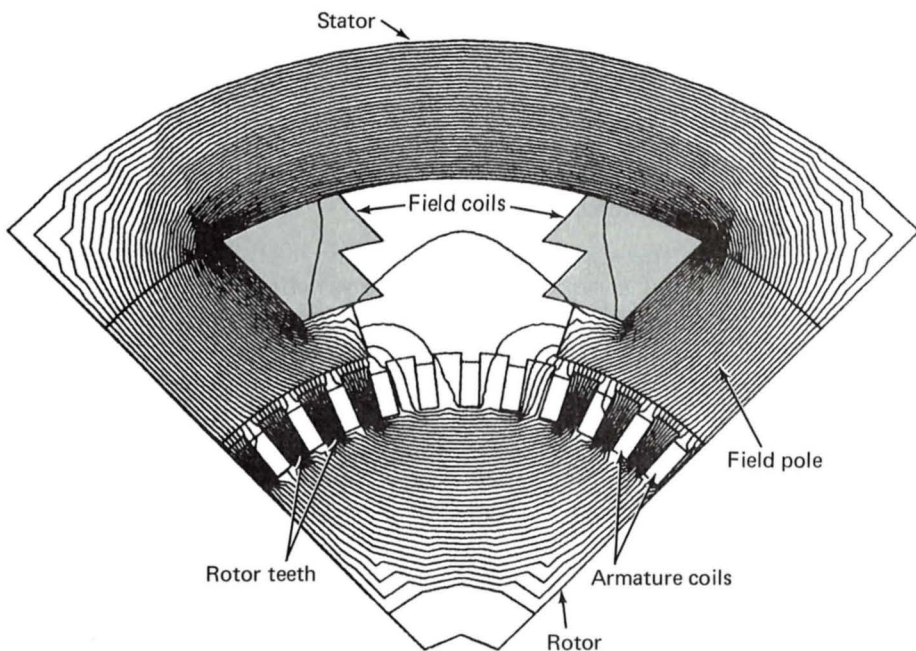


Fig. 4-27. Finite-element solution of the magnetic field distribution in a salient-pole dc generator. Field coils excited; no current in armature coils. (General Electric Company.)

winding. Attention will be focused on a two-pole machine or one pair of a P -pole winding. To develop insight into the polyphase situation, it is helpful to begin with an analysis of a single-phase winding.

a. Single-Phase Winding

Figure 4-28a shows the space-fundamental mmf distribution of a single-phase winding, where, from Eq. 4-8,

$$\mathcal{F}_{a1} = \frac{4}{\pi} k_w \frac{N_{ph}}{P} i_a \cos \theta \quad (4-17)$$

When this winding is excited by a sinusoidally varying current in time

$$i_a = I_a \cos \omega t \quad (4-18)$$

the mmf distribution is given by

$$\mathcal{F}_{a1} = (F_{\max} \cos \theta) \cos \omega t \quad (4-19)$$

Equation 4-19 has been written in a form to emphasize the fact that the re-

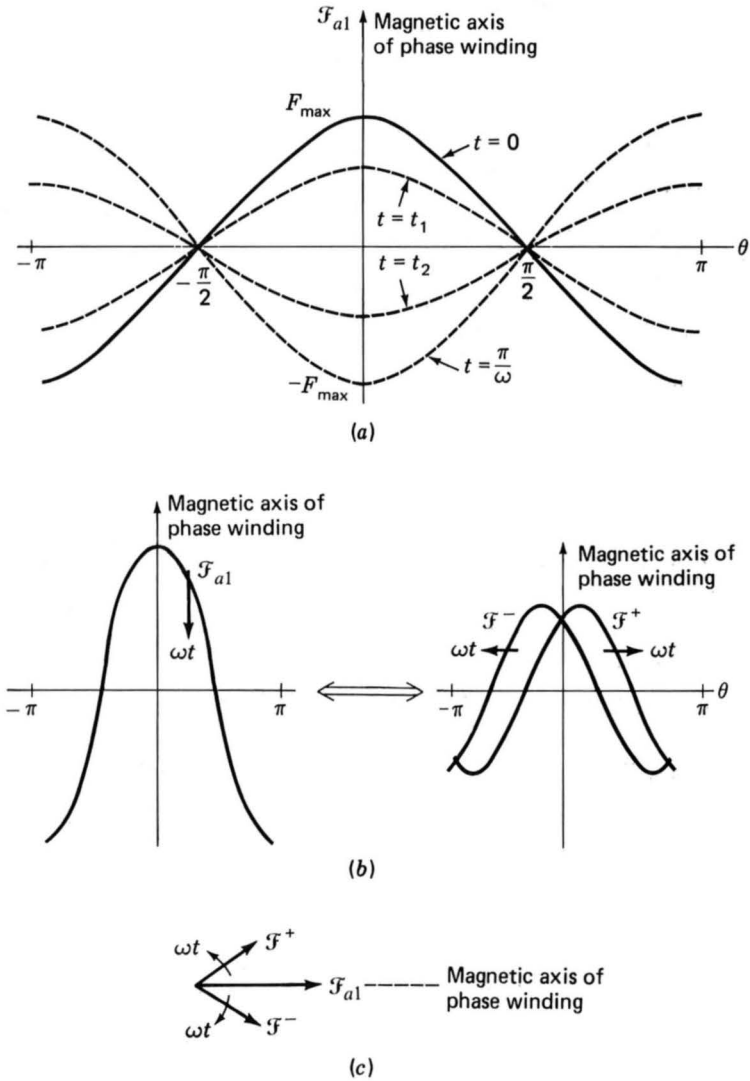


Fig. 4-28. Single-phase-winding fundamental mmf: (a) mmf distribution of a single-phase winding at various times; (b) total mmf \mathcal{F}_{a1} decomposed into two traveling waves \mathcal{F}^+ and \mathcal{F}^- ; (c) phasor decomposition of \mathcal{F}_{a1} .

sult is an mmf distribution of maximum amplitude

$$F_{\max} = \frac{4}{\pi} k_w \frac{N_{\text{ph}}}{P} I_a \quad (4-20)$$

which remains fixed in space but whose amplitude varies sinusoidally in time at frequency ω , as shown in Fig. 4-28a.

Use of a common trigonometric identity[†] permits Eq. 4-19 to be rewritten in the form

$$\mathcal{F}_{a1} = F_{\max} \left[\frac{1}{2} \cos (\theta - \omega t) + \frac{1}{2} \cos (\theta + \omega t) \right] \quad (4-21)$$

which shows that the mmf of a single-phase winding can be resolved into two rotating mmf waves each of amplitude one-half the maximum amplitude of \mathcal{F}_{a1} , with one, \mathcal{F}^+ , traveling in the $+\theta$ direction and the other, \mathcal{F}^- , traveling in the $-\theta$ direction, both with angular velocity ω :

$$\mathcal{F}^+ = \frac{1}{2} F_{\max} \cos (\theta - \omega t) \quad (4-22)$$

$$\mathcal{F}^- = \frac{1}{2} F_{\max} \cos (\theta + \omega t) \quad (4-23)$$

This decomposition is shown graphically in Fig. 4-28*b* and in a phasor representation in Fig. 4-28*c*.

The fact that the mmf of a single-phase winding excited by a source of alternating current can be resolved into rotating traveling waves is an important conceptual step in understanding ac machinery. As shown in the next section, in polyphase ac machinery the windings are equally displaced in space phase and the winding currents are similarly displaced in time phase, with the result that the negative-traveling flux waves of the various windings add to zero while the positive-traveling flux waves reinforce, giving a single positive-traveling flux wave. In single-phase ac machinery, the machine is designed so that the effects of the positive-traveling flux wave are maximized and those of the negative-traveling flux wave are minimized.

b. Polyphase Winding

In this section we study the mmf patterns of three-phase windings such as those found on the stator of three-phase induction and synchronous machines. The analyses presented can be readily extended to a polyphase winding with any number of phases. Once again attention is focused on a two-pole machine or one pair of poles of a P -pole winding.

In a three-phase machine, the windings of the individual phases are displaced from each other by 120 electrical degrees in space around the air-gap circumference, as shown by coils a , $-a$, b , $-b$, and c , $-c$ in Fig. 4-29. The concentrated full-pitch coils shown here may be considered to represent distributed windings, producing sinusoidal mmf waves centered on the magnetic axes of the respective phases. The three space-fundamental sinusoidal mmf waves are accordingly displaced 120 electrical degrees in *space*. But each phase is excited by an alternating current which varies in magnitude sinusoidally with *time*. Under balanced three-phase conditions, the instantaneous currents are

[†] $\cos \alpha \cos \beta = \frac{1}{2} \cos (\alpha - \beta) + \frac{1}{2} \cos (\alpha + \beta)$.

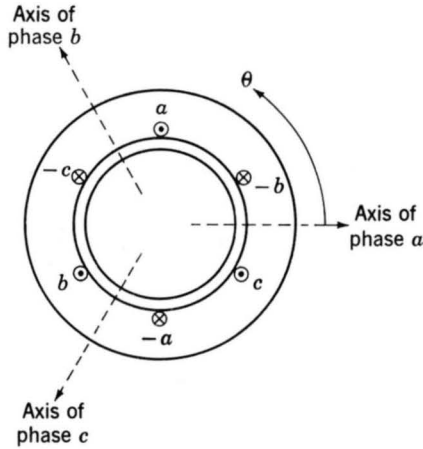


Fig. 4-29. Simplified two-pole three-phase stator winding.

$$i_a = I_m \cos \omega t \quad (4-24)$$

$$i_b = I_m \cos (\omega t - 120^\circ) \quad (4-25)$$

$$i_c = I_m \cos (\omega t + 120^\circ) \quad (4-26)$$

where I_m is the maximum value of the current and the time origin is arbitrarily taken as the instant when the phase- a current is a positive maximum. The phase sequence is assumed to be abc . The instantaneous currents are shown in Fig. 4-30. The dots and crosses in the coil sides (Fig. 4-29) indicate the reference directions for positive phase currents.

The mmf of phase a has been shown to be

$$\mathcal{F}_{a1} = \mathcal{F}_{a1}^+ + \mathcal{F}_{a1}^- \quad (4-27)$$

where

$$\mathcal{F}_{a1}^+ = \frac{1}{2} F_{\max} \cos (\theta - \omega t) \quad (4-28)$$

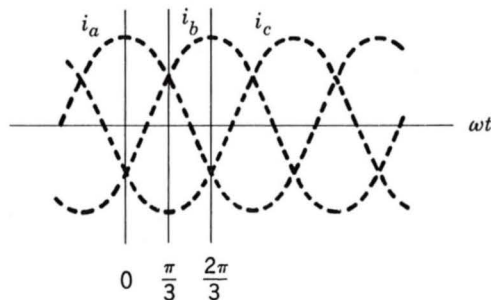


Fig. 4-30. Instantaneous phase currents under balanced three-phase conditions.

$$\mathcal{F}_{a1}^- = \frac{1}{2}F_{\max} \cos(\theta + \omega t) \quad (4-29)$$

and

$$F_{\max} = \frac{4}{\pi} k_w \frac{N_{\text{ph}}}{P} I_m \quad (4-30)$$

Similarly, for phases *b* and *c*, whose axes are at $\theta = 120^\circ$ and $\theta = -120^\circ$ respectively,

$$\mathcal{F}_{b1} = \mathcal{F}_{b1}^+ + \mathcal{F}_{b1}^- \quad (4-31)$$

$$\mathcal{F}_{b1}^+ = \frac{1}{2}F_{\max} \cos(\theta - \omega t) \quad (4-32)$$

$$\mathcal{F}_{b1}^- = \frac{1}{2}F_{\max} \cos(\theta + \omega t + 120^\circ) \quad (4-33)$$

and

$$\mathcal{F}_{c1} = \mathcal{F}_{c1}^+ + \mathcal{F}_{c1}^- \quad (4-34)$$

$$\mathcal{F}_{c1}^+ = \frac{1}{2}F_{\max} \cos(\theta - \omega t) \quad (4-35)$$

$$\mathcal{F}_{c1}^- = \frac{1}{2}F_{\max} \cos(\theta + \omega t - 120^\circ) \quad (4-36)$$

The total mmf is the sum of the contributions from each of the three phases

$$\mathcal{F}(\theta, t) = \mathcal{F}_{a1} + \mathcal{F}_{b1} + \mathcal{F}_{c1} \quad (4-37)$$

This summation can be performed quite easily in terms of the positive- and negative-traveling waves. The negative-traveling waves sum to zero

$$\begin{aligned} \mathcal{F}^-(\theta, t) &= \mathcal{F}_{a1}^- + \mathcal{F}_{b1}^- + \mathcal{F}_{c1}^- \\ &= \frac{1}{2}F_{\max} [\cos(\theta + \omega t) + \cos(\theta + \omega t - 120^\circ) + \cos(\theta + \omega t + 120^\circ)] \\ &= 0 \end{aligned} \quad (4-38)$$

and the positive-traveling waves reinforce

$$\mathcal{F}^+(\theta, t) = \mathcal{F}_{a1}^+ + \mathcal{F}_{b1}^+ + \mathcal{F}_{c1}^+ = \frac{3}{2}F_{\max} \cos(\theta - \omega t) \quad (4-39)$$

Thus, the result of displacing the three windings by 120° in space phase and displacing the winding currents by 120° in time phase is a single positive-traveling wave

$$\mathcal{F}(\theta, t) = \frac{3}{2}F_{\max} \cos(\theta - \omega t) \quad (4-40)$$

The wave described by Eq. 4-40 is a sinusoidal function of the space angle θ . It has a constant amplitude and a space-phase angle ωt which is a linear function of time. The angle ωt provides rotation of the entire wave around the air gap at constant angular velocity ω . Thus, at a fixed time t_1 the wave is a sinusoid in space with its positive peak displaced ωt_1 electri-

cal radians from the fixed point on the winding which is the origin for θ ; at a later instant, t_2 , the positive peak of the same wave is displaced ωt_2 from the origin, and the wave has moved $\omega(t_2 - t_1)$ around the gap. At $t = 0$ the current in phase a is a maximum, and the positive peak of the resultant mmf wave is located at the axis of phase a ; one-third of a cycle later the current in phase b is a maximum, and the positive peak is located at the axis of phase b ; and so on. The angular velocity of the wave is $\omega = 2\pi f$ electrical radians per second. For a P -pole machine the rotational speed is

$$\omega_m = \frac{2}{P} \omega \quad \text{rad/s} \quad (4-41)$$

$$\text{or} \quad n = \frac{120f}{P} \quad \text{r/min} \quad (4-42)$$

results, which is consistent with Eqs. 4-2 and 4-3.

In general, a rotating field of constant amplitude will be produced by a q -phase winding excited by balanced q -phase currents of frequency f when the respective phase axes are located $2\pi/q$ electrical radians apart in space. The constant amplitude will be $q/2$ times the maximum contribution of any one phase, and the speed will be $\omega = 2\pi f$ electrical radians per second.

A polyphase winding excited by balanced polyphase currents is thus seen to produce the same general effect as spinning a permanent magnet about an axis perpendicular to the magnet, or as the rotation of dc-excited field poles.

c. Graphical Analysis of Polyphase MMF

For balanced three-phase currents as given by Eqs. 4-24 to 4-26, the resultant rotating mmf can also be shown graphically. Consider the state of affairs at $t = 0$ (Fig. 4-30) the moment when the phase- a current is at its maximum value I_m . The mmf of phase a then has its maximum value F_{\max} , as shown by the vector $\mathbf{F}_a = \mathbf{F}_{\max}$ drawn along the magnetic axis of phase a in Fig. 4-31a. At this moment, currents i_b and i_c are both $I_m/2$ in the negative direction, as shown by the dots and crosses in Fig. 4-31a indicating the *actual instantaneous* directions. The corresponding mmf's of phases b and c are shown by the vectors \mathbf{F}_b and \mathbf{F}_c , both equal to $\mathbf{F}_{\max}/2$ drawn in the negative direction along the magnetic axes of phases b and c , respectively. The resultant, obtained by adding the individual contributions of the three phases, is a vector $\mathbf{F} = \frac{3}{2}\mathbf{F}_{\max}$ centered on the axis of phase a . It represents a sinusoidal space wave with its positive half wave centered on the axis of phase a and having an amplitude $\frac{3}{2}$ times that of the phase- a contribution alone.

At a later time $\omega t_1 = \pi/3$ (Fig. 4-30), the currents in phases a and b are a positive half maximum, and that in phase c is a negative maximum.

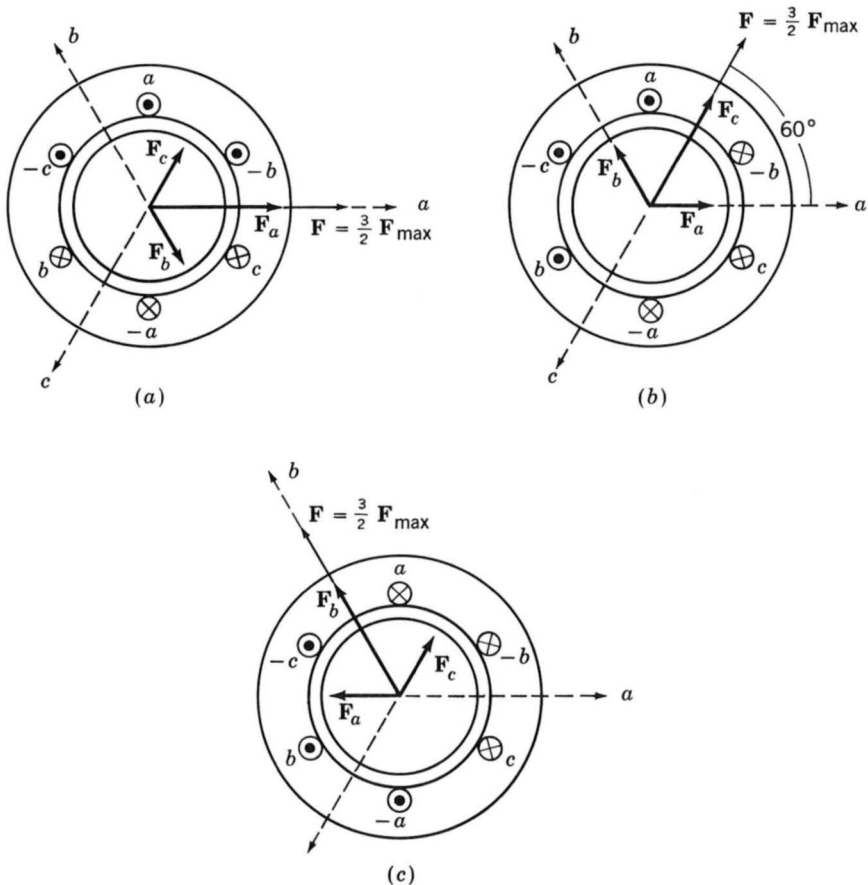


Fig. 4-31. The production of a rotating magnetic field by means of three-phase currents.

The individual mmf components and their resultant are now shown in Fig. 4-31b. The resultant has the same amplitude as at $t = 0$, but it has now rotated counterclockwise 60 electrical degrees in space. Similarly, at $\omega t_2 = 2\pi/3$ (when the phase- b current is a positive maximum and the phase- a and phase- c currents are a negative half maximum) the same resultant mmf distribution is again obtained, but it has rotated counterclockwise 60 electrical degrees still farther and is now aligned with the magnetic axis of phase b (see Fig. 4-31c). As time passes, then, the resultant mmf wave retains its sinusoidal form and amplitude but shifts progressively around the air gap. This shift corresponds to a field rotating uniformly around the circumference of the air gap. Results consistent with this conclusion can be obtained by sketching the distribution at any arbitrary instant of time.

In one cycle the resultant mmf must be back in the position of Fig. 4-31a. The mmf wave therefore makes one revolution per cycle in a two-pole ma-

chine. In a P -pole machine the wave travels one wavelength in $2/P$ revolutions per cycle.

4-6 GENERATED VOLTAGE

The general nature of the induced voltage has already been discussed in Art. 4-2. Quantitative expressions for the induced voltage will now be determined.

a. AC Machines

An elementary ac machine is shown in cross section in Fig. 4-32. The coils on both the rotor and the stator have been shown as single multiple-turn full-pitch coils. The analysis can readily be extended to distributed windings. The field winding on the rotor is assumed to produce a sinusoidal space wave of flux density B at the stator surface. The rotor is spinning at a constant angular velocity of ω electrical radians per second. Although a two-pole machine is shown, the derivations presented here are for the general case of a P -pole machine.

When the rotor poles are in line with the magnetic axis of the stator coil, the flux linkage with the stator N -turn coil is $N\Phi$, where Φ is the air-gap flux per pole. For the assumed sinusoidal flux-density wave

$$B = B_{\text{peak}} \cos \theta \quad (4-43)$$

where B_{peak} is its peak value at the rotor pole center and θ is measured in

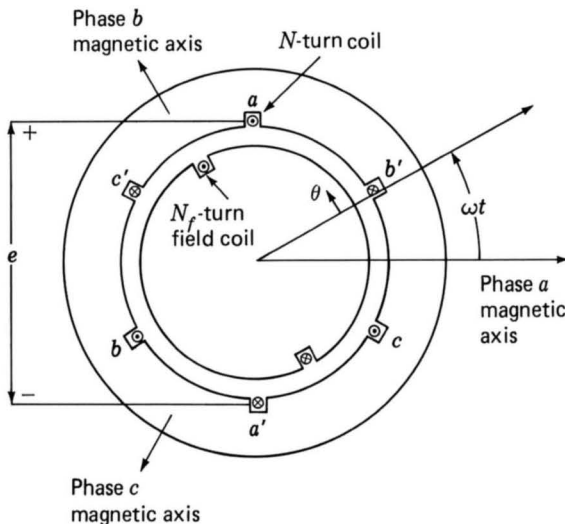


Fig. 4-32. Cross-sectional view of an elementary three-phase ac machine.

electrical radians from the rotor pole axis. The air-gap flux per pole is the integral of the flux density over the pole area; thus, for a two-pole machine

$$\Phi = \int_{-\pi/2}^{+\pi/2} B_{\text{peak}} \cos \theta \, l r \, d\theta = 2B_{\text{peak}} l r \quad (4-44)$$

where l is the axial length of the stator and r is its radius at the air gap. For a P -pole machine

$$\Phi = \frac{2}{P} 2B_{\text{peak}} l r \quad (4-45)$$

because the pole area is $2/P$ times that of a two-pole machine of the same length and diameter.

As the rotor turns, the flux linkage varies as the cosine of the angle α between the magnetic axes of the stator coil and rotor. With the rotor spinning at constant angular velocity ω , the flux linkage with the stator coil is

$$\lambda = N\Phi \cos \omega t \quad (4-46)$$

where time t is arbitrarily chosen as zero when the peak of the flux-density wave coincides with the magnetic axis of the stator coil. By Faraday's law, the voltage induced in the stator coil is

$$e = \frac{d\lambda}{dt} = N \frac{d\Phi}{dt} \cos \omega t - \omega N\Phi \sin \omega t \quad (4-47)$$

The polarity of this induced voltage is such that if the stator coil were short-circuited, the induced voltage would cause a current to flow in the direction that would oppose any change in the flux linkage of the stator coil. Although Eq. 4-47 was derived on the assumption that only the field winding was producing air-gap flux, the equation applies equally well to the general situation where Φ is the net air-gap flux per pole produced by currents on both the rotor and the stator.

The first term on the right-hand side of Eq. 4-47 is a transformer voltage and is present only when the amplitude of the flux-density wave changes with time. The second term is a *speed voltage* generated by the relative motion of the air-gap flux wave and the stator coil. In the normal steady-state operation of most rotating machines, the amplitude of the air-gap flux wave is constant, and the generated voltage is simply the speed voltage. The term *electromotive force* (emf) is often used for the speed voltage. Thus

$$e = -\omega N\Phi \sin \omega t \quad (4-48)$$

Equation 4-48 was derived directly from Faraday's law. Alternatively, the voltage e induced in a conductor of length l moving with linear velocity v in a non-time-varying magnetic field of flux density B is given by the "cutting-of-flux" equation

$$e = Blv \quad (4-49)$$

where B , l , and v are mutually perpendicular. Properly interpreted, this equation also applies to rotating machines and gives a useful alternative basis for visualizing induced voltages. To show that Eq. 4-49 applies to rotating machines, we now derive it from Eq. 4-48.

Substitution of Eq. 4-45 in Eq. 4-48 gives

$$e = -\omega N \frac{2}{P} 2B_{\text{peak}} l r \sin \omega t \quad (4-50)$$

$$e = -\frac{2}{P} \omega r (2lN) B_{\text{peak}} \sin \omega t \quad (4-51)$$

Now $B_{\text{peak}} \sin \omega t$ is the flux density B_{coil} at the stator coil side (Fig. 4-32), $2\omega/P$ is the mechanical angular velocity ω_m , and $2lN$ is the total active length of conductors in the two coil sides. Thus, for a concentrated full-pitch coil

$$e = B_{\text{coil}} (2lN) (-r\omega_m) = B_{\text{coil}} (2lN) v \quad (4-52)$$

where $v = -r\omega_m$ is the linear velocity of the conductor relative to the field. Even though the conductors are embedded in slots, the voltage can be computed by the cutting-of-flux concept, Eq. 4-49, just as if the conductors were lifted out of the slots and placed directly in the air-gap field.

In the normal steady-state operation of ac machines, we are usually interested in the rms values of voltages and currents rather than their instantaneous values. From Eq. 4-48 the maximum value of the induced voltage is

$$E_{\text{max}} = \omega N \Phi = 2\pi f N \Phi \quad (4-53)$$

and its rms value is

$$E_{\text{rms}} = \frac{2\pi}{\sqrt{2}} f N \Phi = \sqrt{2} \pi f N \Phi \quad (4-54)$$

where f is the frequency in hertz. These equations are identical in form to the corresponding emf equations for a transformer. Relative motion of a coil and a constant-amplitude spatial flux-density wave in a rotating machine

produces the same voltage effect as does a time-varying flux in association with stationary coils in a transformer. Rotation, in effect, introduces the time element and transforms a *space* distribution of flux density into a *time* variation of voltage.

The voltage induced is a single-phase voltage. For the production of a set of three-phase voltages, it follows that three coils displaced 120 electrical degrees in space must be used, as shown in elementary form in Fig. 4-12. Equation 4-54 then gives the rms voltage per phase when N is the total series turns per phase. All these elementary windings are full-pitch concentrated windings because the two sides of any coil are 180 electrical degrees apart and all the turns of that coil are concentrated in one pair of slots. In actual ac machine windings, the armature coils of each phase are distributed in a number of slots, as discussed in Art. 4-3. A distributed winding makes better use of the iron and copper and improves the waveform. For distributed windings a reduction factor k_w must be applied because the emf's induced in the individual coils of any one phase group are not in time phase. Their phasor sum is then less than their numerical sum when they are connected in series. (See Appendix B for details. For most three-phase windings, k_w is about 0.85 to 0.95.) For distributed windings Eq. 4-54 becomes

$$E_{\text{rms}} = \sqrt{2} \pi f k_w N_{\text{ph}} \Phi \quad \text{V rms/phase} \quad (4-55)$$

where N_{ph} is the number of series turns per phase.

EXAMPLE 4-1

A two-pole three-phase Y-connected 60-Hz round-rotor synchronous generator has a field winding on the rotor with N_f distributed turns and winding factor k_f and an armature winding on the stator with N_a turns per phase (line to neutral) and winding factor k_a . The air-gap length is g , and the mean air-gap radius is r . The active length of the armature is l . The dimensions and winding data are

$$\begin{aligned} N_f &= 46 \text{ series turns} & k_f &= 0.90 & N_a &= 24 \text{ series turns/phase} \\ k_a &= 0.833 & r &= 0.50 \text{ m} & g &= 0.075 \text{ m} & l &= 4.0 \text{ m} \end{aligned}$$

The field current $I_f = 1500$ A dc. The rotor is driven by a steam turbine at a speed of 3600 r/min. Compute (a) the peak fundamental mmf $F_{1,\text{peak}}$ produced by the field winding, (b) the peak fundamental flux density $B_{1,\text{peak}}$ in the air gap, (c) the fundamental flux per pole Φ , and (d) the rms value of the open-circuit voltage generated in the armature.

Solution

(a) From Eq. 4-9

$$\begin{aligned}
 F_{1,\text{peak}} &= \frac{4}{\pi} \frac{k_f N_f}{P} I_f = \frac{4}{\pi} \frac{0.90(46)}{2} (1500) \\
 &= \frac{4}{\pi} (20.7) (1500) = \frac{4}{\pi} (31,000) \text{ A} \cdot \text{turns/pole}
 \end{aligned}$$

(b) Using Eq. 4-13, we get

$$B_{1,\text{peak}} = \frac{\mu_0 F_{1,\text{peak}}}{g} = \frac{4\pi \times 10^{-7}}{7.5 \times 10^{-2}} \frac{4}{\pi} (31,000) = 0.661 \text{ T}$$

Because of the effect of the slots containing the armature winding, most of the air-gap flux is confined to the stator teeth. The flux density in the teeth at a pole center is higher than the value calculated in part (b), probably by a factor of about 2. In a detailed design this flux density would be calculated to determine whether the teeth were excessively saturated.

(c) From Eq. 4-44 or 4-45

$$\Phi = 2B_{1,\text{peak}} l r = 2(0.661) (4.0) (0.50) = 2.64 \text{ Wb}$$

(d) From Eq. 4-54 with $f = 60 \text{ Hz}$

$$\begin{aligned}
 E_{\text{rms}} &= \sqrt{2} \pi f k_a N_a \Phi = \sqrt{2} \pi (60) (0.833) (24) (2.64) \\
 &= 14.1 \text{ kV rms/phase line to neutral}
 \end{aligned}$$

The three phases are connected in Y, as in Fig. 4-12. The voltage between line terminals is

$$\sqrt{3} (14.1 \text{ kV}) = 24.4 \text{ kV}$$

b. DC Machines

Even if the ultimate purpose is the generation of a direct voltage, clearly the speed voltage generated in an armature coil is an alternating voltage. The alternating waveform must therefore be rectified. Mechanical rectification is provided by the commutator, the device already described in elementary form in Art. 4-2c. For the single coil of Fig. 4-17 the commutator provides full-wave rectification. With the continued assumption of sinu-

soidal flux distribution, the voltage waveform between brushes is transformed to that of Fig. 4-33. The average, or dc, value of the voltage between brushes is

$$E_a = \frac{1}{\pi} \int_0^{\pi} \omega N \Phi \sin \omega t d(\omega t) = \frac{2}{\pi} \omega N \Phi \quad (4-56)$$

For dc machines it is usually more convenient to express the voltage E_a in terms of the mechanical speed ω_m rad/s or n r/min. Substitution of Eq. 4-3 in Eq. 4-56 for a P -pole machine then yields

$$E_a = \frac{PN}{\pi} \Phi \omega_m = 2PN \Phi \frac{n}{60} \quad (4-57)$$

The single-coil dc winding implied here is, of course, unrealistic in the practical sense, and it will be essential later to examine the action of commutators more carefully. Actually, Eq. 4-57 gives correct results for the more practical distributed ac armature windings as well, provided N is taken as the total number of turns in series between armature terminals. Usually the voltage is expressed in terms of the total number of active conductors C_a and the number m of parallel paths through the armature winding. Because it takes two coil sides to make a turn and $1/m$ of these are connected in series, the number of series turns $N = C_a/(2m)$. Substitution in Eq. 4-57 then gives

$$E_a = \frac{PC_a}{2\pi m} \Phi \omega_m = \frac{PC_a}{m} \Phi \frac{n}{60} \quad (4-58)$$

4-7 TORQUE IN NON-SALIENT-POLE MACHINES

The behavior of any electromagnetic device as a component in an electromechanical system can be described in terms of its Kirchhoff-law voltage equations and its electromagnetic torque. The purpose of this article is to derive the voltage and torque equations for an idealized elementary machine, results which can be readily extended later to more complex ma-

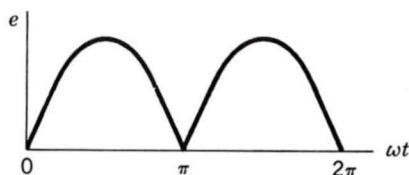


Fig. 4-33. Voltage between brushes in an elementary dc machine.

chines. We derive these equations from two viewpoints and show that basically they stem from the same ideas.

The first viewpoint is essentially the same as that of Art. 3-5. The machine will be regarded as a circuit element whose inductances depend on the angular position of the rotor. The flux linkages λ and magnetic field coenergy will be expressed in terms of the currents and inductances. The torque can then be found from the partial derivative of the magnetic field energy or coenergy with respect to angle and the terminal voltages from the sum of the resistance drops Ri and the Faraday-law voltages $d\lambda/dt$. The result will be a set of nonlinear differential equations describing the dynamic performance of the machine.

The second viewpoint regards the machine as two groups of windings producing magnetic fields in the air gap, one group on the stator and the other on the rotor. By making suitable assumptions regarding these fields, simple expressions can be derived for the flux linkages and magnetic field energy stored in the air gap in terms of the field quantities. The torque and generated voltage can then be found in terms of these quantities. Thus torque is expressed explicitly as the tendency for two magnetic fields to line up in the same way as permanent magnets tend to align themselves, and generated voltage is expressed as the result of relative motion between a field and a winding. These expressions lead to a simple physical picture of the normal steady-state behavior of rotating machines.

a. Coupled-Circuit Viewpoint

Consider the elementary machine of Fig. 4-34 with one winding on the stator and one on the rotor. These windings are distributed over a number of slots so that their mmf waves can be approximated by space sinusoids. In Fig. 4-34a the coil sides s , $-s$ and r , $-r$ mark the positions of the centers of the belts of conductors comprising the distributed windings. An alternative

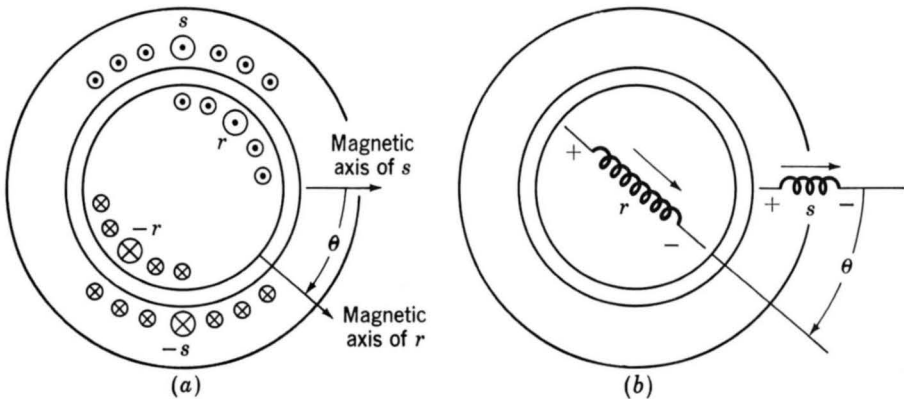


Fig. 4-34. Elementary two-pole machine with smooth air gap: (a) winding distribution and (b) schematic representation.

way of drawing these windings is shown in Fig. 4-34*b*, which also shows reference directions for voltages and currents. Here it is assumed that current in the arrow direction produces a magnetic field in the air gap in the arrow direction, so that a single arrow defines reference directions for both current and flux. The stator and rotor are concentric cylinders, and slot openings are neglected. Consequently, our elementary model does not include the effects of salient poles, which are investigated in later chapters. We also assume that the reluctances of the stator and rotor iron are negligible.

On these assumptions the stator and rotor self-inductances L_{ss} and L_{rr} are constant, but the stator-rotor mutual inductance depends on the angle θ between the magnetic axes of the stator and rotor windings. The mutual inductance is a positive maximum when $\theta = 0$ or 2π , is zero when $\theta = \pm\pi/2$, and is a negative maximum when $\theta = \pm\pi$. On the assumption of sinusoidal mmf waves and a uniform air gap, the space distribution of the air-gap flux wave is sinusoidal, and the mutual inductance is

$$\mathcal{L}_{sr}(\theta) = L_{sr} \cos \theta \quad (4-59)$$

where the script letter \mathcal{L} denotes an inductance which is a function of the electrical angle θ . The italic capital letter L denotes a constant value. Thus L_{sr} is the value of the mutual inductance when the magnetic axes of the stator and rotor are aligned. In terms of the inductances, the stator and rotor flux linkages λ_s and λ_r are

$$\lambda_s = L_{ss}i_s + \mathcal{L}_{sr}(\theta)i_r = L_{ss}i_s + L_{sr}i_r \cos \theta \quad (4-60)$$

$$\lambda_r = \mathcal{L}_{sr}(\theta)i_s + L_{rr}i_r = L_{sr}i_s \cos \theta + L_{rr}i_r \quad (4-61)$$

where the inductances can be calculated as in Appendix B. In matrix notation

$$\begin{bmatrix} \lambda_s \\ \lambda_r \end{bmatrix} = \begin{bmatrix} L_{ss} & \mathcal{L}_{sr}(\theta) \\ \mathcal{L}_{sr}(\theta) & L_{rr} \end{bmatrix} \begin{bmatrix} i_s \\ i_r \end{bmatrix} \quad (4-62)$$

The terminal voltages v_s and v_r are

$$v_s = R_s i_s + p\lambda_s \quad (4-63)$$

$$v_r = R_r i_r + p\lambda_r \quad (4-64)$$

where R_s and R_r are the winding resistances and p is the time-derivative operator d/dt . When the rotor is revolving, θ must be treated as a variable. Differentiation of Eqs. 4-60 and 4-61 and substitution of the results in Eqs. 4-63 and 4-64 then give

$$v_s = R_s i_s + L_{ss} p i_s + L_{sr} (\cos \theta) p i_r - L_{sr} i_r (\sin \theta) p \theta \quad (4-65)$$

$$v_r = R_r i_r + L_{rr} p i_r + L_{sr} (\cos \theta) p i_s - L_{sr} i_s (\sin \theta) p \theta \quad (4-66)$$

where $p\theta$ is the instantaneous speed ω in *electrical* radians per second. In a two-pole machine, θ and ω are equal to the instantaneous shaft angle θ_m and the speed ω_m , respectively. In a P -pole machine, they are related by Eqs. 4-1 and 4-3. The second and third terms on the right-hand sides of Eqs. 4-65 and 4-66 are $L di/dt$ induced voltages like those induced in stationary coupled circuits such as the windings of transformers. The fourth terms are caused by mechanical motion and are proportional to the instantaneous speed. They are the coupling terms relating the interchange of power between the electric and mechanical systems.

The electromagnetic torque can be found from the coenergy in the magnetic field in the air gap. From Eq. 3-51

$$W'_{fld} = \frac{1}{2} L_{ss} i_s^2 + \frac{1}{2} L_{rr} i_r^2 + L_{sr} i_s i_r \cos \theta \quad (4-67)$$

and from Eq. 3-53

$$T = + \frac{\partial W'_{fld}(\theta_m, i_s, i_r)}{\partial \theta_m} = + \frac{\partial W'_{fld}(\theta, i_s, i_r)}{\partial \theta} \frac{d\theta}{d\theta_m} \quad (4-68)$$

where T is the electromagnetic torque acting in the positive direction of θ_m and the derivative must be taken with respect to actual *mechanical* angle θ_m because we are dealing here with mechanical variables. Differentiation of Eqs. 4-67 and 4-1 for a P -pole machine then gives

$$T = - \frac{P}{2} L_{sr} i_s i_r \sin \theta = - \frac{P}{2} L_{sr} i_s i_r \sin \frac{P}{2} \theta_m \quad (4-69)$$

with T in newton-meters. The negative sign in Eq. 4-69 means that the electromagnetic torque acts in the direction to bring the magnetic fields of the stator and rotor into alignment.

Equations 4-65, 4-66, and 4-69 are a set of three equations relating the electrical variables v_s , i_s , v_r , i_r and the mechanical variables T and θ_m . These equations, together with the constraints imposed on the electrical variables by the networks connected to the terminals (sources or loads and external impedances) and the constraints imposed on the mechanical variables (applied torques and inertial, frictional, and spring torques), determine the performance of the device as a coupling element. These are nonlinear differential equations and are difficult to solve except under special circumstances. We are not concerned with their solution here because we are using them merely as steps in the development of the theory of rotating machines.

Now consider a uniform-air-gap machine with several stator and rotor windings. The same general principles that apply to the elementary model of Fig. 4-34 also apply to the multiwinding machine. Each winding has its own self-inductance and mutual inductances with other windings. The self-inductances and mutual inductances between pairs of windings on the same side of the air gap are constant on the assumption of a uniform gap and negligible magnetic saturation. But the mutual inductances between pairs of stator and rotor windings vary as the cosine of the angle between the magnetic axes of the windings. The torque results from the tendency of the magnetic field of the rotor windings to line up with that of the stator windings. It can be expressed as the sum of terms like Eq. 4-69.

EXAMPLE 4-2

Consider the elementary rotating machine of Fig. 4-34. Its shaft is coupled to a mechanical device which can be made to absorb or deliver mechanical torque over a wide range of speeds. This machine can be connected and operated in several ways. For example, suppose that the rotor winding is excited with direct current I_r and the stator winding is connected to an ac source which can either absorb or deliver electric power. Let the stator current be

$$i_s = I_s \cos \omega_s t$$

where $t = 0$ is arbitrarily chosen as the moment when the stator current has its peak value.

(a) Derive an expression for the magnetic torque developed by the machine as the speed is varied by control of the mechanical device connected to its shaft.

(b) Find the speed at which average torque will be produced if the stator frequency is 60 Hz.

(c) With the assumed current-source excitations, what voltages are induced in the stator and rotor windings at synchronous speed?

Solution

(a) From Eq. 4-69 for a two-pole machine

$$T = -L_{sr} i_s i_r \sin \theta_m$$

For the conditions of this problem

$$T = -L_{sr} I_s I_r \cos \omega_s t \sin (\omega_m t + \delta)$$

where ω_m is the clockwise angular velocity impressed on the rotor by the mechanical drive and δ is the angular position of the rotor at $t = 0$. Using a trigonometric identity,[†] we have

$$T = -\frac{1}{2}L_{sr}I_sI_r\{\sin[(\omega_m + \omega_s)t + \delta] + \sin[(\omega_m - \omega_s)t + \delta]\}$$

The torque consists of two sinusoidally time-varying terms of frequencies $\omega_m + \omega_s$ and $\omega_m - \omega_s$. As shown in Art. 4-5, the single stator winding in the machine of Fig. 4-34 creates two flux waves, one traveling in the positive θ direction with angular velocity ω_s and the second traveling in the negative θ direction also with angular velocity ω_s . It is the interaction of the rotor with these two flux waves which results in the two components of the torque expression.

(b) Except when $\omega_m = \pm\omega_s$, the torque averaged over a sufficiently long time is zero. But if $\omega_m = +\omega_s$, the rotor is traveling in synchronism with the positive-traveling stator flux wave, and the torque becomes

$$T = -\frac{1}{2}L_{sr}I_sI_r[\sin(2\omega_s t + \delta) + \sin\delta]$$

The first sine term is a double-frequency component whose average value is zero. The second term is the average torque

$$T_{av} = -\frac{1}{2}L_{sr}I_sI_r \sin\delta$$

The other possibility is $\omega_m = -\omega_s$, which merely means rotation in the counterclockwise direction; the rotor is now traveling in synchronism with the negative-traveling stator flux wave. The negative sign in the expression for T_{av} means that the magnetic torque tends to reduce δ . The machine is an idealized single-phase synchronous machine. (With polyphase synchronous machines the direction of rotation is determined by the phase sequence, as shown in Art. 4-5b.)

With a stator frequency of 60 Hz

$$\omega_m = \omega_s = 2\pi(60) \text{ rad/s} = 60 \text{ Hz} = 3600 \text{ r/min}$$

(c) From the second and fourth terms of Eq. 4-65 with $\omega_m = \omega_s$, the voltage induced in the stator is

$$e_s = -\omega_s L_{ss}I_s \sin\omega_s t - \omega_s L_{sr}I_r \sin(\omega_s t + \delta)$$

From the third and fourth terms of Eq. 4-66, the voltage induced in the rotor is

[†] $\sin\alpha \cos\beta = \frac{1}{2}\sin(\alpha + \beta) + \frac{1}{2}\sin(\alpha - \beta)$.

$$\begin{aligned}
 e_r &= -\omega_s L_{sr} I_s [\sin \omega_s t \cos (\omega_s t + \delta) + \cos \omega_s t \sin (\omega_s t + \delta)] \\
 &= -\omega_s L_{sr} I_s \sin (2\omega_s t + \delta)
 \end{aligned}$$

The stator current induces a double-frequency voltage in the rotor.

b. Magnetic Field Viewpoint

In the foregoing discussion the characteristics of the device as viewed from its electric and mechanical terminals have been expressed in terms of its inductances. This viewpoint gives very little insight into the internal phenomena and gives no conception of the effects of physical dimensions. An alternative formulation in terms of the interacting magnetic fields in the air gap should supply some of these missing features.

Currents in the machine windings create magnetic flux in the air gap between the stator and rotor, the flux paths being completed through the stator and rotor iron. This condition corresponds to the appearance of magnetic poles on both the stator and the rotor, centered on their respective magnetic axes, as shown in Fig. 4-35*a* for a two-pole machine with a smooth air gap. Torque is produced by the tendency of the two component magnetic fields to line up their magnetic axes. The simple physical picture is like that of two bar magnets pivoted at their centers on the same shaft. The torque is proportional to the product of the amplitudes of the stator and rotor mmf waves and is also a function of the angle δ_{sr} between their magnetic axes. We shall show that for a smooth-air-gap machine the torque is proportional to $\sin \delta_{sr}$.

Most of the flux produced by the stator and rotor windings (roughly 90 percent in typical machines) crosses the air gap and links both windings; this flux is termed the *mutual flux*. Small percentages of the flux,

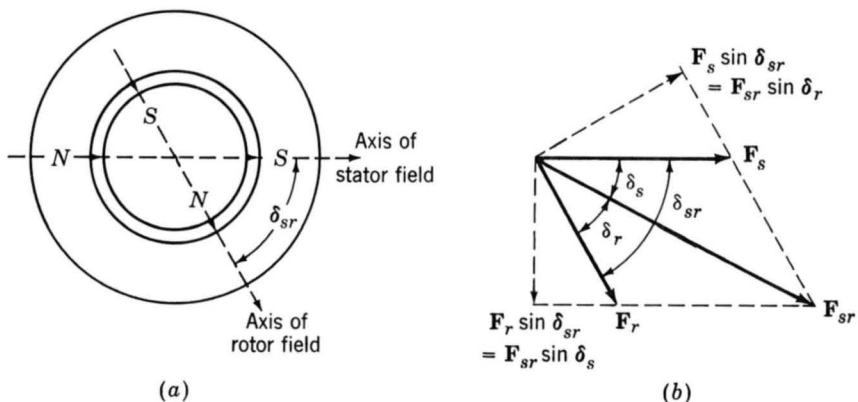


Fig. 4-35. Simplified two-pole machine: (a) elementary model and (b) vector diagram of mmf waves. Torque is produced by the tendency of the rotor and stator magnetic fields to align.

however, do not cross the air gap but link only the rotor or stator winding; these are, respectively, the *rotor leakage flux* and the *stator leakage flux*. They comprise slot and toothtip leakage, end-turn leakage, and space harmonics in the air-gap field. Only the mutual flux is of direct concern in torque production. The leakage fluxes do affect machine performance, however, by virtue of the voltages they induce in their own windings. Their effect on the electrical characteristics is accounted for by means of *leakage inductances* like those of a transformer. This effect, however, is an auxiliary one rather than a fundamental part of torque production.

Our analysis, then, will be in terms of the resultant mutual flux. We shall derive an expression for the magnetic coenergy stored in the air gap in terms of the stator and rotor mmfs and the angle δ_{sr} between their magnetic axes. The torque can then be found from the partial derivative of the coenergy with respect to angle δ_{sr} .

We now assume that the tangential component of the magnetic field in the air gap is negligible compared with the radial component; in other words, the mutual flux goes straight across the gap. We also assume that the radial length g of the gap (the clearance between the rotor and stator) is small compared with the radius of the rotor or stator. On this assumption there is negligible difference between the flux density at the rotor surface, at the stator surface, or at any intermediate radial distance in the air gap, say, halfway between. The air-gap field then reduces to a radial field H or B whose intensity varies with the angle around the periphery. The line integral of H across the gap then is simply Hg and equals the resultant mmf \mathcal{F}_{sr} of the stator and rotor windings; thus

$$Hg = \mathcal{F}_{sr} \quad (4-70)$$

where the script \mathcal{F} denotes the mmf wave as a function of the angle around the periphery.

The mmf waves of the stator and rotor are spatial sine waves with δ_{sr} the phase angle between their magnetic axes in electrical degrees. They can be represented by the space vectors \mathbf{F}_s and \mathbf{F}_r drawn along the magnetic axes of the stator- and rotor-mmfs waves, respectively, as in Fig. 4-35b. The resultant mmf \mathbf{F}_{sr} acting across the air gap, also a sine wave, is the vector sum. From the trigonometric formula for the diagonal of a parallelogram, its peak value is found from

$$F_{sr}^2 = F_s^2 + F_r^2 + 2F_s F_r \cos \delta_{sr} \quad (4-71)$$

in which the F 's are the peak values of the mmf waves. The resultant radial H field is a sinusoidal space wave whose peak value H_{peak} is, from Eq. 4-70,

$$H_{\text{peak}} = \frac{F_{sr}}{g} \quad (4-72)$$

Now consider the magnetic field coenergy stored in the air gap. The coenergy density at a point where the magnetic field intensity is H is $(\mu_0/2)H^2$ in SI units. The coenergy density averaged over the volume of the air gap is $\mu_0/2$ times the average value of H^2 . The average value of the square of a sine wave is half its peak value. Hence,

$$\text{Average coenergy density} = \frac{\mu_0}{2} \frac{H_{\text{peak}}^2}{2} = \frac{\mu_0}{4} \left(\frac{F_{sr}}{g} \right)^2 \quad (4-73)$$

The total coenergy is

$$\begin{aligned} W'_{\text{fld}} &= (\text{average coenergy density}) (\text{volume of air gap}) \\ &= \frac{\mu_0}{4} \left(\frac{F_{sr}}{g} \right)^2 \pi D l g = \frac{\mu_0 \pi D l}{4g} F_{sr}^2 \end{aligned} \quad (4-74)$$

where D = average diameter of air gap, m

l = axial length of air gap, m

g = air-gap length, m

μ_0 = permeability of free space = $4\pi \times 10^{-7}$ H/m

From Eq. 4-71 the coenergy stored in the air gap can now be expressed in terms of the peak amplitudes of the stator- and rotor-mmfs and the space-phase angle between them; thus

$$W'_{\text{fld}} = \frac{\mu_0 \pi D l}{4g} (F_s^2 + F_r^2 + 2F_s F_r \cos \delta_{sr}) \quad (4-75)$$

An expression for the electromagnetic torque T can now be obtained in terms of the interacting magnetic fields by taking the partial derivative of the field coenergy with respect to angle. For a two-pole machine

$$T = + \frac{\partial W'_{\text{fld}}}{\partial \delta_{sr}} = - \frac{\mu_0 \pi D l}{2g} F_s F_r \sin \delta_{sr} \quad (4-76)$$

For a P -pole machine Eq. 4-76 gives the torque per pair of poles. The torque for a P -pole machine then is

$$T = - \frac{P}{2} \frac{\mu_0 \pi D l}{2g} F_s F_r \sin \delta_{sr} \quad (4-77)$$

This important equation states that the torque is proportional to the peak values of the stator- and rotor-mmfs F_s and F_r and to the sine of the electrical space-phase angle δ_{sr} between them. The minus sign means that the fields tend to align themselves. Equal and opposite torques are ex-

erted on the stator and rotor. The torque on the stator is transmitted through the frame of the machine to the foundation.

One can now compare the results of Eq. 4-77 with that of Eq. 4-69. Recognizing that F_s is proportional to i_s and F_r is proportional to i_r , one sees that they are similar in form. In fact, they must be equal, as can be verified by substitution of the appropriate expressions for F_s , F_r (Art. 4-3), and L_{sr} (Appendix B). Note that these results have been derived with the assumption that the iron reluctance is negligible. However, the two techniques are equally valid for finite iron permeability.

On referring to Fig. 4-35*b* it can be seen that $F_r \sin \delta_{sr}$ is the component of the F_r wave in electrical space quadrature with the F_s wave. Similarly $F_s \sin \delta_{sr}$ is the component of the F_s wave in quadrature with the F_r wave. Thus, the torque is proportional to the product of one magnetic field and the component of the other in quadrature with it, much like the cross product of vector analysis. Also note that in Fig. 4-35*b*

$$F_s \sin \delta_{sr} = F_{sr} \sin \delta_r \quad (4-78)$$

and

$$F_r \sin \delta_{sr} = F_{sr} \sin \delta_s \quad (4-79)$$

The torque can then be expressed in terms of the *resultant mmf wave* F_{sr} by substitution of either Eq. 4-78 or 4-79 in Eq. 4-77; thus

$$T = -\frac{P}{2} \frac{\pi}{2} \frac{\mu_0 D l}{g} F_s F_{sr} \sin \delta_s \quad (4-80)$$

$$T = -\frac{P}{2} \frac{\pi}{2} \frac{\mu_0 D l}{g} F_r F_{sr} \sin \delta_r \quad (4-81)$$

Comparison of Eqs. 4-77, 4-80, and 4-81 shows that the torque can be expressed in terms of the component magnetic fields due to *each* current acting alone, as in Eq. 4-77, or in terms of the *resultant* field and *either* of the components, as in Eqs. 4-80 and 4-81, *provided that we use the corresponding angle between the axes of the fields*. Ability to reason in any of these terms is a convenience in machine analysis.

In Eqs. 4-77, 4-80, and 4-81 the fields have been expressed in terms of the peak values of their mmf waves. When magnetic saturation is neglected, the fields can, of course, be expressed in terms of the peak values of their flux-density waves or in terms of total flux per pole. Thus the peak value B of the field due to a sinusoidally distributed mmf wave in a uniform-air-gap machine is $\mu_0 F/g$, where F is the peak value of the mmf wave. For example, the resultant mmf F_{sr} produces a resultant flux-density wave whose peak value is $\mu_0 F_{sr}/g$. Thus,

$$T = -\frac{P}{2} \frac{\pi D l}{2} B_{sr} F_r \sin \delta_r \quad (4-82)$$

One of the inherent limitations in the design of electromagnetic apparatus is the saturation flux density of magnetic materials. Because of saturation in the armature teeth the peak value B_{sr} of the resultant flux-density wave in the air gap is limited to about 1.5 to 2.0 T. The maximum permissible value of the mmf wave is limited by the temperature rise of the winding and other design requirements. Because the resultant flux density and mmf appear explicitly in Eq. 4-82, this equation is in a convenient form for design purposes.

Alternative forms arise when it is recognized that the resultant flux per pole is

$$\Phi = (\text{average value of } B \text{ over a pole}) (\text{pole area}) \quad (4-83)$$

and that the average value of a sinusoid over one-half wavelength is $2/\pi$ times its peak value. Thus

$$\Phi = \frac{2}{\pi} B \frac{\pi D l}{P} = \frac{2 D l}{P} B \quad (4-84)$$

where B is the peak value of the corresponding flux-density wave. For example, substitution of Eq. 4-84 into Eq. 4-82 gives

$$T = -\frac{\pi}{2} \left(\frac{P}{2} \right)^2 \Phi_{sr} F_r \sin \delta_r \quad (4-85)$$

where Φ_{sr} is the resultant flux produced by the combined effect of the stator and rotor mmf's.

To recapitulate, we now have several forms in which the torque of a uniform-air-gap machine can be expressed in terms of its magnetic fields. *All are merely statements that the torque is proportional to the interacting fields and to the sine of the electrical space angle between their magnetic axes.* The negative sign indicates that the electromagnetic torque acts in a direction to decrease the displacement angle between the fields. In a preliminary discussion of machine types, Eq. 4-85 will be the preferred form.

One further remark can be made concerning the torque equations and the thought process leading to them. There is no restriction that the mmf wave or flux-density wave remain stationary in space. They may remain stationary, or they may be traveling waves, as shown in Art. 4-5. If the magnetic fields of the stator and rotor are constant in amplitude and travel around the air gap at the same speed, a steady torque will be produced by the efforts of the stator and rotor fields to align themselves in accordance with the torque equations.

4-8 LINEAR MACHINES

In general, each of the machine types discussed in this book can be produced in linear versions in addition to the rotary versions which are commonly found and which are discussed extensively in the following chapters. In fact, for clarity of discussion, many of the machine types discussed in this book are drawn in their developed (cartesian coordinate) form, such as in Fig. 4-19.

Perhaps the most widely known use of linear motors is in the transportation field. In these applications, linear induction motors are used, typically with the ac "stator" on the moving vehicle and with a conducting stationary "rotor" constituting the rails. In these systems, in addition to providing propulsion, the induced currents in the rail provide levitation, thus offering a mechanism for high-speed transportation without the difficulties associated with wheel-rail interactions on more conventional rail transport.

Linear motors have also found application in the machine tool industry and in robotics where linear motion (required for positioning and in the operation of manipulators) is a common requirement. In addition, reciprocating linear machines are being constructed for driving reciprocating compressors and alternators.

The analysis of linear machines is quite similar to that of rotary machines. In general, linear dimensions and displacements replace angular ones, and forces replace torques. However, with these exceptions, the expressions for machine parameters are derived in an analogous fashion to those presented here for rotary machines, and the results are similar in form.

Consider the linear winding shown in Fig. 4-36. This winding, consisting of N turns per slot and carrying a current i , is directly analogous to the rotary winding shown in developed form in Fig. 4-25. In fact, the only difference is that the angular position θ is replaced by the linear position z .

The fundamental component of the mmf wave of Fig. 4-36 can be found directly from Eq. 4-14 simply by recognizing that this winding has a wavelength β and that the fundamental component of this mmf wave varies as $\cos(2\pi z/\beta)$. Thus replacing the angle θ in Eq. 4-14 by $2\pi z/\beta$, we can find the fundamental component of the mmf wave directly as

$$H_{a1} = \frac{4}{\pi} \frac{Ni}{2g} \cos \frac{2\pi z}{\beta} \quad (4-86)$$

If an actual machine has a distributed winding (similar to its rotary counterpart, shown in Fig. 4-20) consisting of a total of N_{ph} turns distributed over m periods in z (i.e., over a length of $m\beta$), the fundamental com-

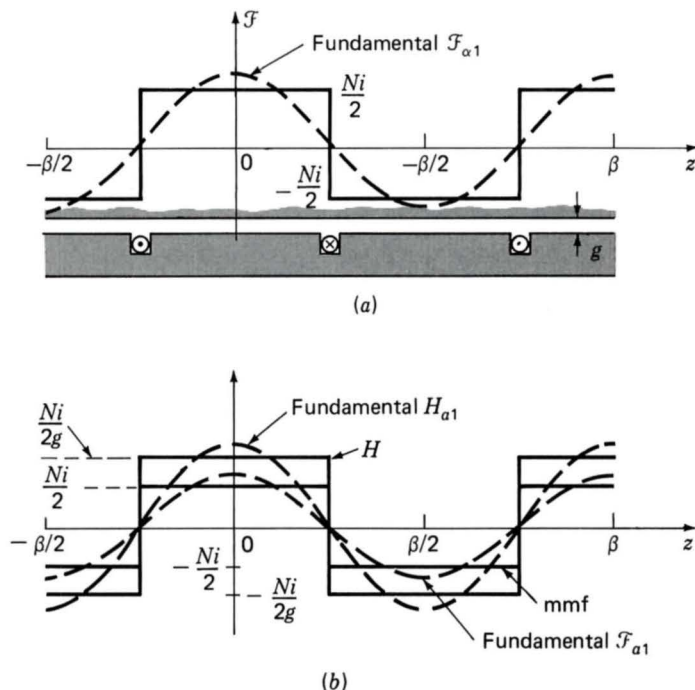


Fig. 4-36. The mmf and H field of a concentrated full-pitch linear winding.

ponent of H can be found by analogy with Eq. 4-16

$$H_{a1} = \frac{4}{\pi} k_w \frac{N_{ph} i}{2mg} \cos \frac{2\pi z}{\beta} \quad (4-87)$$

where k_w is the winding factor.

In a fashion analogous to Art. 4-5b, a three-phase linear winding can be made from three windings such as that of Fig. 4-31, with each phase displaced in position by a distance $\beta/3$ and with each phase excited by balanced three-phase currents of angular frequency ω

$$i_a = I_m \cos \omega t \quad (4-88)$$

$$i_b = I_m \cos (\omega t - 120^\circ) \quad (4-89)$$

$$i_c = I_m \cos (\omega t + 120^\circ) \quad (4-90)$$

Following the development of Eqs. 4-27 through 4-39, we can see that there will be a single positive-traveling mmf which can be written directly from Eq. 4-39 simply by replacing θ by $2\pi z/\beta$ as

$$\mathcal{F}^+(\theta, t) = \frac{3}{2} F_{\max} \cos \left(\frac{2\pi z}{\beta} - \omega t \right) \quad (4-91)$$

where F_{\max} is given by

$$F_{\max} = \frac{4}{\pi} k_w \frac{N_{\text{ph}} I_m}{2m} \quad (4-92)$$

From Eq. 4-91 we see that the result is an mmf which travels in the z direction with a linear velocity

$$v = \frac{dz}{dt} = \frac{\omega \beta}{2\pi} = f\beta \quad (4-93)$$

where f is the exciting frequency in hertz.

EXAMPLE 4-3

A three-phase linear ac motor has a winding with a wavelength of $\beta = 0.5$ m and a winding factor $k_w = 0.92$. The air gap is 1.0 cm long, and a total of 45 turns are distributed over a total winding length of $3\beta = 1.5$ m. Assume the windings to be excited with balanced three-phase currents of amplitude 700 A and frequency 25 Hz. Calculate (a) the amplitude of the resultant mmf wave, (b) the corresponding peak air-gap flux density, and (c) the velocity of this traveling mmf wave.

Solution

(a) From Eq. 4-91, the amplitude of the resultant mmf wave is

$$\begin{aligned} F_{\text{peak}} &= \frac{3}{2} \frac{4}{\pi} k_w \frac{N_{\text{ph}} I_m}{2m} \\ &= \frac{3(4)(0.92)(45)(700)}{2(2)(\pi)(3)} \\ &= 8.81 \times 10^3 \text{ A/m} \end{aligned}$$

(b) The peak air-gap flux density can be found from the result of part (a) by dividing by the air-gap length and multiplying by μ_0 :

$$B_{\text{peak}} = \frac{\mu_0 F_{\text{peak}}}{g}$$

$$\begin{aligned}
 &= \frac{(4\pi \times 10^{-7})(8.81 \times 10^3)}{0.01} \\
 &= 1.11 \text{ T}
 \end{aligned}$$

(c) Finally, the velocity of the traveling wave can be determined from Eq. 4-93:

$$v = f\beta = 25(0.5) = 12.5 \text{ m/s}$$

Linear machines are not discussed specifically in this book. Rather, the reader is urged to recognize that the fundamentals of their performance and analysis correspond directly to those of their rotary counterparts. One major difference between these two machine types is that linear machines have "end effects." These effects are beyond the scope of this book and have been treated in detail in the published literature.[†]

4-9 MAGNETIC SATURATION

The characteristics of electric machines depend heavily upon the use of magnetic materials. These materials are required to form the magnetic circuit and are used by the machine designer to obtain specific machine characteristics. As we have seen in Chap. 1, magnetic materials are less than ideal. As their magnetic flux is increased, they begin to saturate, with the result that their magnetic permeabilities begin to decrease, along with their effectiveness in contributing to the overall flux density in the machine.

Both electromagnetic torque and generated voltage in all machines depend on the winding flux linkages. For specific mmf's in the windings, the fluxes depend on the reluctances of the iron portions of the magnetic circuits and on those of the air gaps. Saturation may therefore appreciably influence the characteristics of the machines. Another aspect of saturation, more subtle and more difficult to evaluate without experimental and theoretical comparisons, concerns its influence on the basic premises from which the analytic approach to machinery is developed. Specifically, relations for mmf are typically based on the assumption of negligible reluctance in the iron. When these relations are applied to practical machines with varying degrees of saturation in the iron, the actual machine can be, in effect, replaced for these considerations by an equivalent machine, one whose iron has negligible reluctance but whose air-gap length is increased by an amount sufficient to absorb the magnetic-potential drop in the iron of the actual machine. Incidentally, the effects of air-gap nonuniformities

[†]See, for example, S. Yamamura, *Theory of Linear Induction Motors*, 2d ed., Halsted Press, 1978.

such as slots and ventilating ducts are also incorporated through the medium of an equivalent smooth gap, a replacement which, in contrast to that above, is made explicitly during magnetic circuit computations for the machine structure. Thus, serious efforts must be made to reproduce the magnetic conditions at the air gap correctly, and the computed performance of machines is based largely on those conditions. Final assurance of the legitimacy of the approach must, of course, be the pragmatic one given by close experimental checks. Alternatively, detailed analyses such as those employing finite-element or other numerical techniques can be used in those situations where conventional techniques appear to be inadequate.

Magnetic circuit data essential to handling saturation are given by the *open-circuit characteristic*, also called the *magnetization curve* or *saturation curve*. An example is shown in Fig. 4-37. Basically, this characteristic is the magnetization curve for the particular iron and air geometry of the machine under consideration. Frequently, the abscissa is plotted in terms of the field current or magnetizing current instead of the mmf in ampere-turns. Also the generated voltage with zero armature current is directly proportional to the flux when the speed is constant. For convenience in use, then, the open-circuit terminal voltage is plotted on the ordinate scale rather than the air-gap flux per pole, and the entire curve is drawn for a stated fixed speed, usually the rated speed. The straight line tangent to the lower portion of the curve is the *air-gap line*, indicating very closely the mmf required to overcome the reluctance of the air gap. If it were not for the effects of saturation, the air-gap line and open-circuit characteristic would coincide, so that the departure of the curve from the air-gap line is an indication of the degree of saturation present. In typical machines the ratio at rated voltage of the total mmf to that required by the air gap alone usually is between 1.1 and 1.25.

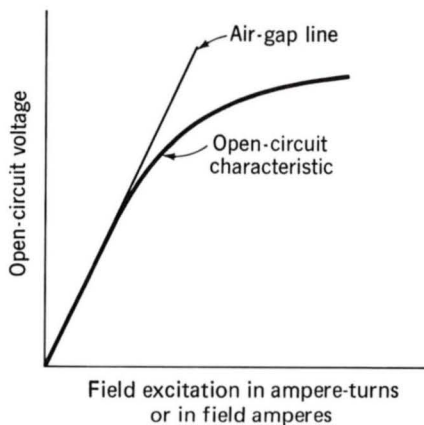


Fig. 4-37. Typical open-circuit characteristic and air-gap line.

The open-circuit characteristic can be calculated from design data by computer-implemented magnetic field solutions based on techniques of finite-element or finite-difference analysis. These techniques can be used to obtain solutions for magnetic fields, including the effects of finite permeability. A typical finite-element solution for the flux distribution around the pole of a salient-pole machine is shown in Fig. 4-38. The distribution of the air-gap flux found from this solution, together with the fundamental and third-harmonic components, is shown in Fig. 4-39.

In addition to saturation effects, Fig. 4-39 clearly illustrates the effect of a nonuniform air gap. As expected, the flux density over the pole face, where the air gap is small, is much higher than that away from the pole. This type of detailed analysis is of great use to a designer in obtaining specific machine properties.

If the machine is an existing one, the magnetization curve is usually determined by operating the machine as an unloaded generator and measuring the values of terminal voltage corresponding to a series of values of field current. For an induction motor the machine is operated at or close to synchronous speed, and values of the magnetizing current are obtained for a series of values of impressed stator voltage. It should be emphasized, however, that saturation in a fully loaded machine occurs as a result of the total mmf acting on the magnetic circuit. Since the flux distribution under

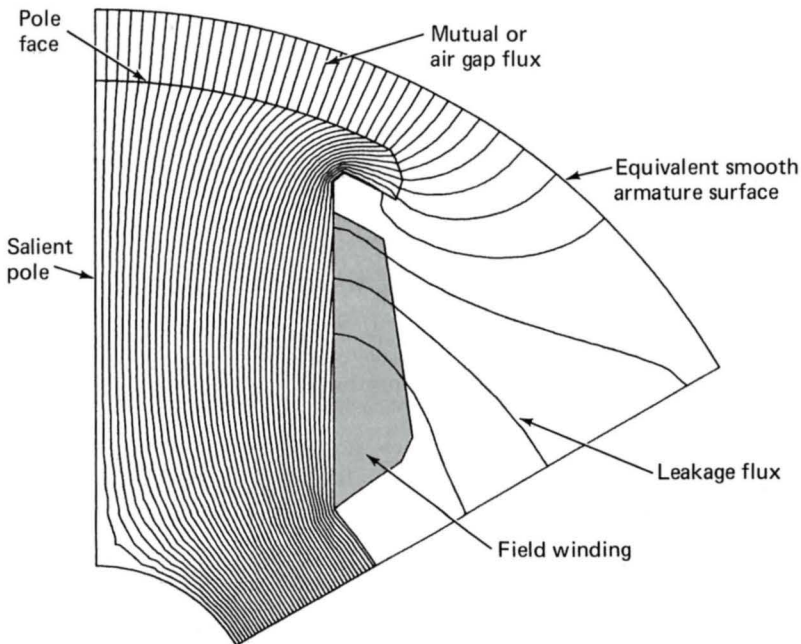


Fig. 4-38. Finite-element solution for the flux distribution around a salient pole. (*General Electric Company.*)

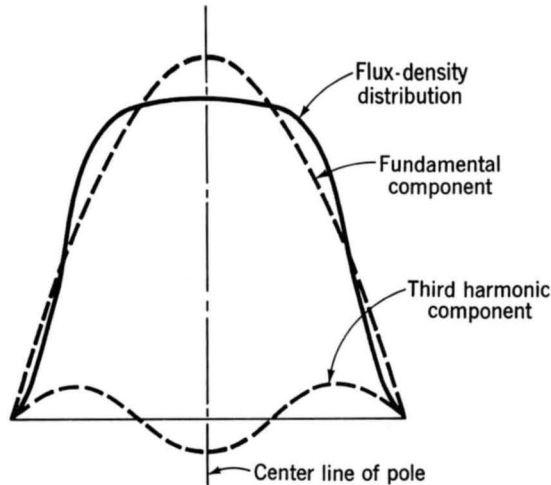


Fig. 4-39. Flux-density wave corresponding to Fig. 4-38 with its fundamental and third harmonic components.

load generally differs from that of no-load conditions, the details of the machine saturation characteristics may vary from the open-circuit curve of Fig. 4-37.

4-10 LEAKAGE FLUXES

In Art. 2-4 we showed that in a two-winding transformer the flux created by each winding can be separated into two components. One component consists of flux which links both windings, and the other consists of flux which links only the winding creating the flux. The first component, called *mutual flux*, is responsible for coupling between the two coils. The second, known as *leakage flux*, contributes only to the self-inductance of each coil.

Note that the concept of mutual and leakage flux is meaningful only in the context of a multiwinding system. For systems of three or more windings, the bookkeeping must be done very carefully. Consider, for example, the three-winding system of Fig. 4-40. Shown schematically are the various components of flux created by a current in winding 1. Here φ_{123} is clearly mutual flux that links all three windings, and φ_{1l} is clearly leakage flux since it links only winding 1. However, φ_{12} is mutual flux with respect to winding 2 yet is leakage flux with respect to winding 3, while φ_{13} is mutual flux with respect to winding 3 and leakage flux with respect to winding 2.

Electric machinery often contains systems of multiple windings, requiring careful bookkeeping to account for the flux contributions of the various windings. Although the details of such analysis are beyond the

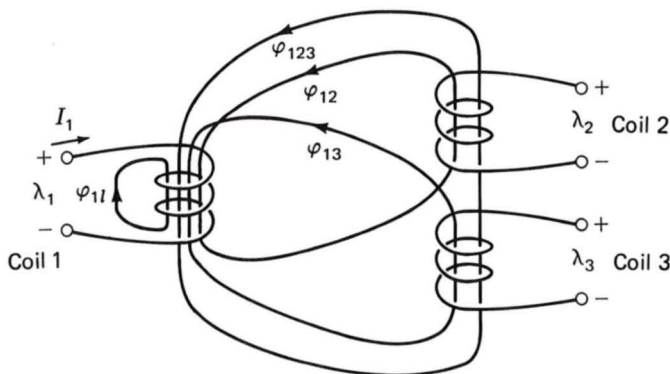


Fig. 4-40. Three-coil system showing components of mutual and leakage flux produced by current in coil 1.

scope of this book, it is useful to discuss these effects in a qualitative fashion and to describe how they affect the basic machine inductances.

Air-Gap Space-Harmonic Fluxes. In this chapter we have seen that although single distributed coils create air-gap flux with a significant amount of space-harmonic content, it is possible to distribute these windings so that the space-fundamental component is emphasized while the harmonic effects are greatly reduced. As a result, we can neglect harmonic effects and consider only space-fundamental fluxes in calculating the self and mutual-inductance expressions of Eqs. B-27 and B-28.

Though often small, the space-harmonic components of air-gap flux do exist. In dc machines they are useful torque-producing fluxes and therefore can be counted as mutual flux between the rotor and stator windings. In ac machines, however, they may generate time-harmonic voltages or asynchronously rotating flux waves. These effects generally cannot be rigorously accounted for in most standard analyses. Nevertheless, it is consistent with the assumptions basic to these analyses to recognize that these fluxes form a part of the leakage flux of the individual windings which produce them.

Slot-Leakage Flux. Figure 4-41 shows the flux created by a single coil side in a slot. Notice that in addition to flux which crosses the air gap, contributing to the air-gap flux, there are flux components which cross the slot. Since this flux links only the coil that is producing it, it also forms a component of the leakage inductance of the winding producing it.

End-Turn Fluxes. Figure 4-42 shows the stator end windings on an ac machine. The magnetic field distribution created by end turns is extremely complex. In general these fluxes do not contribute to useful rotor-to-stator mutual flux, and thus they, too, contribute to leakage inductance.

From this discussion we see that the self-inductance expression of Eq. B-27 must, in general, be modified by an additional term L_l , which

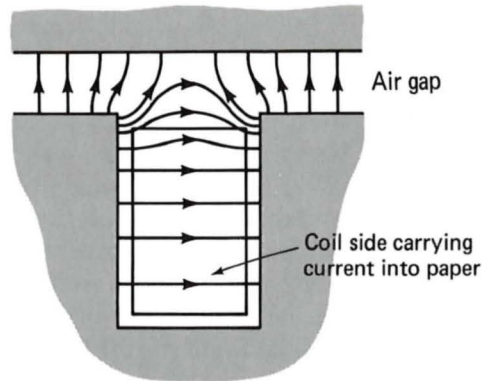


Fig. 4-41. Flux created by a single coil side in a slot.

represents the winding leakage inductance. Although the leakage inductance is usually difficult to calculate analytically and must be determined by approximate or empirical techniques, it plays an important role in machine performance.

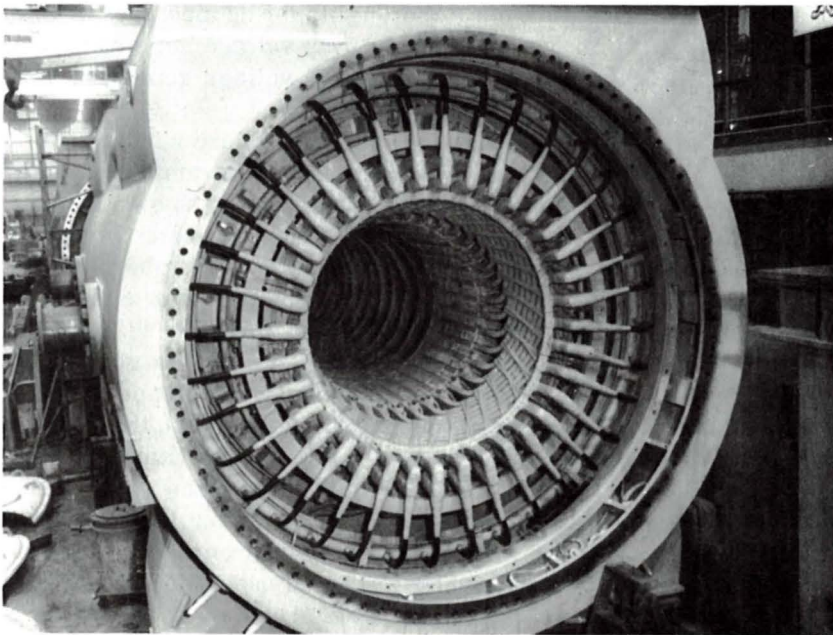


Fig. 4-42. End view of the stator of a 26-kV 908-MVA 3600 r/min turbine generator with water-cooled windings. Hydraulic connections for coolant flow are provided for each winding end turn. (General Electric Company.)

4-11 SUMMARY

In this chapter we have presented a brief and elementary description of three basic types of rotating machines: synchronous, induction, and dc machines. In all of them the basic principles are essentially the same. Voltages are generated by relative motion of a magnetic field with respect to a winding, and torques are produced by the interaction of the magnetic fields of the stator and rotor windings. The characteristics of the various machine types are determined by the methods of connection and excitation of the windings, but the basic principles are essentially similar.

The basic analytical tools for studying rotating machines are expressions for the generated voltages and for the electromagnetic torque. Taken together, they express the coupling between the electric and mechanical systems. To develop a reasonably quantitative theory without the confusion arising from too much detail, we have made several simplifying approximations. In the study of ac machines we have assumed sinusoidal time variations of voltages and currents and sinusoidal space waves of air-gap flux density and mmf. On examination of the mmf of distributed ac windings we found that the space-fundamental component is the most important, but that the mmf of dc machine armature windings is more nearly a sawtooth wave. For our preliminary study in this chapter, however, we have assumed sinusoidal mmf distributions for both ac and dc machines. We examine this assumption more thoroughly for dc machines in Chap. 9. Faraday's law results in Eq. 4-55 for the rms voltage generated in an ac machine winding or Eq. 4-58 for the average voltage generated between brushes in a dc machine.

On examination of the mmf wave of a three-phase winding, we found that balanced three-phase currents produce a constant-amplitude magnetic field rotating in the air gap at synchronous speed, as shown in Fig. 4-31 and Eq. 4-40. The importance of this fact cannot be overestimated, for it means that the double-frequency time-varying torque inherently associated with the double-frequency component of the instantaneous power in a single-phase system is eliminated in balanced three-phase machines, as shown in Appendix A. Imagine a multimewatt 60-Hz generator or a multihorsepower motor subjected to a multimewatt instantaneous power pulsation at 120 Hz! The discovery of rotating fields led to the invention of the simple, rugged, reliable, self-starting polyphase induction motor, which is analyzed in Chap. 7. (A single-phase induction motor will not start; it needs an auxiliary starting winding, as shown in Chap. 11.) It also made possible the construction of multimewatt synchronous generators. The most significant reason for the almost universal use of three-phase generation, transmission, and utilization (for loads above a few kilowatts) is the rotating field in the generators and motors.

Having assumed sinusoidally distributed magnetic fields in the air gap, we then derived expressions for the magnetic torque. The simple physical

picture is like that of two magnets, one on the stator and one pivoted on the rotor, as shown schematically in Fig. 4-35*a*. The torque acts in the direction to align the magnets. To get a reasonably close quantitative analysis without being hindered by details, we assumed a smooth air gap and neglected the reluctance of the magnetic paths in the iron parts, with a mental note to look into these assumptions in later chapters.

In Art. 4-7 we derived expressions for the magnetic torque from two viewpoints, both based on the fundamental principles of Chap. 3. The first viewpoint regards the machine as a group of magnetically coupled circuits with inductances which depend on the angular position of the rotor, as in Art. 4-7*a*. The second regards the machine from the viewpoint of the magnetic fields in the air gap, as in Art. 4-7*b*. It is shown that the torque can be expressed as the product of the stator field, the rotor field, and the sine of the angle between their magnetic axes, as in Eq. 4-77 or any of the forms derived from Eq. 4-77. The two viewpoints are supplementary, and ability to reason in terms of both is helpful in reaching an understanding of how machines work.

This chapter has been concerned with basic principles underlying rotating-machine theory. By itself it is obviously incomplete. Many questions remain unanswered. How do we apply these principles to the determination of the characteristics of synchronous, induction, and dc machines? What are some of the practical problems that arise from the use of iron, copper, and insulation in physical machines? What are some of the economic and engineering considerations affecting rotating-machine applications? What are the physical factors limiting the conditions under which a machine can operate successfully? Appendix C discusses some of these problems. Taken together, Chap. 4 and Appendix C serve as an introduction to the more detailed treatments of rotating machines in Chaps. 5 to 11.

PROBLEMS

4-1. The rotor of a six-pole synchronous generator is rotating at a mechanical speed of 1200 r/min.

- (a) Express this mechanical speed in radians per second.
- (b) What is the frequency of the generated voltage in hertz and in radians per second?
- (c) What mechanical speed in revolutions per minute would be required to generate voltage at a frequency of 50 Hz?

4-2. The voltage generated in one phase of an unloaded three-phase synchronous generator is of the form $v(t) = V_0 \cos \omega t$. Write expressions for the voltage in the remaining two phases.

4-3. A three-phase motor is used to drive a pump. It is observed (by the use of a stroboscope) that the motor speed decreases from 998 r/min at no load to 950 r/min at full load.

- (a) Is this a synchronous or induction motor?
- (b) Estimate the frequency of the applied armature voltage in hertz.
- (c) How many poles does this motor have?

4-4. The object of this problem is to illustrate how the armature windings of certain machines, i.e., dc machines, can be approximately represented by uniform current sheets, the degree of correspondence growing better as the winding is distributed in a greater number of slots around the armature periphery. For this purpose, consider an armature with eight slots uniformly distributed over 360 electrical degrees or one pair of poles. The air gap is of uniform length, the slot openings are very small, and the reluctance of the iron is negligible.

Lay out 360 electrical degrees of the armature with its slots in developed form in the manner of Fig. 4-23a, and number the slots 1 to 8 from left to right. The winding consists of eight single-turn coils, each carrying a direct current of 10 A. Coil sides which can be placed in slots 1 to 4 carry current directed into the paper; those which can be placed in slots 5 to 8 carry current out of the paper.

- (a) Consider that all eight coils are placed with one side in slot 1 and the other in slot 5. The remaining slots are empty. Draw the rectangular mmf wave produced by these coils.
- (b) Next consider that four coils have one side in slot 1 and the other in slot 5, while the remaining four have one side in slot 3 and the other in slot 7. Draw the component rectangular mmf waves produced by each group of coils, and superimpose the components to give the resultant mmf wave.
- (c) Now consider that two coils are placed in slots 1 and 5, two in 2 and 6, two in 3 and 7, and two in 4 and 8. Again superimpose the component rectangular waves to produce the resultant wave. Note that the task can be systematized and simplified by recognizing that the mmf wave is symmetric about its axis and takes a step at each slot which is definitely related to the number of ampere-conductors in the slot.
- (d) Let the armature now consist of 16 slots per 360 electrical degrees with one coil side in each slot. Draw the resultant mmf wave.
- (e) Approximate each of the resultant waves of parts (a) to (d) by isosceles triangles, noting that the representation grows better as the winding is more finely distributed.

4-5. This problem investigates the advantages of short-pitching the stator coils of an ac machine. Figure 4-43a shows a single full-pitch coil in a two-

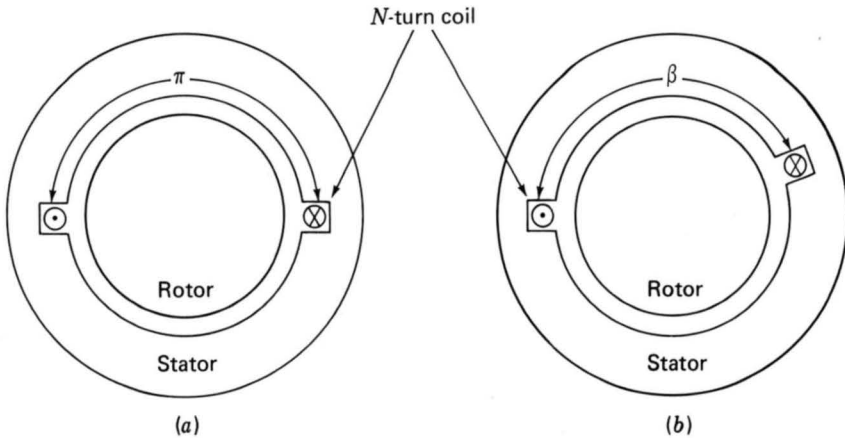


Fig. 4-43. Problem 4-5: (a) full-pitch coil and (b) fractional-pitch coil.

pole machine. Figure 4-43b shows a fractional-pitch coil; the coil sides are β rad apart rather than π rad (180°), as in the full-pitch case.

For an air-gap radial flux distribution of the form

$$B_r = \sum_{n \text{ odd}} B_n \cos n\theta$$

where $n = 1$ corresponds to the fundamental space harmonic, $n = 3$ the third harmonic, etc., the flux linkage of each coil is the integral of B_r over the surface spanned by that coil. Thus for the n th space harmonic, the ratio of the fractional-pitch coil flux linkage to that of the full-pitch coil is

$$\frac{\int_{-\beta/2}^{\beta/2} B_n \cos n\theta d\theta}{\int_{-\pi/2}^{\pi/2} B_n \cos n\theta d\theta} = \frac{\int_{-\beta/2}^{\beta/2} \cos n\theta d\theta}{\int_{-\pi/2}^{\pi/2} \cos n\theta d\theta}$$

It is common to fractional-pitch the coils of an ac machine by 30° ($\beta = 5\pi/6 = 150^\circ$). For $n = 1, 3, 5$ calculate the fractional reduction in flux linkage due to short-pitching.

4-6. A six-pole 60-Hz synchronous machine has a rotor winding with a total of 110 series turns and a winding factor $k_r = 0.92$. The rotor length is 1.82 m, the rotor radius is 55 cm, and the air-gap length is 3.2 cm.

- What is the rated operating speed in revolutions per minute?
- Calculate the rotor winding current required to achieve a peak fundamental air-gap flux density of 1.3 T.
- Calculate the corresponding flux per pole.

4-7. The synchronous machine of Prob. 4-6 has a three-phase armature winding with 44 series turns per phase and a winding factor $k_w = 0.94$. For the flux condition and operating speed of Prob. 4-6, calculate the rms-generated voltage per phase.

4-8. The three-phase synchronous machine of Prob. 4-6 is to be moved to an application which requires that its operating frequency be reduced from 60 to 50 Hz. This application requires that the rms-generated voltage per phase equal 6 kV. As a result, the machine armature will be rewound with a differing number of turns (while maintaining a winding factor $k_w = 0.94$). Calculate the required number of series turns per phase, assuming that the flux per pole remains as given in Prob. 4-6.

4-9. A three-phase Y-connected ac machine is initially operating under balanced three-phase conditions when one of the phase windings becomes open-circuited. Because there is no neutral connection on the winding, this requires that the currents in the remaining two windings become equal and opposite. Under this condition, calculate the relative magnitudes of the resultant positive- and negative-traveling mmf waves.

4-10. What is the effect on the rotating mmf wave of a three-phase winding carrying balanced three-phase currents if two of the phase connections are interchanged?

4-11. In a balanced two-phase machine, the two windings are displaced 90 electrical degrees in space, and the currents in the two windings are phase-displaced 90 electrical degrees in time. For such a machine, carry out the process leading to an equation for the rotating mmf wave corresponding to Eq. 4-40 (which is derived for a three-phase machine).

4-12. The following statements are made in Art. 4-5 just after we derived and discussed Eq. 4-42: In general, a rotating field of constant amplitude will be produced by a q -phase winding excited by balanced q -phase currents of frequency f when the respective phase axes are located $2\pi/q$ electrical radians apart in space. The constant amplitude will be $q/2$ times the maximum contribution of any one phase, and the speed will be $\omega = 2\pi f$ electrical radians per second.

Prove these statements.

4-13. Figure 4-44 shows a two-pole rotor revolving inside a smooth stator which carries a coil of 100 turns. The rotor produces a sinusoidal space distribution of flux at the stator surface; the peak value of the flux-density wave being 0.80 T when the current in the rotor is 10 A. The magnetic circuit is linear. The inside diameter of the stator is 0.10 m, and its axial length is 0.10 m. The rotor is driven at a speed of 60 r/s.

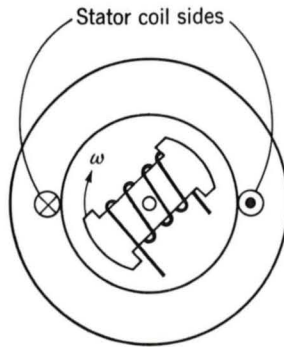


Fig. 4-44. Elementary generator for Prob. 4-13.

- (a) The rotor is excited by a direct current of 10 A. Taking zero time as the instant when the axis of the rotor is vertical, find the expression for the instantaneous voltage generated in the open-circuited stator coil.
- (b) The rotor is now excited by a 60-Hz sinusoidal alternating current whose rms value is 7.07 A. Consequently, the rotor current reverses every half revolution; it is timed to go through zero when the axis of the rotor is vertical. Taking zero time as the instant when the axis of the rotor is vertical, find the expression for the instantaneous voltage generated in the open-circuited stator coil. This scheme is sometimes suggested as a dc generator without a commutator; the thought being that if alternate half cycles of the alternating voltage generated in part (a) are reversed by reversal of the polarity of the field (rotor) winding, then a pulsating direct voltage will be generated in the stator. Explain whether this invention will work as described.

4-14. A three-phase two-pole winding is excited by balanced three-phase 60-Hz currents as described by Eqs. 4-24 to 4-26. Although the winding distribution has been designed to minimize harmonics, there remains some third and fifth spatial harmonics. Thus the phase-*a* mmf can be written as

$$\mathcal{F}_a = (A_1 \cos \theta + A_3 \cos 3\theta + A_5 \cos 5\theta)i_a$$

Similar expressions can be written for phases *b* (replace θ by $\theta - 120^\circ$) and *c* (replace θ by $\theta + 120^\circ$). Calculate the total three-phase mmf. What are the angular velocity and the rotational direction of each component of the mmf?

4-15. The nameplate of a dc generator indicates that it will produce an output voltage of 24 V dc when operated at a speed of 1200 r/min. By what

factor must the number of armature turns be changed if the generator is modified to produce an output voltage of 12 V at a speed of 1500 r/min?

4-16. The design of a four-pole three-phase 480-V 60-Hz induction motor is to be based on a stator core length of 10.5 in and a stator inner diameter of 8.5 in. The stator winding distribution which has been chosen has a winding factor $k_w = 0.91$. The armature is to be Y-connected, and thus the rated voltage of each phase is $480/\sqrt{3}$ V.

- (a) The designer must pick the number of armature turns so that the flux density in the machine is large enough to make efficient use of the magnetic material without being so large that it results in excessive saturation. In this case, the optimal performance is achieved with a peak fundamental air-gap flux density of 1.1 T. Calculate the number of turns per phase.
- (b) For an air-gap length of 0.011 in, calculate the self-inductance of an armature phase based on the results of part (a), using the inductance formulas of Appendix B. Neglect the reluctance of the rotor and stator iron and the armature leakage inductance.

4-17. A two-pole 60-Hz three-phase laboratory-size synchronous generator has a rotor radius of 2.25 in, an air-gap length of 0.010 in, and a rotor length of 7.1 in. The rotor field winding has 248 turns and a winding factor of 0.95. The armature winding consists of 60 turns per phase with a winding factor of 0.93.

- (a) Calculate the flux per pole and peak fundamental air-gap flux density for an armature voltage of 120 V rms/phase.
- (b) Calculate the dc field current in amperes required to achieve the conditions of part (a).

4-18. A four-pole 60-Hz synchronous generator has a rotor length of 3.9 m, diameter of 1.12 m, and air-gap length of 6.2 cm. The rotor winding consists of 55 turns per pole with a winding factor of $k_r = 0.89$. The peak value of fundamental air-gap flux density is limited to 1.0 T and the rotor winding current to 2900 A. Calculate the maximum torque in newton-meters and power output in megawatts which can be supplied by the machine under these conditions.

4-19. Figure 4-45 shows in cross section a machine having a rotor winding f and two identical stator windings a and b . The self-inductance of each stator winding is L_{aa} and of the rotor winding is L_{ff} . The air gap is uniform. The stator windings are in quadrature. The mutual inductance between a stator winding and the rotor winding depends on the angular position θ_0 of the rotor and may be assumed to be

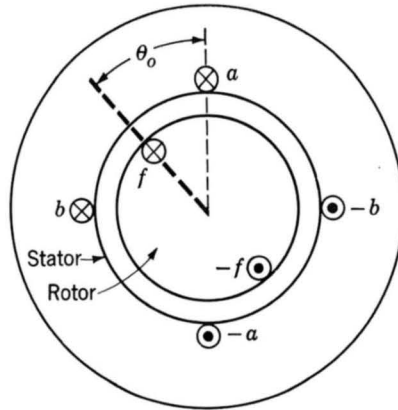


Fig. 4-45. Elementary cylindrical-rotor two-phase synchronous machine for Prob. 4-19.

$$M_{af} = M \cos \theta_0 \quad M_{bf} = M \sin \theta_0$$

where M is the maximum value of the mutual inductance. The resistance of each stator winding is R_a .

- Derive a general expression for the torque T in terms of the angle θ_0 , the inductance constants, and the instantaneous currents i_a , i_b , and i_f . Does this expression apply at standstill? When the rotor is revolving?
- Suppose the rotor is stationary and constant direct currents $I_a = 5$ A, $I_b = 5$ A, and $I_f = 10$ A are supplied to the windings in the directions indicated by the dots and crosses in Fig. 4-45. If the rotor is allowed to move, will it rotate continuously or will it tend to come to rest? If the latter, at what value is θ_0 ?
- The rotor winding is now excited by a constant direct current I_f , and the stator windings carry balanced two-phase currents

$$i_a = \sqrt{2}I_a \cos \omega t \quad i_b = \sqrt{2}I_a \sin \omega t$$

The rotor is revolving at synchronous speed so that its instantaneous angular position θ_0 is given by $\theta_0 = \omega t - \delta$, where δ is a phase angle describing the position of the rotor at $t = 0$. The machine is an elementary two-phase synchronous machine. Derive an expression for the torque under these conditions. Describe its nature.

- Under the conditions of part (c), derive an expression for the instantaneous terminal voltages of stator phases a and b .

4-20. Consider the two-phase synchronous machine of Prob. 4-19. Derive an expression for the torque acting on the rotor if the rotor is rotating at

constant angular velocity ($\theta = \omega t + \delta$) and the phase currents become unbalanced such that

$$i_a = \sqrt{2}I_a \cos \omega t \quad i_b = \sqrt{2}(I_a + I') \sin \omega t$$

What is the instantaneous and time-averaged torque under this condition?

4-21. Figure 4-46 shows in cross section a machine having two identical stator windings a and b arranged in quadrature on a laminated steel core. The salient-pole rotor is made of steel and carries a winding f connected to slip rings. The machine is an elementary two-phase salient-pole synchronous machine.

Because of the nonuniform air gap, the self- and mutual inductances of the stator windings are functions of the angular position θ_0 of the rotor, as follows:

$$L_{aa} = L_0 + L_2 \cos 2\theta_0 \quad L_{bb} = L_0 - L_2 \cos 2\theta_0 \quad M_{ab} = L_2 \sin 2\theta_0$$

where L_0 and L_2 are positive constants. The mutual inductances between the rotor and the stator windings are functions of θ_0

$$M_{af} = M \cos \theta_0 \quad M_{bf} = M \sin \theta_0$$

where M is a positive constant. The self-inductance L_{ff} of the rotor winding is constant, independent of θ_0 .

The rotor (or field) winding f is excited with direct current I_f , and the stator windings are connected to a balanced two-phase voltage source. The currents in the stator windings are

$$i_a = \sqrt{2}I_a \cos \omega t \quad i_b = \sqrt{2}I_a \sin \omega t$$

The rotor is revolving at synchronous speed so that its instantaneous angular position is given by

$$\theta_0 = \omega t - \delta$$

where δ is a phase angle describing the position of the rotor at $t = 0$.

- Derive an expression for the electromagnetic torque acting on the rotor. Describe its nature.
- Can the machine be operated as a motor? As a generator? Explain.
- Will the machine continue to run if the field current I_f is reduced to zero? If so, give an expression for the torque and a physical explanation.

4-22. A three-phase linear ac motor has an armature winding of wavelength 0.7 m. A three-phase balanced set of currents at a frequency of

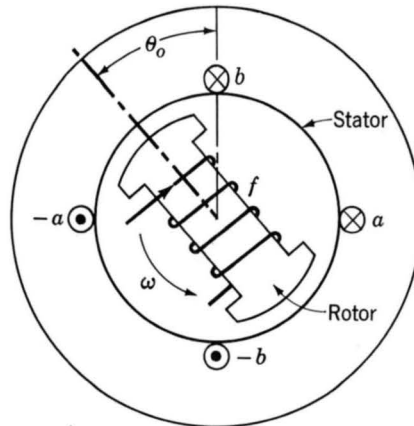


Fig. 4-46. Elementary salient-pole two-phase synchronous machine for Prob. 4-21.

60 Hz is applied to the armature. Calculate the velocity of the resultant traveling mmf wave.

4-23. The linear motor of Prob. 4-22 has a total length of 5 wavelengths, a total of 180 turns per phase, and a winding factor of $k_w = 0.89$. For an air-gap length of 0.75 cm, calculate the magnitude of the balanced three-phase currents which must be applied to the armature to achieve a peak fundamental air-gap flux density of 1.65 T.

Synchronous Machines: Steady State

A synchronous machine is an ac machine whose speed under steady-state conditions is proportional to the frequency of the current in its armature. The magnetic field created by the armature currents rotates at the same speed as that created by field current on the rotor (which is rotating at synchronous speed), and a steady torque results. An elementary picture of how a synchronous machine works is given in Art. 4-2a with emphasis on torque production in terms of the interactions between its magnetic fields.

Analytical methods of examining the steady-state performance of polyphase synchronous machines will be developed in this chapter. Initial consideration will be given to cylindrical-rotor machines; the effects of salient poles are taken up in Arts. 5-6 and 5-7.

5-1 INTRODUCTION TO POLYPHASE SYNCHRONOUS MACHINES

As indicated in Art. 4-2*a*, a synchronous machine is one in which alternating current flows in the armature winding and dc excitation is supplied to the field winding. The armature winding is almost invariably on the stator and is usually a three-phase winding, as described in Chap. 4. The field winding is on the rotor. The cylindrical-rotor construction shown in Figs. 4-10 and 4-11 is used for two- and four-pole turbine generators. The salient-pole construction shown in Fig. 4-9 is best adapted to multipolar slow-speed hydroelectric generators and to most synchronous motors. The dc power required for excitation—approximately one to a few percent of the rating of the synchronous machine—usually is supplied through *slip rings* from a dc generator called an *exciter*, which is often mounted on the same shaft as the synchronous machine. Various excitation systems using ac exciters and solid-state rectifiers are used with large turbine generators. One of these systems is described in Appendix C.

A single synchronous generator supplying power to an impedance load acts as a voltage source whose frequency is determined by its prime-mover speed, as in Eq. 4-2. The current and power factor are then determined by the generator field excitation and the impedance of the generator and load.

Synchronous generators can be readily operated in parallel, and, in fact, the electricity supply systems of industrialized countries may have scores or even hundreds of them operating in parallel, interconnected by thousands of miles of transmission lines, and supplying electric energy to loads scattered over areas of hundreds of thousands of square miles. These huge systems have grown in spite of the necessity for designing the system so that synchronism will be maintained following disturbances and the problems, both technical and administrative, which must be solved to coordinate the operation of such a complex system of machines and personnel. The principal reasons for these interconnected systems are continuity of service and economies in plant investment and operating costs.

When a synchronous generator is connected to a large interconnected system containing many other synchronous generators, the voltage and frequency at its armature terminals are substantially fixed by the system. As a result, armature currents will produce a component of the air-gap magnetic field which rotates at synchronous speed (Eq. 4-41 or 4-42) as determined by the system frequency. For the production of a steady unidirectional electromagnetic torque, the fields of the stator and rotor must rotate at the same speed, and therefore the rotor must turn at precisely synchronous speed. Because any individual generator is a small fraction of the total system generation, it cannot significantly affect the system voltage or frequency. It is often useful for the purposes of analysis to represent the system as a constant-frequency, constant-voltage source known as an *infinite bus*. Many important features of synchronous-machine behavior

can be understood from analysis of a single machine connected to an infinite bus.

The steady-state behavior of a synchronous machine can be visualized in terms of the torque equation. From Eq. 4-85, with changes in notation appropriate to synchronous-machine theory,

$$T = \frac{\pi}{2} \left(\frac{\text{poles}}{2} \right)^2 \Phi_R F_f \sin \delta_{RF} \quad (5-1)$$

where Φ_R = resultant air-gap flux per pole

F_f = mmf of dc field winding

δ_{RF} = phase angle between magnetic axes of Φ_R and F_f

The minus sign of Eq. 4-85 has been omitted with the understanding that the electromagnetic torque acts in the direction to bring the interacting fields into alignment. In normal steady-state operation, the electromagnetic torque balances the mechanical torque applied to the shaft. In a generator, the prime-mover torque acts in the direction of rotation of the rotor, pushing the rotor mmf wave ahead of the resultant air-gap flux. The electromagnetic torque then opposes rotation. The opposite situation exists in a synchronous motor, where the electromagnetic torque is in the direction of rotation, in opposition to the retarding torque of the mechanical load on the shaft.

Variations in the electromagnetic torque result in corresponding variations in the torque angle δ_{RF} , as seen from Eq. 5-1. The relationship is shown in the form of a *torque-angle curve* in Fig. 5-1, where the field current (rotor mmf) and resultant air-gap flux are assumed constant. Positive values of torque represent generator action, and positive values of δ_{RF} represent angles of lead of the rotor mmf wave with respect to the resultant air-gap flux.

As the prime-mover torque is increased, the magnitude of δ_{RF} must increase until the electromagnetic torque balances the shaft torque. The

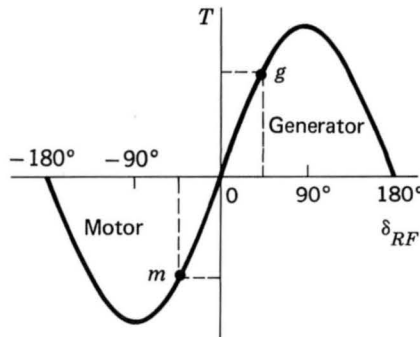


Fig. 5-1. Torque-angle characteristic.

readjustment process is actually a dynamic one, accompanied by a temporary change in the instantaneous mechanical speed of the rotor and a damped mechanical oscillation, called *hunting*, of the rotor about its new steady-state torque angle. In a practical machine, some changes in the amplitudes of the resultant flux-density and mmf waves may also occur because of factors, e.g., saturation and leakage impedance, neglected in the present argument. The adjustment of the rotor to its new angular position following a load change can be observed experimentally in the laboratory by viewing the machine rotor with stroboscopic light having a flashing frequency which causes the rotor to appear stationary when it is turning at its normal synchronous speed. Synchronous-machine transient behavior is discussed in Chap. 6.

As the prime-mover torque is further increased, δ_{RF} increases. When δ_{RF} becomes 90° , the electromagnetic torque reaches its maximum value, known as the *pull-out torque*. Any further increase in prime-mover torque cannot be balanced by a corresponding increase in synchronous electromagnetic torque, with the result that the rotor will speed up and synchronous operation will not be maintained. This phenomenon is known as *losing synchronism* or *pulling out of step*. Under these conditions, the generator is usually disconnected from the line by the automatic operation of circuit breakers, and the prime mover is quickly shut down to prevent dangerous overspeed. Note from Eq. 5-1 that the value of the pull-out torque can be increased by increasing either the field current or the resultant air-gap flux.

As seen from Fig. 5-1, a similar situation occurs in a synchronous motor for which an increase in the shaft load beyond the pull-out torque will cause the rotor to lose synchronism and thus to slow down.

Since a synchronous motor per se has no net starting torque, means must be provided for bringing it up to synchronous speed by induction-motor action, as described briefly at the end of Art. 7-1.

5-2 SYNCHRONOUS-MACHINE INDUCTANCES; EQUIVALENT CIRCUITS

In Art. 5-1, we described synchronous-machine torque-angle characteristics in terms of the interacting air-gap flux and mmf waves. Our purpose now is to derive an equivalent circuit which represents the steady-state terminal volt-ampere characteristics.

A cross-sectional sketch of a three-phase cylindrical-rotor synchronous machine is shown schematically in Fig. 5-2. The figure shows a two-pole machine; alternatively, this can be considered as two poles of a P -pole machine. The three-phase armature winding on the stator is of the same type used in the discussion of rotating magnetic fields in Art. 4-5. Coils aa' , bb' , and cc' represent distributed windings producing sinusoidal mmf and flux-density waves in the air gap. The reference directions for the currents

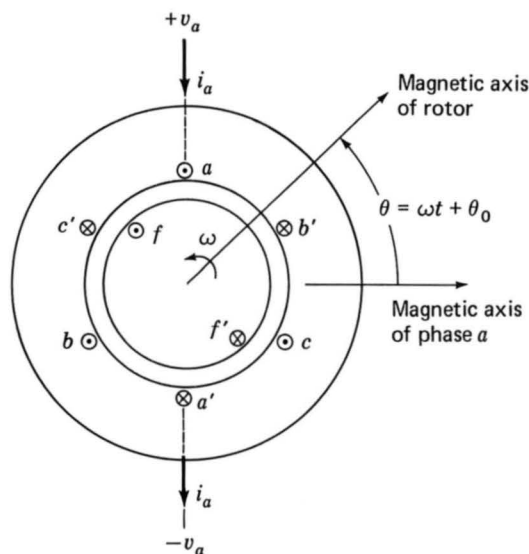


Fig. 5-2. Schematic diagram of a three-phase cylindrical-rotor synchronous machine.

are shown by dots and crosses. The field winding ff' on the rotor also represents a distributed winding which produces a sinusoidal mmf and flux-density wave centered on its magnetic axis and rotating with the rotor.

When the flux linkages with armature phases a, b, c and field winding f are expressed in terms of the inductances and currents as follows,

$$\lambda_a = \mathcal{L}_{aa}i_a + \mathcal{L}_{ab}i_b + \mathcal{L}_{ac}i_c + \mathcal{L}_{af}i_f \quad (5-2)$$

$$\lambda_b = \mathcal{L}_{ba}i_a + \mathcal{L}_{bb}i_b + \mathcal{L}_{bc}i_c + \mathcal{L}_{bf}i_f \quad (5-3)$$

$$\lambda_c = \mathcal{L}_{ca}i_a + \mathcal{L}_{cb}i_b + \mathcal{L}_{cc}i_c + \mathcal{L}_{cf}i_f \quad (5-4)$$

$$\lambda_f = \mathcal{L}_{fa}i_a + \mathcal{L}_{fb}i_b + \mathcal{L}_{fc}i_c + \mathcal{L}_{ff}i_f \quad (5-5)$$

the induced voltages can be found from Faraday's law. Here two like subscripts denote a self-inductance and two unlike subscripts denote a mutual inductance between the two windings. The script \mathcal{L} is used for inductance to conform with the notation in Chap. 6, where the effects of salient poles and transients are analyzed.

Before we proceed, it is useful to investigate the nature of the various inductances. Each of these inductances can be expressed in terms of constants which can be computed from design data or measured by tests on an existing machine.

a. Rotor Self-Inductance

With a cylindrical stator, the self-inductance of the field winding is independent of the rotor position θ when the harmonic effects of stator slot

openings are neglected. Hence

$$\mathcal{L}_{ff} = L_{ff} = L_{ff0} + L_{fl} \quad (5-6)$$

where the italic L is used for an inductance which is independent of θ . The component L_{ff0} takes into account the space-fundamental component of air-gap flux. This component can be computed from air-gap dimensions and winding data, as shown in Appendix B. The additional component L_{fl} accounts for the field-winding leakage flux.

Under transient or unbalanced conditions, the flux linkages with the field winding, Eq. 5-5, vary with time, and the voltages induced in the rotor circuits have an important effect on machine performance, as shown in Chap. 6. With balanced three-phase armature currents, however, the constant-amplitude magnetic field of the armature currents rotates in synchronism with the rotor. Thus the field-winding flux linkages produced by the armature currents do not vary with time, and the voltage induced in the field winding is therefore zero. With constant dc voltage V_f applied to the field-winding terminals, the field direct current I_f is given by Ohm's law, $I_f = V_f/R_f$.

b. Stator-to-Rotor Mutual Inductances

The stator-to-rotor mutual inductances vary periodically with the angle θ between the magnetic axes of the field winding and the armature phase a (Fig. 5-2). With the space-mmF and air-gap flux distribution assumed sinusoidal, the mutual inductance between the field winding f and phase a varies as $\cos \theta$; thus

$$\mathcal{L}_{af} = \mathcal{L}_{fa} = L_{af} \cos \theta \quad (5-7)$$

Similar expressions apply to phases b and c , with θ replaced by $\theta - 120^\circ$ and $\theta + 120^\circ$, respectively. Attention will be focused on phase a . The inductance L_{af} can be calculated as indicated in Appendix B.

With the rotor rotating at synchronous speed ω

$$\theta = \omega t + \theta_0 \quad (5-8)$$

where θ_0 is the angle of the rotor at time $t = 0$. With dc excitation I_f in the field winding, the resultant flux linkage λ_{af} of phase a is

$$\lambda_{af} = L_{af} I_f \cos (\omega t + \theta_0) \quad (5-9)$$

c. Stator Inductances; Synchronous Inductance

With a cylindrical rotor, the air gap is independent of θ if the effects of rotor slots are neglected. The stator self-inductances then are constant; thus

$$\mathcal{L}_{aa} = \mathcal{L}_{bb} = \mathcal{L}_{cc} = L_{aa} = L_{aa0} + L_{al} \quad (5-10)$$

where L_{aa0} is the component of self-inductance due to space-fundamental air-gap flux (Appendix B) and L_{al} is the additional component due to armature leakage flux (Art. 4-9).

The armature phase-to-phase mutual inductances can be found on the assumption that the mutual inductance is due solely to space-fundamental air-gap flux. Because the armature phases are displaced by 120° and $\cos(\pm 120^\circ) = -\frac{1}{2}$, the mutual inductances between armature phases are

$$\mathcal{L}_{ab} = \mathcal{L}_{ba} = \mathcal{L}_{ac} = \mathcal{L}_{ca} = \mathcal{L}_{bc} = \mathcal{L}_{cb} = -\frac{1}{2}L_{aa0} \quad (5-11)$$

The phase- a flux linkages (Eq. 5-2) can be written as

$$\lambda_a = (L_{aa0} + L_{al})i_a - \frac{1}{2}L_{aa0}(i_b + i_c) + \lambda_{af} \quad (5-12)$$

where λ_{af} is given by Eq. 5-9.

With balanced three-phase armature currents (see Fig. 4-30 and Eqs. 4-24 to 4-26)

$$i_a + i_b + i_c = 0 \quad \text{or} \quad i_b + i_c = -i_a \quad (5-13)$$

Substitution of Eq. 5-13 in Eq. 5-12 gives

$$\lambda_a = (L_{aa0} + L_{al})i_a + \frac{1}{2}L_{aa0}i_a + \lambda_{af} = (\frac{3}{2}L_{aa0} + L_{al})i_a + \lambda_{af} \quad (5-14)$$

It is useful to define the *synchronous inductance* L_s as

$$L_s = \frac{3}{2}L_{aa0} + L_{al} \quad (5-15)$$

and thus

$$\lambda_a = L_s i_a + \lambda_{af} \quad (5-16)$$

The synchronous inductance L_s is the effective inductance seen by phase a under the balanced three-phase conditions of normal machine operation. It is made up of three components. The first, L_{aa0} , is due to the space-fundamental air-gap component of phase- a self-flux linkages. The second, L_{al} , is due to the leakage component of phase- a flux linkages. The third component, $\frac{1}{2}L_{aa0}$, is due to the phase- a flux linkages from the space-fundamental component of air-gap flux produced by currents in phases b and c . Under balanced three-phase conditions, the phase- b and $-c$ currents are related to the current in phase a by Eq. 5-13; thus the synchronous inductance is an apparent inductance which accounts for the flux linkages of phase a in terms of the current in phase a , even though this is not truly the self-inductance of phase a alone.

The significance of the synchronous inductance can be further appreciated with reference to the discussion of rotating magnetic fields in Art. 4-5,

where it was shown that under balanced three-phase conditions, the armature currents create a rotating magnetic flux wave in the air gap $\frac{3}{2}$ times the magnitude of that due to phase a alone, the additional component being due to the phase- b and $-c$ currents. This corresponds directly to the $\frac{3}{2}L_{aa0}$ component of the synchronous inductance in Eq. 5-15; this component of the synchronous inductance accounts for the total space-fundamental air-gap component of phase- a flux linkages produced by the three armature currents under balanced three-phase conditions.

The phase- a terminal voltage is the sum of the armature-resistance voltage drop $R_a i_a$ and the induced voltages. From the derivative of Eq. 5-16

$$v_{ta} = R_a i_a + \frac{d\lambda_a}{dt} = R_a i_a + L_s \frac{di_a}{dt} + \frac{d\lambda_{af}}{dt} \quad (5-17)$$

From Eq. 5-9 the corresponding voltage e_{af} is

$$e_{af} = \frac{d\lambda_{af}}{dt} = -\omega L_{af} I_f \sin(\omega t + \theta_0) \quad (5-18)$$

Here e_{af} is the voltage generated by the flux produced by the rotating field winding and is defined as the *excitation voltage*. From the trigonometric identity

$$\begin{aligned} \sin \alpha &= -\cos \left(\alpha + \frac{\pi}{2} \right) \\ e_{af} &= +\omega L_{af} I_f \cos \left(\omega t + \theta_0 + \frac{\pi}{2} \right) \end{aligned} \quad (5-19)$$

The excitation voltage e_{af} leads the flux linkage λ_{af} by 90° . Its rms value E_{af} is

$$E_{af} = \frac{\omega L_{af} I_f}{\sqrt{2}} \quad (5-20)$$

The equation for the rms voltage generated in the armature phases by a rotating flux wave (Eq. 4-55) is repeated here for convenience; thus

$$E_{af} = \sqrt{2} \pi f k_w N_{ph} \Phi_{af} \quad (5-21)$$

where Φ_{af} is the flux per pole produced by the field winding and the other symbols are defined in Chap. 4. It can be shown that Eqs. 5-20 and 5-21 are identical.

In the analysis of steady-state sinusoids, it is convenient to use phasor symbolism. Thus Eq. 5-19 describes a voltage whose rms value is given by

Eq. 5-20 and which leads the flux linkages $\hat{\lambda}_{af}$ by $\pi/2 = 90^\circ$. Similarly the phase- a terminal voltage v_{ta} and armature current i_a can be represented by phasors. The complex impedance equivalent of Eq. 5-17 then is

$$\hat{V}_{ta} = R_a \hat{I}_a + jX_s \hat{I}_a + \hat{E}_{af} \quad (5-22)$$

where $X_s = \omega L_s$ is the *synchronous reactance*. An equivalent circuit in complex form is shown in Fig. 5-3a. The reader should note that Eq. 5-22 and Fig. 5-3a assume the *motor reference direction* for \hat{I}_a , with \hat{I}_a defined as positive into the + terminals of the machine. Alternatively, the *generator reference direction* (\hat{I}_a positive out of the + armature terminals) can be chosen; for this choice Eq. 5-22 becomes

$$\hat{V}_{ta} = -R_a \hat{I}_a - jX_s \hat{I}_a + \hat{E}_{af} \quad (5-23)$$

and the equivalent circuit is that of Fig. 5-3b. Although these two representations are equivalent, the generator reference direction is more common and is generally used from this point on in the text.

Figure 5-4 shows an alternative form of the equivalent circuit in which the synchronous reactance is shown in terms of its components. From Eq. 5-15

$$X_s = \omega L_s = \omega L_{al} + \omega(\frac{3}{2}L_{aa0}) = X_{al} + X_A \quad (5-24)$$

where $X_{al} = \omega L_{al}$ is the *armature leakage reactance* and $X_A = \omega(\frac{3}{2}L_{aa0})$ is reactance corresponding to the rotating space-fundamental air-gap flux produced by the three armature currents. The reactance X_A is defined as the *reactance of armature reaction*. The voltage \hat{E}_R is the internal voltage generated by the resultant air-gap flux and is usually referred to as the *air-gap voltage* or the voltage "behind" leakage reactance. Its rms value E_R is related to the resultant air-gap flux Φ_R , as in Eq. 4-55. As a phasor, \hat{E}_R leads the resultant flux $\hat{\Phi}_R$ by 90° .

It is helpful to have a rough idea of the order of magnitude of the impedance components. For machines with ratings above a few hundred kilo-

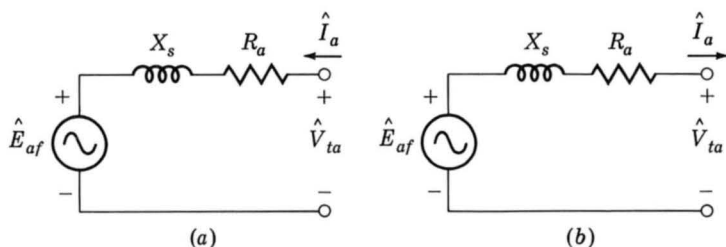


Fig. 5-3. Synchronous-machine equivalent circuits: (a) motor reference direction and (b) generator reference direction.

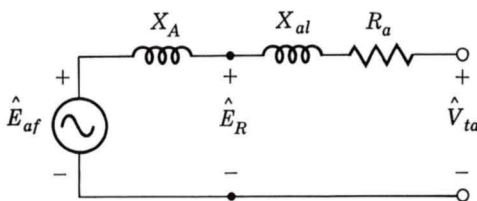


Fig. 5-4. Synchronous-machine equivalent circuit showing air-gap and leakage components of synchronous reactance and air-gap voltage.

voltamperes, the armature-resistance voltage drop at rated current usually is less than 0.01 times rated voltage; i.e., the armature resistance usually is less than 0.01 per unit on the machine rating as a base. (The per unit system is described in Art. 2-8.) The armature leakage reactance usually is in the range of 0.1 to 0.2 per unit, and the synchronous reactance is typically in the range of 1.0 to 2.0 per unit. In general, the per unit armature resistance increases and the per unit synchronous reactance decreases with decreasing size of the machine. In small machines, such as those in educational laboratories, the armature resistance may be in the vicinity of 0.05 per unit and the synchronous reactance in the vicinity of 0.5 per unit. In all but small machines, the armature resistance usually is neglected except insofar as its effect on losses and heating is concerned.

5-3 OPEN- AND SHORT-CIRCUIT CHARACTERISTICS

Two basic sets of characteristic curves for a synchronous machine are involved in the inclusion of saturation effects and in the determination of the appropriate machine constants. These sets are discussed here. Except for a few remarks on the degree of validity of certain assumptions, the discussions apply to both cylindrical-rotor and salient-pole machines.

a. Open-Circuit Characteristic and No-Load Rotational Losses

Like the magnetization curve for a dc machine, the *open-circuit characteristic* of a synchronous machine is a curve of the armature terminal voltage on open circuit as a function of the field excitation when the machine is running at synchronous speed, as shown by curve *occ* in Fig. 5-5a. The curve is often plotted in per unit terms, as in Fig. 5-5b, where unity voltage is the rated voltage and unity field current is the excitation corresponding to the rated voltage on the air-gap line. Essentially, the open-circuit characteristic represents the relation between the space-fundamental component of the air-gap flux and the mmf acting on the magnetic circuit when the field winding constitutes the only mmf source. When the machine is an existing one, the open-circuit characteristic is usually determined experimentally by driving the machine mechanically at synchronous speed with

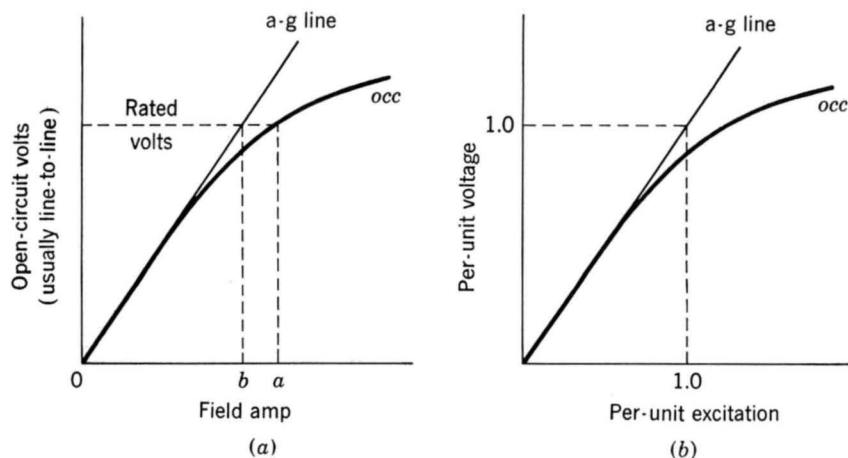


Fig. 5-5. Open-circuit characteristic (a) in terms of volts and field amperes and (b) in per unit.

its armature terminals on open circuit and by reading the terminal voltage corresponding to a series of values of field current. If the mechanical power required to drive the synchronous machine during the open-circuit test is measured, the no-load rotational losses can be obtained. These losses comprise friction, windage, and core loss corresponding to the flux in the machine at no load. The friction and windage losses at synchronous speed are constant, while the open-circuit core loss is a function of the flux, which in turn is proportional to the open-circuit voltage.

The mechanical power required to drive the machine at synchronous speed and unexcited is its friction and windage loss. When the field is excited, the mechanical power equals the sum of the friction, windage, and open-circuit core loss. The open-circuit core loss therefore can be found from the difference between these two values of mechanical power. A curve of open-circuit core loss as a function of open-circuit voltage is shown in Fig. 5-6.

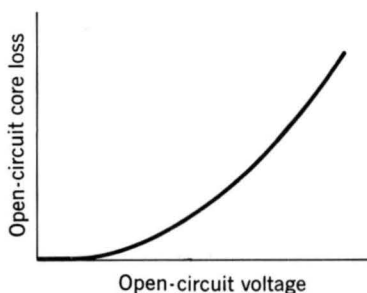


Fig. 5-6. Open-circuit core-loss curve.

b. Short-Circuit Characteristic and Load Loss

If the armature terminals of a synchronous machine which is being driven as a generator at synchronous speed are short-circuited through suitable ammeters, as shown in Fig. 5-7a, and if the field current is gradually increased until the armature current has reached a maximum safe value, then data can be obtained from which the short-circuit armature current can be plotted against the field current. This relation is known as the *short-circuit characteristic*. An open-circuit characteristic *occ* and a short-circuit characteristic *scc* are shown in Fig. 5-7b.

The phasor relation between the excitation voltage \hat{E}_{af} and the steady-state armature current \hat{I}_a under polyphase short-circuit conditions is

$$\hat{E}_{af} = \hat{I}_a(R_a + jX_s) \quad (5-25)$$

The corresponding phasor diagram is shown in Fig. 5-8. Because the resistance is much smaller than the synchronous reactance, the armature current lags the excitation voltage by very nearly 90° . Consequently the armature-reaction-mmf wave is very nearly in line with the axis of the field poles and in opposition to the field mmf, as shown by phasors \hat{A} and \hat{F} representing the space waves of armature reaction and field mmf, respectively.

The resultant mmf creates the resultant air-gap flux wave which generates the air-gap voltage \hat{E}_R equal to the voltage consumed in armature resistance R_a and leakage reactance X_{al} ; as an equation,

$$\hat{E}_R = \hat{I}_a(R_a + jX_{al}) \quad (5-26)$$

In many synchronous machines the armature resistance is negligible, and the leakage reactance is between 0.10 and 0.20 per unit; a representative value is about 0.15 per unit. That is, at rated armature current the leakage-

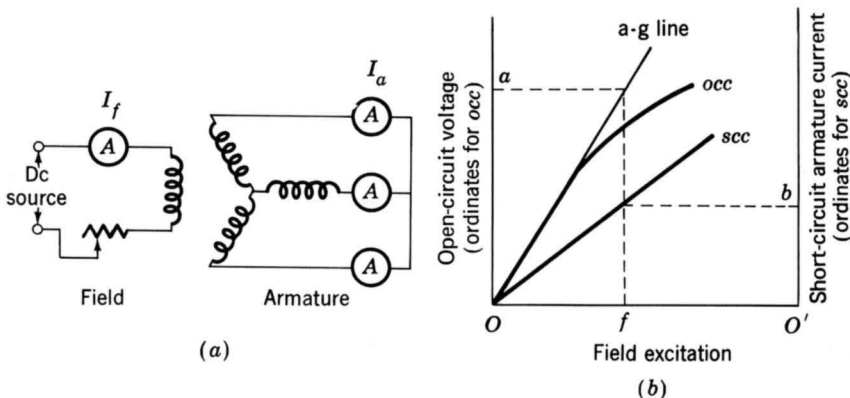


Fig. 5-7. (a) Connections for short-circuit test; (b) open- and short-circuit characteristics.

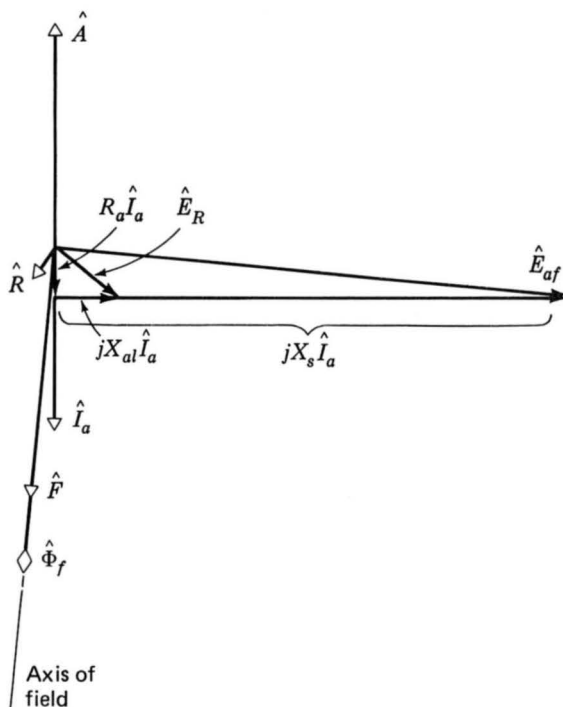


Fig. 5-8. Phasor diagram for short-circuit conditions.

reactance voltage drop is about 0.15 per unit. From Eq. 5-26, therefore, the air-gap voltage at rated armature current on short circuit is about 0.15 per unit; i.e., the resultant air-gap flux is only about 0.15 times its normal voltage value. Consequently, the machine is operating in an unsaturated condition. The short-circuit armature current therefore is directly proportional to the field current over the range from zero to well above rated armature current.

The *unsaturated synchronous reactance* (corresponding to unsaturated operating conditions within the machine) can be found from the open- and short-circuit data. At any convenient field excitation, such as $O'f$ in Fig. 5-7b, the armature current on short circuit is $O'b$, and the excitation voltage for the same field current corresponds to Oa read from the air-gap line. Note that the voltage on the air-gap line should be used because the machine is assumed to be operating in an unsaturated condition. If the voltage per phase corresponding to Oa is $E_{af,ag}$ and the armature current per phase corresponding to $O'b$ is $I_{a,sc}$, then from Eq. 5-25, with armature resistance neglected, the unsaturated value $X_{s,ag}$ of the synchronous reactance is

$$X_{s,ag} = \frac{E_{af,ag}}{I_{a,sc}} \quad (5-27)$$

where the subscripts "ag" indicate air-gap line conditions and "sc" short-circuit conditions. If $E_{af,ag}$ and $I_{a,sc}$ are expressed in per unit, the synchronous reactance will be in per unit. If $E_{af,ag}$ and $I_{a,sc}$ are expressed in rms volts per phase and rms amperes per phase, respectively, the synchronous reactance will be ohms per phase.

Note that the synchronous reactance in ohms is calculated by using the phase or line-neutral voltage. Often the open-circuit saturation curve is given in terms of the line-line voltage, in which case the voltage must be converted to the line-neutral value by dividing by $\sqrt{3}$.

For operation at or near the rated terminal voltage, it is sometimes assumed that the machine is equivalent to an unsaturated one whose magnetization curve is a straight line through the origin and the rated-voltage point on the open-circuit characteristic, as shown by the dashed line Op in Fig. 5-9. According to this approximation, the *saturated value of the synchronous reactance at rated voltage V_{ta}* is

$$X_s = \frac{V_{ta}}{I'_{a,sc}} \quad (5-28)$$

where $I'_{a,sc}$ is the armature current $O'c$ read from the short-circuit characteristic at the field current Of' corresponding to V_{ta} on the open-circuit characteristic, as shown in Fig. 5-9. This method of handling the effects of saturation usually gives satisfactory results when great accuracy is not required.

The *short-circuit ratio* (SCR) is defined as the ratio of the field current required for rated voltage on open circuit to the field current required for rated armature current on short circuit. That is, in Fig. 5-9

$$\text{SCR} = \frac{Of'}{Of''} \quad (5-29)$$

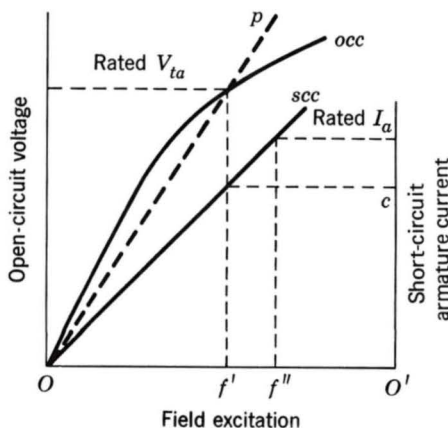


Fig. 5-9. Open- and short-circuit characteristics.

It can be shown that the SCR is the reciprocal of the per unit value of the saturated synchronous reactance given by Eq. 5-28.

EXAMPLE 5-1

The following data are taken from the open- and short-circuit characteristics of a 45-kVA three-phase Y-connected 220-V (line-to-line) six-pole 60-Hz synchronous machine. From the open-circuit characteristic

$$\text{Line-to-line voltage} = 220 \text{ V} \quad \text{Field current} = 2.84 \text{ A}$$

From the short-circuit characteristic

Armature current, A	118	152
Field current, A	2.20	2.84

From the air-gap line

$$\text{Field current} = 2.20 \text{ A} \quad \text{Line-to-line voltage} = 202 \text{ V}$$

Compute the unsaturated value of the synchronous reactance, its saturated value at rated voltage in accordance with Eq. 5-28, and the short-circuit ratio. Express the synchronous reactance in ohms per phase and in per unit on the machine rating as a base.

Solution

At a field current of 2.20 A the voltage to neutral on the air-gap line is

$$E_{af,ag} = \frac{202}{\sqrt{3}} = 116.7 \text{ V}$$

and for the same field current the armature current on short circuit is

$$I_{a,sc} = 118 \text{ A}$$

From Eq. 5-27

$$X_{s,ag} = \frac{116.7}{118} = 0.987 \text{ } \Omega/\text{phase}$$

Note that rated armature current is $45,000/[\sqrt{3}(220)] = 118 \text{ A}$. Therefore, $I_{a,sc} = 1.00$ per unit. The corresponding air-gap-line voltage is

$$E_{af, ag} = \frac{202}{220} = 0.92 \text{ per unit}$$

From Eq. 5-27 in per unit

$$X_{s, ag} = \frac{0.92}{1.00} = 0.92 \text{ per unit}$$

From the open- and short-circuit characteristics and Eq. 5-28

$$X_s = \frac{220}{\sqrt{3}(152)} = 0.836 \Omega/\text{phase}$$

In per unit $I'_{a, sc} = \frac{152}{118} = 1.29$, and from Eq. 5-28

$$X_s = \frac{1.00}{1.29} = 0.775 \text{ per unit}$$

From the open- and short-circuit characteristics and Eq. 5-29

$$\text{SCR} = \frac{2.84}{2.20} = 1.29$$

If the mechanical power required to drive the machine is measured while the short-circuit test is being made, information can be obtained regarding the losses caused by the armature current. The mechanical power required to drive the synchronous machine during the short-circuit test equals the sum of friction and windage plus losses caused by the armature current. The losses caused by the armature current can then be found by subtracting friction and windage from the driving power. The losses caused by the short-circuit armature current are known collectively as the *short-circuit load loss*. A curve of short-circuit load loss plotted against armature current is shown in Fig. 5-10. Typically, it is approximately parabolic.

The short-circuit load loss comprises I^2R loss in the armature winding, local core losses caused by the armature leakage flux, and a very small core loss caused by the resultant flux. The dc resistance loss can be computed if the dc resistance is measured and corrected, when necessary, for the temperature of the windings during the short-circuit test. For copper conductors

$$\frac{R_T}{R_t} = \frac{234.5 + T}{234.5 + t} \quad (5-30)$$

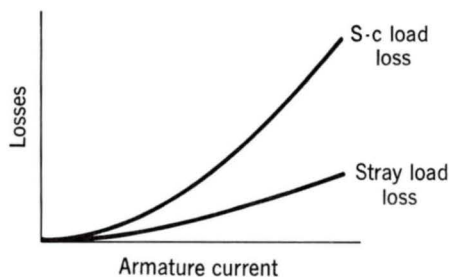


Fig. 5-10. Short-circuit load-loss and stray load-loss curves.

where R_T and R_t are the resistances at Celsius temperatures T and t , respectively. If this dc resistance loss is subtracted from the short-circuit load loss, the difference will be the loss due to skin effect and eddy currents in the armature conductors plus the local core losses caused by the armature leakage flux. (The core loss caused by the resultant flux on short circuit is customarily neglected.) This difference between the short-circuit load loss and the dc resistance loss is the additional loss caused by the alternating current in the armature. It is the stray load loss described in Appendix C, commonly considered to have the same value under normal load conditions as on short circuit. It is a function of the armature current, as shown by the curve in Fig. 5-10.

As with any ac device, the effective resistance of the armature is the power loss attributable to the armature current divided by the square of the current. On the assumption that the stray load loss is a function of only the armature current, the effective resistance $R_{a,\text{eff}}$ of the armature can be determined from the short-circuit load loss:

$$R_{a,\text{eff}} = \frac{\text{short-circuit load loss}}{(\text{short-circuit armature current})^2} \quad (5-31)$$

If the short-circuit load loss and armature current are in per unit, the effective resistance will be in per unit. If they are in watts per phase and amperes per phase, respectively, the effective resistance will be in ohms per phase. Usually it is sufficiently accurate to find the value of $R_{a,\text{eff}}$ at rated current and then to assume it to be constant.

EXAMPLE 5-2

For the 45-kVA three-phase Y-connected synchronous machine of Example 5-1, at rated armature current (118 A) the short-circuit load loss (total for three phases) is 1.80 kW at a temperature of 25°C. The dc resistance of the armature at this temperature is 0.0335 Ω /phase. Compute the effective armature resistance in per unit and in ohms per phase at 25°C.

Solution

In per unit the short-circuit load loss is

$$\frac{1.80}{45} = 0.040$$

at $I_a = 1.00$ per unit. Therefore,

$$R_{a,\text{eff}} = \frac{0.040}{(1.00)^2} = 0.040 \text{ per unit}$$

On a per phase basis the short-circuit load loss is

$$\frac{1800}{3} \text{ W/phase}$$

and consequently the effective resistance is

$$R_{a,\text{eff}} = \frac{1800}{3(118)^2} = 0.043 \text{ } \Omega/\text{phase}$$

The ratio of ac-to-dc resistance is

$$\frac{R_{a,\text{eff}}}{R_{a,\text{dc}}} = \frac{0.043}{0.0335} = 1.28$$

Because this is a small machine, its per unit resistance is relatively high. The armature resistance of machines with ratings above a few hundred kilovoltamperes usually is less than 0.01 per unit.

5-4 STEADY-STATE POWER-ANGLE CHARACTERISTICS

The maximum power a synchronous machine can deliver is determined by the maximum torque which can be applied without loss of synchronism with the external system to which it is connected. The purpose of this article is to derive expressions for the steady-state power limits of simple situations in which the external system can be represented as an impedance in series with a voltage source.

Since the machine itself can be represented by a simple impedance in series with a voltage source, the study of power limits becomes merely a special case of the more general problem of the limitations on power flow through a series impedance. The impedance can include that of a line and transformer bank as well as the synchronous impedance of the machine.

Consider the simple circuit of Fig. 5-11a, comprising two ac voltages \hat{E}_1 and \hat{E}_2 connected by an impedance Z through which the current is \hat{I} . The phasor diagram is shown in Fig. 5-11b. The power P_2 delivered through the impedance to the load end \hat{E}_2 is

$$P_2 = E_2 I \cos \phi_2 \quad (5-32)$$

where ϕ_2 is the phase angle of \hat{I} with respect to \hat{E}_2 . The phasor current is

$$\hat{I} = \frac{\hat{E}_1 - \hat{E}_2}{Z} \quad (5-33)$$

If the phasor voltages and the impedance are expressed in polar form,

$$\hat{I} = \frac{E_1 \angle \delta - E_2 \angle -0^\circ}{|Z| \angle \phi_z} = \frac{E_1}{|Z|} \angle \delta - \phi_z - \frac{E_2}{|Z|} \angle -\phi_z \quad (5-34)$$

where E_1, E_2 = magnitudes of voltages \hat{E}_1 and \hat{E}_2

δ = phase angle by which \hat{E}_1 leads \hat{E}_2

$|Z|$ = magnitude of impedance

ϕ_z = angle of impedance in polar form

The real part of the phasor equation 5-34 is the component of \hat{I} in phase in \hat{E}_2 , whence

$$I \cos \phi_2 = \frac{E_1}{|Z|} \cos (\delta - \phi_z) - \frac{E_2}{|Z|} \cos (-\phi_z) \quad (5-35)$$

Noting that

$$\cos (-\phi_z) = \cos \phi_z = \frac{R}{|Z|}$$

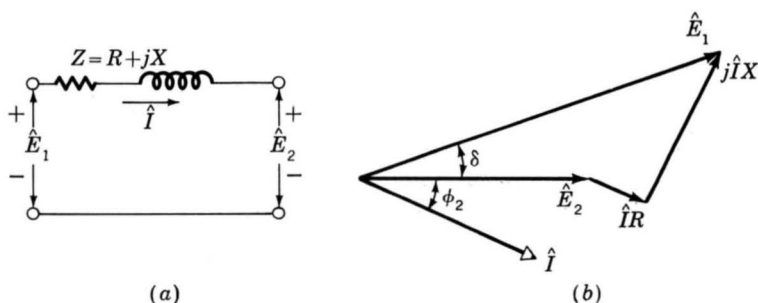


Fig. 5-11. (a) Impedance interconnecting two voltages; (b) phasor diagram.

we see that substitution of Eq. 5-35 in Eq. 5-32 gives

$$P_2 = \frac{E_1 E_2}{|Z|} \cos(\delta - \phi_z) - \frac{E_2^2 R}{|Z|^2} \quad (5-36)$$

and

$$P_2 = \frac{E_1 E_2}{|Z|} \sin(\delta + \alpha_z) - \frac{E_2^2 R}{|Z|^2} \quad (5-37)$$

where

$$\alpha_z = 90^\circ - \phi_z = \tan^{-1} \frac{R}{X} \quad (5-38)$$

usually is a small angle.

Similarly power P_1 at source end \hat{E}_1 of the impedance can be expressed as

$$P_1 = \frac{E_1 E_2}{|Z|} \sin(\delta - \alpha_z) + \frac{E_1^2 R}{|Z|^2} \quad (5-39)$$

If, as is frequently the case, the resistance is negligible, then $\alpha_z \approx 0$ and

$$P_1 = P_2 = \frac{E_1 E_2}{X} \sin \delta \quad (5-40)$$

Equation 5-40 is commonly referred to as the *power-angle characteristic* for a synchronous machine, and the angle δ is known as the *power angle*. If the resistance is negligible and the voltages are constant, the maximum power

$$P_{1,\max} = P_{2,\max} = \frac{E_1 E_2}{X} \quad (5-41)$$

occurs when $\delta = 90^\circ$.

Equation 5-40 is valid for any voltage sources \hat{E}_1 and \hat{E}_2 separated by a reactive impedance jX . Thus for a synchronous machine connected to a system whose Thevenin equivalent is a voltage source \hat{V}_{EQ} in series with a reactive impedance jX_{EQ} , as shown in Fig. 5-12, the power-angle characteristic can be written

$$P = \frac{E_{af} V_{\text{EQ}}}{X_s + X_{\text{EQ}}} \sin \delta \quad (5-42)$$

where P is the power transferred from the synchronous machine to the system and δ is the phase angle of \hat{E}_{af} with respect to \hat{V}_{EQ} .

In a similar fashion it is possible to write a power-angle characteristic in terms of X_s , E_{af} , the terminal voltage V_{ta} , and the relative angle between

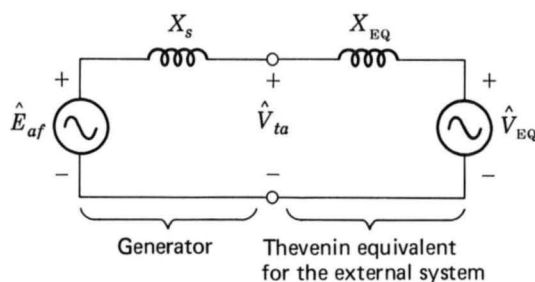


Fig. 5-12. Representation of a synchronous machine connected to an external system.

them, or alternatively X_{EQ} , V_{ta} , and V_{EQ} . Although both expressions are equally valid, they are not equally useful. For example, while E_{af} and V_{EQ} remain constant as P is varied, V_{ta} will not. Thus, while Eq. 5-42 gives an easily solved relation between P and δ , a power-angle characteristic based upon V_{ta} cannot be solved without an additional expression relating V_{ta} to P .

It should be emphasized that the derivation of Eqs. 5-32 to 5-42 is based on a single-phase ac circuit. For a balanced three-phase system, if E_1 and E_2 are the line-neutral voltages, the results must be multiplied by 3 to get the total three-phase power; alternatively E_1 and E_2 can be expressed in terms of the line-to-line voltage (equal to $\sqrt{3}$ times the line-neutral voltage), in which case the equations give three-phase power directly.

When Eq. 5-40 is compared with Eq. 5-1 for torque in terms of interacting flux and mmf waves, they are seen to be of the same form. This is no coincidence. Remember that torque and power are proportional when, as here, speed is constant. What we are really saying is that Eq. 5-1 applied specifically to the idealized cylindrical-rotor machine and translated to circuit terms becomes Eq. 5-40. A quick mental review of the background of each relation should show that they stem from the same fundamental considerations.

From Eq. 5-42 we see that the maximum power transfer associated with synchronous-machine operation is proportional to the magnitude of the system voltage, corresponding to V_{EQ} , and the generator internal voltage E_{af} . Thus for constant system voltage, the maximum power transfer can be increased by increasing the synchronous-machine field current and thus the internal voltage. Of course, this cannot be done without limit; neither the field current nor the machine fluxes can be raised past the point where cooling requirements fail to be met.

In general, stability considerations dictate that a synchronous machine achieve steady-state operation for a power angle considerably less than 90° . Thus, for a given system configuration it is necessary to ensure that the machine will be able to achieve its rated operation and that this operating condition will be within acceptable operating limits for both the machine and the system.

EXAMPLE 5-3

A 2000-hp 1.0-power-factor three-phase Y-connected 2300-V 30-pole 60-Hz synchronous motor has a synchronous reactance of $1.95 \Omega/\text{phase}$. For this problem all losses may be neglected.

(a) Compute the maximum torque in pound-feet which this motor can deliver if it is supplied with power from a constant-frequency, constant-voltage, three-phase source, commonly called an *infinite bus* (in this case 60 Hz and 2300 V line-line), and if its field excitation is constant at the value which would result in 1.00 power factor at rated load.

(b) Instead of the infinite bus of part (a), suppose that the motor is supplied with power from a three-phase Y-connected 2300-V 1750-kVA two-pole 3600 r/min turbine generator whose synchronous reactance is $2.65 \Omega/\text{phase}$. The generator is driven at rated speed, and the field excitations of generator and motor are adjusted so that the motor runs at 1.00 power factor and rated terminal voltage at full load. The field excitations of both machines are then held constant, and the mechanical load on the synchronous motor is gradually increased. Compute the maximum motor torque under these conditions and the terminal voltage when the motor is delivering its maximum torque.

Solution

Although this machine is undoubtedly of the salient-pole type, we solve the problem by simple cylindrical-rotor theory. The solution accordingly neglects reluctance torque. The machine actually would develop a maximum torque somewhat greater than our computed value, as discussed in Art. 5-7.

(a) The equivalent circuit is shown in Fig. 5-13a and the phasor diagram at full load in Fig. 5-13b, where \hat{E}_{afm} is the excitation voltage of the motor and X_{sm} is its synchronous reactance. From the motor rating with losses neglected,

$$\begin{aligned}\text{Rated kVA} &= 2000(0.746) = 1492 \text{ kVA, three-phase} \\ &= 497 \text{ kVA/phase}\end{aligned}$$

$$\text{Rated voltage} = \frac{2300}{\sqrt{3}} = 1330 \text{ V to neutral}$$

$$\text{Rated current} = \frac{497,000}{1330} = 374 \text{ A/phase Y}$$

The synchronous-reactance voltage drop in the motor is

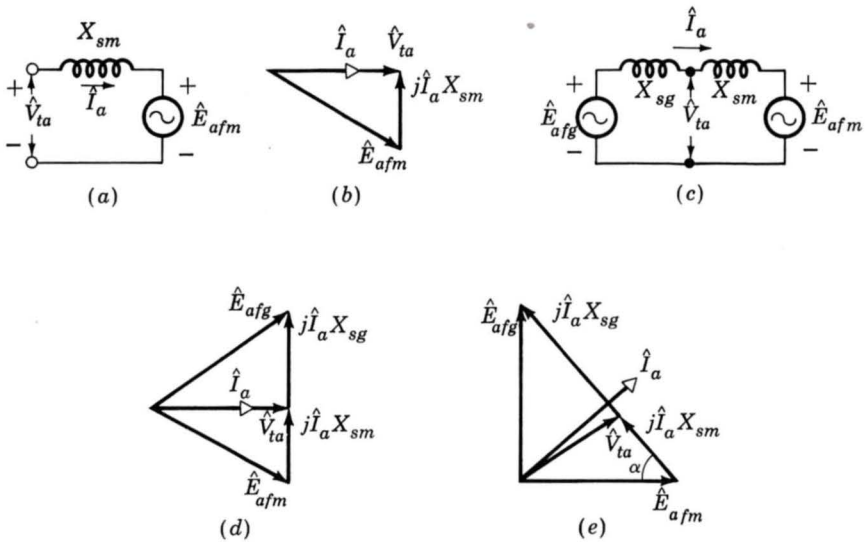


Fig. 5-13. Equivalent circuits and phasor diagrams for Example 5-3.

$$I_a X_{sm} = 374(1.95) = 730 \text{ V/phase}$$

From the phasor diagram at full load

$$E_{afm} = \sqrt{V_{ta}^2 + (I_a X_{sm})^2} = 1515 \text{ V}$$

When the power source is an infinite bus and the field excitation is constant, V_{ta} and E_{afm} are constant. Substitution of V_{ta} for E_1 , E_{afm} for E_2 , and X_{sm} for X in Eq. 5-41 then gives

$$\begin{aligned} P_{\max} &= \frac{V_{ta} E_{afm}}{X_{sm}} = \frac{1330(1515)}{1.95} = 1030 \text{ kW/phase} \\ &= 3090 \text{ kW for three phases} \end{aligned}$$

(In per unit, $P_{\max} = 3090/1492 = 2.07$.) With 30 poles at 60 Hz and synchronous speed = 4 r/s,

$$\begin{aligned} T_{\max} &= \frac{P_{\max}}{\omega_s} = \frac{3090 \times 10^3}{2\pi(4)} = 123,000 \text{ N} \cdot \text{m} \\ &= 0.738(123,000) = 90,800 \text{ lb} \cdot \text{ft} \end{aligned}$$

(b) When the power source is the turbine generator, the equivalent circuit becomes that shown in Fig. 5-13c, where \hat{E}_{afg} is the excitation voltage of the generator and X_{sg} is its synchronous reactance. The phasor diagram

at full motor load, 1.00 power factor, is shown in Fig. 5-13*d*. As before,

$$V_{ta} = 1330 \text{ V at full load} \quad E_{afm} = 1515 \text{ V}$$

The synchronous-reactance voltage drop in the generator is

$$I_a X_{sg} = 374(2.65) = 991 \text{ V}$$

and from the phasor diagram

$$E_{afg} = \sqrt{V_{ta}^2 + (I_a X_{sg})^2} = 1655 \text{ V}$$

Since the field excitations and speeds of both machines are constant, E_{afg} and E_{afm} are constant. Substitution of E_{afg} for E_1 , E_{afm} for E_2 , and $X_{sg} + X_{sm}$ for X in Eq. 5-41 then gives

$$\begin{aligned} P_{\max} &= \frac{E_{afg} E_{afm}}{X_{sg} + X_{sm}} = \frac{1655(1515)}{4.60} = 545 \text{ kW/phase} \\ &= 1635 \text{ kW for three phases} \end{aligned}$$

(In per unit, $P_{\max} = 1635/1492 = 1.095$.)

$$T_{\max} = \frac{P_{\max}}{\omega_s} = \frac{1635 \times 10^3}{2\pi(4)} = 65,000 \text{ N} \cdot \text{m} = 48,000 \text{ lb} \cdot \text{ft}$$

Synchronism would be lost if a load torque greater than this value were applied to the motor shaft. The motor would stall, the generator would tend to overspeed, and the circuit would be opened by protective relays and circuit-breaker action.

With fixed excitations, maximum power occurs when \hat{E}_{afg} leads \hat{E}_{afm} by 90° , as shown in Fig. 5-13*e*. From this phasor diagram

$$I_a (X_{sg} + X_{sm}) = \sqrt{E_{afg}^2 + E_{afm}^2} = 2240 \text{ V}$$

$$I_a = \frac{2240}{4.60} = 488 \text{ A}$$

$$I_a X_{sm} = 488(1.95) = 951 \text{ V}$$

$$\cos \alpha = \frac{E_{afm}}{I_a (X_{sg} + X_{sm})} = \frac{1515}{2240} = 0.676$$

$$\sin \alpha = \frac{E_{afg}}{I_a (X_{sg} + X_{sm})} = \frac{1655}{2240} = 0.739$$

The phasor equation for the terminal voltage is

$$\begin{aligned}\hat{V}_{ta} &= \hat{E}_{afm} + j\hat{I}_a X_{sm} = \hat{E}_{afm} - I_a X_{sm} \cos \alpha + jI_a X_{sm} \sin \alpha \\ &= 1515 - 643 + j703 = 872 + j703\end{aligned}$$

The magnitude of \hat{V}_{ta} is

$$V_{ta} = 1120 \text{ V to neutral} = 1940 \text{ V line to line}$$

When the source is the turbine generator, as in part (b), the effect of its impedance causes the terminal voltage to decrease with increasing load, thereby reducing the maximum power from 3090 kW in part (a) to 1635 kW in part (b).

5-5 STEADY-STATE OPERATING CHARACTERISTICS

The principal steady-state operating characteristics are the interrelations between terminal voltage, field current, armature current, power factor, and efficiency. A selection of performance curves of importance in practical application of the machines are presented here. Each of them can be computed for application studies by the methods presented in this chapter.

Consider a synchronous generator delivering power at constant frequency to a load whose power factor is constant. The curve showing the field current required to maintain rated terminal voltage as the constant-power-factor load is varied is known as a *compounding curve*. Three compounding curves at various constant power factors are shown in Fig. 5-14.

Synchronous generators are usually rated in terms of the maximum apparent power (kVA or MVA) load at a specific voltage and power factor (often 80, 85, or 90 percent lagging) which they can carry continuously without overheating. The active power output of the generator is usually limited to a value within the apparent power rating by the capability of its prime mover. By virtue of its voltage-regulating system, the machine normally operates at a constant voltage whose value is within ± 5 percent of rated voltage. When the real power loading and voltage are fixed, the

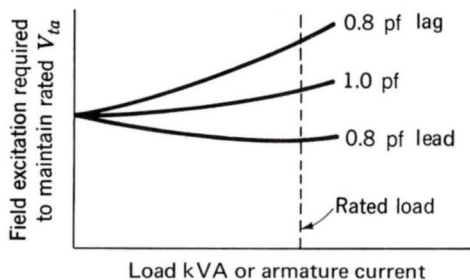


Fig. 5-14. Synchronous-generator compounding curves.

allowable reactive-power loading is limited by either armature or field-winding heating. A typical set of *capability curves* for a large turbine generator is shown in Fig. 5-15. They give the maximum reactive-power loadings corresponding to various power loadings with operation at rated voltage. Armature heating is the limiting factor in the region from unity to rated power factor (0.85 lagging power factor in Fig. 5-15). For lower power factors, field heating is the limiting factor. Such a set of curves forms a valuable guide in planning and operating the system of which the generator is a part. Also shown in Fig. 5-15 is the effect of increased hydrogen pressure (resulting in increased cooling) on allowable machine loadings.

The derivation of Fig. 5-15 can be seen as follows. Operation under conditions of constant terminal voltage and armature current (at the maximum value permitted by heating limitations) corresponds to a constant value of apparent output power determined by the product of terminal voltage and current. Since the per unit apparent power is given by

$$\text{Apparent power} = \sqrt{P^2 + Q^2} = V_{ta} I_a \quad (5-43)$$

where P represents the per unit real power and Q represents the per unit reactive power, we see that a constant apparent power corresponds to a

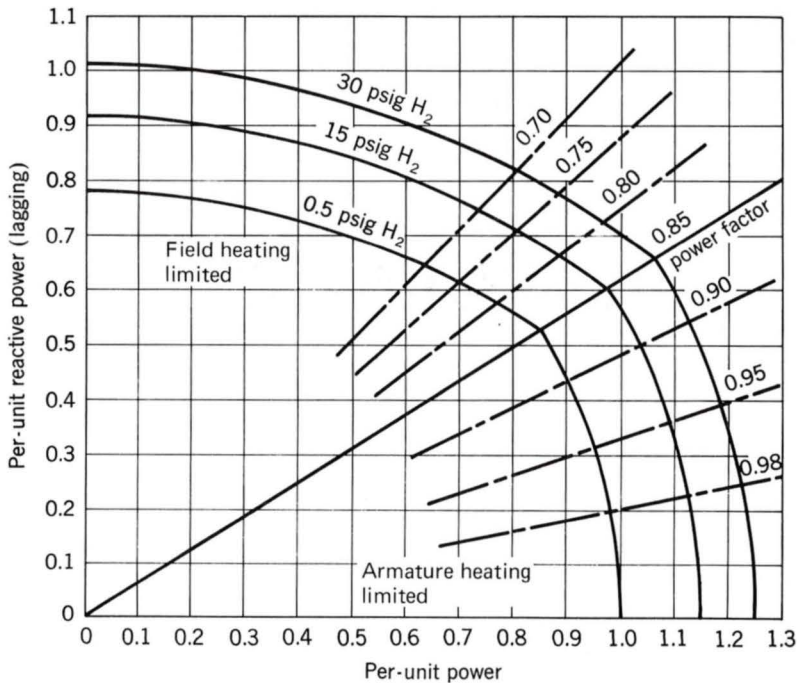


Fig. 5-15. Capability curves of an 0.85 power factor, 0.80 short-circuit ratio hydrogen-cooled turbine generator. Base kVA is rated kVA at 0.5 lb/in² hydrogen.

circle centered on the origin on a plot of reactive power versus real power. This is shown in Fig. 5-16.

Similarly, consider operation when terminal voltage is constant and field current (and hence E_{af}) is limited to a maximum value as determined by heating limitations. In per unit,

$$P - jQ = \hat{V}_{ta} \hat{I}_a \quad (5-44)$$

From Eq. 5-25 (with $R_a = 0$)

$$\hat{E}_{af} = \hat{V}_{ta} + jX_s \hat{I}_a \quad (5-45)$$

Equations 5-44 and 5-45 can be solved to yield

$$P^2 + \left(Q + \frac{V_{ta}^2}{X_s} \right)^2 = \left(\frac{V_{ta} E_{af}}{X_s} \right)^2 \quad (5-46)$$

This equation corresponds to a circle centered on $Q = -(V_{ta}^2/X_s)$ in Fig. 5-16 and determines the field heating limitation on machine operation shown in Fig. 5-15. It is common to specify the rating (apparent power and power factor) of the machine as the point of intersection of these two curves.

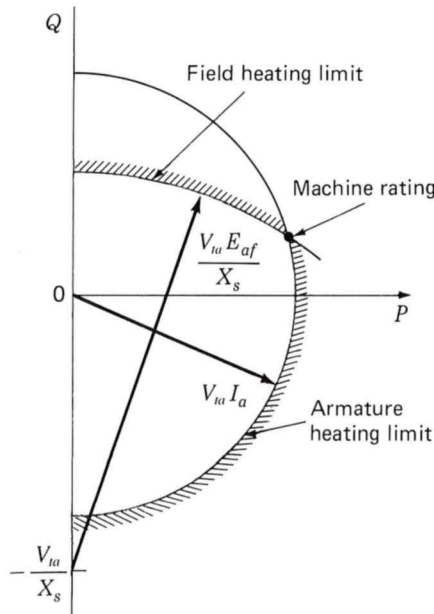


Fig. 5-16. Construction used for the derivation of a synchronous generator capability curve.

The power factor at which a synchronous machine operates, and hence its armature current, can be controlled by adjusting its field excitation. The curve showing the relation between armature current and field current at a constant terminal voltage and with a constant real power is known as a *V curve* because of its characteristic shape. A family of V curves for a synchronous generator is shown in Fig. 5-17. For constant power output, the armature current is, of course, a minimum at unity power factor and increases as the power factor decreases. The dashed lines are loci of constant power factor. They are the synchronous-generator compounding curves (see Fig. 5-14) showing how the field current must be varied as the load is changed to maintain constant power factor. Points to the right of the unity-power-factor compounding curve correspond to overexcitation and leading power factor; points to the left correspond to underexcitation and lagging power factor. Synchronous-motor V curves and compounding curves are very similar to those of synchronous generators. In fact, if it were not for the small effects of armature resistance, motor and generator compounding curves would be identical except that the lagging- and leading-power-factor curves would be interchanged.

As in all electromagnetic machines, the losses in synchronous machines consist of I^2R losses in the windings, core losses, and mechanical losses. The conventional efficiency is computed in accordance with a set of rules agreed upon by ANSI. The general principles upon which these rules are based are described in Appendix C. The following example shows how these rules are applied specifically to synchronous machines.

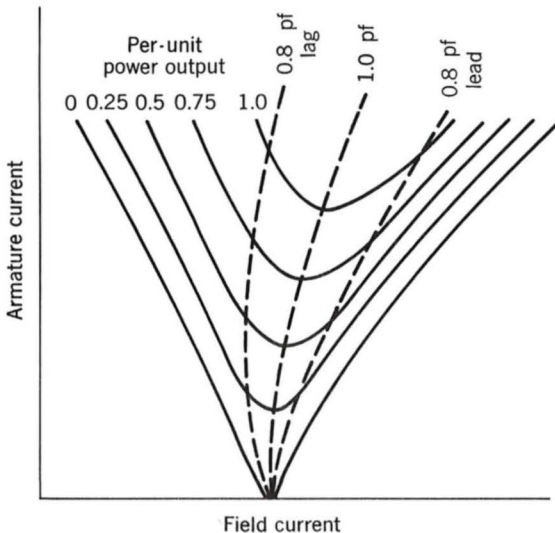


Fig. 5-17. Synchronous-generator V curves.

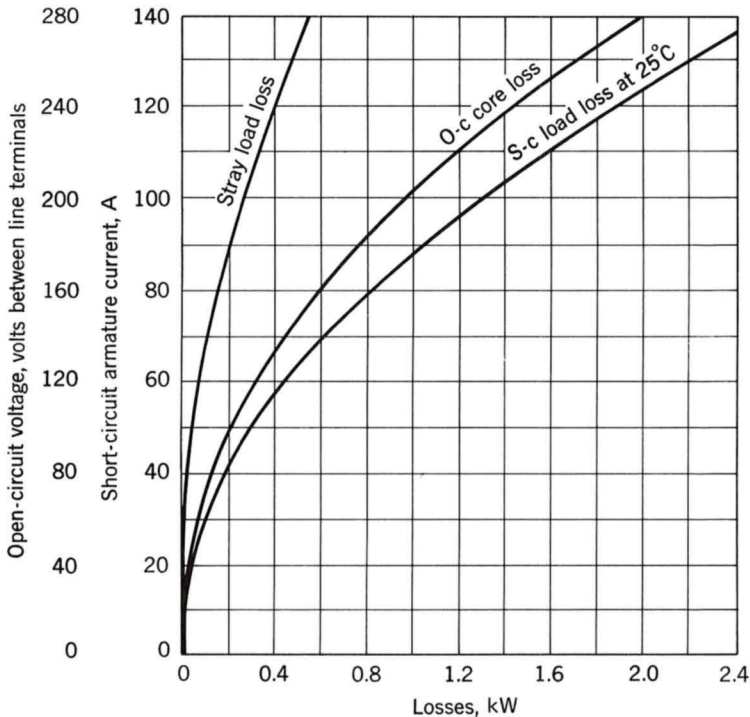
EXAMPLE 5-4

Data are given in Fig. 5-18 with respect to the losses of the 45-kVA synchronous machine of Examples 5-1 and 5-2. Compute its efficiency when it is running as a synchronous motor at a terminal voltage of 230 V and with a power input to its armature of 45 kW at 0.80 leading power factor. The field current measured in a load test taken under these conditions is I_f (test) = 5.50 A.

Solution

For the specified operating conditions, the armature current is

$$I_a = \frac{45,000}{\sqrt{3} (230) (0.80)} = 141 \text{ A}$$



Friction and windage loss = 0.91 kW

Armature dc resistance at 25°C = 0.0335 Ω per phase

Field-winding resistance at 25°C = 29.8 Ω

Fig. 5-18. Losses in a three-phase, 45-kVA, Y-connected, 220-V, 60-Hz, six-pole synchronous machine (Example 5-4).

The I^2R losses are to be computed on the basis of the dc resistances of the windings at 75°C . Correcting the winding resistances by means of Eq. 5-30 gives

$$\text{Field-winding resistance } R_f \text{ at } 75^\circ\text{C} = 35.5 \, \Omega$$

$$\text{Armature dc resistance } R_a \text{ at } 75^\circ\text{C} = 0.0399 \, \Omega/\text{phase}$$

The field I^2R loss is

$$I_f^2 R_f = (5.50^2)(35.5) = 1.07 \, \text{kW}$$

According to ANSI standards, field-rheostat and exciter losses are not charged against the machine. The armature I^2R loss is

$$3I_a^2 R_a = 3(141^2)(0.0399) = 2.38 \, \text{kW}$$

and from Fig. 5-18 at $I_a = 141 \, \text{A}$ the stray load loss = $0.56 \, \text{kW}$. According to ANSI standards, no temperature correction is to be applied to the stray load loss.

The core loss is read from the open-circuit core-loss curve at a voltage equal to the internal voltage behind the resistance of the machine. The stray load loss is considered to account for the losses caused by the armature leakage flux. For motor action this internal voltage is, as a phasor,

$$\hat{V}_{ta} - \hat{I}_a R_a = \frac{230}{\sqrt{3}} - 141(0.80 + j0.60)(0.0399) = 128.4 - j3.4$$

The magnitude is $128.4 \, \text{V}/\text{phase}$, or $222 \, \text{V}$ between line terminals. From Fig. 5-18 open-circuit core loss is $1.20 \, \text{kW}$. Also the friction and windage loss is $0.91 \, \text{kW}$. All losses have now been found:

$$\text{Total losses} = 1.07 + 2.38 + 0.56 + 1.20 + 0.91 = 6.12 \, \text{kW}$$

The power input is the sum of the ac input to the armature and the dc input to the field, or

$$\text{Input} = 46.07 \, \text{kW}$$

Therefore

$$\text{Efficiency} = 1 - \frac{\text{losses}}{\text{input}} = 1 - \frac{6.12}{46.1} = 0.867 = 86.7\%$$

5-6 EFFECTS OF SALIENT POLES; INTRODUCTION TO DIRECT- AND QUADRATURE-AXIS THEORY

The essential features of salient-pole machines are developed in this article based on physical reasoning. A mathematical treatment, based on an inductance formulation like that presented in Art. 5-2, is given in Arts. 6-2 and 6-3, where the dq0 transformation is developed.

a. Flux and MMF Waves

The flux produced by an mmf wave in a uniform-air-gap machine is independent of the spatial alignment of the wave with respect to the field poles. The salient-pole machine, however, has a preferred direction of magnetization determined by the protruding field poles. The permeance along the polar axis, commonly referred to as the rotor *direct axis*, is appreciably greater than that along the interpolar axis, commonly referred to as the rotor *quadrature axis*.

In the derivations that follow note that the field winding produces flux which is oriented along the rotor direct axis. Thus, when phasor diagrams are drawn, the field-winding mmf and its resultant flux $\hat{\phi}_f$ are found along the rotor direct axis. The excitation voltage is the time derivative of the field-winding flux, and thus its phasor \hat{E}_{af} leads the flux ϕ_f by 90° . Since by convention the quadrature axis leads the direct axis by 90° , we see that the excitation voltage phasor \hat{E}_{af} lies along the quadrature axis. Thus a key point in the analysis of synchronous-machine phasor diagrams is that by locating the phasor \hat{E}_{af} , the location of both the quadrature axis and the direct axis is immediately determined; as a result, all machine voltages and currents can be resolved into their *direct*- and *quadrature-axis components*.

We have seen that the armature-reaction flux wave $\hat{\phi}_{ar}$ lags the field flux wave by a space angle of $90^\circ + \phi_{lag}$, where ϕ_{lag} is the time-phase angle by which the armature current in the direction of the excitation emf lags the excitation emf. If the armature current \hat{I}_a lags the excitation emf \hat{E}_{af} by 90° , the armature-reaction flux wave is directly opposite the field poles and in the opposite direction to the field flux $\hat{\phi}_f$, as shown in the phasor diagram of Fig. 5-19a. The corresponding component flux-density waves at the armature surface produced by the field current and by the synchronously rotating space-fundamental component of armature-reaction mmf are shown in Fig. 5-19b, in which the effects of slots are neglected. The waves consist of a space fundamental and a family of odd-harmonic components. In a well-designed machine the harmonic effects usually are small. Accordingly only the space-fundamental components will be considered. It is the fundamental components which are represented by the flux per pole phasors $\hat{\phi}_f$ and $\hat{\phi}_{ar}$ in Fig. 5-19a.

Conditions are quite different when the armature current is in phase with the excitation emf, as shown in the phasor diagram of Fig. 5-20a. The axis of the armature-reaction wave then is opposite an interpolar space, as

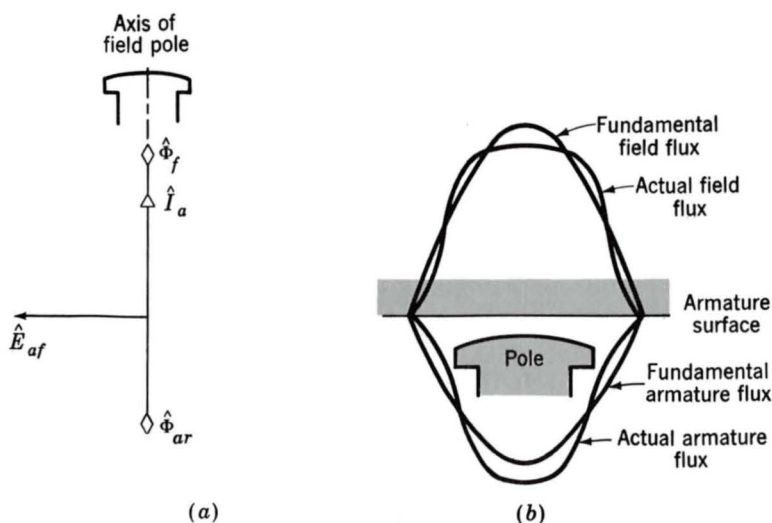


Fig. 5-19. Direct-axis air-gap fluxes in a salient-pole synchronous machine.

shown in Fig. 5-20*b*. The armature-reaction flux wave is badly distorted, comprising principally a fundamental and a prominent third space harmonic. The third-harmonic flux wave generates third-harmonic emf's in the armature phases, but these voltages do not appear between the line terminals.

Because of the high reluctance of the air gap between poles, the space-fundamental armature-reaction flux when the armature reaction is in quadrature with the field poles (Fig. 5-20) is less than the space-fundamental armature-reaction flux which would be created by the same

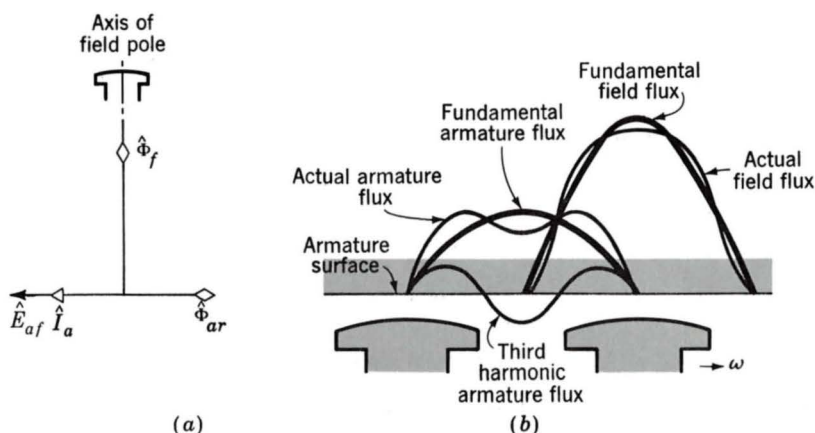


Fig. 5-20. Quadrature-axis air-gap fluxes in a salient-pole synchronous machine.

armature current if the armature flux wave were directly opposite the field poles (Fig. 5-19). Hence, the magnetizing reactance is less when the armature current is in time phase with the excitation emf (Fig. 5-20) than when it is in time quadrature with respect to the excitation emf (Fig. 5-19).

The effects of salient poles can be taken into account by resolving the armature current \hat{I}_a into two components, one in time quadrature with, and the other in time phase with, the excitation voltage \hat{E}_{af} , as shown in the phasor diagram of Fig. 5-21. This diagram is drawn for an unsaturated salient-pole generator operating at a lagging power factor. The direct-axis component \hat{I}_d of the armature current, in time quadrature with the excitation voltage, produces a component fundamental armature-reaction flux $\hat{\Phi}_{ad}$ along the axis of the field poles (the direct axis), as in Fig. 5-19. The quadrature-axis component \hat{I}_q , in phase with the excitation voltage, produces a component fundamental armature-reaction flux $\hat{\Phi}_{aq}$ in space quadrature with the field poles, as in Fig. 5-20. The subscripts d ("direct") and q ("quadrature") refer to the space phase of the armature-reaction fluxes, and not to the time phase of the component currents producing them. Thus a *direct-axis quantity* is one whose magnetic effect is centered on the axes of the field poles. Direct-axis mmf's act on the main magnetic circuit. A *quadrature-axis quantity* is one whose magnetic effect is centered on the interpolar space. For an unsaturated machine, the armature-reaction flux $\hat{\Phi}_{ar}$ is the sum of the components $\hat{\Phi}_{ad}$ and $\hat{\Phi}_{aq}$. The resultant flux $\hat{\Phi}_R$ is the sum of $\hat{\Phi}_{ar}$ and the main-field flux $\hat{\Phi}_f$.

b. Phasor Diagrams for Salient-Pole Machines

With each of the component currents \hat{I}_d and \hat{I}_q there is associated a component synchronous-reactance voltage drop, $j\hat{I}_d X_d$ and $j\hat{I}_q X_q$, respectively.

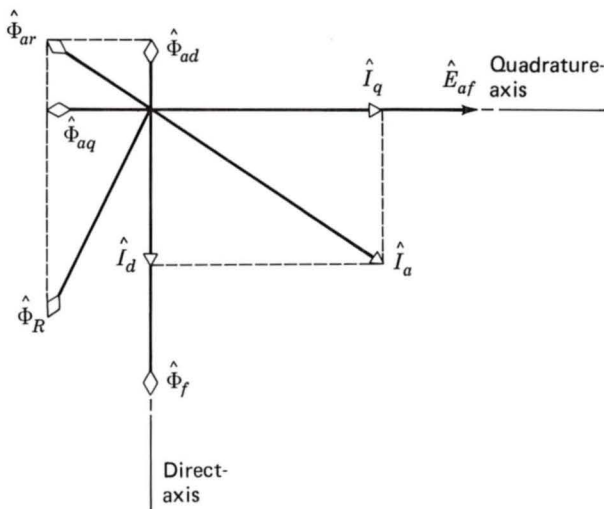


Fig. 5-21. Phasor diagram of a salient-pole synchronous generator.

The reactances X_d and X_q are, respectively, the *direct-* and *quadrature-axis synchronous reactances*; they account for the inductive effects of all the fundamental-frequency-generating fluxes created by the armature currents, along the direct and quadrature axes, including both armature-leakage and armature-reaction fluxes. Thus, the inductive effects of the direct- and quadrature-axis armature-reaction flux waves can be accounted for by *direct-* and *quadrature-axis magnetizing reactances* $X_{\varphi d}$ and $X_{\varphi q}$, respectively, similar to the magnetizing reactance X_φ of cylindrical-rotor theory. The direct- and quadrature-axis synchronous reactances then are

$$X_d = X_{al} + X_{\varphi d} \quad (5-47)$$

$$X_q = X_{al} + X_{\varphi q} \quad (5-48)$$

where X_{al} is the armature leakage reactance, assumed to be the same for direct- and quadrature-axis currents. Compare Eqs. 5-47 and 5-48 with Eq. 5-24 for the non-salient-pole case. As shown in the generator phasor diagram (Fig. 5-22), the excitation voltage \hat{E}_{af} equals the phasor sum of the terminal voltage \hat{V}_{ta} plus the armature-resistance drop $\hat{I}_a R_a$ and the component synchronous-reactance drops $j\hat{I}_d X_d + j\hat{I}_q X_q$.

The reactance X_q is less than the reactance X_d because of the greater reluctance of the air gap in the quadrature axis. Usually X_q is between $0.6X_d$ and $0.7X_d$. Typical values are given in Table 6-1. Note that a small salient-pole effect is also present in turboalternators, even though they are cylindrical-rotor machines, because of the effect of the rotor slots on the quadrature-axis reluctance.

In using the phasor diagram of Fig. 5-22, the armature current must be resolved into its direct- and quadrature-axis components. This resolution assumes that the phase angle $\phi + \delta$ of the armature current with respect to the excitation voltage is known. Often, however, the power factor angle ϕ at the machine terminals is explicitly known, rather than the internal power factor angle $\phi + \delta$. The phasor diagram of Fig. 5-22 is repeated by the solid-line phasors in Fig. 5-23. Study of this phasor diagram shows that the dashed phasor $o'a'$, perpendicular to \hat{I}_a , equals $j\hat{I}_a X_q$. This result follows geometrically from the fact that triangles $o'a'b'$ and oab are

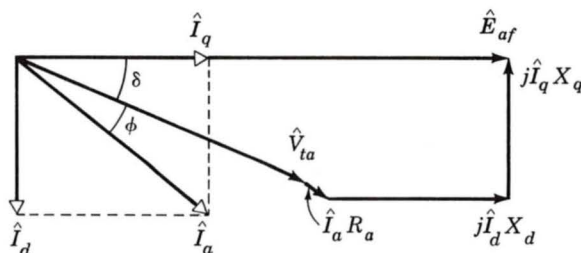


Fig. 5-22. Phasor diagram for a synchronous generator.

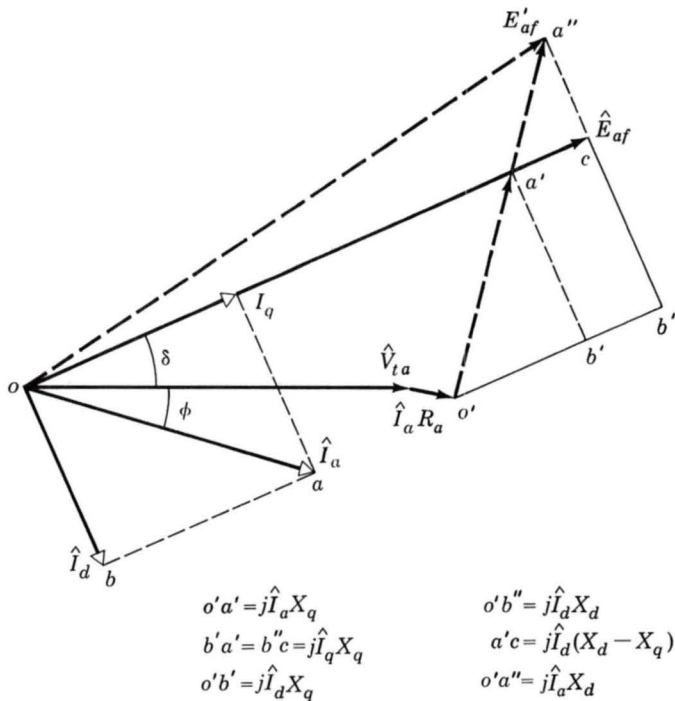


Fig. 5-23. Relations between component voltages in a phasor diagram.

similar, because their corresponding sides are perpendicular. Thus

$$\frac{o'a'}{oa} = \frac{b'a'}{ba} \quad (5-49)$$

or

$$o'a' = \frac{b'a'}{ba} oa = \frac{j\hat{I}_q X_q}{\hat{I}_q} \hat{I}_a = jX_q \hat{I}_a \quad (5-50)$$

The phasor sum $\hat{V}_{ta} + \hat{I}_a R_a + j\hat{I}_a X_q$ then locates the angular position of the excitation voltage \hat{E}_{af} (which in turn lies along the quadrature axis) and therefore the direct and quadrature axes. Physically this must be so, because all the field excitation in a normal machine is in the direct axis. One use of these relations in determining the excitation requirements for specified operating conditions at the terminals of a salient-pole machine is illustrated in Example 5-5.

EXAMPLE 5-5

The reactances X_d and X_q of a salient-pole synchronous generator are 1.00 and 0.60 per unit, respectively. The armature resistance is negligible. Com-

pute the excitation voltage when the generator delivers rated kilovolt-amperes at 0.80 power factor, lagging current, and rated terminal voltage.

Solution

First, the phase of \hat{E}_{af} must be found so that \hat{I}_a can be resolved into its direct- and quadrature-axis components. The phasor diagram is shown in Fig. 5-24.

$$\begin{aligned}\hat{I}_a &= 0.80 - j0.60 = 1.00 \angle -36.9^\circ \\ j\hat{I}_a X_q &= j(0.80 - j0.60)(0.60) = 0.36 + j0.48 \\ \hat{V}_{ta} &= \text{reference phasor} = 1.00 + j0 \\ \text{Phasor sum} &= \hat{E}' = 1.36 + j0.48 = 1.44 \angle 19.4^\circ\end{aligned}$$

The angle $\delta = 19.4^\circ$, and the phase angle between \hat{E}_{af} and \hat{I}_a is $36.9^\circ + 19.4^\circ = 56.3^\circ$.

The armature current can now be resolved into its direct- and quadrature-axis components. Their magnitudes are

$$I_d = 1.00 \sin 56.3^\circ = 0.832 \quad I_q = 1.00 \cos 56.3^\circ = 0.555$$

As phasors,

$$\hat{I}_d = 0.832 \angle -90^\circ + 19.4^\circ = 0.832 \angle -70.6^\circ$$

and

$$\hat{I}_q = 0.555 \angle 19.4^\circ$$

We can now find E_{af} by adding the length

$$a'c = I_d(X_d - X_q)$$

numerically to the magnitude of \hat{E}' ; thus, the magnitude of the excitation voltage is the algebraic sum

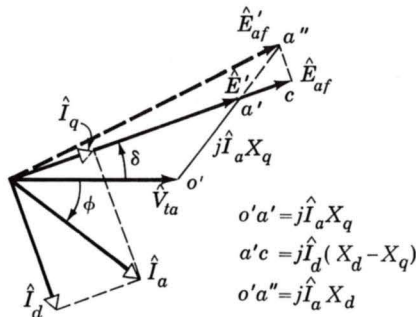


Fig. 5-24. Generator phase diagram for Example 5-5.

$$E_{af} = E' + I_d(X_d - X_q) = 1.44 + 0.832(0.40) = 1.77 \text{ per unit}$$

As a phasor, $\hat{E}_{af} = 1.77/\underline{19.4^\circ}$.

In the simplified theory of Art. 5-2, the synchronous machine is assumed to be representable by a single reactance, the synchronous reactance of Eq. 5-24. The question naturally arises: How serious an approximation is involved if a salient-pole machine is treated in this simple fashion? Suppose the salient-pole machine of Figs. 5-23 and 5-24 were treated by cylindrical-rotor theory as if it had a single synchronous reactance equal to its direct-axis value X_d . For the same conditions at its terminals, the synchronous-reactance drop $j\hat{I}_a X_d$ would be the phasor $o'a''$, and the equivalent excitation voltage would be \hat{E}'_{af} , as shown in these figures. Because ca'' is perpendicular to \hat{E}'_{af} , there is little difference in magnitude between the correct value \hat{E}_{af} and the approximate value \hat{E}'_{af} for a normally excited machine. Recomputation of the excitation voltage on this basis for Example 5-5 gives a value of $1.79/\underline{26.6^\circ}$.

Insofar as the interrelations between terminal voltage, armature current, power, and excitation over the normal operating range are concerned, the effects of salient poles usually are of minor importance, and such characteristics of a salient-pole machine usually can be computed with satisfactory accuracy by the simple cylindrical-rotor theory. Only at small excitations will the differences between cylindrical-rotor and salient-pole theory become important.

There is, however, considerable difference in the phase angles of \hat{E}_{af} and \hat{E}'_{af} in Figs. 5-23 and 5-24. This difference is caused by the reluctance torque in a salient-pole machine. Its effect is investigated now.

5-7 POWER-ANGLE CHARACTERISTICS OF SALIENT-POLE MACHINES

We limit the discussion to the simple system shown in the schematic diagram of Fig. 5-25a, comprising a salient-pole synchronous machine SM connected to an infinite bus of voltage \hat{E}_e through a series impedance of reactance X_e per phase. Resistance will be neglected because usually it is small. Consider that the synchronous machine is acting as a generator. The phasor diagram is shown by the solid-line phasors in Fig. 5-25b. The dashed phasors show the external reactance drop resolved into components due to \hat{I}_d and \hat{I}_q . The effect of the external impedance is merely to add its reactance to the reactances of the machine; i.e., the total values of reactance interposed between the excitation voltage \hat{E}_{af} and the bus voltage \hat{E}_e are

$$X_{dT} = X_d + X_e \quad (5-51)$$

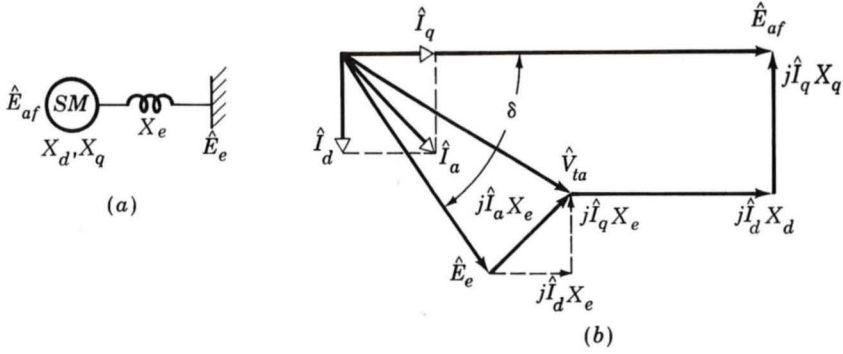


Fig. 5-25. Salient-pole synchronous machine and series impedance: (a) single-line diagram and (b) phasor diagram.

$$X_{qT} = X_q + X_e \quad (5-52)$$

If the bus voltage \hat{E}_e is resolved into components $E_e \sin \delta$ and $E_e \cos \delta$ in phase with \hat{I}_d and \hat{I}_q , respectively, the power P delivered to the bus per phase is

$$P = I_d E_e \sin \delta + I_q E_e \cos \delta \quad (5-53)$$

Also, from Fig. 5-25b,

$$I_d = \frac{E_{af} - E_e \cos \delta}{X_{dT}} \quad (5-54)$$

and

$$I_q = \frac{E_e \sin \delta}{X_{qT}} \quad (5-55)$$

Substitution of Eqs. 5-54 and 5-55 in Eq. 5-53 gives

$$P = \frac{E_{af} E_e}{X_{dT}} \sin \delta + E_e^2 \frac{X_{dT} - X_{qT}}{2X_{dT} X_{qT}} \sin 2\delta \quad (5-56)$$

As discussed in Art. 5-4, Eq. 5-56 gives the power per phase when E_{af} and E_e are expressed as line-neutral voltages. The result must be multiplied by 3 to get three-phase power; alternatively, expressing E_{af} and E_e as line-to-line voltages will result in three-phase power directly.

This power-angle characteristic is shown in Fig. 5-26. The first term is the same as the expression obtained for a cylindrical-rotor machine. This term is merely an extension of the basic concepts of Arts. 4-7 and 5-4 to include the effects of series reactance. The second term introduces the effect of salient poles. It represents the fact that the air-gap flux wave creates torque, tending to align the field poles in the position of minimum reluctance.

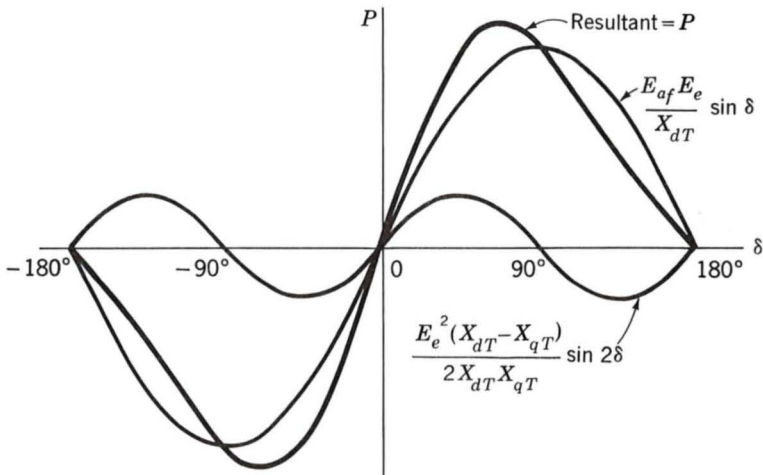


Fig. 5-26. Power-angle characteristic of a salient-pole synchronous machine showing fundamental component due to field excitation and second-harmonic component due to reluctance torque.

tance. This term is the power corresponding to the *reluctance torque* and is of the same general nature as the reluctance torque discussed in Art. 3-5. Note that the reluctance torque is independent of field excitation. Note, also, that if $X_{dT} = X_{qT}$, as in a uniform-air-gap machine, there is no preferential direction of magnetization, the reluctance torque is zero, and Eq. 5-56 reduces to the power-angle equation for a cylindrical-rotor machine whose synchronous reactance is X_{dT} (see Eq. 5-40).

Notice that the characteristic for negative values of δ is the same except for a reversal in the sign of P . That is, the generator and motor regions are alike if the effects of resistance are negligible. For generator action \hat{E}_{af} leads \hat{E}_e ; for motor action \hat{E}_{af} lags \hat{E}_e . Steady-state operation is stable over the range where the slope of the power-angle characteristic is positive. Because of the reluctance torque, a salient-pole machine is "stiffer" than one with a cylindrical rotor; i.e., for equal voltages and equal values of X_{dT} , a salient-pole machine develops a given torque at a smaller value of δ , and the maximum torque which can be developed is somewhat greater.

EXAMPLE 5-6

The 2000-hp 1.0-power-factor three-phase Y-connected 2300-V synchronous motor of Example 5-3 has reactances of $X_d = 1.95$ and $X_q = 1.40 \Omega/\text{phase}$. Neglecting all losses, compute the maximum mechanical power in kilowatts which this motor can deliver if it is supplied with electric power from an infinite bus (Fig. 5-27a) at rated voltage and frequency and if its field excitation is constant at the value which would result in 1.00 power factor

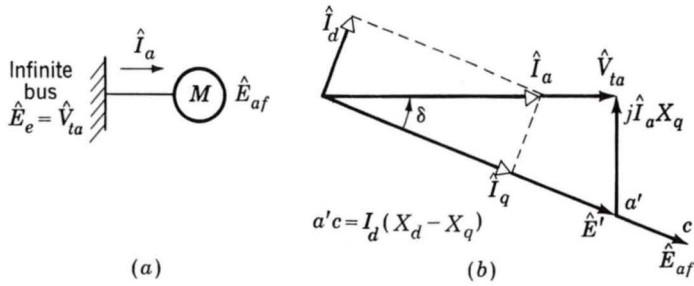


Fig. 5-27. (a) Single-line diagram and (b) phasor diagram for motor of Example 5-6.

at rated load. The shaft load is assumed to be increased gradually so that transient swings are negligible and the steady-state power limit applies. Include the effects of salient poles.

Solution

The first step is to compute the synchronous motor excitation at rated voltage, full load, and unity power factor. As in Example 5-4, the full-load terminal voltage and current are 1330 V to neutral and 374 A/phase Y, respectively. The phasor diagram for the specified full-load conditions is shown in Fig. 5-27b. The only essential difference between this phasor diagram and the generator phasor diagram of Fig. 5-24 is that \hat{I}_a in Fig. 5-27 represents motor *input* current; i.e., we have switched to the motor reference direction for \hat{I}_a . The phasor voltage equation then becomes

$$\hat{E}_{af} = \hat{V}_{ta} - j\hat{I}_d X_d - j\hat{I}_q X_q$$

In Fig. 5-27b,

$$\hat{E}' = \hat{V}_{ta} - j\hat{I}_a X_q = 1330 + j0 - j374(1.40) = 1429/\underline{-21.5^\circ}$$

That is, the angle δ is 21.5° , with \hat{E}_{af} lagging \hat{V}_{ta} . The magnitude of \hat{I}_d is

$$I_d = I_a \sin \delta = 374(0.367) = 137 \text{ A}$$

The magnitude of \hat{E}_{af} can now be found by adding the length $a'c = I_d(X_d - X_q)$ numerically to the magnitude of \hat{E}' ; thus

$$E_{af} = E' + I_d(X_d - X_q) = 1429 + 137(0.55) = 1504 \text{ V to neutral}$$

From Eq. 5-56 the power-angle characteristic for this motor is

$$\begin{aligned} P &= \frac{E_{af} E_e}{X_d} \sin \delta + E_e^2 \frac{X_d - X_q}{2X_d X_q} \sin 2\delta \\ &= 1030 \sin \delta + 178 \sin 2\delta \quad \text{kW/phase} \end{aligned}$$

The maximum power occurs when $dP/d\delta = 0$

$$\frac{dP}{d\delta} = 1030 \cos \delta + 356 \cos 2\delta$$

Setting this equal to zero and using the trigonometric identity

$$\cos 2\alpha = 2 \cos^2 \alpha - 1$$

permit us to solve for the angle δ at which the maximum power occurs:

$$\delta = 73.2^\circ$$

Therefore the maximum power is

$$P_{\max} = 1080 \text{ kW/phase} = 3240 \text{ kW for three phases}$$

Compare with $P_{\max} = 3090 \text{ kW}$ found in Example 5-3, where the effects of salient poles were neglected. The error caused by neglecting saliency is slightly less than 5 percent in this case.

The effect of salient poles on the power limit increases as the excitation voltage is decreased, as can be seen from Eq. 5-56. For a normally excited machine the effect of salient poles usually amounts to a few percent at most. Only at small excitations does the reluctance torque become important. Thus, except at small excitations or when very accurate results are required, a salient-pole machine usually can be adequately treated by simple cylindrical-rotor theory.

5-8 INTERCONNECTED SYNCHRONOUS GENERATORS

As discussed in Art. 5-1, electric power systems consist of the interconnection of large numbers of synchronous generators operating in parallel, interconnected by transmission lines, and supplying large numbers of widely distributed loads. To illustrate the basic features of parallel operation on a very simplified scale, consider an elementary system comprising two identical three-phase generators G_1 and G_2 with their prime movers PM_1 and PM_2 supplying power to a load L , as shown in the single-line diagram of Fig. 5-28. Suppose generator G_1 is supplying the load at rated voltage and frequency, with generator G_2 disconnected. Generator G_2 can be *paralleled* with G_1 by driving it at synchronous speed and adjusting its field excitation so that its terminal voltage equals that of the bus. If the frequency of the incoming machine is not exactly equal to that of the bus, the phase rela-

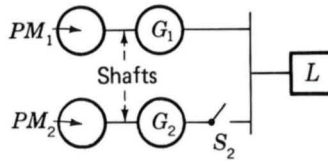


Fig. 5-28. Parallel operation of two synchronous generators.

tion between its voltage and that of the bus will vary at a frequency equal to the difference between the frequencies of the two voltages—perhaps a fraction of a cycle per second. Switch S_2 should be closed when the two voltages are momentarily in phase and the voltage across the switch is zero. A device for indicating the appropriate moment is known as a *synchroscope*. After G_2 has been synchronized in this manner, each machine can be made to take its share of the active- and reactive-power load by appropriate adjustments of the prime-mover throttles and field excitations.

In contrast with dc generators, paralleled synchronous generators must run at exactly the same steady-state speed (for the same number of poles). Consequently, how the active power divides between them depends almost wholly on the speed-power characteristics of their prime movers. In Fig. 5-29 the sloping solid lines PM_1 and PM_2 represent the speed-power characteristics of the two prime movers for constant throttle openings. All practical prime movers have drooping speed-power characteristics. The total load P_L is shown by the solid horizontal line AB , and the generator power outputs are P_1 and P_2 (losses being neglected). Now suppose the throttle opening of PM_2 is increased, translating its speed-power curve upward to the dashed line PM'_2 . The dashed line $A'B'$ now represents the load power. Note that the power output of generator 2 has now increased from P_2 to P'_2 while that of generator 1 has decreased from P_1 to P'_1 . At the same time, the system frequency has increased. The frequency can be restored to normal with a further load shift from generator 1 to generator 2 by closing the throttle on generator 1, lowering its speed-power curve to the dashed line PM'_1 . The load power is now represented by $A''B''$, and the power outputs of the generators are P'_1 and P'_2 . Thus, the system frequency

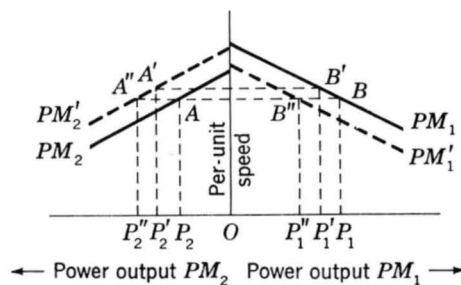


Fig. 5-29. Prime-mover speed-power characteristics.

and the division of active power between the generators can be controlled by the prime-mover throttles.

Changes in excitation affect the terminal voltage and reactive-power distribution. For example, let the two identical generators of Fig. 5-28 be adjusted to share the active and reactive loads equally. The phasor diagram is shown by the solid lines in Fig. 5-30, where \hat{V}_{ta} is the terminal voltage, \hat{I}_L is the load current, \hat{I}_a is the armature current in each generator, and \hat{E}_{af} is the excitation voltage. The synchronous-reactance voltage drop in each generator is $j\hat{I}_a X_s$, and the resistance drops are neglected. Now suppose the excitation of generator 1 is increased. The bus voltage \hat{V}_{ta} will increase. It can then be restored to normal by decreasing the excitation of generator 2. The final condition is shown by the dashed phasors in Fig. 5-30. The terminal voltage, load current, and load power factor have been unchanged. Since the prime-mover throttles have not been touched, the power output and in-phase components of the generator armature currents have not been changed. The excitation voltages \hat{E}_{af1} and \hat{E}_{af2} have shifted in phase so that $\hat{E}_{af} \sin \delta$ remains constant. The generator with the increased excitation has now taken on more of the lagging reactive-KVA load. For the condition shown by the dashed phasors in Fig. 5-30, generator 1 is supplying all the reactive kilovoltamperes, and generator 2 is operating at unity power factor. Thus the terminal voltage and reactive-power distribution between the generators can be controlled by means of the field excitation.

Usually the prime-mover throttles are controlled by governors and automatic frequency regulators so that the system frequency is maintained very nearly constant and power is divided properly among the generators. Voltage and reactive-power flow often are automatically regulated by voltage regulators acting on the field circuits of the generators and by transformers with automatic tap-changing devices.

5-9 SUMMARY

The physical picture of the internal workings of a synchronous machine in terms of rotating magnetic fields is rather simple. It is that of Art. 4-7: interaction of component fields of rotor and stator when the two are stationary with respect to each other. For both round-rotor and salient-pole machines, the component fields and mmf's, together with the associated voltages and currents, can be represented on phasor diagrams such as that of Fig. 5-21. The phasor diagrams in turn lead to the concept of the synchronous reactances X_s , X_d , and X_q .

The unsaturated synchronous reactance X_s or X_d can be found from the results of an open-circuit and a short-circuit test. These test methods are a variation of a testing technique applicable not only to synchronous machines but also to anything whose behavior can be approximated by a linear equivalent circuit to which Thevenin's theorem applies. From the

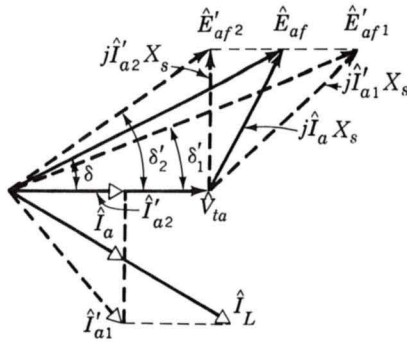


Fig. 5-30. Effects of changing excitations of two paralleled synchronous generators.

Thevenin theorem viewpoint, an open-circuit test gives the internal voltage, and a short-circuit test gives information regarding the internal impedance. From the more specific viewpoint of electromagnetic machinery, an open-circuit test gives information regarding excitation requirements, core losses, and (for rotating machines) friction and windage losses; a short-circuit test gives information regarding the magnetic reactions of the load current, leakage impedances, and losses associated with the load current such as I^2R and stray load losses. The only real complication arises from the effects of magnetic nonlinearity, effects which can be taken into account approximately by considering the machine to be equivalent to an unsaturated one whose magnetization curve is the straight line Op of Fig. 5-9 and whose synchronous reactance is empirically adjusted for saturation as in Eq. 5-28.

Prediction of the steady-state synchronous-machine characteristics then becomes merely a study of power flow through a simple impedance with constant or easily determinable voltages at its ends. Study of the maximum power limits for short-time overloads is simply a special case of the limitations on power flow through an inductive impedance. The power flow through such an impedance can be expressed conveniently in terms of the voltages at its sending and receiving ends and the phase angles associated with these voltages, as in Eq. 5-40 for a cylindrical-rotor machine and 5-56 for a salient-pole machine. These analyses show that saliency has relatively little effect on the interrelations between field excitation, terminal voltage, armature current, and power; but the power-angle characteristics are affected by the presence of a reluctance-torque component. Because of the reluctance torque, a salient-pole machine is stiffer than one with a cylindrical rotor.

In the next chapter we extend our analysis of synchronous machines to include transient conditions. This includes both the transient behavior of the currents and fluxes in the machine and the transient interactions of the machine with the system with which it is connected.

PROBLEMS

5-1. The full-load torque angle δ_{RF} of a synchronous motor at rated voltage and frequency is 30 electrical degrees. Neglect the effects of armature resistance and leakage reactance. If the field current is constant, how would the torque angle be affected by the following changes in operating conditions?

- (a) Frequency reduced 10 percent, load torque constant
- (b) Frequency reduced 10 percent, load power constant
- (c) Both frequency and applied voltage reduced 10 percent, load torque constant
- (d) Both frequency and applied voltage reduced 10 percent, load power constant

5-2. The armature phase windings of a two-phase synchronous machine are displaced by 90 electrical degrees in space.

- (a) What is the mutual inductance between these two windings?
- (b) Repeat the derivation leading to Eq. 5-15, and show that for a two-phase machine the synchronous inductance is simply equal to the armature phase inductance, that is, $L_s = L_{aa0} + L_{al}$, where L_{aa0} is the component of armature phase inductance due to space-fundamental air-gap flux and L_{al} is the armature leakage inductance.

5-3. Design calculations show the following parameters for a round-rotor synchronous generator.

$$\text{Phase-}a \text{ self-inductance } L_{aa} = 2.87 \text{ mH}$$

$$\text{Armature leakage inductance } L_{al} = 0.260 \text{ mH}$$

Calculate the phase-phase mutual inductance and the machine synchronous inductance.

5-4. The manufacturer's data sheet for a 26-kV, 720-MVA, 60-Hz three-phase synchronous generator indicates that it has a synchronous reactance $X_s = 1.92$ and a leakage reactance $X_{al} = 0.19$, both in per unit on the generator base. Calculate (a) the synchronous inductance in millihenrys, (b) the armature leakage inductance in millihenrys, and (c) the armature phase inductance L_{aa} in millihenrys and in per unit.

5-5. The phase- a terminal voltage of a three-phase, 60-Hz synchronous generator is measured to be 15.5 kV rms when the field current is 370 A.

- (a) Calculate the stator-to-rotor mutual inductance L_{af} .
- (b) Calculate the terminal voltage if the field current is held constant while the generator speed is reduced so that the frequency of the generated voltage is 50 Hz.

5-6. The following readings are taken from the results of an open- and a short-circuit test on a 900-MVA three-phase Y-connected 26-kV (line-to-line) two-pole 60-Hz turbine generator driven at synchronous speed:

Field current, A	1710	3290
Armature current, short-circuit test, kA	10.4	20.0
Line voltage, open-circuit characteristic, kV	26.0	(31.8)
Line voltage, air-gap line, V	29.6	(56.9)

The numbers in parentheses are extrapolations based on the measured data. Find (a) the unsaturated value of the synchronous reactance in ohms per phase and per unit, (b) the short-circuit ratio, and (c) the saturated synchronous reactance in per unit and in ohms per phase.

5-7. The following readings are taken from the results of an open- and a short-circuit test on a 9375-kVA three-phase Y-connected 13,800-V (line-to-line) two-pole 60-Hz turbine generator driven at synchronous speed:

Field current, A	169	192
Armature current, short-circuit test, A	392	446
Line voltage, open-circuit characteristic, V	13,000	13,800
Line voltage, air-gap line, V	15,400	17,500

The armature resistance is $0.064 \Omega/\text{phase}$. The armature leakage reactance is 0.10 per unit on the generator rating as a base. Find (a) the unsaturated value of the synchronous reactance in ohms per phase and per unit, (b) the short-circuit ratio, and (c) the saturated synchronous reactance in per unit and ohms per phase.

5-8. (a) Compute the field current required in the generator of Prob. 5-7 at rated voltage, rated-kVA load, 0.80 power factor lagging. Account for saturation under load by the method described in the paragraph relating to Eq. 5-28.

(b) In addition to the data given in Prob. 5-7, more points on the open-circuit characteristic are given below:

Field current, A	200	250	300	350
Line voltage, V	14,100	15,200	16,000	16,600

Find the voltage regulation for the load of part (a). *Voltage regulation* is defined as the rise in voltage when load is removed, the

speed and field excitation being held constant. It is usually expressed as a percentage of the voltage under load.

5-9. Loss data for the generator of Prob. 5-7 are as follows:

Open-circuit core loss at 13,800 V = 68 kW

Short-circuit load loss at 392 A, 75°C = 50 kW

Friction and windage = 87 kW

Field-winding resistance at 75°C = 0.285 Ω

Compute the efficiency at rated load, 0.80 power factor lagging.

5-10. The following data are obtained from tests on a 158-MVA 13.8-kV three-phase 60-Hz 72-pole hydroelectric generator.

Open-circuit characteristic:

I_f , A	100	200	300	400	500	600	700	775	800
Voltage, kV (line-line)	2.21	4.42	6.49	8.42	10.1	11.6	13.1	13.8	14.1

Short-circuit test:

$$I_f = 710 \text{ A} \quad I_a = 6610 \text{ A}$$

(a) Draw the open-circuit saturation curve, the air-gap line, and the short-circuit characteristic. Then find (b) the unsaturated value of the synchronous reactance in ohms per phase and per unit (generator base), (c) the short-circuit ratio, and (d) the saturated synchronous reactance in per unit and ohms per phase.

5-11. What is the maximum per unit reactive power that can be supplied by a synchronous machine operating at its rated terminal voltage whose synchronous reactance is 1.5 per unit and whose maximum field current is limited to 2.3 times that required to achieve rated terminal voltage under open-circuit conditions?

5-12. A 20-MVA 11.5-kV synchronous machine is operating as a synchronous condenser, as discussed in Appendix C-4a. The generator short-circuit ratio is 0.54, and the field current at rated voltage and no load is 275 A. Assume the generator to be connected directly to an 11.5-kV source.

(a) What is the saturated synchronous reactance of the generator in per unit and in ohms per phase?

The generator field current is adjusted to 225 A.

- (b) Draw a phasor diagram, indicating the terminal voltage, excitation voltage, and armature current.
- (c) Calculate the armature current magnitude (per unit and amperes) and its phase angle with respect to the terminal voltage.
- (d) Under these conditions, does the synchronous condenser appear inductive or capacitive to the 11.5-kV system?
- (e) Repeat parts (b) through (d) for a field current of 325 A.

5-13. A synchronous generator with synchronous reactance of 1.47 per unit is operating at a real power loading of 0.5 per unit connected to a system with a series impedance of $j0.08$ per unit. An increase in its field current is observed to cause a decrease in armature current.

- (a) Before the increase, was the generator supplying or absorbing reactive power from the power system?
- (b) As a result of this increase in excitation, does the generator terminal voltage decrease or increase?
- (c) Repeat parts (a) and (b) if the synchronous generator is replaced by a synchronous motor.

5-14. Consider the synchronous machine of Prob. 5-12 to be operating on a power system which can be represented by an 11.5-kV voltage source in series with a reactive impedance of $j0.12$ per unit (generator base).

- (a) Find the maximum power output (in per unit and in megawatts) that can be delivered to the system if the field current is maintained at 275 A.
- (b) Find (i) the generator terminal voltage under the operating condition of part (a), (ii) the magnitude (in per unit and amperes) and phase (with respect to the terminal voltage) of the armature current, and (iii) the corresponding power factor. Is it leading or lagging?
- (c) The field current is increased until the generator terminal voltage is 11.5 kV while the generator output power is held constant at the value found in part (a). Find (i) the magnitude (per unit and amperes) and phase (with respect to the terminal voltage) of the armature current, (ii) the corresponding value of field current, and (iii) the corresponding power factor. Is it leading or lagging?

5-15. Superconducting synchronous generators are designed with superconducting field windings which can carry large current densities and create large magnetic flux densities. Since typical operating magnetic flux densities exceed the saturation flux densities of iron, these machines are designed without iron in the magnetic circuit; as a result, these machines exhibit no saturation effects.

A two-pole 60-Hz 13.8-kV 10-MVA superconducting generator achieves rated open-circuit armature voltage at a field current of 842 A. It achieves rated armature current into a terminal three-phase short circuit with a field

current of 226 A. Consider this generator to be connected to a 13.8-kV distribution feeder of negligible impedance with an output power of 8.5 MW at 0.85 power factor lagging. Calculate (a) the per unit synchronous inductance; (b) the field current in amperes and the rotor angle for this loading; and (c) the resultant rotor angle and reactive-power output in megavolt-amperes if the field current is reduced to 842 A while the prime-mover torque is held constant.

5-16. For a synchronous machine with constant synchronous reactance X_s operating at constant terminal voltage V_{ta} and constant excitation voltage E_{af} , show that the locus of the tip of the armature-current phasor is a circle. On a phasor diagram with terminal voltage chosen as the reference phasor, indicate the position of the center of this circle and its radius. Express the coordinates of the center and the radius of the circle in terms of V_{ta} , E_{af} , and X_s .

5-17. A four-pole 60-Hz 24-kV 600-MVA synchronous generator with a synchronous reactance of 1.67 per unit is operating on a power system which can be represented by a 24-kV infinite bus in series with a reactance impedance of $j0.24 \Omega$. The generator is equipped with a voltage regulator that adjusts the field excitation such that the generator terminal voltage remains at 24 kV independent of the generator loading.

- (a) The generator output power is adjusted to 300 MW.
 - (i) Draw a phasor diagram for this operating condition.
 - (ii) Find the magnitude (in kiloamperes) and phase (with respect to the generator terminal voltage) of the armature current. What is the generator power factor at this operating condition?
 - (iii) Find the magnitude (in kilovolts) of the generator excitation voltage E_{af} .
- (b) Repeat part (a) if the generator output power is increased to 600 MVA.

5-18. The 158-MVA hydroelectric generator of Prob. 5-10 is to be operating on a 13.8-kV power system. Normally the generator is to be operated with its automatic voltage regulator maintaining the terminal voltage at 1.0 per unit. However, the operating utility wishes to investigate the possible consequences should the operator forget to switch over to the automatic voltage regulator and instead leave the excitation constant at a field current of 775 A (corresponding to rated open-circuit voltage). For the purposes of this problem, neglect the effects of saliency and assume that the generator can be represented by the saturated synchronous reactance found in Prob. 5-10.

- (a) If the power system is represented simply by a 13.8-kV infinite bus with no series impedance, can the generator be loaded to an output power of 158 MW without losing synchronism?

- (b) If the power system actually must be represented by a 13.8-kV infinite bus in series with a reactive impedance of $j0.14 \Omega$, what is the maximum generator loading that can be achieved before synchronism is lost?

5-19. Repeat Example 5-5, assuming the generator is operating at one-half of its rated kilovoltamperes at 0.8 power factor (lagging) and rated terminal voltage.

5-20. Repeat Prob. 5-18, assuming that the saturated reactance X_d is equal to that found in Prob. 5-10 and that X_q is equal to 75 percent of this value. Compare the values found here to those found in Prob. 5-18.

5-21. Draw the steady-state direct-quadrature phasor diagram for an over-excited synchronous motor, i.e., one whose field current is high enough for lagging reactive kVA to be delivered to the supply system. From this phasor diagram show that the torque angle δ between the excitation and terminal voltage phasors is given by

$$\tan \delta = \frac{I_a X_q \cos \phi + I_a R_a \sin \phi}{V_{ta} + I_a X_q \sin \phi - I_a R_a \cos \phi}$$

Consider ϕ to be negative when \hat{I}_a lags \hat{V}_{ta} .

5-22. What percentage of its rated output will a salient-pole synchronous machine deliver without loss of synchronism when operating as a motor with rated applied voltage and with the field excitation zero if $X_d = 0.85$ per unit and $X_q = 0.60$ per unit? Compute the per unit armature current for this operating condition.

5-23. If the synchronous machine of Prob. 5-22 is operated as a synchronous generator connected to an infinite bus of rated voltage, find the minimum per-unit excitation for which the machine will stay in synchronism at (a) half load and (b) full load.

5-24. A salient-pole synchronous generator with saturated synchronous reactances $X_d = 1.80$ per unit and $X_q = 1.65$ per unit is connected to an infinite bus (of voltage $V_\infty = 1.0$ per unit) through an external reactance $X_e = 0.12$ per unit. The generator is supplying its rated voltamperes at 0.95 power factor lagging, as measured at the generator terminals.

- (a) Draw a phasor diagram, indicating the infinite bus voltage, armature current, generator terminal voltage, excitation voltage, and rotor angle.
- (b) Calculate the rotor angle in degrees.
- (c) Calculate the per unit terminal and excitation voltages.

6

Synchronous Machines: Transient Performance

In Chap. 5 the steady-state performance of synchronous machines was described. This steady-state behavior is based on the interaction between the armature flux wave, which rotates at synchronous speed, and the synchronously rotating rotor flux wave. The steady-state torque level and the magnitude of the flux waves determine the constant angular separation between these flux waves.

During transient conditions, various disturbances can cause these fluxes to change magnitude and angular displacement as the rotor deviates from synchronous speed. Since electrical windings and solid-iron structures tend to oppose changes in flux linkages, these disturbances induce transient currents in the rotor and stator windings as well as in the rotor body of solid-rotor machines. The transient analysis of synchronous machines is thus concerned with determining transient fluxes and currents and their influence upon the electrical and electromechanical behavior of the machine.

In Art. 5-6 the concept of direct- and quadrature-axis analysis was introduced. This technique, based on viewing the machine from a reference frame attached to the rotor, is extremely valuable in transient analysis of synchronous machines and is developed further in this chapter.

6-1 SYNCHRONOUS-MACHINE TRANSIENTS

The inherent complexity of synchronous-machine transient phenomena can be appreciated by inspecting the main structure details of the machine with the object of discussing the significant circuits when transient conditions prevail. A salient-pole structure is shown in the schematic diagram of Fig. 6-1. *Damper bars* are used in such machines to provide induction-motor-type torques, which aid in damping electromechanical rotor oscillations following transient disturbances; the damper bars and field collar are all short-circuited together at the end of the rotor, forming a structure which appears much like the squirrel cage in an induction motor and whose function is quite similar.

Although solid cylindrical-rotor machines are generally not constructed with damper windings, currents which are induced directly in the rotor body following transients play the same role as damper currents in a salient-pole machine. The rotors of salient-pole machines are normally made of stacks of thin insulated laminations, and hence rotor body currents are not induced in these machines. In fact, in the analysis of solid-rotor machines these rotor body currents are often referred to as damper currents. The salient-pole structure also emphasizes the difference be-

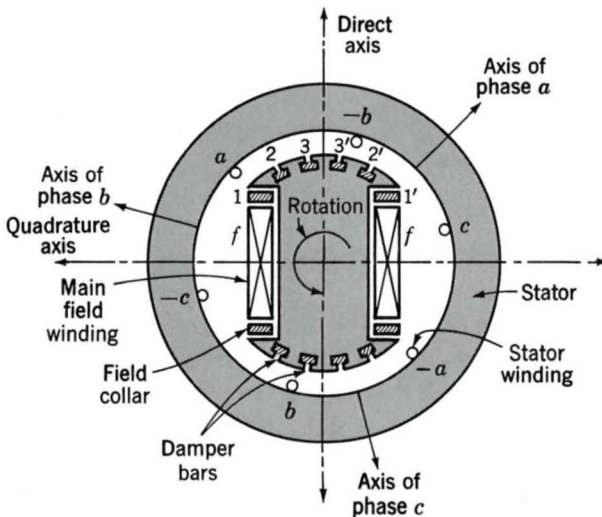


Fig. 6-1. Schematic diagram for synchronous machine showing significant circuits for transient conditions.

tween the polar, or direct, axis and the interpolar, or quadrature, axis; similar differences exist between the two axes of cylindrical-rotor machines in transient analysis, so that the two types of machines are treated in similar fashion in most transient analyses.

Under balanced steady-state conditions, the mmf wave of the stator winding and its associated flux wave revolve at the same speed as the rotor and are of essentially fixed waveform. As a result, the flux linkages with the rotor circuits do not change with time, and no voltages are induced in these circuits. Thus the main-field winding is the only rotor circuit which carries current, and its excitation is determined by the voltage applied to the field terminals.

Under transient conditions the magnitudes of the rotor and stator fluxes change, and often the rotor speed changes, causing the rotor to change its alignment with respect to the synchronously rotating stator flux. As a consequence, the flux linkages with all the rotor circuits change with time, and currents are induced in each—in the damper windings, in the rotor body, and in the field winding. Since the net rotor mmf is produced by all the windings, the resultant electrical and electromechanical behavior of the machine is determined by the transient behavior of each of these currents. Transient analysis is most often accomplished by representing the machine as a set of mutually coupled circuits.

In Fig. 6-1 there is a stator circuit for each of the three phases, a , b , and c , and there are rotor circuits corresponding to the field winding and to the damper bars 2-2' and 3-3' and the conducting field collars 1-1'. An additional rotor circuit may be formed by the bolts and iron of the rotor structure. Currents induced in the rotors of cylindrical-rotor machines can also be represented in terms of current induced in equivalent rotor circuits although the exact current paths are not easily identifiable.

Each of these circuits has its own resistance, self-inductance, and mutual inductances with respect to every other circuit. Basic analysis of synchronous-machine transient behavior can thus be accomplished by the solution of a set of simultaneous coupled-circuit differential equations. This analysis is often assumed linear in the sense that saturation effects are often ignored or at best represented by changing the magnetizing inductance as a function of the net flux. Nevertheless, the solution of these equations can be a formidable task. The solution is expedited appreciably by a linear transformation of variables (known as the dq0 transformation) in which the stator currents, voltages, and fluxes are replaced by equivalent quantities rotating at rotor speed. For example, the three stator-phase currents i_a , i_b , and i_c are replaced by three transformed quantities: the *direct-axis component* i_d , the *quadrature-axis component* i_q , and the *zero-sequence component* i_0 which is zero under balanced terminal conditions of the sort considered in this chapter.

The mathematical formalization of this transformation (Art. 6-2) permits machine analysis to be performed in a reference frame fixed with respect to the rotor; the transformed variables are the equivalent armature quantities as seen by an observer in this reference frame. The physical sig-

nificance of the direct- and quadrature-axis quantities is that given in Art. 5-6; direct-axis quantities lie along the axis of the field winding, whereas quadrature-axis quantities lie along an axis perpendicular to the field winding. The idea of making this transformation arose from an extension of the physical picture corresponding to the steady-state analysis.

This change of variables permits the simultaneous equations to be separated into two sets of equations (one for each axis) based on inductances which are constant in time. This can easily be seen by recognizing that the actual mutual inductances between the stator-phase windings and the rotor circuits change with rotor position (and hence with time), whereas the transformed stator variables remain fixed in the rotor frame and thus the mutual inductances remain unchanged with time. Furthermore, this type of analysis quickly leads to the identification of various reactances and time constants which have proven quite useful in the analysis and characterization of synchronous machines and which are discussed at various points throughout this chapter.

The most common situation in which synchronous-machine transient analysis is required occurs when a synchronous machine is interconnected into a system consisting of many machines, loads, and a large transmission network. For some sorts of analyses it is sufficient to represent the system by a Thevenin-equivalent series impedance and voltage source (infinite bus), as discussed in Art. 5-1. In these cases, the emphasis is on the behavior of the single machine under the assumption that the transient disturbance can be considered localized to that particular unit.

In most cases, however, the disturbance is not so localized, and the analysis must involve a number of machines (perhaps even up to a few hundred units). In addition, the dynamics of turbine-governor and excitation systems may play an important role in the transient behavior and must be modeled. Although it is, in theory, possible to represent each machine by a complex model with a large number of differential equations to be solved, as a practical matter such a procedure often leads to formulations which are at best very slow and at worst too large to be implemented in any form. Thus, many levels of representation are used, ranging from a complex, multiwinding model down to a model in which the machine is represented as a constant voltage in series with a transient reactance.

This chapter cannot begin to cover the range of issues involved in the transient analysis of synchronous machines. It is intended rather to provide a basic understanding of the transient phenomena and to introduce the various models and analytical tools which are available.

6-2 TRANSFORMATION TO DIRECT- AND QUADRATURE-AXIS VARIABLES

In Art. 5-6 the concept of resolving armature quantities into two rotating components—one aligned with the field-winding axis, the direct-axis component, and one in quadrature with the field-winding axis, the quadrature-

axis component—was introduced as a means of facilitating analysis of salient-pole machines. The usefulness of this concept stems from the fact that although each of the stator phases sees a time-varying inductance due to the saliency of the rotor, the transformed quantities rotate with the rotor and hence see constant magnetic paths. Additional saliency effects are present under transient conditions, due to the different conducting paths in the rotor, rendering the concept of this transformation all the more useful.

The idea behind the transformation is an old one, stemming from the work of André Blondel in France, and the technique is sometimes referred to as the *Blondel two-reaction method*. Much of the development in the form used here was carried out by R. E. Doherty, C. A. Nickle, R. H. Park, and their associates in the United States. The transformation itself, known as the *dq0 transformation*, can be represented in a straightforward fashion in terms of the electrical angle θ (equal to poles/2 times the spatial angle) between the rotor direct axis and the stator phase-*a* axis, as shown in Fig. 6-2. Letting *S* represent the stator quantity to be transformed (current, voltage, or flux), we can write the transformation[†] in matrix form as

$$\begin{bmatrix} S_d \\ S_q \\ S_0 \end{bmatrix} = \frac{2}{3} \begin{bmatrix} \cos \theta & \cos (\theta - 120^\circ) & \cos (\theta + 120^\circ) \\ -\sin \theta & -\sin (\theta - 120^\circ) & -\sin (\theta + 120^\circ) \\ \frac{1}{2} & \frac{1}{2} & \frac{1}{2} \end{bmatrix} \begin{bmatrix} S_a \\ S_b \\ S_c \end{bmatrix} \quad (6-1)$$

[†]Although the dq0 transformation is often written in the form of Eqs. 6-1 and 6-2, an equally valid form is

$$\begin{bmatrix} S_d \\ S_q \\ S_0 \end{bmatrix} = \sqrt{\frac{2}{3}} \begin{bmatrix} \cos \theta & \cos (\theta - 120^\circ) & \cos (\theta + 120^\circ) \\ -\sin \theta & -\sin (\theta - 120^\circ) & -\sin (\theta + 120^\circ) \\ \frac{1}{\sqrt{2}} & \frac{1}{\sqrt{2}} & \frac{1}{\sqrt{2}} \end{bmatrix} \begin{bmatrix} S_a \\ S_b \\ S_c \end{bmatrix}$$

and its inverse

$$\begin{bmatrix} S_a \\ S_b \\ S_c \end{bmatrix} = \sqrt{\frac{2}{3}} \begin{bmatrix} \cos \theta & -\sin \theta & \frac{1}{\sqrt{2}} \\ \cos (\theta - 120^\circ) & -\sin (\theta - 120^\circ) & \frac{1}{\sqrt{2}} \\ \cos (\theta + 120^\circ) & -\sin (\theta + 120^\circ) & \frac{1}{\sqrt{2}} \end{bmatrix} \begin{bmatrix} S_d \\ S_q \\ S_0 \end{bmatrix}$$

This form of the transformation has the advantage of being unitary (i.e., the transformation matrix and its inverse matrix are the transpose of each other), and it is *power-invariant* in the sense that using this transformation, Eq. 6-30 becomes simply the sum of the *vi* products

$$p_s = v_d i_d + v_q i_q + v_0 i_0$$

and Eq. 6-31 becomes

$$T = \left(\frac{\text{poles}}{2} \right) (\lambda_d i_q - \lambda_q i_d)$$

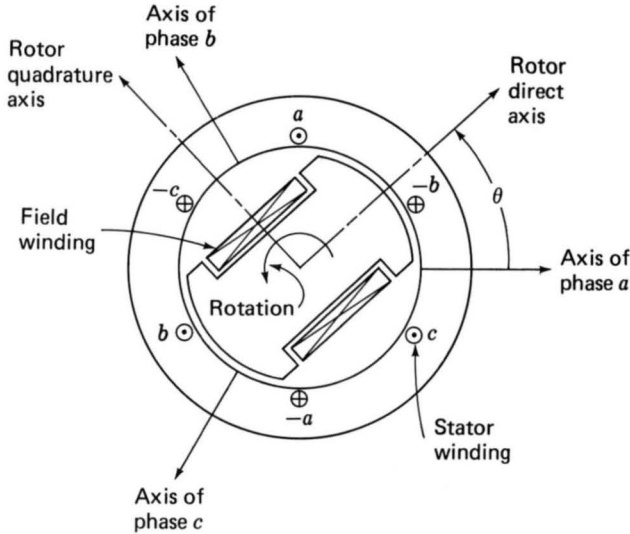


Fig. 6-2. Idealized synchronous machine.

and the inverse transformation as

$$\begin{bmatrix} S_a \\ S_b \\ S_c \end{bmatrix} = \begin{bmatrix} \cos \theta & -\sin \theta & 1 \\ \cos (\theta - 120^\circ) & -\sin (\theta - 120^\circ) & 1 \\ \cos (\theta + 120^\circ) & -\sin (\theta + 120^\circ) & 1 \end{bmatrix} \begin{bmatrix} S_d \\ S_q \\ S_0 \end{bmatrix} \quad (6-2)$$

Here the letter S refers to the quantity to be transformed and the subscripts d and q represent the direct and quadrature axes, respectively. A third component, the *zero-sequence component*, indicated by the subscript 0, is also included. This component is required to yield a unique transformation of the three stator-phase quantities; it corresponds to components of armature current which produce no net air-gap flux and hence no net flux linking the rotor circuits. As can be seen from Eq. 6-1, under balanced three-phase conditions, there are no zero-sequence components. Only balanced three-phase conditions are considered in this book, and hence zero-sequence components are not discussed in any detail.

EXAMPLE 6-1

A two-pole synchronous machine is carrying balanced three-phase armature currents

$$i_a = I_a \cos \omega t \quad i_b = I_a \cos (\omega t - 120^\circ) \quad i_c = I_a \cos (\omega t + 120^\circ)$$

The rotor is rotating at synchronous speed ω , and the rotor direct axis is

aligned with the stator phase- a axis at $t = 0$. Find the direct- and quadrature-axis current components.

Solution

The angle between the rotor direct axis and the stator phase- a axis can be expressed as

$$\theta = \omega t$$

From Eq. 6-1

$$\begin{aligned} i_d &= \frac{2}{3}[i_a \cos \omega t + i_b \cos (\omega t - 120^\circ) + i_c \cos (\omega t + 120^\circ)] \\ &= \frac{2}{3}I_a[\cos^2 \omega t + \cos^2 (\omega t - 120^\circ) + \cos^2 (\omega t + 120^\circ)] \end{aligned}$$

Using the trigonometric identity $\cos^2 \alpha = \frac{1}{2}(1 + \cos 2\alpha)$ gives

$$i_d = I_a$$

Similarly,

$$\begin{aligned} i_q &= -\frac{2}{3}[i_a \sin \omega t + i_b \sin (\omega t - 120^\circ) + i_c \sin (\omega t + 120^\circ)] \\ &= -\frac{2}{3}I_a[\cos \omega t \sin \omega t + \cos (\omega t - 120^\circ) \sin (\omega t - 120^\circ) \\ &\quad + \cos (\omega t + 120^\circ) \sin (\omega t + 120^\circ)] \end{aligned}$$

and using the trigonometric identity $\cos \alpha \sin \alpha = \frac{1}{2} \sin 2\alpha$ gives

$$i_q = 0$$

This result corresponds directly to our physical picture of the dq0 transformation. From the discussion of Art. 4-5 we recognize that the balanced three-phase currents correspond to a synchronously rotating current (or mmf) wave which is aligned with the stator phase- a axis at $t = 0$. This stator-current wave is thus aligned with the rotor direct axis at $t = 0$ and remains so since the rotor is rotating at the same speed. Hence the stator current consists only of a direct-axis component.

6-3 BASIC MACHINE RELATIONS IN dq0 VARIABLES

Equation 5-9 gives the flux-current relationships for a synchronous machine consisting of a field winding and three stator-phase windings. This simple machine is sufficient to demonstrate the basic features of the machine representation in dq0 variables; the effects of additional rotor circuits can be introduced in a straightforward fashion.

The flux-current relationships in terms of phase variables (Eqs. 5-2 to 5-5) are repeated here for convenience

$$\begin{bmatrix} \lambda_a \\ \lambda_b \\ \lambda_c \\ \lambda_f \end{bmatrix} = \begin{bmatrix} \mathcal{L}_{aa} & \mathcal{L}_{ab} & \mathcal{L}_{ac} & \mathcal{L}_{af} \\ \mathcal{L}_{ba} & \mathcal{L}_{bb} & \mathcal{L}_{bc} & \mathcal{L}_{bf} \\ \mathcal{L}_{ca} & \mathcal{L}_{cb} & \mathcal{L}_{cc} & \mathcal{L}_{cf} \\ \mathcal{L}_{fa} & \mathcal{L}_{fb} & \mathcal{L}_{fc} & \mathcal{L}_{ff} \end{bmatrix} \begin{bmatrix} -i_a \\ -i_b \\ -i_c \\ i_f \end{bmatrix} \quad (6-3)$$

where the negative signs have been added consistent with a choice of generator reference for the armature currents. Unlike the analysis of Art. 5-2, this analysis will include the effects of saliency, which cause the stator self- and mutual inductances to vary with rotor position.

For the purposes of this analysis the idealized synchronous machine of Fig. 6-2 is assumed to satisfy two conditions: (1) the air-gap permeance has a constant component as well as a smaller component which varies cosinusoidally with rotor angle as measured from the direct axis, and (2) the effects of space harmonics in the air-gap flux can be ignored. Although these approximations may appear somewhat restrictive, they form the basis of classical dq0 machine analysis and give excellent results in a wide variety of applications. Essentially they involve neglecting effects which result in time-harmonic stator voltages and currents and are thus consistent with our previous assumptions neglecting harmonics produced by discrete windings.

The various machine inductances can then be written in terms of the electrical rotor angle θ (between the rotor direct axis and the stator phase- a axis), using the notation of Art. 5-2, as follows. For the stator self-inductances

$$\mathcal{L}_{aa} = L_{aa0} + L_{al} + L_{g2} \cos 2\theta \quad (6-4)$$

$$\mathcal{L}_{bb} = L_{aa0} + L_{al} + L_{g2} \cos (2\theta + 120^\circ) \quad (6-5)$$

$$\mathcal{L}_{cc} = L_{aa0} + L_{al} + L_{g2} \cos (2\theta - 120^\circ) \quad (6-6)$$

For the stator-to-stator mutual inductances

$$\mathcal{L}_{ab} = \mathcal{L}_{ba} = -\frac{1}{2}L_{aa0} + L_{g2} \cos (2\theta - 120^\circ) \quad (6-7)$$

$$\mathcal{L}_{bc} = \mathcal{L}_{cb} = -\frac{1}{2}L_{aa0} + L_{g2} \cos 2\theta \quad (6-8)$$

$$\mathcal{L}_{ac} = \mathcal{L}_{ca} = -\frac{1}{2}L_{aa0} + L_{g2} \cos (2\theta + 120^\circ) \quad (6-9)$$

For the field-winding self-inductance

$$\mathcal{L}_{ff} = L_{ff} \quad (6-10)$$

and for the stator-to-rotor mutual inductances

$$\mathcal{L}_{af} = \mathcal{L}_{fa} = L_{af} \cos \theta \quad (6-11)$$

$$\mathcal{L}_{bf} = \mathcal{L}_{fb} = L_{af} \cos (\theta - 120^\circ) \quad (6-12)$$

$$\mathcal{L}_{cf} = \mathcal{L}_{fc} = L_{af} \cos (\theta + 120^\circ) \quad (6-13)$$

Comparison with Art. 5-2 shows that the effects of saliency appear only in the stator self- and mutual-inductance terms as an inductance term which varies with 2θ . This twice-angle variation can be understood with reference to Fig. 6-2, where it can be seen that rotation of the rotor through 180° reproduces the original geometry of the magnetic circuit. Notice that the self-inductance of each stator phase is a maximum when the rotor direct axis is aligned with the axis of that phase and that the phase-phase mutual inductance is maximum when the rotor direct axis is aligned midway between the two phases. This is the expected result since the rotor direct axis is the path of lowest reluctance (maximum permeance) for air-gap flux.

The flux-linkage expressions of Eq. 6-3 become much simpler when they are expressed in terms of dq0 variables. This can be done by application of the transformation of Eq. 6-1 to both the flux linkages and the currents of Eq. 6-3. The manipulations are somewhat laborious and are omitted here because they are simply algebraic. The results are

$$\lambda_d = -L_d i_d + L_{af} i_f \quad (6-14)$$

$$\lambda_q = -L_q i_q \quad (6-15)$$

$$\lambda_f = -\frac{3}{2} L_{af} i_d + L_{ff} i_f \quad (6-16)$$

$$\lambda_0 = -L_0 i_0 \quad (6-17)$$

In these equations, new inductance terms appear:

$$L_d = L_{al} + \frac{3}{2}(L_{aa0} + L_{g2}) \quad (6-18)$$

$$L_q = L_{al} + \frac{3}{2}(L_{aa0} - L_{g2}) \quad (6-19)$$

$$L_0 = L_{al} \quad (6-20)$$

The quantities L_d and L_q are the *direct-axis* and *quadrature-axis synchronous inductances*, respectively, as discussed in Art. 5-6. The inductance L_0 is the *zero-sequence inductance*. Notice that the transformed flux-current relationship expressed in Eqs. 6-14 to 6-17 no longer contains inductances which are functions of rotor position. This feature is responsible for the usefulness of the dq0 transformation.

Transformation of the voltage equations (where $p = d/dt$)

$$v_a = -R_a i_a + p\lambda_a \quad (6-21)$$

$$v_b = -R_a i_b + p\lambda_b \quad (6-22)$$

$$v_c = -R_a i_c + p\lambda_c \quad (6-23)$$

$$v_f = R_f i_f + p\lambda_f \quad (6-24)$$

results in

$$v_d = -R_a i_d + p\lambda_d - \omega\lambda_q \quad (6-25)$$

$$v_q = -R_a i_q + p\lambda_q + \omega\lambda_d \quad (6-26)$$

$$v_f = R_f i_f + p\lambda_f \quad (6-27)$$

$$v_0 = -R_a i_0 + p\lambda_0 \quad (6-28)$$

(algebraic details are again omitted), where $\omega = p\theta = d\theta/dt$ is the rotor electrical angular velocity.

In Eqs. 6-25 and 6-26 the terms $\omega\lambda_q$ and $\omega\lambda_d$ are speed-voltage terms which come as a result of the fact that we have chosen to define our variables in a reference frame rotating at angular velocity ω . These speed-voltage terms are directly analogous to the speed-voltage terms found in the dc machine analysis of Chap. 9. In the dc machine the commutator-brush system performs the transformation of transferring armature (rotor) voltages to the field-winding (stator) reference frame.

We now have the basic relations for analysis of our simple synchronous machine. They consist of the flux-current equations 6-14 to 6-17, the voltage equations 6-25 to 6-28, and the transformation equations 6-1 and 6-2. When the machine speed ω is constant, the differential equations are linear with constant coefficients. In addition, the transformer terms $p\lambda_d$ and $p\lambda_q$ in Eqs. 6-25 and 6-26 are often negligible with respect to the speed-voltage terms $\omega\lambda_q$ and $\omega\lambda_d$, providing further simplification. As illustrated later, omission of these terms corresponds to neglecting the harmonics and dc component in the transient solution for stator voltages and currents. In any case, the transformed equations are generally much easier to solve, both analytically and by computer simulation, than the equations expressed directly in terms of phase variables.

In using these equations and the corresponding equations in the machinery literature, careful note should be made of the sign convention and units employed. Here we have chosen the generator convention for armature currents, with positive armature current flowing out of the machine. Also, SI units (volts, amperes, ohms, henrys, etc.) are used here; often in the literature one of several per unit systems is used to provide numerical simplifications.[†]

To complete the basic array, relations for power and torque are needed. The instantaneous power output from the three-phase stator is

[†]See A. W. Rankin, "Per-Unit Impedances of Synchronous Machines," *Trans. AIEE*, 64:569-573, 839-841 (1945).

$$p_s = v_a i_a + v_b i_b + v_c i_c \quad (6-29)$$

Phase quantities can be eliminated from Eq. 6-29 by using Eq. 6-2 written for voltages and currents. The result is[†]

$$p_s = \frac{3}{2}(v_d i_d + v_q i_q + 2v_0 i_0) \quad (6-30)$$

The electromagnetic torque developed, which acts to decelerate the shaft, is readily obtained by using the techniques of Chap. 3 as the power output corresponding to the speed voltages divided by the shaft speed (in mechanical radians per second). From Eq. 6-30 with the speed-voltage terms from 6-25 and 6-26, by recognizing ω as the speed in electrical radians per second, we get

$$T = \frac{3}{2} \frac{\text{poles}}{2} (\lambda_d i_q - \lambda_q i_d) \quad (6-31)$$

The torque of Eq. 6-31 is positive for generator action. This result is in general conformity with torque production from interacting magnetic fields as expressed in Eq. 4-85. In Eq. 6-31 we are superimposing the interaction of components: direct-axis magnetic field with quadrature-axis mmf and quadrature-axis magnetic field with direct-axis mmf. For both interactions the sine of the space-displacement angle has unity magnitude. Again the use of the dq0 transformation leads to a compact result which can be related to our earlier work.

6-4 ANALYSIS OF A SUDDEN THREE-PHASE SHORT CIRCUIT

To demonstrate the application of the dq0 transformation and to begin to develop an understanding of the transient behavior of synchronous machines, it is useful to analyze the transient following a sudden three-phase short circuit at the armature terminals. The machine is assumed to be initially unloaded and to continue operating at synchronous speed ω after the short circuit occurs. Since the short circuit is balanced, zero-sequence quantities do not appear. For the purposes of this analysis, the only rotor circuit to be considered is a field winding, and hence the machine can be described by Eqs. 6-14 to 6-16 and 6-25 to 6-27.

a. Physical Description of the Transient

Before we investigate the analytical solution to this problem, it is useful to start with a physical description of the transient. Since the machine is ini-

[†]See footnote on page 270.

tially unloaded, the only predisturbance current flowing in the machine is the field current. Each armature phase sees a resultant time-varying flux linkage as the rotor rotates.

The situation changes radically upon application of the three-phase short circuit. Currents now flow in the armature windings in such a fashion as to maintain the armature winding flux linkages at the value they had at the time of the short circuit. There are two components of these currents. One is an ac component, corresponding to the armature current required to oppose the time-varying flux produced by the field winding as it rotates. The other is a dc component, corresponding to the initial flux linkage which existed at the time of the short circuit. The net result of these currents is an armature flux linkage which is fixed in space, each armature phase holding constant its own portion of the initial armature flux linkage.

A similar situation occurs on the field winding. It is now rotating in a stationary trapped armature-flux wave and hence must respond with an alternating component of field current to oppose the tendency of this trapped armature flux to change the field-winding flux linkages. In addition, there must be an induced dc component of field current to oppose the synchronously rotating component of flux created by the ac components of armature current, which, to oppose the tendency of the rotating-field flux to change the armature flux linkages, in turn create a rotating flux which attempts to demagnetize (reduce) the flux created by the field winding.

Quite clearly, all these things happen simultaneously, and it is difficult to give a description in terms of cause and effect. However, it is possible to recognize that during this transient, alternating currents in the stator correspond to direct currents on the rotor and vice versa. It should also be clear that these conditions do not remain indefinitely. Resistance in the armature and field windings means that the transient direct currents tend to decay since there is no source to drive them. As a result, the direct armature current and the corresponding alternating field current decay with a time constant determined by the armature resistance R_a . Similarly, the transient direct field current and corresponding transient ac component of armature current decay with a time constant determined by the field resistance R_f .

Figure 6-3 shows the waveforms of the three phase currents and the field current following a sudden three-phase short circuit. In the armature current waveform, the amount of direct current offset in each phase is determined by the flux in that phase at the time of the short circuit. The armature currents are balanced, and thus, like the ac components, the dc components sum to zero at any given instant. The ac component of field current is due to the dc component of armature current and decays at the same rate, determined by the armature resistance. The transient dc component of field current and the corresponding transient ac component of armature current decay together at a rate determined by the field-winding resistance.

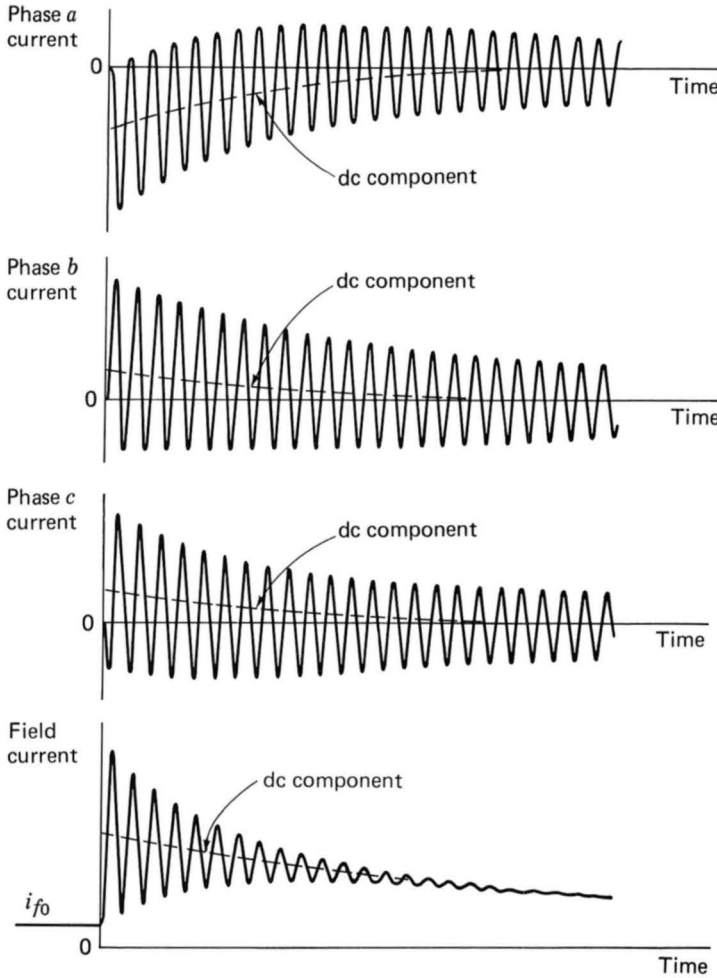


Fig. 6-3. Armature and field currents following a sudden short circuit on an initially unloaded synchronous machine.

b. Armature and Field Resistances Neglected

An analysis based on the assumption that the armature and field resistances are negligibly small will result in a transient similar to that discussed above. However, the dc components of armature and field current will not decay with time. The basic machine equations under these conditions become

$$\lambda_f = L_{ff}i_f - \frac{3}{2}L_{af}i_d \quad (6-32)$$

$$\lambda_d = L_{af}i_f - L_d i_d \quad (6-33)$$

$$\lambda_q = -L_q i_q \quad (6-34)$$

$$v_d = p\lambda_d - \lambda_q \omega \quad (6-35)$$

$$v_q = p\lambda_q + \lambda_d \omega \quad (6-36)$$

$$v_f = p\lambda_f \quad (6-37)$$

Currents i_d and i_q are initially zero, and i_f is initially I_{f0} .

It is now necessary to represent the short circuit in mathematical form. This can be done by noting its effect on the machine voltages. Both before and after the short circuit

$$v_d = 0 \quad (6-38)$$

Hence the short circuit has no effect on v_d . The voltage v_q , however, is $\omega L_{af} I_{f0}$ before the short circuit and zero afterward. Since the short circuit causes v_q to vanish suddenly, its effect can be found by suddenly impressing on the machine the voltage

$$v_q = -\omega L_{af} I_{f0} \quad (6-39)$$

The transient currents found in this way must be added to the initial values of the currents existing before the short circuit to obtain the resultant currents after the short circuit.

The response to the voltage of Eq. 6-39 must be the response for this voltage alone, not for the combined effect of this voltage and the initial excitation. Accordingly, the response must be evaluated with the field winding considered closed and initially unexcited, i.e., with

$$v_f = 0 \quad (6-40)$$

The subscript t (for transient) will be added to the symbols i_f , λ_f , λ_d , and λ_q to denote the values under these conditions. Then the true initial values are added, as in

$$i_f = I_{f0} + i_{ft} \quad (6-41)$$

to find the resultant quantities after the short circuit, thereby superimposing the effect of the true initial excitation. No added subscripts are necessary for i_d and i_q because their initial values are obviously zero for an unloaded machine.

From Eqs. 6-37 and 6-40 we see that the field-winding linkages λ_{ft} must be zero. In other words, with R_f neglected, the field-winding flux linkages λ_f cannot change. This is a specific case of what is sometimes called the *principle of constant flux linkages*, which simply states that the flux linkages of a closed circuit having zero resistance and no voltage source cannot change. To maintain field linkages constant, a current must

be induced in the field winding to counteract the magnetic effects of i_d . From Eq. 6-32, with $\lambda_f = 0$, this current is

$$i_{ft} = + \frac{3}{2} \frac{L_{af}}{L_{ff}} i_d \quad (6-42)$$

Upon substitution of Eq. 6-42 in 6-33,

$$\lambda_{dt} = - \left(L_d - \frac{3}{2} \frac{L_{af}^2}{L_{ff}} \right) i_d \quad (6-43)$$

$$= -L'_d i_d \quad (6-44)$$

where

$$L'_d = L_d - \frac{3}{2} \frac{L_{af}^2}{L_{ff}} \quad (6-45)$$

is the *direct-axis transient inductance*. As we shall see, it is an important constant in machine-transient theory.

The transient inductance of the armature winding can be interpreted in a physical fashion which offers further insight into the behavior of coupled magnetic circuits and electric machinery. Specifically, the armature winding and field windings share a common flux linkage (due to mutual flux). As a result, under conditions where the field winding is trapping flux, a certain fraction of the armature flux linkages are also trapped and held fixed by the field winding. This means that a change in armature current will result in a smaller change in armature flux linkage than would normally be the case under slowly varying conditions. Hence, since the apparent armature inductance is equal to the ratio of the change in armature flux linkage to the corresponding change in armature current, we see that the apparent inductance of the armature L'_d is smaller than the steady-state value L_d .

The specific values of voltages v_d and v_q are now introduced. From Eqs. 6-34 and 6-35, with $v_d = 0$,

$$0 = p\lambda_{dt} + \omega L_q i_q \quad (6-46)$$

or, after Eq. 6-44 is used to obtain $p\lambda_{dt}$,

$$0 = -L'_d p i_d + \omega L_q i_q \quad (6-47)$$

Similarly, from Eqs. 6-36 and 6-39

$$-\omega L_{af} I_{f0} = p\lambda_q + \lambda_d \omega \quad (6-48)$$

which, with Eqs. 6-34 and 6-44, becomes

$$\omega L_{af} I_{f0} = L_q p i_q + \omega L'_d i_d \quad (6-49)$$

Equations 6-47 and 6-49 are two simultaneous equations in i_d and i_q . With i_q eliminated and the resulting equation written in differential equation form, we have

$$\frac{d^2 i_d}{dt^2} + \omega^2 i_d = \frac{\omega^2}{L'_d} L_{af} I_{f0} \quad (6-50)$$

The solution of Eq. 6-50 is

$$i_d = \frac{L_{af} I_{f0}}{L'_d} (1 - \cos \omega t) \quad (6-51)$$

From Eq. 6-47

$$i_q = \frac{L'_d}{\omega L_q} \frac{di_d}{dt} = \frac{L_{af} I_{f0}}{L_q} \sin \omega t \quad (6-52)$$

From Eqs. 6-41 and 6-42

$$i_f = I_{f0} + \frac{3}{2} \frac{L_{af}}{L_{ff}} \frac{L_{af} I_{f0}}{L'_d} (1 - \cos \omega t) \quad (6-53)$$

The waveforms of i_d , i_q , and i_f as given by these results are sketched in Fig. 6-4.

Upon substitution in the dq0 transformation (Eq. 6-2), with θ taken as $\omega t + \theta_0$, the phase current is

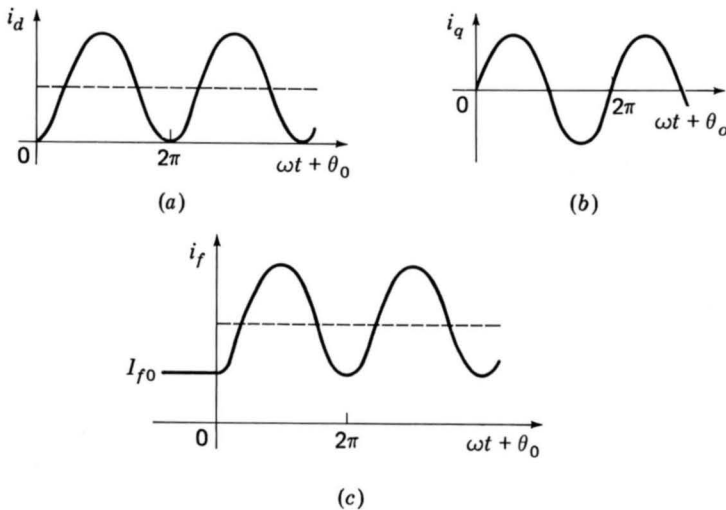


Fig. 6-4. Waveforms of (a) i_d , (b) i_q , and (c) i_f following short circuit. Machine resistances are ignored.

$$i_a = \frac{L_{af}I_{f0}}{L'_d} \cos(\omega t + \theta_0) - \frac{L_{af}I_{f0}}{2} \left(\frac{1}{L'_d} + \frac{1}{L_q} \right) \cos \theta_0 \\ - \frac{L_{af}I_{f0}}{2} \left(\frac{1}{L'_d} - \frac{1}{L_q} \right) \cos(2\omega t - \theta_0) \quad (6-54)$$

From Eqs. 6-3 and 6-21 the peak value of the prefault armature-voltage magnitude is $\sqrt{2}E_{af0} = \omega L_{af}I_{f0}$. Thus Eq. 6-54 can be rewritten

$$i_a = \frac{\sqrt{2}E_{af0}}{X'_d} \cos(\omega t + \theta_0) - \frac{\sqrt{2}E_{af0}}{2} \left(\frac{1}{X'_d} + \frac{1}{X_q} \right) \cos \theta_0 \\ - \frac{\sqrt{2}E_{af0}}{2} \left(\frac{1}{X'_d} - \frac{1}{X_q} \right) \cos(2\omega t + \theta_0) \quad (6-55)$$

where $X'_d = \omega L'_d$ (6-56)

is the *direct-axis transient reactance*.

The phase current is seen to consist of a fundamental-frequency term, a dc component, and a second-harmonic term. The fundamental component is the most important. Its magnitude depends on the prefault excitation and the transient reactance. The dc term depends on θ_0 and hence on the instant when the short circuit appears. The rotor position θ_0 at the time of the short circuit determines the initial flux linkages of each armature phase; the direct currents flow to maintain these flux linkages. If, for example, the fault occurs at the instant when the direct axis is 90° from the axis of phase *a* and hence when the phase-*a* flux linkages are initially zero, no dc component appears in the phase-*a* current. Even then, dc components do appear in the phase-*b* and phase-*c* currents because of the 120° displacement between phases. The second-harmonic term depends on *transient saliency*, or the differences in transient circuitry in the two rotor axes as represented by the quantity $1/X'_d - 1/X_q$. The second-harmonic amplitude is usually small and often neglected.

Notice that as a result of the transformation from dq0 to phase variables, the dc component of i_d corresponds to the ac component of i_a and the ac components of i_d and i_q correspond to the dc and second-harmonic components of i_a . This is the expected result of a transformation from rotating to fixed-frame variables.

Because the field and armature resistances were neglected, none of the terms in Eqs. 6-51 to 6-55 dies away with time. Actually, exponential decays are encountered, as they are in any inductive circuit when resistance is present. This fact is illustrated in Fig. 6-3, which shows the phase currents with their dc components after a short circuit. Before investigating the rates of decay, however, we wish to simplify our basic relations somewhat. This will be done by showing that neglecting the *transformer voltage terms* $p\lambda_d$ and $p\lambda_q$ in Eqs. 6-35 and 6-36 corresponds to eliminating the dc and second-harmonic terms from the above solutions.

c. Resistances and Transformer Voltages Neglected

When the $p\lambda_d$ and $p\lambda_q$ terms are omitted from Eqs. 6-35 and 6-36, very simple expressions for the machine currents are obtained:

$$i_d = \frac{L_{af}L_{f0}}{L'_d} \quad (6-57)$$

$$i_q = 0 \quad (6-58)$$

$$i_f = I_{f0} + i_{ft} = I_{f0} + \frac{3}{2} \frac{L_{af}}{L_{ff}} \frac{L_{af}I_{f0}}{L'_d} \quad (6-59)$$

Substitution in the dq0 transformation (Eq. 6-2) and use of Eq. 6-56 give

$$i_a = \frac{\sqrt{2}E_{af0}}{X'_d} \cos(\omega t + \theta_0) \quad (6-60)$$

The dc and second-harmonic terms have now dropped out of the phase current, as have the fundamental-frequency terms in i_d , i_q , and i_f . Currents i_d and i_f now follow the dashed lines in Fig. 6-4a and c; they have a sudden step at $t = 0$.

Neglect of the second-harmonic and dc components in the phase currents is very common in machine analysis. The former is usually quite small, and the latter dies away very rapidly. Neither has a significant influence on the average torque of the machine for an appreciable time, so that their influence on dynamic performance is relatively small. Accordingly, many machine analyses are carried out with the $p\lambda_d$ and $p\lambda_q$ terms omitted. The advantage is that the resulting equations are much simpler.

d. Field Resistance Included, Transformer Voltages Neglected

We now wish to investigate the decay of currents i_d and i_{ft} of Eqs. 6-57 and 6-59. To do so, we follow substantially the approach of part b of this article except that the $p\lambda_d$ and $p\lambda_q$ terms are omitted but the $R_f i_{ft}$ term is retained in Eq. 6-27. Again,

$$i_q = 0 \quad (6-61)$$

The equation followed by the induced field current i_{ft} becomes

$$\frac{L_{ff}}{L_d} \left(L_d - \frac{3}{2} \frac{L_{af}^2}{L_{ff}} \right) \frac{di_{ft}}{dt} + R_f i_{ft} = 0 \quad (6-62)$$

or, by using Eq. 6-45 and dividing through by R_f ,

$$\frac{L_{ff}}{R_f} \frac{L'_d}{L_d} \frac{di_{ft}}{dt} + i_{ft} = 0 \quad (6-63)$$

Now the fraction

$$\frac{L_{ff}}{R_f} = T'_{d0} \quad (6-64)$$

is the open-circuit time constant of the field winding. (The symbol T is used for time constant in this chapter to conform with standard notation. Elsewhere the symbol τ is used; however, there is practically no possibility of confusion with torque here.) It is called the *direct-axis open-circuit transient time constant*.[†] It characterizes the decay of transients with the armature open-circuited.[†] With the armature short-circuited, however, the apparent field inductance is lower because of coupling to the armature winding. From Eq. 6-63 the time constant is then

$$T'_d = T'_{d0} \frac{L'_d}{L_d} = T'_{d0} \frac{X'_d}{X_d} \quad (6-65)$$

and is called the *direct-axis short-circuit transient time constant*. Both T'_{d0} and T'_d are important constants of the synchronous machine. Typical values for large machines are about 5 s for T'_{d0} and 1 to 2 s for T'_d .

Equation 6-63 can then be written

$$T'_d \frac{di_{ft}}{dt} + i_{ft} = 0 \quad (6-66)$$

Similarly, for current i_d

$$T'_d \frac{di_d}{dt} + i_d = \frac{L_{af} L_{f0}}{L_d} \quad (6-67)$$

Currents i_d and i_f become, subject to their being given by Eqs. 6-57 and 6-59 immediately prior to the application of the short circuit at time $t = 0$,

$$i_d = \frac{L_{af} I_{f0}}{L_d} + L_{af} I_{f0} \left(\frac{1}{L'_d} - \frac{1}{L_d} \right) e^{-t/T'_d} \quad (6-68)$$

$$i_f = I_{f0} + \frac{3}{2} \frac{L_{af}}{L_{ff}} \frac{L_{af} I_{f0}}{L'_d} e^{-t/T'_d} \quad (6-69)$$

[†]The formal definition of the direct-axis open-circuit transient time constant T'_{d0} is the longest time constant associated with rotor transients when the armature is open-circuited. In practical machines with additional conducting paths in the rotor, this time constant will be somewhat modified from that determined simply by the inductance-to-resistance ratio of the field winding given in Eq. 6-64. A similar comment applies for the short-circuit transient time constant of Eq. 6-65. This is discussed further in Art. 6-6.

Finally, the phase current is

$$i_a = \frac{\sqrt{2}E_{af0}}{X_d} \cos(\omega t + \theta_0) + \sqrt{2}E_{af0} \left(\frac{1}{X'_d} - \frac{1}{X_d} \right) e^{-t/T'_d} \cos(\omega t + \theta_0) \quad (6-70)$$

The first term on the right in Eq. 6-70 is the steady-state short-circuit current. The second is the transient term. The phase current is a damped sinusoid. Its initial amplitude is limited by the transient reactance X'_d and its final amplitude by the synchronous reactance X_d . It passes from one to the other exponentially as determined by the time constant T'_d .

The machine-current solutions obtained in this article can be readily adapted to include the external reactance X_e between the machine terminals and the short circuit. Such external reactance merely plays the same role as the armature leakage reactance ωL_{al} , which is a component of X_d , X'_d , and X_q . All that need be done is to add X_e to X_d , X'_d , and X_q wherever they appear (or the corresponding inductance L_e to L_d , L'_d , and L_q). The results are thus made more widely applicable.

To summarize the results of this article, note first that we avoid a frontal attack on the basic machine equations with all terms retained. We do so to avoid complex and cumbersome analysis in which it would be difficult to distinguish between the important and the unimportant. By comparison of the results of parts *b* and *c* of the article, we find the neglect of the $p\lambda_d$ and $p\lambda_q$ terms to be an admissible approximation in most cases. In part *d* we adopt this approximation and investigate how the transients die away. The results are quite simple, and we have established valuable guides to the conduct of other machine-transient analyses. Due to the presence of additional rotor circuits (see Art. 6-6) the transient behavior of actual machines is more complex than the single time-constant behavior described by Eqs. 6-68 to 6-70. However, in many cases a single-time-constant representation will constitute a useful approximation.

6-5 TRANSIENT POWER-ANGLE CHARACTERISTICS

It can be seen from Art. 6-4 that in the first instant following a transient disturbance in the armature circuit of a synchronous machine, the total field linkage λ_f remains constant at its value before the disturbance. Thereafter, in the absence of voltage regulator action, λ_f decays to a new steady-state value. The time constant of the decay is an appropriately adjusted value of the direct-axis open-circuit transient time constant T'_{d0} . For periods of time which are short compared with this time constant, the decrement in field linkages may be neglected. This approximation leads to a simplified representation of the machine which is especially useful in investigating dynamic problems.

The field and direct-axis armature linkages are, from Eqs. 6-14 and 6-16,

$$\lambda_f = L_{ff}i_f - \frac{3}{2}L_{af}i_d \quad (6-71)$$

$$\lambda_d = L_{af}i_f - L_d i_d \quad (6-72)$$

Solving Eq. 6-72 for i_f and substituting in 6-71 give

$$\lambda_f = \frac{L_{ff}}{L_{af}} (\lambda_d + L_d i_d) - \frac{3}{2}L_{af}i_f \quad (6-73)$$

$$\text{or} \quad \frac{L_{af}}{L_{ff}} \lambda_f = \lambda_d + \left(L_d - \frac{3}{2} \frac{L_{af}^2}{L_{ff}} \right) i_d \quad (6-74)$$

$$\frac{L_{af}}{L_{ff}} \lambda_f = \lambda_d + L_d' i_d \quad (6-75)$$

where Eq. 6-45 is used for the transient inductance L_d' . When both sides of Eq. 6-75 are multiplied by ω , we have

$$\omega \frac{L_{af}}{L_{ff}} \lambda_f = \omega \lambda_d + X_d' i_d \quad (6-76)$$

In terms of rms values

$$E_q' = V_q + X_d' i_d \quad (6-77)$$

$$\text{where} \quad E_q' = \omega \frac{L_{af}}{L_{ff}} \frac{\lambda_f}{\sqrt{2}} \quad (6-78)$$

and V_q is written by virtue of Eq. 6-26 with the resistance omitted and the $p\lambda_q$ term ignored.

The voltage E_q' , being directly proportional to λ_f , is constant whenever field flux linkages can be considered constant. It is shown on a phasor diagram in Fig. 6-5. If now the analysis in Art. 5-7 leading to Eq. 5-56 is repeated with E_q' and X_{dT}' replacing E_{af} and X_{dT} , the result is

$$P = \frac{E_q' E_e}{X_{dT}'} \sin \delta + E_e^2 \frac{X_{dT}' - X_{qT}'}{2X_{dT}' X_{qT}'} \sin 2\delta \quad (6-79)$$

$$\text{where} \quad X_{dT}' = X_d' + X_e \quad (6-80)$$

$$\text{and} \quad X_{qT}' = X_q + X_e \quad (6-81)$$

We now have in Eq. 6-79 a power-angle expression which is useful in the analysis of sudden disturbances or of sudden load application. It is applicable only over a period of time short compared with the time constant T_{d0}' ,

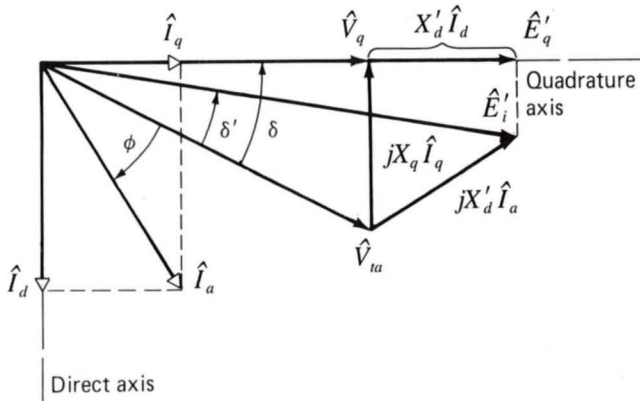


Fig. 6-5. Phasor diagram showing \hat{E}'_q .

but this covers the critical period in many dynamic analyses. However, the steady-state power-angle expression (Eq. 5-56) is applicable during changes which are sufficiently slow for the machine to be always in the steady state. Note that the coefficient of the second term on the right of Eq. 6-79 often is numerically negative because X_q for a normal machine is greater than X'_d (and hence $X_{qT} > X'_{dT}$).

The transient power-angle curve will have an amplitude significantly greater than that of the steady-state curve. The relative amplitudes in a specific instance can be seen in Fig. 6-6. The suddenly induced component of field current following a disturbance is the physical reason for the greater transient amplitude. The practical consequence is that the machine is a stiffer system element in the transient state; e.g., it can withstand a large, suddenly applied power or torque overload if the duration of the overload is relatively short.

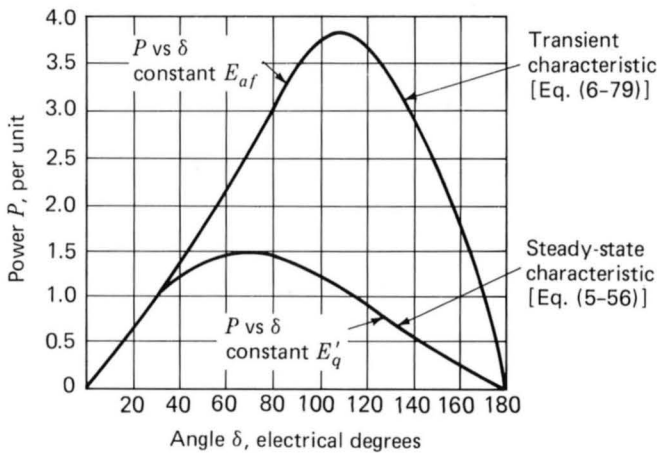


Fig. 6-6. Transient and steady-state power-angle curves.

The assumption of constant field-winding flux linkages[†] results in the transient power-angle characteristic of Fig. 6-6. In fact, as discussed in Arts. 6-6 and 6-7, there are additional current-carrying elements in the rotor. In the case of salient-pole machines with laminated rotor construction, these elements consist of bar or cage windings connected together at their ends. In the case of solid-rotor machines, current paths exist naturally in the rotor body.

Much as does the field winding, under transient conditions these windings also trap flux for a time following the onset of the transient. Thus in addition to transient flux trapped in the direct axis by the field winding, there will be flux trapping by current-carrying elements in the quadrature axis. The time constant associated with the decay of the quadrature-axis transient flux typically is significantly shorter than that of the field winding because these quadrature-axis circuits have a shorter time constant than that of the field winding.

As a result, a detailed analysis of the transient behavior of these machines is more complex than for the trapped-field-winding-flux model presented here which results in the transient power-angle characteristic of Fig. 6-6. Such an analysis is best performed by using the more detailed models discussed briefly in Art. 6-7 in which additional rotor circuits are explicitly represented. Although such models are difficult to solve analytically, they can be readily solved numerically in digital computer simulations and thus are commonly used in the analysis of synchronous-machine transient behavior.

The recognition that both the direct and quadrature axes trap flux can be used to motivate a transient representation which is even simpler than the trapped-field-winding-flux model. This representation is based on the net rotor flux remaining trapped, with each axis trapping its own fraction of the flux. To simplify matters, it is assumed that transient saliency can be neglected and that under these conditions a single transient reactance (equal to the direct-axis transient reactance X'_d) can be associated with each axis.

Neglecting transient saliency permits this representation to use the cylindrical-rotor theory of Art. 5-4. In this case, the transient model becomes that of a constant voltage source E'_i in series with the direct-axis transient reactance X'_d . This model, known as the *constant-voltage-behind-transient-reactance model*, is shown in Fig. 6-7. Note that the voltage \hat{E}'_i can be found from a knowledge of the pretransient terminal voltage and current:

$$\hat{E}'_i = \hat{V}_{ta} + jX'_d \hat{I}_a \quad (6-82)$$

This voltage is shown in the phasor diagram of Fig. 6-5. Note that it is lo-

[†]During the period when the flux linkages of a winding remain essentially constant, it is customary to say that the winding is *trapping flux*.

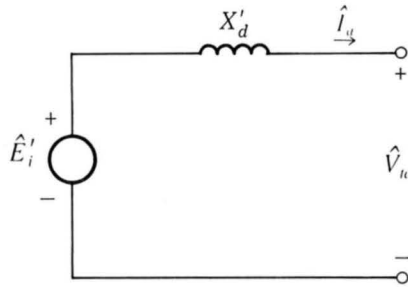


Fig. 6-7. Approximate transient equivalent circuit for a synchronous machine.

cated at an angle δ' (known as the *transient power angle*) with respect to the terminal voltage and that this angle is smaller than the angle δ .

The transient power-angle characteristic of this model can be written by direct analogy with Eq. 5-42 (using the notation of Eq. 6-79) as

$$P = \frac{E'_i E_e}{X'_{dT}} \sin \delta' \quad (6-83)$$

Corresponding to Eq. 6-79, this equation has been written to include the effects of an external system; E_e is its voltage magnitude, X'_{dT} is given by Eq. 6-80, and δ' now is the angle between \hat{E}_e and \hat{E}'_i . Note that this equation is simpler than Eq. 6-79. However, there is not a direct correspondence between these equations because Eq. 6-79 is expressed in terms of the power angle δ and Eq. 6-83 is expressed in terms of the transient power angle δ' .[†]

The validity of this model is severely limited by the approximations upon which it is based, including the assumption that transient saliency is negligible and the corresponding assumption that the time constants associated with the decay of transient flux are of similar magnitudes in both axes. As a result, it no longer sees widespread use in detailed analyses of complex multimachine systems performed on digital computers where more detailed models can be readily implemented. However, it may still be used in such studies to represent machines whose dynamics play only a minor role in the problem under study. In addition, it remains an invaluable tool to the engineer for use in "back-of-the-envelope" calculations.

6-6 EFFECTS OF ADDITIONAL ROTOR CIRCUITS

Up to this point we have considered that the only current-carrying element on the rotor is the field winding on the direct axis. As a result, we have

[†]Note that the assumption of trapped flux means that E'_i is fixed both in magnitude and in angular position with respect to the rotor. As a result, the angle between δ and δ' remains constant, and it is thus a relatively simple matter to calculate the transient behavior of δ based on a transient analysis in terms of δ' .

been able to concentrate on the most important aspects of machine performance without distracting algebraic complications. This permitted us to derive relatively simple expressions for the machine transient currents in Art. 6-5.

In most synchronous machines, there are a number of additional paths in the rotor in which induced currents can flow. In salient-pole machines with laminated rotor construction, which does not permit current to flow in the rotor body, these additional paths are formed by bar or cage windings embedded in the pole faces and connected at their ends by short-circuiting end rings. These are commonly called *damper*, or *amortisseur circuits*. They are specifically included by the machine designer to produce damping torques following electromechanical transients and starting torques for synchronous motors. Still, additional conducting paths may be formed by the bolts and iron of the rotor structure.

In cylindrical-rotor machines which are formed from solid-steel forgings, transient rotor currents can be induced in the solid-rotor body. Although the current paths are not as well defined as in the damper circuits of salient-pole machines, their effects are quite similar and can be represented in a similar fashion. In fact, induced currents in cylindrical-rotor machines are commonly referred to as *damper currents* in keeping with the nomenclature developed for salient-pole machines.

In this section, the effects of induced rotor currents are discussed in a qualitative fashion. Article 6-7 discusses techniques for modeling these currents.

a. Effects on Current-Voltage Relations

In Art. 6-4, the principle of constant flux linkages is described as stating that a closed conducting circuit with zero resistance and no applied voltage must maintain constant flux linkage. If an externally applied magnetic flux distribution attempts to change the flux linkage of this circuit, a current will be induced of sufficient magnitude to oppose this change.

With the exception of closed loops of superconducting wire, normal conducting paths do not have zero resistance and hence cannot maintain their flux linkages indefinitely. However, the principle of constant flux linkages can be applied to these situations with the following modification: *The flux linkage of any closed conduction path with finite resistance cannot change instantaneously.* Furthermore, this flux linkage can be considered to remain essentially constant for times short compared with an appropriate L/R time constant associated with that conducting path (and perhaps additional paths with which it is magnetically coupled).

Based on this principle, we can see how the transient analyses of Art. 6-4 can be extended to include the effects of additional conducting paths in the rotor. In Art. 6-4d, we saw that the effect of trapped flux in the rotor circuit was to decrease the apparent inductance of the armature winding to a value known as the direct-axis transient inductance L'_d . This

is due to the fact that part of the armature flux is common with the trapped field flux and hence cannot be affected by changes in the armature current. Since the apparent inductance of the armature is given by the ratio of the change in armature flux linkages to the change in armature current, the net effect is a reduction in the apparent armature inductance during the period that the field winding traps flux. As the trapped flux in the field winding decays with a time constant known as the direct-axis short-circuit transient time constant T'_d , the apparent armature inductance in turn increases toward its steady-state value L_d .

The phenomenon associated with additional rotor circuits is based on exactly the same principles discussed above for the case of the field winding alone. Each additional rotor circuit tends to trap flux (a portion of which couples to the armature), and this flux in turn decays with a time constant related to the resistance of that circuit and an inductance associated with that circuit and its coupling to the remaining circuits in the machine.

Although in a solid-rotor structure such as a cylindrical-rotor machine there are, in effect, an infinite number of additional rotor circuits associated with the solid-rotor forging, as a practical matter transient phenomena in these machines can be described in terms of the field winding and one or two additional apparent rotor windings on each of the direct and quadrature axes of the rotor. This corresponds quite well to the system of damper windings in salient-pole machines, and hence it is common to employ the same analytical techniques for both types of machines.

If the analysis of Art. 6-4b (in which resistance and hence all flux decay were neglected) were repeated with a single damper circuit included on each of the rotor direct and quadrature axes, two additional equations would appear to express the damper-winding flux linkages and two further equations would be needed to express the fact that the damper windings are short-circuited and hence their terminal voltages are zero. In addition, the flux-current relationships would appear slightly more complex than those of Eqs. 6-32 to 6-34 because there is coupling between all the windings on each axis.

The resulting phase current would be the same as in Eq. 6-55 except that because the direct-axis damper winding traps additional flux, the apparent armature inductance would be smaller than that with field-winding trapped flux alone. As a result, reactances X'_d and X'_q of Eq. 6-55 would be replaced by the reactances X''_d and X''_q , representing the new apparent transformed armature inductances including the effects of damper-winding trapped fluxes. The reactance X''_d is known as the *direct-axis subtransient reactance*, and X''_q is known as the *quadrature-axis subtransient reactance*.

Typically, because the damper circuits have relatively high resistance, the induced damper currents die out rapidly. After a few cycles, these currents have decayed, leaving only the field-winding trapping flux (and perhaps an additional longer-time-constant conducting path on the rotor quadrature axis). At this time, the analysis of Art. 6-4 describes the re-

maining armature current transient.[†] This is illustrated in Fig. 6-8, which shows a symmetric trace of a short-circuit waveform (with the dc component absent or taken out) such as might be obtained on an oscillograph, a storage scope, or a data acquisition system following the sudden application of an armature short circuit. The waveform, whose envelope is shown in Fig. 6-9, can be divided into three periods, or time regimes: the *subtransient period*, lasting only for the first few cycles, during which the current decrement is very rapid; the *transient period*, covering a relatively longer time, during which the current decrement is more moderate; and, finally, the *steady-state period*.

As we have seen, during the subtransient period, both the damper circuits and the field winding are trapping flux. As the induced damper currents decay, only transient field current remains, corresponding to the transient period. The fundamental-frequency component of armature current following the sudden application of a short circuit to the armature of an initially unloaded machine can then be expressed similar to Eq. 6-70 as

$$i_a = \frac{\sqrt{2}E_{af0}}{X_d} \cos(\omega t + \theta_0) + \sqrt{2}E_{af0} \left(\frac{1}{X'_d} - \frac{1}{X_d} \right) \varepsilon^{-t/T'_d} \cos(\omega t + \theta_0) \\ + \sqrt{2}E_{af0} \left(\frac{1}{X''_d} - \frac{1}{X'_d} \right) \varepsilon^{-t/T''_d} \cos(\omega t + \theta_0) \quad (6-84)$$

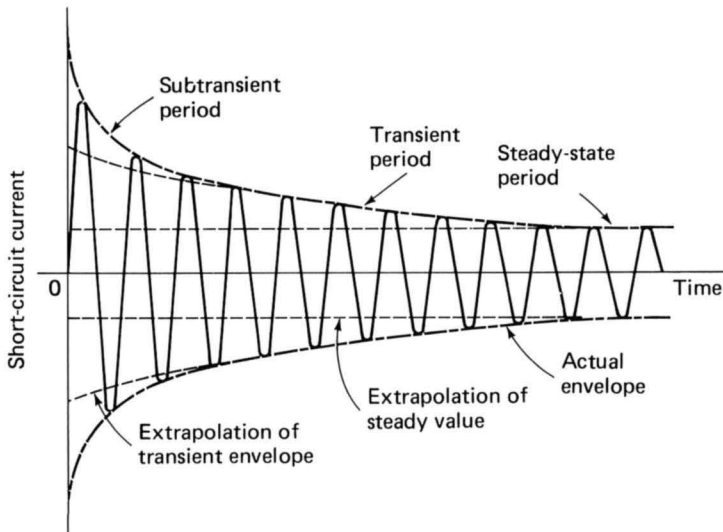


Fig. 6-8. Symmetric trace of armature short-circuit current in a synchronous machine.

[†]For a detailed analysis, including the effects of damper circuits, see B. Adkins and R. G. Harley, *The General Theory of Alternating Current Machines: Applications to Practical Problems*, Chapman and Hall, London, 1975 (distributed in the United States by Halsted Press, a division of Wiley, New York); also C. Concordia, *Synchronous Machines: Theory and Practice*, Wiley, New York, 1951.

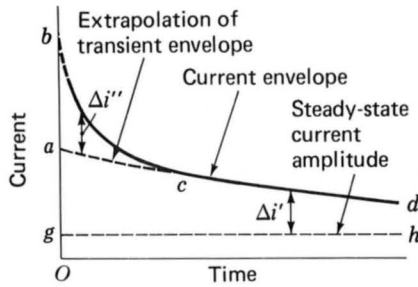


Fig. 6-9. Envelope of a synchronous-machine symmetric short-circuit current.

where T_d'' is the *direct-axis short-circuit subtransient time constant*.

As shown in Art. 6-4b, there will also be dc and second-harmonic components in the armature current following a sudden short circuit, corresponding to the decay of trapped armature flux. These components do not appear in analyses which neglect the transformer voltage terms $p\lambda_d$ and $p\lambda_q$.

It should be emphasized that, especially in the case of solid-rotor generators, the representation of induced direct-axis rotor-body currents by a single equivalent damper circuit is an approximation to the actual situation in which there are a number of conducting paths. However, this approximation has been found to be quite valid in many cases and is generally used to describe machine behavior. This is discussed further in Art. 6-7. Thus, following a three-phase short circuit from open-circuit conditions, the armature current can be shown to be of the form of Eq. 6-82 by appropriate semilogarithmic plots. The difference $\Delta i'$ (Fig. 6-9) between the transient envelope and the steady-state amplitude is plotted to a logarithmic scale as a function of time in Fig. 6-10. In similar fashion, the difference $\Delta i''$ between the subtransient envelope and an extrapolation of the transient envelope is plotted in Fig. 6-10. When the work is done carefully, both plots closely approximate straight lines, illustrating the essentially exponential nature of the decrement.

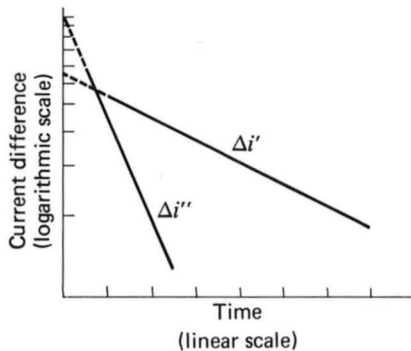


Fig. 6-10. Current differences plotted on semilogarithmic coordinates.

The subtransient reactance X_d'' determines the initial value Ob of the symmetric subtransient envelope bc (Fig. 6-9); X_d'' is equal to the rms value of the prefault open-circuit phase voltage divided by $Ob/\sqrt{2}$, the factor $\sqrt{2}$ appearing because bc is the envelope of peak current values. The time constant T_d'' determines the decay of the subtransient envelope bc ; it is equal to the time required for the envelope to decay to the point where the difference between it and the transient envelope acd is $1/\varepsilon$, or 0.368 times the initial difference ab .

Under the assumption of negligible transformer voltages, the short-circuit oscillogram (Fig. 6-8) of an unloaded machine involves only direct-axis quantities. In a more general case, such as that of a machine with an initial real-power loading, a comparable set of quadrature-axis constants must be available. In addition to X_q and X_q'' these include the *quadrature-axis short-circuit subtransient time constant* T_q'' , the *quadrature-axis transient reactance* X_q' , and the *quadrature-axis short-circuit transient time constant* T_q' . Typical values of synchronous-machine reactances and time constants are given in Table 6-1.[†]

These constants enter into the initial magnitude and decay of quadrature current i_q in the same manner as the direct-axis constants do for i_d . When X_q , X_q' , and X_q'' all have different values, the implication is that there are two equivalent quadrature-axis rotor circuits. The induced currents in one are decremented at an appreciably slower rate than in the other. Greater insight into the effects of damper circuits will be gained during the study of induction machines in the next two chapters.

[†]For a detailed description of standard techniques for measuring and evaluating synchronous-machine transient parameters, see *IEEE Guide: Test Procedures for Synchronous Machines*, IEEE Std. 115-1983, Institute of Electrical and Electronics Engineers, New York, 1983.

TABLE 6-1
TYPICAL VALUES OF MACHINE CONSTANTS*

Machine constant	Generators		Synchronous condensers	Salient-pole motors	
	Solid-rotor	Salient-pole		Low-speed	High-speed
X_d	1.9	1.7	2.2	1.5	1.4
X_d'	0.25	0.30	0.50	0.40	0.35
X_d''	0.20	0.18	0.30	0.25	0.20
X_q	1.85	1.0	1.3	1.0	1.0
X_q'	0.50	1.0	1.3	1.0	1.0
X_q''	0.20	0.25	0.35	0.30	0.25
T_d	0.55	0.50	1.5	0.35	0.50
T_d''	0.02	0.02	0.03	0.01	0.01
T_a	0.17	0.05	0.25	0.04	0.04

*Reactances are per unit values based on the machine rating; time constants are in seconds.

b. Effects on Power and Torque

Damper bars form the starting winding for synchronous motors. The principal reason for installing them in generators is, as their name implies, to produce torques which help to damp out oscillations of the machine rotor about its equilibrium position following transient disturbances. When the speed of the rotor departs from synchronous speed, currents are induced in the damper circuits which produce induction-motor torques, as discussed in some detail in Chap. 7. It is sufficient for present purposes to state that their magnitude is approximately proportional to the departure of rotor speed from synchronous speed as long as that departure is small. The torques produce damping because they act to decelerate the rotor when the rotor speed is above synchronous speed and accelerate the rotor when its speed is less than synchronous speed.

A detailed analysis of synchronous-machine dynamics must include the effects of both synchronous and asynchronous (induction-motor) torques. Clearly the effects of these additional rotor circuits must be included. This can be done by representing them explicitly (see Art. 6-7) or approximately by including a term in the torque equation proportional to the deviation of the rotor speed from synchronous speed (Art. 6-8).

6-7 MODELS OF SYNCHRONOUS MACHINES FOR TRANSIENT ANALYSES

Depending on the type of analysis and the capability of the analysis program being used, a variety of representations can be utilized for synchronous-machine transient behavior. Among the simplest models is that shown in Fig. 6-7, in which transient saliency is ignored and the machine is represented by a constant voltage E'_i behind transient reactance X'_d .

Based on this model, the transient power-angle characteristic is given by Eq. 6-83, where it is assumed that the machine is connected to a system which can be represented by a constant voltage E_e in series with a reactance X_e .

The validity of this model is based on two assumptions: (1) During the period of interest (the transient-time period, generally on the order of 0.5 s), both the direct and quadrature axes of the rotor can be assumed to maintain their flux linkages constant at their pretransient values. This is the constant-voltage assumption. (2) The apparent reactances of each axis under this condition are approximately equal. It is this assumption which permits us to neglect transient saliency and to model the machine by a single transient reactance.

Figure 6-11 shows a phasor diagram from which \hat{E}'_i can be found for the general case of an initially loaded synchronous generator. In this figure ϕ_T is the power-factor angle at the generator terminals, and ϕ is the power-factor angle at the external source. Note that the \hat{E}'_i does not lie

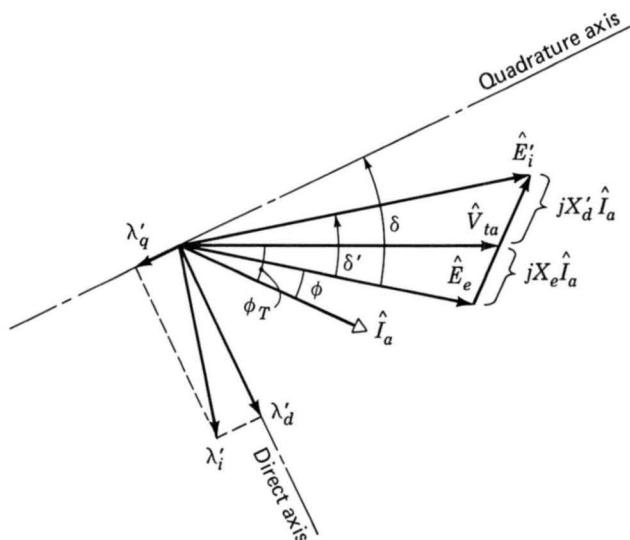


Fig. 6-11. Phasor diagram showing voltage \hat{E}'_i and trapped flux in the direct axis ($\hat{\lambda}'_d$) and quadrature axis ($\hat{\lambda}'_q$).

along the quadrature axis. The phasor diagram shows that the corresponding trapped flux $\hat{\lambda}'_i$ can be resolved into two components. The direct-axis component $\hat{\lambda}'_d$ represents flux trapped by the transient windings on the direct axis, and $\hat{\lambda}'_q$ represents flux trapped by the corresponding circuits on the quadrature axis. Note also that transient power angle δ' is smaller than the steady-state power angle δ and that the assumption of constant rotor flux linkages requires the angle between \hat{E}'_i and the quadrature axis to remain fixed during the transient time period.

EXAMPLE 6-2

The salient-pole generator of Example 5-5 has the parameters (obtained from test data)

$$\begin{aligned}
 X_d &= 1.00 \text{ per unit} & X_q &= 0.60 \text{ per unit} & X'_d &= 0.18 \text{ per unit} \\
 X'_q &= 0.15 \text{ per unit} & T'_{d0} &= 3.0 \text{ s} & T'_{q0} &= 1.6 \text{ s} \\
 T'_d &= 0.52 \text{ s} & T'_q &= 0.43 \text{ s}
 \end{aligned}$$

For the loading of Example 5-5 (rated kilovoltamperes at 0.80 lagging power factor and rated terminal voltage) calculate the steady-state and transient power-angle characteristics, assuming the generator to be connected to an infinite bus directly at its armature terminals.

Solution

With reference to Example 5-5 and Fig. 6-12a,

$$\hat{E}_{af} = 1.77 \angle 19.4^\circ$$

and thus the steady-state power-angle characteristic is (from Eq. 6-52)

$$P = \frac{V_{ta} \hat{E}_{af}}{X_d} \sin \delta + V_{ta}^2 \frac{X_d - X_q}{X_d X_q} \sin 2\delta = 1.77 \sin \delta + 0.67 \sin 2\delta$$

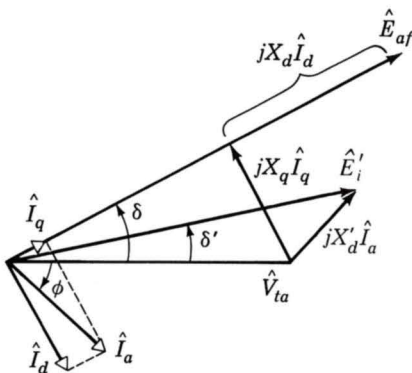
As shown in Fig. 6-12b, the peak of this curve occurs at $\delta = 63.4^\circ$ and has magnitude $P_{\max} = 2.12$ per unit.

The transient power-angle characteristic can be found from Eq. 6-83 under the assumption that transient saliency can be neglected and the generator represented simply as a voltage \hat{E}'_i behind transient reactance X'_d . This assumption is reasonable in this case both because the direct- and quadrature-axis transient reactances are approximately equal and because their time constants are both reasonably long.

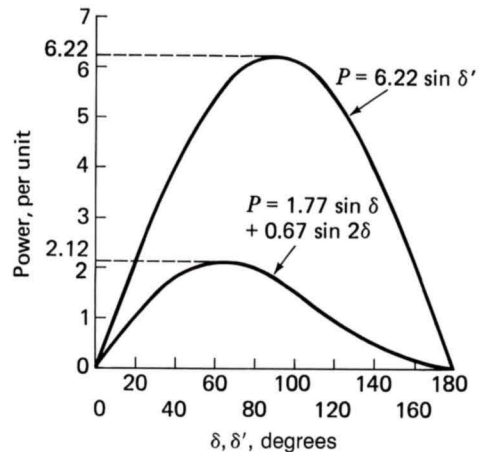
From Eq. 6-83

$$P = \frac{V_{ta} \hat{E}'_i}{X'_d} \sin \delta'$$

and from Fig. 6-12a with $\hat{I}_a = 0.80 - j0.60$,



(a)



(b)

Fig. 6-12. Example 6-2: (a) generator phasor diagram and (b) steady-state and transient power-angle characteristics.

$$\begin{aligned}
 \hat{E}'_i &= \hat{V}_{ta} + jX'_d \hat{I}'_a \\
 &= 1.00 + j(0.18)(0.80 - j0.60) \\
 &= 1.108 + j0.144 = 1.12 \angle 7.4^\circ
 \end{aligned}$$

$$E'_i = 1.12 \text{ per unit}$$

and

$$P = 6.22 \sin \delta'$$

This transient characteristic is also plotted in Fig. 6-12*b*. Note that the effect of induced currents in the rotor windings is to increase the torque-producing capability of the machine significantly. However, this effect lasts only through the transient-time period and disappears as the induced transient rotor currents decay.

A logical extension of the model just presented would include the effects of transient saliency and represent the machine by a separate voltage behind transient reactance on each rotor axis. Although this representation is perhaps somewhat more exact, it is still subject to the same limitations as the simpler model; specifically its validity is limited by the extent to which the rotor fluxes can be assumed to remain constant. All such models suffer from the fact that they neglect damping effects, which can be of great significance in studies of synchronous-machine dynamics.

An alternative to these trapped flux models is to represent the effects of currents in each of the rotor windings specifically. For example, Fig. 6-13 shows the per unit equivalent circuits for a synchronous machine represented by a field winding and a damper circuit on the rotor direct axis and a single damper circuit on the quadrature axis. The equations corresponding

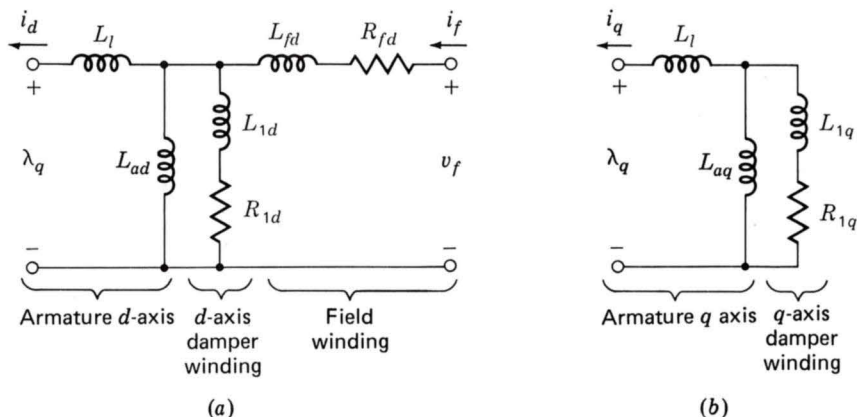


Fig. 6-13. Per unit synchronous-machine equivalent circuits including one damper circuit on each rotor axis: (a) direct-axis equivalent circuit and (b) quadrature-axis equivalent circuit.

to this representation are similar to Eqs. 6-14 to 6-16 and 6-25 to 6-27 with the addition of equations representing the additional short-circuited damper windings. The torque expression of Eq. 6-31 continues to apply. Use of this type of representation (perhaps with additional damper windings) includes directly both synchronous and damping torques. When properly applied, it can lead to accurate representation of synchronous-machine dynamics in a wide variety of situations.

One of the difficulties of using equivalent circuits of the form of Fig. 6-13 is the determination of parameter values for the model elements (resistances and inductances). Traditionally, open- and short-circuit tests such as those described in Arts. 5-5, 6-4, and 6-6 have been used to determine parametric values for the direct-axis equivalent circuit of Fig. 6-13a.[†]

It is much more difficult to obtain parameter values for the quadrature-axis equivalent circuit of Fig. 6-13b. This is due in large part to the fact that standard testing is performed on an unloaded machine for which there is only flux along the direct axis. When the machine is tested under open-circuit conditions, the only source of excitation is the field winding. Similarly, a sudden short-circuit test is initiated by applying a short circuit to an initially open-circuited machine excited only by field current, and thus there is no involvement of the quadrature axis in the transient (with the exception of currents induced by trapped armature flux which do not play a role in the transient behavior of the rotor). Although traditional tests provide a few measurement techniques for the quadrature axis, accurate parameter values have been difficult to obtain and most quadrature-axis parameters have been obtained from manufacturer-provided values.

In recent years, these difficulties in obtaining quadrature-axis parameters from measurements, combined with the need in some cases for more accurate representations of transient rotor currents (using additional equivalent damper circuits on the rotor), have resulted in the development of alternative testing methods. These techniques are based on impedance measurements made directly upon the direct and quadrature axes and are known as *frequency-response testing*.

The most common method for performing these tests is known as *standstill frequency-response testing*.[‡] These tests are made with the rotor held stationary. By appropriate alignment of the rotor, the armature can be excited so as to apply flux along the rotor direct or quadrature axis. In either case, the armature is then excited with variable-frequency currents, ranging from as low as 0.001 to around 100 Hz, and the corresponding

[†]*IEEE Guide: Test Procedures for Synchronous Machines*, IEEE Std. 115-1983, Institute of Electrical and Electronics Engineers, New York, 1983.

[‡]See, for example, *Procedures for Obtaining Synchronous Machine Parameters by Standstill Frequency Response Testing*, IEEE Std. 115A-1987, Institute of Electrical and Electronics Engineers, New York, 1987. Also, "Supplementary Definitions and Associated Test Methods for Synchronous Machine Stability Study Simulations," *IEEE Trans. Power Apparatus and Systems*, PAS-99(4) (July/Aug. 1980).

impedance is measured. These impedances correspond to the input impedances of direct- and quadrature-axis equivalents such as those of Fig. 6-13.

In addition, by recognizing that the direct axis has a second terminal pair (the field winding), additional direct-axis measurements can be made, including the induced field current (if the armature is excited with the field winding short-circuited) or induced field-winding voltage (if the armature is excited with the field winding open-circuited). The input impedance of the field winding can also be measured.

These measurements can be used to obtain parameter values for the elements of the direct- and quadrature-axis equivalent circuits. Experience has shown that for certain types of analyses, models based on frequency-response measurements may exhibit increased accuracy over analyses based on parameters obtained by the traditional methods.[†] This is due in part to the ability to obtain quadrature-axis parameters for which corresponding traditional tests are not available. Difficulties with standstill frequency-response testing include the fact that the measurements are typically made at low excitation levels (corresponding to low flux levels in the machine) and the fact that contact resistances of rotor elements such as slot wedges and retaining rings are different when the rotor is stationary from when the rotor is rotating and centrifugal forces are acting on them.

The choice of model for a given situation must, in general, depend on the type of study being conducted as well as the data available and the type of results desired. This article has briefly indicated the types of models available. Many discussions of modeling are found in the growing literature on synchronous machines.

6-8 SYNCHRONOUS-MACHINE DYNAMICS

Important dynamic problems arise in synchronous-machine systems because (1) successful operation of the machines demands equality of the mechanical speed of the rotor and the speed of the stator field and (2) synchronizing forces tending to maintain this equality are brought into play whenever the relationship is disturbed. If the instantaneous speed of a synchronous machine in a system containing other synchronous equipment should decrease slightly, the decrease would be associated with a decrease in torque angle if the machine were a generator and an increase if it were a motor. For example, if a large load is suddenly applied to the shaft of a synchronous motor, the motor must slow down at least momentarily so that the torque angle can assume the increased value necessary to supply the added load. In fact, until the new angle is reached, an appreciable portion of the energy furnished to the load comes from stored energy in the ro-

[†]P. L. Dandeno, P. Kundur, and R. P. Shulz, "Recent Trends and Progress in Synchronous Machine Modelling in the Electric Utilities Industry," *Proc. IEEE*, **67**(7) (July 1974).

tating mass as it slows down. When the newly required value of the angle is first reached, equilibrium is not yet attained, for the mechanical speed is then below synchronous speed. The angle must momentarily increase further to permit replacing the deficit of stored energy in the rotating mass. The ensuing processes involve a series of oscillations about the final position even when equilibrium is ultimately restored. An exact description of such events can be given only in terms of the associated electromechanical differential equations.

Similar oscillations or hunting, with the accompanying power and current pulsations, may be particularly troublesome in synchronous motors driving loads whose torque requirements vary cyclically at a fairly rapid frequency, as in motors driving reciprocating air or ammonia compressors. If the natural frequency of mechanical oscillation of the synchronous motor is close to the frequency of an important torque harmonic in the compressor cycle, intolerable oscillations result. Electrodynamic transients of a very complicated form but of the same basic nature occur in electric power systems. Unless they are carefully investigated during system planning, they may result in complete shutdowns over wide areas.

a. Basic Electromechanical Equation

The electromechanical equation for a synchronous machine follows directly from equating the inertia torque (equal to the moment of inertia J times the angular acceleration) to the net mechanical and electric torque acting on the rotor. Thus

$$J \frac{d^2\theta}{dt^2} = T_{\text{mech}} - T_{\text{elec}} \quad (6-85)$$

where θ = angular position of rotor

T_{mech} = mechanical accelerating shaft torque applied to rotor

T_{elec} = electromagnetic torque acting to decelerate rotor

This equation, like those which follow, is written with a generator specifically in mind. The same equations can be applied to a motor, although a change in sign of the torque terms is often convenient.

It is often convenient to express the rotor angular position θ in terms of a synchronously rotating reference frame as

$$\theta = \frac{2}{\text{poles}} (\omega t + \delta) \quad (6-86)$$

where ω is the synchronous electric frequency and δ is the electrical angle between a point on the rotor and the synchronous reference frame. Often δ is taken equal to the synchronous-machine power angle. Equation 6-85

thus becomes

$$\frac{2}{\text{poles}} J \frac{d^2\delta}{dt^2} = T_{\text{mech}} - T_{\text{elec}} \quad (6-87)$$

Known as the *swing equation*, Eq. (6-87) can be used to solve for the electromechanical dynamics of the synchronous machine. The key to its use is the accurate representation of the torques acting on the rotor. The mechanical shaft torques must be determined from a representation of the dynamics of the prime mover (or load in the case of a motor).

As discussed in Art. 6-7, when a detailed representation of the synchronous machine is used, the electromagnetic torque T_{elec} can be obtained directly from Eq. 6-31. This type of representation, which finds torque directly from a knowledge of the machine fluxes and currents, includes both synchronous and damping torques. It can be expected to yield accurate results in many types of analyses, provided sufficient equivalent rotor circuits are included to represent the effects of rotor currents adequately and provided proper values for the model parameters can be obtained.[†]

The model of constant voltage behind transient reactance, discussed in Arts. 6-6 and 6-7, can be used in situations where detailed analytical solutions are not possible or are deemed unnecessary. Since this model yields an expression for electric power output, Eq. 6-83, as a function of rotor angle, it is convenient to rewrite Eq. 6-87 in terms of power. This can be done by multiplying by the rotor mechanical velocity ω_m

$$\frac{2}{\text{poles}} J \omega_m \frac{d^2\delta}{dt^2} = P_{\text{mech}} - P_{\text{elec}} \quad (6-88)$$

Since for most situations of practical interest deviations of ω_m from synchronous speed are very small, ω_m can be replaced by the synchronous rotor velocity $\omega_s = (2/\text{poles})\omega$, giving the approximate equation

$$\frac{2}{\text{poles}} J \omega_s \frac{d^2\delta}{dt^2} = P_{\text{mech}} - P_{\text{elec}} \quad (6-89)$$

In this case the electromagnetic power P_{elec} can be represented by two components. One is the *damping power*, discussed in Art. 6-7 and often considered to vary linearly with the departure $d\delta/dt$ from synchronous speed. The second is the *synchronous power*, resulting from synchronous-machine action and characterized by Eq. 5-42 or 5-56 in the steady state and Eq. 6-79 or 6-83 in the transient state. The electromechanical equation 6-89 then becomes

[†]See, for example, P. M. Anderson and A. A. Fouad, *Power System Control and Stability*, Iowa State University Press, Ames, 1977.

$$\frac{2}{\text{poles}} J \omega_s \frac{d^2 \delta}{dt^2} = P_{\text{mech}} - P_d \frac{d\delta}{dt} - P_s(\delta) \quad (6-90)$$

where P_d is the damping power per unit departure in speed from synchronous and $P_s(\delta)$ represents the synchronous power as a function of δ .

The specific nature of the external network must be known before the function $P_s(\delta)$ can be identified. When consideration is restricted to one machine connected directly to the terminals of a very large system (see Art. 5-4) and saliency is ignored, the function is $P_m \sin \delta$ (Eq. 5-42), where P_m is the amplitude of the sinusoidal power-angle curve. Equation 6-90 becomes

$$\frac{2}{\text{poles}} J \omega_s \frac{d^2 \delta}{dt^2} = P_{\text{mech}} - P_d \frac{d\delta}{dt} - P_m \sin \delta \quad (6-91)$$

Positive values of δ denote generator action and therefore energy conversion from mechanical to electric form, positive values of P_{mech} denote mechanical power input to the shaft, positive values of $d\delta/dt$ denote speeds above synchronous speed, and positive values of $d^2\delta/dt^2$ denote acceleration. Alternatively, the reverse convention may be used: positive values of δ denote motor action; positive values of P_{mech} , mechanical power output from the shaft; positive values of $d\delta/dt$, speeds below synchronous speed; and positive values of $d^2\delta/dt^2$, deceleration.

It should be emphasized that for transients occurring in times on the order of the transient time constant or faster, the transient power-angle characteristic (Eq. 6-79 or 6-83) should be used and Eq. 6-91 should be written in terms of the transient power angle δ' . However, for the purposes of this article the distinction need not be made.

Both Eqs. 6-90 and 6-91 are nonlinear. One method of analysis, applicable for small oscillations and illustrated below, is to linearize the power-angle expression. It is simply a special case of linearization about an operating point.

b. Linearized Analysis

When a single machine connected to a large system is under study, only a single differential equation rather than a group of such equations is involved. If, in addition, the variations of δ are small, the term $P_s(\delta)$ in Eq. 6-90 may be replaced by the equation for the slope of the power-angle curve at the operating point. For example, when δ varies between about $+\pi/6$ and $-\pi/6$ electrical radians, the sine of the angle is closely equal to the angle in radians. The term $P_m \sin \delta$ in Eq. 6-91 can then be replaced by the term $P_s \delta$, where P_s is the *synchronizing power* or slope of the power-angle characteristic evaluated at the origin; P_s has units of power per unit angle. Equation 6-91 then becomes

$$\frac{2}{\text{poles}} J \omega_s \frac{d^2 \delta}{dt^2} = P_{\text{mech}} - P_d \frac{d\delta}{dt} - P_s \delta \quad (6-92)$$

Since this equation is now linear, its solution for a particular case can be readily obtained, as illustrated in the following example.

EXAMPLE 6-3

A 200-hp 2300-V three-phase 60-Hz 28-pole 257-r/min synchronous motor is directly connected to a large power system. The motor has the following characteristics:

$$Wk^2 = 10,500 \text{ lb} \cdot \text{ft}^2 \text{ (motor plus load)}$$

$$\text{Synchronizing power } P_s = 11.0 \text{ kW/elec deg}$$

$$\text{Damping torque} = 1770 \text{ lb} \cdot \text{ft}/(\text{mech rad/s})$$

- (a) Investigate the mode of electromechanical oscillation of the machine.
- (b) Rated mechanical load is suddenly thrown on the motor shaft at a time when it is operating in the steady state but unloaded. Study the electrodynamic transient which will ensue.

Solution

(a) Throughout this solution, angle δ will be measured in electrical degrees rather than radians. This fact must be recognized in obtaining P_d and P_s from the given data.

The inertia is given as Wk^2 (weight times the square of the radius of gyration) in U.S. Customary System (USCS) units, a common practice for large machines. In SI units (see table of conversion factors in Appendix D)

$$J = \frac{Wk^2}{23.7} = \frac{10,500}{23.7} = 444 \text{ kg} \cdot \text{m}^2$$

When we use the factor $\pi/180$ to convert angular measurement to degrees, the coefficient of the angular acceleration term becomes

$$\frac{2}{\text{poles}} J \omega_s = \frac{2}{28} (444) \frac{2\pi(257)}{60} \frac{\pi}{180} = 14.9 \text{ W}/(\text{elec deg/s}^2)$$

The remaining motor constants in the appropriate units are

$$P_d = 2\pi(257)(1770) \frac{746}{33,000} \frac{\pi}{180} \frac{2}{28} = 80.6 \text{ W}/(\text{elec deg/s})$$

$$P_s = 11.0(1000) = 11,000 \text{ W/elec deg}$$

The force-free equation which determines the mode of oscillation is then

$$14.9 \frac{d^2\delta}{dt^2} + 80.6 \frac{d\delta}{dt} + 11,000\delta = 0$$

The undamped angular frequency and damping ratio are, respectively,

$$\omega_n = \sqrt{\frac{11,000}{14.9}} = 27 \text{ rad/s}$$

$$\zeta = \frac{80.6}{2\sqrt{14.9(11,000)}} = 0.10$$

The magnitude of ζ places the transient response decidedly in the oscillatory region, as it does for all synchronous machines. Any operating disturbance will be followed by a relatively slowly damped oscillation, or swing, of the rotor before steady operation at synchronous speed is resumed. A large disturbance may, of course, be followed by complete loss of synchronism. The damped angular velocity of the motor is

$$\omega_d = 27\sqrt{1 - 0.10^2} = 26.9 \text{ rad/s}$$

corresponding to a damped oscillation frequency of

$$f_d = \frac{26.9}{2\pi} = 4.3 \text{ Hz}$$

(b) The full load of 200 hp is equivalent to $200(746) = 149,200 \text{ W}$. The steady-state operating angle is

$$\delta_\infty = \frac{149,000}{11,000} = 13.6 \text{ elec deg}$$

A detailed solution of the linearized swing equation would show that the angular excursions characterized by the equation

$$\delta = 13.6^\circ [1 - 1.004e^{-2.7t} \sin(26.9t + 84.3^\circ)]$$

c. Nonlinear Analysis: Equal-Area Methods

In most of the serious dynamics problems, the oscillations are of such magnitude that linearization is not permissible. The equations of motion must

be retained in nonlinear form. Analog or digital computers are often used to aid the analysis. For programming the study on a digital computer, use is made of numerical methods for solving sets of differential equations.[†] The object of the study is usually to find whether synchronism is maintained, i.e., whether the angle δ settles down to a steady operating value after the machine has been subjected to a sizable disturbance.

For simple synchronous-machine systems, damping may be neglected and use may be made of a graphical interpretation of the energy stored in the rotating mass as an aid to determining the maximum rotor angle following a disturbance and to settling the question of maintenance of synchronism. Because of the physical insight it gives to the dynamic process, application of the method to analysis of a single machine connected to a large system is discussed.

Consider specifically a synchronous motor having the power-angle curve of Fig. 6-14. With the motor initially unloaded, the operating point is at the origin of the curve. When a mechanical load P_{mech} is suddenly applied, the operating point travels along sinusoid ABC and, if synchronism is maintained, finally comes to rest at point B with a new torque angle δ_{∞} . To reach this new operating point, the motor must decelerate at least momentarily under the influence of the difference $P_{\text{mech}} - P_m \sin \delta$ between the power required by the load and that resulting from electromechanical energy conversion. Now recall from the thought process leading to Eq. 6-91 that both P_{mech} and $P_m \sin \delta$ are proportional to the corresponding torques. It can be shown that the integral $\int T d\delta$ of the net rotor torque with respect to the angle is equal to the change in rotor kinetic energy. Area OAB in Fig. 6-14 is then seen to be proportional to the energy abstracted from the rotating mass during the initial period when electromagnetic energy

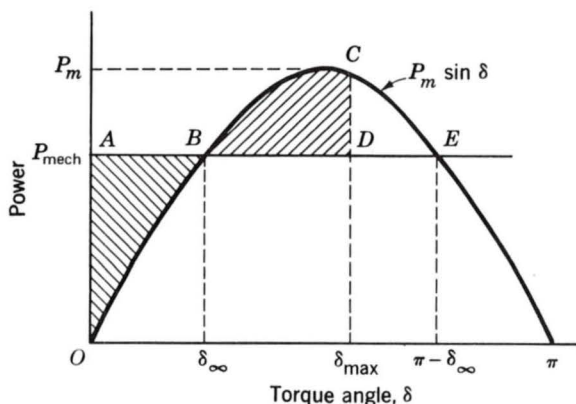


Fig. 6-14. Synchronous-motor power-angle curve and power required by load.

[†]See, for instance, G. W. Stagg and A. H. El-Abiad, *Computer Methods in Power System Analysis*, McGraw-Hill, New York, 1968; also P. M. Anderson and A. A. Fouad, *Power System Control and Stability*, Iowa State Press, Ames, 1977.

conversion is insufficient to supply the shaft load. When point B is reached on the first excursion, therefore, the rotor has a momentum in the direction of deceleration. Acting under this momentum, the rotor must swing past point B until an equal amount of energy is recovered by the rotating mass. The result is that the rotor swings to point C and the angle δ_{\max} , at which point

$$\text{Area } BCD = \text{area } OAB \quad (6-93)$$

Thereafter, in the absence of damping, the rotor will continue to oscillate between points O and C at its natural frequency. The damping present in any physical machine causes successive oscillations to be of decreasing amplitude and finally results in dynamic equilibrium at point B . The analogy to the oscillations of a pendulum may be noted.

This *equal-area method* provides a ready means of finding the maximum angle of swing. It also provides a simple indication of whether synchronism is maintained and a rough measure of the margin of stability. Thus, if area $BCED$ in Fig. 6-14 is less than area OAB , then the decelerating momentum can never be overcome, the angle-time curve follows the course of curve A in Fig. 6-15, and synchronism is lost. But if area $BCED$ is greater than area OAB , then synchronism is maintained with a margin indicated by the difference in areas and the angle-time curve follows curve B of Fig. 6-15. Equality of areas $BCED$ and OAB yields a borderline solution of unstable equilibrium for which curve C is followed.

EXAMPLE 6-4

Determine the maximum shaft load which can be suddenly applied to the motor of Example 6-3 when it is initially operating unloaded. The synchronizing power of 11.0 kW/elec deg quoted in that example is the initial slope of the power-angle curve followed under these conditions. Damping is to be ignored.

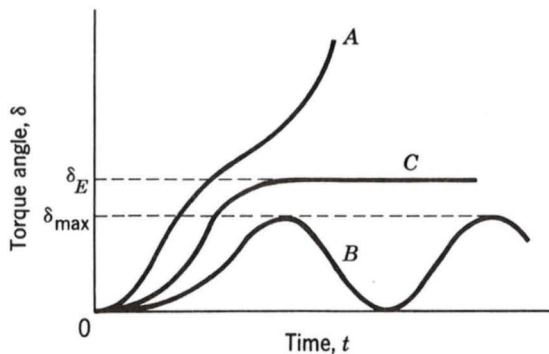


Fig. 6-15. Simple synchronous-machine swing curves showing instability (curve A), stability (curve B), and marginal or critical case (curve C).

Solution

The initial slope of the sinusoidal power-angle curve expressed in kilowatts per radian is equal to the amplitude of the curve in kilowatts. Hence

$$P_m = 11.0 \times \frac{180}{\pi} = 630 \text{ kW}$$

The load P_{mech} must be adjusted so that δ_{max} in Fig. 6-14 achieves the maximum possible value of $\pi - \delta_{\infty}$. In this case, from Fig. 6-16

$$\text{Area } OAB = \text{area } BCD$$

$$\text{or} \quad P_{\text{mech}} \delta_{\infty} - \int_0^{\delta_{\infty}} 630 \sin \delta \, d\delta = \int_{\delta_{\infty}}^{\pi - \delta_{\infty}} 630 \sin \delta \, d\delta - P_{\text{mech}}(\pi - 2\delta_{\infty})$$

where δ_{∞} is the steady-state angle which will be achieved, assuming that synchronism is maintained. Also

$$P_{\text{mech}} = 630 \sin \delta_{\infty}$$

Trial-and-error solution yields

$$P_{\text{mech}} = 455 \text{ kW} = 610 \text{ hp}$$

Notice that the result is independent of inertia when damping is neglected. Under these circumstances, inertia determines the period of oscillation but does not influence its amplitude.

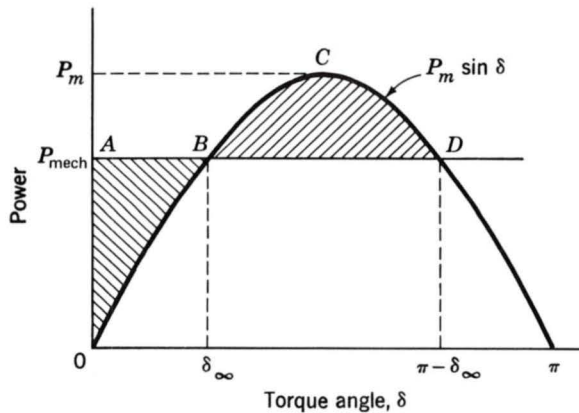


Fig. 6-16. Graphical application of equal-area criterion in Example 6-4.

6-9 SUMMARY

Electric power systems are complex dynamic entities. Although they can often be considered to be operating under steady-state conditions, in actual fact, loads are continually changing and the system is continually reacting in response to these changes. Occasionally, disturbances occur, ranging from the loss of a transmission line due to a lightning strike or the flash-over of a dirty insulator string to a multiple sequence of events resulting in a major blackout over a significant portion of the system. In each case, the synchronous generator plays a significant role in the subsequent transient response of the system; hence an accurate representation of its transient behavior is essential for both predicting and controlling the dynamic characteristics of electric power systems.

Under transient conditions currents are induced in the rotor circuits of synchronous machines. In salient-pole machines these circuits are composed of damper bars arranged much like the rotor bars in a squirrel-cage induction motor. In solid-rotor machines these currents flow directly in the rotor iron. In both cases, currents are also induced in the field winding.

It is the nature of these currents which determines the transient behavior of synchronous machines. Simple transient models can be derived from the concept of trapped rotor flux. Based on the idea that the circuits on the rotor keep their flux constant following a transient, simple mathematical models can be derived in which the machine is represented as a voltage proportional to this trapped flux in series with a transient reactance. The transient reactance is the apparent reactance seen from the armature terminals under the condition of constant rotor flux linkages.

Although such a model is useful for some simple studies of synchronous-machine dynamics, it is not adequate for many situations. It does not predict the damping of rotor oscillations. It cannot predict machine behavior as the various transient rotor currents decay. Thus, more sophisticated models of synchronous machines must explicitly include the effects of the various rotor circuits.

Analysis of synchronous machines is greatly facilitated by transforming armature quantities to a reference frame rotating at rotor speed via the dq0 transformation. In such a reference frame, the armature quantities can be resolved into two components, one along the field-winding axis, also known as the direct axis, and the second along an orthogonal axis, known as the quadrature axis. The rotor can then be represented as a set of direct-axis windings consisting of the field winding and additional windings representing the damper or rotor-body circuits, which produce flux along the direct-axis, and a set of quadrature-axis windings, which corresponds to rotor circuits which produce flux along the quadrature axis. In general, such a model is cast in the form of a set of differential equations which can then be solved via digital or analog computer.

The object of such modeling is to predict dynamic behavior. The basic electromechanical equation, often known as the swing equation, states that the product of the rotor moment of inertia and its angular acceleration is equal to the net torque applied to the rotor (mechanical shaft torque and electromagnetic torque). Under steady-state conditions, the net torque is zero and the rotor remains at constant (synchronous) speed. Transient analysis is performed to investigate the nature of the transients resulting from a disturbance and whether stable steady-state operation will be reestablished.

PROBLEMS

6-1. A 60-Hz 24-kV 250-MVA Y-connected salient-pole synchronous generator ($X_d = 1.75$ per unit, $X_q = 1.40$ per unit) is operating with a phase- a -to-neutral voltage of $14.0 \cos \omega t$ kV and a phase- a current of $5.75 \cos \omega t$ kA; the currents and voltages are balanced three-phase. The rotor angle is known to be $\theta = \omega t + 37^\circ$.

- (a) Draw a phasor diagram for this condition, indicating the terminal voltage, armature current, location of direct and quadrature axes, and direct- and quadrature-axis components of armature terminal voltage and current.
- (b) Using the phasor diagram of part (a) calculate the magnitude of the direct- and quadrature-axis armature voltage and current.
- (c) Repeat the calculation of part (b), using the dq0 transformation of Eq. 6-1.

6-2. This problem is concerned with analysis of a two-phase synchronous machine instead of the three-phase machine of the text. Consider that the machine is idealized as in Art. 6-3 except that there are two distributed windings a and b on the stator, one in each phase, with magnetic axes 90° apart. The salient-pole rotor has only the main-field winding f in the direct axis and no winding in the quadrature axis. The angle from the axis of phase a to the direct axis is θ . That from the phase- b axis to the direct axis is $\theta + 270^\circ$ or, what amounts to the same thing, $\theta - 90^\circ$. Use the same general assumptions, conventions, and notation as in Arts. 5-2, 6-2, and 6-3.

- (a) Write the flux-linkage equations in matrix form corresponding to Eq. 6-3.
- (b) In the manner of Arts. 5-2 and 6-3, show that the inductance matrix $[\mathcal{L}_{abf}]$ is given by

$$\begin{bmatrix} L_{aa0} + L_{g2} \cos 2\theta & L_{g2} \sin 2\theta & L_{af} \cos \theta \\ L_{g2} \sin 2\theta & L_{aa0} - L_{g2} \cos 2\theta & L_{af} \sin \theta \\ L_{af} \cos \theta & L_{af} \sin \theta & L_{ff} \end{bmatrix}$$

- (c) Show that the appropriate dq0 transformation of variables is typified by

$$\begin{bmatrix} i_d \\ i_q \end{bmatrix} = \begin{bmatrix} \cos \theta & \sin \theta \\ -\sin \theta & \cos \theta \end{bmatrix} \begin{bmatrix} i_a \\ i_b \end{bmatrix}$$

Also write the relations for i_a and i_b in terms of i_d , i_q , and θ .

- (d) Show that the flux linkages are given by

$$\lambda_f = L_{ff}i_f - L_{af}i_d \quad \lambda_d = L_{af}i_f - L_{dd}i_d \quad \lambda_q = -L_{qf}i_f$$

Also identify the direct- and quadrature-axis synchronous inductances L_d and L_q in terms of L_{aa0} and L_{g2} .

- (e) Show that Eqs. 6-25 to 6-27 are correct for voltages v_f , v_d , and v_q in this case.
 (f) Show that the instantaneous power output from the two-phase stator is

$$p_s = v_d i_d + v_q i_q$$

- (g) Show that the motor torque is given by

$$T = \frac{\text{poles}}{2} (\lambda_d i_q - \lambda_q i_d)$$

- 6-3.** (a) By carrying out the manipulations described in Art. 6-3 show that Eqs. 6-14 to 6-17 are correct.

- (b) Similarly, show that Eqs. 6-25 to 6-28 are correct.

6-4. A two-pole synchronous motor has a two-phase winding with negligible resistance on the rotor. Its stator has salient poles with a field winding on the direct axis having resistance R_f and excited by a constant voltage V_f . There is a short-circuited stator winding in the quadrature axis.

The motor is running in the steady state with balanced two-phase voltages given by

$$v_a = -V \sin \omega t \quad \text{and} \quad v_b = -V \cos \omega t$$

applied to the rotor windings. The angle from the direct axis to the magnetic axis of rotor phase a is

$$\theta = \omega t + \delta$$

That between the phase- b axis and the direct axis is 90° greater than this. (The statement or solution of Prob. 6-2 can be used as a guide in the solu-

tion of this problem. Note very carefully the conditions stated here, however, to ensure the correct signs.)

- (a) Show that the direct- and quadrature-axis rotor currents into the motor are given by

$$i_d = \frac{-\omega L_{af} I_f + V \cos \delta}{\omega L_d} \quad \text{and} \quad i_q = \frac{V \sin \delta}{\omega L_q}$$

- (b) Show that the motor torque is given by

$$T = -\frac{L_{af} V_f V}{\omega L_d R_f} \sin \delta - \frac{V^2 (L_d - L_q)}{2\omega^2 L_d L_q} \sin 2\delta$$

- (c) Show that the phase-*a* rotor current is

$$i_a = i_d \cos \theta + i_q \sin \theta$$

6-5. Prove that the unitary transformation described in the footnote preceding Eq. 6-1 is power-invariant, as described in the footnote.

6-6. Consider a two-winding transformer whose equivalent circuit is shown in Fig. 6-17. A dc voltage V_0 is applied to winding 1 at $t = 0$.

- Assuming the secondary winding to be open-circuited ($i_2 = 0$), write an expression for the primary current as a function of time.
- Assuming the secondary winding to be short-circuited ($v_2 = 0$) and the secondary resistance to be negligible ($R_2 = 0$), write an expression for (i) the primary current as a function of time and (ii) the secondary current as a function of time. (iii) What is the apparent inductance as seen from the primary terminals?
- Compare the primary open-circuit time constant found in part (a) with the primary short-circuit time constant found in part (b).
- Discuss in general terms the effects of a finite but small R_2 .

6-7. A three-phase turbine generator is rated 13.8 kV (line to line), 125 MVA. Its constants, with reactances expressed in per unit on the machine rating as a base, are

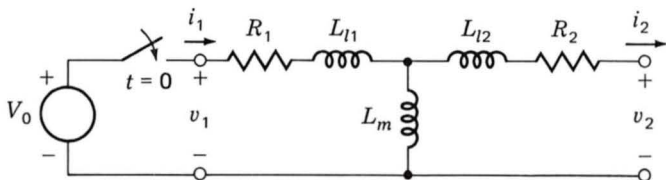


Fig. 6-17. Transformer equivalent circuit for Prob. 6-6.

$$X_d = 1.18 \quad X'_d = 0.23 \quad T'_d = 1.2 \text{ s}$$

It is operating unloaded at a terminal voltage of 1.00 per unit when a three-phase short circuit occurs at its terminals. Except in part (g), ignore the dc component in the short-circuit current. Express numerical answers both in per unit and in amperes.

- (a) What is the rms steady-state short-circuit current? Does it make sense physically for the steady-state short-circuit current to be lower than rated current, as it is here? Explain.
- (b) Write the numerical equation for the instantaneous phase-*a* current as a function of time. Consider the fault to occur when the angle between the axis of phase *a* and the direct axis is 90° . Because of the neglect of the dc component, this is the *symmetric* short-circuit current.
- (c) Write the numerical equation for the envelope of the short-circuit current wave as a function of time.
- (d) Using the result of part (c), write the numerical equation showing how the rms value of short-circuit current varies with time.
- (e) What value is given by the expression in part (d) at $t = 0$? This is known as the *initial symmetric rms short-circuit current*.
- (f) Generalize the result in part (d) by writing the equation for rms symmetric short-circuit current as a function of time, initial voltage behind transient reactance, and machine constants.
- (g) In part (b) suppose the fault occurs when the magnitude of the initial angle is other than 90° . The value of i_a at $t = 0$ will then be nonzero. But since the phase-*a* winding is a resistance-inductance circuit, the complete phase-*a* current cannot change instantaneously from zero. Hence a dc component must be present in i_a to reconcile the situation. This component dies away rapidly. Give the maximum possible initial magnitude of the dc component.

6-8. The machine in Prob. 6-7 has the constants

$$X''_d = 0.13 \quad T''_d = 0.30 \text{ s}$$

in addition to those given there. Work Prob. 6-7, except for part (b), with the subtransient effects included as well as the transient effects. In part (f), the initial voltage behind subtransient reactance must also be reflected. In part (g), the principle still holds that the dc component must preserve continuity of instantaneous phase current just before and just after the short circuit.

6-9. The manufacturer's data sheet for a 50-MVA 13.8-kV three-phase 60-Hz two-pole synchronous generator indicates that it has the following parameters:

$$\begin{aligned}
 X_d &= 1.35 & X_q &= 0.85 & X'_d &= 0.35 & X'_q &= 0.85 \\
 T'_{d0} &= 6.5 & T'_d &= 1.67
 \end{aligned}$$

where the reactances are in per unit and correspond to unsaturated conditions within the machine and the time constants are in seconds. In addition, from the open-circuit characteristics, the field current at rated open-circuit voltage is 675 A, and the field current at rated open-circuit-voltage on the air-gap line is 530 A.

The generator is undergoing a steady-state three-phase short-circuit test at rated speed. The field excitation is adjusted so that the armature current is equal to 25 percent of its rated value.

- (a) Find the field current required to achieve this condition.

The short circuit is suddenly removed. Assume that the exciter maintains constant field voltage throughout the ensuing transient.

- (b) Find the magnitude of the steady-state open-circuit voltage on the machine after all the transients have died out following removal of the short circuit.
- (c) Find a numerical expression for the field current (in per unit and in amperes) as a function of time following the removal of the short circuit.
- (d) Find a numerical expression for the magnitude of the open-circuit armature voltage as a function of time.
- (e) If the initial short-circuit current had been equal to the rated armature current, what effect would this have had on the final value of (i) the field current and (ii) the open-circuit armature voltage following removal of the short circuit?

6-10. A non-salient-pole synchronous generator is characterized by the following parameters:

$$X_d = X_q = 1.67 \text{ per unit}$$

$$X'_d = 0.32 \text{ per unit}$$

$$T'_{d0} = 4.7 \text{ s}$$

$$\text{Field resistance} = 0.18 \, \Omega$$

$$\text{Field voltage required to achieve rated open-circuit terminal voltage} = 470 \text{ V}$$

For the purposes of this problem, neglect the effects of saturation and armature resistance.

- (a) The machine is operating at rated speed, open-circuited, with no excitation applied to the field winding. A voltage of 470 V is sud-

denly applied to the field winding.

- (i) What is the field current as a function of time?
 - (ii) Write an expression for the per unit armature voltage as a function of time.
- (b) The same machine with 470 V applied to the field winding has been operating with a three-phase terminal short circuit long enough for all transients to have died out. What is the steady-state field current in amperes and the per unit armature current?
- (c) The steady-state armature short circuit is suddenly removed. For the purposes of this analysis, assume that all three phase currents are simultaneously interrupted.
- (i) What is the magnitude of the field current in amperes immediately after interrupting of the armature current?
 - (ii) Write expressions for the field current and terminal voltage as a function of time.

6-11. Particularly severe dips in generator terminal voltage are produced by the application of inductive loads at or close to zero power factor. The starting inrush to a large motor is one such type of load. Consider that a synchronous generator is operating initially unloaded at normal terminal voltage. A balanced inductive load X_L is suddenly applied to its terminals. The field voltage is not changed, and the generator continues to operate at synchronous speed. Ignore saturation.

- (a) Show that the variation of terminal voltage with time after load application is given by

$$V_{ta} = E_{f0} \frac{X_L}{X_d + X_L} + E_{f0} \left(\frac{X_L}{X'_d + X_L} - \frac{X_L}{X_d + X_L} \right) e^{-t/T'_d}$$

where E_{f0} is the preload excitation voltage and

$$T'_d = T_{d0} \frac{X'_d + X_L}{X_d + X_L}$$

- (b) Give per unit voltage magnitudes when $X_d = 1.50$, $X'_d = 0.20$, $X_L = 0.95$, and $T_{d0} = 5.5$ s. The reactances are per unit values.

6-12. A salient-pole generator has the following constants in per unit (machine rating base):

$$X_d = 1.17 \quad X_q = 0.75 \quad X'_d = 0.35$$

Assume that the machine is connected directly to an infinite bus at its terminals (voltage = 1.0 per unit) and is operating at rated output power, unity power factor.

- (a) Using the representation of Eq. 6-79, assume E'_q to be constant and compute and plot the transient power-angle curve of the machine in terms of the true power angle δ .
- (b) Compute the transient power-angle characteristic of Eq. 6-83 based on the constant-voltage-behind-transient-reactance model of Fig. 6-7 in terms of the transient power angle δ' .
- (c) The constant-voltage-behind-transient-reactance model of Fig. 6-7 assumes that the angular difference between the angle transient rotor angle δ' and the power angle δ remains constant at its initial pretransient value. As a result, the transient power-angle characteristic of part (b) can be plotted in terms of the true power angle δ simply by adding this value to δ' . Plot the transient power-angle characteristic of part (b) in terms of δ on the plot which you created for part (a).

6-13. Repeat Prob. 6-12 for a cylindrical-rotor generator whose per unit constants are

$$X_d = 2.22 \quad X_q = 2.10 \quad X'_d = 0.24$$

6-14. The ideal condition for synchronizing an alternator with an electric power system is that the alternator voltage be the same as that of the system bus in magnitude, phase, and frequency. Departure from these conditions results in undesirable current and power surges accompanying electro-mechanical oscillation of the alternator rotor. As long as the oscillations are not too violent, they can be investigated by a linearized analysis.

Consider that a 30-MVA 0.85-power-factor 60-Hz two-pole alternator driven by a gas turbine is to be synchronized with a system large enough to be considered an infinite bus. The moment of inertia of the alternator and turbine is $3780 \text{ kg} \cdot \text{m}^2$. The damping power coefficient P_d is $17 \text{ kW}/(\text{elec deg/s})$, and the synchronizing power coefficient P_s is $1.85 \text{ MW}/\text{elec deg}$. Both P_d and P_s may be assumed to remain constant. In all cases below, the terminal voltage is adjusted to its correct magnitude. The turbine governor is sufficiently insensitive not to act during the synchronizing period.

- (a) Consider that the alternator is initially adjusted to the correct speed but that it is synchronized out of phase by 20 electrical degrees, with the alternator leading the bus. Obtain a numerical expression for the ensuing electromechanical oscillations. Also give the largest value of torque exerted on the rotor during the synchronizing period. Ignore losses, and express this torque as a percentage of that corresponding to the nameplate rating.
- (b) Repeat part (a) with the alternator synchronized at the proper angle but with its speed initially adjusted 1.0 Hz fast.
- (c) Repeat part (a) with the alternator initially leading the bus by 20 electrical degrees and its speed initially adjusted 1.0 Hz fast.

6-15. A 1000-kVA 6.9-kV 60-Hz synchronous condenser has the following direct-axis parameters:

$$\begin{aligned} X_d &= 1.98 & X'_d &= 0.46 & X''_d &= 0.26 \\ T'_{d0} &= 8.5 \text{ s} & T''_{d0} &= 0.40 \text{ s} \end{aligned}$$

where the reactances are in per unit on the machine base. This machine is connected to a system through a transformer of reactance 0.23 per unit and of negligible resistance. The synchronous condenser has just been paralleled to the system and is operating at no load and rated terminal voltage when a three-phase short circuit occurs on the system side of the transformer.

- Compute the prefault values of the per unit voltages behind synchronous, transient, and subtransient reactances.
- Give the numerical equation for the fundamental-frequency rms short-circuit current (in amperes) at the generator terminals as a function of time following the fault. Ignore the dc component.
- Compute the largest possible initial value of the dc component of the short-circuit current at the machine terminals in per unit and in amperes. Use the results of part (b) and the fact that the total armature current in each phase at the instant of the fault is zero.

6-16. Consider a synchronous machine with a direct-axis damper winding. The damper winding (labeled by subscript $1d$) is described by the following per unit parameters as referred to the stator:

$\mathcal{L}_{1d1d} = L_{1d1d}$ = damper self-inductance

$\mathcal{L}_{a1d} = L_{a1d} \cos \theta$ = phase- a -to-damper mutual inductance

$\mathcal{L}_{f1d} = L_{f1d}$ = field-to-damper mutual inductance

R_{1d} = damper resistance

- Write the flux-current relationships for this machine corresponding to Eq. 6-3.
- Apply the dq0 transformation to the flux-current relationship of part (a). *Hint:* Note that the dq0 transformation treats both the damper and the field windings in the same manner. As a result, it is possible to obtain the desired results directly from inspection of Eqs. 6-14 to 6-17.
- What are the transformed voltage equations for this machine? Note that the damper winding is short-circuited and thus $v_{1d} = 0$.

6-17. In Prob. 6-16 a synchronous machine with a direct-axis damper winding is analyzed. In this problem, repeat the analysis of Prob. 6-16 with the

addition of a quadrature-axis damper winding (labeled by subscript $1q$). Note that the quadrature axis leads the direct axis, and thus the mutual inductance between phase a and the quadrature-axis damper winding is $\mathcal{L}_{a1q} = -L_{a1q} \sin \theta$.

6-18. A 750-kVA 4160-V six-pole 60-Hz non-salient-pole synchronous generator is driven by a wind turbine and coupled to a 4160-V distribution system (considered here to be an infinite bus) through an impedance of 0.12 per unit (generator base). The generator parameters are

$$X_d = 1.63 \text{ per unit} \quad X'_d = 0.23 \text{ per unit} \quad T'_{d0} = 3.7 \text{ s}$$

The total moment of inertia of the wind turbine and generator combination is $2.1 \times 10^3 \text{ kg} \cdot \text{m}^2$. The generator is initially operating with a terminal voltage of 4160 V at 600-kW output.

- (a) Calculate the initial values (per unit magnitudes and angles with respect to the infinite bus) of the excitation voltage \hat{E}_{af} and the voltage behind transient reactance \hat{E}'_i .

A sudden increase in wind speed causes the wind torque to double. Assume that the voltage behind transient reactance remains constant throughout the ensuing transient.

- (b) Using the equal-area criterion, calculate the maximum value of the transient rotor angle.
 (c) Upon decay of the rotor oscillations, what is the final value of the transient rotor angle?
 (d) Using a linearized analysis, estimate the frequency of the rotor oscillations. The linearization should be performed around the operating point found in part (c).

6-19. A synchronous motor whose input under rated operating conditions is 12,000 kVA is connected to an infinite bus over a short feeder whose impedance is purely reactive. The motor is rated at 60 Hz, 600 r/min and has a total Wk^2 of 550,000 lb · ft² (including the shaft load). The power-angle curve under transient conditions is $2.30 \sin \delta$, where the amplitude is in per unit on a 10,000-kVA base.

- (a) With the motor operating initially unloaded, a 10,000-kW shaft load is suddenly applied. Does the motor remain in synchronism?
 (b) How large a shaft load can be applied suddenly without loss of synchronism?
 (c) Consider now that the suddenly applied load is on for only 0.2 s, after which a comparatively long time elapses before any load is applied again. Determine the maximum value of such a load which will still allow synchronism to be maintained. Use the equal-area

criterion as an aid in the process. For purposes of computing the angle δ at 0.2 s, ignore damping and use a linearized analysis in which the power-angle curve is approximated by a straight line through the origin and the 60° point.

6-20. Two identical 150-MVA 13.8-kV synchronous generators are operating in parallel at a power station. They each have per unit direct-axis reactances of $X_d = 1.37$ and $X'_d = 0.29$. They are connected at their terminals to a power system which can be represented as an infinite bus in series with an impedance of 0.1 per unit on the 150-MVA 13.8-kV generator base.

These generators are each initially operating at 100 MW and rated voltage as measured at their terminals. Due to a problem within the plant, one of the generators is suddenly tripped offline. Using the constant-voltage-behind-transient-reactance model and the equal-area criterion, determine whether this generator will remain in synchronism following this disturbance.

6-21. Reciprocating air and ammonia compressors require a torque which fluctuates periodically about a steady average value. For a two-cycle unit the torque harmonics have frequencies in hertz which are multiples of the speed in revolutions per second. When, as is commonly the case, the compressors are driven by synchronous motors, the torque harmonics cause periodic fluctuation of the torque angle δ and may result in undesirably high pulsations of power and current to the motor. It is therefore essential that, for the significant harmonics, the electrodynamic response of the motor be held to a minimum.

- (a) To investigate the response of the motor to torque harmonics, use a linearized analysis. Let

$$P_{\text{mech}} = P_{\text{sh,max}} \cos \omega t$$

where $P_{\text{sh,max}}$ corresponds to the amplitude of the harmonic-torque pulsation whose angular frequency is ω . Then show that the differential equation can be written

$$\frac{d^2\delta}{dt^2} + 2\zeta\omega_n \frac{d\delta}{dt} + \omega_n^2\delta = \frac{P_{\text{sh,max}}}{P_j} \cos \omega t$$

Identify these quantities in terms of P_s , P_d , and $P_j = (2/\text{poles})J\omega$.

- (b) Show that the phasor expression for the steady-state solution is

$$\Delta = \frac{P_{\text{sh,max}}/P_j}{\omega_n^2 - \omega^2 + j2\zeta\omega_n\omega}$$

- (c) The motor driving the compressor is that of Example 6-3. The compressor has a first-order torque harmonic with an amplitude of $630 \text{ lb} \cdot \text{ft}$ and a frequency of 4.3 Hz . Determine the maximum deviation in power angle δ and the corresponding pulsation of synchronous power.
- (d) Consider that a flywheel is added to bring the total Wk^2 up to $14,890 \text{ lb} \cdot \text{ft}^2$. Repeat the computation of part (c) and compare the results.

7

Polyphase Induction Machines

The objectives of this chapter are to develop equivalent circuits for the polyphase induction motor from which both the effects of the motor on its supply circuit and the characteristics of the motor itself can be determined and to study these effects and characteristics. The general form of equivalent circuit is suggested by the similarity of an induction machine to a transformer.

7-1 INTRODUCTION TO POLYPHASE INDUCTION MACHINES

As indicated in Art. 4-2*b*, an induction motor is one in which alternating current is supplied to the stator directly and to the rotor by induction or transformer action from the stator. As in the synchronous machine, the stator winding is of the type discussed in Art. 4-5. When excited from a

balanced polyphase source, it will produce a magnetic field in the air gap rotating at synchronous speed as determined by the number of poles P and the applied stator frequency f (Eq. 4-42). The rotor may be one of two types. A *wound rotor* carries a polyphase winding similar to, and wound with, the same number of poles as the stator. The terminals of the rotor winding are connected to insulated slip rings mounted on the shaft. Carbon brushes bearing on these rings make the rotor terminals available external to the motor, as shown in the cutaway view in Fig. 7-1. The motor in Fig. 4-14 has a *squirrel-cage rotor* with a winding consisting of conducting bars embedded in slots in the rotor iron and short-circuited at each end by conducting end rings. The extreme simplicity and ruggedness of the squirrel-cage construction are outstanding advantages of this type of induction motor.

Now assume that the rotor is turning at the steady speed n r/min in the same direction as the rotating stator field. Let the synchronous speed of the stator field be n_1 r/min as given by Eq. 4-42. The rotor is then traveling at a speed $n_1 - n$ r/min backward with respect to the stator field, or the *slip* of the rotor is $n_1 - n$ r/min. Slip is more usually expressed as a fraction of synchronous speed.[†] The per unit slip s is

$$s = \frac{n_1 - n}{n_1} \quad (7-1)$$

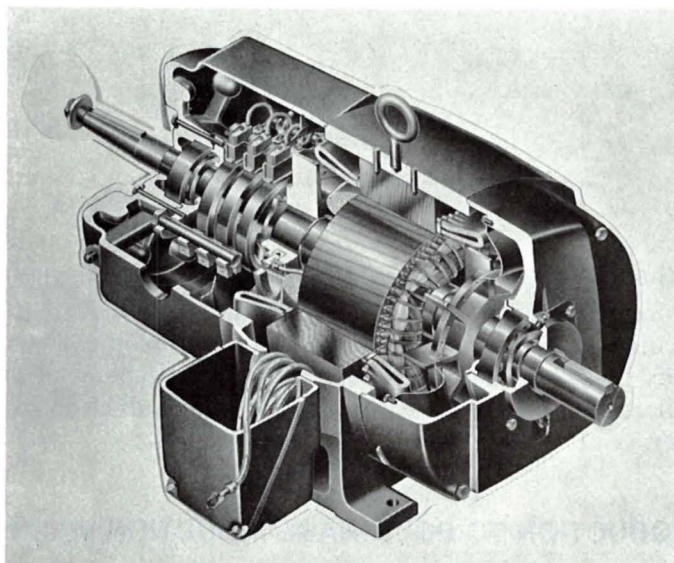


Fig. 7-1. Cutaway view of a three-phase induction motor with a wound rotor and slip rings connected to the three-phase rotor winding. (General Electric Company.)

[†]Alternatively, slip is often expressed in percent, where a slip of 100 percent is equivalent to a per unit slip of unity (1.0).

or

$$n = n_1(1 - s) \quad (7-2)$$

This relative motion of the stator flux and the rotor conductors induces voltages of frequency sf , called *slip frequency*, in the rotor. Thus, the electrical behavior of an induction machine is similar to that of a transformer but with the additional feature of frequency transformation. In fact, a wound-rotor induction machine can be used as a frequency changer.

When it is used as an induction motor, the rotor terminals are short-circuited. The rotor currents are then determined by the magnitudes of the induced voltages and the rotor impedance at slip frequency. At starting, the rotor is stationary, the slip $s = 1$, and the rotor frequency equals the stator frequency f . The field produced by the rotor currents therefore revolves at the same speed as the stator field, and a starting torque results, tending to turn the rotor in the direction of rotation of the stator-inducing field. If this torque is sufficient to overcome the opposition to rotation created by the shaft load, the motor will come up to its operating speed. The operating speed can never equal the synchronous speed n_1 , however, since the rotor conductors would then be stationary with respect to the stator field and no current would be induced in them.

With the rotor revolving in the same direction of rotation as the stator field, the frequency of the rotor currents is sf , and the component rotor field set up by them will travel at sn_1 r/min *with respect to the rotor* in the forward direction. But superimposed on this rotation is the mechanical rotation of the rotor at n r/min. The speed of the rotor field in space is the sum of these two speeds and equals

$$sn_1 + n = sn_1 + n_1(1 - s) = n_1 \quad (7-3)$$

The stator and rotor fields are therefore stationary with respect to each other, a steady torque is produced, and rotation is maintained. Such a torque existing at any mechanical speed n other than synchronous speed is called an *asynchronous torque*.

Figure 7-2 shows a typical squirrel-cage induction-motor torque-speed curve. The factors influencing the shape of this curve can be appreciated in terms of the torque equation 4-85. In this equation recognize that the resultant air-gap flux Φ_{sr} is approximately constant when the stator-applied voltage and frequency are constant. Also recall that the rotor mmf F_r is proportional to the rotor current I_r . Equation 4-85 then reduces to

$$T = KI_r \sin \delta_r \quad (7-4)$$

where K is a constant. The rotor current is determined by the voltage induced in the rotor and its leakage impedance, both at slip frequency. The rotor-induced voltage is proportional to slip. Under normal running conditions the slip is small—3 to 10 percent at full load in most squirrel-cage

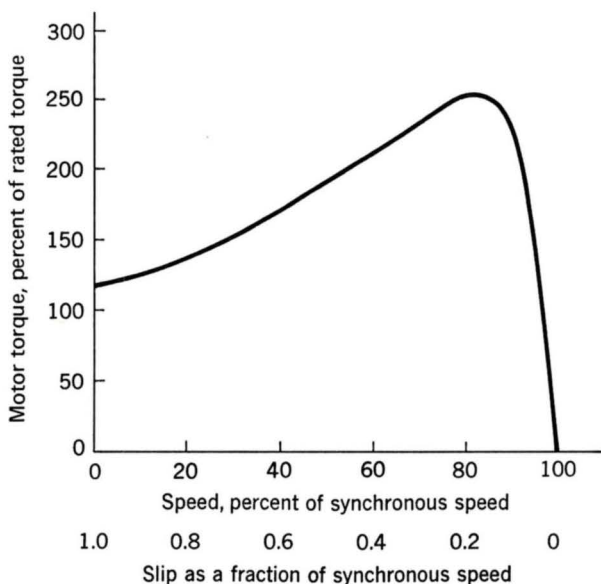


Fig. 7-2. Typical induction-motor torque-speed curve.

motors. The rotor frequency sf therefore is very low (of the order of 2 to 6 Hz in 60-Hz motors). Consequently, in this range the rotor impedance is largely resistive, and the rotor current is very nearly proportional to, and in phase with, the rotor voltage and is therefore very nearly proportional to slip. Furthermore, the rotor-mmf wave lags approximately 90 electrical degrees behind the resultant flux wave, and therefore $\sin \delta_r \approx 1$. (This point is discussed in Art. 7-2a.) Approximate linearity of torque as a function of slip is therefore to be expected in the range where the slip is small. As slip increases, the rotor impedance increases because of the increasing effect of rotor leakage inductance. Thus the rotor current is less than proportional to slip. Also the rotor current lags farther behind the induced voltage, the mmf wave lags farther behind the resultant flux wave, and $\sin \delta_r$ decreases. The result is that the torque increases with increasing slip up to a maximum value and then decreases, as shown in Fig. 7-2. The maximum torque, or *breakdown torque*, limits the short-time overload capability of the motor.

The squirrel-cage motor is substantially a constant-speed motor having a few percent drop in speed from no load to full load. Speed variation can be obtained by using a wound-rotor motor and inserting external resistance in the rotor circuit. In the normal operating range, external resistance simply increases the rotor impedance, necessitating a higher slip for a desired rotor mmf and torque.

In Art. 5-1 it was mentioned that a synchronous motor per se has no starting torque. To make a synchronous motor self-starting, a squirrel-cage winding, called an *amortisseur* or *damping winding*, is inserted in the rotor

pole faces, as shown in Fig. 7-3. The rotor then comes up almost to synchronous speed by induction-motor action with the field winding unexcited. If the load and inertia are not too great, the motor will pull into synchronism when the field winding is energized from a dc source.

7-2 CURRENTS AND FLUXES IN INDUCTION MACHINES

For a coil-wound rotor, the flux-mmf situation can be seen with the aid of Fig. 7-4. This sketch shows a development of a simple two-pole three-phase rotor winding in a two-pole field. It therefore conforms with the restriction that a wound rotor must have the same number of poles as the stator (although the number of phases need not be the same). The flux-density wave is moving to the right at synchronous angular velocity ω_s and at slip angular velocity $s\omega_s$ with respect to the winding, which in turn is rotating to the right at angular velocity $(1 - s)\omega_s$. It is shown in Fig. 7-4 in the position of maximum instantaneous voltage in phase a .

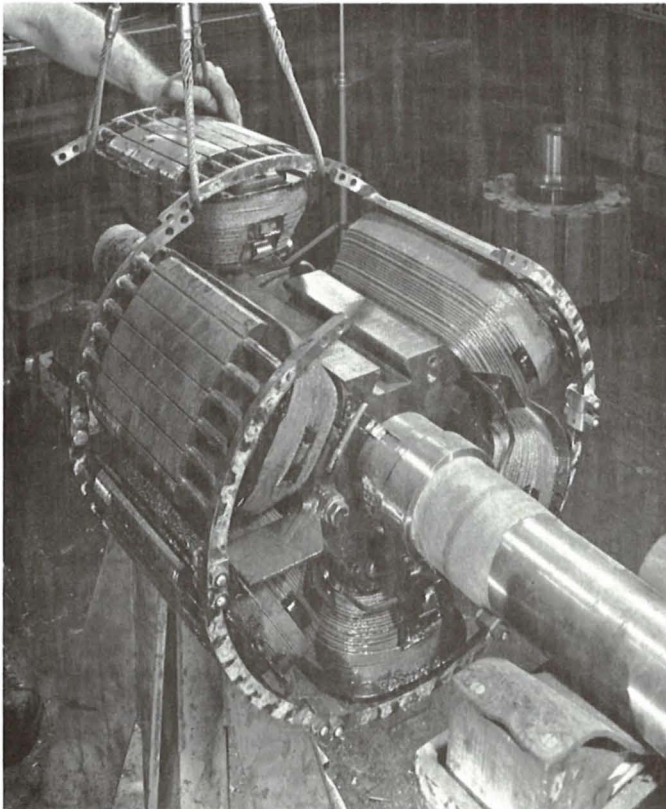


Fig. 7-3. Rotor of a six-pole 1200 r/min synchronous motor showing field coils, pole-face damper winding, and construction. (*General Electric Company.*)

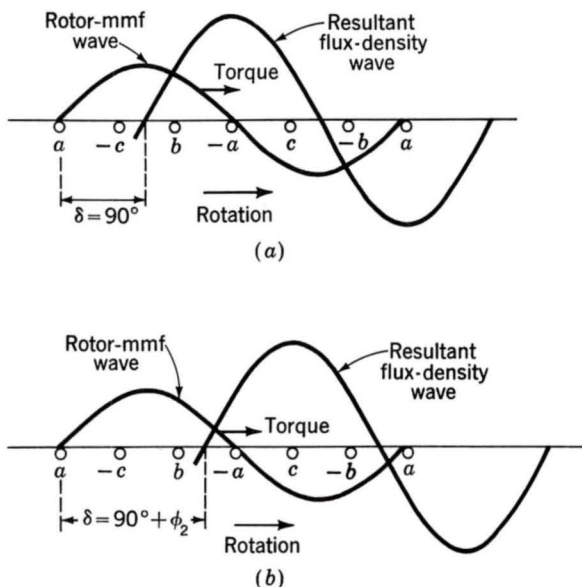


Fig. 7-4. Developed rotor winding of an induction motor with its flux-density and mmf waves in their relative positions for (a) zero and (b) nonzero rotor leakage reactance.

If the rotor leakage reactance, equal to $s\omega_s$ times the rotor leakage inductance, is very small compared with the rotor resistance (which is typically the case at the small slips corresponding to normal operation), the phase- a current will also be a maximum. As shown in Art. 4-5, the rotor-mmf wave will then be centered on phase a . It is so shown in Fig. 7-4a. The displacement angle, or torque angle, δ under these conditions is at its optimum value of 90° .

If the rotor leakage reactance is appreciable, however, the phase- a current lags the induced voltage by the power-factor angle ϕ_2 of the leakage impedance. The phase- a current will not be at maximum until a correspondingly later time. The rotor-mmf wave will then not be centered on phase a until the flux wave has traveled ϕ_2 degrees farther down the gap, as shown in Fig. 7-4b. The angle δ is now $90^\circ + \phi_2$. In general, therefore, the torque angle of an induction motor is

$$\delta = 90^\circ + \phi_2 \quad (7-5)$$

It departs from the optimum value by the power-factor angle of the rotor leakage impedance at slip frequency. The electromagnetic rotor torque is directed toward the right in Fig. 7-4, or in the direction of the rotating flux wave.

The comparable picture for a squirrel-cage rotor is given in Fig. 7-5. A 16-bar rotor placed in a two-pole field is shown in developed form. For sim-

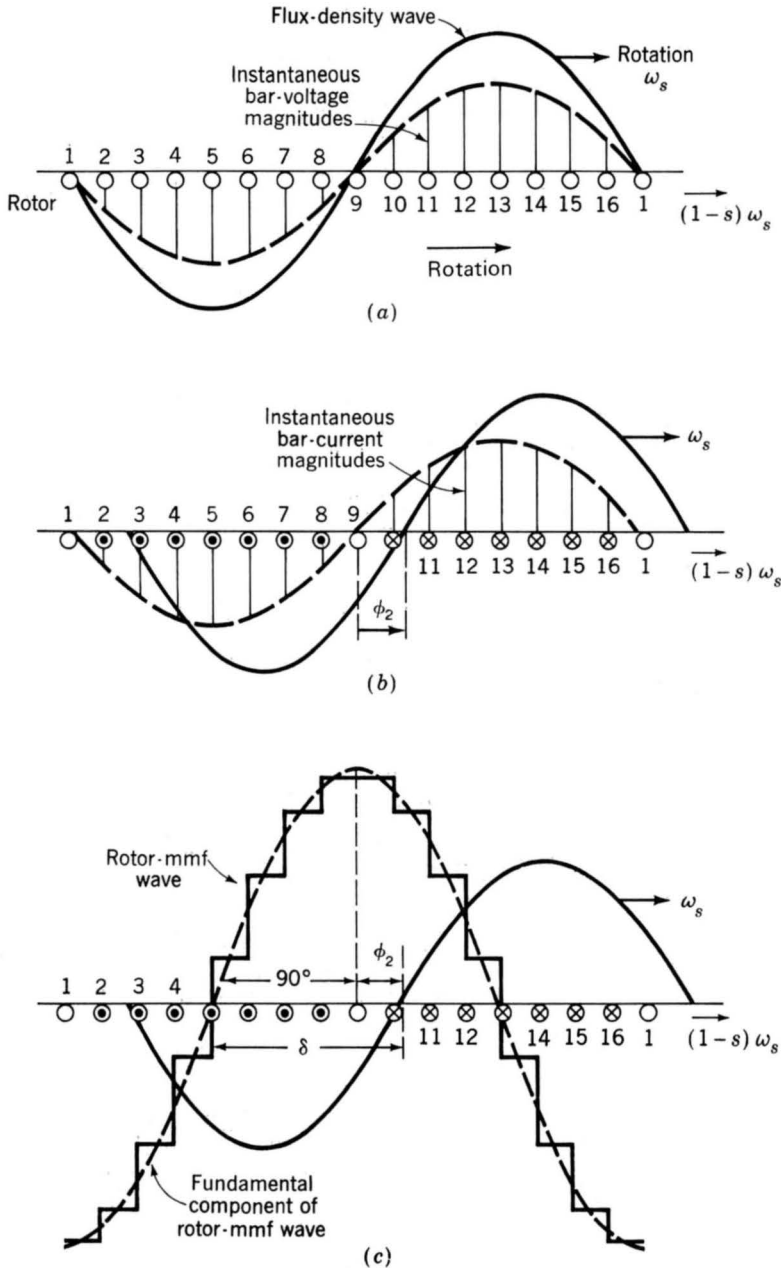


Fig. 7-5. Reactions of a squirrel-cage rotor in a two-pole field.

plicity of drafting, only a relatively small number of rotor bars are chosen, and the number is an integral multiple of the number of poles, a choice normally avoided in order to prevent harmful harmonic effects. In Fig. 7-

5a the sinusoidal flux-density wave induces a voltage in each bar which has an instantaneous value indicated by the solid vertical lines. At a somewhat later instant of time, the bar currents assume the instantaneous values indicated by the solid vertical lines in Fig. 7-5b, the time lag corresponding to the rotor power-factor angle ϕ_2 . In this time interval, the flux-density wave has traveled in its direction of rotation with respect to the rotor through a space angle ϕ_2 and is then in the position shown in Fig. 7-5b. The corresponding rotor-mmfs wave is shown by the step wave of Fig. 7-5c. The fundamental component is shown by the dashed sinusoid and the flux-density wave by the solid sinusoid. Study of these figures confirms the general principle that the number of rotor poles in a squirrel-cage rotor is determined by the inducing flux wave.

7-3 INDUCTION-MOTOR EQUIVALENT CIRCUIT

The foregoing considerations of flux and mmf waves can readily be translated to the steady-state equivalent circuit for the machine. Only machines with symmetric polyphase windings excited by balanced polyphase voltages are considered. As in many other discussions of polyphase devices, it is helpful to think of three-phase machines as being Y-connected, so that currents are always line values and voltages always line-to-neutral values.

First, consider conditions in the stator. The synchronously rotating air-gap flux wave generates balanced polyphase counter emfs in the phases of the stator. The stator terminal voltage differs from the counter emf by the voltage drop in the stator leakage impedance, the phasor relation for the phase under consideration being

$$\hat{V}_1 = \hat{E}_1 + \hat{I}_1(R_1 + jX_1) \quad (7-6)$$

where \hat{V}_1 = stator terminal voltage
 \hat{E}_1 = counter emf generated by resultant air-gap flux
 \hat{I}_1 = stator current
 R_1 = stator effective resistance
 X_1 = stator leakage reactance

The positive directions are shown in the equivalent circuit of Fig. 7-6.

The resultant air-gap flux is created by the combined mmf's of the stator and rotor currents. Just as in the transformer analog, the stator current can be resolved into two components, a load component and an exciting component. The load component \hat{I}_2 produces an mmf which exactly counteracts the mmf of the rotor current. The exciting component \hat{I}_ϕ is the additional stator current required to create the resultant air-gap flux and is a function of the emf \hat{E}_1 . The exciting current can be resolved into a core-loss component \hat{I}_c in phase with \hat{E}_1 and a magnetizing component \hat{I}_m lagging \hat{E}_1 by 90° . In the equivalent circuit the exciting current can be

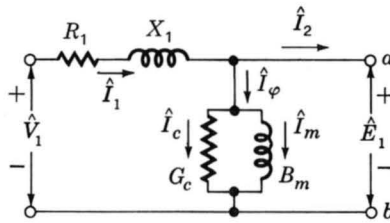


Fig. 7-6. Stator equivalent circuit for a polyphase induction motor.

accounted for by means of a shunt branch, formed by core-loss conductance G_c and magnetizing susceptance B_m in parallel, connected across \hat{E}_1 , as in Fig. 7-6. Both G_c and B_m are usually determined at rated stator frequency and for a value of E_1 close to the expected operating value; they are then assumed to remain constant for the small departures from that value associated with normal operation of the motor.

So far, the equivalent circuit representing stator phenomena is exactly like that for the primary of a transformer. To complete the circuit, the effects of the rotor must be incorporated. This is done by considering stator and rotor voltages and currents in terms of rotor quantities as referred to the stator.

In Art. 7-2 we saw that, insofar as fundamental components are concerned, both squirrel-cage and wound rotors react by producing an mmf wave having the same number of poles as the inducing flux wave, traveling at the same speed as the flux wave, and with a torque angle 90° greater than the rotor power-factor angle. The reaction of the rotor-mmf wave on the stator induces an emf which results in a compensating load component of stator current and thereby enables the stator to absorb from the line the power needed to sustain the torque created by the interaction of the flux and mmf waves. The only way the stator knows what is happening is through the medium of the air-gap flux and rotor-mmf waves. Consequently, if the rotor were replaced by an equivalent one having the same mmf and power factor at the same speed, the stator would be unable to detect the change. Such replacement leads to the idea of referring rotor quantities to the stator, an idea which is of great value in translating flux-mmf considerations into an equivalent circuit for the motor. This concept is especially useful in modeling squirrel-cage rotors for which the identity of the rotor "phase windings" is in no way obvious.

Consider, for example, a coil-wound rotor, wound for the same number of poles and phases as the stator. The number of effective turns per phase in the stator winding is a times the number in the rotor winding. Compare the magnetic effect of this rotor with that of a magnetically equivalent rotor having the same number of turns as the stator. This process is equivalent to referring a transformer secondary to the primary as reflected via the transformer turns ratio. In the case of the induction machine, we will see that in addition to referring the rotor impedance by the square of the

stator/rotor turns ratio, we must take into account the fact that the rotor current is at slip frequency and thus that the rotor inductive reactance is proportionally lowered.

For the same flux and speed, the relation between the voltage \hat{E}_{rotor} induced in the actual rotor and the voltage \hat{E}_{2s} induced in the equivalent rotor is

$$\hat{E}_{2s} = a\hat{E}_{\text{rotor}} \quad (7-7)$$

If the rotors are to be magnetically equivalent, their ampere-turns must be equal, and the relation between the actual rotor current \hat{I}_{rotor} and the current \hat{I}_{2s} in the equivalent rotor must be

$$\hat{I}_{2s} = \frac{\hat{I}_{\text{rotor}}}{a} \quad (7-8)$$

Consequently the relation between the slip-frequency leakage impedance Z_{2s} of the equivalent rotor and the slip-frequency leakage impedance Z_{rotor} of the actual rotor must be

$$Z_{2s} = \frac{\hat{E}_{2s}}{\hat{I}_{2s}} = \frac{a^2 \hat{E}_{\text{rotor}}}{\hat{I}_{\text{rotor}}} = a^2 Z_{\text{rotor}} \quad (7-9)$$

The voltages, currents, and impedances in the equivalent rotor are defined as their values referred to the stator. The thought process is essentially like that involved in referring secondary quantities to the primary in static-transformer theory (see Arts. 2-3 and 2-4). The referring factors are ratios of effective turns and are the same in essence as in transformer theory.

The referring factors must, of course, be known when one is concerned specifically with what is happening in the actual rotor circuits. From the viewpoint of the stator, however, the reflected effects of the rotor show up in terms of the referred quantities, and the theory of both coil-wound and cage rotors can be formulated in terms of the referred rotor. We assume, therefore, that the referred rotor constants are known.

Since the rotor is short-circuited, the phasor relation between the slip-frequency emf \hat{E}_{2s} generated in the reference phase of the referred rotor and the current \hat{I}_{2s} in this phase is

$$\frac{\hat{E}_{2s}}{\hat{I}_{2s}} = Z_{2s} = R_2 + jsX_2 \quad (7-10)$$

where Z_{2s} = slip-frequency rotor leakage impedance per phase referred to stator

R_2 = referred effective resistance

sX_2 = referred leakage reactance at slip frequency

The reactance is expressed in this way because it is proportional to rotor frequency and therefore to slip. Thus X_2 is defined as the value the referred rotor leakage reactance would have at stator frequency. The slip-frequency equivalent circuit of one phase of the referred rotor is shown in Fig. 7-7. This is the equivalent circuit of the rotor as seen in the rotor reference frame.

The stator sees a flux wave and an mmf wave rotating at synchronous speed. This flux wave induces both the slip-frequency rotor voltage \hat{E}_{2s} and the stator counter emf \hat{E}_1 . If it were not for the effect of speed, the referred rotor voltage would equal the stator voltage, since the referred rotor winding is identical with the stator winding. Because the relative speed of the flux wave with respect to the rotor is s times its speed with respect to the stator, the relation between the effective values of stator and rotor emf's is

$$E_{2s} = sE_1 \quad (7-11)$$

The rotor-mmf wave must counteract the mmf of the load component \hat{I}_2 of the stator current, and therefore, since the stator and referred rotor windings have the same number of turns,

$$I_{2s} = I_2 \quad (7-12)$$

Division of Eq. 7-11 by 7-12 then gives

$$\frac{E_{2s}}{I_{2s}} = \frac{sE_1}{I_2} \quad (7-13)$$

When we recognize that torque can be calculated in terms of mmf and the resultant air-gap flux, as in Eq. 4-85, and that equal and opposite torques act on the rotor and stator, we see that the mmf wave created by the stator load current \hat{I}_2 must be space-displaced from the resultant flux wave by the same space angle as that between the rotor-mmf wave and the resultant air-gap flux, namely the torque angle δ . The time-phase angle between the stator voltage \hat{E}_1 and the stator load current \hat{I}_2 therefore must equal the corresponding time angle for the rotor voltage \hat{E}_{2s} and current \hat{I}_{2s} , namely, the rotor power-factor angle ϕ_2 . The fact that the rotor and stator torques are in opposition is accounted for, since the rotor current \hat{I}_{2s} is

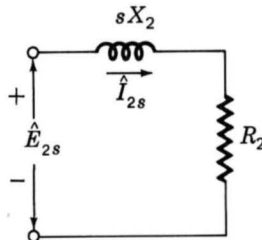


Fig. 7-7. Rotor equivalent circuit for a polyphase induction motor at slip frequency.

created by the rotor emf \hat{E}_{2s} , whereas the stator current \hat{I}_2 is flowing against the stator counter emf \hat{E}_1 . Therefore Eq. 7-13 is true, not only for effective values, but also in a phasor sense. Through substitution of Eq. 7-10 in the phasor equivalent of Eq. 7-13 we have

$$\frac{s\hat{E}_1}{\hat{I}_2} = \frac{\hat{E}_{2s}}{\hat{I}_{2s}} = R_2 + jsX_2 \quad (7-14)$$

Division by s then gives

$$\frac{\hat{E}_1}{\hat{I}_2} = \frac{R_2}{s} + jX_2 \quad (7-15)$$

That is, the stator sees magnetic conditions in the air gap which result in induced stator voltage \hat{E}_1 and stator load current \hat{I}_2 , and by Eq. 7-15 these conditions are identical with the result of connecting an impedance $R_2/s + jX_2$ across \hat{E}_1 . Consequently, the effect of the rotor can be incorporated in the equivalent circuit of Fig. 7-6 by this impedance connected across the terminals ab . The final result is shown in Fig. 7-8. The combined effect of shaft load and rotor resistance appears as a reflected resistance R_2/s , a function of slip and therefore of the mechanical load. The current in the reflected rotor impedance equals the load component \hat{I}_2 of stator current; the voltage across this impedance equals the stator voltage \hat{E}_1 . Note that when rotor currents and voltages are reflected into the stator, their frequency is also changed to stator frequency. All rotor electrical phenomena, when viewed from the stator, become stator-frequency phenomena, because the stator winding simply sees mmf and flux waves traveling at synchronous speed.

7-4 ANALYSIS OF THE EQUIVALENT CIRCUIT

Among the important performance aspects in the steady state are the variations of current, speed, and losses as the load-torque requirements change,

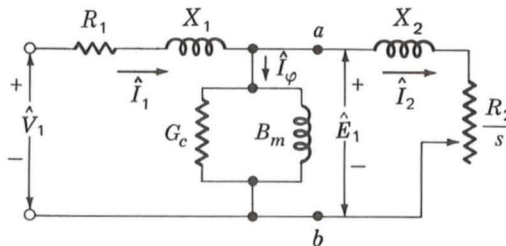


Fig. 7-8. Equivalent circuit for a polyphase induction motor.

as well as the starting torque, and the maximum torque. All these characteristics can be determined from the equivalent circuit.

The equivalent circuit shows that the total power P_{g1} transferred across the air gap from the stator is

$$P_{g1} = q_1 I_2^2 \frac{R_2}{s} \quad (7-16)$$

where q_1 is the number of stator phases. The total rotor I^2R loss is evidently

$$\text{Rotor } I^2R \text{ loss} = q_1 I_2^2 R_2 \quad (7-17)$$

The internal mechanical power P developed by the motor is therefore

$$P = P_{g1} - \text{rotor } I^2R \text{ loss} = q_1 I_2^2 \frac{R_2}{s} - q_1 I_2^2 R_2 \quad (7-18)$$

equivalently
$$P = q_1 I_2^2 R_2 \frac{1-s}{s} \quad (7-19)$$

or
$$P = (1-s)P_{g1} \quad (7-20)$$

We see, then, that of the total power delivered to the rotor the fraction $1-s$ is converted to mechanical power and the fraction s is dissipated as rotor-circuit I^2R loss. From this it is evident that an induction motor operating at high slip is an inefficient device. When power aspects are to be emphasized, the equivalent circuit can be redrawn in the manner of Fig. 7-9. The internal mechanical power per stator phase is equal to the power absorbed by the resistance $R_2(1-s)/s$.

The internal electromagnetic torque T corresponding to the internal power P can be obtained by recalling that mechanical power equals torque times angular velocity. Thus, when ω_s is the synchronous angular velocity of the rotor in mechanical radians per second,

$$P = (1-s)\omega_s T \quad (7-21)$$

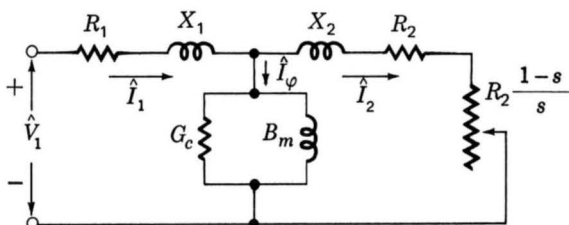


Fig. 7-9. Alternative form of equivalent circuit.

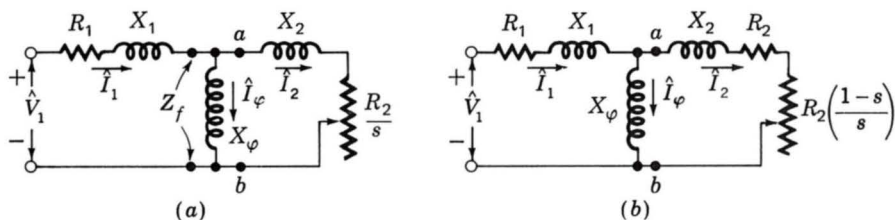


Fig. 7-10. Equivalent circuits.

with T in newton-meters. Use of Eq. 7-19 leads to

$$T = \frac{1}{\omega_s} q_1 I_2^2 \frac{R_2}{s} \quad (7-22)$$

the synchronous angular velocity ω_s being given by

$$\omega_s = \frac{4\pi f}{\text{poles}} \quad (7-23)$$

The internal torque T and internal power P are not the output values available at the shaft because friction, windage, and stray load losses remain to be accounted for. It is obviously correct to subtract friction and windage effects from T or P , and it is generally assumed that stray load effects can be subtracted in the same manner. The final remainder is available in mechanical form at the shaft for useful work.

In static-transformer theory, analysis of the equivalent circuit is often simplified by either neglecting the exciting branch entirely or adopting the approximation of moving it out directly to the primary terminals. Such approximations are not permissible for the induction motor under normal running conditions because the presence of the air gap results in a much lower magnetizing impedance and correspondingly a much higher exciting current—30 to 50 percent of full-load current—and because the leakage reactances are also necessarily higher. Some simplification of the induction-motor equivalent circuit results if the shunt conductance G_c is omitted and the associated core-loss effect is deducted from T or P at the same time that friction, windage, and stray load effects are subtracted. The equivalent circuit then becomes that of Fig. 7-10a or b, and the error introduced is negligible. Such a procedure also has an advantage during motor testing, for then the no-load core loss need not be separated from friction and windage. These last circuits are used in subsequent discussions.

EXAMPLE 7-1

A three-phase Y-connected 220-V (line-to-line) 10-hp 60-Hz six-pole induction motor has the following constants in ohms per phase referred to

the stator:

$$\begin{aligned} R_1 &= 0.294 & R_2 &= 0.144 \\ X_1 &= 0.503 & X_2 &= 0.209 & X_\phi &= 13.25 \end{aligned}$$

The total friction, windage, and core losses may be assumed to be constant at 403 W, independent of load.

For a slip of 2.00 percent, compute the speed, output torque and power, stator current, power factor, and efficiency when the motor is operated at rated voltage and frequency. Neglect the impedance of the source.

Solution

The impedance Z_f (Fig. 7-10a) represents physically the per phase impedance presented to the stator by the air-gap field, both the reflected effect of the rotor and the effect of the exciting current being included therein. From Fig. 7-10a

$$Z_f = R_f + jX_f = \left(\frac{R_2}{s} + jX_2 \right) \text{ in parallel with } jX_\phi$$

Substitution of numerical values gives, for $s = 0.02$,

$$R_f + jX_f = 5.41 + j3.11$$

$$R_1 + jX_1 = 0.29 + j0.50$$

$$\text{Sum} = 5.70 + j3.61 = 6.75 \angle 32.4^\circ \Omega$$

$$\text{Applied voltage to neutral} = \frac{220}{\sqrt{3}} = 127 \text{ V}$$

$$\text{Stator current } I_1 = \frac{127}{6.75} = 18.8 \text{ A}$$

$$\text{Power factor} = \cos 32.4^\circ = 0.844 \text{ lagging}$$

$$\text{Synchronous speed} = \frac{2f}{\text{poles}} = \frac{120}{6} = 20 \text{ r/s} = 1200 \text{ r/min}$$

$$\omega_s = 2\pi(20) = 125.6 \text{ rad/s}$$

$$\text{Rotor speed} = (1 - s)(\text{synchronous speed}) = 0.98(1200) = 1176 \text{ r/min}$$

From Eq. 7-16,

$$P_{g1} = q_1 I_2^2 \frac{R_2}{s} = q_1 I_1^2 R_f = 3(18.8)^2(5.41) = 5740 \text{ W}$$

From Eqs. 7-16 and 7-19 the internal mechanical power is

$$P = 0.98(5740) = 5630 \text{ W}$$

Deducting losses of 403 W gives

$$\text{Output power} = 5630 - 403 = 5230 \text{ W} = 7.00 \text{ hp}$$

$$\text{Output torque} = \frac{\text{output power}}{\omega_{\text{rotor}}} = \frac{5230}{0.98(125.6)} = 42.5 \text{ N} \cdot \text{m} = 31.4 \text{ lb} \cdot \text{ft}$$

The efficiency is calculated from the losses.

$$\begin{aligned} \text{Total stator } I^2R \text{ loss} &= 3(18.8)^2(0.294) = 312 \text{ W} \\ \text{Rotor } I^2R \text{ loss (from Eq. 7-17)} &= 0.02(5740) = 115 \\ \text{Friction, windage, and core losses} &= \underline{403} \\ \text{Total losses} &= 830 \text{ W} \\ \text{Output} &= \underline{5230} \\ \text{Input} &= 6060 \text{ W} \end{aligned}$$

$$\frac{\text{Losses}}{\text{Input}} = \frac{830}{6060} = 0.137$$

$$\text{Efficiency} = 1.000 - 0.137 = 0.863 = 86.3\%$$

The complete performance characteristics of the motor can be determined by repeating these calculations for other assumed values of slip.

7-5 TORQUE AND POWER BY USE OF THEVENIN'S THEOREM

When torque and power relations are to be emphasized, considerable simplification results from application of Thevenin's network theorem to the induction-motor equivalent circuit.

In its general form, Thevenin's theorem permits the replacement of any network of linear circuit elements and constant-phasor voltage sources, as viewed from two terminals a and b (Fig. 7-11a), by a single-phasor voltage source \hat{V}_s in series with a single impedance Z (Fig. 7-11b). The voltage \hat{V}_s is that appearing across terminals a and b of the original network when these terminals are open-circuited; the impedance Z is that viewed from the same terminals when all voltage sources within the network are short-circuited. For application to the induction-motor equivalent circuit, points a and b are taken as those so designated in Fig. 7-10a and b. The equivalent circuit then assumes the forms given in Fig. 7-12 where Thevenin's theorem has been used to transform the network to the left of points a and b into an equivalent voltage source \hat{V}_{1a} in series with an equivalent impedance $R_{e1} + jX_{e1}$.

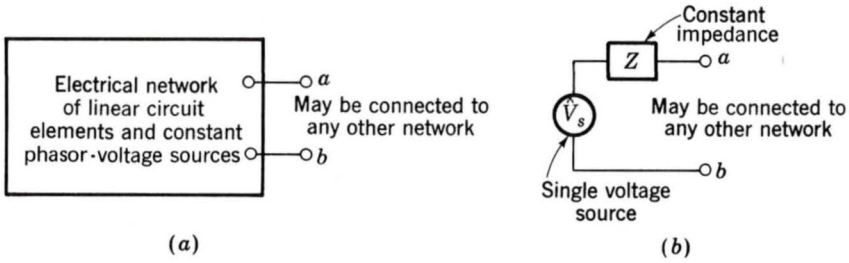


Fig. 7-11. (a) General linear network and (b) its equivalent at terminals ab by Thevenin's theorem.

According to Thevenin's theorem, the equivalent source voltage \hat{V}_{1a} is the voltage that would appear across terminals a and b of Fig. 7-10 with the rotor circuits open and is

$$\hat{V}_{1a} = \hat{V}_1 - \hat{I}_0(R_1 + jX_1) = \hat{V}_1 \frac{jX_\phi}{R_1 + jX_{11}} \quad (7-24)$$

where \hat{I}_0 is the zero-load exciting current and

$$X_{11} = X_1 + X_\phi \quad (7-25)$$

is the self-reactance of the stator per phase, which very nearly equals the reactive component of the zero-load motor impedance. For most induction motors, negligible error results from neglecting the stator resistance in Eq. 7-24. The Thevenin-equivalent stator impedance $R_{e1} + jX_{e1}$ is the impedance between terminals a and b of Fig. 7-10 viewed toward the source with the source voltage short-circuited and therefore is

$$R_{e1} + jX_{e1} = (R_1 + jX_1) \text{ in parallel with } jX_\phi \quad (7-26)$$

From the Thevenin-equivalent circuit (Fig. 7-12) and the torque expression (Eq. 7-22)

$$T = \frac{1}{\omega_s} \frac{q_1 V_{1a}^2 (R_2/s)}{(R_{e1} + R_2/s)^2 + (X_{e1} + X_2)^2} \quad (7-27)$$

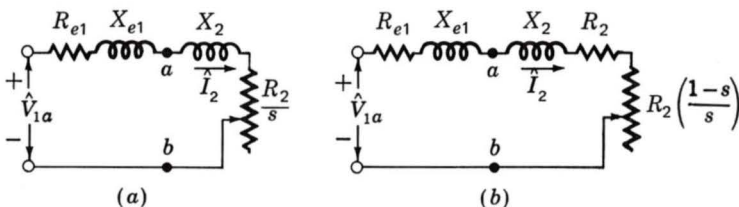


Fig. 7-12. Induction-motor equivalent circuits simplified by Thevenin's theorem.

The general shape of the torque-speed or torque-slip curve with the motor connected to a constant-voltage, constant-frequency source is shown in Figs. 7-13 and 7-14.

In normal motor operation, the rotor revolves in the direction of rotation of the magnetic field produced by the stator currents, the speed is between zero and synchronous speed, and the corresponding slip is between 1.0 and 0, labeled "Motor region" in Fig. 7-13. Motor starting conditions are those of $s = 1.0$.

To obtain physical operation in the region of s greater than 1, the motor must be driven backward, against the direction of rotation of its magnetic field, by a source of mechanical power capable of counteracting the internal torque T . The chief practical usefulness of this region is in bringing motors to a quick stop by a method called *plugging*. By interchanging two stator leads in a three-phase motor, the phase sequence, and hence the direction of rotation of the magnetic field, is reversed suddenly; the motor comes to a stop under the influence of torque T and is disconnected from the line before it can start in the other direction. Accordingly, the region from $s = 1.0$ to $s = 2.0$ is labeled "Braking region" in Fig. 7-13.

The induction machine will operate as a generator if its stator terminals are connected to a constant-frequency voltage source and its rotor is driven above synchronous speed by a prime mover, as shown in Fig. 7-13. The source fixes the synchronous speed and supplies the reactive power input required to excite the air-gap magnetic field. The slip then is negative.

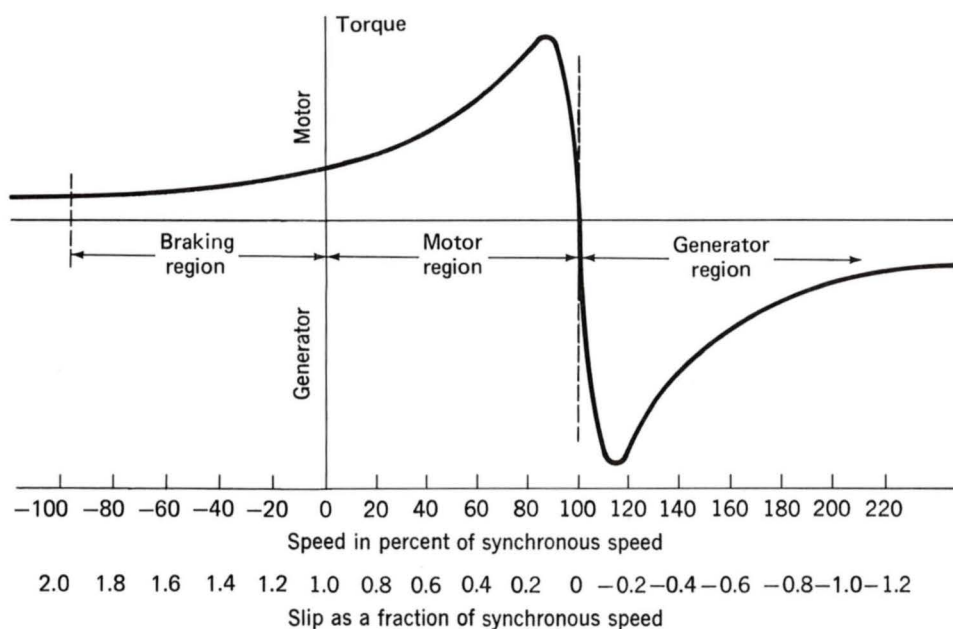


Fig. 7-13. Induction-machine torque-slip curve showing braking, motor, and generator regions.

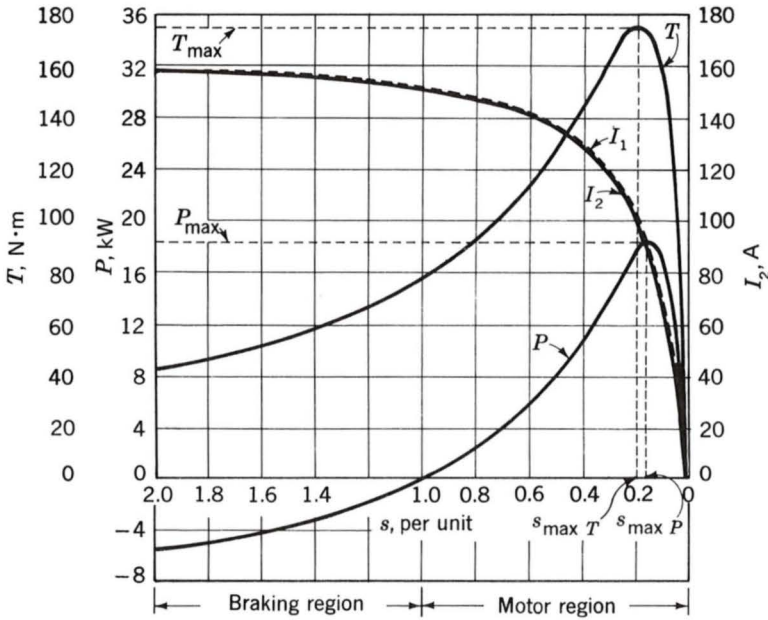


Fig. 7-14. Computed torque, power, and current curves for 10-hp motor in Examples 7-1 and 7-2.

One interesting application is that of an induction generator connected to a power system and driven by a wind turbine.

The *maximum internal*, or *breakdown*, torque T_{\max} , indicated in Fig. 7-14, can be obtained readily from circuit considerations. Internal torque is a maximum when the power delivered to R_2/s in Fig. 7-12a is a maximum. It can be shown that this power will be greatest when the impedance of R_2/s equals the magnitude of the impedance $R_2 + j(X_{e1} + X_2)$ between it and the constant voltage \hat{V}_{1a} , or at a value $s_{\max T}$ of slip for which

$$\frac{R_2}{s_{\max T}} = \sqrt{R_{e1}^2 + (X_{e1} + X_2)^2} \quad (7-28)$$

The slip $s_{\max T}$ at maximum torque is therefore

$$s_{\max T} = \frac{R_2}{\sqrt{R_{e1}^2 + (X_{e1} + X_2)^2}} \quad (7-29)$$

and the corresponding torque is, from Eq. 7-27,

$$T_{\max} = \frac{1}{\omega_s} \left[\frac{0.5q_1 V_{1a}^2}{R_{e1} + \sqrt{R_{e1}^2 + (X_{e1} + X_2)^2}} \right] \quad (7-30)$$

EXAMPLE 7-2

For the motor of Example 7-1, determine (a) the load component I_2 of the stator current, the internal torque T , and the internal power P for a slip $s = 0.03$; (b) the maximum internal torque and the corresponding speed; and (c) the internal starting torque and the corresponding stator load current I_2 .

Solution

First reduce the circuit to its Thevenin-theorem form. From Eq. 7-24, $V_{1a} = 122.3$; from Eq. 7-26, $R_{e1} + jX_{e1} = 0.273 + j0.490$.

(a) At $s = 0.03$, $R_2/s = 4.80$. Then, from Fig. 7-12a,

$$I_2 = \frac{V_{1a}}{\sqrt{(R_{e1} + R_2/s)^2 + (X_{e1} + X_2)^2}} = \frac{122.3}{\sqrt{(5.07)^2 + (0.699)^2}} = 23.9 \text{ A}$$

From Eq. 7-22

$$T = \frac{1}{125.6} (3) (23.9)^2 (4.80) = 65.5 \text{ N} \cdot \text{m}$$

From Eq. 7-19

$$P = 3(23.9)^2 (4.80) (0.97) = 7970 \text{ W}$$

Data for the curves of Fig. 7-14 were computed by repeating these calculations for a number of assumed values of s .

(b) At the maximum-torque point, from Eq. 7-29,

$$s_{\max T} = \frac{0.144}{\sqrt{(0.273)^2 + (0.699)^2}} = \frac{0.144}{0.750} = 0.192$$

$$\text{Speed at } T_{\max} = (1 - 0.192)(1200) = 970 \text{ r/min}$$

From Eq. 7-30

$$T_{\max} = \frac{1}{125.6} \frac{0.5(3)(122.3)^2}{0.273 + 0.750} = 175 \text{ N} \cdot \text{m}$$

(c) At starting, $s = 1$. Therefore,

$$\frac{R_2}{s} = R_2 = 0.144 \quad R_{e1} + \frac{R_2}{s} = 0.417$$

$$I_{2, \text{start}} = \frac{122.3}{\sqrt{(0.417)^2 + (0.699)^2}} = 150.5 \text{ A}$$

From Eq. 7-22

$$T_{\text{start}} = \frac{1}{125.6} (3) (150.5)^2 (0.144) = 78.0 \text{ N} \cdot \text{m}$$

A conventional induction motor with a squirrel-cage rotor is substantially a constant-speed motor having about 5 percent drop in speed from no load to full load. Induction-motor-speed variation can be obtained by using a wound-rotor motor and inserting external resistance in the rotor circuit. In the normal operating range, the external resistance simply increases the rotor impedance, necessitating a higher slip for a desired rotor mmf and torque. The influence of increased rotor resistance on the torque-speed characteristic is shown by the dashed curves in Fig. 7-15. Variation of starting torque with rotor resistance can be seen from these curves by noting the variation of the zero-speed ordinates.

Notice from Eqs. 7-29 and 7-30 that the slip at maximum torque is directly proportional to rotor resistance R_2 , but the value of the maximum torque is independent of R_2 . When R_2 is increased by inserting external resistance in the rotor of a wound-rotor motor, the maximum internal torque

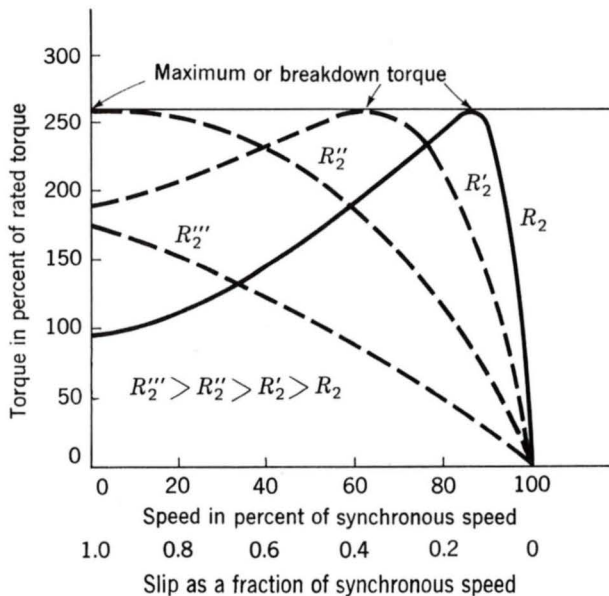


Fig. 7-15. Induction-motor torque-slip curves showing effect of changing rotor-circuit resistance.

is therefore unaffected but the speed at which it occurs can be directly controlled.

In applying the induction-motor equivalent circuit, the idealizations on which it is based should be kept in mind. This is particularly necessary when investigations are carried out over a wide speed range, as in motor-starting problems. Saturation under the heavy inrush currents associated with starting has a significant effect on the motor reactances. Moreover, the rotor currents are at slip frequency, which, of course, varies from stator frequency at zero speed to a low value at full-load speed. The current distribution in the rotor conductors and hence the rotor resistance may vary very significantly over this range. Errors from these causes can be kept to a minimum by using equivalent-circuit constants determined by simulating the proposed operating conditions as closely as possible.[†]

7-6 PERFORMANCE CALCULATIONS FROM NO-LOAD AND BLOCKED-ROTOR TESTS

The data needed for computing the performance of a polyphase induction motor under load can be obtained from the results of a no-load test, a blocked-rotor test, and measurements of the dc resistances of the stator windings. Stray load losses, which must be taken into account when accurate values of efficiency are to be calculated, can also be measured by tests which do not require loading the motor. The stray-load-loss tests are not described here, however.[‡]

Like the open-circuit test on a transformer, the *no-load test* on an induction motor gives information with respect to exciting current and no-load losses. The test is ordinarily taken at rated frequency and with balanced polyphase voltages applied to the stator terminals. Readings are taken at rated voltage, after the motor has been running long enough for the bearings to be properly lubricated. The total rotational loss at rated voltage and frequency under load usually is considered to be constant and equal to its no-load value.

At no load, the rotor current is only the very small value needed to produce sufficient torque to overcome friction and windage. The no-load rotor I^2R loss therefore is negligibly small. Unlike that of a transformer, whose no-load primary I^2R loss is negligible, the no-load stator I^2R loss of an induction motor may be appreciable because of its larger exciting current. Neglecting rotor I^2R losses, the rotational loss P_R for normal running conditions is

[†]See, for instance, R. F. Horrell and W. E. Wood, "A Method of Determining Induction Motor Speed-Torque-Current Curves from Reduced Voltage Tests," *Trans. AIEE*, 73(3):670-674 (1954).

[‡]For information concerning test methods, see *IEEE Standard Test Procedures for Polyphase Induction Motors and Generators*, IEEE Standard 112, 1984, Institute of Electrical and Electronics Engineers, Inc.

$$P_R = P_{nl} - q_1 I_{nl}^2 R_1 \quad (7-31)$$

where P_{nl} = total polyphase power input

I_{nl} = current per phase

q_1 = number of stator phases

R_1 = stator resistance per phase

Because the slip at no load is very small, the reflected rotor resistance R_2/s_{nl} is very large. The parallel combination of rotor and magnetizing branches then becomes jX_ϕ shunted by a very high resistance, and the reactance of this parallel combination therefore very nearly equals X_ϕ . Consequently the apparent reactance X_{nl} measured at the stator terminals at no load very nearly equals $X_1 + X_\phi$, which is the self-reactance X_{11} of the stator; i.e.,

$$X_{11} = X_1 + X_\phi = X_{nl} \quad (7-32)$$

The self-reactance of the stator can therefore be determined from the instrument readings at no load. For a three-phase machine considered to be Y-connected, the magnitude of the no-load impedance Z_{nl} per phase is

$$Z_{nl} = \frac{V_{nl}}{\sqrt{3} I_{nl}} \quad (7-33)$$

where V_{nl} is the line-to-line terminal voltage in the no-load test. The no-load resistance R_{nl} is

$$R_{nl} = \frac{P_{nl}}{3 I_{nl}^2} \quad (7-34)$$

where P_{nl} is the total three-phase power input at no load. The no-load reactance X_{nl} then is

$$X_{nl} = \sqrt{Z_{nl}^2 - R_{nl}^2} \quad (7-35)$$

Usually the no-load power factor is about 0.1, so that the no-load reactance very nearly equals the no-load impedance.

Like the short-circuit test on a transformer, the *blocked-rotor test* on an induction motor gives information with respect to the leakage impedances. The rotor is blocked so that it cannot rotate, and balanced polyphase voltages are applied to the stator terminals. Sometimes the blocked-rotor torque also is measured.

The equivalent circuit for blocked-rotor conditions is identical to that of a short-circuited transformer. An induction motor is more complicated than a transformer, however, because its leakage impedance may be af-

ected by magnetic saturation of the leakage-flux paths and by rotor frequency. The blocked impedance may also be affected by rotor position, although this effect generally is small with cage rotors. The guiding principle is that the blocked-rotor test should be taken under conditions of current and rotor frequency approximately the same as those existing in the operating condition for which the performance is later to be calculated. For example, if one is interested in the characteristics at slips near unity, as in starting, the blocked-rotor test should be taken at normal frequency and with currents near the values encountered in starting. If, however, one is interested in the normal running characteristics, the blocked-rotor test should be taken at a reduced voltage which results in about rated current; the frequency also should be reduced, since the values of rotor effective resistance and leakage inductance at the low rotor frequencies corresponding to small slips may differ appreciably from their values at normal frequency, particularly with double-cage or deep-bar rotors, as discussed in Art. 8-1.

The IEEE Test Procedure suggests a blocked-rotor test frequency of 25 percent of rated frequency. The total leakage reactance at normal frequency can be obtained from this test value by considering the reactance to be proportional to frequency. The effects of frequency often are negligible for normal motors of less than 25-hp rating, and the blocked impedance can then be measured directly at normal frequency. The importance of maintaining test currents near their rated value stems from the fact that these leakage reactances are significantly affected by saturation.

If exciting current is neglected, the blocked-rotor reactance X_{bl} , corrected to normal frequency, equals the sum of the normal-frequency stator and rotor leakage reactances X_1 and X_2 . The performance of the motor is affected relatively little by the way in which the total leakage reactance $X_1 + X_2$ is distributed between the stator and rotor. The IEEE Test Procedure recommends the empirical distribution shown in Table 7-1.

TABLE 7-1
EMPIRICAL DISTRIBUTION OF LEAKAGE REACTANCES
IN INDUCTION MOTORS

Motor class	Description	Fraction of $X_1 + X_2$	
		X_1	X_2
A	Normal starting torque, normal starting current	0.5	0.5
B	Normal starting torque, low starting current	0.4	0.6
C	High starting torque, low starting current	0.3	0.7
D	High starting torque, high slip	0.5	0.5
Wound rotor		0.5	0.5

The magnetizing reactance X_φ now can be determined from the no-load test and the value of X_1 ; thus

$$X_\varphi = X_{nl} - X_1 \quad (7-36)$$

The stator resistance R_1 can be considered equal to its dc value. The rotor resistance then can be determined as follows. From the blocked-rotor test, the blocked resistance R_{bl} can be computed by means of a relation similar to Eq. 7-34. The difference between the blocked resistance and the stator resistance then can be determined from the test data. Denoting this resistance R , we have

$$R = R_{bl} - R_1 \quad (7-37)$$

From the equivalent circuit, with $s = 1$, the resistance R is the resistance of the combination of $R_2 + jX_2$ in parallel with jX_φ . For this parallel combination

$$R = R_2 \frac{X_\varphi^2}{R_2^2 + X_{22}^2} \approx R_2 \left(\frac{X_\varphi}{X_{22}} \right)^2 \quad (7-38)$$

where $X_{22} = X_2 + X_\varphi$ is the self-reactance of the rotor. If X_{22} is greater than $10R_2$, as is usually the case, less than 1 percent error results from use of the approximate form of Eq. 7-38. Substitution of this approximate form in Eq. 7-37 and solving for R_2 then give

$$R_2 = R \left(\frac{X_{22}}{X_\varphi} \right)^2 = (R_{bl} - R_1) \left(\frac{X_{22}}{X_\varphi} \right)^2 \quad (7-39)$$

All the equivalent-circuit constants have now been determined, and the motor performance under load can be computed.

EXAMPLE 7-3

The following test data apply to a 7.5-hp three-phase 220-V 19-A 60-Hz four-pole induction motor with a double-squirrel-cage rotor of the high-starting-torque low-starting-current type (design class C):

Test 1: No-load test at 60 Hz

Applied voltage $V = 219$ V line to line

Average line current $I_{nl} = 5.70$ A

Power $P_{nl} = 380$ W

Test 2: Blocked-rotor test at 15 Hz

$$V = 26.5 \text{ V} \quad I = 18.57 \text{ A} \quad P_{bl} = 875 \text{ W}$$

Test 3: Average dc resistance per stator phase (measured immediately after test 2)

$$R_1 = 0.262 \text{ } \Omega/\text{phase (Y connection assumed)}$$

Test 4: Blocked-rotor test at 60 Hz

$$V = 212 \text{ V} \quad I = 83.3 \text{ A} \quad P_{bl} = 20,100 \text{ W}$$

$$\text{Measured starting torque } T_{\text{start}} = 54.6 \text{ lb} \cdot \text{ft}$$

(a) Compute the no-load rotational loss and the equivalent-circuit constants applying to the normal running conditions. Assume the same temperature as in test 3.

(b) Compute the internal starting torque from the input measurements of test 4. Assume the same temperature as in test 3.

Solution

(a) From tests 1 and 3 and Eq. 7-31

$$P_R = 380 - 3(5.70)^2(0.262) = 354 \text{ W}$$

From test 1 and Eqs. 7-33 and 7-35

$$Z_{nl} = \frac{219}{\sqrt{3}(5.70)} = 22.2 \text{ } \Omega/\text{phase Y}$$

$$R_{nl} = \frac{380}{3(5.70)^2} = 3.9 \text{ } \Omega \quad X_{nl} = 21.8 \text{ } \Omega$$

The blocked-rotor test at reduced frequency and rated current reproduces approximately normal running conditions in the rotor. From test 2

$$Z'_{bl} = \frac{26.5}{\sqrt{3}(18.57)} = 0.825 \text{ } \Omega/\text{phase at 15 Hz}$$

$$R'_{bl} = \frac{675}{3(18.57)^2} = 0.654 \text{ } \Omega \quad X'_{bl} = 0.503 \text{ } \Omega \text{ at 15 Hz}$$

where the primes indicate 15-Hz values. The blocked reactance referred to normal frequency then is

$$X_{bl} = \frac{60}{15}(0.503) = 2.01 \Omega/\text{phase at 60 Hz}$$

According to Table 7-1,

$$X_1 = 0.3(2.01) = 0.603 \Omega/\text{phase} \quad X_2 = 0.7(2.01) = 1.407 \Omega/\text{phase}$$

and by Eq. 7-36

$$X_\phi = 21.8 - 0.6 = 21.2 \Omega/\text{phase}$$

From test 3 and Eqs. 7-37 and 7-39

$$R = 0.654 - 0.262 = 0.392 \quad R_2 = 0.392 \left(\frac{22.6}{21.2} \right)^2 = 0.445 \Omega/\text{phase}$$

The constants of the equivalent circuit for small values of slip have now been calculated.

(b) The internal starting torque can be computed from the input measurements in test 4. From the power input and stator I^2R losses, the air-gap power P_{g1} is

$$P_{g1} = 20,100 - 3(83.3)^2(0.262) = 14,650 \text{ W}$$

Synchronous speed $\omega_s = 188.5 \text{ rad/s}$, and

$$T_{\text{start}} = \frac{14,650}{188.5} = 77.6 \text{ N} \cdot \text{m} = 57.3 \text{ lb} \cdot \text{ft}$$

The test value, $T_{\text{start}} = 54.6 \text{ lb} \cdot \text{ft}$, is a few percent less than the calculated value because the calculations do not account for the power absorbed in stator core loss and in stray load losses.

7-7 SUMMARY

In a polyphase induction motor, slip-frequency currents are induced in the rotor windings as the rotor slips past the synchronously rotating stator flux wave. These rotor currents in turn produce a flux wave which rotates in synchronism with the stator flux wave; the torque stems from the interaction of these two flux waves. For increased load on the motor, the rotor speed decreases, resulting in larger slip and increased induced rotor currents, and greater torque.

Examination of the flux-mmF interactions in a polyphase induction motor shows that, electrically, the machine is a generalized transformer.

The synchronously rotating air-gap flux wave in the induction machine is the counterpart of the mutual core flux in the transformer. The rotating field induces emf's of stator frequency in the stator windings and of slip frequency in the rotor windings for all rotor speeds other than synchronous speed. Thus, the induction machine transforms voltages and at the same time changes frequency. When viewed from the stator, all rotor electrical and magnetic phenomena are transformed to stator frequency. The rotor mmf reacts on the stator windings in the same manner as the mmf of the secondary current in a transformer reacts on the primary.

Pursuit of this line of reasoning leads to equivalent circuits for induction machines. The effects of saturation on the equivalent circuit are less serious than in the corresponding steady-state circuit for synchronous machines. This is largely because, as in the transformer, the performance is determined to a considerably greater extent by the leakage impedances than by the magnetizing impedance. Care must be taken in both testing and analysis, however, to reflect the effects of saturation on leakage reactances as well as of nonuniformity of current distribution on rotor resistance.

One of the salient facts affecting induction-motor applications is that the slip at which maximum torque occurs can be controlled by varying the rotor resistance. A high rotor resistance gives optimum starting conditions but poor running performance. A low rotor resistance, however, may result in unsatisfactory starting conditions. The design of a squirrel-cage motor is therefore quite likely to be a compromise.

For applications requiring a substantially constant speed without excessively severe starting conditions, the squirrel-cage motor usually is unrivaled because of its ruggedness, simplicity, and relatively low cost. Its only disadvantage is its relatively low power factor (about 0.85 to 0.90 at full load for four-pole 60-Hz motors and considerably lower at light loads and for lower-speed motors). The low power factor is a consequence of the fact that all the excitation must be supplied by lagging reactive power taken from the ac source. At speeds below about 500 r/min and ratings above about 50 hp or at medium speeds (500 to 900 r/min) and ratings above about 500 hp, a synchronous motor may cost less than an induction motor.

In the next chapter issues of the dynamics and control of induction motors are discussed. The use of induction motors in variable-speed applications is considered. Marked improvement in the starting performance with relatively little sacrifice in running performance can be built into a squirrel-cage motor by using a deep-bar or double-cage rotor whose effective resistance increases with slip. A wound-rotor motor can be used for very severe starting conditions or when speed control by rotor resistance is required. A wound-rotor motor is more expensive than a squirrel-cage motor. Variable-frequency solid-state motor drives lend considerable flexibility to the application of induction motors in variable-speed applications.

PROBLEMS

7-1. The nameplate on a 460-V 50-hp 60-Hz four-pole induction motor indicates that its speed at rated load is 1760 r/min. Assume the motor to be operating at rated load.

- (a) What is the slip of the rotor?
- (b) What is the frequency of the rotor currents?
- (c) What is the angular velocity of the stator field with respect to the stator? With respect to the rotor?
- (d) What is the angular velocity of the rotor field with respect to the rotor? With respect to the stator?

7-2. Stray leakage fields will induce rotor-frequency voltages in a pickup coil mounted along the shaft of an induction motor. Measurements of the frequency of these induced voltages can be used to determine the rotor speed.

- (a) What is the rotor speed in revolutions per minute of a 60-Hz six-pole induction motor if 0.95-Hz voltages are measured?
- (b) Calculate the frequency of the voltage which will be induced when a two-pole 50-Hz induction motor is operating at a slip of 3 percent. What is the corresponding rotor speed in revolutions per minute?

7-3. A three-phase induction motor runs at almost 900 r/min at no load and 873 r/min at full load when supplied with power from a 60-Hz three-phase source.

- (a) How many poles has the motor?
- (b) What is the percent slip at full load?
- (c) What is the corresponding frequency of the rotor currents?
- (d) What is the corresponding speed of the rotor field with respect to the rotor? With respect to the stator?
- (e) What speed would the rotor have at a slip of 10 percent?
- (f) What is the rotor frequency at this speed?
- (g) Repeat part (d) for a slip of 10 percent.

7-4. Linear induction motors have been proposed for a variety of applications including high-speed ground transportation. A linear motor based on the induction-motor principle consists of a car riding on a track. The track is a developed squirrel-cage winding, and the car, which is 16 ft long and $3\frac{1}{2}$ ft wide, has a developed three-phase 16-pole winding. The centerline distance between adjacent poles is $16/16 = 1$ ft. Power at 60 Hz is fed to the car from arms extending through slots to rails below ground level.

- (a) What is the synchronous speed in miles per hour?
- (b) Will the car reach this speed? Explain your answer.

- (c) To what slip frequency does a car speed of 75 mi/h correspond? What is the frequency of currents induced in the track when the car is traveling at this speed?

7-5. Describe the effect on the torque-speed characteristic of an induction motor produced by (a) halving the applied voltage and (b) halving both the applied voltage and the frequency. Sketch the associated torque-speed characteristics in their approximate relative positions with respect to the rated-voltage rated-frequency characteristic. Neglect the effects of stator resistance and leakage reactance.

7-6. Figure 7-16 shows a three-phase wound-rotor induction machine whose shaft is rigidly coupled to the shaft of a three-phase synchronous motor. The terminals of the three-phase rotor winding of the induction machine are brought out to slip rings as shown. The induction machine is driven by the synchronous motor at the proper speed and in the proper direction of rotation so that three-phase 120-Hz voltages are available at the slip rings. The induction machine has a six-pole stator winding.

- (a) How many poles must the rotor winding of the induction machine have?
- (b) If the stator field in the induction machine rotates in a clockwise direction, what must the direction of rotation of its rotor be?
- (c) What must the speed be in revolutions per minute?
- (d) How many poles must the synchronous motor have?

7-7. The system shown in Fig. 7-16 is used to convert balanced 60-Hz voltages to other frequencies. The synchronous motor has two poles and drives the interconnecting shaft in the clockwise direction. The induction machine has 12 poles, and its stator windings are connected to the lines to produce a counterclockwise rotating field (in the opposite direction to the

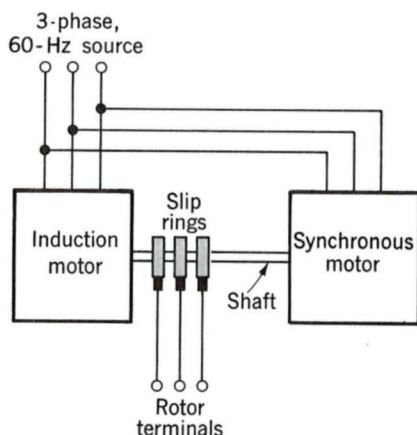


Fig. 7-16. Interconnected induction and synchronous machines (Probs. 7-6 and 7-7).

synchronous motor). The machine has a wound rotor whose terminals are brought out through slip rings.

- (a) At what speed does the motor run?
- (b) What is the frequency of the rotor voltages in the induction machine?

7-8. A three-phase eight-pole 60-Hz 4160-V 1000-hp squirrel-cage induction motor has the following equivalent-circuit constants in ohms per phase Y referred to the stator:

$$R_1 = 0.295 \quad R_2 = 0.277 \quad X_1 = 2.61 \quad X_2 = 3.24 \quad X_\phi = 61.3$$

Determine the changes in these constants which will result from the following proposed design modifications. Consider each modification separately.

- (a) Replace the stator winding with an otherwise identical winding with a wire size whose cross-sectional area is increased by 4 percent.
- (b) Decrease the inner diameter of the stator laminations such that the air gap is decreased by 15 percent.
- (c) Replace the aluminum rotor bars (conductivity 3.5×10^7 mhos/m) with copper bars (conductivity 5.8×10^7 mhos/m).
- (d) The stator winding, originally connected in Y for 4160-V operation, is reconnected in Δ for 2.4-kV operation.

7-9. A three-phase Y-connected 480-V (line-to-line) 30-hp 60-Hz four-pole induction motor has the following equivalent-circuit constants in ohms per phase referred to the stator:

$$R_1 = 0.21 \quad R_2 = 0.20 \quad X_1 = 1.2 \quad X_2 = 1.1 \quad X_\phi = 39$$

The total friction, windage, and core losses may be assumed constant at 1340 W. The motor is connected directly to a 480-V source. Compute the speed, shaft output torque in newton-meters, power in horsepower, efficiency, and terminal power factor for slips of 1, 2, and 3 percent.

7-10. A 15-hp 230-V three-phase Y-connected 60-Hz four-pole squirrel-cage induction motor develops full-load internal torque at a slip of 0.03 when operated at rated voltage and frequency. For the purposes of this problem, rotational and core losses can be neglected. Impedance data on the motor in ohms per phase are as follows:

$$R_1 = 0.24 \quad X_1 = X_2 = 0.31 \quad X_\phi = 10.4$$

Determine the maximum internal torque at rated voltage and frequency, the slip at maximum torque, and the internal starting torque at rated voltage and frequency. Express the torques in newton-meters.

7-11. Suppose the induction motor of Prob. 7-10 is supplied from a 240-V constant-voltage 60-Hz source through a feeder whose impedance is $0.30 + j0.22 \Omega/\text{phase}$. Determine the maximum internal torque that the motor can deliver and the corresponding values of stator current and terminal voltage.

7-12. A three-phase induction motor, operating at rated voltage and frequency, has a starting torque of 165 percent and a maximum torque of 210 percent of full-load torque. Neglect stator resistance and rotational losses, and assume constant rotor resistance. Determine (a) the slip at full load, (b) the slip at maximum torque, and (c) the rotor current at starting, in per unit of full-load rotor current.

7-13. When operated at rated voltage and frequency, a three-phase squirrel-cage induction motor (of the design classification known as a high-slip motor) delivers full load at a slip of 8.3 percent and develops a maximum torque of 240 percent of full-load torque at a slip of 50 percent. Neglect core and rotational losses, and assume that the resistances and inductances of the motor are constant.

Determine the torque and rotor current at starting with rated voltage and frequency. Express the torque and rotor current in per unit based on their full-load values.

7-14. A 275-kW 600-V (line-to-line) six-pole 60-Hz induction motor has the following impedance data in ohms per phase Y referred to the stator:

$$R_1 = 0.0139 \quad R_2 = 0.0360 \quad X_1 = 0.155 \quad X_2 = 0.150 \quad X_\varphi = 5.20$$

It achieves rated shaft output at a slip of 3.4 percent with an efficiency of 93.5 percent. The motor is to be used as a generator driven by a wind turbine. It will be connected to a distribution system which can be represented by a 600-V infinite bus.

- (a) From the given data calculate the total rotational and core losses at rated load. Assume them to remain constant.
- (b) With the wind turbine driving the induction machine at a slip of -3.4 percent, calculate (i) the electric power output in kilowatts, (ii) the efficiency (electric output power per shaft input power), and (iii) the power factor measured at the machine terminals.
- (c) The actual distribution system has an effective impedance of $0.015 + j0.045 \Omega/\text{phase}$. For a slip of -3.4 percent, calculate (i) the induction-machine terminal voltage and power factor and (ii) the electric output power in kilowatts measured at the machine terminals.

7-15. For a 25-hp 230-V three-phase 60-Hz squirrel-cage motor operated at rated voltage and frequency, the rotor I^2R loss at maximum torque is 9.0

times that at full-load torque, and the slip at full-load torque is 0.028. Stator resistance and rotational losses may be neglected and the reactances and rotor resistance assumed to remain constant. Find (a) the slip at maximum torque, (b) the maximum torque, and (c) the starting torque. Express the torques in per unit of full-load torque.

7-16. A squirrel-cage induction motor runs at a slip of 4.0 percent at full load. The rotor current at starting is 5.0 times the rotor current at full load. The rotor resistance is independent of rotor frequency, and rotational losses, stray load losses, and stator resistance may be neglected. Compute (a) the starting torque and (b) the maximum torque and the slip at which maximum torque occurs. Express the torques in per unit of full-load torque.

7-17. A Δ -connected 25-hp 230-V (line-to-line) three-phase six-pole 60-Hz squirrel-cage induction motor has the following equivalent-circuit parameters in ohms per phase Y:

$$R_1 = 0.060 \quad R_2 = 0.055 \quad X_1 = 0.34 \quad X_2 = 0.33 \quad X_\phi = 10.6$$

- (a) Calculate the starting current and torque for this motor connected directly to a 230-V source.
- (b) To limit the starting current, it is proposed to connect the stator winding in Y for starting and then to switch to the Δ connection for normal operation. (i) What are the equivalent-circuit parameters in ohms per phase for the Y connection? (ii) With the motor connected directly to a 230-V source, calculate the starting current and torque.

7-18. The following test data apply to a 150-hp 2300-V three-phase four-pole 60-Hz squirrel-cage induction motor:

No-load test at rated voltage and frequency:

$$\text{Line current} = 8.1 \text{ A} \quad \text{Three-phase power} = 3025 \text{ W}$$

Blocked-rotor test at 15 Hz:

$$\text{Line voltage} = 268 \text{ V} \quad \text{Line current} = 52.5 \text{ A}$$

$$\text{Three-phase power} = 19.2 \text{ kW}$$

$$\text{Stator resistance between line terminals} = 2.35 \text{ } \Omega$$

Compute the stator current and power factor, horsepower output, and efficiency when this motor is operating at rated voltage and frequency with a slip of 2.85 percent.

7-19. Two 50-hp 440-V 59.8-A three-phase six-pole 60-Hz squirrel-cage induction motors have identical stators. The dc resistance measured between any pair of stator line terminals is $0.204\ \Omega$. The blocked-rotor tests at 60 Hz are as follows:

Motor	Volts line to line	Amperes	Three-phase power, kW
1	67.2	60.0	3.28
2	89.5	60.0	8.63

Determine the ratio of the internal starting torque developed by motor 2 to that developed by motor 1 (*a*) for the same current and (*b*) for the same applied voltage.

7-20. The results of a blocked-rotor test at 60 Hz on a 25-hp three-phase 230-V 60-Hz six-pole squirrel-cage induction motor are

$$\text{Line-to-line voltage} = 105\ \text{V} \quad \text{Line current} = 215\ \text{A}$$

$$\text{Three-phase power} = 21.0\ \text{kW} \quad \text{Torque} = 62\ \text{lb} \cdot \text{ft}$$

Determine the starting torque at a line-to-line voltage of 190 V and 50 Hz.

7-21. A 220-V three-phase four-pole 60-Hz squirrel-cage induction motor develops a maximum internal torque of 250 percent at a slip of 14 percent when operating at rated voltage and frequency. If the effect of stator resistance is neglected, determine the maximum internal torque that this motor would develop if it were operated at 180 V and 50 Hz. Under these conditions, at what speed in revolutions per minute would maximum torque be developed?

Polyphase-Induction-Machine Dynamics and Control

The polyphase induction motor is most often used to drive essentially constant loads at constant speed. As seen in Chap. 7, this operation is typically at low slips, where motor efficiency is high.

To complete our discussion of induction-motor performance, it is necessary to consider the behavior of such motors under non-steady-state conditions. This chapter investigates the start-up behavior of induction machines as well as the dynamics associated with transient mechanical and electric disturbances. Various methods of speed control are also described.

Until recently, induction motors found little application in situations where widely varying speed or precision control of speed was required. The advent of power semiconductors has changed that. Solid-state variable-frequency motor drives can now permit induction motors to be used in situations previously considered the domain of dc motors. This flexibility, com-

bined with the simplicity, low cost, and reliability of induction motors, guarantees their increased use in such applications as electric vehicles (trains and cars) and industrial processes. The use of variable-frequency solid-state drives is discussed in Art. 8-5.

8-1 EFFECTS OF ROTOR RESISTANCE; DOUBLE-SQUIRREL-CAGE ROTORS

A basic limitation of induction motors with constant rotor resistance is that the rotor design has to be a compromise. High efficiency under normal running conditions requires a low rotor resistance; but a low rotor resistance results in a low starting torque and high starting current at a low starting power factor.

a. Wound-Rotor Motors

The use of a wound rotor is one effective way of avoiding the need for compromise. The terminals of the rotor winding are connected to slip rings in contact with brushes. For starting, resistors may be connected in series with the rotor windings, the result being increased starting torque and reduced starting current at an improved power factor. The general nature of the effects on the torque-speed characteristics caused by varying rotor resistance is shown in Fig. 7-15. By use of the appropriate value of rotor resistance, the maximum torque can be made to occur at standstill if high starting torque is needed. As the rotor speeds up, the external resistances can be decreased, making maximum torque available throughout the accelerating range. Since most of the rotor I^2R loss is dissipated in the external resistors, the rotor temperature rise during starting is lower than it would be if the resistance were incorporated in the rotor winding. For normal running, the rotor winding can be short-circuited directly at the brushes. The rotor winding is designed to have low resistance so that running efficiency is high and full-load slip is low. Besides their use when starting requirements are severe, wound-rotor induction motors can be used for adjustable-speed drives. Their chief disadvantage is greater cost and complexity than squirrel-cage motors.

The principal effects of varying rotor resistance on the starting and running characteristics of induction motors can be shown quantitatively by the following example.

EXAMPLE 8-1

A 500-hp wound-rotor induction motor, with its slip rings short-circuited, has the following properties:

Full load slip = 1.5 percent

Rotor I^2R at full-load torque = 5.69 kW

Slip at maximum torque = 6.0 percent

Rotor current at maximum torque = $2.82 I_{2fl}$, where I_{2fl} is the full-load rotor current

Torque at 20 percent slip = $1.20 T_{fl}$, where T_{fl} is the full-load torque

Rotor current at 20 percent slip = $3.95 I_{2fl}$

If the rotor-circuit resistance is increased to $5R_{\text{rotor}}$ by connecting non-inductive resistances in series with each rotor slip ring, determine (a) the slip at which the motor will develop the same full-load torque, (b) total rotor-circuit I^2R loss at full-load torque, (c) horsepower output at full-load torque, (d) slip at maximum torque, (e) rotor current at maximum torque, (f) starting torque, and (g) rotor current at starting. Express the torques and rotor currents in per unit based on the full-load torque values.

Solution

The solution involves recognition of the fact that the only way the stator becomes aware of the happenings in the rotor is through the effect of the resistance R_2/s . Examination of the equivalent circuit shows that for specified applied voltage and frequency everything concerning the stator performance is fixed by the value of R_2/s , the other impedance elements being constant. For example, if R_2 is doubled and s is simultaneously doubled, the stator is unaware that any change has been made. The stator current and power factor, the power delivered to the air gap, and the torque are constant as long as the ratio R_2/s is the same.

Added physical significance can be given to the argument by examining the effects of simultaneously doubling R_2 and s from the viewpoint of the rotor. Observers on the rotor then see the resultant air-gap flux wave traveling past them at twice the original slip speed, generating twice the original rotor voltage at twice the original slip frequency. The rotor reactance therefore is doubled, and since the original premise is that the rotor resistance also is doubled, the rotor impedance is doubled but the rotor power factor is unchanged. Since rotor voltage and impedance are both doubled, the effective value of the rotor current remains the same; only its frequency is changed. The air gap still has the same synchronously rotating flux and mmf waves with the same torque angle. Observers on the rotor therefore agree with their counterparts on the stator that the torque is unchanged when both rotor resistance and slip are changed proportionally.

Observers on the rotor, however, are aware of two changes not apparent in the stator: (1) the rotor I^2R loss has doubled, and (2) the rotor is turning more slowly and therefore developing less mechanical power with the same torque. In other words, more of the power absorbed from the sta-

tor goes into I^2R heat in the rotor, and less is available for mechanical power.

The preceding thought processes can be readily applied to the solution of this example.

(a) If the rotor resistance is increased 5 times, the slip must increase 5 times for the same value of R_2/s and therefore for the same torque. But the original slip at full load is 0.015. The new slip at full-load torque therefore is $5(0.015) = 0.075$.

(b) The effective value of the rotor current is the same as its full-load value before addition of the series resistance, and therefore the rotor I^2R loss is 5 times the full-load value of 5.69 kW, or

$$\text{Rotor } I^2R = 5(5.69) = 28.45 \text{ kW}$$

(c) The increased slip has caused the per unit speed at full-load torque to drop from $1 - s = 0.985$ down to $1 - s = 0.925$ with added rotor resistance. The torque is the same. The power output therefore has dropped proportionally, or

$$P = \frac{0.925}{0.985}(500) = 469.5 \text{ hp}$$

The decrease in output equals the increase in rotor I^2R loss.

(d) If rotor resistance is increased 5 times, the slip at maximum torque simply increases 5 times. But the original slip at maximum torque is 0.060. The new slip at maximum torque with the added rotor resistance therefore is

$$s_{\max T} = 5(0.060) = 0.30$$

(e) The effective value of the rotor current at maximum torque is independent of rotor resistance; only its frequency is changed when rotor resistance is varied. Therefore,

$$I_{2\max T} = 2.82I_{2fl}$$

(f) With the rotor resistance increased 5 times, the starting torque will be the same as the original running torque at a slip of 0.20 and therefore equals the running torque without the series resistors, namely,

$$T_{\text{start}} = 1.20T_{fl}$$

(g) The rotor current at starting with the added rotor resistances will be the same as the rotor current when running at a slip of 0.20 with the

slip rings short-circuited, namely,

$$I_{2,\text{start}} = 3.95I_{2f}$$

b. Deep-Bar and Double-Squirrel-Cage Rotors

An ingenious and simple way of obtaining a rotor resistance which will automatically vary with speed makes use of the fact that at standstill the rotor frequency equals the stator frequency; as the motor accelerates, the rotor frequency decreases to a very low value—perhaps 2 or 3 Hz at full load in a 60-Hz motor. With suitable shapes and arrangements for rotor bars, squirrel-cage rotors can be designed so that their effective resistance at 60 Hz is several times their resistance at 2 or 3 Hz. The various schemes all make use of the inductive effect of the slot-leakage flux on the current distribution in the rotor bars. The phenomena are basically the same as the skin and proximity effect in any system of conductors with alternating current in them.

Consider first a squirrel-cage rotor having deep, narrow bars like that shown in cross section in Fig. 8-1. The general character of the slot-leakage field produced by the current in the bar within this slot is shown in the figure. If the rotor iron had infinite permeability, all the leakage-flux lines would close in paths below the slot, as shown. Now imagine the bar to consist of an infinite number of layers of differential depth; one at the bottom and one at the top are indicated crosshatched in Fig. 8-1. The leakage inductance of the bottom layer is greater than that of the top layer because the bottom layer is linked by more leakage flux. But all the layers are electrically in parallel. Consequently, with alternating current, the current in the low-reactance upper layers will be greater than that in the high-reactance lower layers; the current will be forced toward the top of the slot, and the phase of current in the upper layers will lead that of the current in the lower ones. The nonuniform current distribution results in an increase in the effective bar resistance and a smaller decrease in the effective leakage inductance of the bar. Since the distortion in current distribution depends on an inductive effect, the effective resistance is a function of the

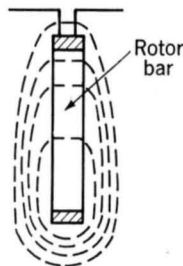


Fig. 8-1. Deep rotor bar and slot-leakage flux.

frequency. It is also a function of the depth of the bar and of the permeability and resistivity of the bar material. Figure 8-2 shows a curve of the ratio of ac effective resistance to dc resistance as a function of frequency computed for a copper bar 1.00 in deep. A squirrel-cage rotor with deep bars can be readily designed to have an effective resistance at stator frequency (standstill) several times greater than its dc resistance. As the motor accelerates, the rotor frequency decreases and therefore the rotor effective resistance decreases, approaching its dc value at small slips.

An alternative way of attaining similar results is the double-cage arrangement shown in Fig. 8-3. The squirrel-cage winding consists of two layers of bars short-circuited by end rings. The upper bars are of smaller cross-sectional area than the lower bars and consequently have higher resistance. The general nature of the slot-leakage field is shown in Fig. 8-3, from which it can be seen that the inductance of the lower bars is greater than that of the upper ones because of the flux crossing the slot between the two layers. The difference in inductance can be made quite large by properly proportioning the constriction in the slot between the two bars. At standstill, when rotor frequency equals stator frequency, there is relatively little current in the lower bars because of their high reactance; the effective resistance of the rotor at standstill then approximates that of the high-resistance upper layer. At the low rotor frequencies corresponding to small slips, however, reactance becomes negligible, and the rotor resistance then approaches that of the two layers in parallel.

Note that since the effective resistance and leakage inductance of double-cage and deep-bar rotors vary with frequency, the parameters R_2 and X_2 , representing the referred effects of rotor resistance and leakage inductance as viewed from the stator, are not constant. A more complicated form of equivalent circuit is required if the reactions of the rotor are to be represented by the effects of slip together with constant resistance and reactance elements.

The simple equivalent circuit derived in Art. 7-3 still correctly represents the motor, however, but now R_2 and X_2 are functions of slip. All the basic relations still apply to the motor if the values of R_2 and X_2 are prop-

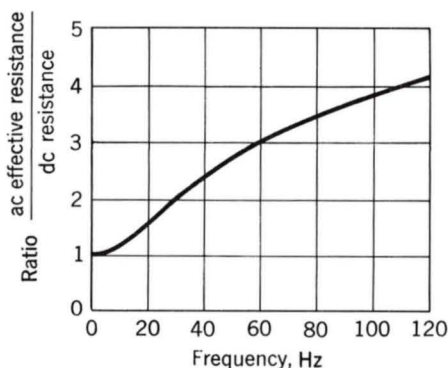


Fig. 8-2. Skin effect in a copper rotor bar 1.00 in deep.

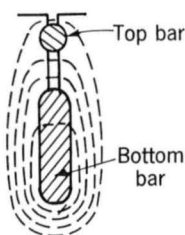


Fig. 8-3. Double-squirrel-cage rotor bars and slot-leakage flux.

erly adjusted with changes in slip. For example, in computing the starting performance, R_2 and X_2 should be taken as their effective values at stator frequency; in computing the running performance at small slips, however, R_2 should be taken as its effective value at a low frequency, and X_2 should be taken as the stator-frequency value of the reactance corresponding to a low-frequency effective value of the rotor leakage inductance. Over the normal running range of slips, the rotor resistance and leakage inductance usually can be considered constant at substantially their dc values.

c. Motor-Application Considerations

By use of double-cage and deep-bar rotors, squirrel-cage motors can be designed to have the good starting characteristics resulting from high rotor resistance and at the same time the good running characteristics resulting from low rotor resistance. The design is necessarily somewhat of a compromise, however, and the motor lacks the flexibility of the wound-rotor machine with external rotor resistance. The wound-rotor motor should be used when starting requirements are very severe. Alternatively, solid-state motor drives can be used, as discussed in Art. 8-5.

To meet the usual needs of industry, integral-horsepower three-phase squirrel-cage motors are available from manufacturers' stock in a range of standard ratings up to 200 hp at various standard frequencies, voltages, and speeds. (Larger motors are generally regarded as special-purpose rather than general-purpose motors.) According to the terminology established by NEMA, several standard designs are available to meet various starting and running requirements. Representative torque-speed characteristics of the four most common designs are shown in Fig. 8-4. These curves are fairly typical of 1800 r/min (synchronous-speed) motors in ratings from 7.5 to 200 hp, although it should be understood that individual motors may differ appreciably from these average curves. Briefly, the characteristic features of these designs are as follows.

Design Class A: Normal Starting Torque, Normal Starting Current, Low Slip. This design usually has a low-resistance single-cage rotor. It emphasizes good running performance at the expense of starting. The full-load slip is low, and the full-load efficiency is high. The maximum torque usually is well over 200 percent of full-load torque and occurs at a small slip (less than 20 percent). The starting torque at full voltage varies from about 200 percent of full-load torque in small motors to about 100 percent

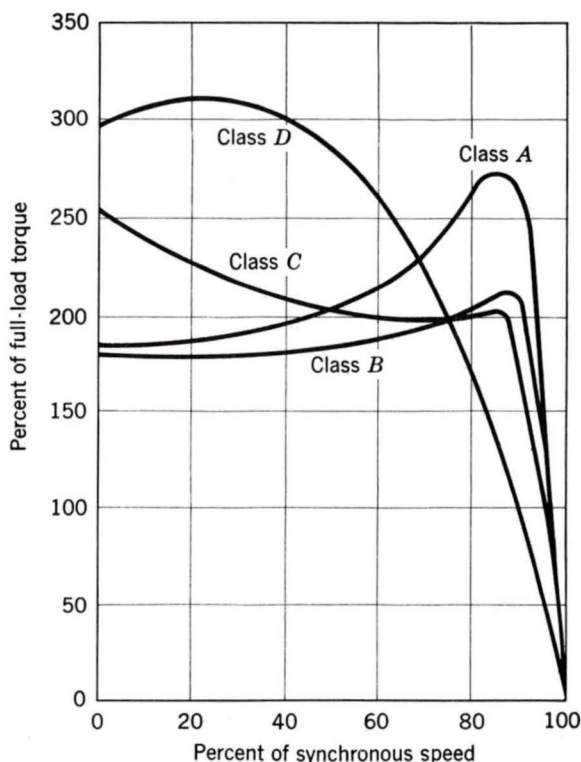


Fig. 8-4. Typical torque-speed curves for 1800-r/min general-purpose induction motors.

in large motors. The high starting current (500 to 800 percent of full-load current when started at rated voltage) is the principal disadvantage of this design. In sizes below about 7.5 hp, these starting currents usually are within the limits on inrush current which the distribution system supplying the motor can withstand, and across-the-line starting at full voltage then can be used; otherwise, reduced-voltage starting must be used. Reduced-voltage starting results in a decrease in starting torque because the starting torque is proportional to the voltampere input to the motor, which in turn is proportional to the square of the voltage applied to the motor terminals. The reduced voltage for starting is usually obtained from an autotransformer, called a *starting compensator*, which may be manually operated or automatically operated by relays which cause full voltage to be applied after the motor is up to speed. A circuit diagram of one type of compensator is shown in Fig. 8-5. If a smoother start is necessary, series resistance or reactance in the stator may be used.

The class A motor is the basic standard design in sizes below about 7.5 and above about 200 hp. It is also used in intermediate ratings where design considerations may make it difficult to meet the starting-current limitations of the class B design. Its field of application is about the same as that of the class B design described next.

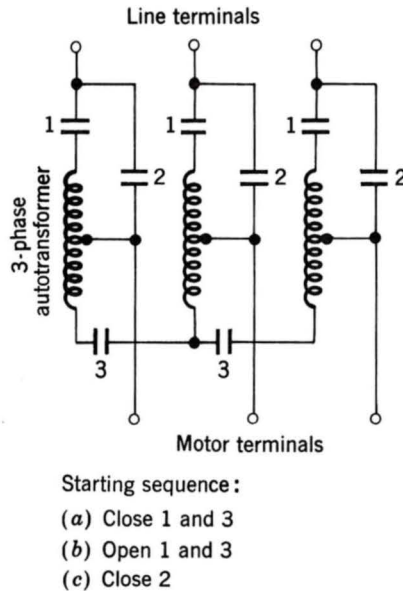


Fig. 8-5. Connections of a one-step starting autotransformer.

Design Class B: Normal Starting Torque, Low Starting Current, Low Slip. This design has approximately the same starting torque as the class A design with but 75 percent of the starting current. Full-voltage starting therefore may be used with larger sizes than with class A. The starting current is reduced by designing for relatively high leakage reactance, and the starting torque is maintained by use of a double-cage or deep-bar rotor. The full-load slip and efficiency are good—about the same as for the class A design. However, the use of high reactance slightly decreases the power factor and decidedly lowers the maximum torque (usually only slightly over 200 percent of full-load torque being obtainable).

This design is the most common in the 7.5- to 200-hp range of sizes. It is used for substantially constant speed drives where starting-torque requirements are not severe, such as in driving fans, blowers, pumps, and machine tools.

Design Class C: High Starting Torque, Low Starting Current. This design uses a double-cage rotor with higher rotor resistance than the class B design. The result is higher starting torque with low starting current but somewhat lower running efficiency and higher slip than the class A and class B designs. Typical applications are in driving compressors and conveyers.

Design Class D: High Starting Torque, High Slip. This design usually has a single-cage high-resistance rotor (frequently brass bars). It produces very high starting torque at low starting current, high maximum torque at

50 to 100 percent slip, but runs at a high slip at full load (7 to 11 percent) and consequently has low running efficiency. Its principal uses are for driving intermittent loads involving high accelerating duty and for driving high-impact loads such as punch presses and shears. When driving high-impact loads, the motor is generally aided by a flywheel which helps supply the impact and reduces the pulsations in power drawn from the supply system. A motor whose speed falls appreciably with an increase in torque is required so that the flywheel can slow down and deliver some of its kinetic energy to the impact.

8-2 INDUCTION-MACHINE DYNAMICS

Among integral-horsepower induction motors, i.e., those used primarily for power purposes, the most common dynamic problems are associated with starting and stopping and with the ability of the motor to continue operation during serious disturbances of the supply system. For example, a typical problem in an industrial plant may concern the ability to start a large motor without causing other parallel motors to cease normal operation because of the voltage reduction caused by the heavy inrush current to the motor being started.

The methods of induction-motor representation in dynamic analyses depend to a considerable extent on the nature and complexity of the problem and the associated precision requirements. When the electric transients in the motor are to be included (Art. 8-4), the equivalent circuit of Fig. 8-15 may be used. In many problems, however, the electric transients in the induction machine may be ignored. This simplification is possible, because as illustrated in Example 8-3, the electric transients subside rapidly—most commonly in a time short compared with the duration of the motional transient. (Among the principal exceptions to this statement are large 3600-r/min motors.) We confine ourselves here to this type of problem.

Representation of the machine under these conditions can be based on steady-state theory. The problem then becomes one of arriving at a sufficiently simple yet reasonably realistic representation which will not unduly complicate the dynamic analysis, particularly through the introduction of nonlinearities. One approach applicable to relatively simple problems is a graphical one. Both the torque produced by the motor and the torque required to turn the load are considered to be nonlinear functions of speed for which data are given in the form of curves. The procedure is illustrated in the following example.

EXAMPLE 8-2

A polyphase induction motor has the torque-speed curve for rated impressed voltage shown in Fig. 8-6. A curve of the torque required to main-

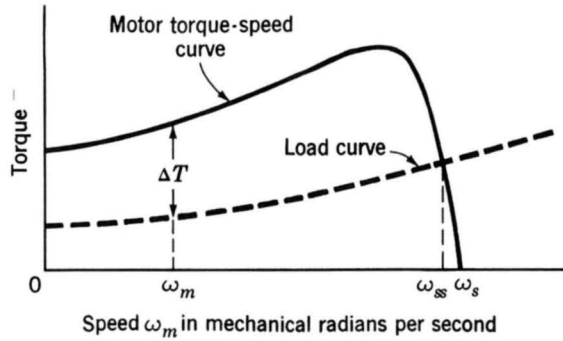


Fig. 8-6. Induction-motor torque-speed curve and curve of load torque.

tain rotation of the load is also given in Fig. 8-6. The inertia of the load and rotor is J in SI units.

Consider that across-the-line starting at rated voltage is used and that the steady-state torque-speed curve represents the performance under transient conditions with sufficient accuracy. Show how a curve of speed as a function of time can be obtained.

Solution

At any motor speed ω_m mechanical radians per second, the torque differential ΔT between that produced by the motor and that required to turn the load is available to accelerate the rotating mass. Consequently,

$$J \frac{d\omega_m}{dt} = \Delta T$$

The time required to attain the speed ω_m is therefore

$$t = J \int_0^{\omega_m} \frac{1}{\Delta T} d\omega_m$$

This integral can be evaluated graphically by plotting a curve of $1/\Delta T$ as a function of ω_m and finding the area between the curve and the ω_m axis up to the value corresponding to the upper limit of the integral, a procedure illustrated in Fig. 8-7. The area can be found by planimeter, by counting small squares on the curve sheet, or by dividing it into uniform segments and using the average ordinate for each section. Alternatively, a mathematical function can be fitted to the $1/\Delta T$ curve, and the integration can be performed numerically or analytically. This area, in units of radians per newton-meter-second multiplied by the inertia J in SI units, gives the time t in seconds. The computations can be carried out conveniently in tabular form to yield a result of the type shown in Fig. 8-8.

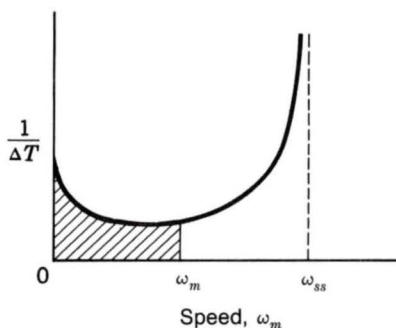


Fig. 8-7. Graphical analysis of induction-motor starting.

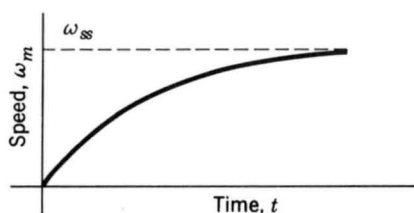


Fig. 8-8. Speed-time curve of induction motor during starting.

Once the motor speed versus time is known, the corresponding current-versus-time characteristic can be obtained from either a current-versus-speed curve or analytic expressions. The magnitude of armature current remains large until the speed increases to the point where the effective rotor impedance is on the order of the magnetizing reactance; at this point the current begins to drop toward its steady-state operating value. At no load, this current is essentially the magnetizing current of the motor. Under full-load conditions, the current includes both this magnetizing current and the stator-load-current component.

In some cases the rated-voltage motor starting current may exceed that considered desirable. In such cases, a number of options are available.

Series Impedance. A series reactive impedance can be used to limit starting current. After an appropriate time, this impedance can be automatically short-circuited, connecting the motor directly to the source voltage.

Reduced Voltage. The motor can be connected to the source via an auto-transformer supplying reduced voltage, as shown in Fig. 8-5. The motor is then switched to full voltage at a predetermined operating condition.

Y-Δ Switching. An induction motor designed for a Δ armature connection can be started with the armature connect in Y. As shown in Eq. 2-38,

this results in an armature impedance 3 times that of the Δ connection and hence one-third of the starting current (and torque).

Split-Winding Starting. In the split-winding scheme, multiple parallel circuits are provided for each phase and are connected in parallel for running; for starting, however, the circuits on one or more phases are connected in series.

These schemes provide reduced starting currents and correspondingly reduced starting torques. Their applicability to any particular situation must be carefully considered along with other issues related to their implementation. Alger[†] discusses these issues in some detail.

8-3 SPEED CONTROL OF INDUCTION MOTORS

The simple induction motor fulfills admirably the requirements of substantially constant speed drives. Many motor applications, however, require several speeds or even a continuously adjustable range of speeds. From the earliest days of ac power systems, engineers have been interested in the development of adjustable-speed ac motors.

The synchronous speed of an induction motor can be changed by (a) changing the number of poles or (b) varying the line frequency. The operating slip can be changed by (c) varying the line voltage, (d) varying the rotor resistance, or (e) applying voltages of the appropriate frequency to the rotor circuits. The salient features of speed-control methods based on these five possibilities are discussed in the following five sections of this article. Control methods involving solid-state devices are mentioned only briefly because they are more fully treated in Art. 8-5.

a. Pole-Changing Motors

The stator winding can be designed so that by simple changes in coil connections the number of poles can be changed in the ratio 2 to 1. Either of two synchronous speeds can be selected. The rotor is almost always of the squirrel-cage type. A cage winding always reacts by producing a rotor field having the same number of poles as the inducing stator field. If a wound rotor is used, additional complications are introduced because the rotor winding also must be rearranged for pole changing. With two independent sets of stator windings, each arranged for pole changing, as many as four synchronous speeds can be obtained in a squirrel-cage motor, for example, 600, 900, 1200, and 1800 r/min for 60-Hz operation.

The basic principles of the pole-changing winding are shown in Fig. 8-9, in which aa and $a'a'$ are two coils comprising part of the phase- a stator winding. An actual winding would, of course, consist of several coils in each group. The windings for the other stator phases (not shown in the fig-

[†]P. L. Alger, *Induction Machines*, 2d ed., chap. 8, Gordon and Breach, New York, 1970.

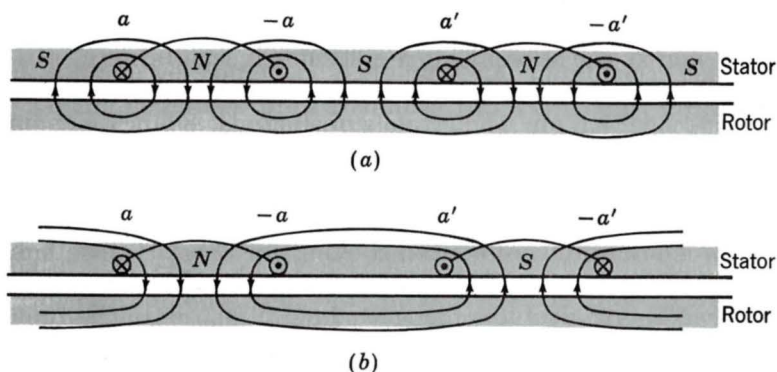


Fig. 8-9. Principles of the pole-changing winding.

ure) would be similarly arranged. In Fig. 8-9a the coils are connected to produce a four-pole field; in Fig. 8-9b the current in the $a'a'$ coil has been reversed by means of a controller, the result being a two-pole field.

Figure 8-10 shows the four possible arrangements of these two coils: they can be connected in series or in parallel and with their currents either in the same direction (four-pole operation) or in the opposite direction (two-pole operation). Additionally, the machine phases can be connected either in Y or Δ , resulting in eight possible combinations.

Note that for a given phase voltage, the different connections will result in differing levels of air-gap flux density. For example, a change from a Δ to a Y connection will reduce the coil voltage (and hence the air-gap flux density) for a given coil arrangement by $\sqrt{3}$. Similarly, changing from a connection with two coils in series to two in parallel will double the voltage across each coil and therefore double the magnitude of the air-gap flux density. These changes in flux density can, of course, be compensated for by changes in the applied winding voltage. In any case, they must be con-

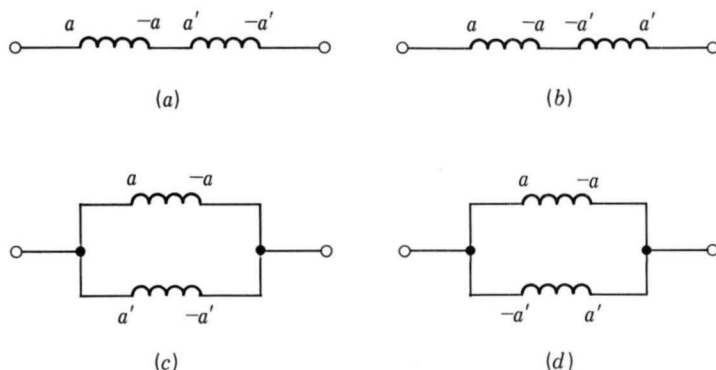


Fig. 8-10. Four possible arrangements of phase-a stator coils in a pole-changing induction motor: (a) series-connected, four-pole; (b) series-connected, two-pole; (c) parallel-connected, four-pole; (d) parallel-connected, two-pole.

sidered, along with corresponding changes in motor torque, when the configuration to be used in a specific application is considered.

b. Line-Frequency Control

The synchronous speed of an induction motor can be controlled by varying the line frequency. To maintain approximately constant flux density, the line voltage should also be varied directly with the frequency. The maximum torque then remains very nearly constant. An induction motor used in this way has characteristics similar to those of a separately excited dc motor with constant flux and variable armature voltage.

The major problem is to determine the most effective and economical source of adjustable frequency. One method is to use a wound-rotor induction machine as a frequency changer. Another, considered in Art. 8-5, is to use solid-state frequency converters.

c. Line-Voltage Control

The internal torque developed by an induction motor is proportional to the square of the voltage applied to its primary terminals, as shown by the two torque-speed characteristics in Fig. 8-11. If the load has the torque-speed characteristic shown by the dashed line, the speed will be reduced from n_1 to n_2 . This method of speed control is commonly used with small squirrel-cage motors driving fans.

d. Rotor-Resistance Control

The possibility of speed control of a wound-rotor motor by changing its rotor-circuit resistance has already been pointed out in Art. 8-1a. The torque-speed characteristics for three different values of rotor resistance are shown in Fig. 8-12. If the load has the torque-speed characteristic shown by the dashed line, the speeds corresponding to each of the values of rotor resistance are n_1 , n_2 , and n_3 . This method of speed control has characteristics similar to those of dc shunt-motor speed control by means of resistance in series with the armature.

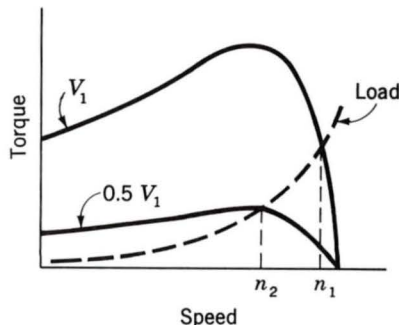


Fig. 8-11. Speed control by means of line voltage.

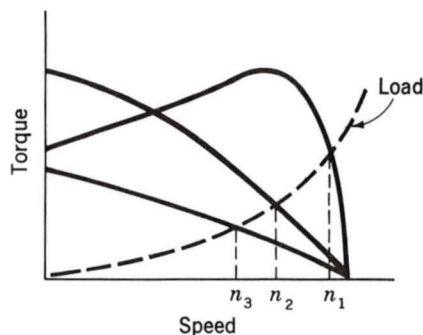


Fig. 8-12. Speed control by means of rotor resistance.

The principal disadvantages of both line-voltage and rotor-resistance control are low efficiency at reduced speeds and poor speed regulation with respect to change in load.

e. Control of Slip by Auxiliary Devices

In considering schemes for speed control by varying the slip, the fundamental laws relating the flow of power in induction machines should be kept in mind. The fraction s of the power absorbed from the stator is transformed by electromagnetic induction to electric power in the rotor circuits. If the rotor circuits are short-circuited, this power is wasted as rotor I^2R loss and operation at reduced speeds is inherently inefficient.

Numerous schemes have been invented for recovering this slip-frequency electric power. Although some are rather complicated in detail, they all comprise a means for introducing adjustable voltages of slip frequency into the rotor circuits of a wound-rotor induction motor. They can be broadly classified in two types, as shown in Fig. 8-13, where *IM* represents a three-phase wound-rotor induction motor whose speed is to be regulated. In Fig. 8-13*a* the rotor circuits of *IM* are connected to auxiliary frequency-changing apparatus, represented by the box *FC*, in which the slip-frequency electric power generated in the rotor of the main motor is

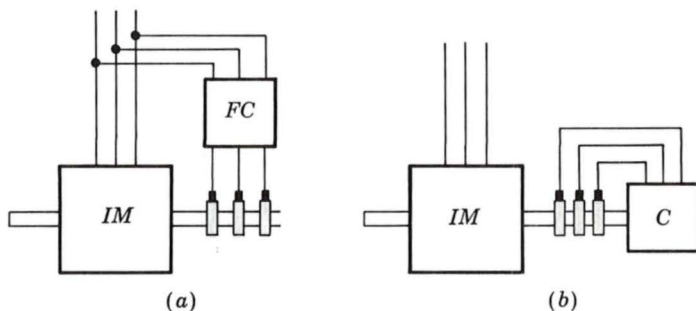


Fig. 8-13. Two basic schemes for induction-motor speed control by auxiliary machines.

converted to electric power at line frequency and returned to the line. In Fig. 8-13*b* the rotor circuits of *IM* are connected to auxiliary apparatus, represented by box *C*, in which the slip-frequency electric power is converted to mechanical power and added to the shaft power developed by the main motor. In both these schemes the speed and power factor of the main motor can be adjusted by controlling the magnitude and phase of the slip-frequency voltages of the auxiliary machines. The auxiliary apparatus may be a fairly complicated system of rotating machines and adjustable-ratio transformers or, in the case of Fig. 8-13*a*, may consist of solid-state frequency conversion.

8-4 ELECTRIC TRANSIENTS IN INDUCTION MACHINES

The transient behavior of induction machines can be examined by following substantially the same approach as that in Art. 6-4 for synchronous machines. The results will be very similar to those in the synchronous case.

Consider that the induction machine is acting as either a motor or a generator when a three-phase short circuit occurs at its terminals. In either case, the machine will feed current into the fault because of the "trapped" flux linkages with the rotor circuits. This current will, in time, decay to zero because, unlike the synchronous machine with its field winding, there is no source of excitation connected to the rotor windings of an induction machine. In addition to an ac component, the stator current will, in general, have a decaying dc component in order to keep the flux linkages with the associated phase initially constant. The ac component of the short-circuit current as a function of time appears as in Fig. 8-14.

The analysis of a symmetric three-phase short circuit on an initially unloaded synchronous machine in Art. 6-4 is greatly simplified by the use of the dq0 transformation, which refers all stator quantities to a syn-

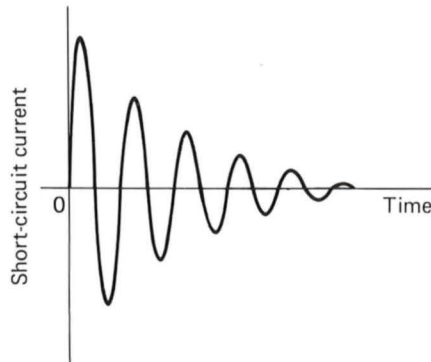


Fig. 8-14. Waveform of symmetric short-circuit current in an induction machine.

chronously rotating reference frame. A similar transformation is possible for an induction machine; however, the choice of reference frame is not so obvious. One choice is a reference frame rotating with the rotor. In this case the transformed steady-state stator quantities vary at slip frequency, as do the rotor quantities.

A second choice of reference frame is one which rotates at synchronous speed. In this case there would be speed-voltage terms in both the stator and rotor equations; mechanical speed would multiply the stator fluxes, and slip speed would multiply the rotor fluxes. In either case, analysis of a three-phase short circuit on an induction machine would yield results similar to those found in Art. 6-4 for the synchronous machine. Thus, instead of rederiving this solution for the induction machine, we can use the synchronous-machine solution to obtain our solution directly.

The initial magnitude of the ac component of stator current can be determined in terms of a *transient reactance* X' and a voltage E'_1 behind that reactance, assumed equal to its prefault value. The decay of the ac component can be characterized in terms of a *short-circuit transient time constant* T' . Since the ac stator currents are driven by dc decaying rotor currents, the frequency of the stator currents is determined by the rotor angular velocity. For low slips this frequency is essentially the synchronous electric frequency; for higher slips the frequency will be determined accordingly. It is usually assumed that the machine speed remains constant during the short-circuit transient since the transient is of short duration.

Much of the analytical development of Art. 6-4 can be applied by making the appropriate changes in notation. The currents i_d and i_f , for example, become the stator and rotor currents i_1 and i_2 , respectively. The reactances X_{al} , X_f , and $X_{\phi d}$ become the stator and rotor leakage reactances X_1 and X_2 and the magnetizing reactance X_ϕ , respectively. Because of the cylindrical structure of the induction-machine rotor, the distinction between direct and quadrature axis need not be maintained. The results corresponding to Eqs. 6-45, 6-56, 6-64, and 6-65 are, respectively,

$$X' = X_1 + X_\phi - \frac{X_\phi^2}{X_\phi + X_2} \quad (8-1)$$

equivalently
$$X' = X_1 + \frac{X_\phi X_2}{X_\phi + X_2} \quad (8-2)$$

$$T'_0 = \frac{X_2 + X_\phi}{2\pi f R_2} \quad (8-3)$$

and
$$T' = T'_0 \frac{X'}{X_1 + X_\phi} \quad (8-4)$$

where T'_0 is the *open-circuit transient time constant* of the induction machine and R_2 is the rotor-circuit resistance. The initial transient-current

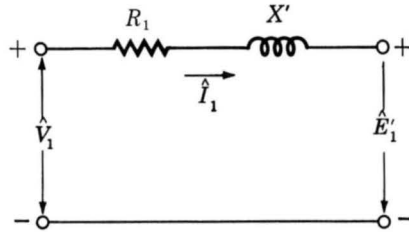


Fig. 8-15. Simplified transient equivalent circuit of an induction machine.

magnitude is given by

$$I_1 = \frac{E'_1}{X'} \quad (8-5)$$

The induction machine can then be represented by the simple transient equivalent circuit of Fig. 8-15. The reactance is the transient reactance X' , defined by Eqs. 8-1 and 8-2. Although it has been ignored so far, the stator resistance R_1 can also be added if somewhat greater precision is desired. The voltage E'_1 behind transient reactance is a voltage proportional to rotor flux linkages. It changes with these linkages and, for a three-phase short circuit, decreases to zero at a rate determined by the short-circuit transient time constant T' (Eq. 8-4). Adjustment of the time constant for external reactance between the machine terminals and the fault can readily be carried out by adding the reactance to the numerator and denominator of the fraction in Eq. 8-4.

EXAMPLE 8-3

A 400-hp 440-V (line-to-line) 60-Hz Y-connected six-pole squirrel-cage induction motor has a full-load efficiency of 93 percent and a power factor of 90 percent. The motor constants in ohms per phase referred to the stator are

$$X_1 = 0.060 \quad X_2 = 0.060 \quad X_\phi = 2.50 \quad R_1 = 0.0073 \quad R_2 = 0.0064$$

While the motor is operating in the steady state under rated conditions, a three-phase short circuit occurs on its supply line near the motor terminals. Determine the motor rms short-circuit current.

Solution

From Eq. 8-1 the motor transient reactance is

$$X' = 0.060 + 2.50 - \frac{(2.50)^2}{0.06 + 2.50} = 0.12 \, \Omega/\text{phase}$$

The prefault stator current is

$$I_1 = \frac{400(746)}{0.90(0.93)(440\sqrt{3})} = 467 \text{ A}$$

With terminal voltage as the reference phasor, the prefault voltage behind transient reactance is then

$$\hat{E}'_1 = \frac{440}{\sqrt{3}} - (0.0073 + j0.12)(467 \angle -\cos^{-1}0.90) = 232 \angle -12.2^\circ$$

From Eq. 8-5, the initial rms short-circuit current is

$$\frac{232}{0.12} = 1940 \text{ A}$$

The open-circuit time constant (Eq. 8-3) is

$$T'_0 = \frac{2.50 + 0.060}{2\pi(60)(0.0064)} = 1.06 \text{ s}$$

and the short-circuit time constant (Eq. 8-4) is

$$T' = 1.06 \left(\frac{0.12}{2.56} \right) = 0.050 \text{ s}$$

The rms short-circuit current is therefore

$$I_1 = 1940 e^{-t/0.050} \text{ A}$$

The short-circuit time constant is three cycles on a 60-Hz base. Accordingly, in three cycles the short-circuit current decreases to 36.8 percent of its initial value. It has substantially disappeared in about 10 cycles. Thus while the initial short-circuit current of an induction machine is relatively high compared with its normal current, the transient usually disappears rapidly. Because of this fact, the electric transients in induction machines are often neglected.

8-5 APPLICATION OF ADJUSTABLE-SPEED SOLID-STATE AC MOTOR DRIVES

As discussed briefly in Art. 8-3, induction-motor speed control can be obtained by such means as frequency and voltage control as well as recov-

ering the slip-frequency rotor power via auxiliary devices. The use of solid-state electronics in implementing these techniques in ac motor drive systems has led to the increased use of induction machines in situations where speed control is required. Solid-state ac drive systems are considerably more complex than their dc counterparts; however, although dc motors have dominated the adjustable-speed drive field, ac motors are used in drive systems where their special features, such as the absence of commutators and brushes, must be utilized. As is discussed in Chaps. 10 and 11, advances in ac drive system technology resulting in increased flexibility and large decreases in size, weight, and cost have increased interest in other types of ac machines such as permanent-magnet and variable-reluctance machines for variable-speed applications. Thus although the induction motor will continue to be used in these applications, the number of options available to the drive system engineer is increasing.

Adjustable-frequency power can be generated by a *thyristor*[†] circuit called an *inverter*. Inverters are used to transfer energy from a dc source to an ac load of arbitrary frequency and phase. They are used in ac drive systems to provide power of adjustable frequency to ac motors and to regenerate rotor-circuit power back to the ac line in wound-rotor induction motors. A typical motor drive consists of a rectifier to convert power from the ac supply to dc form, an inverter to form the adjustable-frequency alternating current from the dc bus, and a control system to set the frequency, adjust the motor voltage, and ensure that the maximum torque of the motor will not be exceeded.

Inverters for providing power at adjustable frequency for ac motor drive systems are usually three-phase inverters. A battery may be floated on the dc bus to ensure an uninterrupted supply of energy for critical applications if power from the ac supply to the rectifier is interrupted. The three-phase inverter has a minimum of six thyristors arranged in a bridge configuration, as shown in schematic form in Fig. 8-16; these thyristors (labeled TR) are switched sequentially to synthesize at the ac terminals of the inverter bridge a set of three-phase voltages that is applied to the motor. Practical inverter circuits must include provisions for commutating current from thyristor to thyristor as the thyristors are switched.[‡]

Typical waveforms for the line-to-neutral voltages v_{a0} and v_{b0} and the line-to-line voltage v_{ab} are shown in Fig. 8-17, which is drawn for the case where each thyristor conducts for exactly one-half cycle (180° conduction). Table 8-1 shows the status of each thyristor in the bridge of Fig. 8-16 at the various steps of the waveform of Fig. 8-17. Each step corresponds to 60° on the output waveform. The line-to-neutral voltages are three-step-per-half-

[†]A thyristor (also known as a *silicon controlled rectifier*, or SCR) is a three-terminal device which is similar to a diode except that it must be turned on by a signal to its gate lead before it will begin conduction of current when it is forward-biased.

[‡]For a description of practical inverter circuits, see B. D. Bedford and R. G. Hoft, *Principles of Inverter Circuits*, Wiley, New York, 1964; also S. B. Dewan and A. Straughen, *Power Semiconductor Circuits*, Wiley, New York, 1975.

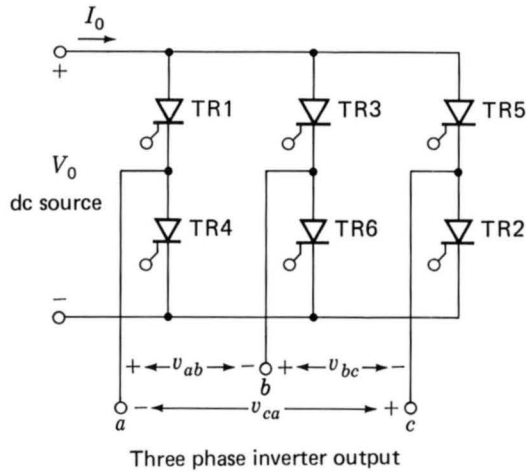


Fig. 8-16. Three-phase inverter-bridge configuration.

cycle approximations to sine waves while the line-to-line voltages are positive and negative pulses 120° wide. When the inverter voltages are applied to a motor, the motor responds to the fundamental and the harmonics of the waveforms to produce positive and braking torques and both normal and additional losses. Inverters can be built that produce output waveforms with less harmonic content by various techniques. For example, the outputs of two inverters whose waveforms are phase-displaced can be added, resulting in cancellation of some of the harmonics.

The output of a three-phase inverter is applied to synchronous and induction motors to obtain adjustable-speed operation by means of frequency control.[†] Where closely regulated speed is required from one or more motors, as in textile applications, synchronous motors are used; they will operate in synchronism with the oscillator that controls the inverter independently of their loading. But where nominally regulated speed is re-

[†]See A. Kusko, *Solid-State AC Motor Drives*, M.I.T. Press, Cambridge, Mass., 1971.

TABLE 8-1

Step	Thyristor					
	TR1	TR2	TR3	TR4	TR5	TR6
I	On	Off	Off	Off	On	On
II	On	On	Off	Off	Off	On
III	On	On	On	Off	Off	Off
IV	Off	On	On	On	Off	Off
V	Off	Off	On	On	On	Off
VI	Off	Off	Off	On	On	On

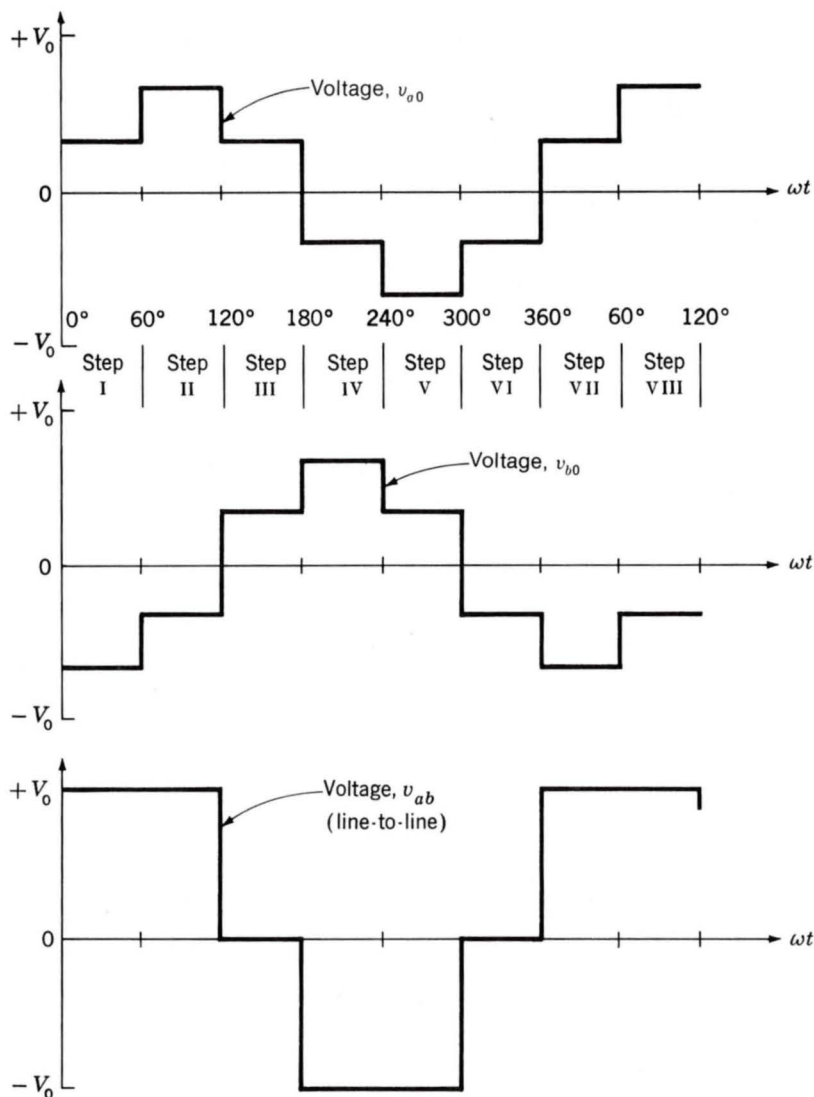


Fig. 8-17. Waveforms generated by a three-phase inverter, 180° conduction.

quired, as in high-speed grinders or special vehicle drives, induction motors are used. Special types of motors are frequently employed because the operation is different from the usual fixed-frequency application. The synchronous motors are usually hybrid induction-synchronous motors which synchronize by reluctance torque (see Fig. 8-18) or by using permanent-magnet fields. The induction motors are either squirrel-cage or solid-iron rotor types. Operation is frequently carried out both above and below the nominal frequency of the motor, for example, 10 to 120 Hz for a 60-Hz motor.

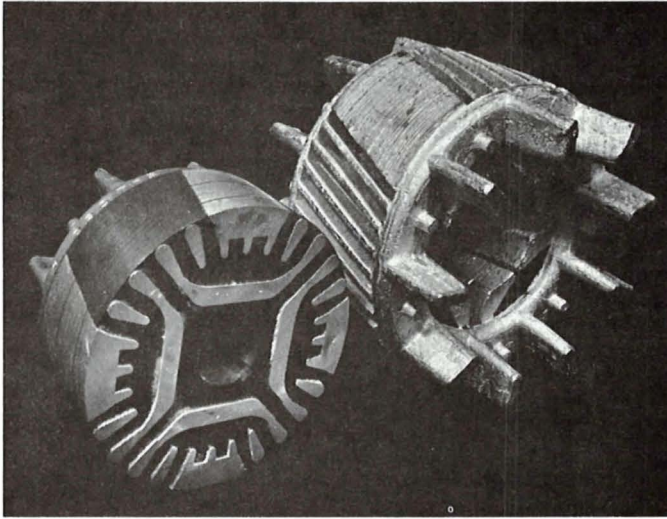


Fig. 8-18. Cutaway views of a rotor of a Synchrospeed motor. (Left) The magnetic laminations are shown dark, the conductors light. (Right) Only the rotor conductors are shown; the iron has been etched away. (The Louis Allis Company.)

The synchronous speed is directly proportional to frequency. Of primary interest is the shape of the torque-speed curve of the induction motor at each frequency in the operating range, including the starting and break-down torques. The torques are determined by how the terminal voltage of the motor is managed as the frequency is adjusted. It is clear that to secure operation of a given motor at the maximum air-gap flux density over its speed range, the air-gap voltage must be adjusted proportional to frequency f . By so doing we obtain the maximum available torque from the induction motor at each frequency setting. In a practical system, the terminal voltage V_1 is controlled so that V_1/f is constant; this type of control is termed *constant volts per hertz*. For a voltage waveform that changes shape as a function of frequency, the half-wave average voltage rather than the rms voltage is controlled in the above-described manner. Present practice is to maintain V_1 constant below a specific frequency to overcome the $I_1 R_1$ drop; in some drives, the voltage V_1 is held constant for operation above the nominal motor frequency and for obtaining constant-horsepower operation.

The torque-speed curve of an induction motor for a given frequency can be calculated by using the methods of Chap. 7 within the accuracy of the motor parameters at that frequency. The torque-speed curves for the motor operated over a range of frequency, but at constant air-gap flux density, are practically the same on a slip-speed scale, as shown in Fig. 8-19. This can be confirmed by viewing the air gap from the rotor; the rotor behavior is determined only by the slip speed, which sets the rotor induced voltage, frequency, current, and the torque produced. Note that a speed regulation

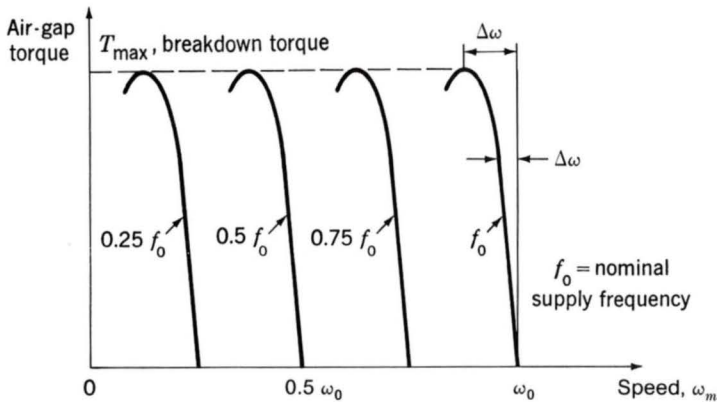


Fig. 8-19. Idealized torque-speed curves of an induction motor under adjustable-frequency control.

of 3 percent at nominal frequency ω_0 becomes a speed regulation of 30 percent at $\omega_s = 0.1\omega_0$.

An adjustable-frequency drive can be started in several ways. It can be started at the lowest frequency and brought up to speed by raising the frequency. It can be started at any frequency in the range as a constant-frequency induction motor is started. Or it can be started from the ac supply line and transferred to the inverter after it is up to speed. The problems of starting are the dual ones of obtaining sufficient starting torque and of not exceeding the current rating of the inverter, which is usually based on the ability of the inverter to commutate the current, rather than the thyristor ratings.

The measured torque-speed curves on an actual adjustable-frequency drive system correspond closely with the curves of Fig. 8-19 for the ideal motor. The terminal voltage of the motor is usually held constant for operation above nominal frequency. Hence, the inverter-rectifier system requires no modification other than to provide thyristor gating pulses for such operation. The breakdown torque, instead of remaining constant as in Fig. 8-19, declines. The drive operates in a constant-horsepower mode. The operation is directly analogous to field-weakening control of a dc drive with fixed armature voltage over the nominal speed.

The waveform of each half cycle of the motor voltage must be controlled below nominal speed to maintain constant air-gap flux density. The method of such control should minimize the harmonic content to avoid undue losses and braking torques. It should also be done without complicating or penalizing the inverter. The waveforms for two typical methods for such control are shown in Fig. 8-20.

Figure 8-20a shows control of a line-to-line voltage by amplitude variation of a 120° -wide pulse. Such control is obtained by varying the dc voltage from the rectifier portion of the drive. If self-commutation is em-

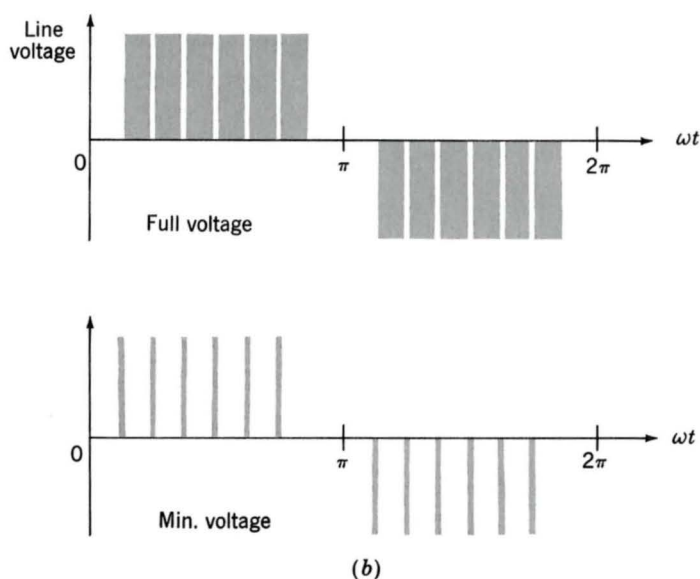
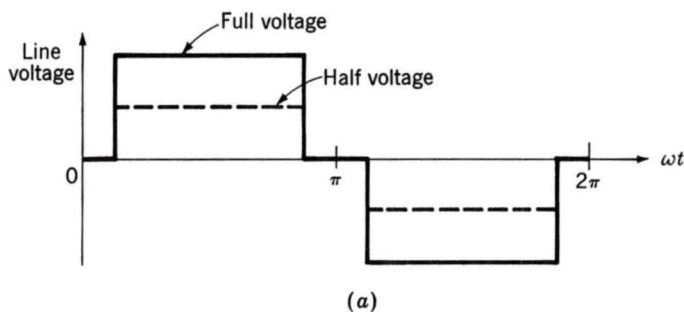


Fig. 8-20. Voltage control by (a) amplitude and (b) pulse-width control.

ployed in the inverter, it may not be possible to charge the commutation capacitors from the dc bus to commute the full motor current properly at low frequencies. The inverter may have to be derated or a separate fixed-voltage dc bus set up just to supply the commuting capacitors.

Figure 8-20b shows waveform control by pulse-width control of each half cycle of the ac voltage. The 120° width of the waveform is divided typically into six 20° -wide pulses where maximum voltage is obtained at 20° and minimum voltage at, say, 2° for a 10-to-1 speed range. The inverter dc voltage level remains unchanged, but auxiliary commutation must be used to turn off the thyristors at prescribed points in the half cycle.

8-6 SUMMARY

The dynamic performance of induction machines can often be analyzed by use of a steady-state speed-torque characteristic, as developed in Art. 7-5. Such an analysis neglects the effects of electric transients which generally occur much faster than the electromechanical dynamics of interest.

The design of an induction machine must often be a compromise between running requirements (speed regulation, efficiency, etc.) and those of start-up. High torque at start-up generally requires relatively high rotor resistance, while acceptable running characteristics dictate lower resistances.

Engineers have a range of options available to achieve these objectives. They may use a deep-bar or double-squirrel-cage design, in which the effective rotor resistance changes with slip. Alternatively, they may choose a wound-rotor design, in which the rotor resistance can be varied via external resistors or a regeneration scheme which absorbs slip-frequency rotor power (as a simple resistor does) and feeds this power back to the ac supply at the armature terminals.

Solid-state variable-frequency motor drives permit the application of induction motors in situations which previously were the almost exclusive domain of dc motors. This allows the engineer to benefit from the simplicity, reliability, and lower cost of induction motors. On the other hand, because of the necessity to generate variable-frequency and/or variable-voltage alternating current, these solid-state drive systems are more complex and expensive than their dc counterparts.

PROBLEMS

8-1. A 100-hp 60-Hz six-pole 460-V three-phase wound-rotor induction motor develops full-load torque at 1152 r/min with the rotor short-circuited. An external noninductive resistance of $1\ \Omega$ is placed in series with each phase of the rotor, and the motor is observed to develop its rated torque at a speed of 1116 r/min. Calculate the resistance per phase of the original motor.

8-2. A 50-hp 460-V three-phase four-pole 60-Hz wound-rotor induction motor develops a maximum internal torque of 225 percent at a slip of 18 percent when operating at rated voltage and frequency with its rotor short-circuited directly at the slip rings. Stator resistance and rotational losses may be neglected, and the rotor resistance may be assumed to be constant, independent of rotor frequency. Determine (a) the slip at full load in percent, (b) the rotor I^2R loss at full load in watts, and (c) the starting torque at rated voltage and frequency in newton-meters.

If the rotor resistance is now doubled (by inserting external series resistances), determine (d) the torque in newton-meters when the stator current has its full-load value and (e) the corresponding slip.

8-3. A 50-hp three-phase 440-V six-pole wound-rotor induction motor develops its rated full-load output at a speed of 1164 r/min when operated at rated voltage and frequency with its slip rings short-circuited. The maximum torque it can develop at rated voltage and frequency is 250 percent of full-load torque. The resistance of the rotor winding is $0.10\ \Omega/\text{phase Y}$. Neglect rotational and stray load losses and stator resistance.

- (a) Compute the rotor I^2R loss at full load.
- (b) Compute the speed at maximum torque.
- (c) How much resistance must be inserted in series with the rotor to produce maximum starting torque?

The motor is now run from a 50-Hz supply with the applied voltage adjusted so that the air-gap flux wave has the same amplitude at the same torque as on 60 Hz.

- (d) Compute the 50-Hz applied voltage.
- (e) Compute the speed at which the motor will develop a torque equal to its 60-Hz full-load value with its slip rings short-circuited.

8-4. A 230-V three-phase four-pole 60-Hz wound-rotor induction motor develops an internal torque of 180 percent with a line current of 190 percent at a slip of 5.5 percent when running at rated voltage and frequency with its rotor terminals short-circuited. (Torque and current are expressed as percentages of their full-load values.) The rotor resistance is $0.175\ \Omega$ between each pair of rotor terminals and may be assumed to be constant. What should be the resistance of each of three balanced Y-connected resistors inserted in series with each rotor terminal if the starting current at rated voltage and frequency is to be limited to 190 percent? What internal starting torque will be developed?

8-5. The resistance measured between each pair of slip rings of a three-phase 60-Hz 300-hp 16-pole induction motor is $0.065\ \Omega$. With the slip rings short-circuited, the full-load slip is 0.035, and it may be assumed that the slip-torque curve is a straight line from no load to full load. This motor drives a fan which requires 300 hp at the full-load speed of the motor. The torque required to drive the fan varies as the square of the speed. What resistances should be connected in series with each slip ring so that the fan will run at 325 r/min?

8-6. A polyphase induction motor has negligible rotor rotational losses and is driving a pure-inertia load. The moment of inertia of the rotor plus load is J SI units.

- (a) Obtain an expression for the rotor energy loss during starting. Express the result in terms of J and the synchronous angular velocity ω_s .

- (b) Obtain an expression for the rotor energy loss associated with reversal from full speed forward by reversing the phase sequence of the voltage supply (a process known as *plugging*). Express the result in terms of J and ω_s .
- (c) State and discuss the degree of dependence of the results in parts (a) and (b) on the current-limiting scheme which can be used during starting and reversal.
- (d) A 20-hp three-phase four-pole 60-Hz squirrel-cage induction motor has a full-load efficiency of 89.0 percent. The total inertia of rotor plus load is $0.51 \text{ kg} \cdot \text{m}^2$. The total motor losses for a reversal may be assumed to be 2.25 times the rotor losses. The impairment of ventilation arising from the lower average speed during reversing is to be ignored.

Using the result in part (b), compute the number of times per minute that the motor can be reversed without exceeding its allowable temperature rise.

- (e) Discuss the optimism or pessimism of the result in part (d).

8-7. A 460-V three-phase Y-connected six-pole 60-Hz wound-rotor induction motor has a stator-plus-rotor leakage reactance of $0.22 \Omega/\text{phase}$ referred to the stator, a rotor-plus-load moment of inertia of $1.3 \text{ kg} \cdot \text{m}^2$, negligible losses (except for rotor I^2R loss), and negligible exciting current. It is connected to a balanced 460-V source and drives a pure-inertia load. Across-the-line starting is used, and the rotor-circuit resistance is to be adjusted so that the motor brings its load from rest to one-half synchronous speed in the shortest possible time.

Determine the value of the rotor resistance referred to the stator and the minimum time to reach one-half of synchronous speed.

8-8. Consider an induction machine with equivalent-circuit parameters which can be considered to be constant independent of slip.

- (a) Show that in the limit of negligible armature resistance R_1 , the torque expression of Eq. 7-27 can be written as

$$\frac{T}{T_{\max}} = \frac{2}{s/s_{\max T} + s_{\max T}/s}$$

where T_{\max} is the maximum torque and $s_{\max T}$ is the slip at maximum torque, defined by Eqs. 7-29 and 7-30.

- (b) The period of heavy current inrush to an induction motor during starting usually lasts for about the time required to reach the slip $s_{\max T}$ at maximum torque, after which it decreases to the normal running value. Develop an expression for the time t required to reach the speed corresponding to $s_{\max T}$ for an induction motor being

started at full voltage. The combined inertia of the rotor and the connected mechanical equipment is J . The motor is unloaded at starting, and rotational losses are to be neglected.

8-9. A three-phase induction motor is operating in the steady state at slip s_1 . By suddenly interchanging two stator leads, the motor is to be plugged to a quick stop. Use the notation and assumptions of Prob. 8-8 and consider the motor to be unloaded.

- (a) Develop an expression for the braking time of the motor.
- (b) Suppose that the motor is to be reversed instead of simply brought to a stop. Develop an expression for the reversing time.

8-10. A 4160-V 3000-hp two-pole three-phase 60-Hz squirrel-cage induction motor is driving a boiler-feed pump in an electric generating plant. The table below lists points on the motor torque-speed curve at rated voltage, speed being in percentage of synchronous speed and torque in percentage of rated torque. Also listed are the torque requirements of the boiler-feed pump expressed in percentage of motor rated torque. The drive is started at rated voltage with the discharge valve open but working against a check valve until the pump head equals the system head. The straight-line portion of the pump characteristic between 0 and 10 percent speed represents the breakaway-torque requirements. At 92 percent speed the check valve opens, and there is a discontinuity in the slope of the pump curve. At 98 percent speed the motor produces its maximum torque.

Percent speed	0	10	30	50	70	90	92	98	99.5
Percent motor torque	75	75	75	75	80	125	155	240	100
Percent pump torque	15	0+	4	12	26	42	44	87	100

The inertia of the drive is such that $6700 \text{ kW} \cdot \text{s}$ of energy is stored in the rotating mass at synchronous speed. Determine (a) the time required for the check valve to open after rated voltage is applied to the motor and (b) the time required to reach the motor maximum-torque point.

8-11. For the boiler-feed-pump drive in Prob. 8-10, consider that the motor must occasionally be started with the motor voltage at 75 percent of its rated value. The motor torque may be assumed to be proportional to the square of the voltage.

- (a) Determine the time required for the check valve to open.
- (b) To what value may the motor starting voltage be reduced without making it impossible to reach a speed at which water is delivered to the system?

8-12. A frequency-changer set is to be designed for supplying variable-frequency power to induction motors driving the propellers on scale-model airplanes for wind-tunnel testing, as described in Art. 8-3*b*. The frequency changer is a wound-rotor induction machine driven by a dc motor whose speed can be controlled. The three-phase stator winding of the induction machine is excited from a 60-Hz source, and variable-frequency three-phase power is taken from its rotor winding. The set must meet the following specifications:

Output frequency range = 100 to 475 Hz

Maximum speed = 3000 r/min

Maximum power output = 75 kW at 0.85 power factor and 475 Hz

The power required by the induction-motor load drops off rapidly with decreasing frequency, so that the maximum-speed condition determines the sizes of the machines.

On the basis of negligible exciting current, losses, and voltage drops in the induction machine, find (a) the minimum number of poles for the induction machine, (b) the corresponding maximum and minimum speeds, (c) the kVA rating of the stator winding of the induction machine, and (d) the horsepower rating of the dc machine.

8-13. An adjustable-speed drive is to be furnished for a large fan in an industrial plant. The fan is to be driven by two wound-rotor induction motors coupled mechanically to the fan shaft and arranged so that lower speeds will be carried on the smaller motor and higher speeds on the larger motor. The speed control is to be arranged in steps so that the control will be uninterrupted from minimum to maximum speed and so that there will not be a sudden change in speed during the transfer from one motor to the other.

The larger motor is to be a 2300-V three-phase 500-hp 60-Hz six-pole motor; the smaller motor is to be a 200-hp 60-Hz eight-pole motor. The following motor data are furnished by the manufacturer:

Constant	200-hp motor	500-hp motor
Stator resistance, Ω	0.55	0.13
Rotor resistance, Ω	0.91	0.21
Stator plus rotor leakage reactance, Ω	2.4	0.93

These values are per phase values (Y connection) referred to the stator. Motor rotational losses and exciting requirements may be ignored.

The minimum operating speed of the fan is to be 460 r/min; the maximum speed is to be approximately 1165 r/min. The fan requires 460 hp at 1165 r/min, and the power required at other speeds varies nearly as the cube of the speed.

The proposed control scheme is based on the stators of both motors being connected to the line at all times when the drive is in operation. In the lower speed range, the rotor of the 500-hp motor is open-circuited. This lower range is obtained by adjustment of external resistance in the rotor of the 200-hp motor. Above this lower speed range, the rotor of the 200-hp motor is open-circuited; speed adjustment in the upper range is obtained by adjustment of external resistance in the rotor of the 500-hp motor.

The transition between motors from the lower to the upper speed range is to be handled as follows:

- 1 All external rotor resistance is cut out of the 200-hp motor.
- 2 By means of a closed-before-open type of contactor, the rotor circuit of the 500-hp motor is closed, and then the rotor circuit of the 200-hp motor is opened. The external rotor resistance in the 500-hp motor for this step has such a value that the speed will be the same as in the first step.
- 3 Higher speeds are obtained by cutting out rotor resistance in the 500-hp motor.

This procedure is essentially reversed in going from the higher to the lower speed range.

As plant engineer, you are asked to consider some features of this proposal. In particular, you are asked to (a) determine the range of external rotor resistance (referred to the stator) which must be available for insertion in the 200-hp motor, (b) determine the range of external rotor resistance which must be available for insertion in the 500-hp motor, and (c) discuss any features of the scheme which you do not like and suggest alternatives.

8-14. A six-pole 460-V 400-hp three-phase 60-Hz Y-connected squirrel-cage induction motor has the following constants in ohms per phase referred to the stator: $X_1 = X_2 = 0.049$, $X_\phi = 2.32$, $R_1 = 0.0048$, and $R_2 = 0.0069$. The motor is supplied at normal terminal voltage through a series reactance of $0.025 \Omega/\text{phase}$ representing a step-down transformer bank. It is fully loaded, the slip rings are short-circuited, and the efficiency and power factor are 92.3 and 90.0 percent, respectively.

A three-phase short circuit occurs at the high-voltage terminals of the transformer bank. Determine the initial symmetric short-circuit current in the motor, and show how it is decremented.

8-15. Following are points on the torque-speed curve of a three-phase squirrel-cage induction motor with balanced rated voltage applied:

Torque, per unit	0	1.00	2.00	3.00	3.50	3.25	3.00
Speed, per unit	1.00	0.97	0.93	0.80	0.47	0.20	0

Unit speed is synchronous speed; unit torque is rated torque. The motor is coupled to a machine tool which requires rated torque regardless of speed. The inertia of the motor plus load is such that it requires 1.3 s to bring them to rated speed with a constant accelerating torque equal to rated torque.

With the motor driving the load under normal steady conditions, the voltage at its terminals suddenly drops to 45 percent of rated value because of a short circuit in the neighborhood. It remains at this reduced value for 0.8 s and is then restored to its full value by clearing of the short circuit. The undervoltage relays on the motor do not operate. Will the motor stop? If not, what is its lowest speed? If it does stop, find the maximum time that the motor could have operated at 45 percent terminal voltage without stopping. Neglect any effects of secondary importance.

8-16. Induction-motor transient and dynamic considerations are important factors in the industrial application of these motors, as in refineries, chemical process plants, auxiliary drives in steam stations, etc. It is common practice to provide two sources of electric power to critical drives, a normal source and an emergency source to which the motor bus is automatically transferred in the event of failure of the normal source. When the normal source has been tripped, flux linkages are "trapped" by the closed rotor circuits of the operating motors. A motor terminal voltage (often called the *residual voltage*) is therefore produced which may require an appreciable time to decay to zero. If the motor is transferred almost immediately to the emergency source, the residual voltage and the emergency-source voltage may be so phase-displaced that the resulting heavy inrush current may damage the motor. One solution is to install a voltage-sensitive relay which delays transfer until the residual voltage has decayed to about 30 percent of normal motor voltage. In the meantime the motor is slowing down and may have real difficulty in reaccelerating when the emergency source is connected.

To investigate these problems, consider a 4160-V 3000-hp two-pole three-phase 3570-r/min 60-Hz squirrel-cage induction motor driving a boiler-feed pump. The motor has an open-circuit transient time constant of 3.9 s, short-circuit time constant of 0.14 s, and transient reactance of $1.8 \Omega/\text{phase Y}$. The motor is operating fully loaded at rated voltage and draws 2590 kVA at 0.90 power factor from the mains. (This problem is based on a single motor. In a practical case, the effects of other parallel motors must be considered.[†])

- (a) Determine the time required after interruption of the normal supply for the residual voltage to decay to 30 percent of the normal bus voltage.

[†]See D. G. Lewis and W. D. Marsh, "Transfer of Steam-Electric Generating Station Auxiliary Buses," *Trans. AIEE*, 74:322-330 (1955).

- (b) Determine the speed to which the motor decelerates in this interval. The inertia of the motor rotor and pump impeller is $68.0 \text{ kg} \cdot \text{m}^2$. Consider that the load torque varies as the square of the speed, and neglect losses.
- (c) Assume that the emergency source consists of a constant 100 percent voltage behind a reactive impedance of 0.13Ω (representing a step-down transformer bank). Assume also that torque-slip and current-slip curves at rated voltage are available for the motor. Outline a method by which a speed-time curve can be obtained for the reacceleration period. A step-by-step method arranged for either hand computation or digital-computer programming is suggested.
- (d) Let the torque-slip curve be that given for the motor in Prob. 8-10. Corresponding data for the current-slip curve are given below, the current being percentage of current under rated conditions.

Percentage of speed	0	30	50	70	90	92	98	99.5
Percentage of current	620	620	620	620	580	540	390	100

By the method you have outlined in part (c), plot motor speed as a function of time during reacceleration.

- (e) The practical problem may be to determine the maximum allowable impedance and hence the size of the emergency step-down transformer bank which will permit both motor starting and successful reacceleration of all the motor drives after transfer. Describe how you would carry out such an investigation.

8-17. An induction motor is being selected to drive a pump. The speed of the motor and pump will be controlled by adjustment of the primary stator voltage. The motor slip is 0.03 per unit for rated torque.

Sketch the profile of the allowable motor torque as a function of slip from $s = 0$ to 1.0 per unit for the following levels of rotor power dissipation:

- (a) nominal, corresponding to dissipation at $s = 0.03$ per unit; (b) twice the value for part (a); (c) 4 times the value for part (a).

8-18. A variable-frequency variable-voltage three-phase ac motor drive is used to drive a squirrel-cage induction motor. The output frequency can be varied from 30 to 60 Hz and, in order to maintain essentially constant flux in the motor, the output voltage varies linearly with frequency (constant volts per hertz).

- (a) For this motor-drive-motor combination, rewrite Eq. 7-27 in terms of the synchronous speed ω_s , the shaft mechanical speed ω_m , V_{t0} , the applied voltage at 60 Hz, and $\omega_0 = 2\pi \times 60$, the 60-Hz angular frequency.

- (b) Show that in the limit of negligible stator resistance the magnitude of the peak torque remains constant, independent of the applied frequency.
- (c) Show that in the limit of negligible stator resistance the shape of the torque-speed characteristic is independent of the applied frequency and is simply shifted up or down in speed as determined by the applied frequency.
- (d) Express quantitatively the criterion for the validity of negligible-stator-resistance approximation used in parts (b) and (c).

8-19. The motor drive of Prob. 8-18 is used to drive the three-phase 220-V (line-to-line) 10-hp 60-Hz six-pole induction motor of Examples 7-1 and 7-2. This problem repeats the calculations of Examples 7-1 and 7-2 with the motor-drive output at 30 Hz and 110 V (line to line). Assume that the total friction, windage, and core loss under these conditions is 100 W, independent of load.

- (a) Based on the results of part (c) of Prob. 8-18, the shaft torque at a slip of 4 percent should correspond to the 2 percent 60-Hz 220-V case of Example 7-1. Calculate the motor speed, output torque and power, stator current, power factor, and efficiency for a slip of 4 percent.
- (b) Calculate the maximum torque and the corresponding speed and slip.
- (c) Calculate the starting torque and current.

DC Machines: Steady State

Dc machines are characterized by their versatility. By means of various combinations of shunt-, series-, and separately excited field windings they can be designed to display a wide variety of volt-ampere or speed-torque characteristics for both dynamic and steady-state operation. Because of the ease with which they can be controlled, systems of dc machines are often used in applications requiring a wide range of motor speeds or precise control of motor output. In recent years, solid-state ac drive system technology has developed sufficiently that these systems are beginning to be found in applications previously associated almost exclusively with dc machines. However, dc machines will continue to find application because of their flexibility and the relative simplicity of their drive systems as compared with ac machines.

9-1 INTRODUCTION

The essential features of a dc machine are shown schematically in Fig. 9-1. The stator has salient poles and is excited by one or more field coils. The air-gap flux distribution created by the field windings is symmetric about the centerline of the field poles. This axis is called the *field axis* or *direct axis*.

As discussed in Art. 4-2c, the ac voltage generated in each rotating armature coil is converted to dc in the external armature terminals by means of a rotating commutator and stationary brushes to which the armature leads are connected. The commutator-brush combination forms a mechanical rectifier, resulting in a dc armature voltage as well as an armature-mmf wave which is fixed in space. Commutator action is discussed in detail in Art. 9-2.

The brushes are located so that commutation occurs when the coil sides are in the neutral zone, midway between the field poles. The axis of the armature-mmf wave then is 90 electrical degrees from the axis of the field poles, i.e., in the *quadrature axis*. In the schematic representation of Fig. 9-1a, the brushes are shown in the quadrature axis because this is the position of the coils to which they are connected. The armature-mmf wave then is along the brush axis, as shown. (The geometric position of the brushes in an actual machine is approximately 90 electrical degrees from their position in the schematic diagram because of the shape of the end connections to the commutator. For example, see Fig. 9-7.) For simplicity, the circuit representation usually will be drawn as in Fig. 9-1b.

Although the magnetic torque and the speed voltage appearing at the brushes are somewhat dependent on the spatial waveform of the flux distribution, for convenience we continue to assume a sinusoidal flux-density

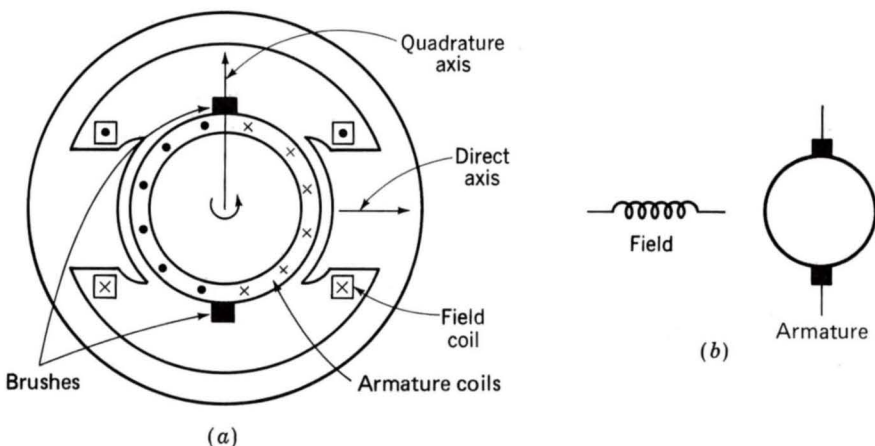


Fig. 9-1. Schematic representations of a dc machine.

wave in the air gap. The torque can then be found from the magnetic field viewpoint of Art. 4-7*b*.

The torque can be expressed in terms of the interaction of the direct-axis air-gap flux per pole Φ_d and the space-fundamental component F_{a1} of the armature-mm*f* wave, in a form similar to Eq. 4-85. With the brushes in the quadrature axis, the angle between these fields is 90 electrical degrees, and its sine equals unity. Substitution in Eq. 4-85 then gives for a *P*-pole machine

$$T = \frac{\pi}{2} \left(\frac{P}{2} \right)^2 \Phi_d F_{a1} \quad (9-1)$$

in which the minus sign has been dropped because the positive direction of the torque can be determined from physical reasoning. The peak value of the sawtooth armature-mm*f* wave is given by Eq. 4-10, and its space fundamental F_{a1} is $8/\pi^2$ times its peak. Substitution in Eq. 9-1 then gives

$$T = \frac{PC_a}{2\pi m} \Phi_d i_a = K_a \Phi_d i_a \quad (9-2)$$

where i_a = current in external armature circuit

C_a = total number of conductors in armature winding

m = number of parallel paths through winding

and

$$K_a = \frac{PC_a}{2\pi m} \quad (9-3)$$

is a constant fixed by the design of the winding.

The rectified voltage generated in the armature has already been found in Art. 4-6*b* for an elementary single-coil armature, and its waveform is shown in Fig. 4-33. The effect of distributing the winding in several slots is shown in Fig. 9-2, in which each of the rectified sine waves is

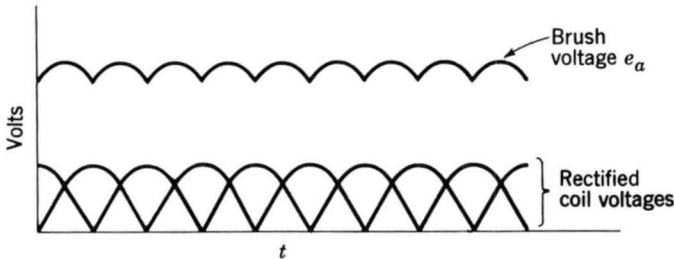


Fig. 9-2. Rectified coil voltages and resultant voltage between brushes in a dc machine.

the voltage generated in one of the coils, commutation taking place at the moment when the coil sides are in the neutral zone. The generated voltage as observed from the brushes is the sum of the rectified voltages of all the coils in series between brushes and is shown by the rippling line labeled e_a in Fig. 9-2. With a dozen or so commutator segments per pole, the ripple becomes very small and the average generated voltage observed from the brushes equals the sum of the average values of the rectified coil voltages. From Eq. 4-58 the rectified voltage e_a between brushes, known also as the *speed voltage*, is

$$e_a = \frac{PC_a}{2\pi m} \Phi_d \omega_m = K_a \Phi_d \omega_m \quad (9-4)$$

where K_a is the winding constant defined in Eq. 9-3. The rectified voltage of a distributed winding has the same average value as that of a concentrated coil. The difference is that the ripple is greatly reduced.

From Eqs. 9-2 and 9-4, with all variables expressed in SI units,

$$e_a i_a = T \omega_m \quad (9-5)$$

This equation simply says that the instantaneous electric power associated with the speed voltage equals the instantaneous mechanical power associated with the magnetic torque, the direction of power flow being determined by whether the machine is acting as a motor or generator.

The direct-axis air-gap flux is produced by the combined mmf $\Sigma N_f i_f$ of the field windings, the flux-mmF characteristic being the *magnetization curve* for the particular iron geometry of the machine. A magnetization curve is shown in Fig. 9-3a, in which it is assumed that the armature mmf has no effect on the direct-axis flux because the axis of the armature-mmF wave is perpendicular to the field axis. It will be necessary to reexamine this assumption later in this chapter, where the effects of saturation are investigated more thoroughly. Because the armature emf is proportional to flux times speed, it is usually more convenient to express the magnetization curve in terms of the armature emf e_{a0} at a constant speed ω_{m0} as shown in Fig. 9-3b. The voltage e_a for a given flux at any other speed ω_m is proportional to the speed; i.e., from Eq. 9-4

$$\frac{e_a}{\omega_m} = K_a \Phi_d = \frac{e_{a0}}{\omega_{m0}} \quad (9-6)$$

or

$$e_a = \frac{\omega_m}{\omega_{m0}} e_{a0} \quad (9-7)$$

Figure 9-3c shows the magnetization curve with only one field winding excited. This curve can easily be obtained by test methods, no knowledge of any design details being required.

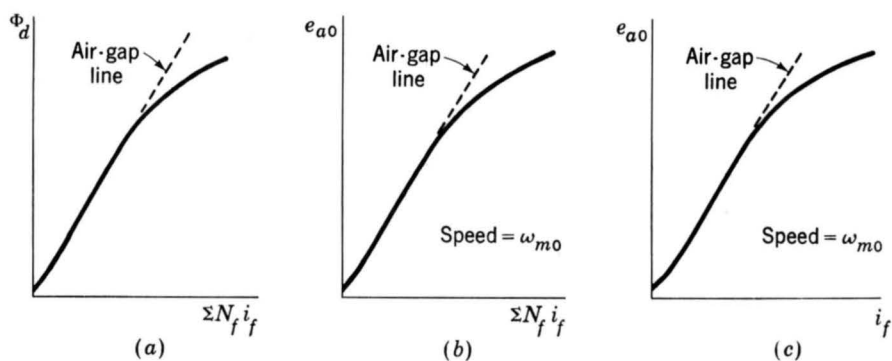


Fig. 9-3. Magnetization curves of a dc machine.

Over a fairly wide range of excitation the reluctance of the iron is negligible compared with that of the air gap. In this region the flux is linearly proportional to the total mmf of the field windings, the constant of proportionality being the *direct-axis air-gap permeance* \mathcal{P}_d ; thus

$$\Phi_d = \mathcal{P}_d \sum N_f i_f \quad (9-8)$$

The dashed straight line through the origin coinciding with the straight portion of the magnetization curves in Fig. 9-3 is called the *air-gap line*.

The outstanding advantages of dc machines arise from the wide variety of operating characteristics which can be obtained by selection of the method of excitation of the field windings. The field windings may be *separately excited* from an external dc source, or they may be *self-excited*, i.e., the machine may supply its own excitation. Connection diagrams are shown in Fig. 9-4. The method of excitation profoundly influences both the

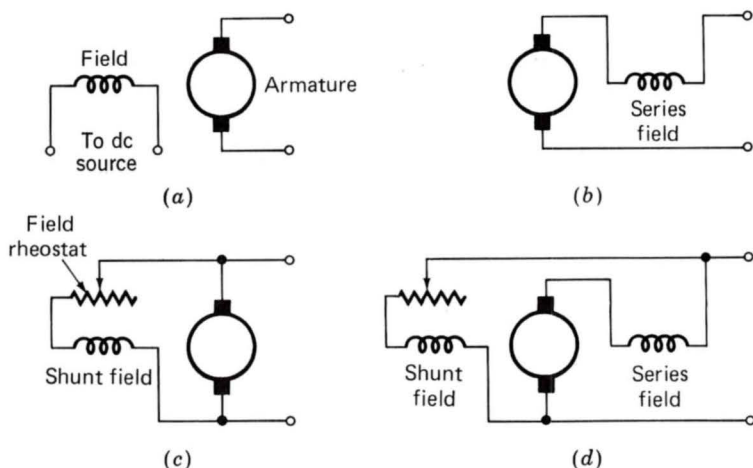


Fig. 9-4. Field circuit connections of dc machines: (a) separate excitation, (b) series, (c) shunt, (d) compound.

steady-state characteristics and the dynamic behavior of the machine in control systems.

The connection diagram of a *separately excited generator* is given in Fig. 9-4a. The required field current is a very small fraction of the rated armature current—on the order of 1 to 3 percent in the average generator. A small amount of power in the field circuit may control a relatively large amount of power in the armature circuit; i.e., the generator is a power amplifier. Separately excited generators are often used in feedback control systems when control of the armature voltage over a wide range is required.

The field windings of self-excited generators may be supplied in three different ways. The field may be connected in series with the armature (Fig. 9-4b), resulting in a *series generator*. The field may be connected in shunt with the armature (Fig. 9-4c), resulting in a *shunt generator*, or the field may be in two sections (Fig. 9-4d), one of which is connected in series and the other in shunt with the armature, resulting in a *compound generator*. With *self-excited generators*, residual magnetism must be present in the machine iron to get the self-excitation process started. The effects of residual magnetism can be clearly seen in Fig. 9-3, where the flux and voltage are seen to have nonzero values when the field current is zero.

Typical steady-state volt-ampere characteristics of dc generators are shown in Fig. 9-5, constant-speed prime movers being assumed. The relation between the steady-state generated emf E_a and the terminal voltage V_t is

$$V_t = E_a - I_a R_a \quad (9-9)$$

where I_a is the armature current output and R_a is the armature circuit re-

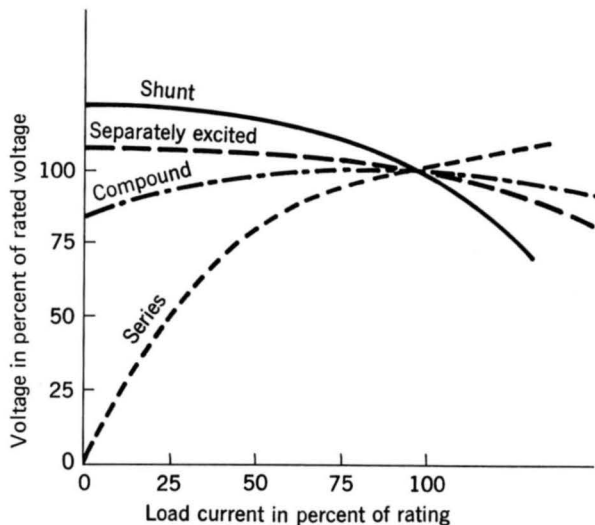


Fig. 9-5. Volt-ampere characteristics of dc generators.

sistance. In a generator, E_a is larger than V_t , and the electromagnetic torque T is a countertorque opposing rotation.

The terminal voltage of a separately excited generator decreases slightly with an increase in the load current, principally because of the voltage drop in the armature resistance. The field current of a series generator is the same as the load current, so that the air-gap flux and hence the voltage vary widely with load. As a consequence, series generators are not often used. The voltage of shunt generators drops off somewhat with load, but not in a manner which is objectionable for many purposes. Compound generators are normally connected so that the mmf of the series winding aids that of the shunt winding. The advantage is that through the action of the series winding the flux per pole can increase with load, resulting in a voltage output which is nearly constant or which even rises somewhat as load increases. The shunt winding usually contains many turns of relatively small wire. The series winding, wound on the outside, consists of a few turns of comparatively heavy conductor because it must carry the full armature current of the machine. The voltage of both shunt and compound generators can be controlled over reasonable limits by means of rheostats in the shunt field.

Any of the methods of excitation used for generators can also be used for motors. Typical steady-state speed-torque characteristics are shown in Fig. 9-6, in which it is assumed that the motor terminals are supplied from a constant-voltage source. In a motor the relation between the emf E_a generated in the armature and the terminal voltage V_t is

$$V_t = E_a + I_a R_a \quad (9-10)$$

or
$$I_a = \frac{V_t - E_a}{R_a} \quad (9-11)$$

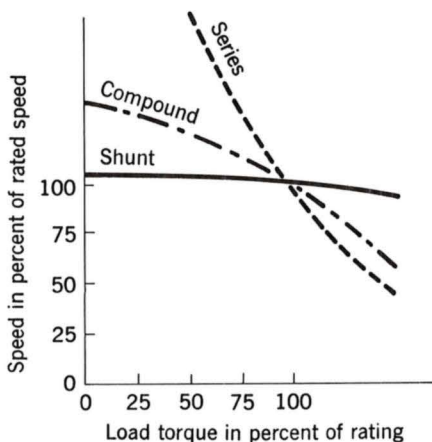


Fig. 9-6. Speed-torque characteristics of dc motors.

where I_a is now the armature current input. The generated emf E_a is now smaller than the terminal voltage V_t , the armature current is in the opposite direction to that in a generator, and the electromagnetic torque is in the direction to sustain rotation of the armature.

In shunt and separately excited motors, the field flux is nearly constant. Consequently, increased torque must be accompanied by a very nearly proportional increase in armature current and hence by a small decrease in counter emf E_a to allow this increased current through the small armature resistance. Since counter emf is determined by flux and speed (Eq. 9-4), the speed must drop slightly. Like the squirrel-cage induction motor, the shunt motor is substantially a constant-speed motor having about 5 percent drop in speed from no load to full load. A typical speed-load characteristic is shown by the solid curve in Fig. 9-6. Starting torque and maximum torque are limited by the armature current that can be successfully commutated.

An outstanding advantage of the shunt motor is ease of speed control. With a rheostat in the shunt-field circuit, the field current and flux per pole can be varied at will, and variation of flux causes the inverse variation of speed to maintain counter emf approximately equal to the impressed terminal voltage. A maximum speed range of about 4 or 5 to 1 can be obtained by this method, the limitation again being commutating conditions. By variation of the impressed armature voltage, very wide speed ranges can be obtained.

In the series motor, increase in load is accompanied by increases in the armature current and mmf and the stator field flux (provided the iron is not completely saturated). Because flux increases with load, speed must drop in order to maintain the balance between impressed voltage and counter emf; moreover, the increase in armature current caused by increased torque is smaller than in the shunt motor because of the increased flux. The series motor is therefore a varying-speed motor with a markedly drooping speed-load characteristic of the type shown in Fig. 9-6. For applications requiring heavy torque overloads, this characteristic is particularly advantageous because the corresponding power overloads are held to more reasonable values by the associated speed drops. Very favorable starting characteristics also result from the increase in flux with increased armature current.

In the compound motor, the series field may be connected either *cumulatively*, so that its mmf adds to that of the shunt field, or *differentially*, so that it opposes. The differential connection is very rarely used. As shown by the broken-dash curve in Fig. 9-6, a cumulatively compounded motor has speed-load characteristics intermediate between those of a shunt and a series motor, the drop of speed with load depending on the relative number of ampere-turns in the shunt and series fields. It does not have the disadvantage of very high light-load speed associated with a series motor, but it retains to a considerable degree the advantages of series excitation.

The application advantages of dc machines lie in the variety of performance characteristics offered by the possibilities of shunt, series, and compound excitation. Some of these characteristics have been touched upon briefly in this article. Still greater possibilities exist if additional sets of brushes are added so that other voltages can be obtained from the commutator. Thus the versatility of dc-machine systems and their adaptability to control, both manual and automatic, are their outstanding features.

9-2 COMMUTATOR ACTION

The dc machine differs in several respects from the ideal model of Art. 4-2c. Although the basic concepts of Art. 4-2c are still valid, a reexamination of the assumptions and a modification of the model are desirable. The crux of the matter is the effect of the commutator shown in Figs. 4-1 and 4-16.

Figure 9-7 shows diagrammatically the armature winding of Figs. 4-22 and 4-23a with the addition of the commutator, brushes, and connections of the coils to the commutator segments. The commutator is represented by the ring of segments in the center of the figure. The segments are insulated from each other and from the shaft. Two stationary brushes are shown by the black rectangles inside the commutator. Actually the brushes usually contact the outer surface, as shown in Fig. 4-16. The coil sides in the slots are shown in cross section by the small circles with dots and crosses in them, indicating currents toward and away from the reader, respectively, as in Fig. 4-22. The connections of the coils to the commutator segments are shown by the circular arcs. The end connections at the back of the armature are shown dashed for the two coils in slots 1 and 7, and the connections of these coils to adjacent commutator segments are shown by the heavy arcs. All coils are identical. The back end connections of the other coils have been omitted to avoid complicating the figure, but they can easily be traced by remembering that each coil has one side in the top of a slot and the other side in the bottom of the diametrically opposite slot.

In Fig. 9-7a the brushes are in contact with commutator segments 1 and 7. Current entering the right-hand brush divides equally between two parallel paths through the winding. The first path leads to the inner coil side in slot 1 and finally ends at the brush on segment 7. The second path leads to the outer coil side in slot 6 and also finally ends at the brush on segment 7. The current directions in Fig. 9-7a can readily be verified by tracing these two paths. They are the same as in Fig. 4-22. The effect is identical to that of a coil wrapped around the armature with its magnetic axis vertical, and a clockwise magnetic torque is exerted on the armature, tending to align its magnetic field with that of the field winding.

Now suppose the machine is acting as a generator driven in the counterclockwise direction by an applied mechanical torque. Figure 9-7b shows

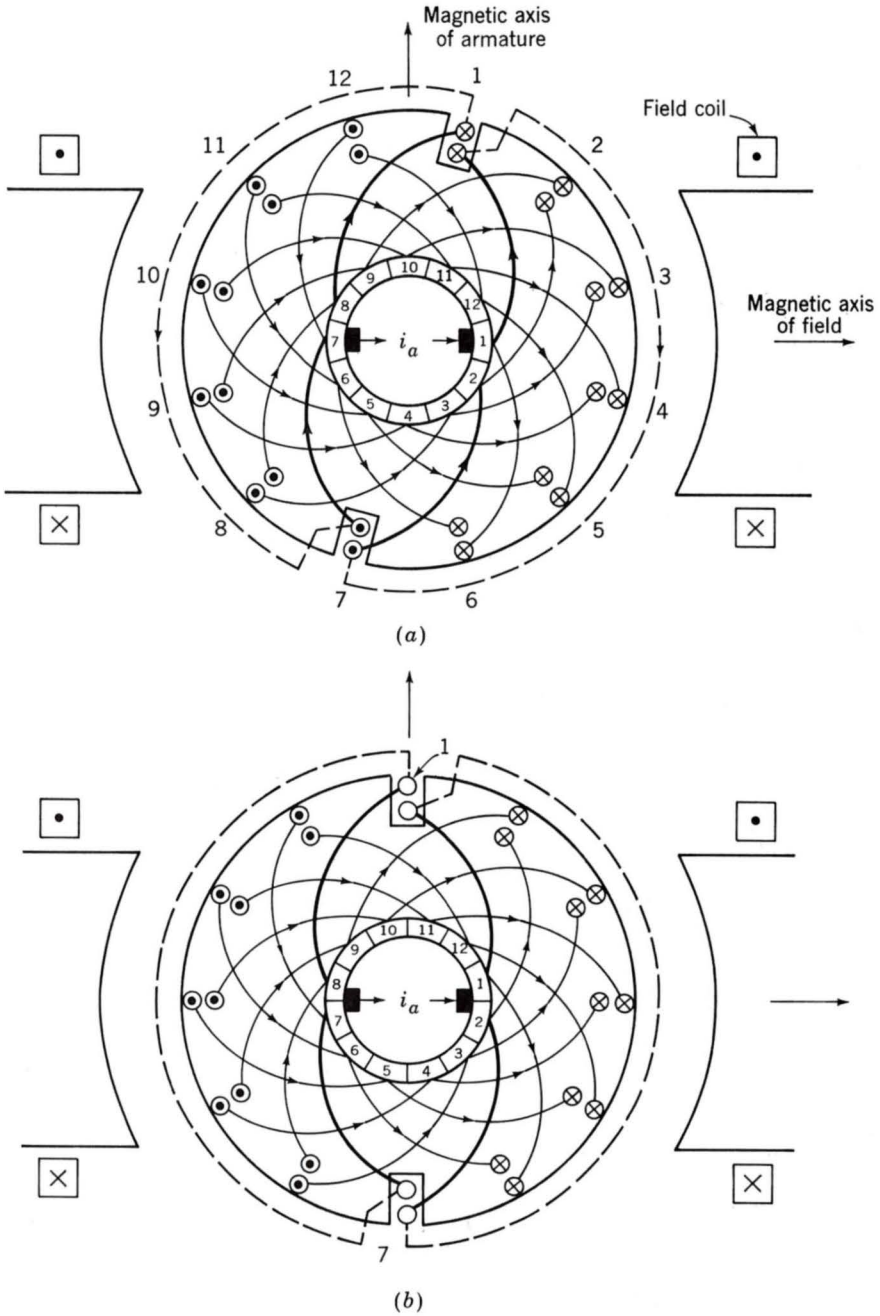


Fig. 9-7. Dc machine armature winding with commutator and brushes. (a), (b) Current directions for two positions of the armature.

the situation after the armature has rotated through the angle subtended by half a commutator segment. The right-hand brush is now in contact with both segments 1 and 2, and the left-hand brush is in contact with both segments 7 and 8. The coils in slots 1 and 7 are now short-circuited by the brushes. The currents in the other coils are shown by the dots and crosses, and they produce a magnetic field whose axis again is vertical.

After further rotation, the brushes will be in contact with segments 2 and 8, and slots 1 and 7 will have rotated into the positions which were previously occupied by slots 12 and 6 in Fig. 9-7a. The current directions will be similar to those of Fig. 9-7a except that the currents in the coils in slots 1 and 7 will have reversed. The magnetic axis of the armature is still vertical.

During the time when the brushes are simultaneously in contact with two adjacent commutator segments, the coils connected to these segments are temporarily removed from the main circuits through the winding, short-circuited by the brushes, and the currents in them are reversed. Ideally, the current in the coils being commutated should reverse linearly with time. Serious departure from linear commutation will result in sparking at the brushes. Means for obtaining sparkless commutation are discussed in Art. 9-8. With linear commutation the waveform of the current in any coil as a function of time is trapezoidal, as shown in Fig. 9-8.

The winding of Fig. 9-7 is simpler than that used in most dc machines. Ordinarily more slots and commutator segments would be used, and except in small machines, more than two poles are common. Nevertheless, the simple winding of Fig. 9-7 includes the essential features of more complicated windings.

9-3 EFFECT OF ARMATURE MMF

Armature mmf has definite effects on both the space distribution of the air-gap flux and the magnitude of the net flux per pole. The effect on flux distribution is important because the limits of successful commutation are directly influenced; the effect on flux magnitude is important because both the generated voltage and the torque per unit of armature current are influenced thereby. These effects and the problems arising from them are described in this article.

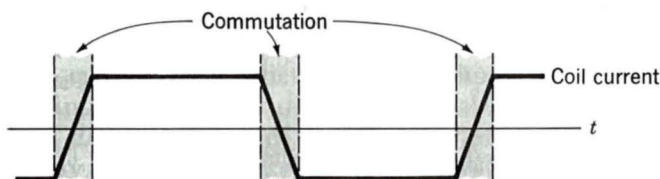


Fig. 9-8. Waveform of current in an armature coil with linear commutation.

It was shown in Art. 4-3*b* and Fig. 4-23 that the armature-mm*f* wave can be closely approximated by a sawtooth, corresponding to the wave produced by a finely distributed armature winding or current sheet. For a machine with brushes in the neutral position, the idealized mm*f* wave is again shown by the dashed sawtooth in Fig. 9-9, in which a positive mm*f* ordinate denotes flux lines leaving the armature surface. Current directions in all windings other than the main field are indicated by black and crosshatched bands. Because of the salient-pole field structure found in almost all dc machines, the associated space distribution of flux will not be triangular. The distribution of air-gap flux density with only the armature excited is given by the solid curve of Fig. 9-9. As can readily be seen, it is appreciably decreased by the long air path in the interpolar space.

The axis of the armature mm*f* is fixed at 90 electrical degrees from the main-field axis by the brush position. The corresponding flux follows the paths shown in Fig. 9-10. The effect of the armature mm*f* is seen to be that of creating flux crossing the pole faces; thus its path in the pole shoes crosses the path of the main-field flux. For this reason, armature reaction of this type is called *cross-magnetizing armature reaction*. It evidently causes a decrease in the resultant air-gap flux density under one half of the pole and an increase under the other half.

When the armature and field windings are both excited, the resultant air-gap flux-density distribution is of the form given by the solid curve of Fig. 9-11. Superimposed on this figure are the flux distributions with only the armature excited (long-dash curve) and only the field excited (short-dash curve). The effect of cross-magnetizing armature reaction in decreas-

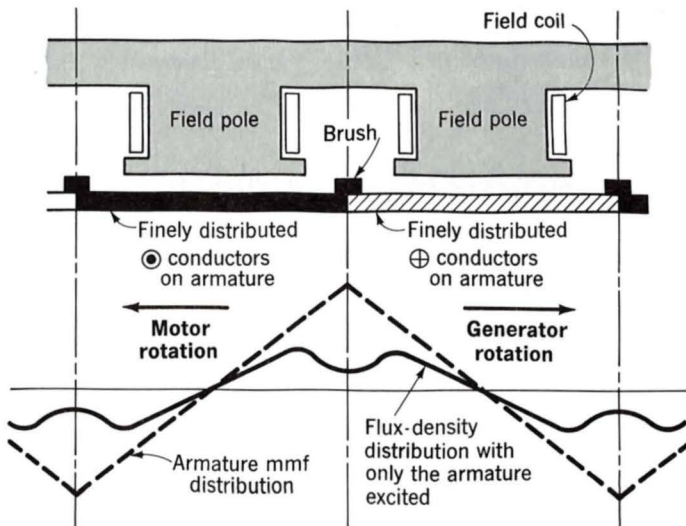


Fig. 9-9. Armature-mm*f* and flux-density distribution with brushes on neutral and only the armature excited.

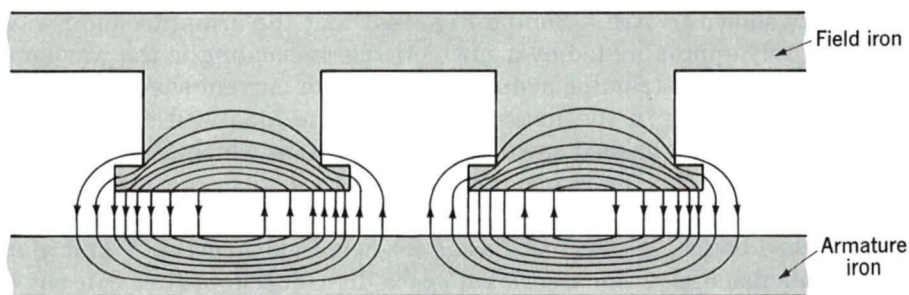


Fig. 9-10. Flux with only the armature excited and brushes on neutral.

ing the flux under one pole tip and increasing it under the other can be seen by comparing the solid and short-dash curves. In general, the solid curve is not the algebraic sum of the two dashed curves because of the non-linearity of the iron magnetic circuit. Because of saturation of the iron, the flux density is decreased by a greater amount under one pole tip than it is increased under the other. Accordingly, the resultant flux per pole is lower

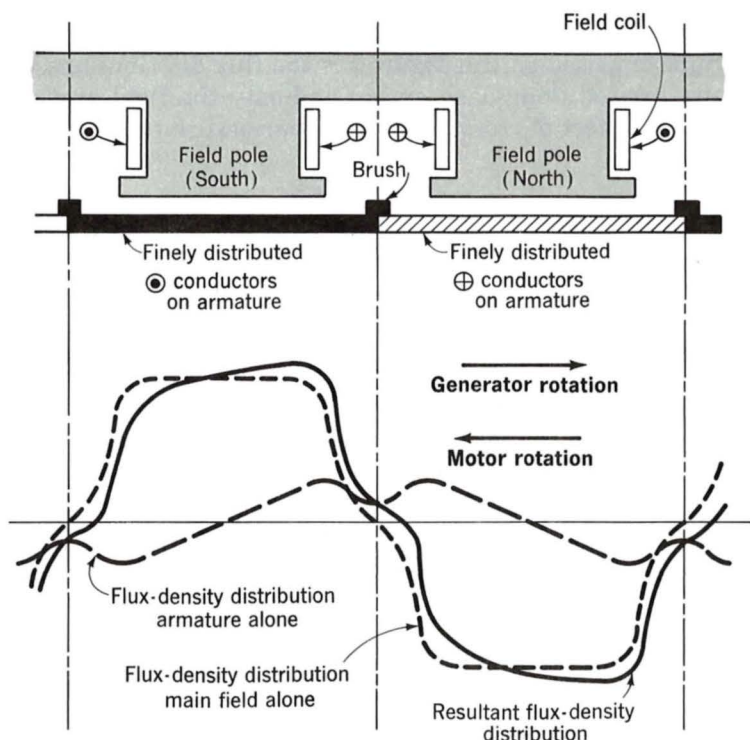


Fig. 9-11. Armature, main-field, and resultant flux-density distributions with brushes on neutral.

than would be produced by the field winding alone, a consequence known as the *demagnetizing effect of cross-magnetizing armature reaction*. Since it is caused by saturation, its magnitude is a nonlinear function of both the field current and the armature current. For normal machine operation at the flux densities used commercially, the effect is usually significant, especially at heavy loads, and must often be taken into account in analyses of performance.

The distortion of the flux distribution caused by cross-magnetizing armature reaction may have a detrimental influence on the ability to commutate the current, especially if the distortion becomes excessive. In fact, this distortion is usually an important factor limiting the short-time overload of a dc machine. Tendency toward distortion of the flux distribution is most pronounced in a machine, such as a shunt motor, where the field excitation remains substantially constant while the armature mmf may reach very significant proportions at heavy loads. The tendency is least pronounced in a series-excited machine, such as the series motor, for both the field and armature mmf increase with load.

The effect of cross-magnetizing armature reaction can be limited in the design and construction of the machine. The mmf of the main field should exert predominating control on the air-gap flux, so that the condition of weak-field mmf and strong armature mmf can be avoided. The reluctance of the cross-flux path—essentially, the armature teeth, pole shoes, and the air gap, especially at the pole tips—can be increased by increasing the degree of saturation in the teeth and pole faces, by avoiding too small an air gap, and by using a chamfered or eccentric pole face, which increases the air gap at the pole tips. These expedients affect the path of the main flux as well, but the influence on the cross flux is much greater. The best, but also the most expensive, curative measure is to compensate the armature mmf by means of a winding embedded in the pole faces, a measure discussed in Art. 9-8.

If the brushes are not in the neutral position, the axis of the armature-mmfm wave is not 90° from the main-field axis. The armature mmf then produces not only cross magnetization but also a direct demagnetizing or magnetizing effect, depending on the direction of brush shift. Shifting of the brushes from the neutral is usually inadvertent due to incorrect positioning of the brushes or a poor brush fit. Before the invention of interpoles, however, shifting the brushes was a common method of securing satisfactory commutation, the direction of the shift being such that demagnetizing action was produced. It can be shown that brush shift in the direction of rotation in a generator or against rotation in a motor produces a direct demagnetizing mmf which may result in unstable operation of a motor or excessive drop in voltage of a generator. Incorrectly placed brushes can be detected by a load test. If the brushes are on neutral, the terminal voltage of a generator or the speed of a motor should be the same for identical conditions of field excitation and armature current when the direction of rotation is reversed.

9-4 ANALYTICAL FUNDAMENTALS: ELECTRIC CIRCUIT ASPECTS

From Eqs. 9-1 and 9-4 the electromagnetic torque and generated voltage of a dc machine are, respectively,

$$T = K_a \Phi_d I_a \quad (9-12)$$

and

$$E_a = K_a \Phi_d \omega_m \quad (9-13)$$

where

$$K_a = \frac{PC_a}{2\pi m} \quad (9-14)$$

Here the capital-letter symbols E_a for generated voltage and I_a for armature current are used to emphasize that we are primarily concerned with steady-state considerations in this chapter. The remaining symbols are as defined in Art. 9-1. These are basic equations for analysis of the machine. The quantity $E_a I_a$ is frequently referred to as the *electromagnetic power*; from Eqs. 9-12 and 9-13 it is related to electromagnetic torque by

$$T = \frac{E_a I_a}{\omega_m} \quad (9-15)$$

The electromagnetic power differs from the mechanical power at the machine shaft by the rotational losses and differs from the electric power at the machine terminals by the shunt-field and armature $I^2 R$ losses. The electromagnetic power is that measured at the points across which E_a exists; numerical addition of the rotational losses for generators and subtraction for motors yield the mechanical power at the shaft.

The interrelations between voltage and current are immediately evident from the connection diagram of Fig. 9-12. Thus,

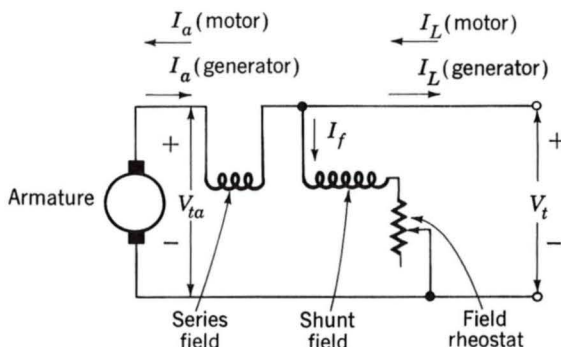


Fig. 9-12. Motor or generator connection diagram with current directions.

$$V_{ta} = E_a \pm I_a R_a \quad (9-16)$$

$$V_t = E_a \pm I_a (R_a + R_s) \quad (9-17)$$

and
$$I_L = I_a \pm I_f \quad (9-18)$$

where the plus sign is used for a motor and the minus sign for a generator and R_a and R_s are the resistances of the armature and series field, respectively. Some of the terms in Eqs. 9-16 to 9-18 may be omitted when the machine connections are simpler than those shown in Fig. 9-12. The resistance R_a is to be interpreted as that of the armature plus brushes unless specifically stated otherwise. Sometimes R_a is taken as the resistance of the armature winding alone and the brush-contact voltage drop is accounted for as a separate item, usually assumed to be 2 V.

EXAMPLE 9-1

A 25-kW 125-V separately excited dc machine is operated at a constant speed of 3000 r/min with a constant field current such that the open-circuit armature voltage is 125 V. The armature resistance is 0.02 Ω .

Compute the armature current, terminal power, and electromagnetic power and torque when the terminal voltage is (a) 128 V and (b) 124 V.

Solution

(a) From Eq. 9-16, with $V_t = 128$ V and $E_a = 125$ V, the armature current is

$$I_a = \frac{V_t - E_a}{R_a} = \frac{128 - 125}{0.02} = 150 \text{ A}$$

in the motor direction, and the terminal power is

$$V_t I_a = 128 \times 150 = 19.20 \text{ kW}$$

The electromagnetic power is given by

$$E_a I_a = 125 \times 150 = 18.75 \text{ kW}$$

It is smaller than the terminal power by the power dissipated in the armature resistance because the machine is operating as a motor.

Finally, the electromagnetic torque is given by Eq. 9-15:

$$T = \frac{E_a I_a}{\omega_m} = \frac{18.75 \text{ kW}}{100\pi} = 59.7 \text{ N} \cdot \text{m}$$

(b) In this case, the armature current is

$$I_a = \frac{E_a - V_t}{R_a} = \frac{125 - 124}{0.02} = 50 \text{ A}$$

in the generator direction, and the terminal power is

$$V_t I_a = 124 \times 50 = 6.20 \text{ kW}$$

The electromagnetic power is

$$E_a I_a = 125 \times 50 = 6.25 \text{ kW}$$

and the electromagnetic torque is

$$T = \frac{6.25 \text{ kW}}{100\pi} = 19.9 \text{ N} \cdot \text{m}$$

Note that in this case the machine is operating as a generator.

For compound machines, another variation may occur. Figure 9-12 shows a *long-shunt connection* in that the shunt field is connected directly across the line terminals with the series field between it and the armature. An alternative possibility is the *short-shunt connection*, illustrated in Fig. 9-13 for a compound generator, with the shunt field directly across the armature and the series field between it and the line terminals. The series-field current is then I_L instead of I_a , and the voltage equations are modified accordingly. There is so little practical difference between these two connections that the distinction can usually be ignored: unless otherwise stated, compound machines will be treated as though they were long-shunt-connected.

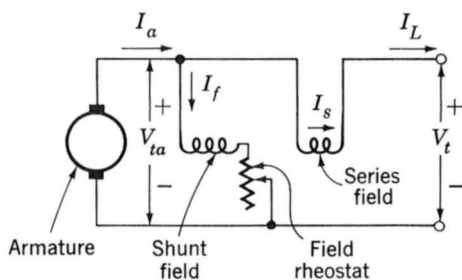


Fig. 9-13. Short-shunt compound-generator connections.

Although the difference between terminal voltage V_t and armature-generated voltage E_a is comparatively small for normal operation, it has a definite bearing on performance characteristics. In effect, this difference, acting in conjunction with the circuit resistances and energy conversion requirements, affects the value of armature current I_a and hence the rotor field strength. Complete determination of machine behavior requires a similar investigation of factors influencing the stator field strength or, more particularly, the net flux per pole Φ_d .

9-5 ANALYTICAL FUNDAMENTALS: MAGNETIC CIRCUIT ASPECTS

The flux per pole is that resulting from the combined armature and field mmf's. The interdependence of armature-generated voltage E_a and magnetic circuit conditions in the machine is accordingly a function of the sum of all the mmf's on the polar- or direct-axis flux path. First we consider the mmf purposely placed on the stator main poles to create the working flux, i.e., the *main-field mmf*, and then we include armature-mmf effects.

a. Armature Reaction Neglected

With no load on the machine or with armature-reaction effects ignored, the resultant mmf is the algebraic sum of the mmf's on the main- or direct-axis poles. For the usual compound generator or motor having N_f shunt-field turns per pole and N_s series-field turns per pole,

$$\text{Main-field mmf} = N_f I_f \pm N_s I_s \quad (9-19)$$

Additional terms will appear in this equation when there are additional field windings on the main poles and when, unlike the compensating windings of Art. 9-9, they are wound concentric with the normal field windings to permit specialized control. In Eq. 9-19 the plus sign is used when the two mmf's are aiding or when the two fields are cumulatively connected; the minus sign is used when the series field opposes the shunt field or for a differential connection. When either the series or the shunt field is absent, the corresponding term in Eq. 9-19 naturally is omitted.

Equation 9-19 thus sums up in ampere-turns per pole the gross mmf of the main-field windings acting on the main magnetic circuit. The magnetization curve for a dc machine is generally given in terms of current in only the principal field winding, which is almost invariably the shunt-field winding when one is present. The mmf units of such a magnetization curve and of Eq. 9-19 can be made the same by one of two rather obvious steps. The field current on the magnetization curve can be multiplied by the turns per pole in that winding, giving a curve in terms of ampere-turns per pole; or both sides of Eq. 9-19 can be divided by N_f , converting the units to

the equivalent current in the N_f coil alone which produces the same mmf. Thus

$$\text{Gross mmf} = I_f \pm \frac{N_s}{N_f} I_s \quad \text{equivalent shunt-field amperes} \quad (9-20)$$

The latter procedure is often the more convenient and the one more commonly adopted.

An example of a *no-load magnetization characteristic* is given by the curve for $I_a = 0$ in Fig. 9-14. The numerical scales on the left-hand and lower axes give representative values for a 100-kW 250-V 1200-r/min generator; the mmf scale is given in both shunt-field current and ampere-turns per pole, the latter being derived from the former on the basis of a 1000-turns-per-pole shunt field. The characteristic can also be presented in normalized, or per unit, form, as shown by the upper mmf and right-hand voltage scale. On these scales, 1.0 per unit field current or mmf is that re-

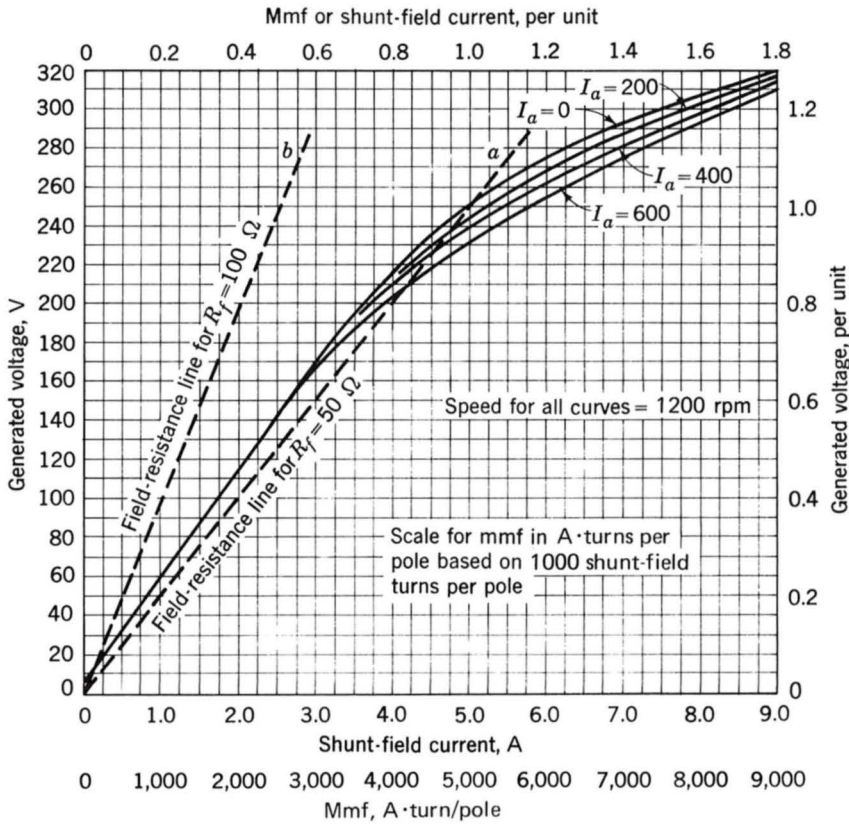


Fig. 9-14. Magnetization curves for a 250-V 1200-r/min dc machine.

quired to produce rated voltage at rated speed when the machine is unloaded; similarly, 1.0 per unit voltage equals rated voltage.

Use of the magnetization curve with generated voltage rather than flux plotted on the vertical axis may be somewhat complicated by the fact that the speed of a dc machine need not remain constant and that speed enters into the relation between flux and generated voltage. Hence generated-voltage ordinates correspond to a unique machine speed. The generated voltage E_a at any speed ω_m is, in accordance with Eq. 9-13, given by

$$E_a = E_{a0} \frac{\omega_m}{\omega_{m0}} \quad (9-21)$$

where ω_{m0} is the magnetization-curve speed and E_{a0} the corresponding armature emf.

EXAMPLE 9-2

A 100-kW 250-V 400-A long-shunt compound generator has armature resistance (including brushes) of 0.025Ω , a series-field resistance of 0.005Ω , and the magnetization curve of Fig. 9-14. There are 1000 shunt-field turns per pole and 3 series-field turns per pole.

Compute the terminal voltage at rated current output when the shunt-field current is 4.7 A and the speed is 1150 r/min. Neglect the armature reaction.

Solution

Now, $I_s = I_a = I_L + I_f = 400 + 4.7 = 405$ A. From Eq. 9-20 the main-field gross mmf is

$$4.7 + \frac{3}{1000}(405) = 5.9 \text{ equivalent shunt-field amperes}$$

By entering the $I_a = 0$ curve of Fig. 9-14 with this current, one reads 274 V. Accordingly, the actual emf is

$$E_a = (274) \frac{1150}{1200} = 262 \text{ V}$$

Then

$$V_t = E_a - I_a(R_a + R_s) = 262 - 405(0.025 + 0.005) = 250 \text{ V}$$

b. Effect of Armature MMF

As described in Art. 9-3, excitation of the armature winding gives rise to a demagnetizing effect caused by a cross-magnetizing armature reaction. Analytical inclusion of this effect is not a straightforward task because of the nonlinearities involved. One common approach is to base the work on experimentally determined data for the machine involved or for one of similar design and frame size. Data are taken with both the field and armature excited, and the tests are conducted so that the effects on generated emf of varying both the main-field excitation and the armature mmf can be noted.

One form of summarizing and correlating the results is illustrated in Fig. 9-14. Curves are plotted not only for the no-load characteristic ($I_a = 0$) but also for a family of values of I_a . In the analysis of machine performance, then, the inclusion of armature reaction becomes simply a matter of using the magnetization curve corresponding to the armature current involved. Note that the ordinates of all these curves give values of armature-generated voltage E_a , not terminal voltage under load. Note also that all the curves tend to merge with the air-gap line as the saturation of the iron decreases.

The load-saturation curves are displaced to the right of the no-load curve by an amount which is a function of I_a . The effect of armature reaction then is approximately the same as a demagnetizing mmf AR acting on the main-field axis. The *net* direct-axis mmf is then assumed to be

$$\text{Net mmf} = \text{gross mmf} - AR = N_f I_f \pm N_s I_s - AR \quad (9-22)$$

The no-load magnetization curve can then be used as the relation between generated emf and net excitation under load with the armature reaction accounted for as a demagnetizing mmf. Over the normal operating range (about 240 to about 300 V for the machine of Fig. 9-14), the demagnetizing effect of armature reaction may be assumed to be approximately proportional to the armature current.

The amount of armature reaction present in Fig. 9-14 is chosen so that some of its disadvantageous effects will appear in a pronounced form in subsequent numerical examples and problems illustrating generator and motor performance features. It is definitely more than one would expect to find in a normal well-designed machine operating at normal currents.

9-6 ANALYSIS OF STEADY-STATE PERFORMANCE

Although exactly the same principles apply to the analysis of a dc machine acting as a generator as to one acting as a motor, the general nature of the problems ordinarily encountered is somewhat different for the two methods of operation. For a generator, the speed is usually fixed by the prime

mover, and problems often encountered are to determine the terminal voltage corresponding to a specified load and excitation or to find the excitation required for a specified load and terminal voltage. For a motor, however, problems frequently encountered are to determine the speed corresponding to a specific load and excitation or to find the excitation required for specified load and speed conditions; terminal voltage is often fixed at the value of the available source. The routine techniques of applying the common basic principles therefore differ to the extent that the problems differ.

a. Generator Analysis

Since the main-field current is independent of the generator voltage, separately excited generators are the simplest to analyze. For a given load, the main-field excitation is given by Eq. 9-20, and the associated armature-generated voltage E_a is determined by the appropriate magnetization curve. This voltage, together with Eq. 9-16 or 9-17, fixes the terminal voltage.

In self-excited generators, the shunt-field excitation depends on the terminal voltage and the series-field excitation on the armature current. Dependence of shunt-field current on terminal voltage can be incorporated graphically in an analysis by drawing the *field-resistance line*, the line $0a$ in Fig. 9-14, on the magnetization curve. The field-resistance line $0a$ is simply a graphical representation of Ohm's law for the shunt field. It is the locus of the terminal voltage versus shunt-field-current operating point. Thus, the line $0a$ is drawn for $R_f = 50 \Omega$ and hence passes through the origin and the point (1.0 A, 50 V).

One instance of the interdependence of magnetic and electric circuit conditions can be seen by examining the buildup of voltage for an unloaded shunt generator. When the field circuit is closed, the small voltage from residual magnetism (the 6-V intercept of the magnetization curve, Fig. 9-14) causes a small field current. If the flux produced by the resulting ampere-turns adds to the residual flux, progressively greater voltages and field currents are obtained. If the field ampere-turns oppose the residual magnetism, the shunt-field terminals must be reversed to obtain buildup.

This can be seen with the aid of Fig. 9-15. In Fig. 9-15, the generated voltage e_a is shown in series with the armature inductance L_a and resistance R_a . The shunt-field winding, shown connected across the armature terminals, is represented by its inductance L_f and resistance R_f . The differential equation describing the buildup of the field current i_f is

$$(L_a + L_f) \frac{di_f}{dt} = e_a - (R_a + R_f)i_f \quad (9-23)$$

From this equation it is clear that as long as the net voltage across the winding inductances $e_a - i_f(R_a + R_f)$ is positive, the field current and the corresponding generated voltage will increase. Buildup continues until

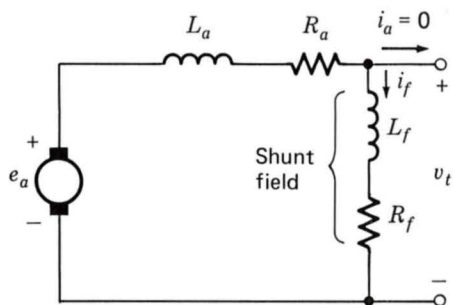


Fig. 9-15. Equivalent circuit for analysis of voltage buildup in a self-excited dc generator.

the volt-ampere relations represented by the magnetization curve and the field-resistance line are simultaneously satisfied, i.e., at their intersection, 250 V for line $0a$ in Fig. 9-14. From Eq. 9-23, it is clear that the field-resistance line should also include the armature resistance. However, this resistance is in general much less than the field and is typically neglected.

Notice that if the field resistance is too high, as shown by line $0b$ for $R_f = 100\ \Omega$, the intersection is at very low voltage and buildup is not obtained. Notice also that if the field-resistance line is essentially tangent to the lower part of the magnetization curve, corresponding to $57\ \Omega$ in Fig. 9-14, the intersection may be anywhere from about 60 to 170 V, resulting in very unstable conditions. The corresponding resistance is the *critical field resistance*, beyond which buildup will not be obtained. The same buildup process and the same conclusions apply to compound generators; in a long-shunt compound generator, the series-field mmf created by the shunt-field current is entirely negligible.

For a shunt generator, the magnetization curve for the appropriate value of I_a is the locus of E_a versus I_f . The field-resistance line is the locus V_t versus I_f . With steady-state operation and at any value of I_f , therefore, the vertical distance between the line and the curve must be the $I_a R_a$ drop at the load corresponding to that condition. Determination of the terminal voltage for a specified armature current is then simply a matter of finding where the line and curve are separated vertically by the proper amount; the ordinate of the field-resistance line at that field current is then the terminal voltage. For a compound generator, however, the series-field mmf causes corresponding points on the line and curve to be displaced horizontally as well as vertically. The horizontal displacement equals the series-field mmf measured in equivalent shunt-field amperes, and the vertical displacement is still the $I_a R_a$ drop.

Great precision is evidently not obtained from the foregoing computational process. The uncertainties caused by magnetic hysteresis in dc machines make high precision unattainable in any event. In general, the magnetization curve on which the machine operates on any given occasion may range from the rising to the falling part of the rather fat hysteresis loop for the magnetic circuit of the machine, depending essentially on the

magnetic history of the iron. The curve used for analysis is usually the mean magnetization curve, and thus the results obtained are substantially correct on the average. Significant departures from the average may be encountered in the performance of any dc machine at a particular time, however.

EXAMPLE 9-3

A 100-kW 250-V 400-A 1200-r/min dc shunt generator has the magnetization curves (including armature-reaction effects) of Fig. 9-14. The armature-circuit resistance, including brushes, is $0.025\ \Omega$. The generator is driven at a constant speed of 1200 r/min, and the excitation is adjusted to give rated voltage at no load.

(a) Determine the terminal voltage at an armature current of 400 A.
 (b) A series field of 4 turns per pole having a resistance of $0.005\ \Omega$ is to be added. There are 1000 turns per pole in the shunt field. The generator is to be *flat-compounded* so that the full-load voltage is 250 V when the shunt-field rheostat is adjusted to give a no-load voltage of 250 V. Show how a resistance across the series field (a *series-field diverter*) can be adjusted to produce the desired performance.

Solution

(a) The field-resistance line $0a$ (Fig. 9-14) passes through the 250-V 5.0-A point of the no-load magnetization curve. At $I_a = 400$ A

$$I_a R_a = 400(0.025) = 10\text{ V}$$

A vertical distance of 10 V exists between the magnetization curve for $I_a = 400$ A and the field-resistance line at a field current of 4.1 A, corresponding to $V_t = 205$ V. The associated line current is

$$I_L = I_a - I_f = 400 - 4 = 396\text{ A}$$

Note that a vertical distance of 10 V also exists at a field current of 1.2 A, corresponding to $V_t = 60$ V. The voltage-load curve is accordingly double-valued in this region. The point for which $V_t = 205$ V is the normal operating point.

(b) For the no-load voltage to be 250 V, the shunt-field resistance must be $50\ \Omega$, and the field-resistance line is $0a$ (Fig. 9-14). At full load, $I_f = 5.0$ A because $V_t = 250$ V. Then

$$I_a = 400 + 5.0 = 405\text{ A}$$

and

$$E_a = 250 + 405(0.025 + R_p)$$

where R_p is the parallel combination of the series-field resistance $R_s = 0.005 \Omega$ and the diverter resistance R_d [$R_p = R_s R_d / (R_s + R_d)$].

The series field and the diverter resistor are in parallel, and thus the shunt-field current can be calculated as

$$I_s = \frac{405R_d}{R_s + R_d} = \frac{405R_p}{R_s}$$

and the equivalent shunt-field amperes can be calculated from Eq. 9-20 as

$$I_{\text{net}} = 5.0 + \frac{4}{1000} I_s = 5.0 + \frac{1.62R_p}{R_s}$$

This equation can be solved for R_p which can be, in turn, substituted along with the numerical value for R_s in the equation for E_a to yield

$$E_a = 253.9 + 1.25I_{\text{net}}$$

This can be plotted on Fig. 9-14 (E_a on the vertical axis and I_{net} on the horizontal axis). Its intersection with the magnetization characteristic for $I_a = 400$ A (strictly speaking, of course, a curve for $I_a = 405$ A should be used, but such a small distinction is obviously meaningless) gives $I_{\text{net}} = 6.0$ A. Thus

$$R_p = \frac{R_s(I_{\text{net}} - 5)}{1.62} = 3.1 \text{ m}\Omega$$

and thus

$$R_d = 82 \text{ m}\Omega$$

b. Motor Analysis

Since the terminal voltage of motors is usually substantially constant at a specific value, there is no dependence of shunt-field excitation on a varying voltage as in shunt and compound generators. Hence, motor analysis most nearly resembles that for separately excited generators, although speed is now an important variable and often the one whose value is to be found. Analytical essentials include Eqs. 9-16 and 9-17 relating terminal voltage and generated voltage (counter emf), Eq. 9-20 for main-field excitation, the magnetization curve for the appropriate armature current as the graphical relation between counter emf and excitation, Eq. 9-12 showing the dependence of electromagnetic torque on flux and armature cur-

rent, and Eq. 9-13 relating counter emf with flux and speed. The last two relations are particularly significant in motor analysis. The former is pertinent because the interdependence of torque and the stator and rotor field strengths must often be examined. The latter is the usual medium for determining motor speed from other specified operating conditions.

Motor speed corresponding to a given armature current I_a can be found by first computing the actual generated voltage E_a from Eq. 9-16 or 9-17. Next obtain the main-field excitation from Eq. 9-20. Since the magnetization curve will be plotted for a constant speed ω_{m0} , which in general will be different from the actual motor speed ω_m , the generated voltage read from the magnetization curve at the foregoing main-field excitation will correspond to the correct flux conditions but to speed ω_{m0} . Substitution in Eq. 9-21 then yields the actual motor speed.

Note that knowledge of the armature current is postulated at the start of this process. When, as is frequently the case, the speed at a stated shaft power or torque output is to be found, successive trials based on assumed values of I_a usually form the simplest procedure. Plotting the successive trials permits speedy determination of the correct armature current and speed at the desired output.

EXAMPLE 9-4

A 100-hp 250-V dc shunt motor has the magnetization curves (including armature-reaction effects) of Fig. 9-14. The armature circuit resistance, including brushes, is $0.025\ \Omega$. No-load rotational losses are 2000 W, and stray load losses equal 1.0 percent of the output. The field rheostat is adjusted for a no-load speed of 1100 r/min.

(a) As an example of computing points on the speed-load characteristic, determine the speed in revolutions per minute and output in horsepower corresponding to an armature current of 400 A.

(b) Because the speed-load characteristic referred to in part (a) is considered undesirable, a *stabilizing winding* consisting of $1\frac{1}{2}$ cumulative series turns per pole is to be added. The resistance of this winding is negligible. There are 1000 turns per pole in the shunt field. Compute the speed corresponding to an armature current of 400 A.

Solution

(a) At no load, $E_a = 250$ V. The corresponding point on the 1200-r/min no-load saturation curve is

$$E_{a0} = 250 \times \frac{1200}{1100} = 273\text{ V}$$

for which $I_f = 5.90$ A. The field current remains constant at this value.

At $I_a = 400$ A, the actual counter emf is

$$E_a = 250 - 400(0.025) = 240 \text{ V}$$

From Fig. 9-14 with $I_a = 400$ and $I_f = 5.90$, the value of E_a would be 261 V if the speed were 1200 r/min. The actual speed is then

$$n = \frac{240}{261}(1200) = 1100 \text{ r/min}$$

The electromagnetic power is

$$E_a I_a = 240(400) = 96,000 \text{ W}$$

Deduction of the rotational losses leaves 94,000 W. With stray load losses accounted for, the power output P_o is given by

$$94,000 - 0.01P_o = P_o$$

or

$$P_o = 93.1 \text{ kW} = 124.7 \text{ hp}$$

Note that the speed at this load is the same as at no load, indicating that armature-reaction effects have caused an essentially flat speed-load curve.

(b) With $I_f = 5.90$ A and $I_s = I_a = 400$ A, the main-field mmf in equivalent shunt-field amperes is

$$5.90 + \frac{1.5}{1000}(400) = 6.50$$

From Fig. 9-14 the corresponding value of E_a at 1200 r/min would be 273 V. Accordingly, the speed is now

$$n = \frac{240}{273}(1200) = 1055 \text{ r/min}$$

The power output is the same as in part (a). The speed-load curve is now drooping, due to the effect of the stabilizing winding.

EXAMPLE 9-5

To limit the starting current to the value which the motor can commutate successfully (see Art. 9-8), all except very small dc motors are started with external resistance in series with their armatures. This resistance is cut out either manually or automatically as the motor comes up to speed. In

Fig. 9-16, for example, the contactors 1A, 2A, and 3A cut out successive steps R_1 , R_2 , and R_3 , respectively, of the starting resistor.

Consider that a motor is to be started with normal field flux. Armature reaction and armature inductance are to be ignored. During starting, the armature current and hence the electromagnetic torque are not to exceed twice the rated values, and a step of the starting resistor is to be cut out whenever the armature current drops to its rated value. Except in part (f), computations are to be made in the per unit system with magnitudes expressed as fractions of base values. (Base voltage equals rated line voltage, base armature current equals full-load armature current, and base resistance equals the ratio of base voltage to base current.)

(a) What is the minimum per unit value of armature resistance which will permit these conditions to be met by a three-step starting resistor?

(b) Above what per unit value of armature resistance will a two-step resistor suffice?

(c) For the armature resistance of part (a), what are the per unit resistance values R_1 , R_2 , and R_3 of the starting resistor?

(d) For a motor with the armature resistance of part (a), the contactors are to be closed by voltage-sensitive relays connected across the armature (called the *counter-emf method*). At what fractions of rated line voltage should the contactors close?

(e) For a motor with the armature resistance of part (a), sketch approximate curves of armature current, electromagnetic torque, and speed during the starting process, and label the ordinates with the appropriate per unit values at significant instants of time.

(f) For a 10-hp 230-V 500 r/min dc shunt motor having a full-load armature current of 37 A and fulfilling the conditions of part (a), list numerical values in their usual units for armature resistance, the results of parts (c) and (d), and the ordinate labelings of part (e).

Solution

(a) To prevent the armature current from exceeding 2.00 per unit at the instant the main contactor M closes,

$$R_1 + R_2 + R_3 + R_a = \frac{V_t}{I_a} = \frac{1.00}{2.00} = 0.50$$

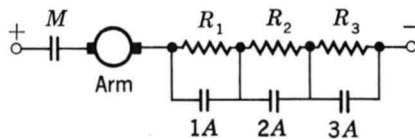


Fig. 9-16. Starting resistors and accelerating contactors for a dc motor.

When the current has dropped to 1.00 per unit,

$$E_{a1} = V_t - I_a(R_1 + R_2 + R_3 + R_a) = 1.00 - 1.00(0.50) = 0.50$$

At the instant the accelerating contactor 1A closes, short-circuiting R_1 , the counter emf has attained this numerical value. Then, to prevent the allowable armature current from being exceeded,

$$R_2 + R_3 + R_a = \frac{V_t - E_{a1}}{I_a} = \frac{1.00 - 0.50}{2.00} = 0.25$$

When the current has again dropped to 1.00 per unit,

$$E_{a2} = V_t - I_a(R_2 + R_3 + R_a) = 1.00 - 1.00(0.25) = 0.75$$

Repetition of this procedure for the closing of accelerating contactors 2A and 3A yields

$$R_3 + R_a = 0.125 \quad E_{a3} = 0.875 \quad R_a = 0.0625$$

and

$$\text{Final } E_a \text{ at full load} = 0.938$$

The desired minimum per unit value of R_a is therefore 0.0625, because a lower value will allow the armature current to exceed twice the rated value when contactor 3A is closed.

(b) If a two-step resistor is to suffice, R_3 must be zero. Since, from part (a),

$$R_3 + R_a = 0.125$$

it follows that a three-step resistor is not required when R_a is equal to or greater than 0.125.

Under the specified starting conditions, a three-step resistor is appropriate for motors whose armature-circuit resistances are between 0.0625 and 0.125 per unit. For general-purpose continuously rated shunt motors, these values correspond to the lower integral-horsepower sizes. On average, motor sizes up to about 10 hp will conform to these requirements, although the size limit will be lower for high-speed motors and higher for low-speed motors. For larger motors, either additional steps must be provided, or the limit on current and torque peaks must be relaxed. The results of this analysis are conservative because the armature resistance under transient conditions is higher than the static value.

(c) From the relations in part (a) the per unit starting resistances are

$$R_3 = 0.125 - 0.0625 = 0.0625$$

$$R_2 = 0.25 - 0.0625 - 0.0625 = 0.125$$

and

$$R_1 = 0.50 - 0.0625 - 0.0625 - 0.125 = 0.25$$

(d) Just before contactor 1A closes,

$$V_{ta1} = E_{a1} + I_a R_a = 0.50 + 1.00(0.0625) = 0.563$$

In like manner,

$$V_{ta2} = 0.75 + 1.00(0.0625) = 0.813$$

and

$$V_{ta3} = 0.875 + 1.00(0.0625) = 0.938$$

Acceleration contactors 1A, 2A, and 3A, respectively, should pick up at these fractions of rated line voltage.

(e) Consider that main contactor *M* closes at $t = 0$ and that accelerating contactors 1A, 2A, and 3A close, respectively, at times t_1 , t_2 , and t_3 . These values of time are not known (when armature and load inertias and torque-speed curve of the load are given, values of time can be computed numerically), so that only the general shapes of the current, electromagnetic torque, and speed curves can be given. They are indicated in Fig. 9-17.

The labeling of the speed curve follows from the fact that a counter emf $E_a = 0.938$ corresponds to rated speed at rated load and hence to unity speed. Other speeds are in proportion to E_a ; thus, at t_1 , t_2 , and t_3 , respectively,

$$n_1 = \frac{0.50}{0.938}(1.00) = 0.534$$

$$n_2 = \frac{0.75}{0.938}(1.00) = 0.800$$

and

$$n_3 = \frac{0.875}{0.938}(1.00) = 0.933$$

(f) Base quantities for this motor are as follows:

$$\text{Base voltage} = 230 \text{ V} \quad \text{Base armature current} = 37 \text{ A}$$

$$\text{Base armature-circuit resistance} = \frac{230}{37} = 6.22 \Omega$$

$$\text{Base speed} = 500 \text{ r/min}$$

$$\text{Base electromagnetic torque} = \frac{60}{2\pi n} E_a I_a$$

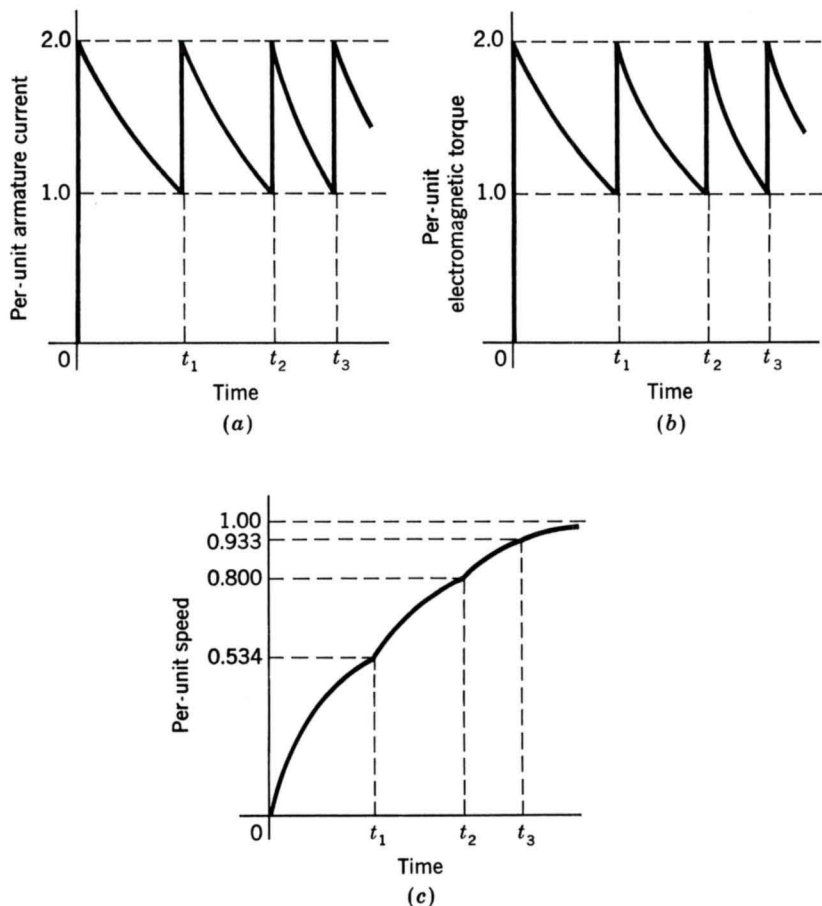


Fig. 9-17. (a) Armature current, (b) electromagnetic torque, and (c) speed during starting of a dc motor.

$$\begin{aligned} &= \frac{60}{2\pi(500)} [230 - 37(0.0625)(6.22)] (37) \\ &= 152 \text{ N} \cdot \text{m} \end{aligned}$$

Note that rated electromagnetic torque will be greater than rated shaft torque because of rotational and stray load losses.

The motor armature resistance is

$$R_a = 0.0625(6.22) = 0.389 \, \Omega$$

Values for the other quantities desired are listed in Table 9-1.

TABLE 9-1
ABSOLUTE VALUES FOR EXAMPLE 9-4

Part (c), Ω	Part (d), V	Part (e) scales of Fig. 9-17
$R_1 = 1.56$	Relay 1A = 129	1.0 armature current = 37 A
$R_2 = 0.778$	Relay 2A = 187	1.0 electromagnetic torque = 152 N · m
$R_3 = 0.389$	Relay 3A = 216	1.0 speed = 500 r/min

9-7 COMMUTATION AND INTERPOLES

One of the most important limiting factors on satisfactory operation of a dc machine is the ability to transfer the necessary armature current through the brush contact at the commutator without sparking and without excessive local losses and heating of the brushes and commutator. Sparking causes destructive blackening, pitting, and wear of both commutator and brushes, conditions which rapidly become worse and burn away the copper and carbon. It may be caused by faulty mechanical conditions, such as chattering of the brushes or a rough, unevenly worn commutator, or, as in any switching problem, by electrical conditions. The latter conditions are seriously influenced by the armature mmf and the resultant flux wave.

As indicated in Art. 9-2, a coil undergoing commutation is in transition between two groups of armature coils: at the end of the commutation period, the coil current must be equal but opposite to that at the beginning. Figure 9-7*b* shows the armature in an intermediate position during which the coils in slots 1 and 7 are being commutated. The commutated coils are short-circuited by the brushes. During this period the brushes must continue to conduct the armature current I_a from the armature winding to the external circuit. The short-circuited coil constitutes an inductive circuit with time-varying resistances at the brush contact, with, in general, rotational voltages induced in the coil and with both conductive and inductive coupling to the rest of the armature winding.

The attainment of good commutation is more an empirical art than a quantitative science. The principal obstacle to quantitative analysis lies in the electrical behavior of the carbon-copper (brush-commutator) contact film. Its resistance is nonlinear and is a function of current density, current direction, temperature, brush material, moisture, and atmospheric pressure. Its behavior in some respects is like that of an ionized gas or plasma. The most significant fact is that an unduly high current density in a portion of the brush surface (and hence an unduly high energy density in that part of the contact film) results in sparking and a breakdown of the film at that point. The boundary film also plays an important part in the mechanical behavior of the rubbing surfaces. At high altitudes, definite

steps must be taken to preserve it, or extremely rapid brush wear takes place.

The empirical basis of securing sparkless commutation, then, is to avoid excessive current densities at any point in the copper-carbon contact. This basis, combined with the principle of utilizing all material to the fullest extent, indicates that optimum conditions are obtained when the current density is uniform over the brush surface during the entire commutation period. A linear change of current with time in the commutated coil, corresponding to *linear commutation* as shown in Fig. 9-8, brings about this condition and is accordingly the optimum.

The principal factors tending to produce linear commutation are changes in brush-contact resistance resulting from the linear decrease in area at the trailing brush edge and linear increase in area at the leading edge. Several electrical factors militate against linearity. Resistance in the commutated coil is one example. Usually, however, the voltage drop at the brush contacts is sufficiently large (of the order of 1.0 V) in comparison with the resistance drop in a single armature coil to permit the latter to be ignored. Coil inductance is a much more serious factor. Both the voltage of self-induction in the commutated coil and the voltage of mutual induction from other coils (particularly those in the same slot) undergoing commutation at the same time oppose changes in current in the commutated coil. The sum of these two voltages is often referred to as the *reactance voltage*. Its result is that current values in the short-circuited coil lag in time the values dictated by linear commutation. This condition is known as *under-commutation* or *delayed commutation*.

Armature inductance thus tends to produce high losses and sparking at the trailing brush tip. For best commutation, inductance must be held to a minimum by using the fewest possible number of turns per armature coil and by using a multipolar design with a short armature. The effect of a given reactance voltage in delaying commutation is minimized when the resistive brush-contact voltage drop is significant compared with it. This fact is one of the main reasons for the use of carbon brushes with their appreciable contact drop. When good commutation is secured by virtue of resistance drops, the process is referred to as *resistance commutation*. It is used today as the exclusive means only in fractional-horsepower machines.

Another important factor in the commutation process is the rotational voltage induced in the short-circuited coil. Depending on its sign, this voltage may hinder or aid commutation. In Fig. 9-11, for example, cross-magnetizing armature reaction creates a definite flux in the interpolar region. The direction of the corresponding rotational voltage in the commutated coil is the same as the current under the immediately preceding pole face. This voltage then encourages the continuance of current in the old direction and, like the resistance voltage, opposes its reversal. To aid commutation, the rotational voltage must oppose the reactance voltage. The general principle of producing in the coil undergoing commutation a

rotational voltage which approximately compensates for the reactance voltage, a principle called *voltage commutation*, is used in almost all modern commutating machines. The appropriate flux density is introduced in the commutating zone by means of small, narrow poles located between the main poles. These auxiliary poles are called *interpoles* or *commutating poles*.

The general appearance of interpoles and an approximate map of the flux produced when they alone are excited are shown in Fig. 9-18. (The interpoles are the smaller poles between the larger main poles in Fig. 9-20.) The polarity of a commutating pole must be that of the main pole just ahead of it, i.e., in the direction of rotation for a generator, and just behind it for a motor. The interpole mmf must be sufficient to neutralize the cross-magnetizing armature mmf in the interpolar region and enough more to furnish the flux density required for the rotational voltage in the short-circuited armature coil to cancel the reactance voltage. Since both the armature mmf and the reactance voltage are proportional to the armature current, the commutating winding must be connected in series with the armature. To preserve the desired linearity, the commutating pole should operate at low saturations. By the use of commutating fields, then, sparkless commutation is secured over a wide range in modern machines. In accordance with the performance standards of NEMA, general-purpose dc machines must be capable of carrying for one minute, with successful commutation, loads of 150 percent of the current corresponding to the continuous rating with the field rheostat set for rated-load excitation.

9-8 COMPENSATING WINDINGS

For machines subjected to heavy overloads, rapidly changing loads, or operation with a weak main field, there is the possibility of trouble other

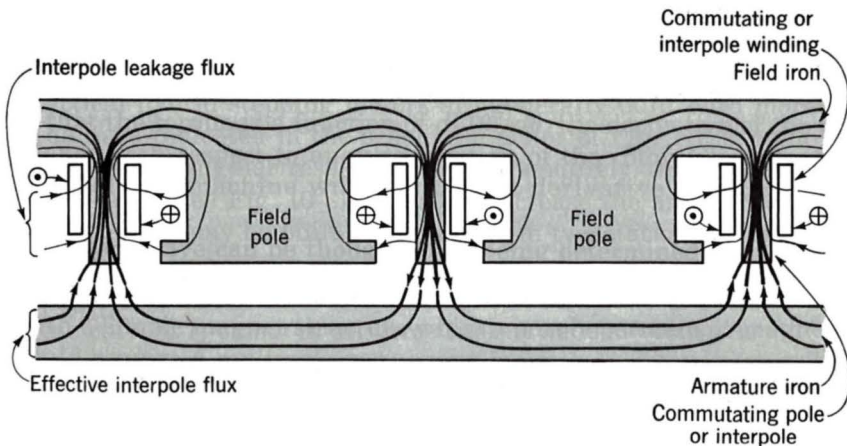


Fig. 9-18. Interpoles and their associated component flux.

than simply sparking at the brushes. At the instant when an armature coil is located at the peak of a badly distorted flux wave, the coil voltage may be high enough to break down the air between the adjacent segments to which the coil is connected and result in flashover, or arcing, between segments. The breakdown voltage here is not high, because the air near the commutator is in a condition favorable to breakdown. The maximum allowable voltage between segments is of the order of 30 to 40 V, a fact which limits the average voltage between segments to lower values and thus determines the minimum number of segments which can be used in a proposed design. Under transient conditions, high voltages between segments may result from the induced voltages associated with growth and decay of armature flux. Inspection of Fig. 9-10, for instance, may enable one to visualize very appreciable voltages of this nature being induced in a coil under the pole centers by the growth or decay of the armature flux shown in the sketch. Consideration of the sign of this induced voltage will show that it adds to the normal rotational emf when load is dropped from a generator or added to a motor. Flashing between segments may quickly spread around the entire commutator and, in addition to its possibly destructive effects on the commutator, constitutes a direct short circuit on the line. Even with interpoles present, therefore, armature reaction under the poles definitely limits the conditions under which a machine can operate.

These limitations can be considerably extended by compensating or neutralizing the armature mmf under the pole faces. Such compensation can be achieved by means of a *compensating*, or *pole-face*, *winding* (Fig. 9-19) embedded in slots in the pole face and having a polarity opposite to that of the adjoining armature winding. The physical appearance of such a winding can be seen in the stator of Fig. 9-20. Since the axis of the compensating winding is the same as that of the armature, it will almost completely neutralize the armature reaction of the armature conductors under the pole faces when it is given the proper number of turns. It must be connected in series with the armature in order to carry a proportional current. The net effect of the main field, armature, commutating winding, and com-

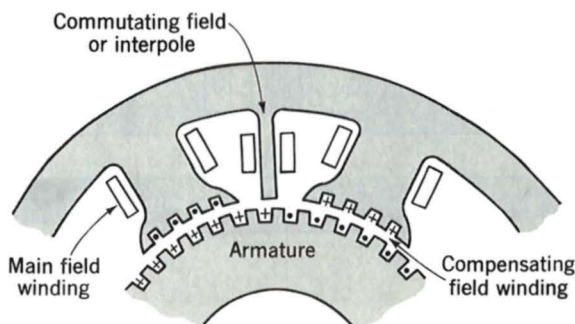


Fig. 9-19. Section of dc machine showing compensating winding.

compensating winding on the air-gap flux is that, except for the commutation zone, the resultant flux-density distribution is substantially the same as that produced by the main field alone (Fig. 9-11). Furthermore, the addition of a compensating winding improves the speed of response because it reduces the armature-circuit time constant.

The main disadvantage of pole-face windings is their expense. They are used in machines designed for heavy overloads or rapidly changing loads (steel-mill motors are a good example of machines subjected to severe duty cycles) or in motors intended to operate over wide speed ranges by shunt-field control. By way of a schematic summary, Fig. 9-21 shows the circuit diagram of a compound machine with a compensating winding. The relative position of the coils in this diagram indicates that the commutating and compensating fields act along the armature axis and the shunt and series fields act along the axis of the main poles. Rather complete control of air-gap flux around the entire armature periphery is thus achieved.

9-9 DC MOTOR SPEED CONTROL

Dc machines are generally much more adaptable to adjustable-speed service than the ac machines associated with a constant-speed rotating field. Indeed, the ready susceptibility of dc motors to adjustment of their operating speed over wide ranges and by a variety of methods is one of the impor-

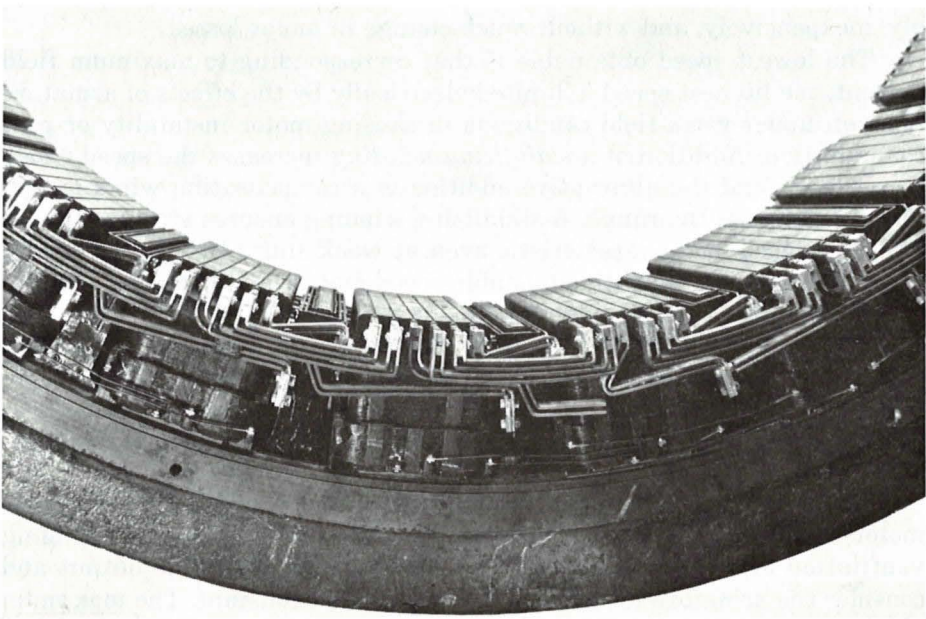


Fig. 9-20. Section of a dc motor stator or field showing shunt and series coils, interpoles, and pole-face compensating winding. (Westinghouse Electric Company.)

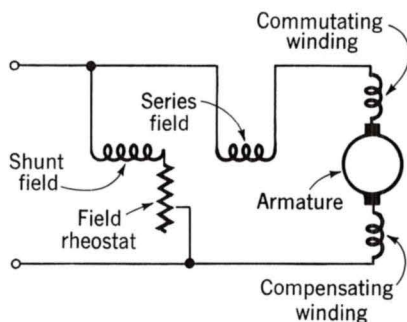


Fig. 9-21. Schematic connection diagram of a dc machine.

tant reasons for the strong competitive position of dc machinery in modern industrial applications.

The three most common speed-control methods are adjustment of the flux, usually by means of field-current control, adjustment of the resistance associated with the armature circuit, and adjustment of the armature terminal voltage.

Field-current control is the most common method and forms one of the outstanding advantages of shunt motors. The method is, of course, also applicable to compound motors. Adjustment of field current and hence the flux and speed by adjustment of the shunt-field circuit resistance or with a solid-state control when the field is separately excited is accomplished simply, inexpensively, and without much change in motor losses.

The lowest speed obtainable is that corresponding to maximum field current; the highest speed is limited electrically by the effects of armature reaction under weak-field conditions in causing motor instability or poor commutation. Addition of a *stabilizing winding* increases the speed range appreciably, and the alternative addition of a compensating winding still further increases the range. A stabilizing winding ensures attainment of a drooping speed-load characteristic even at weak shunt-field currents and heavy loads. It is used with adjustable-speed motors intended for operation over a wide speed range by shunt-field resistance control; its performance was illustrated in Example 9-4. With a compensating winding, the overall range may be as high as 8 to 1 for a small integral-horsepower motor. Economic factors limit the feasible range for very large motors to about 2 to 1, however, with 4 to 1 often being regarded as the limit for the average-size motor.

To examine approximately the limitations on the allowable continuous motor output as the speed is changed, neglect the influence of changing ventilation and changing rotational losses on the allowable output and consider the armature terminal voltage to remain constant. The maximum armature current I_a is then fixed at the nameplate value so that the motor will not overheat, and the speed voltage E_a remains constant because the effect of a speed change is compensated by the change of flux causing it as

the field current is varied. Then the $E_a I_a$ product and hence the allowable motor output remain substantially constant over the speed range. The dc motor with shunt-field-rheostat speed control is accordingly referred to as a *constant-horsepower drive*. Torque, however, varies directly with flux and therefore has its highest allowable value at the lowest speed. Field-current control is thus best suited to drives requiring increased torque at low speeds. When a motor so controlled is used with a load requiring constant torque over the speed range, the rating and size of the machine are determined by the product of the torque and the highest speed. Such a drive is inherently oversize at the lower speeds, which is the principal economic factor limiting the practical speed range of large motors.

Armature-circuit-resistance control consists of obtaining reduced speeds by the insertion of external series resistance in the armature circuit. It can be used with series, shunt, and compound motors; for the last two types, the series resistor must be connected between the shunt field and the armature, not between the line and the motor. It is the common method of speed control for series motors and is generally analogous in action to wound-rotor induction-motor control by series rotor resistance.

For a fixed value of series armature resistance, the speed will vary widely with load, since the speed depends on the voltage drop in this resistance and hence on the armature current demanded by the load. For example, a 1200-r/min shunt motor whose speed under load is reduced to 750 r/min by series armature resistance will return to almost 1200-r/min operation when the load is thrown off because the effect of the no-load current in the series resistance is insignificant. The disadvantage of poor speed regulation may not be important in a series motor, which is used only where varying speed service is required or satisfactory anyway.

Also, the power loss in the external resistor is large, especially when the speed is greatly reduced. In fact, for a constant-torque load, the power input to the motor plus resistor remains constant, while the power output to the load decreases in proportion to the speed. Operating costs are therefore comparatively high for long-time running at reduced speeds. Because of its low initial cost, however, the series-resistance method (or the variation of it discussed in the next paragraph) will often be attractive economically for short-time or intermittent slowdowns. Unlike shunt-field control, armature-resistance control offers a *constant-torque drive* because both flux and, to a first approximation, allowable armature current remain constant as speed changes.

A variation of this control scheme is given by the *shunted-armature method*, which may be applied to a series motor, as in Fig. 9-22a, or a shunt motor, as in Fig. 9-22b. In effect, resistors R_1 and R_2 act as a voltage divider applying a reduced voltage to the armature. Greater flexibility is possible because two resistors can now be adjusted to provide the desired performance. For series motors, the no-load speed can be adjusted to a finite, reasonable value, and the scheme is therefore applicable to the production of slow speeds at light loads. For shunt motors, the speed

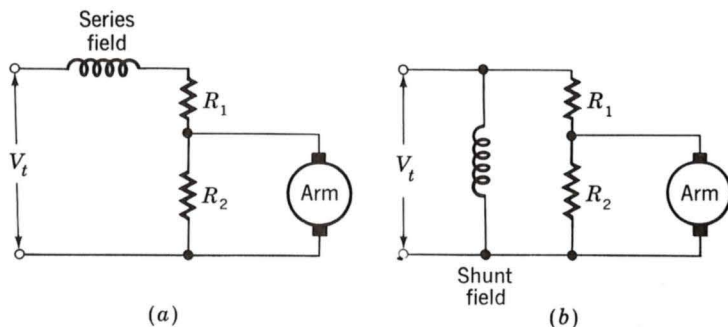


Fig. 9-22. Shunted-armature method of speed control applied to (a) a series motor and (b) a shunt motor.

regulation in the low-speed range is appreciably improved because the no-load speed is definitely lower than the value with no controlling resistors.

Armature-terminal-voltage control utilizes the fact that a change in the armature terminal voltage of a shunt motor is accompanied in the steady state by a substantially equal change in the speed voltage and, with constant motor flux, a consequent proportional change in motor speed. Usually the power available is constant-voltage alternating current, so that auxiliary equipment in the form of a rectifier or a motor-generator set is required to provide the controlled armature voltage for the motor. The development of solid-state controlled rectifiers capable of handling many kilowatts has opened up a whole new field of applications where precise control of motor speed is required.

One common scheme, called the *Ward Leonard system*, shown schematically in Fig. 9-23, requires an individual motor-generator set to supply power to the armature of the motor whose speed is to be controlled. Control of the armature voltage of the main motor M is obtained by field-rheostat adjustment in the separately excited generator G , permitting close control of speed over a wide range. An obvious disadvantage is the initial investment in three full-size machines in contrast to that in a single motor. The speed-control equipment is located in low-power field circuits,

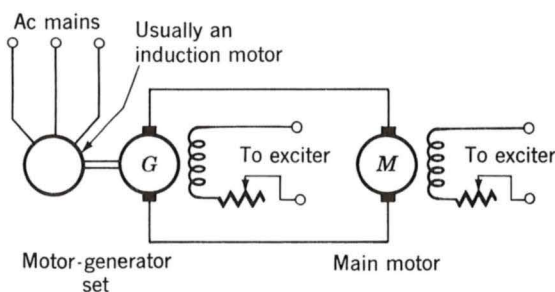


Fig. 9-23. Ward Leonard system of dc motor speed control.

however, rather than in the main power circuits. The smoothness and versatility of control are such that the method or one of its variants is often applied.

Frequently the control of generator voltage is combined with motor-field control, as indicated by the rheostat in the field of motor *M* in Fig. 9-23, in order to achieve the widest possible speed range. With such dual control, base speed can be defined as the normal-armature-voltage full-field speed of the motor. Speeds above base speed are obtained by motor-field control; speeds below base speed are obtained by armature-voltage control. As discussed in connection with field-current control, the range above base speed is that of a constant-horsepower drive. The range below base speed is that of a constant-torque drive because, as in armature-resistance control, the flux and the allowable armature current remain approximately constant. The overall output limitations are therefore as shown in Fig. 9-24*a* for approximate allowable torque and in Fig. 9-24*b* for approximate allowable horsepower. The constant-torque characteristic is well suited to many applications in the machine-tool industry, where many loads consist largely in overcoming the friction of moving parts and hence have essentially constant torque requirements.

The speed regulation and the limitations on the speed range above base speed are those already presented with reference to field-current control; the maximum speed thus does not ordinarily exceed 4 times base speed and preferably not twice base speed. In the region of armature-voltage control, the principal limitation in the basic system is residual magnetism in the generator, although considerations of speed regulation may also be determining. For conventional machines, the lower limit for reliable and stable operation is about one-tenth of base speed, corresponding to a total maximum-to-minimum range not exceeding 40 to 1. With armature reaction ignored, the decrease in speed from no-load to full-load torque is caused entirely by the full-load armature-resistance voltage drop in the dc generator and motor. This full-load armature-resistance voltage

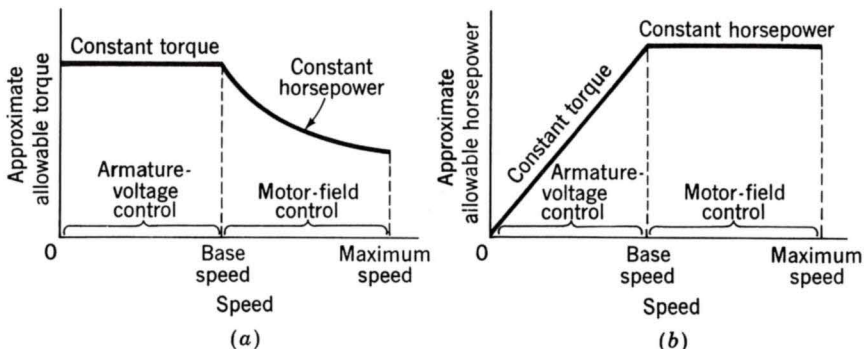


Fig. 9-24. (a) Torque and (b) power limitations of combined armature-voltage and field-rheostat methods of speed control.

drop is constant over the voltage-control range, since full-load torque and hence full-load current are usually regarded as constant in that range. When measured in revolutions per minute, therefore, the speed decrease from no-load to full-load torque is a constant, independent of the no-load speed. The torque-speed curves accordingly are closely approximated by a series of parallel straight lines for the various generator-field adjustments. Note that a speed decrease of, say, 40 r/min from a no-load speed of 1200 r/min is often of little importance; a decrease of 40 r/min from a no-load speed of 120 r/min, however, may at times be of critical importance and require corrective steps in the layout of the system.

9-10 METADYNES AND AMPLIDYNES

So far we have considered dc machines with brushes located only in the quadrature axis. The purpose of this article is to examine the effects of additional brushes located in the direct axis. By these means the armature mmf can be used to provide most of the excitation, and high-power gains can be achieved. Machines with more than two brush sets per pair of poles are called *metadynes*. This article is concerned with metadyne generators, with emphasis on the most common form, the amplidyne.[†]

a. Basic Metadyne Generators

A modification of the basic dc machine is shown in Fig. 9-25. The stator has a control-field winding f on the direct axis. Brushes qq' are located on the commutator so that commutation takes place along the quadrature axis, as in the normal dc generator. With the generator driven at constant speed ω_{m0} and with magnetic saturation neglected, the voltage e_{aq} generated in the armature between the quadrature-axis brushes is

$$e_{aq} = K_{qf} i_f \quad (9-24)$$

where K_{qf} is a constant and i_f is the field current.

Now reduce the field current to a small value and short-circuit the quadrature-axis brushes, as shown in Fig. 9-25. Since the impedance of the short-circuited armature is small, a weak control-field current will produce a relatively much larger quadrature-axis armature current and a corresponding flux-density wave centered on the quadrature axis. By commutator action this magnetic field is stationary in space. Its effect is similar to that of a fictitious stator winding on the quadrature axis.

[†]For a discussion of the steady-state theory and descriptions of a number of applications, see J. M. Pestarini, *Metadyne Statics*, M.I.T.-Wiley, New York, 1952. For discussions of the transient theory, see M. Riaz, "Transient Analysis of the Metadyne Generator," *Trans. AIEE*, **72**(3):52-62 (1953); K. A. Fegley, "Metadyne Transients," *Trans. AIEE*, **74**(III):1179-1188 (1955).

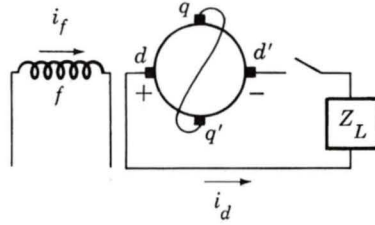


Fig. 9-25. Basic metadyne.

If brushes dd' are now placed on the commutator in the direct axis, as shown in Fig. 9-25, an emf e_{ad} generated in the armature by its rotation in the quadrature-axis flux will appear across these brushes. With the continued assumption of constant speed and negligible saturation

$$e_{ad} = K_{dq} i_q \quad (9-25)$$

where i_q is the quadrature-axis armature current and K_{dq} is a constant.

Now connect a load R_L to the direct-axis brushes. The direct-axis armature current i_d produces an mmf which *opposes* the control-field mmf. Each stage of voltage generation results in a current whose magnetic field is spatially 90° ahead of the flux wave producing the voltage. With two stages of voltage generation, the mmf of the direct-axis output current is shifted 90° twice and therefore opposes the original field excitation. The quadrature-axis-generated emf now is

$$e_{aq} = K_{qf} i_f - K_{qd} i_d \quad (9-26)$$

where K_{qd} is a constant under the assumed conditions of constant speed and negligible saturation.

Under the assumptions of constant speed, constant field current I_{f0} , and resistance R_q short-circuiting the quadrature-axis brushes, Eqs. 9-25 and 9-26 can be used to solve for the load current i_d in terms of the load resistance R_L and the direct-axis winding resistance R_d :

$$i_d = \frac{K_{df} K_{qf}}{(R_L + R_d) R_q + K_{dq} K_{qd}} I_{f0} \quad (9-27)$$

Under these assumptions, which also neglect the effects of saturation, the load current can be seen to be constant independent of the load.

The metadyne generator of Fig. 9-25 is therefore a two-stage power amplifier with strong negative current feedback from the final output stage to the input. For a fixed value of field current it maintains very nearly constant output current i_d over a wide range of load impedance. Its power amplification, however, is reduced by the effect of the negative feedback.

b. Amplidynes

The most common version of the metadyne, the *amplidyne*, consists of the basic metadyne generator plus a cumulative winding on the direct axis connected in series with the direct-axis load current, as shown by the winding labeled "Comp" in the schematic diagram of Fig. 9-26. This winding, called a *compensating winding*, is carefully designed to provide a flux as nearly as possible equal and opposite to the flux produced by the direct-axis armature current. The negative-feedback effect of the load current is thereby canceled, and the control-field winding has almost complete control over the direct-axis flux. Very little control-field power input is required to produce a large current in the short-circuited quadrature axis of the armature. The quadrature-axis current then produces the principal magnetic field. The power required to sustain the quadrature-axis current and the load is supplied mechanically by the motor driving the amplidyne. Power amplification of the order of 20,000 to 1 can be easily obtained. This power amplification may be compared with values in the range from about 20 to 1 and 100 to 1 for conventional generators.

Various auxiliary or control-field windings can be added to either axis of an amplidyne to improve performance characteristics. For example, a cumulative series field can be wound on the quadrature axis and connected in series with the quadrature-axis current. This field decreases the quadrature-axis current for a specified direct-axis voltage output. Quadrature-axis commutation is thereby improved.

Amplidynes are used to provide the power amplification in a variety of feedback control systems requiring controlled power output in the range from about 1 to 50 kW. For example, they are used as the voltage-regulating unit in the excitation systems of large ac generators to insert a buck-or-boost voltage in series with the field winding of the main exciter.[†] Or the main exciter may be an amplidyne when the excitation requirements are within the range where amplidynes are competitive with other types of excitation systems.

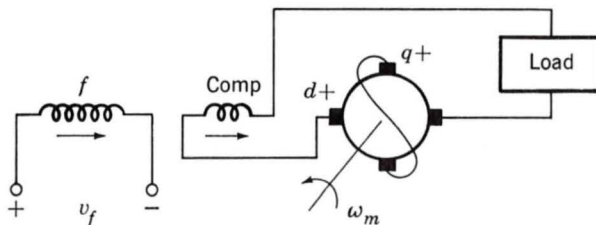


Fig. 9-26. Basic amplidyne.

[†]H. C. Barnes, J. A. Oliver, A. S. Rubenstein, and M. Temoshok, "Alternator-Rectifier Exciter for Cardinal Plant 724-MVA Generator," *IEEE Trans. Power Appar. Syst.*, **87**(4):1189–1198 (1968).

9-11 SUMMARY; DC MACHINE APPLICATIONS

Discussion of dc machine applications involves recapitulation of the highlights of the machine's performance features, together with economic and technical evaluation of the machine's position with respect to competing energy conversion devices. For dc machines in general, the outstanding advantage lies in their flexibility and versatility. The principal disadvantage is likely to be the initial investment concerned. Yet the advantages of dc motors are such that they retain a strong competitive position for industrial applications.

Dc generators are the obvious answer to the problem of converting mechanical energy to electric energy in dc form. When the consumer of electric energy is geographically removed from the site of energy conversion by any appreciable distance, however, the advantages of ac generation, voltage transformation, and transmission are such that energy conversion and transmission in ac form are almost always adopted, ac-to-dc transformation taking place at or near the consumer. For ac-to-dc transformation the dc generator as part of an ac-to-dc motor-generator set must compete with semiconductor rectifier systems. When large-power rectification from ac to constant-voltage dc form is involved, the electronic methods usually offer determining economic advantages. The principal applications of dc generators, therefore, are to cases where the primary energy conversion occurs very near the point of consumption and cases where the ability to control output voltage in a prescribed manner is necessary, although solid-state controlled rectification using silicon controlled rectifiers (SCRs) and Triacs is finding widespread application.

Among dc generators themselves, separately excited and cumulatively compounded self-excited machines are the most common. Separately excited generators have the advantage of permitting a wide range of output voltages, whereas self-excited machines may produce unstable voltages in the lower ranges, where the field-resistance line becomes essentially tangent to the magnetization curve. Cumulatively compounded generators may produce a substantially flat voltage characteristic or one which rises with load, whereas shunt or separately excited generators (assuming no series field in the latter, which, of course, is not at all a practical restriction) produce a drooping voltage characteristic unless external regulating means are added. So far as the control potentialities of dc generators are concerned, the control-type generators (amplidynes and similar machines) discussed in Art. 9-10 represent the results of a fuller exploration of the inherent possibilities.

Among dc motors, the outstanding characteristics of each type are as follows. The series motor operates with a decidedly drooping speed as load is added, the no-load speed usually being prohibitively high; the torque is proportional to almost the square of the current at low saturations and to some power between 1 and 2 as saturation increases. The shunt motor at

constant field current operates at a slightly drooping but almost constant speed as load is added, the torque being almost proportional to armature current; equally important, however, is the fact that its speed can be controlled over wide ranges by shunt-field control, armature-voltage control, or a combination of both. Depending on the relative strengths of shunt and series field, the cumulatively compounded motor is intermediate between the other two and may be given essentially the advantages of one or the other.

By virtue of its ability to handle heavy torque overloads while cushioning the associated power overload with a speed drop, and by virtue of its ability to withstand severe starting duties, the series motor is best adapted to hoist-, crane-, and traction-type loads. Its ability is almost unrivaled in this respect. Speed changes are usually achieved by armature-resistance control. In some instances, the wound-rotor induction motor with rotor-resistance control competes with the series motor, but the principal argument concerns the availability and economics of a dc power supply rather than inherent motor characteristics.

Compound motors with a heavy series field have performance features approaching those of series motors except that the shunt field limits the no-load speed to safe values; the general remarks for series motors therefore apply. Compound motors with lighter series windings often find competition from squirrel-cage induction motors with high-resistance rotors—high-slip motors (referred to in Chap. 7 as class D induction motors). Both motors provide a definitely drooping speed-load characteristic such as is desirable, for example, when flywheels are used as load equalizers to smooth out intermittent load peaks. Complete economic comparison of the two competing types must reflect both the usually higher initial cost of a compound-motor installation and the usually higher cost of losses in the high-slip induction motor.

Because of the comparative simplicity, cheapness, and ruggedness of the squirrel-cage induction motor, the shunt motor is not in a favorable competitive position for constant-speed service except at low speeds, where it becomes difficult and expensive to build high-performance induction motors with the requisite number of poles. The comparison at these low speeds is often likely to be between synchronous and dc motors. The outstanding feature of the shunt motor is its adaptability to adjustable-speed service as discussed in Art. 9-9, by means of armature-resistance control for speeds below the full-field speed, field-rheostat control for speeds above the full-field speed, and armature-voltage, or Ward Leonard, control for speeds below (and, at times, somewhat above) the normal-voltage full-field speed. The combination of armature-voltage control and shunt-field control, together with the possibility of additional field windings in either the motor or the associated generator to provide desirable inherent characteristics, gives the dc drives an enviable degree of flexibility. The use of solid-state motor drives reinforces the competitive position of dc machines where complete control of operation is important.

It should be emphasized that the choice of equipment for an engineering application of adjustable-speed drives is rarely a cut-and-dried matter or one to be decided from a mere verbal list of advantages and disadvantages. In general, specific, quantitative, economic, and technical comparison of all possibilities should be undertaken. Local conditions and the characteristics of the driven equipment (e.g., constant-horsepower, constant-torque, and variable-horsepower variable-torque requirements) invariably play an important role.

Dc machines have seen widespread use in electromechanical systems because of the relative ease with which their dynamics can be controlled by variable levels of dc voltage applied to their armature and/or field terminals. However, solid-state technology now permits the generation of variable-frequency ac voltages of significant power level, resulting in the use of ac machines in applications once considered almost exclusively the domain of dc machines. One should also remember that comparative studies of motor cost and characteristics are based on the combination of motor and control equipment, for the latter plays an important part in determining motor performance under specific conditions and represents a by no means negligible portion of the total initial cost.

PROBLEMS

9-1. (a) Compare the effect on the speed of a dc shunt motor of varying the line voltage with that of varying only the armature terminal voltage, so that the field current remains fixed. (b) Compare both these effects with that of varying only the shunt-field current, the armature terminal voltage remaining fixed.

9-2. State approximately how the armature current and speed of a dc shunt motor would be affected by each of the following changes in the operating conditions:

- (a) Halving the armature terminal voltage while the field current and load torque remain constant
- (b) Halving the armature terminal voltage while the field current and horsepower output remain constant
- (c) Doubling the field flux while the armature terminal voltage and load torque remain constant
- (d) Halving both the field flux and armature terminal voltage while the horsepower output remains constant
- (e) Halving the armature terminal voltage while the field flux remains constant and the load torque varies as the square of the speed

Only brief quantitative statements of the order of magnitude of the changes are expected, e.g., "speed approximately doubled."

9-3. The constant-speed magnetization curve for a 25-hp 250-V dc machine at a speed of 1100 r/min is shown in Fig. 9-27. This machine is separately excited and has an armature resistance of $0.12\ \Omega$. This machine is to be operated as a dc generator while driven from a synchronous motor at a constant speed of 1100 r/min.

- (a) Find the rated armature current of this machine.
- (b) If the armature current is limited to its rated value, calculate the maximum power output of the generator and the corresponding armature voltage for constant field currents of (i) 1.0 A, (ii) 2.0 A, and (iii) 2.5 A.
- (c) Repeat part (b) if the speed of the synchronous generator is reduced to 800 r/min.

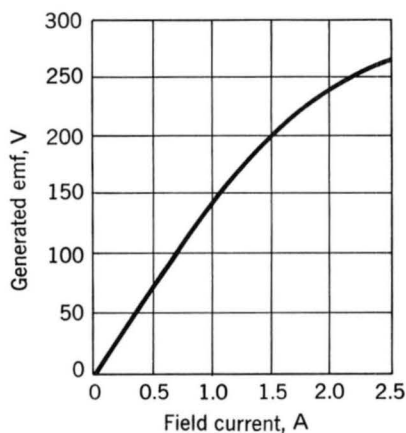


Fig. 9-27. Magnetization curve at 1100 r/min for dc machine of Prob. 9-3.

9-4. A 15-kW 250-V 1150 r/min shunt generator is driven by a prime mover whose speed is 1195 r/min when the generator delivers no load. The speed falls to 1150 r/min when the generator delivers 15 kW and may be assumed to decrease in proportion to the generator output. The generator is to be changed into a short-shunt compound generator by equipping it with a series field which will cause its voltage to rise from 230 V at no load to 250 V for a load of 65.2 A. It is estimated that the series field will have a resistance of $0.06\ \Omega$. The armature resistance (including brushes) is $0.17\ \Omega$. The shunt-field winding has 1800 turns per pole.

To determine the necessary series-field turns, the machine is run as a separately excited generator and the following load data are obtained:

$$\text{Armature terminal voltage} = 254\ \text{V}$$

$$\text{Armature current} = 66.5\ \text{A}$$

Field current = 1.95 A

Speed = 1145 r/min

The magnetization curve at 1195 r/min is as follows:

E_a, V	230	240	250	260	270	280
I_f, A	1.05	1.13	1.25	1.44	1.65	1.91

Determine (a) the necessary number of series-field turns per pole and (b) the armature reaction in equivalent demagnetizing ampere-turns per pole for $I_a = 66.5 \text{ A}$.

9-5. When operating from a 230-V dc supply, a dc series motor operates at 900 r/min with a line current of 75 A. Its armature-circuit resistance is 0.13Ω , and its series-field resistance is 0.09Ω . Due to saturation effects, the flux at an armature current of 25 A is 45 percent of that at an armature current of 75 A. Find the motor speed when the armature voltage is 230 V and the armature current is 25 A.

9-6. (a) A 230-V dc shunt-wound motor is used as an adjustable-speed drive over the range from 0 to 1500 r/min. Speeds from 0 to 750 r/min are obtained by adjusting the armature terminal voltage from 0 to 230 V with the field current kept constant. Speeds from 750 to 1500 r/min are obtained by decreasing the field current with the armature terminal voltage maintained at 230 V. Over the entire speed range the torque required by the load remains constant. Show the general form of the curve of armature current versus speed over the entire range. Ignore machine losses and armature-reaction effects.

(b) Suppose that, instead of keeping the load torque constant, the armature current is not to exceed a specified value. Show the general form of the curve of allowable load torque versus speed assuming conditions otherwise are as in part (a).

9-7. Two adjustable-speed dc shunt motors have maximum speeds of 1850 r/min and minimum speeds of 550 r/min. Speed adjustment is obtained by field-rheostat control. Motor A drives a load requiring constant horsepower over the speed range; motor B drives one requiring constant torque. All losses and armature reaction may be neglected.

(a) If the horsepower outputs are equal at 1850 r/min and the armature currents are each 100 A, what will the armature currents be at 550 r/min?

- (b) If the horsepower outputs are equal at 550 r/min and the armature currents are each 100 A, what will the armature currents be at 1850 r/min?
- (c) Answer parts (a) and (b) for speed adjustment by armature-voltage control with conditions otherwise the same.

9-8. Consider a dc shunt motor connected to a constant-voltage source and driving a load requiring constant electromagnetic torque. Show that if $E_a > 0.5V_t$ (the normal situation), increasing the resultant air-gap flux decreases the speed, whereas if $E_a < 0.5V_t$ (as might be brought about by inserting a relatively high resistance in series with the armature), increasing the resultant air-gap flux increases the speed.

9-9. A dc shunt motor is mechanically coupled to a three-phase cylindrical-rotor synchronous generator. The dc motor is connected to a 230-V constant-voltage dc supply, and the ac generator is connected to a 460-V (line-to-line) constant-voltage constant-frequency three-phase supply. The four-pole Y-connected synchronous machine is rated 25 kVA, 460 V, and has a synchronous reactance of 5.85 Ω /phase. The four-pole dc machine is rated 25 kW, 230 V. All losses are to be neglected.

- (a) If the two machines act as a motor-generator set receiving power from the dc mains and delivering power to the ac supply, what is the excitation voltage of the ac machine in volts per phase (line to neutral) when it delivers rated kilovoltamperes at 1.00 power factor?
- (b) Leaving the field current of the ac machine as in part (a), what adjustment can be made to reduce the power transfer (between ac and dc) to zero? Under this condition of zero transfer, what is the armature current of the dc machine? What is the armature current of the ac machine?
- (c) Leaving the field current of the ac machine as in parts (a) and (b), what adjustment can be made to cause 25 kW to be taken from the ac supply and delivered to the dc supply? Under these conditions, what is the armature current of the dc machine? What are the magnitude and phase of the current of the ac machine?

9-10. A 150-hp 600-V 600-r/min dc series-wound railway motor has a combined field and armature resistance (including brushes) of 0.165 Ω . The full-load current at rated voltage and speed is 186 A. The magnetization curve at 400 r/min is as follows:

Generated emf, V	375	400	425	450	475
Field amperes	169	194	225	261	300

Determine the internal starting torque when the starting current is limited to 340 A. Assume the armature reaction to be equivalent to a demagnetizing mmf which varies as the square of the current.

9-11. A 15-hp 230-V shunt motor has an armature-circuit resistance of $0.19\ \Omega$ and a field resistance of $145\ \Omega$. At no load and rated voltage, the speed is 1150 r/min, and the armature current is 7.65 A. At full load and rated voltage, the line current is 56.1 A, and because of armature reaction, the flux is 5 percent less than its no-load value. What is the full-load speed?

9-12. A 36-in axial-flow disk pressure fan is rated to deliver air at 27,120 ft³/min against a static pressure of $\frac{1}{2}$ in H₂O when rotating at a speed of 1165 r/min. This fan has the following speed-load characteristics:

Speed, r/min	700	800	900	1000	1100	1200
Input, hp	2.9	3.9	5.2	6.7	8.6	11.1

It is proposed to drive the fan by a 10-hp 230-V 37.5-A four-pole dc shunt motor. The motor has an armature winding with two parallel paths and $C_a = 666$ active conductors. Armature-circuit resistance is $0.267\ \Omega$. The armature flux per pole is $\Phi_d = 10^{-2}$ Wb; armature reaction is negligible. No-load rotational losses (considered constant) are estimated at 600 W, a typical value for such a motor. Determine the shaft-horsepower output and the operating speed of the motor when it is connected to the fan load.

9-13. A shunt motor operating from a 230-V line draws a full-load armature current of 38.5 A and runs at a speed of 1200 r/min at both no load and full load. The following data are available on this motor:

Armature-circuit resistance (including brushes) = $0.21\ \Omega$

Shunt-field turns per pole = 1800 turns

The magnetization curve taken as a generator at no load and 1200 r/min is

E_a , V	180	200	220	240	250
I_f , A	0.82	0.96	1.22	1.61	1.89

- Determine the shunt-field current of this motor at no load and 1200 r/min when connected to a 230-V line. Assume negligible armature-circuit resistance drop and armature reaction at no load.
- Determine the effective armature reaction at full load in ampere-turns per pole.

- (c) How many series-field turns should be added to make this machine into a long-shunt cumulatively compounded motor whose speed will be 1115 r/min when the armature current is 38.5 A and the applied voltage is 230 V? The series field will have a resistance of 0.046Ω .
- (d) If a series-field winding having 25 turns per pole and a resistance of 0.046Ω is installed, determine the speed when the armature current is 38.5 A and the applied voltage is 230 V.

9-14. A 10-hp 230-V shunt motor has 1800 shunt-field turns per pole, an armature resistance (including brushes) of 0.23Ω , and a commutating-field resistance of 0.041Ω . The shunt-field resistance (exclusive of rheostat) is 275Ω . When the motor is operated at no load with rated terminal voltage and varying field resistance, the following data are taken:

Speed, r/min	1110	1130	1160	1200	1240
I_f , A	0.746	0.704	0.664	0.616	0.580

The no-load armature current is negligible. When the motor is operated at full load and rated terminal voltage, the armature current is 37.5 A, the field current is 0.616 A, and the speed is 1180 r/min.

- (a) Calculate the full-load armature reaction in equivalent demagnetizing ampere-turns per pole.
- (b) Calculate the full-load electromagnetic torque.
- (c) What starting torque will the motor exert with maximum field current if the starting armature current is limited to 75 A? The armature reaction under these conditions is $160 \text{ A} \cdot \text{turns per pole}$.
- (d) Design a series field to give a full-load speed of 1075 r/min when the no-load speed is 1200 r/min.

9-15. When operated at rated voltage, a 230-V shunt motor runs at 1800 r/min at full load and at no load. The full-load armature current is 50.0 A. The shunt-field winding has 1500 turns per pole. The resistance of the armature circuit (including brushes and interpoles) is 0.20Ω . The magnetization curve at 1800 r/min is

E_a , V	200	210	220	230	240	250
I_f , A	0.53	0.59	0.65	0.73	0.81	0.95

- (a) Compute the demagnetizing effect of armature reaction at full load in ampere-turns per pole.

- (b) A long-shunt cumulative series-field winding having six turns per pole and a resistance of $0.055\ \Omega$ is added to the machine. Compute the speed at full-load current and rated voltage, with the same shunt-field circuit resistance as in part (a).
- (c) With the series-field winding of part (b) installed, compute the internal starting torque in newton-meters if the starting armature current is limited to 90 A and the shunt-field current has its normal value. Assume that the corresponding demagnetizing effect of armature reaction is $230\ \text{A} \cdot \text{turns}$ per pole.

9-16. A 230-V dc shunt motor has an armature-circuit resistance of $0.15\ \Omega$. This motor operates from a 230-V supply and takes an armature current of 75 A. An external resistance of $0.9\ \Omega$ is now inserted in series with the armature, and the electromagnetic torque and field-rheostat setting are unchanged. Give the percentage change in (a) the total current taken by the motor from the supply and (b) the speed of the motor; (c) state whether this will be an increase or a decrease.

9-17. A punch press is found to operate satisfactorily when driven by a 10-hp 230-V compound motor having a no-load speed of 1800 r/min and a full-load speed of 1200 r/min when the torque is $43.8\ \text{lb} \cdot \text{ft}$. The motor is temporarily out of service, and the only available replacement is a compound motor with the following characteristics:

Rating = 230 V, 12.5 hp	No-load current = 4 A
No-load speed = 1820 r/min	Full-load speed = 1600 r/min
Full-load current = 57.0 A	Full-load torque = $43.8\ \text{lb} \cdot \text{ft}$
Armature-circuit resistance = $0.2\ \Omega$	Shunt-field current = 1.6 A

It is desired to use this motor as an emergency drive for the press without making any change in its field windings.

- (a) How can it be made to have the desired speed regulation?
- (b) Draw the pertinent circuit diagram and give complete specifications of the necessary apparatus.

9-18. Two identical 10-hp 230-V 36-A dc shunt machines are to be used as the generator and motor, respectively, in a Ward Leonard system. The generator is driven by a synchronous motor whose speed is constant at 1200 r/min. The armature-circuit resistance of each machine is $0.22\ \Omega$ (including brushes). Armature reaction is negligible. Data for the magnetization curve of each machine at 1200 r/min are as follows:

I_f , A	0.3	0.6	0.9	1.2	1.5	1.8
E_a , V	108	183	230	254	267	276

- Compute the maximum and minimum values of generator-field current needed to give the motor a speed range from 300 to 1500 r/min at full-load armature current (36.0 A) with the motor-field current held constant at 0.80 A.
- Compute the speed regulation of the motor for the conditions of maximum speed and minimum speed found in part (a).
- Compute the maximum motor speed obtainable at full-load armature current if the motor-field current is reduced to 0.30 A and the generator-field current is not allowed to exceed 1.60 A.

9-19. One of the most common industrial applications of dc series motors is crane and hoist drives. This problem relates to the computation of selected motor performance characteristics for such a drive. The specific motor concerned is a series-wound 230-V totally enclosed motor having a $\frac{1}{2}$ -hour crane rating of 65 hp with a 75°C temperature rise. The performance characteristics of the motor alone at 230 V as taken from the manufacturer's catalog are listed in Table 9-2. The resistance of the armature (including brushes) plus commutating field is 0.105 Ω , and that of the series-field winding is 0.050 Ω . Armature reaction should be ignored.

The motor is to be connected as in Fig. 9-28a for hoisting and Fig. 9-28b for lowering. The former connection is simply one for series-resistance control. The latter connection is one for lowering by dynamic braking with the field reconnected in shunt and having an adjustable resistance in series with it.

A few samples of the torque-speed curves determining the suitability of the motor and control for its particular application are to be plotted. Plot all these curves on the same sheet, torque horizontally and speed verti-

TABLE 9-2

Line current, A	Shaft torque, lb · ft	Speed, r/min
50	80	940
100	210	630
150	380	530
200	545	475
250	730	438
300	910	407
350	1105	385
400	1265	370

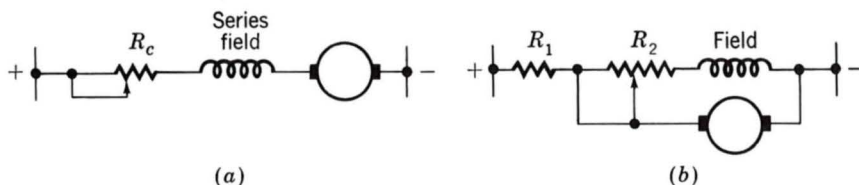


Fig. 9-28. Series crane motor (Prob. 9-19): (a) hoisting connection and (b) lowering connection.

cally, covering about the torque-magnitude range embraced in Table 9-2. Provide for both positive and negative values of speed, corresponding, respectively, to hoisting and lowering; provide also for both positive and negative values of torque, corresponding, respectively, to torque in the direction of raising the load and torque in the direction of lowering the load; thus, use all four quadrants of the conventional rectangular coordinate system.

- (a) For the hoisting connection, plot torque-speed curves for the control resistor R_c set at 0, 0.60, and 1.20 Ω . If any of these curves extend into the fourth quadrant within the range of torques covered, plot them in that region and interpret physically what operation there means.
- (b) For the lowering connection, plot a torque-speed curve for $R_1 = 0.60 \Omega$ and R_2 set at 0.60 Ω . The most important portion of this curve is in the fourth quadrant, but if it extends into the third quadrant, that region should also be plotted and interpreted physically.
- (c) In part (b) what is the lowering speed corresponding to rated torque?
- (d) How is the speed in part (c) affected by decreasing R_2 ? Why?
- (e) How would the speed of part (c) be affected by adding resistance in series with the motor armature? Why?

9-20. A weak shunt-field winding is to be added to a 50-hp 230-V 600 r/min series hoist motor for the purpose of preventing excessive speeds at very light loads. Its resistance will be 230 Ω . The combined resistance of the interpole and armature winding (including brushes) is 0.046 Ω . The series-field winding has 26 turns per pole with a total resistance of 0.023 Ω . To determine its design, the following test data were obtained before the shunt field was installed:

Load test as a series motor (output not measured):

$$V_t = 230 \text{ V} \quad I_a = 184 \text{ A} \quad n = 600 \text{ r/min}$$

No-load test with series field separately excited:

Voltage applied to armature, V	Speed, r/min	Armature current, A	Series-field current, A
230	1500	10.0	55
230	1200	9.2	68
230	900	8.0	95
215	700	7.7	125
215	600	7.5	162
215	550	7.2	186
215	525	7.1	208
215	500	7.0	244

- (a) Determine the number of shunt-field turns per pole if the no-load speed at rated voltage is to be 1450 r/min. The armature, series-field, and interpole winding resistance drops are negligible at no load.
- (b) Determine the speed after installation of the shunt field when the motor is operated at rated voltage with a load which results in a line current of 175 A. Assume that the demagnetizing mmf of armature reaction is unchanged by addition of the shunt field.

9-21. A 20-hp 230-V shunt motor has an armature resistance of $0.124\ \Omega$ and a field-circuit resistance of $95\ \Omega$. The motor delivers rated output power at rated voltage when its armature current is 73.5 A. When the motor is operating at rated voltage, the speed is observed to be 1150 r/min when the machine is loaded such that the armature current is 41.5 A.

- (a) Calculate the rated-load speed of this motor.

In order to protect both the motor and the dc supply under starting conditions, an external resistance will be connected in series with the armature winding (with the field winding remaining directly across the 230-V supply). This resistance will then be automatically adjusted in steps so that the armature current does not exceed 200 percent of rated current. The step size will be determined such that, until all the external resistance is switched out, the armature current will not be permitted to drop below rated value. In other words, the machine is to start with 200 percent of rated armature current, and as soon as the current falls to rated value, sufficient series resistance is to be cut out to restore the current to 200 percent. This process will be repeated until all the series resistance has been eliminated.

- (b) Find the maximum value of the series resistance.
- (c) How much resistance should be cut out at each step in the starting operation, and at what speed should each step occur?

9-22. A 2-kW 200-V metadyne generator of the type shown in Fig. 9-25 is driven by a synchronous motor at 1800 r/min and has the following constants:

Control-field resistance $R_f = 20 \, \Omega$

Control-field inductance $L_{ff} = 2 \, \text{H}$

Voltage constant $K_{qf} = 240 \, \text{V/field amperes}$

Armature resistances $R_{aq} = R_{ad} = 4 \, \Omega$

Armature inductance $L_{aq} = 1.0 \, \text{H}$

Voltage constants $K_{dq} = K_{qd} = 60 \, \text{V/A}$

The metadyne supplies a $20\text{-}\Omega$ resistive load at a voltage of $200 \, \text{V}$. Find the power input to the control field and the power amplification.

9-23. A compensating winding is added to the metadyne of Prob. 9-22, converting it to an amplidyne. The amplidyne supplies $200 \, \text{V}$ to a $20\text{-}\Omega$ load. Find the power input to the control field, and compare with the result of Prob. 9-22. Neglect the resistance of the compensating winding.



Variable Reluctance Machines

Variable-reluctance machines[†] (often abbreviated VRMs) are perhaps the simplest of electrical machines. They consist of a stator with excitation windings and a magnetic rotor with saliency. Rotor conductors are not required because torque is produced by the tendency of the rotor to align with the stator-produced flux wave in such a fashion as to maximize the stator flux linkages that result from a given applied stator current. Torque production in these machines can be evaluated by using the techniques of Chap. 3 and the fact that the stator winding inductances are functions of the angular position of the rotor.

Although the concept of the VRM has been around for a long time, only recently have these machines begun to see widespread use in engi-

[†]Variable-reluctance machines are often referred to as *switched reluctance machines* (SRMs) to indicate the combination of a VRM and the switching inverter required to drive it. This term is popular in the technical literature.

neering applications. This is due in large part to the fact that although they are simple in construction, they are somewhat complicated to control. For example, the position of the rotor must be known in order to properly energize the phase windings to produce torque. It is only relatively recently that the widespread availability and low cost of micro and power electronics have brought the cost of the sensing and control required to successfully operate VRM drive systems down to a level where these systems can be competitive with systems based on dc- and induction-motor technologies.

10-1 BASICS OF VRM ANALYSIS

Variable-reluctance machines can be categorized into two types: singly salient and doubly salient. In either case, their most noticeable features are that there are no windings or permanent magnets on their rotors and that their only source of excitation consists of stator windings. This can be a significant feature because it means that all the resistive winding losses in the VRM occur on the stator. Because the stator can typically be cooled much more effectively and easily than the rotor, the result is often a smaller motor for a given rating and frame size.

To produce torque, VRMs must be designed such that the stator winding inductances vary with the position of the rotor. Figure 10-1a shows a cross-sectional view of a *singly salient VRM* which can be seen to consist of a nonsalient stator and a two-pole salient rotor, both constructed of high-permeability magnetic material. In the figure, a two-phase stator winding is shown although any number of phases are possible. Notice that the inductance of each stator-phase winding varies with rotor position such that the inductance is maximum when the rotor axis is aligned with the magnetic axis of that phase and minimum when the two axes are perpendicular.

Figure 10-1b shows the cross-sectional view of a two-phase *doubly salient VRM*. Note that the salient stator has four poles, each with a winding. However, the windings on opposite poles are of the same phase and can be considered to be connected in either series or parallel for the purposes of this analysis. Thus this machine is quite similar to that of Fig. 10-1a in that there is a two-phase stator winding and a two-pole salient rotor. Similarly, the phase inductance of this configuration varies from a maximum value when the rotor axis is aligned with the axis of that phase to a minimum when they are perpendicular. In fact, the only significant difference between the two machine configurations is that the saliency of the stator enhances the difference between the maximum and minimum inductances, which in turn further enhances the torque-producing characteristics of the machine.

The relationship between flux linkage and current for these two machines is particularly simple because symmetry arguments can be used to

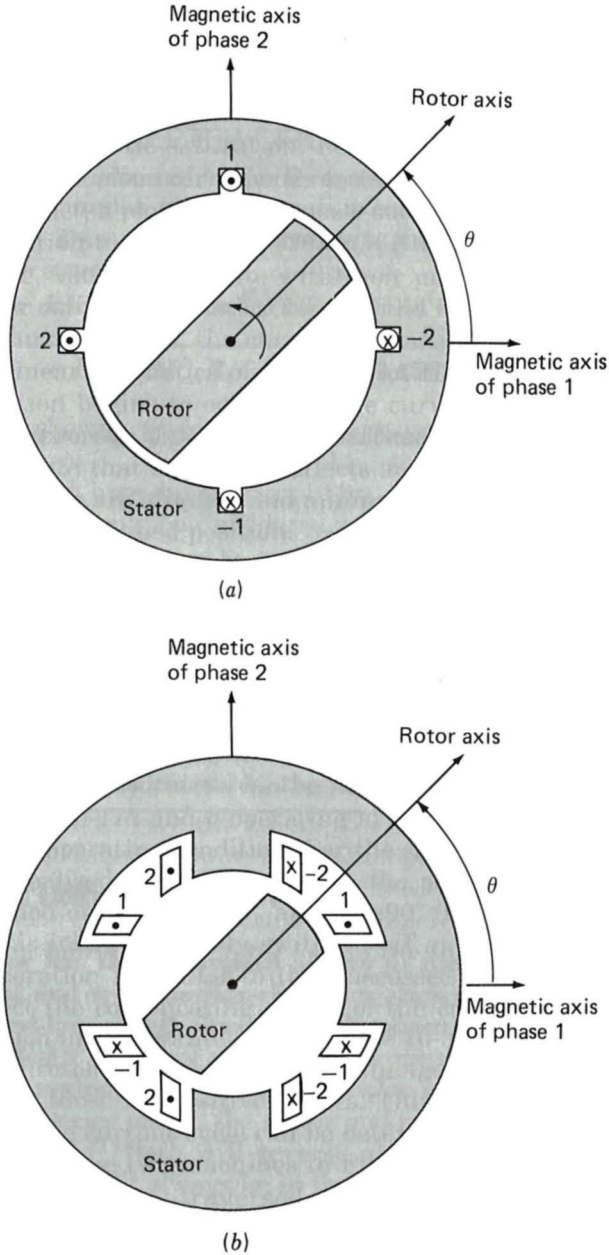


Fig. 10-1. Basic two-phase VRMs: (a) singly salient and (b) doubly salient.

show that if the reluctance of the machine iron is negligible, then there is negligible mutual flux linkage between the two phase windings and hence that their phase-phase mutual inductance can be considered to be zero.

Thus,

$$\lambda_1 = L_{11}(\theta)i_1 = L(\theta)i_1 \quad (10-1)$$

and

$$\lambda_2 = L_{22}(\theta)i_2 = L(\theta - 90^\circ)i_2 \quad (10-2)$$

Here $L_{11}(\theta)$ and $L_{22}(\theta)$ are the self-inductances of phases 1 and 2, respectively, and $L(\theta)$ is an inductance which depends on the angle θ between the magnetic axis of phase 1 and the rotor axis as defined in Fig. 10-1. Figure 10-2 shows typical variations of $L(\theta)$ for the singly and doubly salient configurations of Fig. 10-1. Note that both of these inductances are periodic with a period of 180° because rotation of the rotor through 180° from any given angular position results in no change in the magnetic circuit of the machine.

From Eq. 3-53 the electromagnetic torque of this system can be determined from the coenergy as

$$T = \frac{\partial W'_{\text{fld}}(i_1, i_2, \theta)}{\partial \theta} \quad (10-3)$$

where the partial derivative is taken while holding currents i_1 and i_2 constant. The coenergy can be found from Eq. 3-55, using Eqs. 10-1 and 10-2 and the fact that the mutual inductance between the windings is zero, as

$$W'_{\text{fld}} = \frac{1}{2}L(\theta)i_1^2 + \frac{1}{2}L(\theta - 90^\circ)i_2^2 \quad (10-4)$$

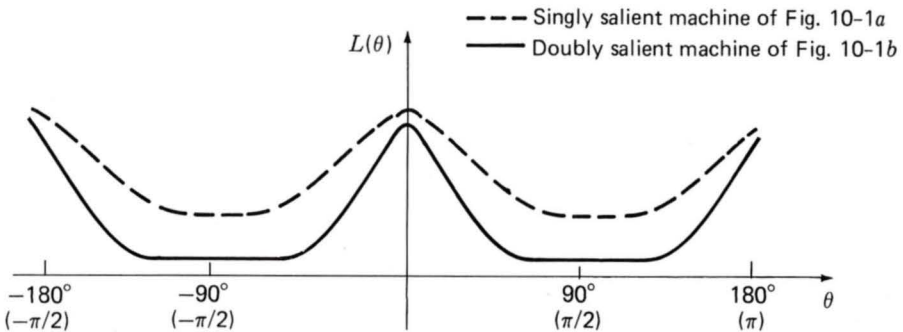


Fig. 10-2. Plots of inductance versus θ for the VRMs of Fig. 10-1.

Thus, combining Eqs. 10-3 and 10-4 gives the torque as

$$T = \frac{1}{2} i_1^2 \frac{dL(\theta)}{d\theta} + \frac{1}{2} i_2^2 \frac{dL(\theta - 90^\circ)}{d\theta} \quad (10-5)$$

Equation 10-5 illustrates an important characteristic of variable-reluctance machines. Notice that the torque is proportional to the square of the phase currents and that as a result it depends on only the magnitude of the phase currents and not on their direction. Thus the motor drive which supplies the phase currents can be unidirectional, i.e., it is not required to supply bidirectional currents. Since the phase currents are typically switched on and off by solid-state switches such as transistors or thyristors and since each switch need only handle currents in a single direction, this means that the motor drive requires only half the number of switches (as well as half the corresponding control electronics) that would be required in a corresponding bidirectional drive. The result is a drive system which is less complex and may be less expensive. Typical motor drives are discussed in Art. 10-4.

Note that Eqs. 10-4 and 10-5 are valid under the assumption that there is no mutual inductance between the phases. Such an assumption is valid for VRMs of Fig. 10-1 in part because of the symmetry of the machine geometry. Such a symmetry argument cannot be made for most VRM geometries. In such machines, the mutual inductance can be shown to be zero only under restrictive assumptions such as the infinite permeability of the rotor and stator magnetic material.

As a result, in practical VRMs there is typically a small mutual flux linkage between the phases. Often this term can be ignored, and as a result expressions for coenergy and torque of the form of Eqs. 10-4 and 10-5 can be assumed valid. However, in some cases this assumption cannot be justified. In practice, it is common to drive the machine iron significantly into saturation such that the relationship between flux linkages and currents becomes more complex than those considered here. In these cases, a mutual inductance term can be included, and coenergy expression will take the form of Eq. 3-55 from which the torque can then be found by using Eq. 10-3. Although the techniques of Chap. 3 and indeed torque expressions of the form of Eq. 10-3 remain valid, analytical expressions are often difficult to obtain (see Art. 10-5).

At the design and analysis stage, the winding flux-current relationships and torque can be determined by using numerical analysis packages which can account for the nonlinearity of the machine magnetic material. Once a machine has been constructed, measurements can be made, both to validate the various assumptions and approximations which have been made and to obtain an accurate measure of actual machine performance.

From this point on, we use the symbol m to indicate the number of stator poles and n to indicate the number of rotor poles, and the corresponding machine is called an m/n machine. Example 10-1 examines a 4/2 VRM.

EXAMPLE 10-1

A 4/2 VRM is shown in Fig. 10-3. Its dimensions are

$$\begin{aligned} R &= 3.8 \text{ cm} & \alpha &= \beta = 60^\circ = \pi/3 \text{ rad} \\ g &= 2.54 \times 10^{-2} \text{ cm} & D &= 0.13 \text{ m} \end{aligned}$$

and the phase windings are connected in series such that there are a total of $N = 100$ turns (50 turns per pole) in each phase winding. Assume the rotor and stator to be of infinite magnetic permeability.

(a) Neglecting leakage and fringing fluxes, plot the phase-1 inductance $L(\theta)$ as a function of θ .

(b) Plot the torque, assuming (i) $i_1 = I_1$ and $i_2 = 0$ and (ii) $i_1 = 0$ and $i_2 = I_2$.

(c) Calculate the net torque (in newton-meters) acting on the rotor when both windings are excited such that $i_1 = i_2 = 5 \text{ A}$ and at angles (i) $\theta = 0^\circ$, (ii) $\theta = 45^\circ$, (iii) $\theta = 75^\circ$.

Solution

(a) Using the magnetic circuit techniques of Chap. 1, we see that the maximum inductance L_{\max} for phase 1 occurs when the rotor axis is aligned with the phase-1 magnetic axis. From Eq. 1-23, we see that L_{\max} is equal to

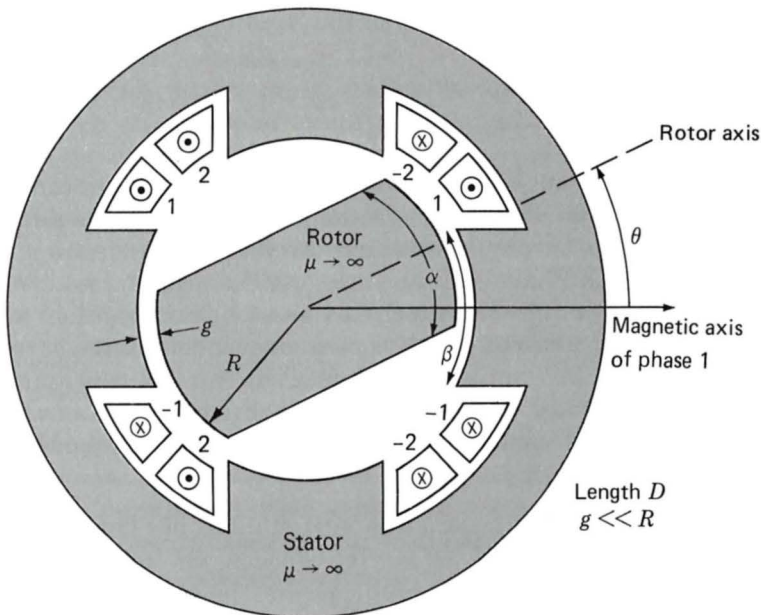


Fig. 10-3. A 4/2 VRM for Example 10-1.

$$L_{\max} = \frac{N^2 \mu_0 \alpha R D}{2g}$$

where $\alpha R D$ is the cross-sectional area of the air gap and $2g$ is the total gap length in the magnetic circuit. For the values given,

$$\begin{aligned} L_{\max} &= \frac{N^2 \mu_0 \alpha R D}{2g} \\ &= \frac{(100)^2 (4\pi \times 10^{-7}) (\pi/3) (3.8 \times 10^{-2}) \times 0.13}{2 \times (2.54 \times 10^{-4})} \\ &= 0.128 \text{ H} \end{aligned}$$

Neglecting fringing, the inductance $L(\theta)$ will vary linearly with the air-gap cross-sectional area as shown in Fig. 10-4a. Note that this idealization predicts that the inductance is zero when there is no overlap when, in fact, there will be some small value of inductance, as shown in Fig. 10-2.

(b) From Eq. 10-5, the torque consists of two terms

$$T = \frac{1}{2} i_1^2 \frac{dL(\theta)}{d\theta} + \frac{1}{2} i_2^2 \frac{dL(\theta - 90^\circ)}{d\theta}$$

and $dL/d\theta$ can be seen to be the stepped waveform of Fig. 10-4b whose maximum values are given by $\pm L_{\max}/\alpha$ (with α expressed in radians!). Thus the torque is as shown in Fig. 10-4c.

(c) The peak torque due to each of the windings is given by

$$T_{\max} = \frac{L_{\max}}{2\alpha} i^2 = \frac{0.128}{2(\pi/3)} 5^2 = 1.53 \text{ N} \cdot \text{m}$$

(i) From the plot in Fig. 10-4c, at $\theta = 0^\circ$, the torque contribution from phase 2 is clearly zero. Although the phase-1 contribution appears to be indeterminate, in an actual machine the torque change from T_{\max_1} to $-T_{\max_1}$ at $\theta = 0^\circ$ would have a finite slope and the torque would be zero at $\theta = 0^\circ$. Thus the net torque from phases 1 and 2 at this position is zero.

Notice that the torque at $\theta = 0^\circ$ is zero independent of the current levels in phases 1 and 2. This is a problem with the 4/2 configuration of Fig. 10-3 since the rotor can get "stuck" at this position (as well as at $\theta = \pm 90^\circ, \pm 180^\circ$) and there is no way that electrical torque can be applied to move it.

(ii) At $\theta = 45^\circ$ both phases are providing torque. That of phase 1 is negative while that of phase 2 is positive. Because the phase currents are equal, the torques are thus equal and opposite and the net torque is zero. However, unlike the case of $\theta = 0^\circ$, the torque at this point can be made

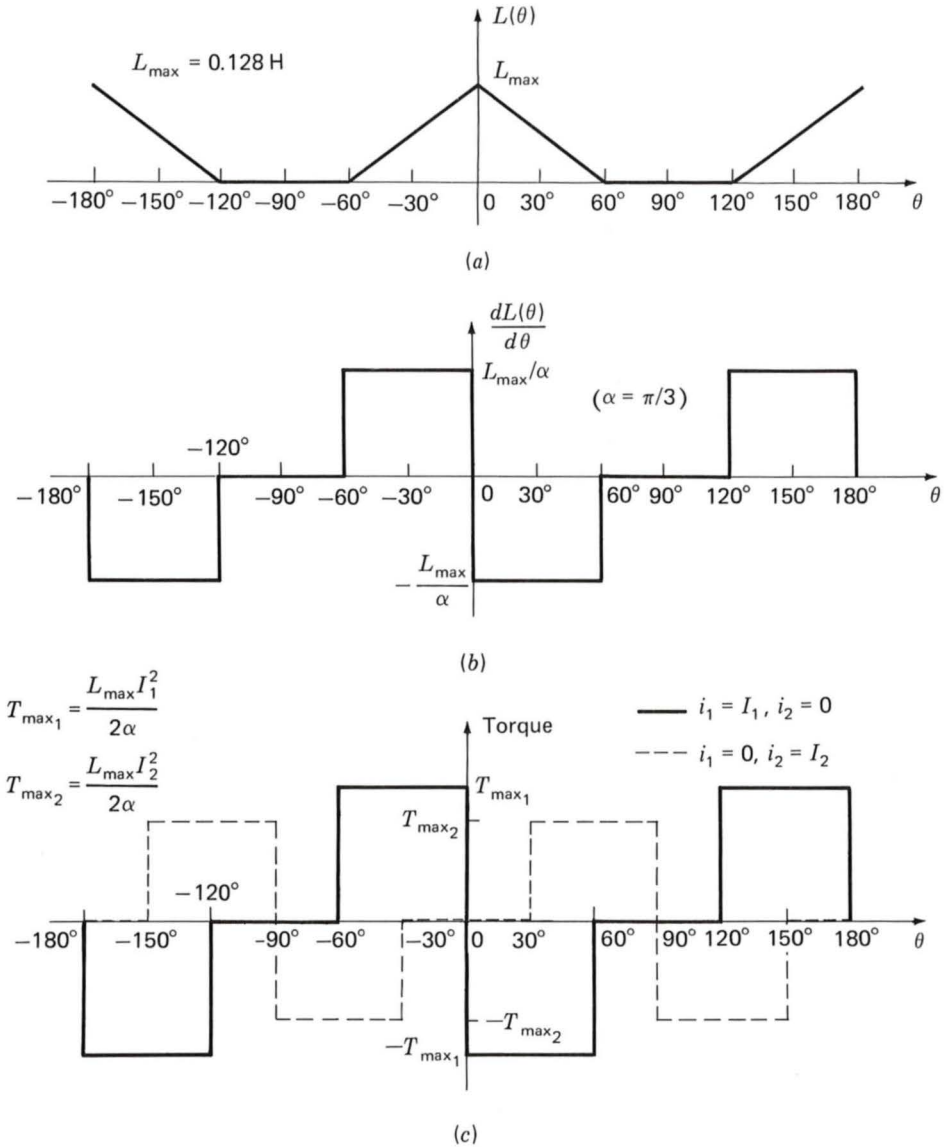


Fig. 10-4. (a) $L(\theta)$ versus θ , (b) $dL(\theta)/d\theta$ versus θ , and (c) torque versus θ .

either positive or negative simply by appropriate selection of the phase currents.

(iii) At $\theta = 75^\circ$ phase 1 produces no torque while phase 2 produces a positive torque of magnitude T_{\max} . Thus the net torque at this position is positive and of magnitude $1.53 \text{ N} \cdot \text{m}$. Notice that there is no combination of phase currents that will produce a negative torque at this position since

the phase-1 torque is always zero while that of phase 2 can be only positive (or zero).

Example 10-1 illustrates a number of important characteristics of VRMs. Clearly these machines must be designed to avoid the occurrence of absolute zero-torque positions at which the torque is zero in all phases simultaneously, independent of the magnitude of the phase currents. This is of concern in the design of 4/2 machines which will always have such torque zeros if they are constructed with uniform, symmetric air gaps.

It is also clear that to operate VRMs with specified torque characteristics, the phase currents must be applied in a fashion consistent with the rotor position. For example, positive torque production from each phase winding in Example 10-1 can be seen from Fig. 10-4c to occur only for specific values of θ . Thus operation of VRMs must include some sort of control which determines both the sequence and the waveform of the phase currents to achieve the desired operation. This is typically implemented by using electronic switching devices (transistors, thyristors, gate-turn-off devices, etc.) under the supervision of a microprocessor-based controller.

Although a 4/2 VRM such as in Example 10-1 can be made to work, as a practical matter it is not particularly useful because of undesirable characteristics such as its zero-torque positions and the fact that there are angular locations at which it is not possible to achieve a positive torque. For example, because of these limitations, this machine cannot be made to generate a constant torque independent of rotor angle; certainly no combination of phase currents can result in torque at the zero-torque positions or in positive torque in the range of angular locations where only negative torque can be produced. As discussed in Art. 10-2, these difficulties can be eliminated by 4/2 designs with asymmetric geometries, and so practical 4/2 machines can be constructed.

As has been seen in this article, the analysis of VRMs is conceptually straightforward. In the case of linear machine iron (no magnetic saturation), finding the torque is simply a matter of finding the stator-phase inductances (self and mutual) as a function of rotor position and then calculating the derivative of the coenergy with respect to angular position (holding the phase currents constant when taking the derivative). Similarly, as discussed in Art. 3-7, the electric terminal voltage for each of the phases can be found from the sum of the time derivative of the phase flux linkage and the iR drop across the phase resistance.

In the case of nonlinear machine iron (where saturation effects are important), as is discussed in Art. 10-5, the coenergy can be found by appropriate integration of the phase flux linkages, and the torque can again be found from the derivative of the coenergy. In either case, there are no rotor windings and typically no other rotor currents in a well-designed variable-reluctance motor, and hence unlike other ac machine types (synchronous

and induction), there are no electrical dynamics associated with the machine rotor. This greatly simplifies their analysis.

Although VRMs are simple in concept and construction, their operation is somewhat complicated and requires sophisticated control and motor-drive electronics to achieve useful and desired operating characteristics. These issues and others are discussed in the following articles.

10-2 PRACTICAL VRM CONFIGURATIONS

Practical VRM drives (the motor and its inverter) are designed to meet operating criteria such as

- Low cost
- Constant torque independent of rotor angular position
- A desired operating speed range
- High efficiency
- A large torque-to-mass ratio

As in any engineering situation, the final design for a specific application will involve a compromise between the variety of options available to the designer. Because VRMs require some sort of electronics and control to operate, often the designer is concerned with optimizing a characteristic of the complete drive system (the VRM and its drive electronics and control), and this will impose additional constraints on the motor design.

VRMs can be built in a wide variety of configurations. In Fig. 10-1, two forms of a 4/2 machine are shown: a singly salient machine in Fig. 10-1a and a doubly salient machine in Fig. 10-1b. Although both types of design can be made to work, a doubly salient design is often the superior choice because it can generally produce a larger torque for a given frame size.

This can be seen qualitatively (under the assumption of a high-permeability, nonsaturating magnetic structure) by reference to Eq. 10-5, which shows that the torque is a function of $dL(\theta)/d\theta$, the derivative of the phase inductance with respect to angular position of the rotor. Clearly, all else being equal, the machine with the largest derivative will produce the largest torque.

This derivative can be thought of as being determined by the ratio of the maximum to minimum phase inductances L_{\max}/L_{\min} . In other words, we can write,

$$\begin{aligned} \frac{dL(\theta)}{d\theta} &\cong \frac{L_{\max} - L_{\min}}{\Delta\theta} \\ &= \frac{L_{\max}}{\Delta\theta} \left(1 - \frac{L_{\min}}{L_{\max}} \right) \end{aligned} \quad (10-6)$$

where $\Delta\theta$ is the angular displacement of the rotor between the positions of maximum and minimum phase inductance and is a function of the rotor geometry only. From Eq. 10-6, we see that the largest value of L_{\max}/L_{\min} will give the largest torque. Because of its geometry, a doubly salient structure will typically have a lower minimum inductance and thus a larger value of L_{\max}/L_{\min} and hence will produce a larger torque for the same rotor structure.

For this reason doubly salient machines are the predominant type of VRM, and hence for the remainder of this chapter we consider only doubly salient VRMs. In general, doubly salient machines can be constructed with two or more poles on each stator and rotor. It should be pointed out that once the basic structure of a VRM is determined, L_{\max} is fairly well determined by such quantities as the number of turns, air-gap length, and basic pole dimensions. The challenge to the VRM designer is to achieve a small value of L_{\min} . This is a difficult task because L_{\min} is dominated by leakage fluxes and other quantities which are difficult to calculate and analyze.

As shown in Example 10-1, the geometry of a symmetric 4/2 VRM with a uniform air gap gives rise to rotor positions for which no torque can be developed for any combination of excitation of the rotor-phase windings. These torque zeros can be seen to occur at rotor positions where all the stator phases are simultaneously at a position of either maximum or minimum inductance. Since the torque depends on the derivative of inductance with respect to angular position, this simultaneous alignment of maximum and minimum inductance points necessarily results in zero torque.

Figure 10-5 shows a 6/4 VRM from which we see that a fundamental feature of the 6/4 machine is that no such simultaneous alignment of phase inductances is possible. As a result, this machine does not have any zero-torque positions. This is a significant point because it eliminates the possibility that the rotor might get stuck in one of these positions at standstill and that it would then have to be mechanically moved to a new position before it could be started. In addition to the fact that there are not positions of simultaneous alignment for the 6/4 VRM, it can be seen that there also are no rotor positions at which only a torque of a single sign (either positive or negative) can be produced. Hence by proper control of the phase currents, it should be possible to achieve a constant-torque output independent of rotor position.

In the case of a symmetric VRM with m stator poles and n rotor poles, a simple test can be used to determine if zero-torque positions exist. If the ratio m/n (or alternatively n/m if n is larger than m) is an integer, there will be zero-torque positions. For example, for a 6/4 machine the ratio is 1.5, and there will be no zero-torque positions. However, the ratio is 2.0 for a 6/3 machine, and there will be zero-torque positions.

In some instances, design constraints may dictate that a machine with an integral pole ratio is desirable. In these cases, it is possible to eliminate the torque-zero positions by constructing a machine with an asymmetric rotor. For example, the rotor radius can be made to vary with angle as

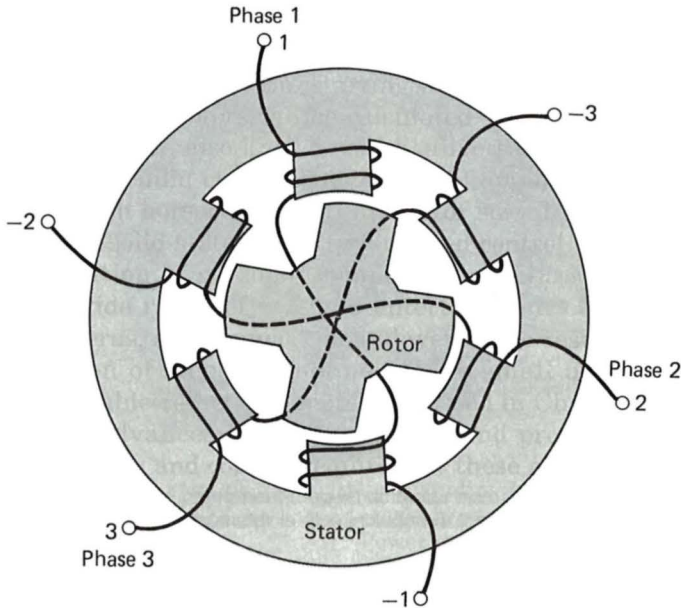


Fig. 10-5. Cross-sectional view of a 6/4 three-phase VRM.

shown in grossly exaggerated fashion in Fig. 10-6a. This design, which also requires that the width of the rotor pole be wider than that of the stator, will not produce zero torque at positions of alignment because $dL(\theta)/d\theta$ is not zero at these points, as can be seen with reference to Fig. 10-6b.

An alternative procedure for constructing an integral-pole-ratio VRM without zero-torque positions is to construct a stack of two or more VRMs in series, aligned such that each of the VRMs is displaced in angle from the others and with all rotors sharing a common shaft. In this fashion, the torque-zero positions of the individual machines will not align, and thus the complete machine will not have any torque zeros. For example, a series stack of two two-phase, 4/2 VRMs such as that of Example 10-1 (Fig. 10-3) with a 45° angular displacement between the individual VRMs will result in a four-phase VRM without torque-zero positions.

Generally VRMs are wound with a single coil on each pole. Although it is possible to control each of these windings separately as individual phases, it is common practice to combine them into groups of poles which are excited simultaneously. For example, the 4/2 VRM of Fig. 10-3 is shown connected as a two-phase machine. As shown in Fig. 10-5, a 6/4 VRM is commonly connected as a three-phase machine with opposite poles connected to the same phase and in such a fashion that the windings drive flux in the same direction through the rotor.

In some cases, VRMs are wound with a parallel set of windings on each phase. This configuration, known as a *bifilar winding*, in some cases can result in a simple inverter configuration and thus a simple, inexpen-

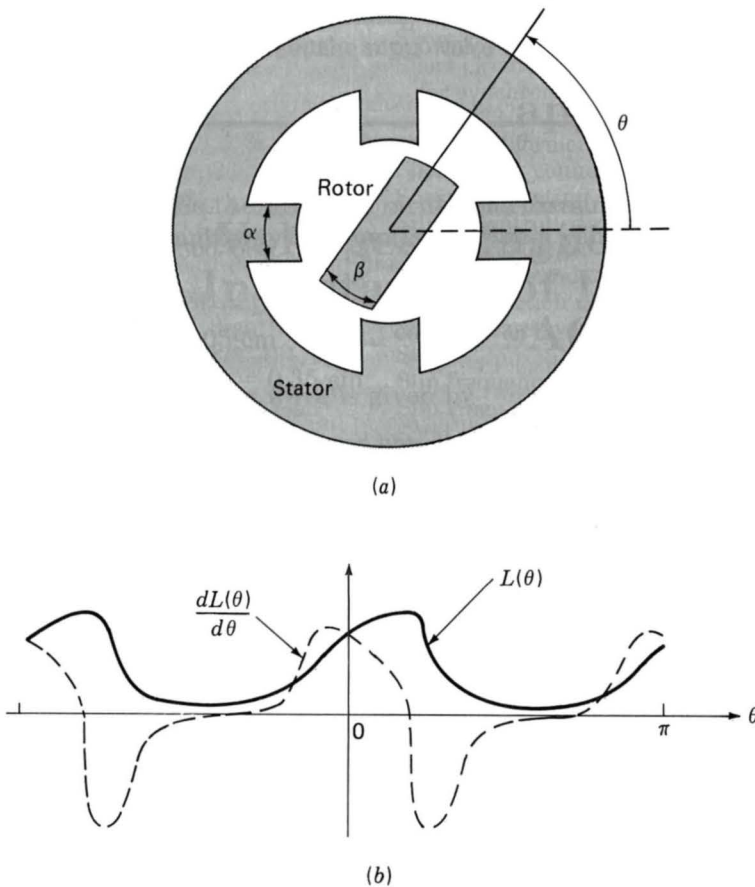


Fig. 10-6. A 4/2 VRM with nonuniform air gap: (a) exaggerated schematic view and (b) plots of $L(\theta)$ and $dL(\theta)/d\theta$ versus θ .

sive motor drive. The use of a bifilar winding in VRM drives is discussed in Art. 10-4.

In general, when a given phase is excited, the torque is such that the rotor is pulled to the nearest position of maximum flux linkage. As excitation is removed from this phase and the next phase is excited, the rotor "follows" as it is then pulled to a new maximum flux-linkage position. However, unlike a conventional synchronous machine, the relationship between the rotor speed and the frequency and sequence of stator-winding excitation can be quite complex, depending on the number of rotor poles and the number of stator poles and phases. This is illustrated in the following example.

EXAMPLE 10-2

Consider a four-phase 8/6 VRM. If the stator phases are excited sequentially with a total time of T_0 s required to excite the four phases (i.e., each phase is excited for a time of $T_0/4$ s), find the angular velocity of the stator flux wave and the corresponding angular velocity of the rotor.

Solution

Figure 10-7 shows in schematic form an 8/6 VRM. The details of the pole shapes are not of importance for this example, and thus the rotor and stator poles are shown simply as arrows indicating their locations. The figure shows the rotor aligned with the stator phase-1 poles. This position corresponds to that which would occur if there were no load on the rotor and the stator phase-1 windings were excited, since it corresponds to a position of maximum phase-1 flux linkage.

Consider next that the excitation on phase 1 is removed and phase 2 is excited. At this point, the stator flux wave has rotated 45° in the clockwise direction. Similarly, as the excitation on phase 2 is removed and phase 3 is excited, the stator flux wave will move an additional 45° clockwise. Thus the angular velocity ω_s of the stator flux wave can be calculated quite simply as $\pi/4$ rad (45°) divided by $T_0/4$ s, or $\omega_s = \pi/T_0$ rad/s.

Note, however, that this is not the angular velocity of the rotor itself. As the phase-1 excitation is removed and phase 2 is excited, the rotor will move in such a fashion as to maximize the phase-2 flux linkages. In this case, Fig. 10-7 shows that the rotor will move 15° counterclockwise since the nearest rotor poles to phase 2 are actually 15° ahead of the phase-2

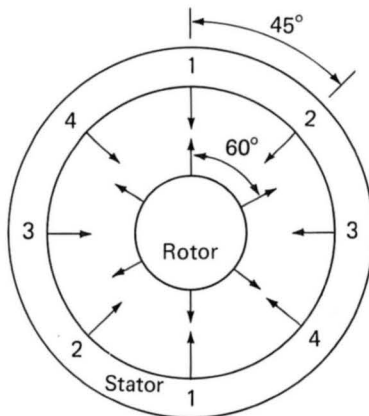


Fig. 10-7. Schematic view of a four-phase 8/6 VRM. Pole locations are indicated by arrows.

poles. Thus the angular velocity of the rotor can be calculated as $-\pi/12$ rad (15° with the minus sign indicating counterclockwise rotation) divided by $T_0/4$ s, or $\omega_r = -\pi/(3T_0)$ rad/s.

In this case, the rotor travels at one-third the angular velocity of the stator excitation and in the opposite direction!

Example 10-2 illustrates the complex relationship that can exist between the excitation frequency of a VRM and the “synchronous” rotor frequency. This relationship is directly analogous to that between two mechanical gears for which the choice of different gear shapes and configurations gives rise to a wide range of speed ratios. It is difficult to derive a single rule which will describe this relationship for the immense variety of VRM configurations which can be envisioned. It is, however, a fairly simple matter to follow a procedure similar to that shown in Example 10-2 to investigate any particular configuration of interest.

Further variations on VRM configurations are possible if the main stator and rotor poles are subdivided by the addition of individual teeth (which can be thought of as a set of small poles excited simultaneously by a single winding). The basic concept is illustrated in Fig. 10-8, which shows a schematic view of three poles of a three-phase VRM with a total of six main stator poles. Such a machine, with the stator and rotor poles subdivided into teeth, is known as a *castleated VRM*, the name resulting from the fact that the stator teeth appear much like the towers on a medieval castle.

In Fig. 10-8 each stator pole has been divided into four subpoles by the addition of four teeth of width $6\frac{3}{7}^\circ$ (indicated by the angle β in the figure), with a slot of the same width between each tooth. The same tooth/slot spac-

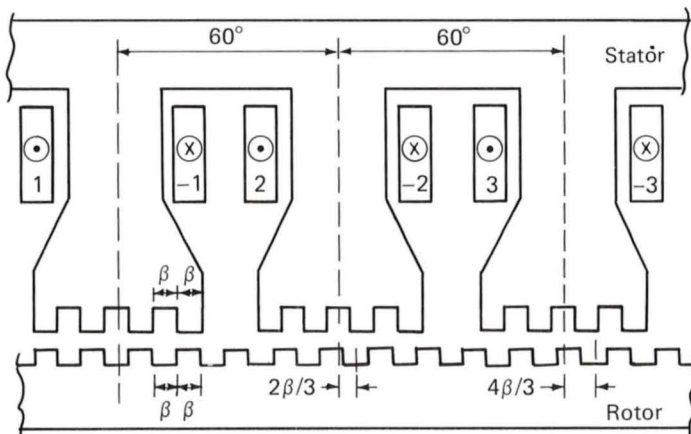


Fig. 10-8. Schematic view of a three-phase castleated VRM with six stator poles and four teeth per pole and 28 rotor poles.

ing is chosen for the rotor, resulting in a total of 28 teeth on the rotor. Notice that this number of rotor teeth and the corresponding value of β were chosen so that when the rotor teeth are aligned with those of the phase-1 stator pole, they are not aligned with those of phases 2 and 3. In this fashion, successive excitation of the stator phases will result in a rotation of the rotor.

Castleation further complicates the relationship between the rotor speed and the frequency and sequence of the stator-winding excitation. For example, from Fig. 10-8 it can be seen that for this configuration, when the excitation of phase 1 is removed and phase 2 is excited (corresponding to a rotation of the stator flux wave by 60° in the clockwise direction), the rotor will rotate by an angle of $(2\beta/3)^\circ = 4\frac{2}{7}^\circ$ in the counterclockwise direction.

From the preceding analysis, we see that the technique of castleation can be used to create VRMs capable of operating at low speeds (and hence high torque for a given stator power input) and with very precise rotor position accuracy. For example, the machine of Fig. 10-8 can be rotated precisely by angular increments of $(2\beta/3)^\circ$. The use of more teeth can further increase the position resolution of these machines. Such machines can be found in applications where low speed, high torque, and precise angular resolution are required.

10-3 CURRENT WAVEFORMS FOR TORQUE PRODUCTION

As is seen in Art. 10-1, the torque produced by a VRM in which saturation and mutual inductance effects can be neglected is determined by the derivatives of the phase inductances with respect to the rotor angular position, each multiplied by the square of the corresponding phase current. For example, from Eq. 10-5, the torque for the 4/2 machines of Fig. 10-1 is given by

$$T = \frac{1}{2} i_1^2 \frac{dL_1(\theta)}{d\theta} + \frac{1}{2} i_2^2 \frac{dL_2(\theta)}{d\theta} \quad (10-7)$$

For each phase of a VRM, the phase inductance is periodic in rotor angular position and thus the area under the curve of $dL/d\theta$ calculated over a complete period of $L(\theta)$ is zero, i.e.,

$$\int_0^{2\pi/n} \frac{dL(\theta)}{d\theta} d\theta = L(2\pi/n) - L(0) = 0 \quad (10-8)$$

where n is the number of rotor poles.

The average torque produced by a VRM can be found by integrating the torque equation (Eq. 10-7) over a complete period of rotation. Clearly, if the stator currents are held constant, Eq. 10-8 shows that the average

torque will be zero. Thus, to produce a time-averaged torque, the stator currents must vary with rotor position. The desired average output torque for a VRM depends on the nature of the application. For example, motor operation requires a positive time-averaged shaft torque. Similarly, braking or generator action requires negative time-averaged torque.

Positive torque is produced when a phase is excited at angular positions with positive $dL/d\theta$ for that phase, and negative torque is produced by excitation at positions at which $dL/d\theta$ is negative. Consider a three-phase, 6/4 VRM (similar to that shown in Fig. 10-5) with 40° rotor and stator poles. The inductance versus rotor position for this machine will be similar to the idealized representation shown in Fig. 10-9.

Operation of this machine as a motor requires a net positive torque. Alternatively, it can be operated as a generator under conditions of net negative torque. Noting that positive torque is generated when excitation is applied at rotor positions at which $dL/d\theta$ is positive, we see that a control system is required that determines rotor position and applies the phase-winding excitations at the appropriate time. It is, in fact, the need for this sort of control that makes VRM drive systems more complex than might perhaps be thought, considering only the simplicity of the VRM itself.

One of the reasons that VRM drive systems have begun to find application in a wide variety of situations is because the widespread availability and low cost of micro and power electronics have brought the cost of the sensing and control required to successfully operate VRM drive systems down to a level where these systems can be competitive with systems

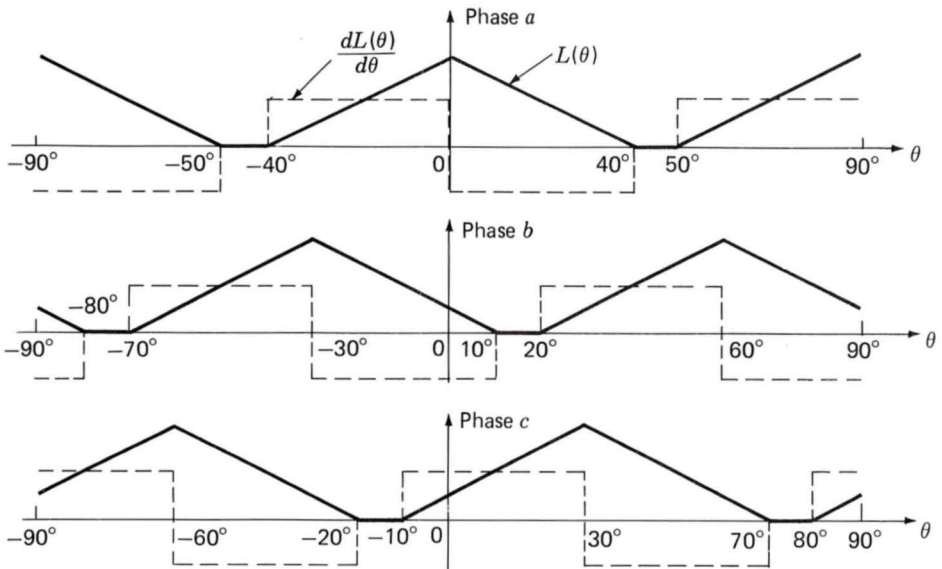


Fig. 10-9. Idealized inductance and $dL/d\theta$ curves for a three-phase 6/4 VRM with 40° rotor and stator poles.

based upon dc and induction-motor technologies. Although the control of VRM drives is more complex than that required for dc, induction, and permanent-magnet ac motor systems, in many applications the overall VRM drive system turns out to be less expensive and more flexible than the competition.

Assuming that the appropriate rotor-position sensor and control system is available, the question still remains as to how to excite the armature phases. From Fig. 10-9, one possible excitation scheme would be to apply a constant current to each phase at those angular positions at which $dL/d\theta$ is positive and zero current otherwise.

If this is done, the resultant torque waveform will be that of Fig. 10-10. Note that because the torque waveforms of the individual phases overlap, the resultant torque will not be constant but rather will have a pulsating component on top of its dc average value. In general, such pulsating torques are to be avoided both because they may produce damaging stresses in the machine and because they may result in the generation of excessive vibration and noise from the machine.

Consideration of Fig. 10-9 shows that there are alternative excitation strategies which can reduce the torque pulsations of Fig. 10-10. Perhaps the simplest strategy is to excite each phase for only 30° of angular position instead of the 40° which resulted in Fig. 10-9. Thus, each phase would simply be turned off as the next phase were turned on, and there would be no torque overlap between phases.

Although this strategy would be an ideal solution to the problem, as a practical matter it is not possible to implement. The problem is that because each phase winding has a self-inductance, it is not possible to instantaneously switch on or off the phase currents. Specifically, for a VRM with independent (uncoupled) phases,[†] the voltage-current relationship of the j th phase is given by

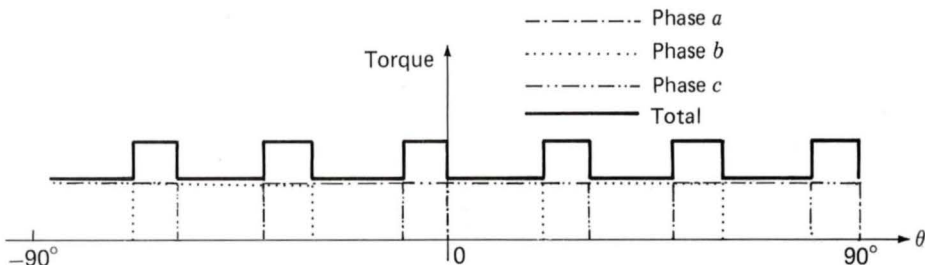


Fig. 10-10. Individual phase torques for the motor of Fig. 10-9. Each phase is excited with a constant current I_0 only at positions where $dL/d\theta > 0$.

[†]The reader is reminded that in some cases the assumption of independent phases is not justified, and then a more complex analysis of the VRM is required (see the discussion following the derivation of Eq. 10-5).

$$v_j = R_j i_j + \frac{d\lambda_j}{dt} \quad (10-9)$$

where

$$\lambda_j = L_j(\theta) i_j \quad (10-10)$$

Thus,

$$v_j = R_j i_j + \frac{d}{dt} [L_j(\theta) i_j] \quad (10-11)$$

Equation 10-11 can be rewritten as

$$v_j = \left\{ R_j + \frac{d}{dt} [L_j(\theta)] \right\} i_j + L_j(\theta) \frac{di_j}{dt} \quad (10-12)$$

or

$$v_j = \left[R_j + \frac{dL_j(\theta)}{d(\theta)} \frac{d\theta}{dt} \right] i_j + L_j(\theta) \frac{di_j}{dt} \quad (10-13)$$

Although Eqs. 10-11 through 10-13 are complex and often require numerical solution, they clearly indicate that some time is required to build up currents in the phase windings following application of voltage to that phase. A similar analysis can be done for conditions associated with removal of the phase currents. Because this typically occurs when the phase inductances are at their maximum, the time required for the removal of current may be even longer than that required for current buildup. These effects are illustrated in Example 10-3 which also shows that in cases where winding resistance can be neglected, an approximate solution to these equations can be found.

EXAMPLE 10-3

Consider the idealized 4/2 VRM of Example 10-1. Assume that it has a winding resistance of $R = 1.5 \, \Omega/\text{phase}$ and a leakage inductance $L_l = 5 \, \text{mH}$ in each phase. For a constant rotor speed of 4000 r/min, calculate (a) the phase-1 current as a function of time during the interval $-60^\circ \leq \theta \leq 0^\circ$, assuming that a constant voltage of $V_0 = 100 \, \text{V}$ is applied to phase 1 just as $dL(\theta)/d\theta$ becomes positive (i.e., at $\theta = -60^\circ = -\pi/3 \, \text{rad}$), and (b) the decay of phase-1 current if a negative voltage of $-100 \, \text{V}$ is applied at $\theta = 0^\circ$ and maintained until the current reaches zero.

Solution

(a) From Eq. 10-13, the differential equation governing the current buildup in phase 1 is given by

$$v = \left[R + \frac{dL(\theta)}{d\theta} \frac{d\theta}{dt} \right] i + L(\theta) \frac{di}{dt}$$

At 4000 r/min,

$$\frac{d\theta}{dt} = 4000 \frac{\text{r}}{\text{min}} \times \frac{\pi}{30} \frac{\text{rad/s}}{\text{r/min}} = \frac{400\pi}{3} \frac{\text{rad}}{\text{s}}$$

From Fig. 10-4 (for $-60^\circ \leq \theta \leq 0^\circ$)

$$\begin{aligned} L(\theta) &= L_l + \frac{L_{\max}}{\pi/3} \left(\theta + \frac{\pi}{3} \right) \\ &= 0.005 + 0.122(\theta + \pi/3) \end{aligned}$$

Thus

$$\frac{dL(\theta)}{d\theta} = 0.122 \frac{\text{H}}{\text{rad}}$$

and

$$\frac{dL(\theta)}{d\theta} \frac{d\theta}{dt} = 51.2 \, \Omega$$

which is much greater than the resistance $R = 1.5 \, \Omega$.

This will enable us to obtain an approximate solution for the current by neglecting the Ri term in Eq. 10-11. We must then solve

$$\frac{d(Li)}{dt} = v$$

for which the solution is

$$\begin{aligned} i(t) &= \frac{\int_0^t v \, dt}{L(t)} = \frac{V_0 t}{L(t)} \\ &= \frac{100t}{0.005 + 51.2t} \quad \text{A} \end{aligned}$$

which is valid until $\theta = 0$ at $t = 2.5$ ms. This solution is plotted in Fig. 10-11a.

(b) During the period of current decay the solution proceeds as in part (a). From Fig. 10-4, for $0^\circ \leq \theta \leq 60^\circ = \pi/3$ rad, $dL(\theta)/dt = -51.2 \Omega$ and the Ri term can again be ignored in Eq. 10-11.

Thus since the applied voltage is $V_0 = -100$ V for this time period [$t \geq 2.5$ ms until $i(t) = 0$] and recognizing that the current must remain continuous at $t = 2.5$ ms, we see that the solution becomes

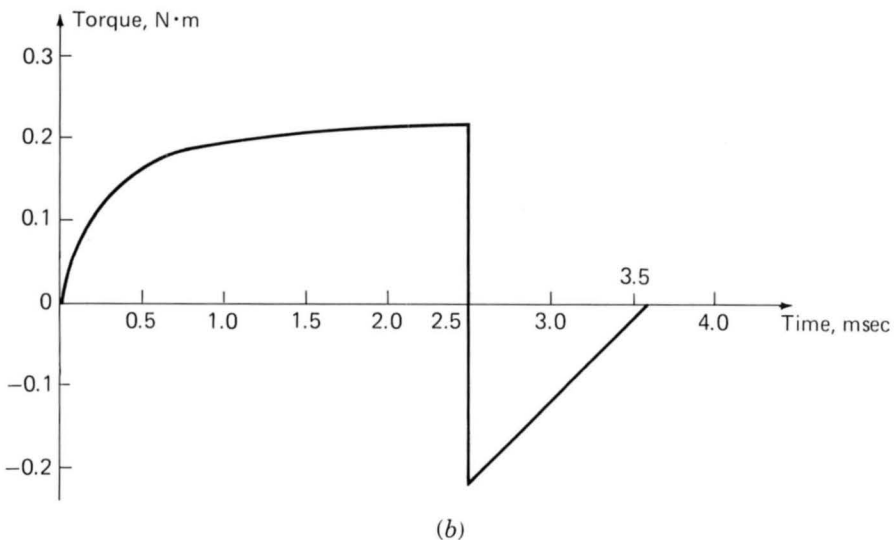
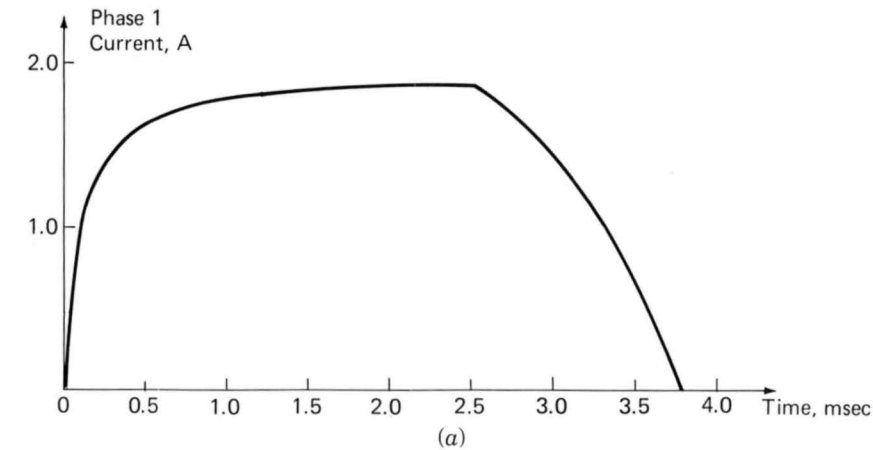


Fig. 10-11. Example 10-3: (a) Phase-1 current and (b) torque profile.

$$\begin{aligned}
 i(t) &= 1.88 + \frac{\int_{2.5 \times 10^{-3}}^t v dt}{L(t)} \\
 &= 1.88 - \frac{100(t - 2.5 \times 10^{-3})}{0.005 + 51.2(5 \times 10^{-3} - t)} \quad \text{A}
 \end{aligned}$$

This current decay is also plotted in Fig. 10-11*a*, where we see that the current reaches zero at $t = 3.77$ ms.

Notice from Fig. 10-11*a* that because much of the current increase occurs while the inductance is relatively low while the current decay begins when the phase inductance is at its maximum, the current buildup occurs more rapidly than does its decay. Also notice that just as the current waveform differs significantly from the ideal, so does the torque profile (plotted in Fig. 10-11*b*) differ from the ideal profile of Fig. 10-4*c*. In fact, we see that significant negative torque is generated due to the slow decay of the phase current following turn-off.

This example also illustrates another important aspect of VRM operation. For a system of resistance of $1.5 \, \Omega$ and constant inductance, one would expect a steady-state current of $100/1.5 = 66.7$ A. Yet in this system the steady-state current is less than 2 A. The reason for this is evident from Eqs. 10-12 and 10-13 where we see that $dL(\theta)/dt = 51.2 \, \Omega$ appears as an apparent resistance in series with the winding resistance and which is much larger than the winding resistance. The corresponding voltage drop (the speed voltage) is of sufficient magnitude to limit the steady-state current to a value of $100/51.2 = 1.90$ A.

Example 10-3 indicates important aspects of VRM performance which do not appear in an idealized analysis such as that of Example 10-1 but which play an extremely important role in practical applications. It is clear that it is not possible to readily apply phase currents of arbitrary waveshapes. Winding inductances (and their time derivatives) significantly affect the current waveforms that can be achieved for a given applied voltage.

In fact, the problem becomes more severe as the rotor speed is increased. Consideration of Example 10-3 shows, for a given applied voltage, (1) that as the speed is increased, the current will take a larger fraction of the available time during which $dL/d\theta$ is positive to achieve a given level, and (2) that the steady-state current which can be achieved is progressively lowered. One common method for maximizing the available torque is to apply the phase voltage somewhat in advance of the time when $dL/d\theta$ begins to increase. This gives the current time to build up to a significant level before torque production begins.

Yet a more significant difficulty (also illustrated in Example 10-3) is that just as the currents require a significant amount of time to increase at

the beginning of a turn-on cycle, they also require time to decrease at the end. Because these currents are typically turned off when the rotor is near its maximum inductance position, the decay time is often longer than the time required for current buildup. As a result, if the phase excitation is removed at or near the end of the positive $dL/d\theta$ period, it is likely that there will be phase current remaining as $dL/d\theta$ becomes negative, so there will be a period of negative torque production, reducing the effective torque-producing capability of the VRM.

One way to avoid such negative torque production would be to turn off the phase excitation sufficiently early in the cycle that the current will have decayed to zero by the time that $dL/d\theta$ becomes negative. However, there is clearly a point of diminishing returns, because turning off the phase current while $dL/d\theta$ is positive also reduces positive torque production. As a result, it is often necessary to accept a certain amount of negative torque (to get the required positive torque) and to compensate for it by the production of additional positive torque from another phase.

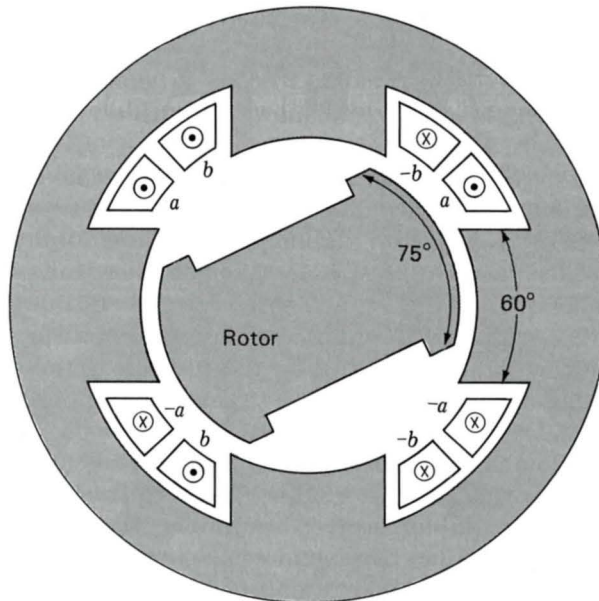
Another possibility is illustrated in Fig. 10-12. Figure 10-12a shows the cross-sectional view of a 4/2 VRM similar to that of Fig. 10-3 with the exception that the rotor pole angle has been increased from 60° to 75° with the result that the rotor pole overhangs that of the stator by 15° . As can be seen from Fig. 10-12b, this results in a region of constant inductance separating the positive and negative $dL/d\theta$ regions, which in turn provides additional time for the phase current to be turned off before the region of negative torque production is reached.

Although Fig. 10-12 shows an example with 15° of rotor overhang, in any particular design the amount of overhang would be determined as part of the overall design process and would depend on such issues as the amount of time required for the phase current to decay and the operating speed of the VRM. Also included in this design process must be recognition that the use of wider rotor poles will result in a larger value of L_{\min} , which itself tends to reduce torque production (see the discussion of Eq. 10-6) and to increase the time for current buildup.

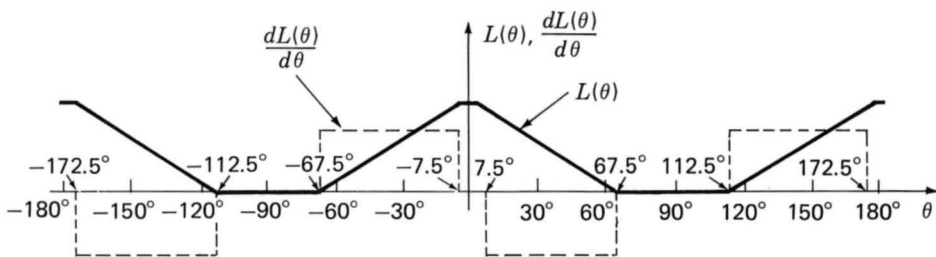
Under conditions of constant-speed operation, it is often desirable to achieve constant torque independent of rotor position. Such operation will minimize pulsating torques which may cause excessive noise and vibration and perhaps ultimately lead to component failure due to material fatigue. This means that as the torque production of one phase begins to decrease, that of another phase must increase to compensate. As can be seen from torque waveforms such as those found in Fig. 10-11, this represents a complex control problem for the phase excitation, and a totally ripple-free torque will be difficult to achieve in many cases.

10-4 VRM DRIVES

Unlike dc and ac (synchronous or induction) machines, VRMs cannot be simply "plugged in" to a dc or ac source and then be expected to run. As



(a)



(b)

Fig. 10-12. A 4/2 VRM with 15° rotor overhang: (a) cross-sectional view and (b) plots of $L(\theta)$ and $dL(\theta)/d\theta$ versus θ .

has been seen in this chapter, the phases must be excited with (typically unipolar) currents, and the timing of these currents must be carefully correlated with the position of the rotor poles in order to produce a useful, time-averaged torque. The result is that although the VRM itself is perhaps the simplest of rotating machines, a practical VRM drive system is relatively complex.

VRM drive systems are competitive only because this complexity can be realized easily and inexpensively through power and microelectronic circuitry. Because these drive systems require a fairly sophisticated level of controllability for even the simplest modes of VRM operation, fairly sophisticated control features can be added (typically in the form of addi-

tional software) at little additional cost, further increasing the competitive position of VRM drives.

In addition to the VRM itself, the basic VRM drive system consists of the following components: a rotor-position sensor, a controller, and an inverter.

The function of the rotor-position sensor is to provide an indication of shaft position which can be used to control the timing and waveform of the phase excitation. This is directly analogous to the timing signal used to control the firing of the cylinders in an automobile engine.

The controller is typically implemented in software in microelectronic (microprocessor) circuitry. Its function is to determine the sequence and waveforms of the phase excitation required to achieve the desired motor speed-torque characteristics. In addition to set points of desired speed and/or torque and shaft position (from the shaft-position sensor), sophisticated controllers often employ additional inputs including shaft-speed and phase-current magnitude. Along with the basic control function of determining the desired torque for a given speed, the more sophisticated controllers attempt to provide excitations which are in some sense optimized (for maximum efficiency, stable transient behavior, etc.).

The control circuitry consists typically of low-level electronics which cannot be used to directly supply the currents required to excite the motor phases. Rather its output consists of signals which control the inverter which in turn supplies the phase currents. In general, the inverter consists of a dc source and a set of controllable switches whose function is to connect the various phases to the dc source at appropriate times as determined by the controller.

Control of the VRM is achieved by the application of currents to the VRM phase windings. A phase winding of a VRM can be thought of as a nonlinear (due to magnetic saturation effects), time-varying (due to changes in rotor position with time) inductance. Many of the issues associated with the control of current in these systems can be investigated by considering the situation of a constant inductance supplied by a dc source. This has the additional advantage of being easily analyzed.

Figure 10-13a shows such a system in which an inductor of constant inductance L is connected to a dc source of voltage V_0 . The resistance of the inductor is R while the source resistance is R_s . An ideal switch is shown connecting the source and the inductor. Finally a *flyback diode* is shown connected across the inductor.

Figure 10-13b shows the system configuration when the switch is closed. Under this condition, the diode is back-biased and carries no current, and the inductor current is governed by the differential equation

$$L \frac{di}{dt} + (R + R_s)i = V_0 \quad (10-14)$$

Assuming that the inductor is carrying an initial current I_1 at time t_1 when the switch is closed, the subsequent current is given by

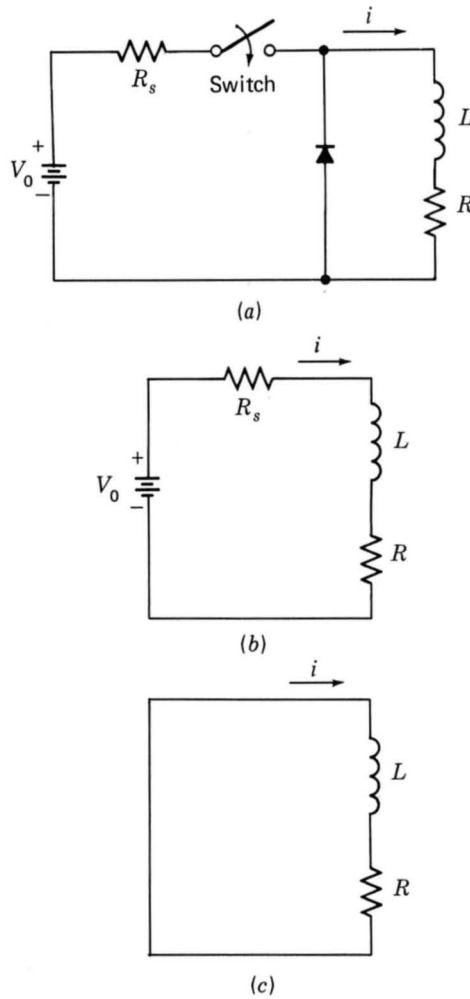


Fig. 10-13. Simplified drive circuit for an inductive load: (a) complete circuit, (b) equivalent circuit with the switch closed, and (c) equivalent circuit with the switch open.

$$i(t) = \frac{V_0}{R + R_s} + \left(I_1 - \frac{V_0}{R + R_s} \right) e^{-(t-t_1)/\tau} \quad (10-15)$$

where

$$\tau = \frac{L}{R + R_s} \quad (10-16)$$

is the time constant associated with the inductance and the total dc resistance of the circuit.

If there were no flyback diode present in the circuit, as the switch is opened, the current would begin to drop and a negative voltage would ap-

pear across the inductor ($L di/dt < 0$) in order to maintain current flow through the inductor. Typically this voltage will become large enough to maintain current flow through the switch (often in the form of an arc) until all the energy has been dissipated from the inductor.

The presence of the flyback diode changes matters considerably. As the inductor voltage becomes negative, it forward-biases the diode, turning it on, and provides an alternate path for the inductor current. Figure 10-13c shows the effective configuration which exists under these conditions. The diode is assumed to be ideal and thus appears as a short circuit across the inductor terminals. In addition to providing an alternative current path for inductor current, the diode prevents excessive voltages from damaging the switch upon opening.

From Fig. 10-13c it can be seen that the inductor current will decay with the L/R time constant of the inductor. Thus if the switch is opened at time t_2 when the inductor is carrying a current I_2 , the inductor will discharge and the subsequent inductor current will be given by

$$i(t) = I_2 e^{-(t-t_2)R/L} \quad (10-17)$$

Thus we can see that by alternately closing and opening the switch it is possible to charge and discharge the inductor. If the switch is operated at a rate slow compared to the time constants of the charge and discharge transients, the resulting current waveform will be as shown in Fig. 10-14a. While the switch is closed, the current will increase with time constant $L/(R + R_s)$ to a dc value of $V_0/(R + R_s)$. When the switch is then opened, the current will in turn decay to zero with time constant L/R .

As is discussed in Art. 10-3, VRM operation requires control of the current applied to each phase. For example, one control strategy for constant-torque production is to apply constant current to each phase during the time that $dL/d\theta$ for that phase is constant. This results in constant torque proportional to the square of the phase-current magnitude. The magnitude of the torque can be controlled by changing the magnitude of the phase current.

Clearly, a current waveform of the form of Fig. 10-14a does not provide sufficient flexibility to achieve arbitrary levels of direct current from a dc voltage source of fixed magnitude. For example, if the time constants associated with charging and discharging the inductor are short compared with the desired on-time of the direct current, turning on the switch will essentially apply a direct current of magnitude $V_0/(R + R_s)$ to the inductor and turning off the switch will remove it. The resultant waveform will be that of Fig. 10-14b.

Figure 10-15 shows a technique that can be used to achieve arbitrary values of direct current I_0 [$I_0 < V_0/(R + R_s)$]. This technique is known as *chopping*. By alternately turning the switch on and off, the current can be made to vary around a dc level. In Fig. 10-15, the switch is first turned on

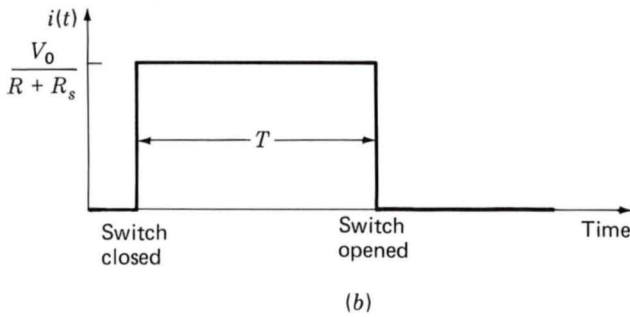
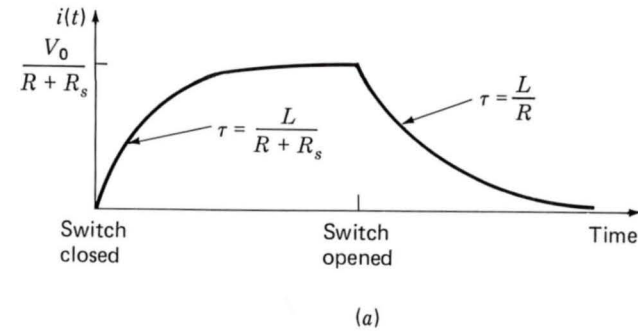


Fig. 10-14. Current waveforms for system of Fig. 10-13. (a) Inductor current following closing and opening of switch; (b) inductor current when switch is closed for time T [$T \gg L/R$, $L/(R + R_s)$].

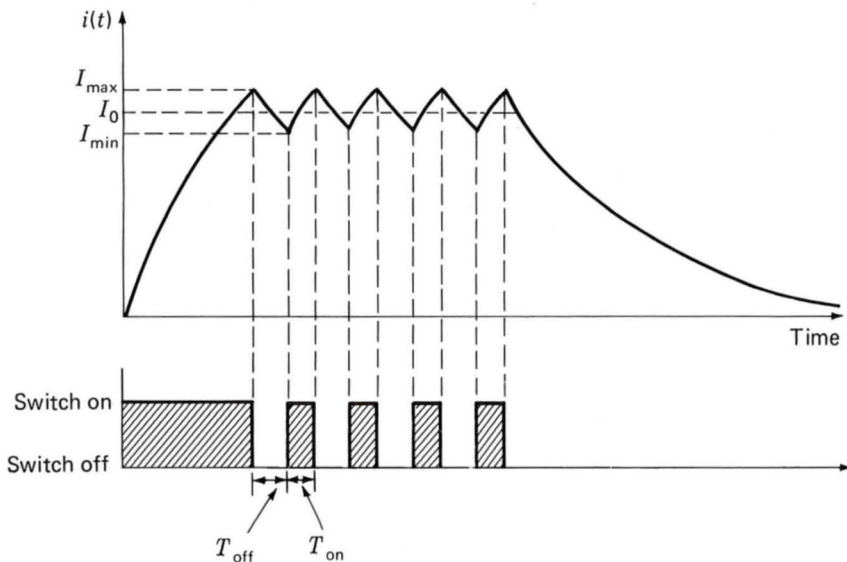


Fig. 10-15. Inductor current showing the effects of chopping for the system of Fig. 10-13.

until the current $i(t)$ reaches the value I_{\max} . It is then turned off for a time T_{off} during which the current decays to a value I_{\min} , following which it is again turned on for a time T_{on} until the current reaches I_{\max} . This cycle is repeated until a time when the switch is left off and the current is allowed to decay to zero.

Depending on the choice of T_{off} and T_{on} , the current waveform upon chopping may be more complex than that of Fig. 10-15. In many cases, T_{off} and T_{on} may be varied during the course of the switching operation, and in the case of a VRM, the winding inductance will vary with time, further complicating the waveform. However, in all such situations, the basic idea remains the same. By alternately opening and closing the switch, the current can be made to vary around an average value I_0 . Depending on how rapidly the switch can be turned on and off subject to practical limits associated with the switching devices and their control circuitry, the current ripple ($I_{\max} - I_{\min}$) can be made arbitrarily small.

EXAMPLE 10-4

Consider the system of Fig. 10-13a with the following parameter values:

$$V_0 = 100 \text{ V} \quad L = 250 \text{ mH} \quad R = 2.5 \, \Omega \quad R_s = 2.5 \, \Omega$$

The system is to be operated in a chopping mode to produce a current waveform such as that of Fig. 10-15.

Calculate the switching times T_{off} and T_{on} such that the inductor current varies between $I_{\min} = 10 \text{ A}$ and $I_{\max} = 12 \text{ A}$.

Solution

Initially the switch is held closed until the current reaches the value $I_{\max} = 12 \text{ A}$. At this point the current begins to decay. From Eq. 10-17, with $I_2 = I_{\max}$ and assuming the switch is turned off at time $t_i = 0$, the subsequent current decay is given by

$$i(t) = I_{\max} e^{-tR/L}$$

Setting $t = T_{\text{off}}$ then gives $i(t = T_{\text{off}}) = I_{\min}$. This can be solved for T_{off} to give

$$\begin{aligned} T_{\text{off}} &= -\frac{L}{R} \ln \frac{I_{\min}}{I_{\max}} \\ &= -\frac{0.25}{2.5} \ln \frac{10}{12} = 18.2 \text{ ms} \end{aligned}$$

At this point the switch is closed until the current reaches the value I_{\max} at time $t = T_{\text{off}} + T_{\text{on}}$. From Eq. 10-15, by setting $I_1 = I_{\min}$ and $t_1 = T_{\text{off}}$, T_{on} can be found as

$$\begin{aligned} T_{\text{on}} &= -\frac{L}{R + R_s} \ln \frac{I_{\max} - V_0/(R + R_s)}{I_{\min} - V_0/(R + R_s)} \\ &= -\frac{0.25}{5} \ln \frac{12 - 20}{10 - 20} = 11.2 \text{ ms} \end{aligned}$$

Example 10-4 shows a typical current waveform which can be achieved with a simple chopping circuit driving a constant-value inductor. This system can be operated "open loop" in that the switching times can be predetermined and the controller can achieve the desired current level based upon these calculated times.

The control required to drive the phase windings of a VRM is made more complex because the phase-winding inductances change both with rotor position and with current levels due to saturation effects in the magnetic material. As a result, it is not possible in general to perform the chopping open-loop based on a precalculated algorithm. However, chopping can be readily accomplished through the use of feedback. The instantaneous phase current can be measured and a switching scheme can be devised such that the switch can be opened when the current has been found to reach the desired level I_{\max} , and the switch can be turned on when the current decays to I_{\min} .

Figure 10-16a to c shows three common configurations found in inverter systems for driving VRMs.[†] In these figures, the switching device is indicated by the symbol for an ideal switch. In practical inverters, the switch will be a solid-state device such as a thyristor, a transistor [bipolar or field effect (FET)], or a GTO (gate-turn-off) device. Each inverter is shown in a two-phase configuration. As is clear from the figure, extension of each configuration to drive additional phases can be readily accomplished.

The configuration of Fig. 10-16a is perhaps the simplest. There are two switches and two diodes per phase. To energize phase 1, for example, both switches S_{1a} and S_{1b} must be closed. This places the phase winding directly across the supply and causes current i_1 to flow in the direction indicated. When the switches are opened, di_1/dt becomes negative and a voltage is developed across the phase winding in such a direction as to forward-bias diodes D_{1a} and D_{1b} . As a result, although current continues to flow through

[†]For a detailed discussion of these inverter systems, see R. M. Davis, W. F. Ray, and R. J. Blake, "Inverter Drive for Switched Reluctance Motor: Circuits and Component Ratings," *IEE Proc.*, **128B**(2) (Mar. 1981).

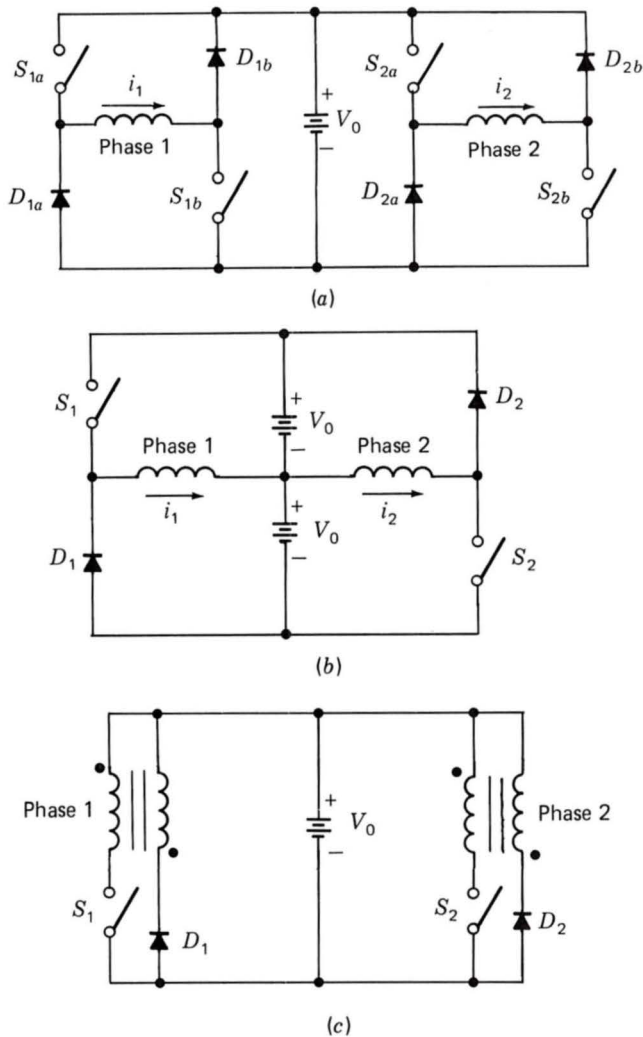


Fig. 10-16. Inverter configurations. (a) Two-phase inverter which uses two switches per phase. (b) Two-phase inverter which uses a split supply and one switch per phase. (c) Two-phase inverter with bifilar phase windings and one switch per phase.

the phase winding, it is now connected across the supply with a reverse polarity, forcing the current to decay to zero.

It is interesting to note an important distinction between this circuit and that of Fig. 10-13a. In the circuit of Fig. 10-13a, all the magnetic energy which is initially stored in the inductor is dissipated (in the resistance of the inductor and in the flyback diode) when the switch is opened and the current decays through the flyback diode. When the switches open in the inverter circuit of Fig. 10-16a, the current flows back through the dc source

and much of the energy is returned to the source. This process is known as *regeneration* and clearly results in an inverter which is much more efficient than one in which all excess magnetic stored energy is dissipated in the form of heat. Similarly, this circuit will permit generator operation with the predominant energy exchange consisting of power being delivered from the VRM to the dc source.

The inverter configuration of Fig. 10-16a is perhaps the simplest of configurations which provide regeneration capability. Its main disadvantage is that it requires two switches per phase. In many applications, the cost of the switches (and their associated drive circuitry) dominates the cost of the inverter, and the result is that this configuration is less attractive in terms of cost when compared to other configurations which require one switch per phase.

Figure 10-16b shows one such configuration. This configuration requires a split supply (i.e., two supplies of voltage V_0) but only a single switch and diode per phase. Closing switch S_1 connects the phase-1 winding to the upper dc source. Opening the switch causes the phase current to transfer to diode D_1 , connecting the winding to the bottom dc source. Phase 1 is thus supplied by the upper dc source and regenerates through the bottom source. Note that to maintain symmetry and to balance the energy supplied from each source equally, phase 2 is connected oppositely so that it is supplied from the bottom source and regenerates into the top source.

The major disadvantages of the configuration of Fig. 10-16b are that it requires a split supply and that when the switch is opened, the switch must withstand a voltage of $2V_0$. This can be readily seen by recognizing that when diode D_1 is forward-biased, the switch is connected across the two supplies. Such switches are likely to be more expensive than the switches required by the configuration of Fig. 10-16a. Both of these issues will tend to offset some of the economic advantage which can be gained by the elimination of one switch and one diode as compared with the inverter circuit of Fig. 10-16a.

A third inverter configuration is shown in Fig. 10-16c. This configuration requires only a single dc source and uses only a single switch and diode per phase. This configuration achieves regeneration through the use of *bifilar* phase windings. In a bifilar winding, each phase is wound with two separate windings which are closely coupled magnetically (this can be achieved by winding the two windings at the same time) and can be thought of as the primary and secondary windings of a transformer.

When switch S_1 is closed, the primary winding of phase 1 is energized, exciting the phase winding. Opening the switch induces a voltage in the secondary winding (note the polarity indicated by the dots in Fig. 10-16c) in such a direction as to forward-bias D_1 . The result is that current is transferred from the primary to the secondary winding with a polarity such that the current in the phase decays to zero and energy is returned to the source.

Although this configuration requires only a single dc source, it requires a switch which must withstand a voltage in excess of $2V_0$ (the degree of excess being determined by the voltage developed across the primary leakage reactance as current is switched from the primary to the secondary windings) and requires the more complex bifilar winding in the machine. In addition, the switches in this configuration must include snubbing circuitry (typically consisting of a resistor-capacitor combination) to protect them from transient overvoltages. These overvoltages result from the fact that although the two windings of the bifilar winding are wound such that they are as closely coupled as possible, perfect coupling cannot be achieved. As a result, there will be energy stored in the leakage fields of the primary winding which must be dissipated when the switch is opened.

This section has provided a brief introduction to the topic of drive systems for variable-reluctance machines. In most cases, many additional issues must be considered before a practical drive system can be implemented. For example, accurate rotor position sensing is required for proper control of the phase excitation, and the control loop must be properly compensated to ensure its stability. In addition, the finite rise and fall times of current buildup in the motor phase windings will ultimately limit the maximum achievable rotor torque and speed.

The performance of a complete VRM drive system is intricately tied to the performance of all its components, including the VRM, its controller, and its inverter. In this sense, the VRM is quite different from the induction, synchronous, and dc machines discussed earlier in this book. As a result, it is useful to design the complete drive system as an integrated package and not to design the individual components (VRM, inverter, controller, etc.) separately. The inverter configurations of Fig. 10-16 are representative of a number of possible inverter configurations which can be used in VRM drive systems. The choice of an inverter for a specific application must be made based on engineering and economic considerations as part of an integrated VRM drive system design.

10-5 NONLINEAR ANALYSIS

Like most electric machines, VRMs employ magnetic materials both to direct and shape the magnetic fields in the machine and to increase the magnetic flux density that can be achieved from a given amount of current. To obtain the maximum benefit from the magnetic material, the magnetic flux density in practical VRMs is high enough so that the magnetic material is in saturation under normal operating conditions.

The actual operating flux density is determined by trading off such quantities as cost, efficiency, and torque/mass ratio. As with the synchronous, induction, and dc machines discussed earlier, these trade-offs continue to exist in the design of VRMs. However, because the VRM and its

inverter are quite closely interrelated, VRMs involve additional trade-offs that in turn affect the choice of operating flux density.

Figure 10-2 shows typical inductance versus angle curves for the VRMs of Fig. 10-1. Such curves are characteristic of all VRMs. It must be recognized that use of the concept of inductance assumes that the magnetic circuit in the machine is linear so that the flux density (and hence the winding flux linkage) is proportional to the winding current. This linear analysis is based on the assumption that the magnetic material in the motor has constant magnetic permeability. This assumption was used for all the analyses earlier in this chapter.

An alternate representation of the flux linkage versus current characteristic of a VRM is shown in Fig. 10-17. This representation consists of a series of plots of the flux linkage versus current at various rotor angles. In this figure, the curves correspond to a machine with a two-pole rotor such

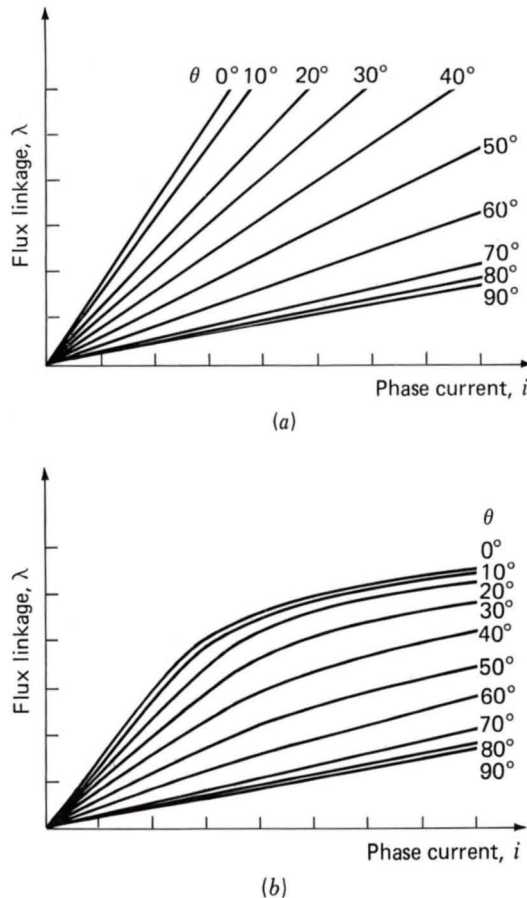


Fig. 10-17. Plots of λ versus i for VRM with (a) linear and (b) nonlinear magnetics.

as in Fig. 10-1, and hence a plot of curves from 0° to 90° is sufficient to completely characterize the machine.

Figure 10-17a shows the set of λ - i characteristics which would be measured in a machine with linear magnetics, i.e., constant magnetic permeability and no magnetic saturation. For each rotor angle, the curve is a straight line whose slope corresponds to the inductance $L(\theta)$ at that angular position. In fact, a plot of $L(\theta)$ versus θ such as in Fig. 10-2 is an equivalent representation to that of Fig. 10-17a.

In practice, VRMs do operate with their magnetic material in saturation, and their λ - i characteristics take on the form of Fig. 10-17b. Notice that for low current levels, the curves are linear, corresponding to the assumption of linear magnetics of Fig. 10-17a. However, for higher current levels, saturation begins to occur and the curves bend over steeply, with the result that there is significantly less flux linkage for a given current level. Finally, note that saturation effects are maximum at $\theta = 0^\circ$ (the rotor and stator poles are aligned) and minimal for higher angles as the rotor approaches the nonaligned position.

Saturation has two important effects on VRM performance. On the one hand, saturation limits flux densities for a given current level and thus tends to limit the amount of torque available from the VRM. On the other hand, it can be shown that saturation tends to lower the required inverter power rating for a given VRM output power and thus tends to make the inverter smaller and less costly. A well-designed VRM system will be based on a trade-off between the two effects.[†]

These effects of saturation can be investigated by considering the two machines of Fig. 10-17a and b operating at the same rotational speed and under the same operating condition. For the sake of simplicity, we assume a somewhat idealized condition in which the phase-1 current is instantaneously switched on to a value I_0 at $\theta = -90^\circ$ (the unaligned position for phase 1) and is instantaneously switched off at $\theta = 0^\circ$ (the aligned position). This operation is similar to that discussed in Example 10-1 in that we will neglect the complicating effects of the current buildup and decay transients which are illustrated in Example 10-3.

Because of rotor symmetry, the flux linkages for negative rotor angles are identical to those for positive angles. Thus, the flux linkage-current trajectories for one current cycle can be determined from Fig. 10-17a and b and are shown for the two machines in Fig. 10-18a and b.

As each trajectory is traversed, the power input to the winding is given by its volt-ampere product (see Chap. 3)

$$p_{in} = i v = i \frac{d\lambda}{dt} \quad (10-18)$$

[†]For a discussion of saturation effects in VRM drive systems, see T. J. E. Miller, "Converter Volt-Ampere Requirements of the Switched Reluctance Motor," *IEEE Trans. Ind. Appl.*, **IA-21**:1136-1144 (1985).

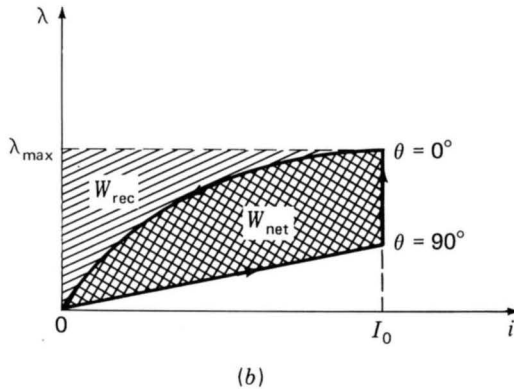
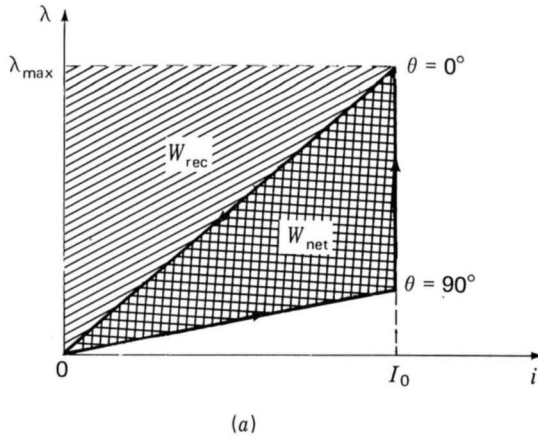


Fig. 10-18. (a) Flux-linkage–current trajectory for the (a) linear and (b) nonlinear machines of Fig. 10-17.

The net electric energy input to the machine (the energy that is converted to mechanical work) in a cycle can be determined by integrating Eq. 10-18 around the trajectory

$$\text{Net work} = \oint p_{\text{in}} dt = \oint i d\lambda \quad (10-19)$$

This can be seen graphically as the area enclosed by the trajectory, labeled W_{net} in Fig. 10-18a and b. Note that the saturated machine converts less useful work per cycle than the unsaturated machine. As a result, to get a machine of the same power output, the saturated machine will have to be larger than a corresponding (hypothetical) unsaturated machine. This analysis demonstrates the effects of saturation in lowering torque and power output.

The peak energy input to the winding from the inverter can also be calculated. It is equal to the integral of the input power from the start of the trajectory to the point (I_0, λ_{\max}) :

$$\text{Peak energy} = \int_0^{\lambda_{\max}} i d\lambda \quad (10-20)$$

This is the total area under the λ - i curve, shown in Fig. 10-18a and b as the sum of the areas labeled W_{rec} and W_{net} .

Since we have seen that the energy represented by the area W_{net} corresponds to useful output energy, it is clear that the energy represented by the area W_{rec} corresponds to energy input that is required to make the VRM operate (i.e., it goes into creating the magnetic fields in the VRM) but must be recycled back into the inverter at the end of the trajectory.

The inverter rating is determined by the average power per phase processed by the inverter as the motor operates, equal to the peak energy input to the VRM divided by the time T between cycles. Similarly, the average output power per phase of the VRM is given by the net energy input per cycle divided by T . Thus the ratio of the inverter rating to power output is

$$\frac{\text{Inverter power rating}}{\text{Net output power}} = \frac{\text{area}(W_{\text{rec}} + W_{\text{net}})}{\text{area } W_{\text{net}}} \quad (10-21)$$

In general, the inverter rating determines its cost and size. Thus, for a given power output from the VRM, a smaller ratio of inverter power rating to output power means that the inverter will be both smaller and cheaper. Comparison of Fig. 10-18a and b shows that this ratio is smaller in the machine which saturates; the effect of saturation is to lower the amount of energy which must be recycled each cycle and hence the power rating of the inverter required to supply the VRM.

It should be emphasized again that, in the design of the VRM system, a trade-off must be made. On the one hand, saturation tends to increase the size of the VRM for a given power output. On the other hand, on comparing two VRM systems with the same power output, the system with the higher level of saturation will require an inverter with a lower power rating. Thus the ultimate design will be determined by a trade-off between VRM size, cost, and efficiency and inverter size, cost, and efficiency.

In Example 10-4 and the preceding analysis, we considered the calculation of the excitation requirements for achieving a specific current level in a constant-value inductor. We then recognized that in a VRM, where rotor position and hence inductances are constantly changing, these calculations are significantly complicated. Clearly, saturation effects further complicate these calculations.

The objective of this section has been to show the effects of saturation on the design performance of VRM systems. Because the VRM and its power inverter and controller system are both strongly affected by saturation effects, consideration of these effects becomes much more critical in the design of VRM drive systems than in conventional systems based on induction, synchronous, or dc motors. This typically requires the use of computer-based analytical techniques as the systems are designed in order to achieve competitive performance.

10-6 SUMMARY

Variable-reluctance machines are perhaps the simplest of electrical machines. They consist of a stator with excitation windings and a magnetic rotor with saliency. Torque is produced by the tendency of the salient-pole rotor to align with excited magnetic poles on the stator.

VRMs are synchronous machines in that they produce net torque only when the rotor motion is in some sense synchronous with the applied stator mmf. This synchronous relationship may be complex, with the rotor speed being some specific fraction of the applied electrical frequency as determined not only by the number of stator and rotor poles but also by the number of stator and rotor teeth on these poles. In fact, in some cases, the rotor will be found to rotate in the direction opposite to the rotation direction of the applied stator mmf.

Successful operation of a VRM depends on exciting the stator-phase windings in a specific fashion correlated to the instantaneous position of the rotor. Thus, rotor position must be measured, and a controller must be employed to determine the appropriate excitation waveforms and to control the output of the inverter. Typically chopping is required to obtain these waveforms. The net result is that although the VRM is itself a simple device, somewhat complex electronics is required to make a complete drive system.

The significance of VRMs in engineering applications stems from their low cost, reliability, and controllability. Because their torque depends only on the square of the applied stator currents and not on their direction, these machines can be operated from unidirectional drive systems, reducing the cost of the power electronics. However, it is only recently, with the advent of low-cost, flexible power electronic circuitry and microprocessor-based control systems that VRMs have begun to see widespread application in systems ranging from traction drives to high-torque, precision position control systems for robotics applications.

Practical experience with VRMs has shown that they have the potential for high reliability. This is due in part to the simplicity of their construction and to the fact that there are no windings on their rotors. In addition, VRM drives can be operated successfully (at a somewhat reduced

rating) following the failure of one or more phases, either in the machine or in the inverter. VRMs typically have a large number of rotor phases (four or more), and significant output can be achieved even if some of these phases are out of service. Because there is no rotor excitation, there will be no voltage generated in a phase winding which fails open-circuited or current generated in a phase winding which fails short-circuited, and thus the machine can continue to be operated without risk of further damage or additional losses and heating.

Because VRMs can be readily manufactured with a large number of rotor and stator teeth (resulting in large inductance changes for small changes in rotor angle), they can be constructed to produce very large torques per unit volume. There is, however, a trade-off between torque and velocity, and such machines will have a low rotational velocity (consistent with the fact that only so much power can be produced by a given machine frame size). On the opposite extreme, the simple configuration of a VRM rotor and the fact that it contains no windings suggest that it is possible to build extremely rugged VRM rotors. These rotors can withstand high speeds, and motors which operate in excess of 200,000 r/min have been built.

Finally, we have seen that saturation plays a large role in VRM performance. As recent advances in power electronic and microelectronic circuitry have brought VRM drive systems into the realm of practicality, so have recent advances in computer-based analytical techniques for magnetic field analysis. Use of these techniques now makes it practical to perform optimized designs of VRM drive systems which are competitive with alternative technologies in many applications.

PROBLEMS

10-1. Repeat Example 10-1 for a machine identical to that considered in the example except that the stator pole-face angle is $\beta = 50^\circ$.

10-2. Consider the 4/2 VRMs of Fig. 10-1. In the paragraph preceding Eq. 10-1, the text states that "symmetry arguments can be used to show that if the reluctance of the machine iron is negligible, then there is negligible mutual flux linkage between the two phase windings and hence that their phase-phase mutual inductance can be considered to be zero." Use magnetic circuit techniques to show that this statement is true.

10-3. Use magnetic circuit techniques to show that the phase-phase mutual inductance in the 6/4 VRM of Fig. 10-5 is zero under the assumption of infinite rotor and stator-iron permeability.

10-4. A 6/4 VRM of the form of Fig. 10-5 has the following properties:

Stator pole angle $\beta = 30^\circ$

Rotor pole angle $\alpha = 30^\circ$

Air-gap length $g = 3 \times 10^{-2}$ cm

Rotor outer radius $R = 3.2$ cm

Active length $D = 8$ cm

This machine is connected as a three-phase motor with opposite poles connected in series to form each phase winding. There are 40 turns per pole (80 turns per phase). The rotor and stator iron can be considered to be of infinite permeability, and hence mutual inductance effects can be neglected.

- (a) Defining the zero of rotor angle θ at the position when the phase-1 inductance is maximum, plot and label the inductance of phase 1 as a function of rotor position.
- (b) On the plot of part (a), plot the inductances of phases 2 and 3.
- (c) Find the phase-1 current I_0 which results in a magnetic flux density of 1.0 T in the air gap under the phase-1 pole face when the rotor is in a position of maximum phase-1 inductance.
- (d) Assuming that the phase-1 current is held constant at the value found in part (c) and that there is no current in phases 2 and 3, plot the torque as a function of rotor position.

The motor is to be driven from a three-phase current-source inverter which can be switched on or off to supply either zero current or a constant current of magnitude I_0 to each phase.

- (e) Under the idealized assumption that the currents can be instantaneously switched, determine the sequence of phase currents (as a function of rotor position) that will result in a constant positive motor torque, independent of rotor position.
- (f) If the frequency of the stator excitation is such that a time $T_0 = 30$ ms is required to sequence through all three phases under the excitation conditions of part (e), find the rotor angular velocity and its direction of rotation.

10-5. In Sec. 10-2, when discussing Fig. 10-5, the text states: "In addition to the fact that there are not positions of simultaneous alignment for the 6/4 VRM, it can be seen that there also are no rotor positions at which only a torque of a single sign (either positive or negative) can be produced." Show that this statement is true.

10-6. Consider a three-phase 6/8 VRM. The stator phases are excited sequentially with a total time of 25 ms required to excite the three phases. Find the angular velocity of the rotor. Express your answers both in radians per second and revolutions per minute.

10-7. The phase windings of the castleated machine of Fig. 10-8 are to be excited by turning the phases on and off individually (i.e., only one phase can be on at any given time).

- (a) Describe the sequence of phase excitations required to move the rotor to the left (counterclockwise) by an angle of approximately 21.4° .
- (b) The stator phases are to be excited as a regular sequence of pulses. Calculate the phase order and the time between pulses required to produce a steady-state rotor rotation of 100 r/min in the clockwise direction.

10-8. Replace the 28-tooth rotor of Prob. 10-7 with a rotor with 26 teeth.

- (a) Phase 1 is excited, and the rotor is allowed to come to rest. If the excitation on phase 1 is removed and excitation is applied to phase 2, calculate the resultant direction and magnitude (in degrees) of rotor rotation.
- (b) The stator phases are to be excited as a regular sequence of pulses. Calculate the phase order and the time between pulses required to produce a steady-state rotor rotation of 100 r/min in the clockwise direction.

10-9. Repeat Example 10-3 for a rotor speed of 3500 r/min.

10-10. The three-phase 6/4 VRM of Prob. 10-4 has a winding resistance of $0.1\ \Omega$ /phase and a leakage inductance of 4 mH in each phase.

- (a) Plot the phase-1 inductance as a function of the rotor angle θ . Define the zero of the rotor angle as occurring at the position of maximum phase-1 inductance.

Assume that the rotor is rotating at a constant angular velocity of 2000 r/min.

- (b) A voltage of 75 V is applied to phase 1 as the rotor reaches the position $\theta = -30^\circ$ and is maintained constant until $\theta = 0^\circ$. Calculate and plot the phase-1 current as a function of time during this period.
- (c) When the rotor reaches $\theta = 0^\circ$, the applied voltage is reversed so that a voltage of $-75\ \text{V}$ is applied to the winding. This voltage is maintained until the winding current reaches zero, at which point the winding is open-circuited. Calculate and plot the current decay during the time until the rotor reaches angle $\theta = 30^\circ$.
- (d) Calculate and plot the torque during the periods investigated in parts (b) and (c).

10-11. Assume that the VRM of Examples 10-1 and 10-3 is modified by replacing its rotor by a rotor with 75° pole-face angles as shown in Fig. 10-12a. All other dimensions and parameters of the VRM are unchanged.

- (a) Calculate and plot $L(\theta)$ for this machine.
- (b) Repeat Example 10-3 except that the constant voltage of 100 V is first applied at $\theta = -67.5^\circ$ when $dL(\theta)/d\theta$ becomes positive and the

constant voltage of -100 V is then applied at $\theta = -7.5^\circ$ [i.e., when $dL(\theta)/d\theta$ becomes zero] and is maintained until the winding current reaches zero.

(c) Plot the corresponding torque.

10-12. Consider the system of Fig. 10-13a with the following parameter values:

$$V_0 = 75 \text{ V} \quad R_s = 1 \, \Omega \quad R = 2.5 \, \Omega \quad L = 325 \text{ mH}$$

The switch is to be alternately turned on and off for times T_{on} and T_{off} , respectively. Calculate these switching times such that the inductor current varies between a minimum current of 8 A and a maximum current of 10.5 A.

10-13. The system of Prob. 10-12 is to be operated such that the switch is alternately turned on and off for equal times of 15 ms. Calculate the maximum and minimum currents when this system is operating in the steady state.



Fractional- and Subfractional-Motors

Fractional- and subfractional-horsepower motors are found in many types of equipment in the home, office, and industry. They differ from integral-horsepower motors in the wide variety of designs and characteristics available, prompted by the economics and special requirements of their applications. Subfractional-horsepower motors, especially, come in a wide variety of designs and configurations. This chapter should not be considered in any way an exhaustive study of these types of electric machines, but rather should be considered an introduction to this rapidly growing and expanding area of electric machinery.

Many fractional-horsepower ac machines are designed for and used in single-phase applications. In the home, single-phase induction motors are found in refrigerators, air conditioners, fans, washers, and dryers. Although they are simple in construction, their single-phase operation makes them more difficult to analyze than larger three-phase motors. In this

chapter, we describe the various types of motors qualitatively in terms of rotating-field theory, and we develop a method of analysis appropriate for two-phase motors from which the starting and running characteristics of single-phase induction motors can be calculated.[†]

The series ac motor, also known as the universal motor, is widely used in portable tools, vacuum cleaners, and kitchen appliances where its high speed results in high horsepower per unit motor size. These motors are frequently used with solid-state circuitry for speed control.

The proliferation of personal computers, auxiliary devices such as printers, and a wide range of personal entertainment equipment such as VCRs, video cameras, and compact disk players have resulted in the widespread application of stepping motors. These small ac motors, closely related to the variable-reluctance motor discussed in Chap. 10, in combination with recent advances in digital control and processing electronics provide the flexibility and control required for these and many other applications to come.

11-1 SINGLE-PHASE INDUCTION MOTORS: QUALITATIVE EXAMINATION

Structurally, the most common types of single-phase induction motors resemble polyphase squirrel-cage motors except for the arrangement of the stator windings. An induction motor with a cage rotor and a single-phase stator winding is represented schematically in Fig. 11-1. Instead of being a concentrated coil, the actual stator winding is distributed in slots to produce an approximately sinusoidal space distribution of mmf. Such a motor inherently has no starting torque, but if it is started by auxiliary means, it will continue to run. Before we consider auxiliary starting methods, the basic properties of the elementary motor of Fig. 11-1 are described.

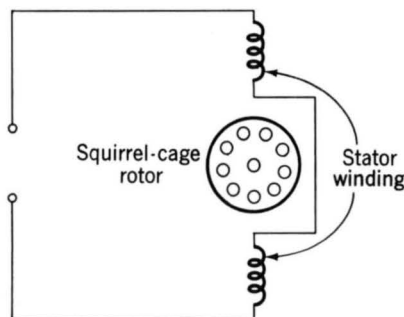


Fig. 11-1. Elementary single-phase induction motor.

[†]For an extensive treatment of fractional-horsepower ac motors, see C. B. Veinott, *Fractional- and Subfractional-Horsepower Electric Motors*, McGraw-Hill, New York, 1970.

For the single-phase stator winding of Fig. 11-1, if the stator current is a cosinusoidal function of time, the mmf wave can be written as a function of space and time as

$$\mathcal{F}_1 = F_{1,\max} \cos \omega t \cos \theta \quad (11-1)$$

which, as shown in Eq. 4-21, can be written as the sum of a positive- and negative-traveling mmf wave of equal magnitude. The positive-traveling wave is given by

$$\mathcal{F}^+ = \frac{1}{2} F_{1,\max} \cos (\theta - \omega t) \quad (11-2)$$

and the negative-traveling wave is given by

$$\mathcal{F}^- = \frac{1}{2} F_{1,\max} \cos (\theta + \omega t) \quad (11-3)$$

Each of these component mmf waves produces induction-motor action, but the corresponding torques are in opposite directions. With the rotor at rest, the forward and backward air-gap flux waves created by the combined mmf's of the stator and rotor currents are equal, the component torques are equal, and no starting torque is produced. If the forward and backward air-gap flux waves remained equal when the rotor is revolving, each of the component fields would produce a torque-speed characteristic similar to that of a polyphase motor with negligible stator leakage impedance, as illustrated by the dashed curves *f* and *b* in Fig. 11-2*a*. The resultant torque-speed characteristic, which is the algebraic sum of the two component curves, shows that if the motor were started by auxiliary means, it would produce torque in whatever direction it was started.

The assumption that the air-gap flux waves remain equal when the rotor is in motion is a rather drastic simplification of the actual state of affairs. First, the effects of stator leakage impedance are ignored. Second, the effects of induced rotor currents are not properly accounted for. Both these effects will ultimately be included in the detailed quantitative theory of Art. 11-3. The following qualitative explanation shows that the performance of a single-phase induction motor is considerably better than would be predicted on the basis of equal forward and backward flux waves.

When the rotor is in motion, the component rotor currents induced by the backward field are greater than at standstill and their power factor is lower. Their mmf, which opposes that of the stator current, results in a reduction of the backward flux wave. Conversely, the magnetic effect of the component currents induced by the forward field is less than at standstill because the rotor currents are less and their power factor is higher. As speed increases, therefore, the forward flux wave increases while the backward flux wave decreases, their sum remaining roughly constant since it must induce the stator counter emf, which is approximately constant if the stator leakage-impedance voltage drop is small. Hence, with the rotor in motion, the torque of the forward field is greater and that of the backward

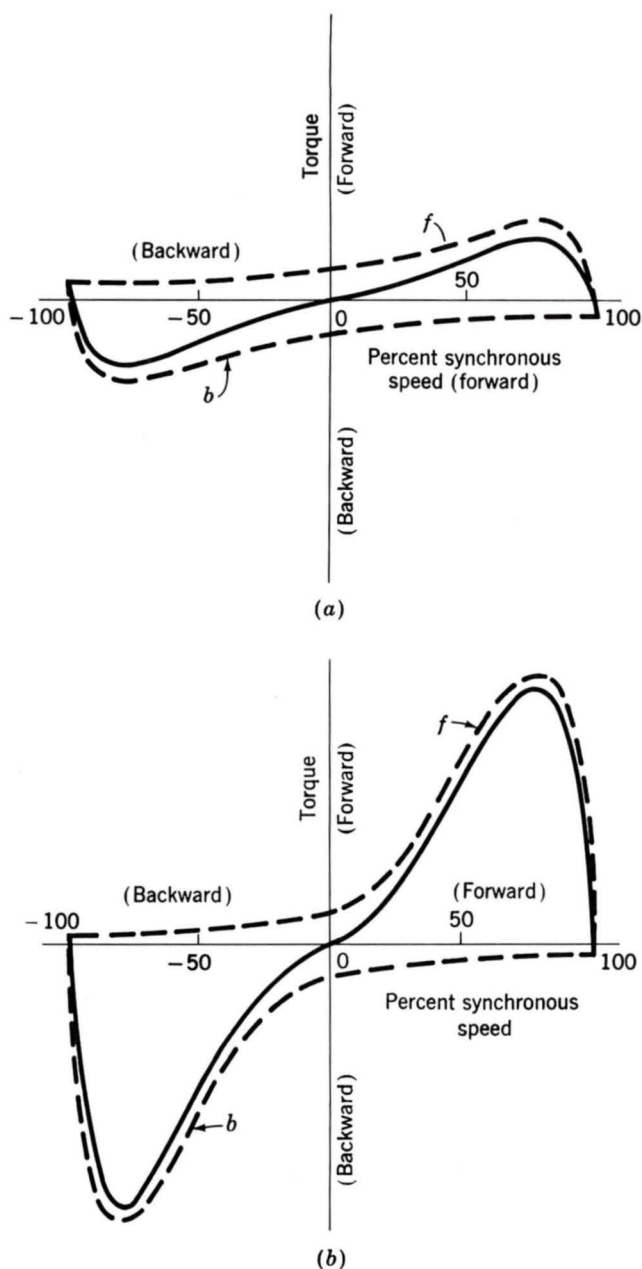


Fig. 11-2. Torque-speed characteristic of a single-phase induction motor (a) on the basis of constant forward and backward flux waves, (b) taking into account changes in the flux waves.

field is less than in Fig. 11-2a, the true situation being about as shown in Fig. 11-2b. In the normal running region at a few percent slip, the forward field is several times greater than the backward field, and the flux wave does not differ greatly from the constant-amplitude revolving field in the

air gap of a balanced polyphase motor. In the normal running region, therefore, the torque-speed characteristic of a single-phase motor is not too greatly inferior to that of a polyphase motor having the same rotor and operating with the same maximum air-gap flux density.

In addition to the torques shown in Fig. 11-2, double-stator-frequency torque pulsations are produced by the interactions of the oppositely rotating flux and mmf waves which glide past each other at twice synchronous speed. These interactions produce no average torque, but they tend to make the motor noisier than a polyphase motor. Such torque pulsations are unavoidable in a single-phase motor because of the pulsations in instantaneous power input inherent in a single-phase circuit. The effects of the pulsating torque can be minimized by using an elastic mounting for the motor. The torque referred to on the torque-speed curves is the time average of the instantaneous torque.

11-2 STARTING AND RUNNING PERFORMANCE OF SINGLE-PHASE INDUCTION AND SYNCHRONOUS MOTORS

Single-phase induction motors are classified in accordance with the methods of starting and are usually referred to by names descriptive of these methods. Selection of the appropriate motor is based on the starting- and running-torque requirements of the load, the duty cycle, and the limitations on starting and running current from the supply line for the motor. The cost of single-phase motors increases with the horsepower and with the performance, such as starting-torque-to-current ratio; hence, the application engineer selects the lowest horsepower and performance motor that meets his or her requirement to minimize the cost. Where a large number of motors are to be used for a specific purpose, a special motor is designed for the application to ensure least cost. In the fractional-horsepower motor business, differences of cost in pennies are important. Starting methods and resulting torque-speed characteristics are considered qualitatively in this article.

a. Split-Phase Motors

Split-phase motors have two stator windings, a main winding m and an auxiliary winding a , with their axes displaced 90 electrical degrees in space. They are connected as shown in Fig. 11-3a. The auxiliary winding has a higher resistance-to-reactance ratio than the main winding, so that the two currents are out of phase, as indicated in the phasor diagram of Fig. 11-3b, which is representative of conditions at starting. Since the auxiliary-winding current \hat{I}_a leads the main-winding current \hat{I}_m , the stator field first reaches a maximum along the axis of the auxiliary winding and then somewhat later in time reaches a maximum along the axis of the main winding. The winding currents are equivalent to unbalanced two-

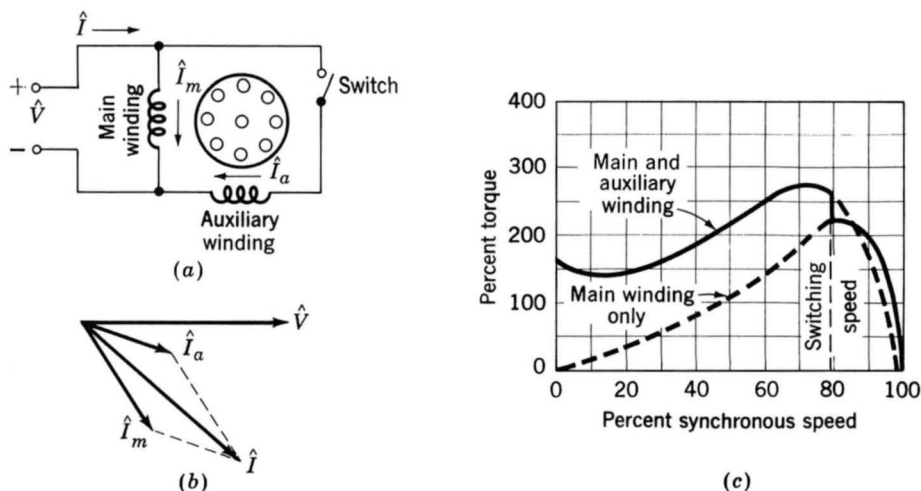


Fig. 11-3. Split-phase motor: (a) connections, (b) phasor diagram at starting, and (c) typical torque-speed characteristic.

phase currents, and the motor is equivalent to an unbalanced two-phase motor. The result is a rotating stator field which causes the motor to start. After the motor starts, the auxiliary winding is disconnected, usually by means of a centrifugal switch that operates at about 75 percent of synchronous speed. The simple way to obtain the high resistance-to-reactance ratio for the auxiliary winding is to wind it with smaller wire than the main winding, a permissible procedure because this winding is in circuit only during starting. Its reactance can be reduced somewhat by placing it in the tops of the slots. A typical torque-speed characteristic is shown in Fig. 11-3c.

Split-phase motors have moderate starting torque with low starting current. Typical applications include fans, blowers, centrifugal pumps, and office equipment. Typical ratings are $\frac{1}{20}$ to $\frac{1}{2}$ hp; in this range they are the lowest-cost motors available.

b. Capacitor-Type Motors

Capacitors can be used to improve the starting performance, running performance, or both, of the motor, depending on the size and connection of the capacitor.

The capacitor-start motor is also a split-phase motor, but the time-phase displacement between the two currents is obtained by means of a capacitor in series with the auxiliary winding, as shown in Fig. 11-4a. Again the auxiliary winding is disconnected after the motor has started, and consequently the auxiliary winding and capacitor can be designed at minimum cost for intermittent service. By using a starting capacitor of appropriate value, the auxiliary-winding current \hat{I}_a at standstill could be made to lead the main-winding current \hat{I}_m by 90 electrical degrees, as it would in a balanced

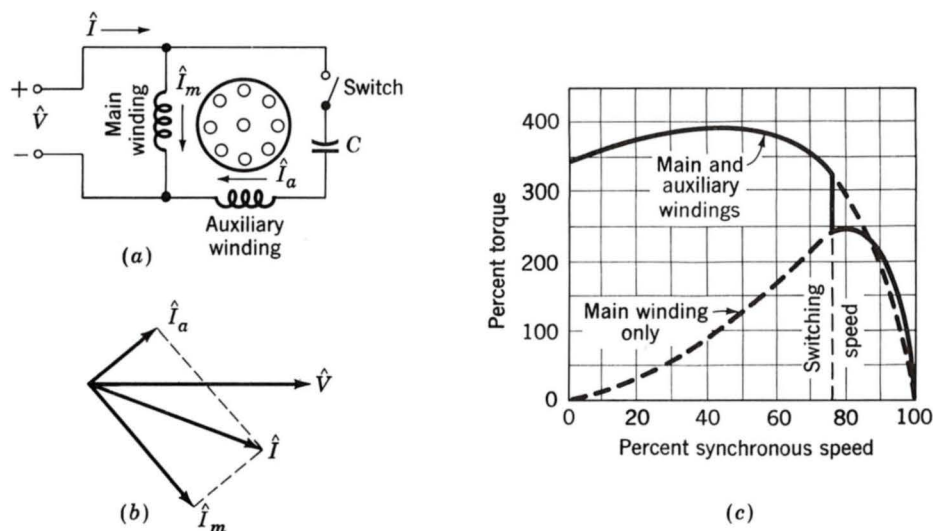


Fig. 11-4. Capacitor-start motor: (a) connections, (b) phasor diagram at starting, and (c) typical torque-speed characteristic.

two-phase motor (see Fig. 11-4b). Actually, the best compromise between the factors of starting torque, starting current, and costs results with a phase angle somewhat less than 90° . A typical torque-speed characteristic is shown in Fig. 11-4c, high starting torque being an outstanding feature. These motors are used for compressors, pumps, refrigeration and air-conditioning equipment, and other hard-to-start loads. A cutaway view of a capacitor-start motor is shown in Fig. 11-5.

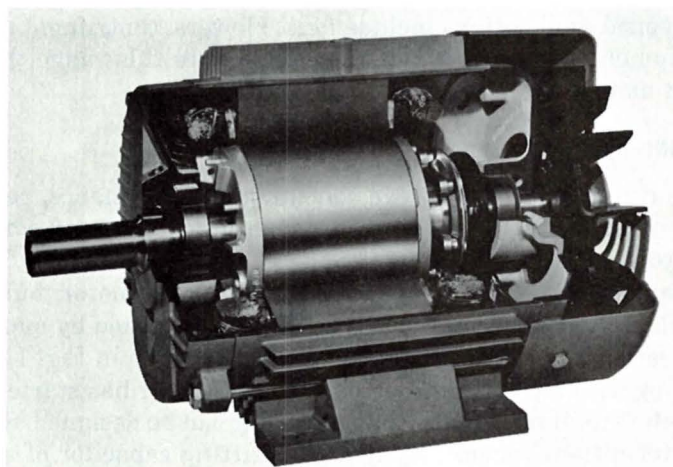


Fig. 11-5. Cutaway view of a capacitor-start induction motor. The starting switch is at the right of the rotor. The motor is of dripproof construction. (General Electric Company.)

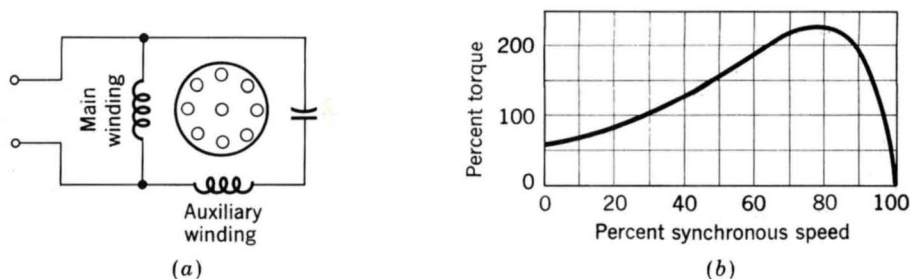


Fig. 11-6. Permanent-split-capacitor motor and typical torque-speed characteristic.

In the permanent-split-capacitor motor, the capacitor and auxiliary winding are not cut out after starting; the construction can be simplified by omission of the switch, and the power factor, efficiency, and torque pulsations improved. For example, the capacitor and auxiliary winding could be designed for perfect two-phase operation at any one desired load. The backward field would then be eliminated, with resulting improvement in efficiency. The double-stator-frequency torque pulsations also would be eliminated, the capacitor serving as an energy storage reservoir for smoothing out the pulsations in power input from the single-phase line. The result is a quiet motor. Starting torque must be sacrificed because the capacitance is necessarily a compromise between the best starting and running values. The resulting torque-speed characteristic and a schematic diagram are given in Fig. 11-6.

If two capacitors are used, one for starting and one for running, theoretically optimum starting and running performance can both be obtained. One way of accomplishing this result is shown in Fig. 11-7a. The small value of capacitance required for optimum running conditions is permanently connected in series with the auxiliary winding, and the much larger value required for starting is obtained by a capacitor connected in parallel

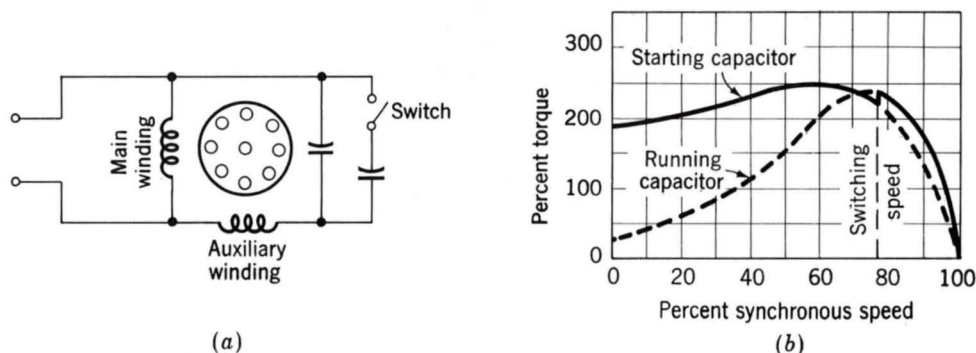


Fig. 11-7. Capacitor-start, capacitor-run motor and typical torque-speed characteristic.

with the running capacitor. The starting capacitor is disconnected after the motor starts.

The capacitor for a capacitor-start motor has a typical value of $300\ \mu\text{F}$ for a $\frac{1}{2}$ -hp motor. Since it must carry current for just the starting time, the capacitor is a special compact ac electrolytic type made for motor-starting duty. The capacitor for the same motor permanently connected has a typical rating of $40\ \mu\text{F}$; since it operates continuously, the capacitor is an ac paper, foil, and oil type. The cost of the motors is related to the performance: the permanent-capacitor motor has the lowest cost, the capacitor-start motor next, and the capacitor-start, capacitor-run motor the highest cost.

EXAMPLE 11-1

A $\frac{1}{3}$ -hp 120-V 60-Hz capacitor-start motor has the following constants for the main and auxiliary windings (at starting):

$$\begin{aligned} Z_m &= 4.5 + j3.7\ \Omega && \text{main winding} \\ Z_a &= 9.5 + j3.5\ \Omega && \text{auxiliary winding} \end{aligned}$$

Find the value of starting capacitance that will place the main and auxiliary winding currents in quadrature at starting.

Solution

The currents \hat{I}_m and \hat{I}_a are shown in Fig. 11-4a and b. The impedance angle of the main winding is

$$\phi_m = \tan^{-1} \frac{3.7}{4.5} = 39.6^\circ$$

The impedance angle of the auxiliary winding must be

$$\phi_a = 39.6^\circ - 90.0^\circ = -50.4^\circ$$

The reactance X_c of the capacitor must satisfy the relationship

$$\tan^{-1} \frac{3.5 - X_c}{9.5} = -50.4^\circ$$

$$\frac{3.5 - X_c}{9.5} = -1.21$$

$$X_c = 1.21(9.5) + 3.5 = 15.0\ \Omega$$

The capacitance C is

$$C = \frac{10^6}{15.0(377)} = 177 \mu\text{F}$$

c. Shaded-Pole Motors

As illustrated schematically in Fig. 11-8a, the shaded-pole motor usually has salient poles with one portion of each pole surrounded by a short-circuited turn of copper called a *shading coil*. Induced currents in the shading coil cause the flux in the shaded portion of the pole to lag the flux in the other portion. The result is like a rotating field moving in the direction from the unshaded to the shaded portion of the pole, and a low starting torque is produced. A typical torque-speed characteristic is shown in Fig. 11-8b. The efficiency is low. Shaded-pole motors are the least expensive type of fractional-horsepower motor and are built up to about $\frac{1}{20}$ hp.

d. Self-Starting Reluctance Motors

Any one of the induction-motor types described above can be made into a self-starting synchronous motor of the reluctance type. Anything which makes the reluctance of the air gap a function of the angular position of the rotor with respect to the stator coil axis will produce reluctance torque when the rotor is revolving at synchronous speed. For example, suppose some of the teeth are removed from a squirrel-cage rotor, leaving the bars and end rings intact, as in an ordinary squirrel-cage induction motor. Figure 11-9a shows a lamination for such a rotor designed for use with a four-pole stator. The stator may be polyphase or any one of the single-phase types described above. The motor will start as an induction motor and at

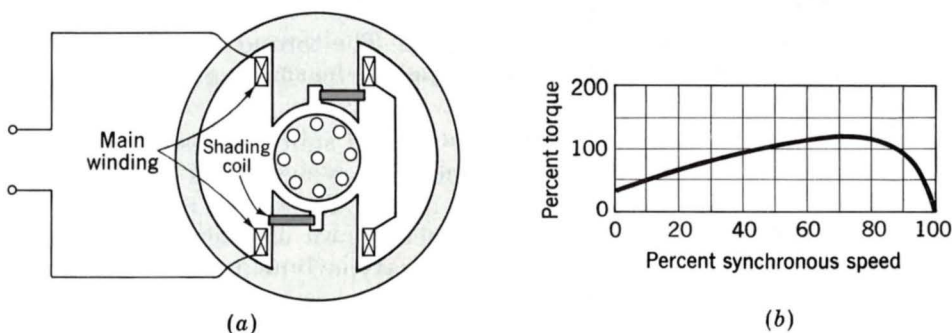


Fig. 11-8. Shaded-pole motor and typical torque-speed characteristic.

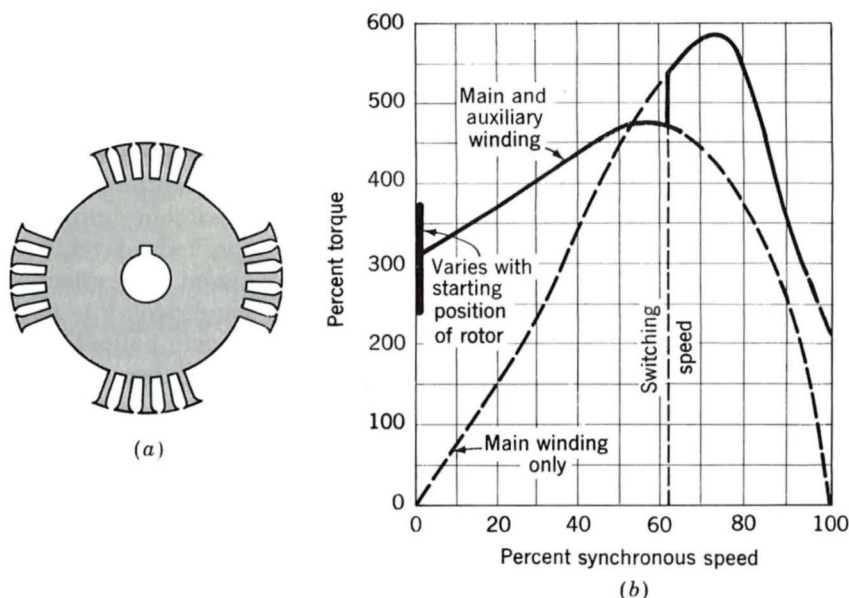


Fig. 11-9. Rotor punching for four-pole reluctance-type synchronous motor and typical torque-speed characteristic.

light loads will speed up to a small value of slip. The reluctance torque arises from the tendency of the rotor to try to align itself in the minimum-reluctance position with respect to the synchronously revolving forward air-gap flux wave, in accordance with the principles explained in Chap. 3. At a small slip, this torque alternates slowly in direction; the rotor is accelerated during a positive half cycle of the torque variation and decelerated during the succeeding negative half cycle. If, however, the moment of inertia of the rotor and its mechanical load are sufficiently small, the rotor will be accelerated from slip speed up to synchronous speed during an accelerating half cycle of the reluctance torque. The rotor will then pull into step and continue to run at synchronous speed. The torque of the backward-revolving field affects the synchronous-motor performance in the same way as an additional shaft load.

A typical torque-speed characteristic for a split-phase-start synchronous motor of the single-phase reluctance type is shown in Fig. 11-9b. Notice the high values of induction-motor torque. The reason for this is that in order to obtain satisfactory synchronous-motor characteristics, it has been found necessary to build reluctance-type synchronous motors on frames which would be suitable for induction motors of 2 or 3 times the synchronous-motor rating. Also notice that the principal effect of the salient-pole rotor on the induction-motor characteristic is at standstill, where considerable "cogging" is evident; i.e., the torque varies considerably with rotor position.

e. Hysteresis Motors

The phenomenon of hysteresis can be used to produce mechanical torque. In its simplest form, the rotor of a hysteresis motor is a smooth cylinder of magnetically hard steel, without windings or teeth. It is placed inside a slotted stator carrying distributed windings designed to produce as nearly as possible a sinusoidal space distribution of flux, since undulations in the flux wave greatly increase the losses. In single-phase motors, the stator windings usually are of the permanent-split-capacitor type, as in Fig. 11-6. The capacitor is chosen so as to result in approximately balanced two-phase conditions within the motor windings. The stator then produces a rotating field, approximately constant in space waveform and revolving at synchronous speed.

Instantaneous magnetic conditions in the air gap and rotor are indicated in Fig. 11-10*a* for a two-pole stator. The axis SS' of the stator-mm*f* wave revolves at synchronous speed. Because of hysteresis, the magnetization of the rotor lags behind the inducing mm*f* wave, and therefore the axis RR' of the rotor flux wave lags behind the axis of the stator-mm*f* wave by the hysteretic lag angle δ (Fig. 11-10*a*). If the rotor is stationary, starting torque is produced proportional to the product of the fundamental components of the stator mm*f* and rotor flux and the sine of the torque angle δ . The rotor then accelerates if the countertorque of the load is less than the developed torque of the motor. As long as the rotor is turning at less than synchronous speed, each particle of the rotor is subjected to a repetitive hysteresis cycle at slip frequency. While the rotor accelerates, the lag angle δ remains constant if the flux is constant, since the angle δ depends merely on the hysteresis loop of the rotor and is independent of the

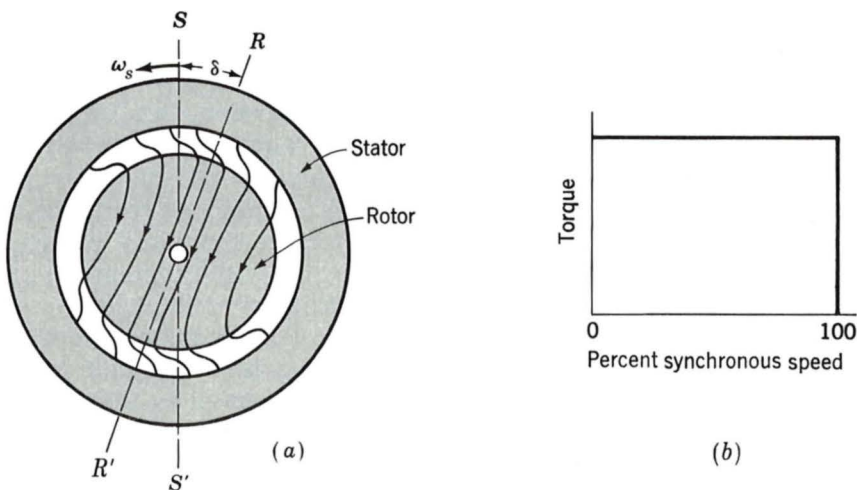


Fig. 11-10. (a) General nature of the magnetic field in the air gap and rotor of a hysteresis motor; (b) idealized torque-speed characteristic.

rate at which the loop is traversed. The motor therefore develops constant torque right up to synchronous speed, as shown in the idealized torque-speed characteristic of Fig. 11-10*b*. This feature is one of the advantages of the hysteresis motor. In contrast with a reluctance motor, which must "snap" its load into synchronism from an induction-motor torque-speed characteristic, a hysteresis motor can synchronize any load which it can accelerate, no matter how great the inertia. After reaching synchronism, the motor continues to run at synchronous speed and adjusts its torque angle so as to develop the torque required by the load.

The hysteresis motor is inherently quiet and produces smooth rotation of its load. Furthermore, the rotor takes on the same number of poles as the stator field. The motor lends itself to multispeed synchronous-speed operation where the stator is wound with several sets of windings and utilizes pole-changing connections. The hysteresis motor can accelerate and synchronize high-inertia loads because its torque is uniform from standstill to synchronous speed.

11-3 REVOLVING-FIELD THEORY OF SINGLE-PHASE INDUCTION MOTORS

In Art. 11-1 the stator-mm*f* wave of a single-phase induction motor is shown to be equivalent to two constant-amplitude mm*f* waves revolving in opposite directions at synchronous speed. Each of these component stator-mm*f* waves induces its own component rotor currents and produces induction-motor action just as in a balanced polyphase motor. This double-revolving-field concept not only is useful for qualitative visualization but also can be developed into a quantitative theory applicable to a wide variety of induction-motor types. A simple and important case is the single-phase induction motor running on only its main winding.

First consider conditions with the rotor stationary and only the main stator winding m excited. The motor then is equivalent to a transformer with its secondary short-circuited. The equivalent circuit is shown in Fig. 11-11*a*, where R_{1m} and X_{1m} are, respectively, the resistance and leakage reactance of the main winding, X_ϕ is the magnetizing reactance, and R_2 and X_2 are the standstill values of the rotor resistance and leakage reactance referred to the main stator winding by use of the appropriate turns ratio. Core loss, which is omitted here, will be accounted for later as if it were a rotational loss. The applied voltage is \hat{V} , and the main-winding current is \hat{I}_m . The voltage \hat{E}_m is the counter em*f* generated in the main winding by the stationary pulsating air-gap flux wave produced by the combined action of the stator and rotor currents.

In accordance with the double-revolving-field concept of Art. 11-1, the stator mm*f* can be resolved into half-amplitude forward and backward rotating fields. At standstill the amplitudes of the forward and backward resultant air-gap flux waves both equal half the amplitude of the pulsating

field. In Fig. 11-11b the portion of the equivalent circuit representing the effects of the air-gap flux is split into two equal portions, representing the effects of the forward and backward fields, respectively.

Now consider conditions after the motor has been brought up to speed by some auxiliary means and is running on only its main winding in the direction of the forward field at a per unit slip s . The rotor currents induced by the forward field are of slip frequency sf , where f is the stator frequency. Just as in any polyphase motor with a symmetric polyphase or cage rotor, these rotor currents produce an mmf wave traveling forward at slip speed with respect to the rotor and therefore at synchronous speed with respect to the stator. The resultant of the forward waves of stator and rotor mmf creates a resultant forward wave of air-gap flux which generates a counter emf \hat{E}_{mf} in the main winding m of the stator. The reflected effect of the rotor as viewed from the stator is like that in a polyphase motor and can be represented by an impedance $0.5R_2/s + j0.5X_2$ in parallel with $j0.5X_\phi$, as in the portion of the equivalent circuit (Fig. 11-11c) labeled f . The factors of 0.5 come from the resolution of the pulsating stator mmf into forward and backward components.

Now consider conditions with respect to the backward field. The rotor is still turning at a slip s with respect to the forward field, and its per unit speed n in the direction of the forward field is

$$n = 1 - s \quad (11-4)$$

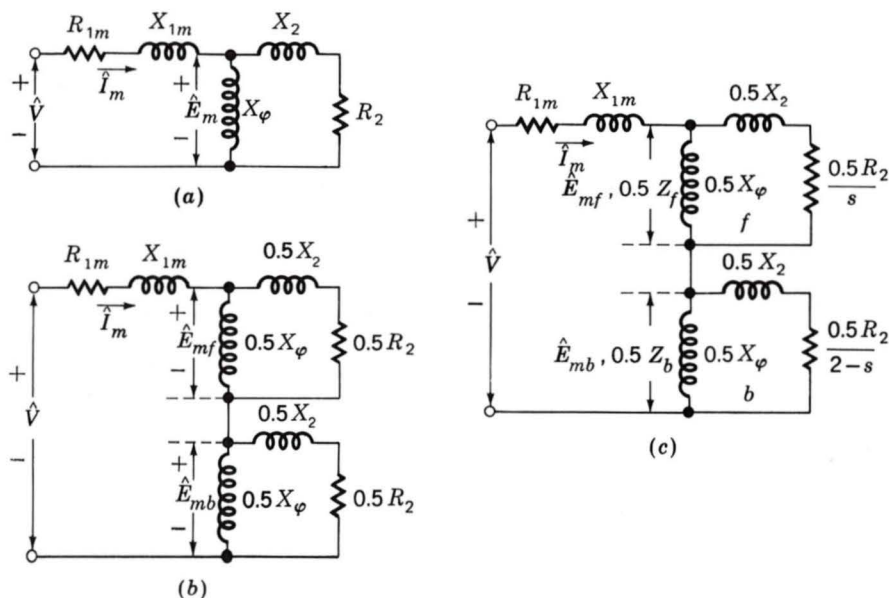


Fig. 11-11. Equivalent circuits for a single-phase induction motor: (a) rotor blocked; (b) rotor blocked, showing effects of forward and backward fields; (c) running conditions.

The relative speed of the rotor with respect to the backward field is $1 + n$, or its slip with respect to the backward field is

$$1 + n = 2 - s \quad (11-5)$$

The backward field then induces rotor currents whose frequency is $(2 - s)f$. For small slips, these rotor currents are of almost twice stator frequency. At a small slip, an oscillogram of rotor current therefore will show a high-frequency component from the backward field superposed on a low-frequency component from the forward field. As viewed from the stator, the rotor-mmF wave of the backward-field rotor currents travels at synchronous speed but in the backward direction. The equivalent circuit representing these internal reactions from the viewpoint of the stator is like that of a polyphase motor whose slip is $2 - s$ and is shown in the portion of the equivalent circuit (Fig. 11-11c) labeled *b*. As with the forward field, the factors of 0.5 come from the resolution of the pulsating stator mmF into forward and backward components. The voltage \hat{E}_{mb} across the parallel combination representing the backward field is the counter emf generated in the main winding *m* of the stator by the resultant backward field.

By use of the equivalent circuit of Fig. 11-11c, the stator current, power input, and power factor can be computed for any assumed value of slip when the applied voltage and the motor impedances are known. To simplify the notation, let

$$Z_f = R_f + jX_f = \left(\frac{R_2}{s} + jX_2 \right) \text{ in parallel with } jX_\phi \quad (11-6)$$

and

$$Z_b = R_b + jX_b = \left(\frac{R_2}{2 - s} + jX_2 \right) \text{ in parallel with } jX_\phi \quad (11-7)$$

The impedances representing the reactions of the forward and backward fields from the viewpoint of the single-phase stator winding *m* are $0.5Z_f$ and $0.5Z_b$, respectively, in Fig. 11-11c.

Examination of the equivalent circuit (Fig. 11-11c) confirms the conclusion, reached by qualitative reasoning in Art. 11-1 (Fig. 11-2b), that the forward air-gap flux wave increases and the backward wave decreases when the rotor is set in motion. When the motor is running at a small slip, the reflected effect of the rotor resistance in the forward field, $0.5R_2/s$, is much larger than its standstill value, while the corresponding effect in the backward field, $0.5R_2/(2 - s)$, is smaller. The forward-field impedance therefore is larger than its standstill value, while that of the backward field is smaller. The forward-field counter emf \hat{E}_{mf} therefore is larger than its

standstill value, while the backward-field counter emf \hat{E}_{mb} is smaller; i.e., the forward air-gap flux wave increases, while the backward flux wave decreases.

Moreover, mechanical output conditions can be computed by application of the torque and power relations developed for polyphase motors in Chap. 7. The torques produced by the forward and backward fields can each be treated in this manner. The interactions of the oppositely rotating flux and mmf waves cause torque pulsations at twice stator frequency but produce no average torque.

As in Eq. 7-22, the internal torque T_f of the forward field in newton-meters equals $1/\omega_s$ times the power P_{gf} in watts delivered by the stator winding to the forward field, where ω_s is the synchronous angular velocity in mechanical radians per second; thus

$$T_f = \frac{1}{\omega_s} P_{gf} \quad (11-8)$$

When the magnetizing impedance is treated as purely inductive, P_{gf} is the power absorbed by the impedance $0.5Z_f$; that is,

$$P_{gf} = I_m^2 0.5R_f \quad (11-9)$$

where R_f is the resistive component of the forward-field impedance defined in Eq. 11-6. Similarly, the internal torque T_b of the backward field is

$$T_b = \frac{1}{\omega_s} P_{gb} \quad (11-10)$$

where P_{gb} is the power delivered by the stator winding to the backward field, or

$$P_{gb} = I_m^2 0.5R_b \quad (11-11)$$

where R_b is the resistive component of the backward-field impedance Z_b defined in Eq. 11-7. The torque of the backward field is in the opposite direction to that of the forward field, and therefore the net internal torque T is

$$T = T_f - T_b = \frac{1}{\omega_s} (P_{gf} - P_{gb}) \quad (11-12)$$

Since the rotor currents produced by the two component air-gap fields are of different frequencies, the total rotor I^2R loss is the numerical sum of the losses caused by each field. In general, as shown by comparison of Eqs. 7-16 and 7-17, the rotor I^2R loss caused by a rotating field equals the

slip of the field times the power absorbed from the stator, whence

$$\text{Forward-field rotor } I^2R = sP_{gf} \quad (11-13)$$

$$\text{Backward-field rotor } I^2R = (2 - s)P_{gb} \quad (11-14)$$

$$\text{Total rotor } I^2R = sP_{gf} + (2 - s)P_{gb} \quad (11-15)$$

Since power is torque times angular velocity and the angular velocity of the rotor is $(1 - s)\omega_s$, the internal power P converted to mechanical form, in watts, is

$$P = (1 - s)\omega_s T = (1 - s)(P_{gf} - P_{gb}) \quad (11-16)$$

As in the polyphase motor, the internal torque T and internal power P are not the output values because rotational losses remain to be accounted for. It is obviously correct to subtract friction and windage effects from T or P , and it is usually assumed that core losses can be treated in the same manner. For the small changes in speed encountered in normal operation, the rotational losses are often assumed to be constant.[†]

EXAMPLE 11-2

A $\frac{1}{4}$ -hp 110-V 60-Hz four-pole capacitor-start motor has the following constants in ohms and losses in watts.

$$R_{1m} = 2.02 \quad X_{1m} = 2.79 \quad R_2 = 4.12 \quad X_2 = 2.12 \quad X_\varphi = 66.8$$

$$\text{Core loss} = 24 \text{ W} \quad \text{Friction and windage} = 13 \text{ W}$$

For a slip of 0.05, determine the stator current, power factor, power output, speed, torque, and efficiency when this motor is running as a single-phase motor at rated voltage and frequency with its starting winding open.

Solution

The first step is to determine the values of the forward- and backward-field impedances at the assigned value of slip. The following relations, derived from Eq. 11-6, simplify the computations:

$$R_f = \frac{X_\varphi^2}{X_{22}} \frac{1}{sQ_2 + 1/(sQ_2)} \quad X_f = \frac{X_2 X_\varphi}{X_{22}} + \frac{R_f}{sQ_2}$$

$$\text{where} \quad X_{22} = X_2 + X_\varphi \quad \text{and} \quad Q_2 = \frac{X_{22}}{R_2}$$

[†]For a treatment of the experimental determination of motor constants and losses, see Veinott, op. cit., chap. 18.

Substitution of numerical values gives, for $s = 0.05$,

$$R_f + jX_f = 31.9 + j40.3 \, \Omega$$

Corresponding relations for the backward-field impedance Z_b are obtained by substituting $2 - s$ for s in these equations. When $(2 - s)Q_2$ is greater than 10, as is usually the case, less than 1 percent error results from use of the following approximate forms:

$$R_b = \frac{R_2}{2 - s} \left(\frac{X_\varphi}{X_{22}} \right)^2 \quad X_b = \frac{X_2 X_\varphi}{X_{22}} + \frac{R_b}{(2 - s)Q_2}$$

Substitution of numerical values gives, for $s = 0.05$,

$$R_b + jX_b = 1.98 + j2.12 \, \Omega$$

Addition of the series elements in the equivalent circuit of Fig. 11-11c gives

$$\begin{aligned} R_{1m} + jX_{1m} &= 2.02 + j2.79 \\ 0.5(R_f + jX_f) &= 15.95 + j20.15 \\ 0.5(R_b + jX_b) &= \underline{0.99 + j1.06} \\ \text{Input } Z = \text{sum} &= 18.96 + j24.00 = 30.6 \angle 51.7^\circ \end{aligned}$$

$$\text{Stator current } I_m = \frac{110}{30.6} = 3.59 \, \text{A}$$

$$\text{Power factor} = \cos 51.7^\circ = 0.620$$

$$\text{Power input} = 110(3.59)(0.620) = 244 \, \text{W}$$

The power absorbed by the forward field (Eq. 11-19) is

$$P_{gf} = (3.59)^2(15.95) = 206 \, \text{W}$$

The power absorbed by the backward field (Eq. 11-11) is

$$P_{gb} = (3.59)^2(0.99) = 12.8 \, \text{W}$$

Internal mechanical power (Eq. 11-16) is

$$P = 0.95(206 - 13) = 184$$

$$\text{Rotational loss} = 24 + 13 = \underline{37}$$

$$\text{Power output} = \text{difference} = 147 \, \text{W} = 0.197 \, \text{hp}$$

$$\text{Synchronous speed} = 1800 \, \text{r/min} = 30 \, \text{r/s}$$

$$\omega_s = 2\pi(30) = 188.5 \, \text{rad/s}$$

$$\begin{aligned}
 \text{Rotor speed} &= (1 - s)(\text{synchronous speed}) \\
 &= 0.95(1800) = 1710 \text{ r/min} \\
 &= 0.95(188.5) = 179 \text{ rad/s}
 \end{aligned}$$

$$\text{Torque} = \frac{\text{power}}{\text{angular velocity}} = \frac{147}{179} = 0.821 \text{ N} \cdot \text{m} = 0.605 \text{ lb} \cdot \text{ft}$$

$$\text{Efficiency} = \frac{\text{output}}{\text{input}} = \frac{147}{244} = 0.602$$

As a check on the power bookkeeping, compute the losses:

$$\begin{aligned}
 \text{Stator } I_m^2 R_{1m} &= (3.59)^2(2.02) = 26.0 \\
 \text{Forward-field rotor } I^2 R, \text{ Eq. 11-13} &= 0.05(206) = 10.3 \\
 \text{Backward-field rotor } I^2 R, \text{ Eq. 11-14} &= 1.95(12.8) = 25.0 \\
 \text{Rotational losses} &= \underline{37.0} \\
 &98.3 \text{ W}
 \end{aligned}$$

From input – output, total losses = 97 W, which checks within accuracy of computations.

Examination of the order of magnitude of the numerical values in Example 11-2 suggests approximations which usually can be made. These approximations pertain particularly to the backward-field impedance. Note that the impedance $0.5(R_b + jX_b)$ is only about 5 percent of the total motor impedance for a slip near full load. Consequently, an approximation as large as 20 percent of this impedance would cause only about 1 percent error in the motor current. Although, strictly speaking, the backward-field impedance is a function of slip, very little error usually results from computing its value at any convenient slip in the normal running region—say, 5 percent—and then assuming R_b and X_b to be constants. With a slightly greater approximation, the shunting effect of jX_ϕ on the backward-field impedance can often be neglected, whence

$$Z_b \approx \frac{R_2}{2 - s} + jX_2 \quad (11-17)$$

This equation gives values of the backward-field resistance that are a few percent high, as can be seen by comparison with the exact expression given in Example 11-2. Neglecting s in Eq. 11-17 would tend to give values of the backward-field resistance that would be too low, and therefore such an approximation would tend to counteract the error in Eq. 11-17. Consequently,

for small slips

$$Z_b \approx \frac{R_2}{2} + jX_2 \quad (11-18)$$

In the polyphase motor (Art. 7-5), maximum internal torque and the slip at which it occurs can easily be expressed in terms of the motor constants; the maximum internal torque is independent of rotor resistance. No such simple relations exist for the single-phase motor. The single-phase problem is much more involved because of the presence of the backward field, the effect of which is twofold: (1) it absorbs some of the applied voltage, thus reducing the voltage available for the forward field and decreasing the forward torque developed; and (2) the backward field then absorbs some of the forward-field torque. Both these effects depend on rotor resistance as well as leakage reactance. Consequently, unlike the polyphase motor, the maximum internal torque of a single-phase motor is influenced by rotor resistance; increasing the rotor resistance decreases the maximum torque and increases the slip at which maximum torque occurs.

Principally because of the effects of the backward field, a single-phase induction motor is somewhat inferior to a polyphase motor using the same rotor and the same stator core. The single-phase motor has a lower maximum torque which occurs at a lower slip. For the same torque, the single-phase motor has a higher slip and greater losses, largely because of the backward-field rotor I^2R loss. The voltampere input to the single-phase motor is greater, principally because of the power and reactive voltamperes consumed by the backward field. The stator I^2R loss also is somewhat higher in the single-phase motor, because one phase, rather than several, must carry all the current. Because of the greater losses, the efficiency is lower, and the temperature rise for the same torque is higher. A larger frame size must be used for a single-phase motor than for a polyphase motor of the same power and speed rating. Because of the larger frame size, the maximum torque can be made comparable with that of a physically smaller but equally rated polyphase motor. In spite of the larger frame size and the necessity for auxiliary starting arrangements, general-purpose single-phase motors in the standard fractional-horsepower ratings cost approximately the same as correspondingly rated polyphase motors because of the much greater volume of production of the former.

11-4 UNBALANCED OPERATION OF SYMMETRICAL TWO-PHASE MACHINES; THE SYMMETRICAL-COMPONENT CONCEPT

Unbalanced operation of an induction motor occurs either when the voltages applied to the stator do not constitute a balanced polyphase set or

when the stator or rotor windings are not symmetrical with respect to the phases. The single-phase motor is the extreme case of a motor operating under unbalanced stator-voltage conditions. In some cases, unbalanced voltages are produced in the supply network to a motor, e.g., when a line fuse is blown. In other cases, unbalanced voltages are produced by the starting impedances of single-phase motors, as described in Art. 11-2. The purpose of this article is to develop the symmetrical-component theory of two-phase induction motors from the double-revolving-field concept and to show how the theory can be applied to a variety of problems involving induction motors having two stator windings in space quadrature.

First, consider in review what happens when balanced two-phase voltages are applied to the stator terminals of a two-phase machine having a uniform air gap, a symmetrical polyphase or cage rotor, and two identical stator windings a and m in space quadrature. The stator currents are equal in magnitude and in time quadrature. When the current in winding a has its instantaneous maximum, the current in winding m is zero and the stator-mmf wave is centered on the axis of winding a . Similarly, the stator-mmf wave is centered on the axis of winding m at the instant when the current in winding m has its instantaneous maximum. The stator-mmf wave therefore travels 90 electrical degrees in space in an interval of 90° in time, the direction of its travel depending on the phase sequence of the currents. A more complete analysis in the manner of Art. 4-5 proves that the traveling wave has constant amplitude and constant angular velocity. This fact is, of course, the basis of the whole theory of balanced operation of induction machines.

The behavior of the motor for balanced two-phase applied voltages of either phase sequence can be readily determined. Thus, if the rotor is turning at a per unit speed n in the direction from winding a toward winding m , the terminal impedance per phase is given by the equivalent circuit of Fig. 11-12a when the applied voltage v_a leads the applied voltage v_m by 90°. Throughout the rest of this treatment, this phase sequence is called *positive sequence* and is designated by subscript f since positive-sequence currents result in a forward field. With the rotor still forced to run at the same speed and in the same direction, the terminal impedance per phase is given by the equivalent circuit of Fig. 11-12b when v_a lags v_m by 90°. This phase sequence is called *negative sequence* and is designated by subscript b , since negative-sequence currents produce a backward field.

Suppose now that *two* balanced two-phase voltage sources of *opposite phase sequence* are connected in series and applied simultaneously to the motor, as indicated in Fig. 11-13a, where phasor voltages \hat{V}_{mf} and $j\hat{V}_{mf}$ applied, respectively, to windings m and a form a balanced system of positive sequence, and phasor voltages \hat{V}_{mb} and $-j\hat{V}_{mb}$ form another balanced system but of negative sequence. The resultant voltage \hat{V}_m applied to winding m is, as a phasor,

$$\hat{V}_m = \hat{V}_{mf} + \hat{V}_{mb} \quad (11-19)$$

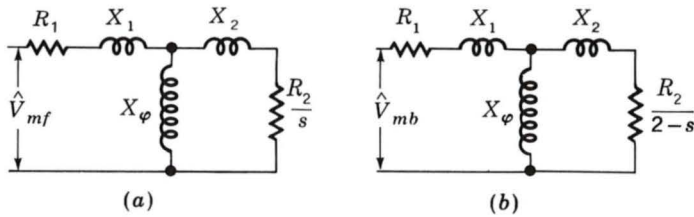


Fig. 11-12. Equivalent circuits for a two-phase motor under unbalanced conditions: (a) forward field and (b) backward field.

and that applied to winding a is

$$\hat{V}_a = j\hat{V}_{mf} - j\hat{V}_{mb} \quad (11-20)$$

If, for example, the forward, or positive-sequence, system is given by the phasors \hat{V}_{mf} and $j\hat{V}_{mf}$ in Fig. 11-13b and the backward, or negative-sequence, system is given by the phasors \hat{V}_{mb} and $-j\hat{V}_{mb}$, then the resultant voltages are given by the phasors \hat{V}_m and \hat{V}_a . An unbalanced two-phase system of applied voltages \hat{V}_m and \hat{V}_a has thus been synthesized by combining two symmetrical systems of opposite phase sequence.

The symmetrical-component systems are, however, much easier to work with than their unbalanced resultant system. Thus, it is easy to compute the component currents produced by each symmetrical-component system of applied voltages because the induction motor operates as a balanced two-phase motor for each component system. By superposition, the actual current in a winding then is the sum of its components. Thus, if \hat{I}_{mf} and \hat{I}_{mb} are, respectively, the positive- and negative-sequence component phasor currents in winding m , then the corresponding positive- and negative-

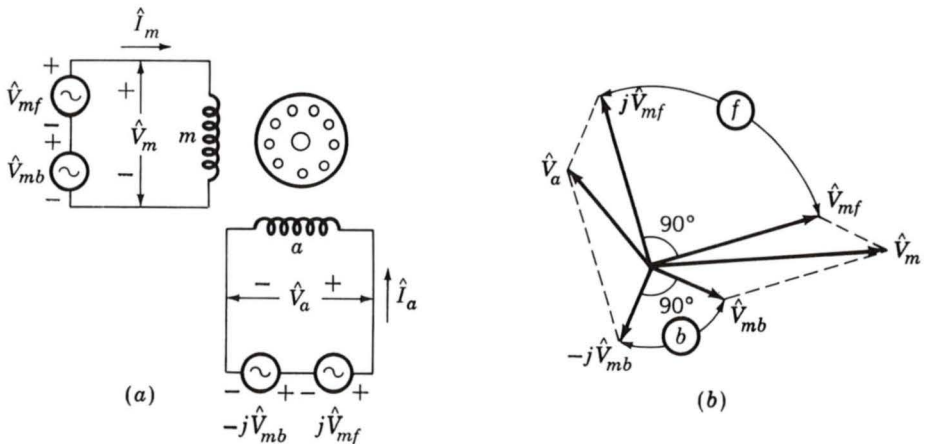


Fig. 11-13. Synthesis of an unbalanced two-phase system from the sum of two balanced systems of opposite phase sequence.

sequence component phasor currents in winding a are, respectively, $j\hat{I}_{mf}$ and $-j\hat{I}_{mb}$, and the actual winding currents \hat{I}_m and \hat{I}_a are

$$\hat{I}_m = \hat{I}_{mf} + \hat{I}_{mb} \quad (11-21)$$

$$\hat{I}_a = j\hat{I}_{mf} - j\hat{I}_{mb} \quad (11-22)$$

The inverse operation of finding the symmetrical components of specified voltages or currents must be performed often. Solution of Eqs. 11-19 and 11-20 for the phasor components \hat{V}_{mf} and \hat{V}_{mb} in terms of known phasor voltages \hat{V}_m and \hat{V}_a gives

$$\hat{V}_{mf} = \frac{1}{2}(\hat{V}_m - j\hat{V}_a) \quad (11-23)$$

$$\hat{V}_{mb} = \frac{1}{2}(\hat{V}_m + j\hat{V}_a) \quad (11-24)$$

These operations are illustrated in the phasor diagram of Fig. 11-14. Obviously, similar relations give the phasor symmetrical components \hat{I}_{mf} and \hat{I}_{mb} of the current in winding m in terms of specified phasor currents \hat{I}_m and \hat{I}_a in the two phases; thus

$$\hat{I}_{mf} = \frac{1}{2}(\hat{I}_m - j\hat{I}_a) \quad (11-25)$$

$$\hat{I}_{mb} = \frac{1}{2}(\hat{I}_m + j\hat{I}_a) \quad (11-26)$$

EXAMPLE 11-3

The equivalent-circuit constants of a 5-hp 220-V 60-Hz four-pole two-phase squirrel-cage induction motor in ohms per phase are

$$R_1 = 0.534 \quad X_1 = 2.45 \quad X_\varphi = 70.1 \quad R_2 = 0.956 \quad X_2 = 2.96$$

This motor is operated from an unbalanced two-phase source whose phase voltages are, respectively, 230 and 210 V, the smaller voltage leading the larger by 80° . For a slip of 0.05, find (a) the positive- and negative-sequence components of the applied voltages, (b) the positive- and negative-sequence

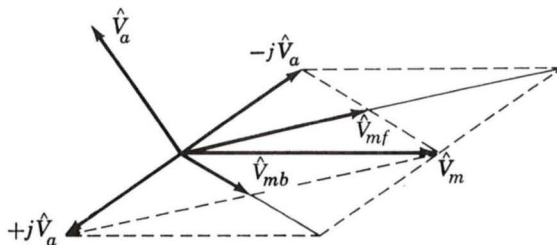


Fig. 11-14. Resolution of unbalanced two-phase voltages into symmetrical components.

components of the stator-phase currents, (c) the effective values of the phase currents, and (d) the internal mechanical power.

Solution

(a) Let \hat{V}_m and \hat{V}_a denote the voltages applied to the two phases, respectively. Then

$$\hat{V}_m = 230 \angle 0^\circ = 230 + j0 \text{ V}$$

$$\hat{V}_a = 210 \angle 80^\circ = 36.4 + j207 \text{ V}$$

From Eqs. 11-23 and 11-24 the forward and backward components of voltages are, respectively,

$$\hat{V}_{mf} = \frac{1}{2}(230 + j0 + 207 - j36.4) = 218.5 - j18.2 = 219.5 \angle -4.8^\circ \text{ V}$$

$$\hat{V}_{mb} = \frac{1}{2}(230 + j0 - 207 + j36.4) = 11.5 + j18.2 = 21.5 \angle 57.7^\circ \text{ V}$$

(b) As in Example 11-2, the forward-field impedance is, for a slip of 0.05,

$$\begin{aligned} Z_f &= 16.46 + j7.15 \ \Omega \\ R_1 + jX_1 &= \frac{0.53 + j2.45 \ \Omega}{16.99 + j9.60} = 19.50 \angle 29.4^\circ \ \Omega \end{aligned}$$

Hence, the forward component of stator current is

$$\hat{I}_{mf} = \frac{219.5 \angle -4.8^\circ}{19.50 \angle 29.4^\circ} = 11.26 \angle -34.2^\circ \text{ A}$$

For the same slip, again as in Example 11-2, the backward-field impedance is

$$\begin{aligned} Z_b &= 0.451 + j2.84 \ \Omega \\ R_1 + jX_1 &= \frac{0.534 + j2.45 \ \Omega}{0.985 + j5.29} = 5.38 \angle 79.5^\circ \ \Omega \end{aligned}$$

Hence, the backward component of stator current is

$$\hat{I}_{mb} = \frac{21.5 \angle 57.7^\circ}{5.38 \angle 79.5^\circ} = 4.0 \angle -21.8^\circ \text{ A}$$

(c) By Eqs. 11-21 and 11-22 the currents in the two phases are, respectively,

$$\begin{aligned} \hat{I}_m &= 13.06 - j7.79 = 15.2 \angle -31^\circ \text{ A} \\ \hat{I}_a &= 4.81 + j5.64 = 7.40 \angle 49.2^\circ \text{ A} \end{aligned}$$

Note that the currents are much more unbalanced than the applied voltages. Even though the motor is not overloaded insofar as shaft load is concerned, the losses are appreciably increased by the current unbalance and the stator winding with the greatest current may overheat.

(d) The power delivered to the forward field by the two stator phases is

$$P_{gf} = 2I_{mf}^2 R_f = 2(126.8)(16.46) = 4175 \text{ W}$$

and the power delivered to the backward field is

$$P_{gb} = 2I_{mb}^2 R_b = 2(16.0)(0.451) = 15 \text{ W}$$

Thus, according to Eq. 11-16, the internal mechanical power developed is

$$P = 0.95(4175 - 15) = 3950 \text{ W}$$

If the core losses, friction and windage, and stray load losses are known, the shaft output can be found by subtracting them from the internal power. The friction and windage losses depend solely on the speed and are the same as they would be for balanced operation at the same speed. The core and stray load losses, however, are somewhat greater than they would be for balanced operation with the same positive-sequence voltage and current. The increase is caused principally by the $(2 - s)$ -frequency core and stray losses in the rotor caused by the backward field.

11-5 SERIES UNIVERSAL MOTORS

A series motor has the convenient ability to run on either alternating or direct current and with similar characteristics, provided both stator and rotor cores are laminated. Such a single-phase series motor therefore is commonly called a *universal motor*. The torque angle is fixed by the brush position and is normally at its optimum value of 90° . If alternating current is supplied to a series motor, the stator and rotor field strengths will vary in exact time phase. Both will reverse at the same instant, and consequently the torque will always be in the same direction, though pulsating in magnitude at twice line frequency. Average torque will be produced, and the performance of the motor will be generally similar to that with direct current.

Small universal motors are used where light weight is important, as in vacuum cleaners, kitchen appliances, and portable tools, and usually operate at high speeds (1500 to 15,000 r/min). Typical characteristics are shown in Fig. 11-15. The ac and dc characteristics differ somewhat for two reasons: (1) With alternating current, reactance-voltage drops in the field

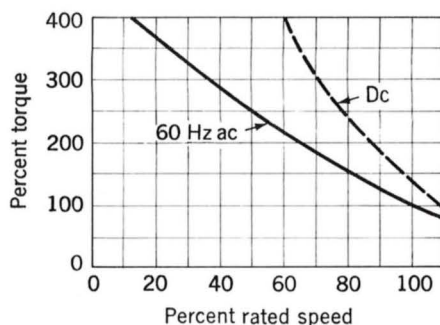


Fig. 11-15. Typical torque-speed characteristics of a series universal motor.

and armature absorb part of the applied voltage, and therefore for a specified current and torque the rotational counter emf generated in the armature is less than with direct current and the speed tends to be lower. (2) With alternating current, the magnetic circuit may be appreciably saturated at the peaks of the current wave, and the rms value of the flux may thus be appreciably less with alternating current than with the same rms value of direct current; the torque therefore tends to be less with alternating than with direct current. The universal motor provides the highest horsepower per dollar in the fractional-horsepower range, at the expense of noise, relatively short life, and high speed.

To obtain control of the speed and torque of the series motor, the ac voltage may be applied in series with a solid-state device which controls the voltage applied to the motor. A thyristor can control alternate half cycles of the voltage so that the motor carries unidirectional current. A bidirectional switch (Triac) can be used to control both half cycles of the applied voltage. The firing angle can be manually adjusted, as in a trigger-controlled electric drill, or can be controlled by a speed control circuit, as in some portable tools and appliances. The combination of a series motor and a solid-state device provides an economical, controllable motor package.

EXAMPLE 11-4

Show that the time-averaged torque of an ac series motor is proportional to the square of the rms current when the magnetic structure is not saturated.

Solution

The instantaneous magnetic flux φ produced by the motor current i_a in the field poles is

$$\varphi = K_f i_a$$

The instantaneous torque is $K_t \varphi i_a$; hence the time-averaged torque T_{av} is

$$T_{av} = \frac{\omega}{\pi} \int_0^{\pi/\omega} K_t K_f i_a^2 dt = K_t K_f I_a^2$$

where I_a is the rms value of the current i_a . This relationship is independent of the waveform of the current i_a .

11-6 STEPPING MOTORS

The stepping motor is a form of ac motor which is designed to rotate a specific number of degrees for each electrical pulse applied to its control unit. Step sizes may range from less than a degree to 15° or larger. The stepping motor is often used in digital control systems, where the motor receives open-loop commands in the form of a train of pulses to turn a shaft or move an object a specific distance.

A significant advantage of the stepping motor is its compatibility with digital electronic systems. These systems are becoming increasingly common in a wide variety of applications and at the same time are becoming both more powerful and less expensive. Typical applications include paper feed motors in typewriters and printers, positioning of print heads, pens in XY plotters, recording heads in computer disk drives, and worktable and tool positioning in numerically controlled machining equipment. In many applications, position information can be obtained simply by keeping count of the pulses sent to the motor, and position sensors and feedback control are not required.

The elementary operation of a four-phase stepping motor with a two-pole rotor is shown in the sequence of Fig. 11-16. The rotor can be either a ferromagnetic element or a permanent magnet. The rotor assumes the angles $\theta = 0, 45, 90^\circ, \dots$ as the windings are excited in the sequence

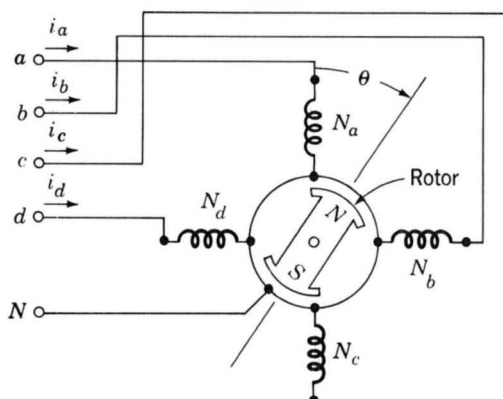


Fig. 11-16. Elementary diagram of a four-phase stepping motor.

$N_a, N_a + N_b, N_b, \dots$. The stepping motor of Fig. 11-16 can also be used for 90° steps by exciting the coils singly. In the latter case, only the permanent-magnet rotor can be used. The torque-angle curves for the two types of rotors are shown in Fig. 11-17; whereas the permanent-magnet rotor produces peak torque when the excitation is shifted 90° , the ferromagnetic rotor produces zero torque and may move in either direction. The permanent-magnet rotor has the additional feature that the rotor position θ is defined by the winding currents with no ambiguity, whereas the ferromagnetic rotor has two possible positions for each pattern of winding currents. Winding patterns can be visualized for steps of 22.5° , 11.25° , and smaller per pulse to the input circuit.

Stepping motors come in a wide variety of designs and configurations. These include variable-reluctance, permanent-magnet, and hybrid configurations. The variable-reluctance motor is discussed in detail in Chap. 10. The angular resolution of the VRM is determined by the number of rotor stator teeth and can be greatly enhanced by techniques such as castellation, as shown in Fig. 10-8.

The VRM configurations discussed in Chap. 10 consist of a single rotor and stator with multiple phases. A stepping motor of this configuration is called a *single-stack variable-reluctance stepping motor*. An alternate form

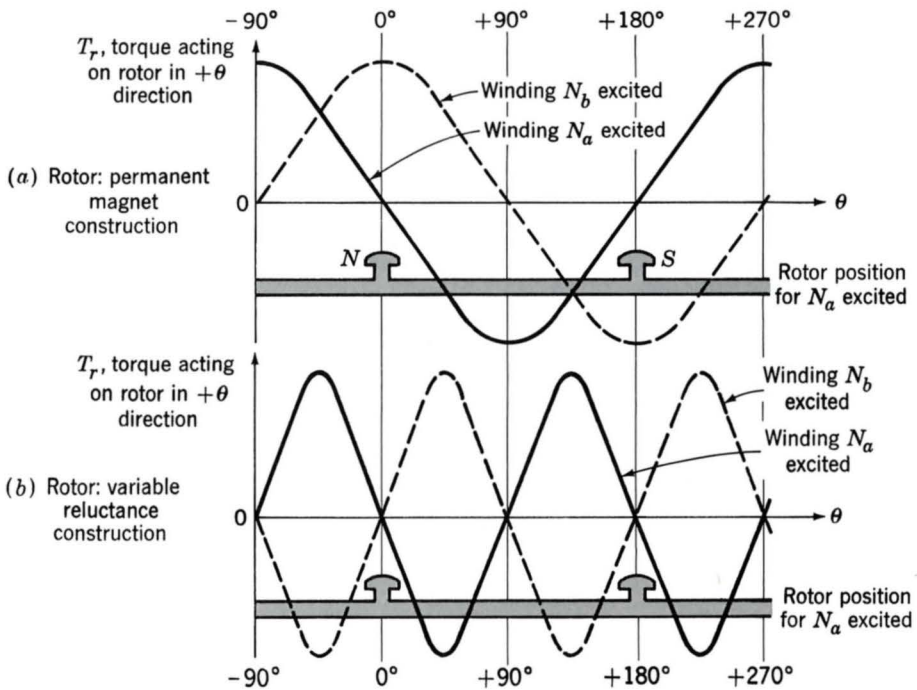


Fig. 11-17. Torque-angle curves for the stepping motor of Fig. 11-16: (a) permanent-magnet rotor and (b) variable-reluctance rotor.

of variable-reluctance stepping motor is known as a *multistack variable-reluctance stepping motor*. In this configuration, the motor can be considered to be made up of a set of axially displaced, single-phase VRMs mounted on a single shaft.

Figure 11-18 shows a multistack variable-reluctance stepping motor. This motor consists of a series of stacks, each axially displaced, of identical geometry and excited by a single phase winding, as shown in Fig. 11-19. This motor has three stacks and three phases, although motors with additional phases and stacks are common. For an n -stack motor, the rotor or stator (but not both) on each stack is displaced by $1/n$ times the pole-pitch angle. In Fig. 11-18, the rotor poles are aligned, but the stators are offset in angular displacement by one-third of the pole pitch. By successively exciting the individual phases, the rotor can be turned in increments of this displacement angle.

Figure 11-20 shows a schematic view of a *permanent-magnet stepping motor*. This motor has a two-pole rotor and a two-phase stator. As an individual phase is excited, the rotor will tend to align with that phase. Unlike the VRM, the rotor alignment in the permanent-magnet stepping motor depends on the direction of the phase currents. Reversing the phase currents

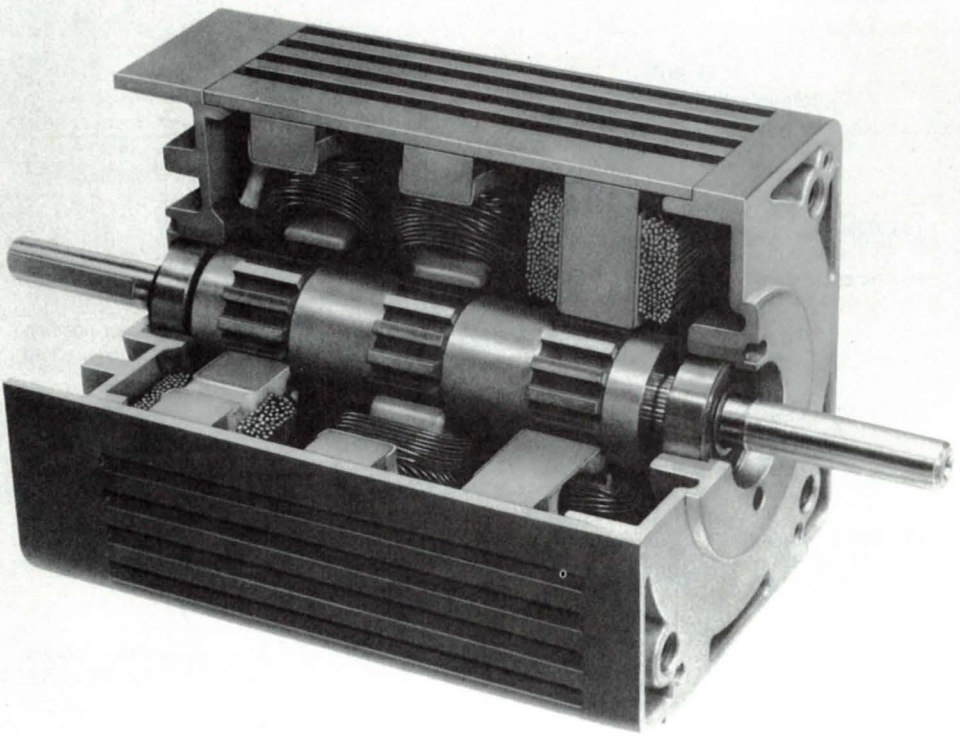


Fig. 11-18. Cutaway view of a three-phase three-stack variable-reluctance stepping motor. (Warner Electric.)

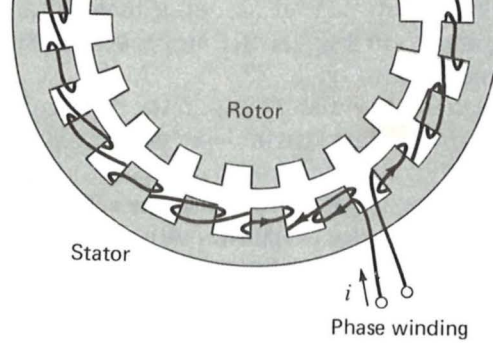


Fig. 11-19. Diagram of one stack and phase of a multiphase, multistack variable-reluctance stepping motor, such as that in Fig. 11-18. For an n -stack motor, the rotor or stator (but not both) on each stack is displaced by $1/n$ times the pole pitch.

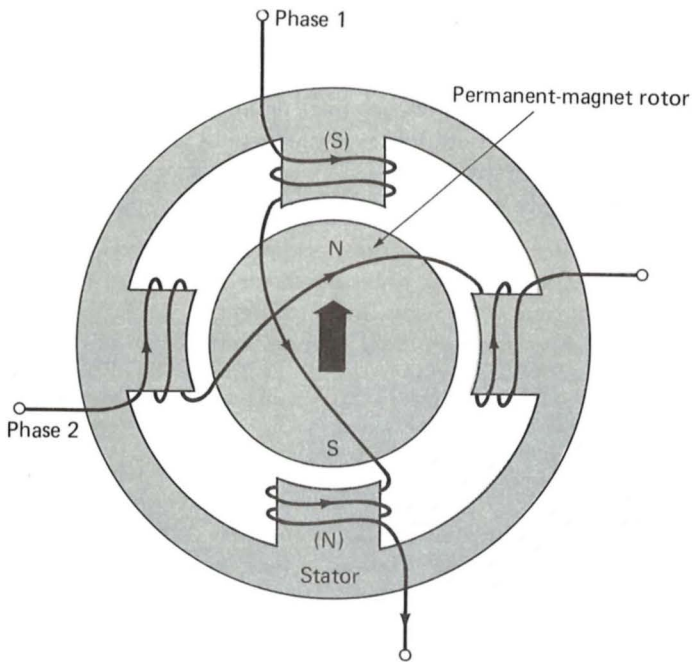


Fig. 11-20. Schematic view of a two-phase permanent-magnet stepping motor. Phase 1 is shown energized in such a fashion as to align the rotor with the north pole vertically up.

reluctance and permanent-magnet stepping motors. A photo of a hybrid stepping motor is shown in Fig. 11-21, and a schematic view of a hybrid stepping motor is shown in Fig. 11-22.

The rotor structure hybrid stepping-motor rotor configuration appears much like that of a multistack variable-reluctance stepping motor. In the rotor of Fig. 11-22a, two identical rotor stacks are displaced axially along the rotor and displaced in angle by one-half the rotor pole pitch. Unlike the multistack variable-reluctance stepping motor, in the hybrid stepping motor, rotor stacks are separated by an axially directed permanent magnet. As a result, in Fig. 11-22a one end of the rotor can be considered to have a north magnetic pole and the other end a south magnetic pole.

The hybrid stepping motor varies significantly from a multistack variable-reluctance stepping motor in that the stator pole structure is continuous along the length of the rotor. Figure 11-22b shows a schematic end view of a hybrid stepping motor. The stator has four poles with the phase-1 winding wound on the vertical poles and the phase-2 winding wound on the horizontal poles. The rotor is shown with its north-pole end at the near end of the motor and the south-pole end (shown crosshatched) at the far end.

In Fig. 11-22b, phase 1 is shown excited such that the top stator pole is a south pole while the bottom pole is a north pole. This stator excitation interacts with the permanent-magnet flux of the rotor to align the rotor with a pole on its north-pole end vertically upward and a pole on its south-pole

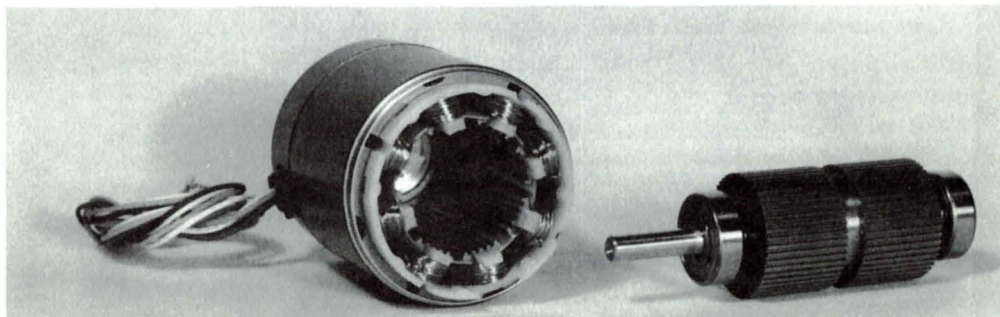


Fig. 11-21. Disassembled 1.8°/step hybrid stepping motor. (*Oriental Motor.*)

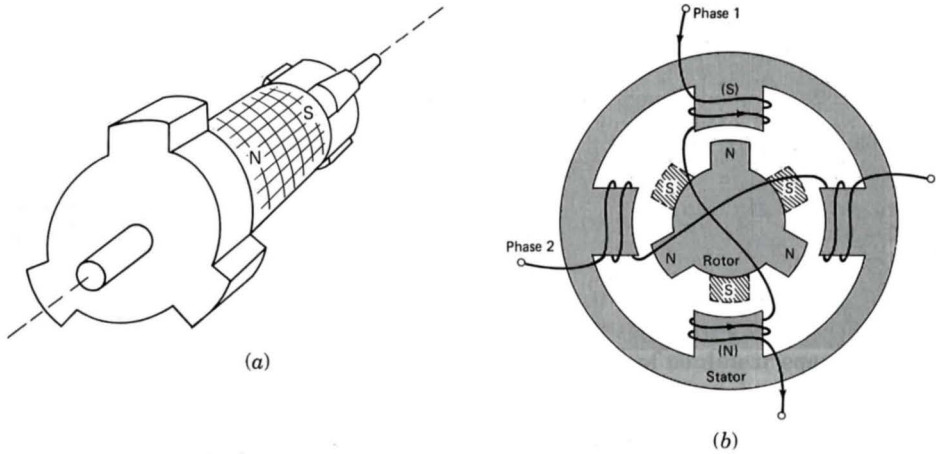


Fig. 11-22. Schematic view of a hybrid stepping motor. (a) Two-stack rotor showing the axially directed permanent magnet and the pole pieces displaced by one-half the pole pitch. (b) End view from the rotor north poles and showing the rotor south poles at the far end (shown crosshatched). Phase 1 of the stator is energized to align the rotor as shown.

end vertically downward, as shown in the figure. Note that if the stator excitation is removed, there will still be a permanent-magnet torque tending to maintain the rotor in the position shown.

To turn the rotor, excitation is removed from phase 1, and phase 2 is excited. If phase 2 is excited such that the right-hand stator pole is a south pole and the left-hand one is a north pole, the rotor will rotate 30° counterclockwise. Similarly, if the opposite excitation is applied to the phase-2 winding, a 30° rotation in the clockwise direction will occur. Thus by alternately applying phase-1 and phase-2 excitation of the appropriate polarity, the rotor can be made to rotate in either direction by a specified angular increment.

Practical hybrid stepping motors are generally built with more rotor poles than are indicated in the schematic motor of Fig. 11-22, in order to give much better angular resolution. Correspondingly, the stator poles are often castleated (see Fig. 10-8) to further increase the angular resolution. In addition, they may be built with more than two stacks per rotor.

The hybrid stepping-motor design offers advantages over the permanent-magnet design discussed earlier. It can achieve small step sizes easily and with a simple magnet structure while a purely permanent-magnet motor would require a multipole permanent magnet. In comparison with the variable-reluctance stepping motor, the hybrid design may require less excitation to achieve a given torque because some of the excitation is sup-

plied by the permanent magnet. In addition, the hybrid stepping motor will tend to maintain its position when the stator excitation is removed, as does the permanent-magnet design.

The actual choice of a stepping-motor design for a particular application is determined based on the desired operating characteristics, availability, size, and cost. In addition to the three classifications of stepping motors discussed in this chapter, a number of differing and often quite clever designs have been developed. Although these encompass a wide range of configurations and construction techniques, the operating principles remain the same.

Stepping motors may be driven by electronic drive components similar to those discussed in Art. 10-4. The reader is referred to that article for further information on the issues of drive systems. Note that the issue of controlling a stepping motor to obtain the desired response under dynamic, transient conditions is quite complex and remains the subject of considerable investigation.[†]

11-7 PERMANENT-MAGNET MOTORS

Permanent-magnet dc motors come in many different configurations and fall into many categories. They may take the form of conventional dc machines in which the stationary field winding is replaced by a permanent magnet. Alternatively, they may take the form of a synchronous machine in which the rotating field winding is replaced by a permanent magnet.

Permanent magnets offer a number of useful benefits in electric machinery applications. Chief among these is that they do not require external excitation, and its associated power dissipation, to create magnetic fields in the machine. In ac machines, slip rings and brushes are not required. In both ac and dc machines, this also means that space is not required for windings, and thus permanent-magnet machines can be smaller, and in some cases cheaper, than their externally excited counterparts.

Alternatively, permanent-magnet machines are subject to limitations imposed by the permanent magnets themselves. These include the risk of demagnetization due to excessive currents in the motor windings or due to overheating of the magnet. In addition, the permanent magnets are somewhat limited in the magnitude of air-gap flux density that they can produce. However, with the development of new magnetic materials such as samarium cobalt and neodymium-iron-boron (Art. 1-6), these characteristics are becoming less and less restrictive for permanent-magnet machine design.

Figure 11-23 shows a disassembled view of a permanent-magnet dc motor. This particular motor is used to rotate the disk in a personal com-

[†]For further information on stepping motors, see P. P. Acarnley, *Stepping Motors: A Guide to Modern Theory and Practice*, rev. 2d ed., Peter Peregrinus Ltd., London, 1982, and Takashi Kenjo, *Stepping Motors and Their Microprocessor Controls*, Clarendon Press, Oxford, 1984.

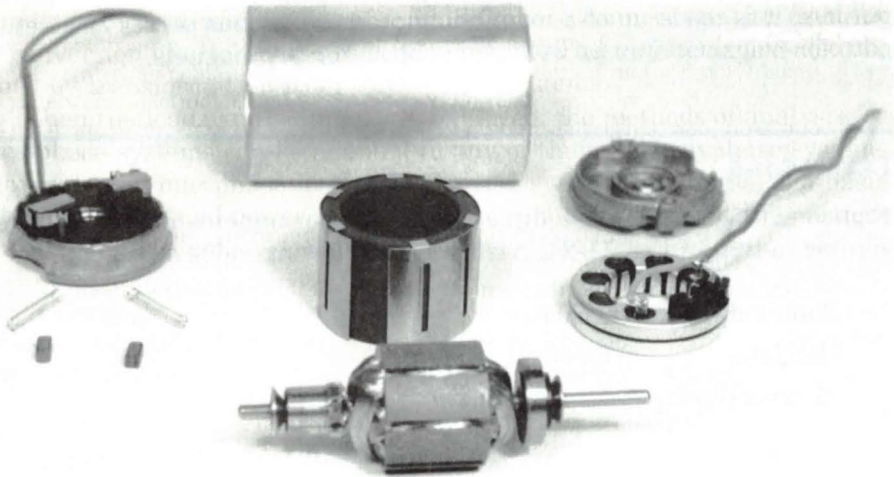


Fig. 11-23. Disassembled permanent-magnet dc motor from a personal computer disk drive. A permanent-magnet ac tachometer is also included in the same housing for speed control. (Buehler Products Inc.)

puter disk drive. Notice that the rotor of this motor consists of a conventional dc armature with commutator segments and brushes. There is also a small permanent magnet on one end which constitutes the field of an ac tachometer, required for speed control in the disk drive.

Unlike the salient-pole field structure characteristic of a dc machine with external field excitation (see Fig. 9-20), permanent-magnet motors such as that of Fig. 11-23 typically have a smooth stator structure consisting of a cylindrical shell (or fraction thereof) of uniform thickness magnetized in the radial direction. Such a structure is illustrated in Fig. 11-24, where the arrows indicate the direction of magnetization. The rotor of Fig. 11-24 has winding slots and has a commutator and brushes, as in all dc machines. Notice also that the outer shell in these motors serves a dual

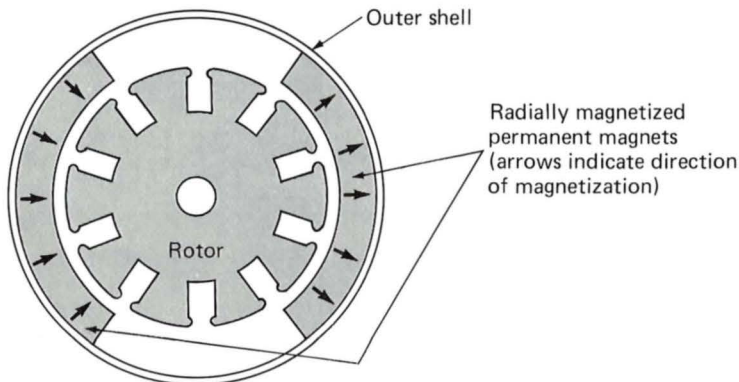


Fig. 11-24. Cross section of a typical permanent-magnet motor. Arrows indicate the direction of magnetization in the permanent magnets.

purpose; it is made up of a magnetic material and thus serves as a return path for magnetic flux as well as a support for the magnets.

EXAMPLE 11-5

Figure 11-25*a* defines the dimensions of a permanent-magnet dc motor similar to that of Fig. 11-24. Assume the following values:

Rotor radius $R_r = 1.2$ cm

Gap length $t_g = 0.05$ cm

Magnet thickness $t_m = 0.35$ cm

Also assume that both the rotor and outer shell are made of infinitely per-

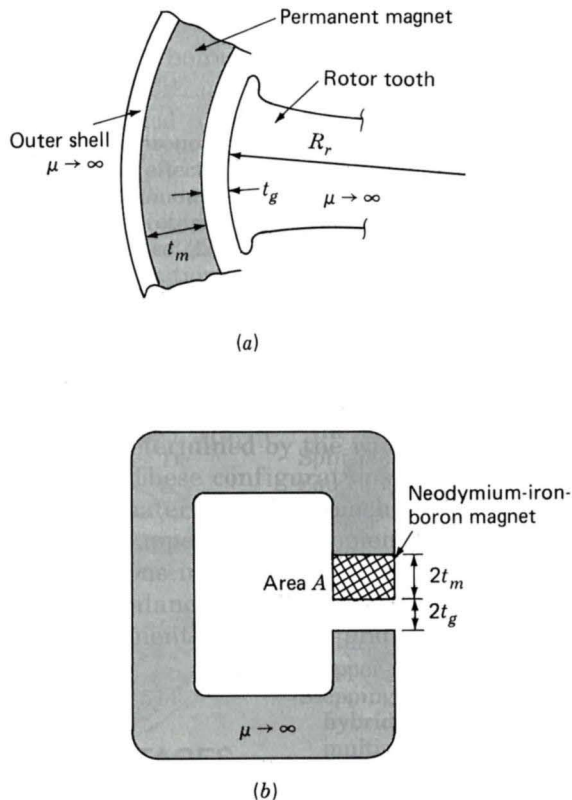


Fig. 11-25. (a) Dimension definitions for the motor of Fig. 11-24; (b) approximate magnetic equivalent circuit.

meable magnetic material ($\mu \rightarrow \infty$) and that the magnet is neodymium-iron-boron (see Fig. 1-18).

Ignoring the effects of rotor slots, estimate the magnetic flux density B in the air gap of this motor.

Solution

Because the rotor and outer shell are assumed to be of infinite magnetic permeability, the motor can be represented by a magnetic equivalent circuit consisting of an air gap of length $2t_g$ in series with a section of neodymium-iron-boron of length $2t_m$ (see Fig. 11-25*b*). Note that this equivalent circuit is approximate because the cross-sectional area of the flux path in the motor increases with increasing radius, whereas it is assumed to be constant in the equivalent circuit.

The solution can be written down by direct analogy with Example 1-7. Replacing the air-gap length g with $2t_g$ and the magnet length l_m with $2t_m$, the equation for the load line can be written as

$$B_m = -\mu_0 \left(\frac{t_m}{t_g} \right) H_m = -7\mu_0 H_m$$

This relationship can be plotted on Fig. 1-18 to find the operating point from its intersection with the dc magnetization curve for neodymium-iron-boron. Alternatively, recognizing that the dc magnetization curve for neodymium-iron-boron is a straight line of the form

$$B_m = 1.06\mu_0 H_m + 1.25 \text{ T}$$

we find that

$$B_m = B_g = 1.09 \text{ T}$$

Figure 11-26 shows an exploded view of an alternate form of permanent-magnet dc motor. In this motor, the armature windings are made into the form of a thin disk (with no iron in the armature). As in any dc motor, brushes are used to commutate the armature current, contacting the commutator portion of the armature which is at its inner radius. Currents in the disk armature flow radially, and the disk is placed between two sets of permanent magnets which create axial flux through the armature winding. The combination of axial magnetic flux and radial currents produces a torque which rotates the rotor as in any dc motor. This motor configuration can be shown to produce large acceleration (due to low rotor inertia), no cogging torque (due to the fact that the rotor is nonmagnetic), and long brush life and high-speed capability (due to the fact that the armature inductance is low and thus there will be little arcing at the commutator segments).

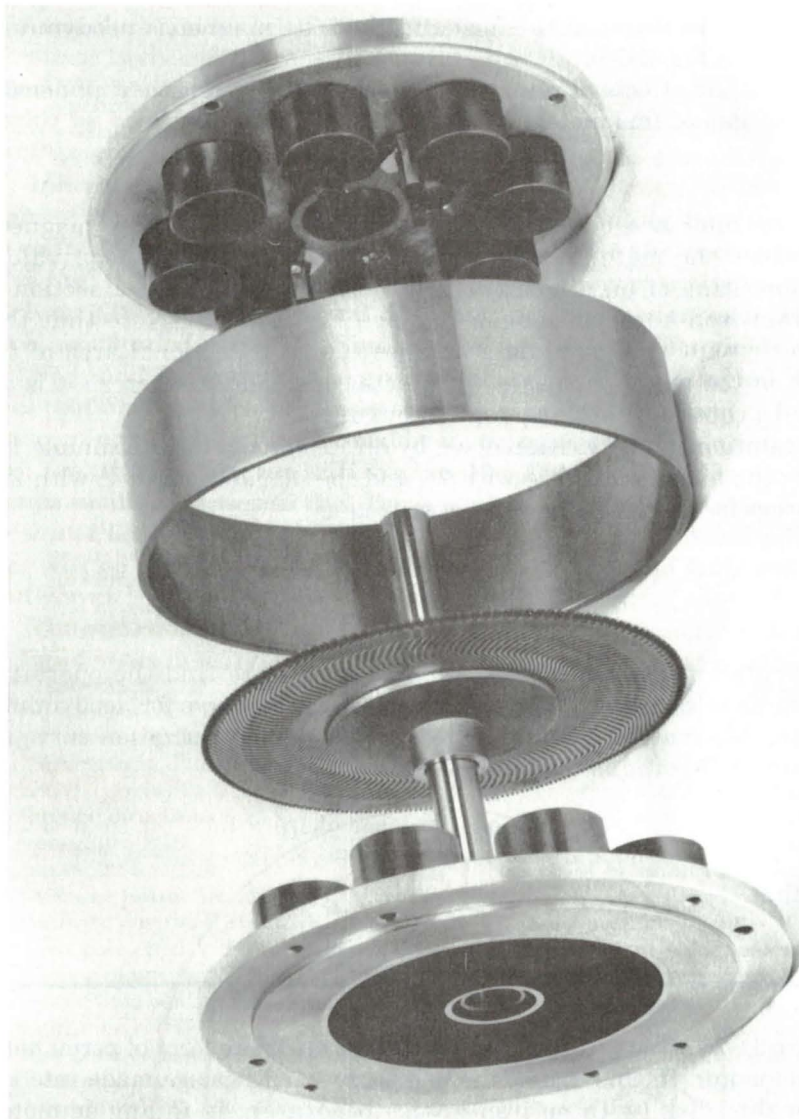


Fig. 11-26. Exploded view of a disk armature permanent-magnet servomotor. Magnets are Alnico. (PMI Motion Technologies.)

The principal difference between permanent-magnet dc machines and those discussed in Chap. 9 is that they have a fixed source of field-winding flux which is supplied by a permanent magnet. As a result, the equivalent circuit for a permanent-magnet dc motor is identical to that of the externally excited dc motor except that there are no field-winding connections. Figure 11-27 shows the equivalent circuit for a permanent-magnet dc motor.

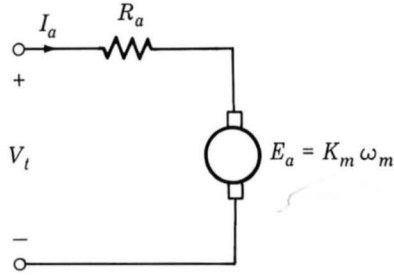


Fig. 11-27. Equivalent circuit of a permanent-magnet dc motor.

From Eq. 9-13, the speed-voltage term for a dc motor can be written in the form

$$E_a = K_a \Phi_d \omega_m \quad (11-27)$$

where Φ_d is the net flux along the field-winding axis and K_a is a geometric constant. In a permanent-magnet dc machine, Φ_d is constant and thus Eq. 11-27 can be reduced to

$$E_a = K_m \omega_m \quad (11-28)$$

where

$$K_m = K_a \Phi_d \quad (11-29)$$

is known as the motor's *torque constant* and is a function of motor geometry and magnet properties.

Finally the torque of the machine can be easily found from Eq. 9-15 as

$$T = \frac{E_a I_a}{\omega_m} = K_m I_a \quad (11-30)$$

EXAMPLE 11-6

A permanent-magnet dc motor is known to have an armature resistance of $1.03 \, \Omega$. When operated at no load from a dc source of 50 V, it is observed to operate at a speed of 2100 r/min and to draw 1.25 A. Find (a) the speed-voltage constant K_m , (b) the no-load rotational losses of the motor, and (c) the hp output of the motor when it is operating at 1700 r/min from a 48-V source.

Solution

(a) From the equivalent circuit of Fig. 11-27, the generated voltage E_a can be found as

$$\begin{aligned} E_a &= V_t - I_a R_a \\ &= 50 - 1.25(1.03) = 48.7 \text{ V} \end{aligned}$$

At a speed of 2100 r/min,

$$\begin{aligned} \omega_m &= 2100 \frac{\text{r}}{\text{min}} \times \frac{2\pi \text{ rad}}{\text{r}} \times \frac{1 \text{ min}}{60 \text{ s}} \\ &= 220 \text{ rad/s} \end{aligned}$$

Therefore, from Eq. 11-28,

$$K_m = \frac{E_a}{\omega_m} = 0.22 \text{ V/(rad/s)}$$

(b) At no load, all the power supplied to the generated voltage E_a is used to supply rotational losses. Therefore

$$\text{Rotational losses} = E_a I_a = 61 \text{ W}$$

(c) At 1700 r/min,

$$\omega_m = 1700 \left(\frac{2\pi}{60} \right) = 178 \text{ rad/s}$$

and

$$E_a = K_m \omega_m = 0.22 \times 178 = 39.2 \text{ V}$$

The input current can now be found as

$$I_a = \frac{V_t - E_a}{R_a} = \frac{48 - 39.2}{1.03} = 8.54 \text{ A}$$

The shaft input power can be calculated as

$$P_{\text{shaft}} = E_a I_a = 39.2 \times 8.54 = 335 \text{ W}$$

Assuming the rotational losses to be constant at their no-load value (certainly an approximation), the output power can be calculated:

$$P_{\text{out}} = P_{\text{shaft}} - \text{rotational losses} = 274 \text{ W} = 0.37 \text{ hp}$$

11-8 PERMANENT-MAGNET AC MOTORS

Permanent-magnet ac motors are polyphase synchronous motors with permanent-magnet rotors. Thus they are similar to the synchronous machines discussed in Chaps. 5 and 6 except that the field windings are replaced by permanent magnets.

Figure 11-28 is a schematic diagram of a three-phase permanent-magnet ac machine. Comparison of this figure with Fig. 5-2 emphasizes the similarities between the permanent-magnet ac machine and the conventional synchronous machine. In fact, the permanent-magnet ac machine can be readily analyzed with the techniques of Chap. 5 simply by assuming that the machine is excited by a field current of constant value, making sure to calculate the various machine inductances based on the effective permeability of the permanent-magnet rotor.

Figure 11-29 shows a cutaway view of a typical permanent-magnet ac motor. This figure also shows a speed and position sensor mounted on the rotor shaft. This sensor is used for control of the motor, just as a shaft-position sensor is required for the operation of a stepping motor. A number of techniques may be used for shaft-position sensing, including Hall-effect devices, light-emitting diodes and phototransistors in combination with a pulsed wheel, and inductance pickups.

In fact, an alternate viewpoint of a permanent-magnet ac motor is that it is a permanent-magnet stepping motor with a nonsalient stator. Under this viewpoint, the only difference between the two is that there will be little, if any, saliency (cogging) torque in the permanent-magnet ac motor.

Operation of the permanent-magnet ac motor is similar to that of the permanent-magnet stepping motor. Based on rotor-position information from the shaft-position sensor, the motor phase windings are excited sequen-

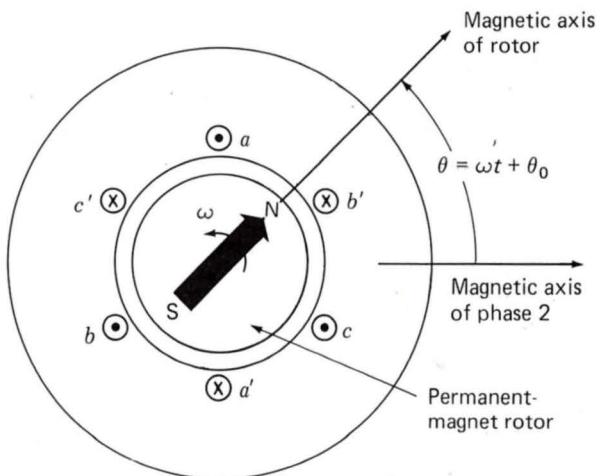


Fig. 11-28. Schematic diagram of a three-phase permanent-magnet ac machine. The arrow indicates the direction of rotor magnetization.

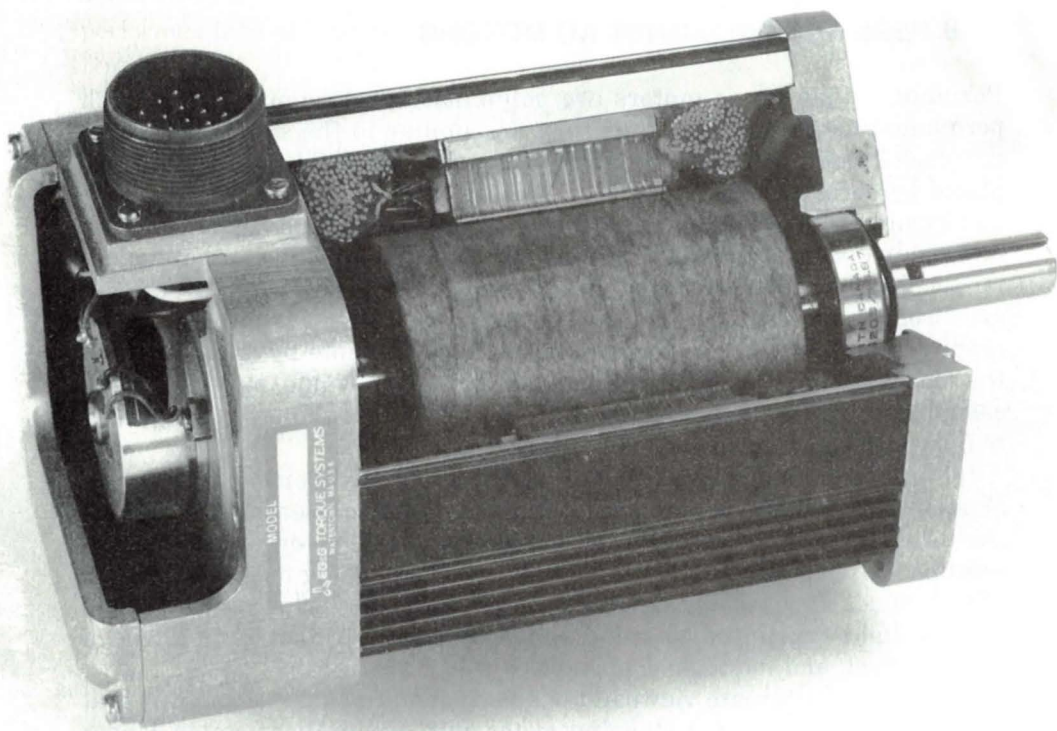


Fig. 11-29. Cutaway view of a permanent-magnet ac motor. Also shown is the shaft speed and position sensor used to control the motor. (EG&G Torque Systems.)

tially in such a fashion as to produce the desired torque and speed. As with the stepping motor, the frequency of the excitation determines the motor speed, and the angular position between the rotor magnetic axis and a given phase when it is excited determines the torque which will be produced.

The capability to measure rotor speed and position and to apply variable frequency and amplitude phase excitation to ac permanent-magnet motors means that they are highly controllable and can be made to exhibit a wide range of operating characteristics when coupled to appropriate control electronics and a drive system. As a result, these motors are now found in many applications previously considered to be almost exclusively the domain of dc motors.

Permanent-magnet ac motors are frequently referred to as *brushless motors* or *brushless dc motors*. This terminology comes about both because of their similarity in characteristics to dc motors and because of the fact that one can view these motors as inside-out dc motors, with their field winding on the rotor and with their armature electronically commutated by the shaft-position sensor and by switches (transistors, thyristors, etc.) connected to the armature windings.

11-9 SUMMARY

One theme of this chapter is a continuation of the induction-machine theory of Chap. 7 and its application to the single-phase induction motor. This theory is expanded by a step-by-step reasoning process from the simple revolving-field theory of the symmetrical polyphase induction motor. The basic concept is the resolution of the stator-mm ϕ wave into two constant-amplitude traveling waves revolving around the air gap at synchronous speed in opposite directions. If the slip for the forward field is s , then that for the backward field is $2 - s$. Each of these component fields produces induction-motor action, just as in a symmetrical polyphase motor. From the viewpoint of the stator, the reflected effects of the rotor can be visualized and expressed quantitatively in terms of simple equivalent circuits. The ease with which the internal reactions can be accounted for in this manner is the essential reason for the usefulness of the double-revolving-field theory.

For a single-phase winding, the forward- and backward-component mm ϕ waves are equal, and their amplitude is half the maximum value of the peak of the stationary pulsating mm ϕ produced by the winding. The resolution of the stator mm ϕ into its forward and backward components then leads to the physical concept of the single-phase motor described in Art. 11-1 and finally to the quantitative theory developed in Art. 11-3 and to the equivalent circuits of Fig. 11-11.

The next step is investigation of the possibilities of applying the double-revolving-field resolution to a symmetrical two-phase motor with unbalanced applied voltages, as in Art. 11-4. This investigation leads to the symmetrical-component concept, whereby an unbalanced two-phase system of currents or voltages can be resolved into the sum of two balanced two-phase component systems of opposite phase sequence. Resolution of the currents into symmetrical-component systems is equivalent to resolving the stator-mm ϕ wave into its forward and backward components, and therefore the internal reactions of the rotor for each symmetrical-component system are the same as those which we have already investigated. A very similar reasoning process, not considered here, leads to the well-known three-phase symmetrical-component method for treating problems involving unbalanced operation of three-phase rotating machines. The ease with which the rotating machine can be analyzed in terms of revolving-field theory is the chief reason for the usefulness of the symmetrical-component method.

This chapter also introduces a number of other commonly used small-motor types. Although they work on the same principles as their larger counterparts, their analysis is complex and their design is often largely empirical. In each motor, however, the electromechanical transduction is achieved by the spatial displacement of the flux distributions associated with the stationary and rotating members.

The remaining motor types discussed in this chapter are found in a wide variety of common applications. The universal motor is simply a series-

connected dc motor with a laminated rotor and stator so that it can be run from both dc and ac sources. It is found in most small ac appliances such as blenders, mixers, vacuum cleaners, and small electric handtools. Besides being inexpensive to manufacture, it is readily adaptable to variable-speed applications, either by the insertion of series resistance or by the use of solid-state voltage controllers.

Stepping motors are the electromechanical companions to digital electronics. By proper application of voltage pulses to the stator windings, these motors can be made to rotate in well-defined steps ranging down to a fraction of a degree per pulse. They are thus essential components of digitally controlled electromechanical systems where a high degree of precision is required. They are found in numerically controlled machine tools, in line printers and disk drives in computer systems, and in *XY* plotters.

Finally this chapter discusses permanent-magnet motors. Permanent-magnet dc machines have been used for many years in applications where the controllability of dc machines is required but where there is no need for a separately excited field winding. As is the case for stepping motors, permanent-magnet ac motors are seeing increased application as the price of digital electronics and controllers decreases and their power increases such that the performance and cost characteristics of permanent-magnet ac machine systems meet or exceed those previously associated with their competition.

PROBLEMS

11-1. What type of motor would you use in the following applications? Vacuum cleaner, refrigerator, compact disk player, video camera, washing machine, food mixer, portable electric drill, electric clock, water pump, window fan, automobile windshield wiper. Justify your selection.

11-2. A $\frac{3}{4}$ -hp 120-V 50-Hz capacitor-start motor has the following constants for the main and auxiliary windings (at starting):

$$\begin{aligned} Z_m &= 6.45 + j8.27 \, \Omega && \text{main winding} \\ Z_a &= 11.5 + j8.15 \, \Omega && \text{auxiliary winding} \end{aligned}$$

- (a) Find the magnitudes and phase angles of the currents in the main and auxiliary windings when rated voltage is applied to the motor under starting conditions.
- (b) Find the value of starting capacitance that will place the main- and auxiliary-winding currents in quadrature at starting.
- (c) Repeat part (a) when the capacitance of part (b) is inserted in series with the auxiliary winding.

11-3. Repeat Prob. 11-2 if the motor is operated from a 120-V 60-Hz source.

11-4. Repeat Example 11-2 for a slip of 0.04.

11-5. A $\frac{1}{2}$ -hp four-pole 115-V 60-Hz single-phase induction motor has the following parameters (resistances and reactances are in ohms per phase):

$$R_{1m} = 1.83 \quad R_2 = 3.29$$

$$X_{1m} = 2.49 \quad X_\phi = 58.7 \quad X_2 = 2.49$$

$$\text{Core loss} = 36 \text{ W} \quad \text{Friction and windage} = 13.8 \text{ W}$$

Find the speed, stator current, torque, power output, power factor, and efficiency of this motor when operating at rated voltage and a slip of 0.045.

11-6. At standstill the currents in the main and auxiliary windings of a capacitor-start induction motor are $I_m = 16.4 \text{ A}$ and $I_a = 7.2 \text{ A}$, respectively. The auxiliary-winding current leads the main-winding current by 57° . The effective turns per pole, i.e., the number of turns corrected for the effects of winding distribution, are $N_m = 70$ and $N_a = 100$. The windings are in space quadrature.

- (a) Determine the amplitudes of the forward and backward stator-mmfs waves.
- (b) Suppose it were possible to adjust the magnitude and phase of the auxiliary-winding current. What magnitude and phase would produce a pure-forward mmf wave?

11-7. Derive an expression in terms of Q_2 for the nonzero speed of a single-phase induction motor at which the internal torque is zero. (See Example 11-2.)

11-8. Repeat Example 11-3 for a slip of 0.04.

11-9. (a) Find the starting torque of the motor given in Example 11-3 for the conditions specified.

- (b) Compare the result of part (a) with the torque which the motor would develop at starting when balanced two-phase voltages of 220 V are applied.

- (c) Show, in general, that if the stator voltages V_m and V_a of a two-phase induction motor are in quadrature but unequal, the starting torque is the same as that developed when balanced two-phase voltages of $\sqrt{V_m V_a}$ are applied.

11-10. The induction motor of Example 11-3 is supplied from an unbalanced two-phase source by a four-wire feeder having an impedance of

$1.2 + j2.8 \Omega/\text{phase}$. The source voltages can be expressed as

$$V_m = 235 \angle 0^\circ \text{ V} \quad V_a = 205 \angle 75^\circ \text{ V}$$

For a slip of 0.05, show that the induction-motor performance is such that the motor's terminal voltages correspond more nearly to those of a balanced two-phase system than do those at the source.

11-11. The equivalent-circuit constants in ohms per phase referred to the stator for a two-phase 1.5-hp 220-V four-pole 60-Hz squirrel-cage induction motor are given below. The no-load rotational loss is 200 W.

$$R_1 = 3.2 \quad R_2 = 2.4 \quad X_1 = X_2 = 3.2 \quad X_\phi = 100$$

- The voltage applied to phase m is $220 \angle 0^\circ \text{ V}$, and the voltage applied to phase a is $220 \angle 60^\circ \text{ V}$. At a slip $s = 0.04$, $Z_f = 41.9 + j27.2 \Omega$ and $Z_b = 1.20 + j3.2 \Omega$. What is the net air-gap torque?
- What is the starting torque with the applied voltages of part (a)?
- The applied voltages are readjusted so that $\hat{V}_m = 220 \angle 0^\circ$ and $\hat{V}_a = 220 \angle 90^\circ$. Full load on the machine occurs at $s = 0.04$. At what value of slip does maximum torque occur? What is the value of maximum air-gap torque in newton-meters?
- While the motor is running as in part (c), phase a is open-circuited. What is the horsepower developed by the machine at slip $s = 0.04$?
- What voltage appears across the open phase- a terminals under the conditions of part (d) at $s = 0.04$?

11-12. Consider a four-phase stepper motor with a permanent-magnet rotor, as shown in Fig. 11-16. The motor is to be controlled using a 4-bit digital signal from a microprocessor. The 4 bits represent phases a to d respectively, and a 1 indicates that the corresponding phase is to be excited. Thus the output 0100 will cause phase b to be excited, 1001 will cause phases a and d to be excited, etc. The digital signal is the input to an electronic circuit which provides the actual excitation.

- Make a table of the 4-bit signals which correspond to rotor angular positions of $0, 45, \dots, 315^\circ$.
- By sequencing through the digital signals found in part (a), the motor can be made to rotate at a constant speed. For a speed of 1000 r/min, at what time interval (in milliseconds) should the digital signal be changed?

11-13. Figure 11-30 shows a two-phase hybrid stepping motor with castle-ated poles on the stator. The rotor is shown in the position it occupies when current is flowing into the positive lead of phase 1.

11-14. Consider a multistack, multiphase variable-reluctance stepping motor such as that shown schematically in Fig. 11-19, with 16 poles on each of the rotor and stator stacks and three stacks with one phase winding per stack.

- (a) Assume that the stator poles are aligned. Calculate the angular displacement between the rotor stacks.
- (b) Determine the frequency of phase currents required to achieve a rotor rotation speed of 650 r/min.

11-15. The manufacturer's data sheet for a permanent-magnet dc motor indicates that it has a torque constant $K_m = 0.24 \text{ V}/(\text{rad/s})$ and an armature resistance of 2.1Ω . For a constant applied armature voltage of 90 V dc, calculate (a) the no-load speed of the motor in revolutions per minute, (b) its stall (zero-speed) current and torque, and (c) its torque as a function of speed.

11-16. Measurements on a small permanent-magnet dc motor indicate that it has an armature resistance of 7.5Ω . With an applied armature voltage of 6 V, the motor is observed to achieve a no-load speed of 10,570 r/min while drawing an armature current of 13 mA.

- (a) Calculate the motor torque constant K_m .
- (b) Find the no-load rotational losses of the motor.

Assume the motor to be operating with an applied armature voltage of 6 V.

- (c) Find the stall current and torque of the motor.
- (d) At what speed will this motor achieve a power output of 1 W? Estimate the efficiency of this motor under this output condition.

11-17. The dc motor of Prob. 11-16 will be used to drive a load which requires a power of 0.75 W at a speed of 8500 r/min. Calculate the armature voltage which must be applied to the motor to achieve this operating condition.

11-18. A two-phase permanent-magnet ac motor has a rated speed of 6000 r/min and a four-pole rotor. Calculate the frequency of armature currents required to achieve this speed.

11-19. Small single-phase permanent-magnet ac generators are frequently used to generate the power for lights on bicycles. For this application, these generators are typically designed with a significant amount of leakage inductance in their armature winding. A simple model for these generators is an ac voltage source $e_a(t) = \omega K_a \cos \omega t$ in series with the armature leakage inductance L_a and the armature resistance R_a . Here ω is the electrical

frequency of the generated voltage which is determined by the speed of the generator as it rubs against the bicycle wheel.

Assuming that the generator is running a light bulb which can be modeled as a resistance R_L , determine the range of generator speed under which the light bulb will operate at constant brightness.

Three-Phase Circuits

Generation, transmission, and heavy-power utilization of ac electric energy almost invariably involve a type of system or circuit called a *polyphase system* or *polyphase circuit*. In such a system, each voltage source consists of a group of voltages having related magnitudes and phase angles. Thus, an n -phase system will employ voltage sources which conventionally consist of n voltages substantially equal in magnitude and successively displaced by a phase angle of $360^\circ/n$. A *three-phase system* will employ voltage sources which conventionally consist of three voltages substantially equal in magnitude and displaced by phase angles of 120° . Because it possesses definite economic and operating advantages, the three-phase system is by far the most common, and consequently emphasis is placed on three-phase circuits in this appendix.

The three individual voltages of a three-phase source may each be connected to its own independent circuit. We would then have three separate

single-phase systems. Alternatively, as will be shown in Art. A-1, symmetrical electric connections can be made between the three voltages and the associated circuitry to form a three-phase system. It is the latter alternative that we are concerned with in this appendix. Note that the word *phase* now has two distinct meanings. It may refer to a portion of a polyphase system or circuit, or, as in the familiar steady-state circuit theory, it may be used in reference to the angular displacement between voltage or current phasors. There is very little possibility of confusing the two.

A-1 GENERATION OF THREE-PHASE VOLTAGES

Consider the elementary three-phase two-pole generator of Fig. A-1. On the armature are three coils aa' , bb' , and cc' whose axes are displaced 120° in space from each other. This winding can be represented schematically as shown in Fig. A-2. When the field is excited and rotated, voltages will be generated in the three phases in accordance with Faraday's law. If the field structure is so designed that the flux is distributed sinusoidally over the

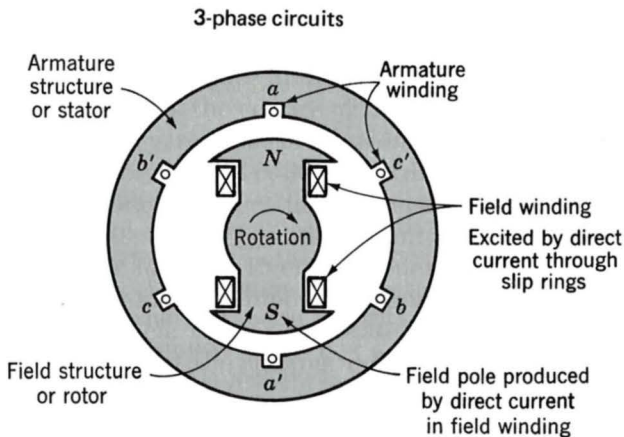


Fig. A-1. Elementary three-phase two-pole generator.

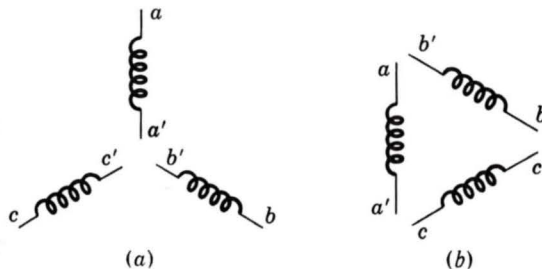


Fig. A-2. Schematic representation of windings of Fig. A-1.

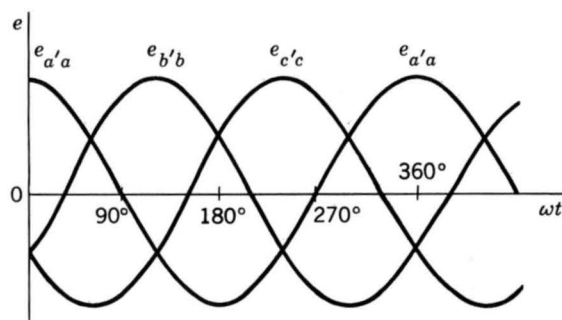


Fig. A-3. Voltage waves generated in windings of Figs. A-1 and A-2.

poles, the flux linking any phase will vary sinusoidally with time and sinusoidal voltages will be induced in the three phases. As shown in Fig. A-3, these three waves will be displaced 120° electrical degrees in time as a result of the phases being displaced 120° in space. The corresponding phasor diagram is shown in Fig. A-4. In general, the time origin and the reference axis in diagrams such as Figs. A-3 and A-4 are chosen on the basis of analytical convenience.

There are two possibilities for the utilization of voltages generated in this manner. The six terminals $a, a', b, b', c,$ and c' of the winding may be connected to three independent single-phase systems, or the three phases of the winding may be interconnected and used to supply a three-phase system. The latter procedure is adopted almost universally. The three phases of the winding may be interconnected in two possible ways, as shown in Fig. A-5. Terminals $a', b',$ and c' may be joined to form the neutral o , yielding a *Y connection*, or terminals a and b', b and $c',$ and c and a' may be joined individually, yielding a *Δ connection*. In the *Y connection*, a *neutral conductor*, shown dashed in Fig. A-5a, may or may not be brought out. If a neutral conductor exists, the system is a *four-wire three-phase system*; if not, it is a *three-wire three-phase system*. In the *Δ connection* (Fig. A-5b), no neutral exists and only a three-wire three-phase system can be formed.

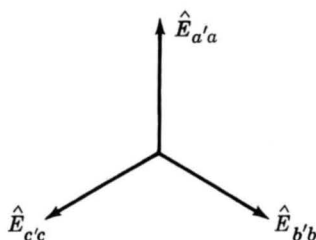


Fig. A-4. Phasor diagram of generated voltages.

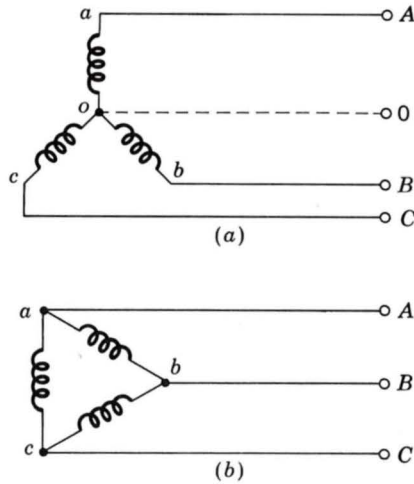


Fig. A-5. Three-phase connections: (a) Y connection and (b) Δ connection.

The three phase voltages, Figs. A-3 and A-4, are equal and phase-displaced by 120 electrical degrees, a general characteristic of a *balanced three-phase system*. Furthermore, in a balanced three-phase system the impedance in any one phase is equal to that in either of the other two phases, so that the resulting phase currents are equal and phase-displaced from each other by 120 electrical degrees. Likewise, equal power and equal reactive power flow in each phase. An *unbalanced three-phase system*, however, may lack any of or all the equalities and 120° displacements. Note that *only balanced systems are treated in this appendix and none of the methods developed or conclusions reached apply to unbalanced systems*. Most practical problems are concerned with balanced systems. Many industrial loads are three-phase loads and therefore inherently balanced, and in supplying single-phase loads from a three-phase source definite efforts are made to keep the three-phase system balanced by assigning approximately equal single-phase loads to each of the three phases.

A-2 THREE-PHASE VOLTAGES, CURRENTS, AND POWER

When the three phases of the winding in Fig. A-1 are Y-connected, as in Fig. A-5a, the phasor diagram of voltages is that of Fig. A-6. The *phase order* or *phase sequence* in Fig. A-6 is *abc*; that is, the voltage of phase *a* reaches its maximum 120° before that of phase *b*. The use of double-subscript notation in Fig. A-6 greatly simplifies the task of drawing the complete diagram. The subscripts indicate the points between which the voltage exists, and the order of subscripts indicates the direction in which the voltage rise is taken. Thus, $\hat{E}_{ao} = -\hat{E}_{oa}$.

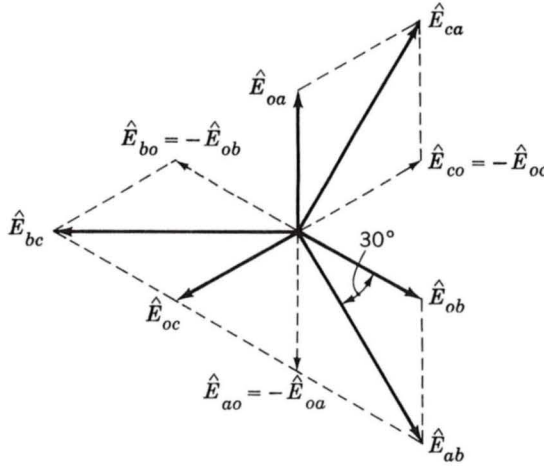


Fig. A-6. Voltage phasor diagram for Y connection.

The three-phase voltages \hat{E}_{oa} , \hat{E}_{ob} , and \hat{E}_{oc} are also called *line-to-neutral voltages*. The three voltages \hat{E}_{ab} , \hat{E}_{bc} , and \hat{E}_{ca} , called *line voltages* or, more specifically, *line-to-line voltages*, are also important. By Kirchhoff's voltage law, the line voltage \hat{E}_{ab} is

$$\hat{E}_{ab} = \hat{E}_{ao} + \hat{E}_{ob} = -\hat{E}_{oa} + \hat{E}_{ob} = \sqrt{3} \hat{E}_{ob} \angle -30^\circ \quad (\text{A-1})$$

as shown in Fig. A-6. Similarly,

$$\hat{E}_{bc} = \sqrt{3} \hat{E}_{oc} \angle -30^\circ \quad (\text{A-2})$$

and

$$\hat{E}_{ca} = \sqrt{3} \hat{E}_{oa} \angle -30^\circ \quad (\text{A-3})$$

Stated in words, these equations show that, for a Y connection, the line voltage is $\sqrt{3}$ times the phase voltage, or the line-to-line voltage is $\sqrt{3}$ times the line-to-neutral voltage.

The corresponding current phasors for the Y connection of Fig. A-5a are given in Fig. A-7. Obviously, for a Y connection, the line currents and phase currents are equal.

When the three phases are Δ -connected, as in Fig. A-5b, the phasor diagram of voltages is that of Fig. A-8. Obviously, for a Δ connection, the line voltages and phase voltages are equal.

The corresponding phasor diagram of currents is given in Fig. A-9. The three-phase currents are \hat{I}_{ab} , \hat{I}_{bc} , and \hat{I}_{ca} , the order of the subscripts indicating the current directions. By Kirchhoff's current law, the line current \hat{I}_{aA} is

$$\hat{I}_{aA} = \hat{I}_{ba} + \hat{I}_{ca} = -\hat{I}_{ab} + \hat{I}_{ca} = \sqrt{3} \hat{I}_{ca} \angle 30^\circ \quad (\text{A-4})$$

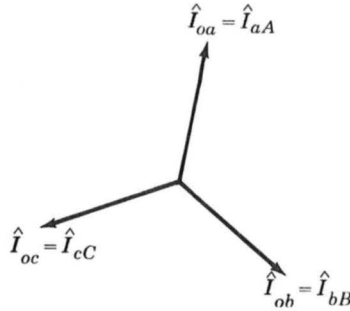
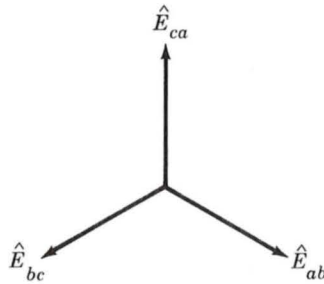


Fig. A-7. Current phasor diagram for Y connection.

Fig. A-8. Voltage phasor diagram for Δ connection.

as shown in Fig. A-9. Similarly,

$$\hat{I}_{bB} = \sqrt{3} \hat{I}_{ab} / 30^\circ \quad (\text{A-5})$$

and

$$\hat{I}_{cC} = \sqrt{3} \hat{I}_{bc} / 30^\circ \quad (\text{A-6})$$

Stated in words, Eqs. A-4 to A-6 show that for a Δ connection, the line current is $\sqrt{3}$ times the phase current. Evidently, the relations between phase and line currents of a Δ connection are similar to those between phase and line voltages of a Y connection.

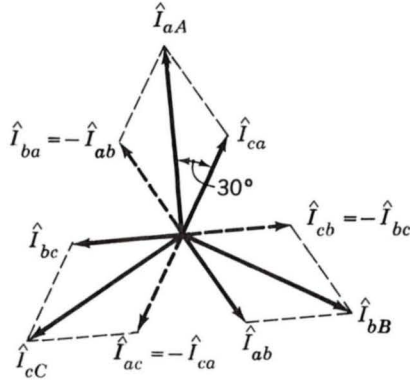
For both Y- and Δ -connected systems it can be shown that the total of the instantaneous power for all three phases of a balanced three-phase circuit does not pulsate with time. Thus, with the time origin taken at the maximum positive point of the phase-*a* voltage wave, the instantaneous voltages of the three phases are

$$e_a = \sqrt{2} E_p \cos \omega t \quad (\text{A-7})$$

$$e_b = \sqrt{2} E_p \cos (\omega t - 120^\circ) \quad (\text{A-8})$$

$$e_c = \sqrt{2} E_p \cos (\omega t + 120^\circ) \quad (\text{A-9})$$

where E_p is the rms value of the phase voltage. When the phase currents

Fig. A-9. Current phasor diagram for Δ connection.

are displaced from the corresponding phase voltages by the angle θ , the instantaneous phase currents are

$$i_a = \sqrt{2}I_p \cos(\omega t + \theta) \quad (\text{A-10})$$

$$i_b = \sqrt{2}I_p \cos(\omega t + \theta - 120^\circ) \quad (\text{A-11})$$

$$i_c = \sqrt{2}I_p \cos(\omega t + \theta + 120^\circ) \quad (\text{A-12})$$

where I_p is the rms value of the phase current.

The instantaneous power in each phase then becomes

$$p_a = e_a i_a = E_p I_p [\cos(2\omega t + \theta) + \cos \theta] \quad (\text{A-13})$$

$$p_b = e_b i_b = E_p I_p [\cos(2\omega t + \theta - 240^\circ) + \cos \theta] \quad (\text{A-14})$$

$$p_c = e_c i_c = E_p I_p [\cos(2\omega t + \theta + 240^\circ) + \cos \theta] \quad (\text{A-15})$$

The total instantaneous power for all three phases is

$$p = p_a + p_b + p_c = 3E_p I_p \cos \theta \quad (\text{A-16})$$

Notice that the sum of the cosine terms which involve time in Eqs. A-13 to A-15 (the first terms in the brackets) is zero. The total instantaneous power is accordingly independent of time. This situation is depicted graphically in Fig. A-10. Instantaneous powers for the three phases are plotted, together with the total instantaneous power, which is the sum of the three individual waves. *The total instantaneous power for a balanced three-phase system is constant and is equal to 3 times the average power per phase.*

In general, the total instantaneous power for any balanced polyphase system is constant. This is one of the outstanding advantages of polyphase systems. It is of particular advantage in the operation of polyphase motors,

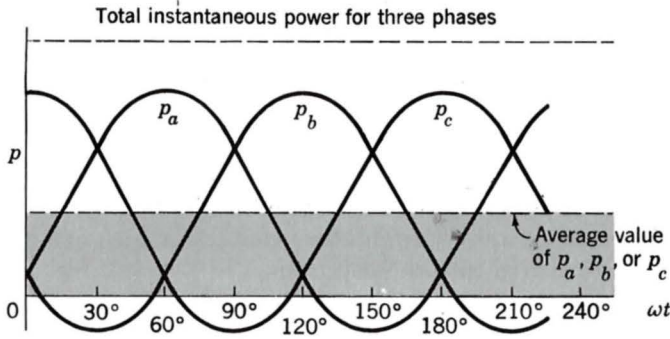


Fig. A-10. Instantaneous power in a three-phase system.

for example, for it means that the shaft-power output is constant and that torque pulsations, with the consequent tendency toward vibration, do not result from pulsations inherent in the supply system.

On the basis of single-phase considerations, the average power per phase P_p for either a Y- or Δ -connected system connected to a balanced three-phase load of impedance $Z_p = R_p + jX_p \Omega/\text{phase}$ is

$$P_p = E_p I_p \cos \theta = I_p^2 R_p \quad (\text{A-17})$$

where E_p , I_p , R_p , and θ are the voltage, current, resistance, and power-factor angle, respectively, per phase. The total three-phase power P is

$$P = 3P_p \quad (\text{A-18})$$

Similarly, for reactive power per phase Q_p and total three-phase reactive power Q ,

$$Q_p = E_p I_p \sin \theta = I_p^2 X_p \quad (\text{A-19})$$

and

$$Q = 3Q_p \quad (\text{A-20})$$

where X_p is the reactance per phase.

The voltamperes per phase (VA)_p and total three-phase voltamperes VA are

$$(\text{VA})_p = E_p I_p = I_p^2 Z_p \quad (\text{A-21})$$

and

$$\text{VA} = 3(\text{VA})_p \quad (\text{A-22})$$

In Eqs. A-17 and A-19, θ is the angle between phase voltage and phase current. As in the single-phase case, it is given by

$$\theta = \tan^{-1} \frac{X_p}{R_p} = \cos^{-1} \frac{R_p}{Z_p} = \sin^{-1} \frac{X_p}{Z_p} \quad (\text{A-23})$$

The power factor of a balanced three-phase system is therefore equal to that of any one phase.

A-3 Y- AND Δ -CONNECTED CIRCUITS

Three specific examples are given to illustrate the computational details of Y- and Δ -connected circuits. Explanatory remarks which are generally applicable are incorporated into the solutions.

EXAMPLE A-1

In Fig. A-11 is shown a 60-Hz transmission system consisting of a line having the impedance $Z_l = 0.05 + j0.20 \, \Omega$, at the receiving end of which is a load of equivalent impedance $Z_L = 10.0 + j3.00 \, \Omega$. The impedance of the return conductor should be considered zero.

(a) Compute (i) the line current I ; (ii) the load voltage E_L ; (iii) the power, reactive power, and voltamperes taken by the load; and (iv) the power and reactive-power loss in the line.

Suppose now that three such identical systems are to be constructed to supply three such identical loads. Instead of drawing the diagrams one below the other, let them be drawn in the fashion shown in Fig. A-12, which is, of course, the same electrically.

(b) For Fig. A-12 give the current in each line; the voltage at each load; the power, reactive power, and voltamperes taken by each load; the power and reactive-power loss in each of the three transmission systems; the total power, reactive power, and voltamperes taken by the loads; and the total power and reactive-power loss in the three transmission systems.

Next consider that the three return conductors are combined into one and that the phase relationship of the voltage sources is such that a balanced four-wire three-phase system results, as in Fig. A-13.

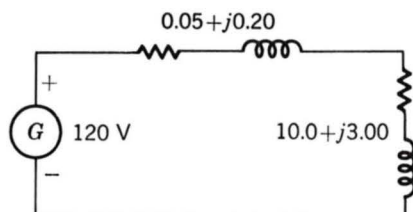


Fig. A-11. Circuit for Example A-1a.

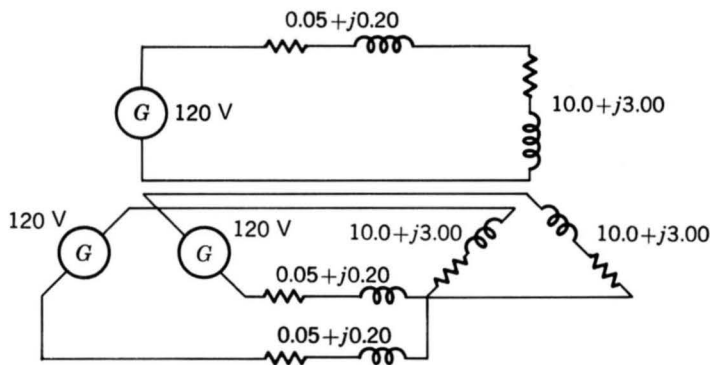


Fig. A-12. Circuit for Example A-1b.

(c) For Fig. A-13 give the line current; the load voltage, both line-to-line and line-to-neutral; the power, reactive power, and voltamperes taken by each phase of the load; the power and reactive-power loss in each line; the total three-phase power, reactive power, and voltamperes taken by the load; and the total power and reactive-power loss in the lines.

(d) In Fig. A-13 what is the current in the combined return or neutral conductor?

(e) Can this conductor be dispensed with in Fig. A-13 if desired?

Assume now that this neutral conductor is omitted. This results in the three-wire three-phase system of Fig. A-14.

(f) Repeat part (c) for Fig. A-14.

(g) On the basis of the results of this example, outline briefly the method of reducing a balanced three-phase Y-connected circuit problem to its equivalent single-phase problem. Be careful to distinguish between the use of line-to-line and line-to-neutral voltages.

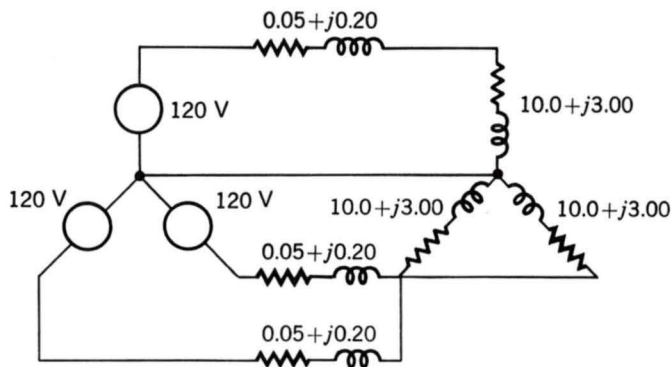


Fig. A-13. Circuit for Example A-1c to e.

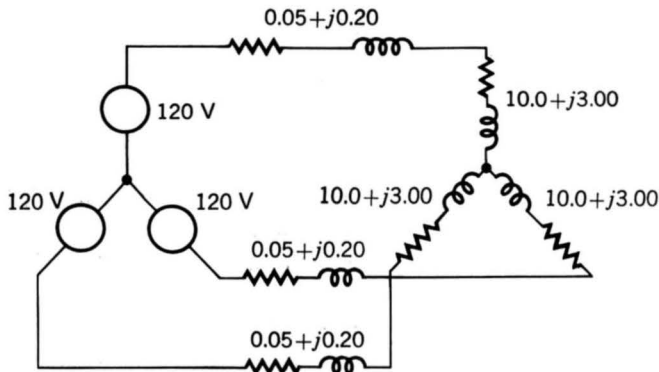


Fig. A-14. Circuit for Example A-1f.

Solution

(a)

$$I = \frac{120}{\sqrt{(0.05 + 10.0)^2 + (0.20 + 3.00)^2}} = 11.4 \text{ A}$$

$$E_L = I|Z_L| = 11.4 \sqrt{(10.0)^2 + (3.00)^2} = 119 \text{ V}$$

$$P_L = I^2 R_L = (11.4)^2 (10.0) = 1300 \text{ W}$$

$$Q_L = I^2 X_L = (11.4)^2 (3.00) = 390 \text{ VA reactive}$$

$$(\text{VA})_L = I^2 |Z_L| = (11.4)^2 \sqrt{(10.0)^2 + (3.00)^2} = 1360 \text{ VA}$$

$$P_l = I^2 R_l = (11.4)^2 (0.05) = 6.5 \text{ W}$$

$$Q_l = I^2 X_l = (11.4)^2 (0.20) = 26 \text{ VA reactive}$$

(b) The first four obviously have the same values as in part (a).

$$\text{Total power} = 3P_L = 3(1300) = 3900 \text{ W}$$

$$\text{Total reactive power} = 3Q_L = 3(390) = 1170 \text{ VA reactive}$$

$$\text{Total VA} = 3(\text{VA})_L = 3(1360) = 4080 \text{ VA}$$

$$\text{Total power loss} = 3P_l = 3(6.5) = 19.5 \text{ W}$$

$$\text{Total reactive-power loss} = 3Q_l = 3(26) = 78 \text{ VA reactive}$$

(c) The results obtained in part (b) are unaffected by this change. The voltage in parts (a) and (b) is now the line-to-neutral voltage. The line-to-line voltage is

$$\sqrt{3}(119) = 206 \text{ V}$$

(d) By Kirchhoff's current law, the neutral current is the phasor sum of the three line currents. These line currents are equal and phase-displaced 120° . Since the phasor sum of three equal phasors 120° apart is zero, the neutral current is zero.

(e) The neutral current being zero, the neutral conductor can be dispensed with if desired.

(f) Since the presence or absence of the neutral conductor does not affect conditions, the values are the same as in part (c).

(g) A neutral conductor can be assumed, regardless of whether one is physically present. Since the neutral conductor in a balanced three-phase circuit carries no current and hence has no voltage drop across it, the neutral conductor should be considered to have zero impedance. Then one phase of the Y, together with the neutral conductor, can be removed for study. Since this phase is uprooted at the neutral, *line-to-neutral voltages must be used*. This procedure yields the single-phase equivalent circuit, in which all quantities correspond to those in one phase of the three-phase circuit. Conditions in the other two phases being the same (except for the 120° phase displacements in the currents and voltages), there is no need for investigating them individually. Line currents in the three-phase system are the same as in the single-phase circuit, and total three-phase power, reactive power, and voltamperes are 3 times the corresponding quantities in the single-phase circuit. If line-to-line voltages are desired, they must be obtained by multiplying voltages in the single-phase circuit by $\sqrt{3}$.

EXAMPLE A-2

Three impedances of value $Z_p = 4.00 + j3.00 = 5.00 / 36.9^\circ \Omega$ are connected in Y, as shown in Fig. A-15. For balanced line-to-line voltages of 208 V, find the line current, the power factor, and the total power, reactive power, and voltamperes.

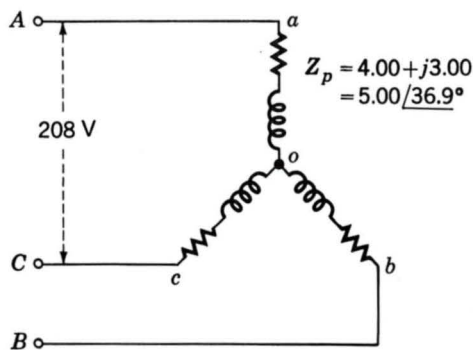


Fig. A-15. Circuit for Example A-2.

Solution

The line-to-neutral voltage across any one phase, such as ao , is

$$E_p = \frac{208}{\sqrt{3}} = 120 \text{ V}$$

Hence

$$I_l = I_p = \frac{E_p}{|Z_p|} = \frac{120}{5.00} = 24.0 \text{ A}$$

$$\text{Power factor} = \cos \theta = \cos 36.9^\circ = 0.80 \text{ lagging}$$

$$P = 3P_p = 3I_p^2 R_p = 3(24.0)^2(4.00) = 6910 \text{ W}$$

$$Q = 3Q_p = 3I_p^2 X_p = 3(24.0)^2(3.00) = 5180 \text{ VA reactive}$$

$$\text{VA} = 3(\text{VA})_p = 3E_p I_p = 3(120)(24.0) = 8640 \text{ VA}$$

Note that phases a and c (Fig. A-15) do not form a simple series circuit. Consequently, the current cannot be found by dividing 208 V by the sum of the phase- a and - c impedances. To be sure, an equation can be written for voltage between points a and c by Kirchhoff's voltage law, but this must be a phasor equation taking account of the 120° phase displacement between the phase- a and phase- c currents. As a result, the method of thought outlined in Example A-1 leads to the simplest solution.

EXAMPLE A-3

Three impedances of value $Z_p = 12.00 + j9.00 = 15.00 \angle 36.9^\circ \Omega$ are connected in Δ , as shown in Fig. A-16. For balanced line-to-line voltages of 208 V, find the line current, the power factor, and the total power, reactive power, and voltamperes.

Solution

The voltage across any one phase, such as ca , is evidently equal to the line-to-line voltage. Consequently,

$$E_p = 208 \text{ V}$$

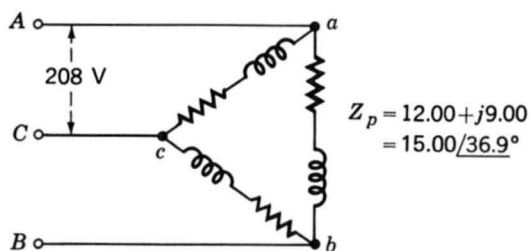


Fig. A-16. Circuit for Example A-3.

and
$$I_p = \frac{E_p}{|Z_p|} = \frac{208}{15.00} = 13.87 \text{ A}$$

Power factor = $\cos \theta = \cos 36.9^\circ = 0.80$ lagging

From Eq. A-4

$$I_l = \sqrt{3}I_p = \sqrt{3}(13.87) = 24.0 \text{ A}$$

Also
$$P = 3P_p = 3I_p^2 R_p = 3(13.87)^2(12.00) = 6910 \text{ W}$$

$$Q = 3Q_p = 3I_p^2 X_p = 3(13.87)^2(9.00) = 5180 \text{ VA reactive}$$

and
$$\text{VA} = 3(\text{VA})_p = 3E_p I_p = 3(208)(13.87) = 8640 \text{ VA}$$

Note that phases ab and bc do not form a simple series circuit, nor does the path cba form a simple parallel combination with the direct path through the phase ca . Consequently, the line current cannot be found by dividing 208 V by the equivalent impedance of Z_{ca} in parallel with $Z_{ab} + Z_{bc}$. Kirchhoff's-law equations involving quantities in more than one phase can be written, but they must be phasor quantities taking account of the 120° phase displacement between phase currents and between phase voltages. As a result, the method outlined above leads to the simplest solution.

Comparison of the results of Examples A-2 and A-3 leads to a valuable and interesting conclusion. Note that the line-to-line voltage, line current, power factor, total power, reactive power, and voltamperes are precisely equal in the two cases; in other words, conditions viewed from the terminals A, B, and C are identical, and one cannot distinguish between the two circuits from their terminal quantities. It will also be seen that the impedance, resistance, and reactance per phase of the Y connection (Fig. A-15) are exactly one-third of the corresponding values per phase of the Δ connection (Fig. A-16). Consequently, a balanced Δ connection can be replaced by a balanced Y connection providing that the circuit constants per phase obey the relation

$$Z_Y = \frac{1}{3}Z_\Delta \quad (\text{A-24})$$

Conversely, a Y connection can be replaced by a Δ connection provided Eq. A-24 is satisfied. The concept of this Y- Δ equivalence stems from the general Y- Δ transformation and is not the accidental result of a specific numerical case.

Two important corollaries follow from this equivalence: (1) A general computational scheme for balanced circuits can be based entirely on Y-connected circuits or entirely on Δ -connected circuits, whichever one prefers. Since it is frequently more convenient to handle a Y connection, the former scheme is usually adopted. (2) In the frequently occurring prob-

lems in which the connection is not specified and is not pertinent to the solution, either a Y or a Δ connection may be assumed. Again the Y connection is more commonly selected. In analyzing three-phase motor performance, for example, the actual winding connections need not be known unless the investigation is to include detailed conditions within the coils themselves. The entire analysis can be based on an assumed Y connection.

A-4 ANALYSIS OF BALANCED THREE-PHASE CIRCUITS; SINGLE-LINE DIAGRAMS

By combining the principle of Δ -Y equivalence with the technique revealed by Example A-1, a simple method of reducing a balanced three-phase-circuit problem to its corresponding single-phase problem can be developed. All the methods of single-phase-circuit analysis thus become available for its solution. The end results of the single-phase analysis are then translated back into three-phase terms to give the final results.

In carrying out this procedure, phasor diagrams need be drawn for only one phase of the Y connection, the diagrams for the other two phases being unnecessary repetition. Furthermore, circuit diagrams can be simplified by drawing only one phase. Examples of such *single-line diagrams* are given in Fig. A-17, showing two three-phase generators with their associated lines or cables supplying a common substation load. Specific connections of apparatus can be indicated if desired. Thus, Fig. A-17b shows that G_1 is Y-connected and G_2 is Δ -connected. Impedances are given in ohms per phase.

When one is dealing with power, reactive power, and voltamperes, it is sometimes more convenient to deal with the entire three-phase circuit at once instead of concentrating on one phase. This possibility arises because simple expressions for three-phase power, reactive power, and voltamperes can be written in terms of line-to-line voltage and line current regardless of whether the circuit is Y- or Δ -connected. Thus, from Eqs. A-17 and A-18, three-phase power is

$$P = 3P_p = 3E_p I_p \cos \theta \quad (\text{A-25})$$

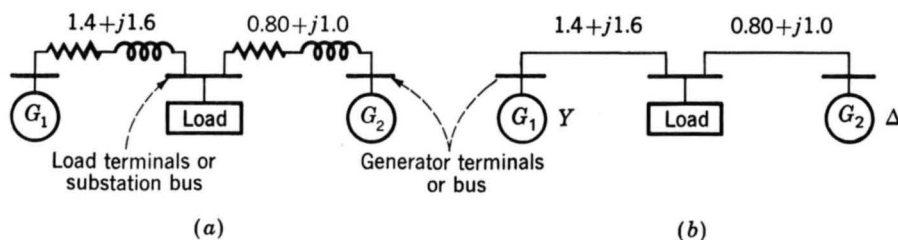


Fig. A-17. Examples of single-line diagrams.

For a Y connection, $I_p = I_{\text{line}}$ and $E_p = E_{\text{line}}/\sqrt{3}$. For a Δ connection, $I_p = I_{\text{line}}/\sqrt{3}$ and $E_p = E_{\text{line}}$. In either case, Eq. A-25 becomes

$$P = \sqrt{3} E_{\text{line}} I_{\text{line}} \cos \theta \quad (\text{A-26})$$

$$\text{Similarly,} \quad Q = \sqrt{3} E_{\text{line}} I_{\text{line}} \sin \theta \quad (\text{A-27})$$

$$\text{and} \quad \text{VA} = \sqrt{3} E_{\text{line}} I_{\text{line}} \quad (\text{A-28})$$

It should be borne in mind, however, that the power-factor angle θ , given by Eq. A-23, is the angle between \hat{E}_p and \hat{I}_p and not that between \hat{E}_{line} and \hat{I}_{line} .

EXAMPLE A-4

Figure A-17 is the equivalent circuit of a load supplied from two three-phase generating stations over lines having the impedances per phase given on the diagram. The load requires 30 kW at 0.80 power factor lagging. Generator G_1 operates at a terminal voltage of 797 V line to line and supplies 15 kW at 0.80 power factor lagging. Find the load voltage and the terminal voltage and power and reactive-power output of G_2 .

Solution

Let I , P , and Q , respectively, denote line current and three-phase active and reactive power. The subscripts 1 and 2 denote the respective branches of the system; the subscript r denotes a quantity measured at the receiving end of the line. We then have

$$I_1 = \frac{P_1}{\sqrt{3} E_1 \cos \theta_1} = \frac{15,000}{\sqrt{3} (797) (0.80)} = 13.6 \text{ A}$$

$$P_{r1} = P_1 - 3I_1^2 R_1 = 15,000 - 3(13.6)^2 (1.4) = 14,220 \text{ W}$$

$$\begin{aligned} Q_{r1} &= Q_1 - 3I_1^2 X_1 = 15,000 \tan (\cos^{-1} 0.80) - 3(13.6)^2 (1.6) \\ &= 10,350 \text{ VA reactive} \end{aligned}$$

The factor 3 appears before $I_1^2 R_1$ and $I_1^2 X_1$ in the last two equations because the current I_1 exists in all three lines. The load voltage is

$$\begin{aligned} E_L &= \frac{\text{VA}}{\sqrt{3} (\text{current})} = \frac{\sqrt{(14,220)^2 + (10,350)^2}}{\sqrt{3} (13.6)} \\ &= 748 \text{ V line to line} \end{aligned}$$

Since the load requires 30,000 W and 30,000 $\tan (\cos^{-1} 0.80)$ or 22,500 VA reactive,

$$P_{r_2} = 30,000 - 14,220 = 15,780 \text{ W}$$

and $Q_r = 22,500 - 10,350 = 12,150 \text{ VA reactive}$

$$I_2 = \frac{\text{VA}}{\sqrt{3}(\text{voltage})} = \frac{\sqrt{(15,780)^2 + (12,150)^2}}{\sqrt{3}(748)} = 15.4 \text{ A}$$

$$P_2 = P_{r_2} + 3I_2^2 R_2 = 15,780 + 3(15.4)^2(0.80) = 16,350 \text{ W}$$

$$Q_2 = Q_{r_2} + 3I_2^2 X_2 = 12,150 + 3(15.4)^2(1.0) = 12,870 \text{ VA reactive}$$

$$E_2 = \frac{\text{VA}}{\sqrt{3}(\text{current})} = \frac{\sqrt{(16,350)^2 + (12,870)^2}}{\sqrt{3}(15.4)}$$

$$= 780 \text{ V line to line}$$

A-5 OTHER POLYPHASE SYSTEMS

Although three-phase systems are by far the most common of all polyphase systems, other numbers of phases are used for specialized purposes. The five-wire four-phase system (Fig. A-18) is sometimes used for low-voltage distribution. It has the advantage that for a phase voltage of 115 V, single-phase voltages of 115 (between a , b , c , or d and o , Fig. A-18) and 230 V (between a and c or b and d) are available as well as a system of polyphase voltages. Essentially the same advantages are possessed by four-wire three-phase systems having a line-to-neutral voltage of 120 V and a line-to-line voltage of 208 V, however.

Four-phase systems are obtained from three-phase systems by means of special transformer connections. Half of the four-phase system—the part ao (Fig. A-18), for example—constitutes a two-phase system. In

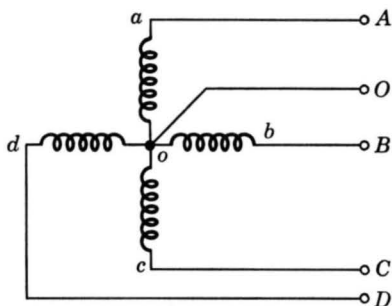


Fig. A-18. A five-wire four-phase system.

mercury-arc rectifiers, 6-, 12-, 18-, and 36-phase connections are used for the conversion of alternating to direct current. These systems are also obtained by transformation from three-phase systems.

When the loads and voltages are balanced, the methods of analysis for three-phase systems can be adapted to any of the other polyphase systems by considering one phase of that polyphase system. Of course, the basic voltage, current, and power relations must be modified to suit the particular polyphase system.

Voltages, Magnetic Fields, and Inductances of Distributed AC Windings

Both amplitude and waveform of the generated voltage and armature mmf's in machines are determined by the winding arrangements and general machine geometry. These configurations in turn are dictated by economic use of space and materials in the machine and by suitability for the intended service. In this appendix we supplement the introductory discussion of these considerations in Chap. 4 by analytical treatment of ac voltages and mmf's in the balanced steady state. Attention is confined to the time-fundamental component of voltages and the space-fundamental component of mmf's.

B-1 GENERATED VOLTAGES

In accordance with Eq. 4-54, the rms generated voltage per phase for a concentrated winding having N_{ph} turns per phase is

$$E = \sqrt{2} \pi f N_{ph} \Phi \quad (B-1)$$

where f is the frequency and Φ the fundamental flux per pole.

A more complex and practical winding will have coil sides for each phase distributed in several slots per pole. Equation B-1 can then be used to compute the voltage distribution of individual coils. To determine the voltage of an entire phase group, the voltages of the component coils must be added as phasors. Such addition of fundamental-frequency voltages is the subject of this article.

a. Distributed Fractional-Pitch Windings

A simple example of a distributed winding is illustrated in Fig. B-1 for a three-phase two-pole machine. This case retains all the features of a more general one with any integral number of phases, poles, and slots per pole per phase. At the same time, a *double-layer winding* is shown. Double-layer windings usually lead to simpler end connections and to a machine which is more economical to manufacture and are found in all machines except some small motors below 10 hp. Generally, one side of a coil, such as a_1 , is placed in the bottom of a slot, and the other side, $-a_1$, is placed in the top of another slot. Coil sides such as a_1 and a_3 or a_2 and a_4 which are in

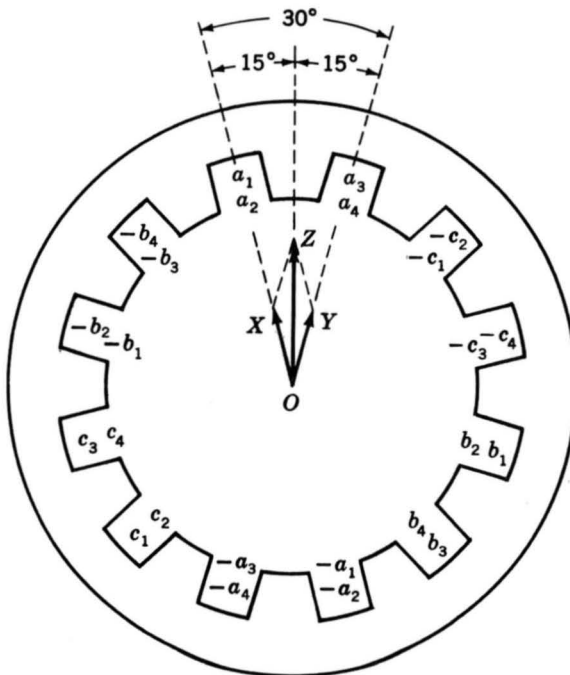


Fig. B-1. Distributed three-phase two-pole full-pitch armature winding with voltage phasor diagram.

adjacent slots and associated with the same phase constitute a *phase belt*. All phase belts are alike when an integral number of slots per pole per phase are used, and for the normal machine the peripheral angle subtended by a phase belt is 60 electrical degrees for a three-phase machine and 90 electrical degrees for a two-phase machine.

Individual coils in Fig. B-1 all span a full pole pitch, or 180 electrical degrees; accordingly, the winding is a *full-pitch winding*. Suppose now that all coil sides in the tops of the slots are shifted one slot counterclockwise, as in Fig. B-2. Any coil, such as $a_1, -a_1$, then spans only five-sixths a pole pitch or $\frac{5}{6}(180) = 150$ electrical degrees, and the winding is a *fractional-pitch*, or *chorded*, winding. Similar shifting by two slots yields a $\frac{2}{3}$ -pitch winding, and so forth. Phase groupings are now intermingled, for some slots contain coil sides in phases a and b , a and c , and b and c . Individual phase groups, such as that formed by a_1, a_2, a_3, a_4 on one side and $-a_1, -a_2, -a_3, -a_4$ on the other, are still displaced by 120 electrical degrees from the groups in other phases so that three-phase voltages are produced. Besides the minor feature of shortening the end connections, fractional-pitch windings will be found to decrease the harmonic content of both voltage and mmf waves.

The end connections between the coil sides are normally in a region of negligible flux density, and hence altering them does not significantly af-

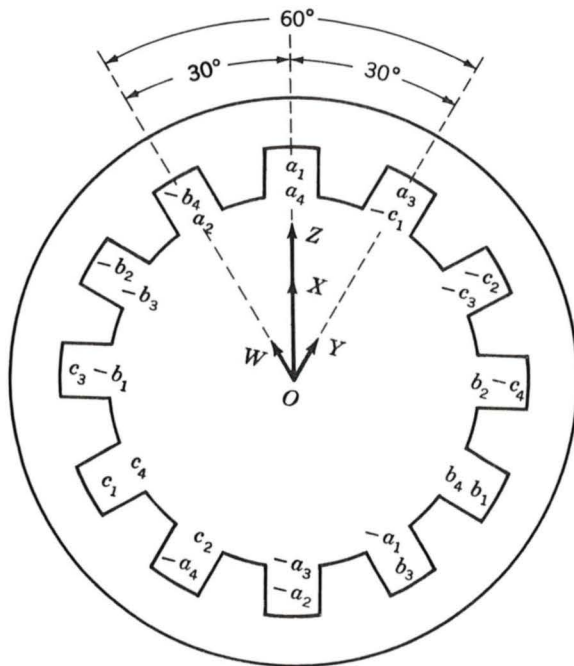


Fig. B-2. Distributed three-phase two-pole fractional-pitch armature winding with voltage phasor diagram.

fect the mutual flux linkages of the winding. Allocation of coil sides in slots is then the factor determining the generated voltages, and only that allocation need be specified in Figs. B-1 and B-2. The only requisite is that all coil sides in a phase be included in the interconnection in such a manner that individual voltages make a positive contribution to the total. The practical consequence is that end connections can be made according to the dictates of manufacturing simplicity; the theoretical consequence is that when computational advantages result, the coil sides in a phase can be combined in an arbitrary fashion to form equivalent coils.

One sacrifice is made in using the distributed and fractional-pitch windings of Figs. B-1 and B-2 compared with a concentrated full-pitch winding: for the same number of turns per phase, the fundamental-frequency generated voltage is lower. The harmonics are, in general, lowered by an appreciably greater factor, however, and the total number of turns which can be accommodated on a fixed iron geometry is increased. The effect of distributing the winding in Fig. B-1 is that the voltages of coils a_1 and a_2 are not in phase with those of coils a_3 and a_4 . Thus, the voltage of coils a_1 and a_2 can be represented by phasor OX in Fig. B-1, and that of coils a_3 and a_4 by the phasor OY . The time-phase displacement between these two voltages is the same as the electrical angle between adjacent slots, so that OX and OY coincide with the centerlines of adjacent slots. The resultant phasor OZ for phase a is obviously smaller than the arithmetic sum of OX and OY .

In addition, the effect of fractional pitch in Fig. B-2 is that a coil links a smaller portion of the total pole flux than if it were a full-pitch coil. The effect can be superimposed on that of distributing the winding by regarding coil sides a_2 and $-a_1$ as an equivalent coil with the phasor voltage OW (Fig. B-2), coil sides a_1 , a_4 , $-a_2$, and $-a_3$ as two equivalent coils with the phasor voltage OX (twice the length of OW), and coil sides a_3 and $-a_4$ as an equivalent coil with phasor voltage OY . The resultant phasor OZ for phase a is obviously smaller than the arithmetic sum of OW , OX , and OY and is also smaller than OZ in Fig. B-1.

The combination of these two effects can be included in a *winding factor* k_w to be used as a reduction factor in Eq. B-1. Thus, the generated voltage per phase is

$$E = \sqrt{2} \pi k_w f N_{ph} \Phi \quad (\text{B-2})$$

where N_{ph} is the total turns in series per phase and k_w accounts for the departure from the concentrated full-pitch case. For a three-phase machine, Eq. B-2 yields the line-to-line voltage for a Δ -connected winding and the line-to-neutral voltage for a Y-connected winding. As in any balanced Y connection, the line-to-line voltage of the latter winding is $\sqrt{3}$ times the line-to-neutral voltage.

b. Breadth and Pitch Factors

By separately considering the effects of distributing and of chording the winding, reduction factors can be obtained in generalized form convenient for quantitative analysis. The effect of distributing the winding in n slots per phase belt is to yield n voltage phasors phase-displaced by the electrical angle γ between slots, γ being equal to 180 electrical degrees divided by the number of slots per pole. Such a group of phasors is shown in Fig. B-3a and, in a more convenient form for addition, again in Fig. B-3b. Each phasor AB , BC , and CD is the chord of a circle with center at O and subtends the angle γ at the center. The phasor sum AD subtends the angle $n\gamma$, which, as noted previously, is 60 electrical degrees for the normal, uniformly distributed three-phase machine and 90 electrical degrees for the corresponding two-phase machine. From triangles OaA and OAd , respectively,

$$OA = \frac{Aa}{\sin(\gamma/2)} = \frac{AB}{2 \sin(\gamma/2)} \quad (\text{B-3})$$

$$OA = \frac{Ad}{\sin(n\gamma/2)} = \frac{AD}{2 \sin(n\gamma/2)} \quad (\text{B-4})$$

Equating these two values of OA yields

$$AD = AB \frac{\sin(n\gamma/2)}{\sin(\gamma/2)} \quad (\text{B-5})$$

But the arithmetic sum of the phasors is $n(AB)$. Consequently, the reduc-

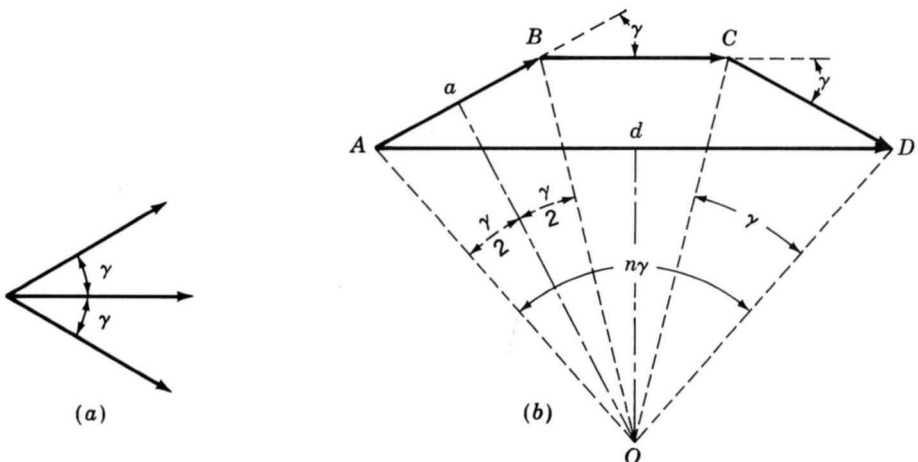


Fig. B-3. (a) Coil voltage phasors and (b) phasor sum.

tion factor arising from distributing the winding is

$$k_b = \frac{AD}{nAB} = \frac{\sin (n\gamma/2)}{n \sin (\gamma/2)} \quad (\text{B-6})$$

The factor k_b is called the *breadth factor* of the winding.

The effect of chording on the coil voltage can be obtained by first determining the flux linkages with the fractional-pitch coil. Thus, in Fig. B-4 coil side $-a$ is only ρ electrical degrees from side a instead of the full 180° . The flux linkages with the coil are

$$\lambda = NB_{\text{peak}} l r \frac{2}{P} \int_{\rho+\alpha}^{\alpha} \sin \theta d\theta \quad (\text{B-7})$$

$$\lambda = NB_{\text{peak}} l r \frac{2}{P} [\cos (\alpha + \rho) - \cos \alpha] \quad (\text{B-8})$$

where l = axial length of coil side

r = coil radius

P = number of poles

With α replaced by ωt to indicate rotation at ω electrical radians per second, Eq. B-8 becomes

$$\lambda = NB_{\text{peak}} l r \frac{2}{P} [\cos (\omega t + \rho) - \cos \omega t] \quad (\text{B-9})$$

The addition of cosine waves required in the brackets of Eq. B-9 may be

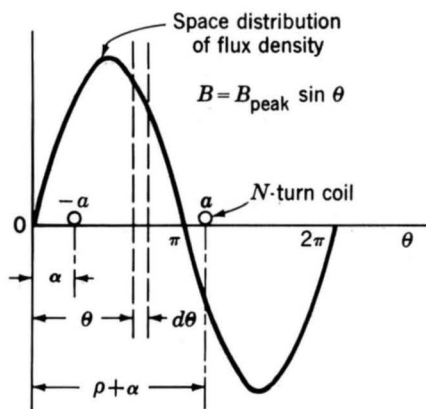


Fig. B-4. Fractional-pitch coil in sinusoidal field.

performed by a phasor diagram as indicated in Fig. B-5, from which it follows that

$$\cos(\omega t + \rho) - \cos \omega t = -2 \cos \frac{\pi - \rho}{2} \cos \left(\omega t - \frac{\pi - \rho}{2} \right) \quad (\text{B-10})$$

a result which can also be obtained directly from the terms in Eq. B-9 by the appropriate trigonometric transformations. The flux linkages are then

$$\lambda = -NB_{\text{peak}} l r \frac{4}{P} \cos \frac{\pi - \rho}{2} \cos \left(\omega t - \frac{\pi - \rho}{2} \right) \quad (\text{B-11})$$

and the instantaneous voltage is

$$e = \omega NB_{\text{peak}} l r \frac{4}{P} \cos \frac{\pi - \rho}{2} \sin \left(\omega t - \frac{\pi - \rho}{2} \right) \quad (\text{B-12})$$

The phase angle $(\pi - \rho)/2$ in Eq. B-12 merely indicates that the instantaneous voltage is no longer zero when α in Fig. B-4 is zero. The factor $\cos[(\pi - \rho)/2]$ is an amplitude-reduction factor, however, so that the rms voltage of Eq. B-1 is modified to

$$E = \sqrt{2} \pi k_p f N_{\text{ph}} \Phi \quad (\text{B-13})$$

where the *pitch factor* k_p is

$$k_p = \cos \frac{\pi - \rho}{2} \quad (\text{B-14})$$

When both the breadth and pitch factors apply, the rms voltage is

$$E = \sqrt{2} \pi k_b k_p f N_{\text{ph}} \Phi \quad (\text{B-15})$$

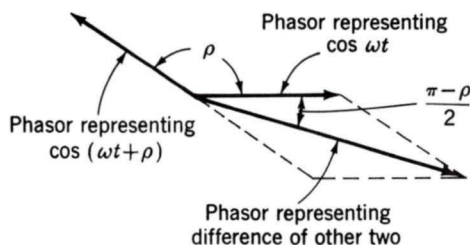


Fig. B-5. Phasor addition for fractional-pitch coil.

which is an alternate form of Eq. B-2; the winding factor k_w is seen to be the product of the pitch and breadth factors.

$$k_w = k_b k_p \quad (\text{B-16})$$

EXAMPLE B-1

Calculate the breadth, pitch, and winding factors for the distributed fractional-pitch winding of Fig. B-2.

Solution

The winding of Fig. B-2 has two coils per phase belt, separated by an electrical angle of 30° . From Eq. B-6 the breadth factor is

$$k_b = \frac{\sin(n\gamma/2)}{n \sin(\gamma/2)} = \frac{\sin[2(30^\circ)/2]}{2 \sin(30^\circ/2)} = 0.966$$

The fractional-pitch coils span $150^\circ = 5\pi/6$ rad, and from Eq. B-14 the pitch factor is

$$k_p = \cos \frac{\pi - \rho}{2} = \cos \frac{\pi - 5\pi/6}{2} = 0.966$$

The winding factor is

$$k_w = k_b k_p = 0.933$$

B-2 ARMATURE MMF WAVES

Distribution of a winding in several slots per pole per phase and the use of fractional-pitch coils influence not only the emf generated in the winding but also the magnetic field produced by it. Space-fundamental components of the mmf distributions are examined in this article.

a. Concentrated Full-Pitch Windings

We have seen in Art. 4-3 that a concentrated winding of N turns in a P -pole machine produces a rectangular mmf wave around the air-gap circumference. With excitation by a sinusoidal rms current I , the time-maximum amplitude of the space-fundamental component of the wave is, in accor-

dance with Eq. 4-5,

$$\frac{4}{\pi} \frac{N}{P} (\sqrt{2} I) \quad A \cdot \text{turns/pole} \quad (\text{B-17})$$

For a polyphase concentrated winding, the amplitude for one phase becomes

$$\frac{4}{\pi} \frac{N_{\text{ph}}}{P} (\sqrt{2} I) \quad A \cdot \text{turns/pole} \quad (\text{B-18})$$

where N_{ph} is the number of series turns per phase.

Each phase of a polyphase concentrated winding creates such a pulsating standing mmf wave in space. This situation forms the basis of the analysis leading to Eq. 4-40. For concentrated windings, Eq. 4-40 can be rewritten as

$$\mathcal{F}(\theta, t) = \frac{3}{2} \frac{4}{\pi} \frac{N_{\text{ph}}}{P} (\sqrt{2} I) \cos(\theta - \omega t) \quad (\text{B-19})$$

The amplitude of the resultant mmf wave in a three-phase machine in ampere-turns per pole is then

$$F_A = \frac{3}{2} \frac{4}{\pi} \frac{N_{\text{ph}}}{P} (\sqrt{2} I) = 0.90 \frac{3N_{\text{ph}}}{P} I \quad (\text{B-20})$$

Similarly, for a q -phase machine, the amplitude is

$$F_A = \frac{q}{2} \frac{4}{\pi} \frac{N_{\text{ph}}}{P} (\sqrt{2} I) = 0.90 \frac{qN_{\text{ph}}}{P} I \quad (\text{B-21})$$

In Eqs. B-20 and B-21, I is the rms current per phase. The equations include only the fundamental component of the actual distribution and apply to concentrated full-pitch windings with balanced excitation.

b. Distributed Fractional-Pitch Winding

When the coils in each phase of a winding are distributed among several slots per pole, the resultant space-fundamental mmf can be obtained by superposition from the preceding simpler considerations for a concentrated winding. The effect of distribution can be seen from Fig. B-6, which is a reproduction of the three-phase two-pole full-pitch winding with two slots per pole per phase given in Fig. B-1. Coils a_1 and a_2 , b_1 and b_2 , and c_1 and c_2 by themselves constitute the equivalent of a three-phase two-pole concentrated winding because they form three sets of coils excited by polyphase currents and mechanically displaced 120° from each other. They therefore produce a rotating space-fundamental mmf; the amplitude of this contribu-

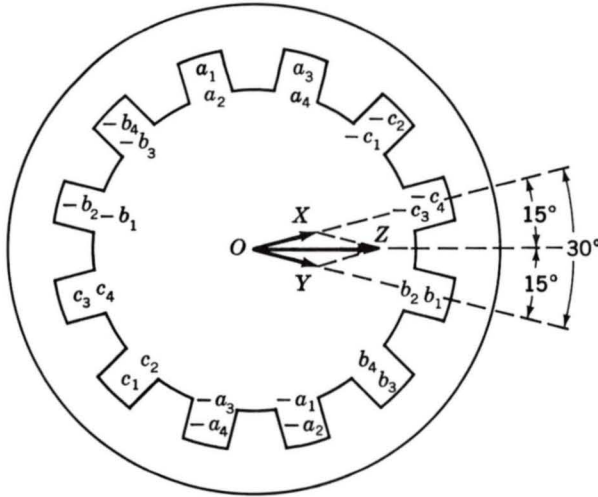


Fig. B-6. Distributed three-phase two-pole full-pitch armature winding with mmf phasor diagram.

tion is given by Eq. B-20 when N_{ph} is taken as the sum of the series turns in coils a_1 and a_2 only. Similarly, coils a_3 and a_4 , b_3 and b_4 , and c_3 and c_4 produce another identical mmf wave, but one which is phase-displaced in space by the slot angle γ from the former wave. The resultant space-fundamental mmf wave for the winding can be obtained by adding these two sinusoidal contributions.

The contribution from the $a_1a_2b_1b_2c_1c_2$ coils can be represented by the phasor OX in Fig. B-6. Such phasor representation is appropriate because the waveforms concerned are sinusoidal, and phasor diagrams are simply convenient means for adding sine waves. These are space sinusoids, however, not time sinusoids. Phasor OX is drawn in the space position of the mmf peak for an instant of time when the current in phase a is a maximum. The length of OX is proportional to the number of turns in the associated coils. Similarly, the contribution from the $a_3a_4b_3b_4c_3c_4$ coils may be represented by the phasor OY . Accordingly, the phasor OZ represents the resultant mmf wave. Just as in the corresponding voltage diagram, the resultant mmf is seen to be smaller than if the same number of turns per phase were concentrated in one slot per pole.

In like manner, mmf phasors can be drawn for fractional-pitch windings as illustrated in Fig. B-7, which is a reproduction of the three-phase two-pole $\frac{5}{6}$ -pitch winding with two slots per pole per phase given in Fig. B-2. Phasor OW represents the contribution for the equivalent coils formed by conductors a_2 and $-a_1$, b_2 and $-b_1$, and c_2 and $-c_1$; OX for a_1a_4 and $-a_3$, $-a_2$, b_1b_4 and $-b_3$, $-b_2$, and c_1c_4 and $-c_3$, $-c_2$; and OY for a_3 and $-a_4$, b_3 and $-b_4$, and c_3 and $-c_4$. The resultant phasor OZ is, of course, smaller than

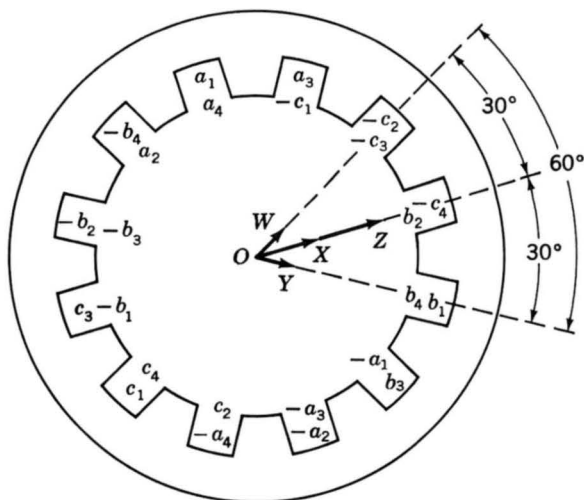


Fig. B-7. Distributed three-phase two-pole fractional-pitch armature winding with mmf phasor diagram.

the algebraic sum of the individual contributions and is also smaller than OZ in Fig. B-6.

By comparison with Figs. B-1 and B-2, these phasor diagrams can be seen to be identical with those for generated voltages. It therefore follows that pitch and breadth factors previously developed can be applied directly to the determination of resultant mmf. Thus, for a distributed fractional-pitch polyphase winding, the amplitude of the space-fundamental component of mmf can be obtained by using $k_b k_p N_{ph}$ instead of simply N_{ph} in Eqs. B-20 and B-21. These equations then become

$$F_A = \frac{3}{2} \frac{4}{\pi} \frac{k_b k_p N_{ph}}{P} (\sqrt{2} I) = 0.90 \frac{3 k_b k_p N_{ph}}{P} I \quad (\text{B-22})$$

for a three-phase machine and

$$F_A = \frac{q}{2} \frac{4}{\pi} \frac{k_b k_p N_{ph}}{P} (\sqrt{2} I) = 0.90 \frac{q k_b k_p N_{ph}}{P} I \quad (\text{B-23})$$

for a q -phase machine, where F_A is in ampere-turns per pole.

B-3 AIR-GAP INDUCTANCES OF DISTRIBUTED WINDINGS

Figure B-8a shows an N -turn full-pitch concentrated armature winding in a magnetic structure with a concentric cylindrical rotor. The mmf of this

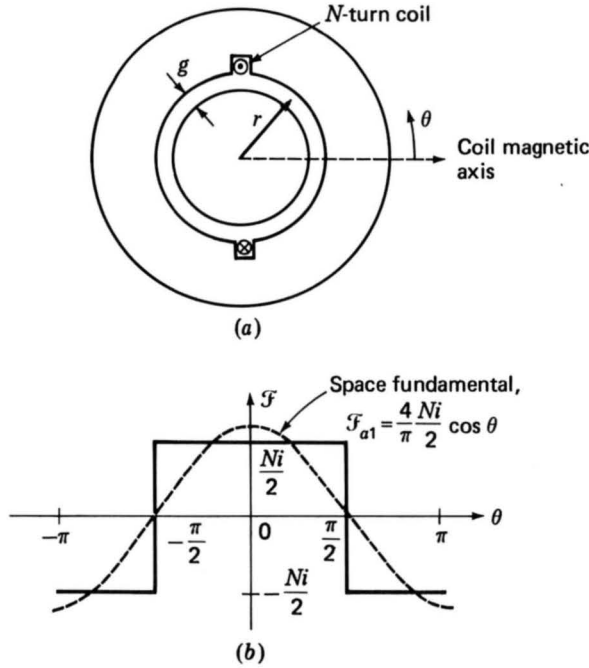


Fig. B-8. (a) N -turn concentrated coil and (b) resultant mmf.

configuration is shown in Fig. B-8b. Since the air-gap length g is much smaller than the average air-gap radius r , the air-gap radial magnetic field can be considered uniform and equal to the mmf divided by g .

From Eq. 4-4 the space-fundamental mmf is given by

$$\mathcal{F}_{a1} = \frac{4}{\pi} \frac{Ni}{2} \cos \theta \quad (\text{B-24})$$

and the corresponding air-gap flux density is

$$\mathcal{B} = \mu_0 \frac{\mathcal{F}_{a1}}{g} = \frac{2\mu_0 Ni}{\pi g} \cos \theta \quad (\text{B-25})$$

Equation B-25 can be integrated to find the fundamental air-gap flux per pole (Eq. 4-4)

$$\Phi = l \int_{-\pi/2}^{\pi/2} \mathcal{B} r d\theta = \frac{4\mu_0 N l r i}{\pi g} \quad (\text{B-26})$$

where l is the axial length of the air gap. The air-gap inductance of the coil

can be found from Eq. 1-22

$$L = \frac{\lambda}{i} = \frac{N\Phi}{i} = \frac{4\mu_0 N^2 lr}{\pi g} \quad (\text{B-27})$$

For a distributed P -pole coil with N_{ph} series turns and a winding factor $k_w = k_b k_p$, the air-gap inductance can be found from Eq. B-27 by substituting for N the effective turns per pole pair ($2k_w N_{ph}/P$)

$$L = \frac{4}{\pi} \mu_0 \left(\frac{2k_w N_{ph}}{P} \right)^2 \frac{lr}{g} = \frac{16\mu_0 (k_w N_{ph})^2 lr}{\pi g P^2} \quad (\text{B-28})$$

Finally, Fig. B-9 shows schematically two coils (labeled 1 and 2) with winding factors k_{w1} and k_{w2} and with $2N_1/P$ and $2N_2/P$ turns per pole pair, respectively; their magnetic axes are separated by an electrical angle α (equal to $P/2$ times their spatial angular displacement). The mutual inductance between these two windings is given by

$$\begin{aligned} L_{12} &= \frac{4}{\pi} \mu_0 \frac{2k_{w1} N_1}{P} \frac{2k_{w2} N_2}{P} \frac{lr}{g} \cos \alpha \\ &= \frac{16\mu_0 (k_{w1} N_1) (k_{w2} N_2) lr}{\pi g P^2} \cos \alpha \end{aligned} \quad (\text{B-29})$$

Although the figure shows one winding on the rotor and the second on the stator, Eq. B-29 is equally valid for the case where both windings are on the same member.

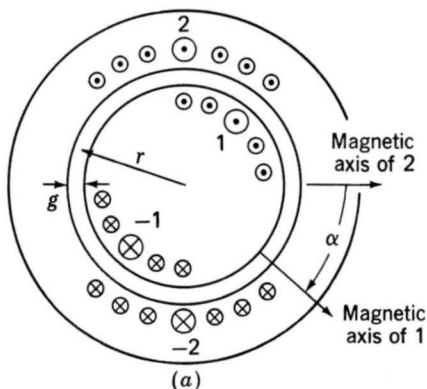


Fig. B-9. Two distributed windings separated by electrical angle α .

EXAMPLE B-2

The two-pole stator-winding distribution of Fig. B-2 is found on an induction motor with an air-gap length of 0.015 in (3.81×10^{-4} m), an average rotor radius of 2.5 in (6.35×10^{-2} m), and an axial length of 8 in (0.203 m). Each stator coil has 15 turns, and the coil phase connections are as shown in Fig. B-10. Calculate the phase-*a* air-gap inductance L_{aa0} and *a*-to-*b* mutual inductance L_{ab} .

Solution

Note that the placement of the coils around the stator is such that the flux linkages of each of the two parallel paths are equal. In addition, the air-gap flux distribution is unchanged if, rather than dividing equally between the two legs, as actually occurs, one path were disconnected and all the current were to flow in the remaining path. Thus, the phase inductances can be found by calculating the inductances associated with only one of the parallel paths.

This result may appear to be somewhat puzzling because the two paths are connected in parallel, and thus it would appear that the parallel inductance should be one-half that of the single-path inductance. However, the inductances share a common magnetic circuit, and their combined inductance must reflect this fact. It should be pointed out that the phase resistance is one-half that of each of the paths.

The winding factor has been calculated in Example B-1. Thus, from Eq. B-28,

$$L_{aa0} = \frac{16\mu_0 k_w^2 N_{ph}^2 l r}{\pi g P^2}$$

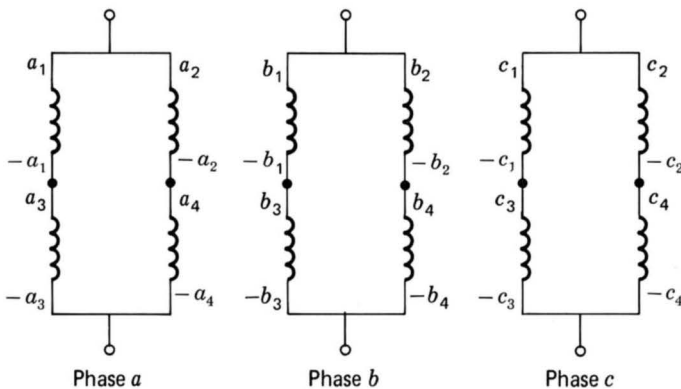


Fig. B-10. Coil phase connections of Fig. B-2 for Example B-2.

$$\begin{aligned}
&= \frac{16(4\pi \times 10^{-7})(0.933)^2(30)^2(0.203)(6.35 \times 10^{-2})}{\pi(3.81 \times 10^{-4})(2^2)} \\
&= 42.4 \text{ mH}
\end{aligned}$$

The winding axes are separated by $\alpha = 120^\circ$, and thus from Eq. B-28

$$L_{ab} = \frac{16\mu_0 k_{ph}^2 N_{ph}^2 l r}{\pi g P^2} \cos \alpha = -21.2 \text{ mH}$$

Engineering Aspects of Practical Electric Machine Performance and Operation

In this book the basic essential features of electric machinery have been discussed; this material forms the basis for understanding the behavior of electric machinery of all types. In this appendix our objective is to introduce practical issues associated with the engineering implementation of the machinery concepts which have been developed. Issues common to all electric machine types such as losses, cooling, and rating are discussed.

C-1 LOSSES

Consideration of machine losses is important for three reasons: (1) Losses determine the efficiency of the machine and appreciably influence its operating cost; (2) losses determine the heating of the machine and hence the

rating or power output that can be obtained without undue deterioration of the insulation; and (3) the voltage drops or current components associated with supplying the losses must be properly accounted for in a machine representation. Machine efficiency, like that of transformers or any energy-transforming device, is given by

$$\text{Efficiency} = \frac{\text{output}}{\text{input}} \quad (\text{C-1})$$

which can also be expressed as

$$\text{Efficiency} = \frac{\text{input} - \text{losses}}{\text{input}} = 1 - \frac{\text{losses}}{\text{input}} \quad (\text{C-2})$$

$$\text{Efficiency} = \frac{\text{output}}{\text{output} + \text{losses}} \quad (\text{C-3})$$

Rotating machines in general operate efficiently except at light loads. The full-load efficiency of average motors, e.g., is in the neighborhood of 74 percent for 1-hp size, 89 percent for 50-hp, 93 percent for 500-hp, and 97 percent for 5000-hp. The efficiency of slow-speed motors is usually lower than that of high-speed motors, the total spread being 3 or 4 percent.

The forms given by Eqs. C-2 and C-3 are often used for electric machines, since their efficiency is most commonly determined by measurement of losses instead of by directly measuring the input and output under load. Efficiencies determined from loss measurements can be used in comparing competing machines if exactly the same methods of measurement and computation are used in each case. For this reason, the various losses and the conditions for their measurement are precisely defined by the American National Standards Institute (ANSI), the Institute of Electrical and Electronics Engineers (IEEE), and the National Electrical Manufacturers Association (NEMA). The following discussion of individual losses incorporates many of these provisions as given in ANSI Standard C50, although no attempt is made to present all the details.

***I*²*R* Losses**

Of course, *I*²*R* losses are found in all windings of the machine. By convention, these losses are computed on the basis of the dc resistances of the winding at 75°C. Actually the *I*²*R* loss depends on the effective resistance of the winding under the operating frequency and flux conditions. The increment in loss represented by the difference between dc and effective resistances is included with stray load losses, discussed below. In the field

circuits of synchronous and dc machines, only the losses in the field winding are charged against the machine; the losses in external sources supplying the excitation are charged against the plant of which the machine is a part. Closely associated with I^2R loss is the *brush-contact loss* at slip rings and commutators. By convention, this loss is normally neglected for induction and synchronous machines, and for industrial-type dc machines the voltage drop at the brushes is regarded as constant at 2 V total when carbon and graphite brushes with shunts (pigtailed) are used.

Mechanical Losses

These losses consist of brush and bearing friction, windage, and the power required to circulate the air through the machine and ventilating system, if one is provided, whether by self-contained or external fans (except for the power required to force air through long or restricted ducts external to the machine). Friction and windage losses can be measured by determining the input to the machine running at the proper speed but unloaded and unexcited. Frequently they are lumped with core loss and determined at the same time.

Open-Circuit, or No-Load, Core Loss

Open-circuit core loss consists of the hysteresis and eddy-current losses arising from changing flux densities in the iron of the machine with only the main exciting winding energized. In dc and synchronous machines, these losses are confined largely to the armature iron, although the flux pulsations arising from slot openings will cause losses in the field iron as well, particularly in the pole shoes or surfaces of the field iron. In inductance machines the losses are confined largely to the stator iron. Open-circuit core loss can be found by measuring the input to the machine when it is operating unloaded at rated speed or frequency and under the appropriate flux or voltage conditions and then deducting the friction and windage loss and, if the machine is self-driven during the test, the no-load armature I^2R loss (no-load stator I^2R loss for an induction motor). Usually, data are taken for a curve of core loss as a function of armature voltage in the neighborhood of rated voltage. The core loss under load is then considered to be the value at a voltage equal to rated voltage corrected for armature ohmic-resistance drop under load (a phasor correction for an ac machine). For induction motors, however, this correction is dispensed with, and the core loss at rated voltage is used. For efficiency determination alone, there is no need to segregate open-circuit core loss and friction and windage loss; the sum of these two losses is termed the *no-load rotational loss*.

Eddy-current loss is dependent on the squares of the flux density, frequency, and thickness of laminations. Under normal machine conditions it

can be expressed to a sufficiently close approximation as

$$P_e = K_e (B_{\max} f \tau)^2 \quad (\text{C-4})$$

where τ = lamination thickness

B_{\max} = maximum flux density

f = frequency

K_e = proportionality constant

The value of K_e depends on the units used, volume of iron, and resistivity of the iron. Variation of hysteresis loss can be expressed in equation form only on an empirical basis. The most commonly used relation is

$$P_h = K_h f B_{\max}^n \quad (\text{C-5})$$

where K_h is a proportionality constant dependent on the characteristics and volume of iron and the units used and the exponent n ranges from 1.5 to 2.5, a value of 2.0 often being used for estimating purposes in machines. In both Eqs. C-4 and C-5 frequency can be replaced by speed and flux density by the appropriate voltage, with the proportionality constants changed accordingly.

When the machine is loaded, the space distribution of flux density is significantly changed by the mmf of the load currents. The actual core losses may increase noticeably. For example, mmf harmonics cause appreciable losses in the iron near the air-gap surfaces. The total increment in core loss is classified as part of the stray load loss.

Stray Load Loss

Stray load loss consists of the losses arising from nonuniform current distribution in the copper and the additional core losses produced in the iron by distortion of the magnetic flux by the load current. It is a difficult loss to determine accurately. By convention it is taken as 1.0 percent of the output for dc machines. For synchronous and induction machines it can be found by test.

Study of the foregoing classification of the losses in a machine shows it to have a few features which, from a fundamental viewpoint, are somewhat artificial. Illustrations are offered by the division of iron losses into no-load core loss and an increment which appears under load, the division of I^2R losses into ohmic I^2R losses and an increment created by nonuniform current distribution, and the lumping of these two increments in the scavengerlike stray-load-loss category. These features are dictated by ease of testing. They are justified by the fact that the principal motivation is the determination of the total losses and efficiency as nearly equal to the actual values as possible but also suitable for economic comparison of ma-

chines. Because of this seeming dominance of efficiency aspects, it may be appropriate to emphasize once more that losses play more than a book-keeping role in machine operation.

In a generator, for example, components of mechanical input torque to the shaft are obviously required to supply I^2R and iron losses as well as friction and windage losses and the generator output. These losses may therefore be appreciable factors in the damping of electric and mechanical transients in the machine. Components of the stray load loss, although they may be individually only a fraction of a percent of the output, may be of first importance in the design of the machine. For example, rotor heating is usually a limiting factor in the design of large high-speed alternators, and the components of stray loss on the surface of the rotor structure are of great importance because they directly affect the dimensions of an alternator of given output. Of more direct concern in theoretical aspects is the influence of hysteresis and eddy currents in causing flux to lag behind mmf. There is a small angle of lag between the rotating mmf waves in a machine and the corresponding component flux-density waves. Associated with this influence is a torque on magnetic material in a rotating field, a torque proportional to the hysteresis and eddy-current losses in the material. Although the torque accompanying these losses is relatively small in normal machines, direct use of it is made in one type of small motor, the hysteresis motor.

C-2 RATING AND HEATING

One of the most common and important questions in the application of machines, transformers, and other electrical equipment is: What maximum output can be obtained? The answer, of course, depends on various factors, since the machine, while providing this output, in general must meet definite performance standards. A universal requirement is that the life of the machine not be unduly shortened by overheating. The temperature rise resulting from the losses considered in the previous article is therefore a major factor in the rating of a machine.

The operating temperature of a machine is closely associated with its life expectancy because deterioration of the insulation is a function of both time and temperature. Such deterioration is a chemical phenomenon involving slow oxidation and brittle hardening and leading to loss of mechanical durability and dielectric strength. In many cases the deterioration rate is such that the life of the insulation can be represented as an exponential

$$\text{Life} = A\varepsilon^{B/T} \quad (\text{C-6})$$

where A and B are constants and T is the absolute temperature. Thus, ac-

cording to Eq. C-6, when life is plotted to a logarithmic scale against the reciprocal of absolute temperature on a uniform scale, a straight line should result. Such plots form valuable guides in the thermal evaluation of insulating materials and systems. A very rough idea of the life-temperature relation can be obtained from the old and more or less obsolete rule of thumb that the time to failure of organic insulation is halved for each 8 to 10°C rise.

The evaluation of insulating materials and complete systems of insulation (which may include widely different materials and techniques in combination) is to a large extent a functional one based on accelerated life tests. Both normal life expectancy and service conditions will vary widely for different classes of electric equipment. Life expectancy, for example, may be a matter of minutes in some military and missile applications, may be 500 to 1000 h in certain aircraft and electronic equipment, and may range from 10 to 30 years or more in large industrial equipment. The test procedures will accordingly vary with the type of equipment. Accelerated life tests on models, called *motorettes*, are commonly used in insulation evaluation. Such tests, however, cannot be easily applied to all equipment, especially the insulation systems of large machines.

Insulation life tests generally attempt to simulate service conditions. They usually include the following elements:

- 1 Thermal shock resulting from heating to the test temperature
- 2 Sustained heating at that temperature
- 3 Thermal shock resulting from cooling to room temperature or below
- 4 Vibration and mechanical stress such as may be encountered in actual service
- 5 Exposure to moisture
- 6 Dielectric testing to determine the condition of the insulation

Enough samples must be tested to permit statistical methods to be applied in analyzing the results. The life-temperature relations obtained from these tests lead to the classification of the insulation or insulating system in the appropriate temperature class.

For the allowable temperature limits of insulating systems used commercially, the latest standards of ANSI, IEEE, and NEMA should be consulted. The three NEMA insulation-system classes of chief interest for industrial machines are class B, class F, and class H. Class B insulation includes mica, glass fiber, asbestos, and similar materials with suitable bonding substances. Class F insulation also includes mica, glass fiber, and synthetic substances similar to those in class B, but the system must be capable of withstanding higher temperatures. Class H insulation, intended for still higher temperatures, may consist of materials such as silicone elastomer and combinations including mica, glass fiber, asbestos, etc., with bonding substances such as appropriate silicone resins. Experience and

tests showing the material or system to be capable of operation at the recommended temperature form the important classifying criteria.

When the temperature class of the insulation is established, the permissible observable temperature rises for the various parts of industrial-type machines can be found by consulting the appropriate standards. Reasonably detailed distinctions are made with respect to type of machine, method of temperature measurement, machine part involved, whether the machine is enclosed, and the type of cooling (air-cooled, fan-cooled, hydrogen-cooled, etc.). Distinctions are also made between general-purpose machines and definite- or special-purpose machines. The term *general-purpose motor* refers to one of standard rating "up to 200 hp with standard operating characteristics and mechanical construction for use under usual service conditions without restriction to a particular application or type of application." In contrast a *special-purpose motor* is "designed with either operating characteristics or mechanical construction, or both, for a particular application." For the same class of insulation, the permissible rise of temperature is lower for a general-purpose motor than for a special-purpose motor, largely to allow a greater factor of safety where service conditions are unknown. Partially compensating the lower rise, however, is the fact that general-purpose motors are allowed a service factor of 1.15 when operated at rated voltage; the *service factor* is a multiplier which, applied to the rated output, indicates a permissible loading which may be carried continuously under the conditions specified for that service factor.

Examples of allowable temperature rises can be seen from Table C-1. The table applies to integral-horsepower induction motors, is based on 40°C ambient temperature, and assumes measurement of temperature rise by determining the increase of winding resistances.

The most common machine rating is the *continuous rating* defining the output (in kilowatts for dc generators, kilovoltamperes at a specified power factor for ac generators, and horsepower for motors) which can be carried indefinitely without exceeding established limitations. For intermittent, periodic, or varying duty, a machine may be given a *short-time rating* defining the load which can be carried for a specific time. Standard periods for short-time ratings are 5, 15, 30, and 60 min. Speeds, voltages,

TABLE C-1
ALLOWABLE TEMPERATURE RISE, °C†

Motor type	Class B	Class F	Class H
1.15 service factor	90	115	
1.00 service factor, encapsulated windings	85	110	
Totally enclosed, fan-cooled	80	105	125
Totally enclosed, nonventilated	85	110	135

†Excerpted from NEMA standards.

and frequencies are also specified in machine ratings, and provision is made for possible variations in voltage and frequency. Motors, for example, must operate successfully at voltages 10 percent above and below rated voltage and, for ac motors, at frequencies 5 percent above and below rated frequency; the combined variation of voltage and frequency may not exceed 10 percent. Other performance conditions are so established that reasonable short-time overloads can be carried. Thus, the user of a motor can expect to be able to apply for a short time an overload of, say, 25 percent at 90 percent of normal voltage with an ample margin of safety.

The converse problem to the rating of machinery, that of choosing the size of machine for a particular application, is a relatively simple one when the load requirements remain substantially constant. For many motor applications, however, the load requirements vary more or less cyclically and over a wide range. The duty cycle of a typical crane or hoist motor offers a good example. From the thermal viewpoint, the average heating of the motor must be found by detailed study of the motor losses during the various parts of the cycle. Account must be taken of changes in ventilation with motor speed for open and semiclosed motors. Judicious selection is based on a large amount of experimental data and considerable experience with the motors involved. For estimating the required size of motors operating at substantially constant speeds, it is sometimes assumed that the heating of the insulation varies as the square of the horsepower load, an assumption which obviously overemphasizes the role of armature I^2R loss at the expense of the core loss. The rms ordinate of the horsepower-time curve representing the duty cycle is obtained by the same technique used to find the rms value of periodically varying currents, and a motor rating is chosen on the basis of the result; i.e.,

$$\text{rms hp} = \sqrt{\frac{\Sigma (\text{hp})^2 \times \text{time}}{\text{running time} + (\text{standstill time}/k)}} \quad (\text{C-7})$$

where the constant k accounts for the poorer ventilation at standstill and equals approximately 4 for an open motor. The time for a complete cycle must be short compared with the time for the motor to reach a steady temperature.

Although crude, the rms-horsepower method is used fairly often. The necessity for rounding the result to a commercially available motor size[†] obviates the need for precise computations; if the rms horsepower were 87, for example, a 100-hp motor would be chosen. Special consideration must be given to motors that are frequently started or reversed, for such operations are thermally equivalent to heavy overloads. Consideration must also be given to duty cycles having such high torque peaks that motors with

[†]Commercially available motors are generally found in standard sizes as defined by NEMA. NEMA Standards on Motors and Generators specify motor rating as well as the type and dimensions of the motor frame.

continuous ratings chosen on purely thermal bases would be unable to furnish the torques required. It is to such duty cycles that special-purpose motors with short-time ratings are often applied. Short-time-rated motors in general have better torque-producing ability than motors rated to produce the same power output continuously, although, of course, they have a lower thermal capacity. Both these properties follow from the fact that a short-time-rated motor is designed for high flux densities in the iron and high current densities in the copper. In general, the ratio of torque capacity to thermal capacity increases as the period of the short-time rating decreases. Higher temperature rises are allowed than for general-purpose motors. A motor with a 150-hp 1-h 50°C rating, for example, may have the torque ability of a 200-hp continuously rated motor; it will be able to carry only about 0.8 times its rated output, or 120 hp, continuously, however. In many cases it will be the economical solution for a drive requiring a continuous thermal capacity of 120 hp but having torque peaks which require the ability of a 200-hp continuously rated motor.

C-3 COOLING MEANS FOR ELECTRIC MACHINES

The cooling problem in electric apparatus in general increases in difficulty with increasing size. The surface area from which the heat must be carried away increases roughly as the square of the dimensions, whereas the heat developed by the losses is roughly proportional to the volume and therefore increases approximately as the cube of the dimensions. This problem is a particularly serious one in large turbine generators, where economy, mechanical requirements, shipping, and erection all demand compactness, especially for the rotor forging. Even in moderate sizes of machines, e.g., above a few thousand kilovoltamperes for generators, a closed ventilating system is commonly used. Rather elaborate systems of cooling ducts must be provided to ensure that the cooling medium will effectively remove the heat arising from the losses.

For turbine generators, hydrogen is commonly used as the cooling medium in the totally enclosed ventilating system. Hydrogen has the following properties which make it well suited to the purpose:

- 1 Its density is only about 0.07 times that of air at the same temperature and pressure, and therefore windage and ventilating losses are much less.
- 2 Its specific heat on an equal-weight basis is about 14.5 times that of air. This means that, for the same temperature and pressure, hydrogen and air are about equally effective in their heat-storing capacity per unit volume, but the heat transfer by forced convection between the hot parts of the machine and the cooling gas is considerably greater with hydrogen than with air.

- 3 The life of the insulation is increased and maintenance expenses decreased because of the absence of dirt, moisture, and oxygen.
- 4 The fire hazard is minimized. A hydrogen-air mixture will not explode if the hydrogen content is above about 70 percent.

The result of the first two properties is that for the same operating conditions the heat which must be dissipated is reduced and at the same time the ease with which it can be carried off is increased.

The machine and its water-cooled heat exchanger for cooling the hydrogen must be sealed in a gastight envelope. The crux of the problem is in sealing the bearings. The system is maintained at a slight pressure (at least 0.5 lb/in^2) above atmospheric so that gas leakage is outward and an explosive mixture cannot accumulate in the machine. At this pressure, the rating of the machine can be increased by about 30 percent above its air-cooled rating, and the full-load efficiency increased by about 0.5 percent. The trend is toward the use of higher pressures (15 to 60 lb/in^2). Increasing the hydrogen pressure from 0.5 to 15 lb/in^2 increases the output for the same temperature rise by about 15 percent; a further increase to 30 lb/in^2 provides about an additional 10 percent.

An important step which has made it possible almost to double the output of a hydrogen-cooled turbine-generator of given physical size is the development of *conductor cooling*, also called *inner cooling*. Here the coolant (liquid or gas) is forced through hollows or ducts inside the conductor or conductor strands. Examples of such conductors can be seen in Fig. C-1. Thus, the thermal barrier presented by the electric insulation is largely circumvented, and the conductor losses can be absorbed directly by the coolant. Hydrogen is usually the cooling medium for the rotor conductors. Either gas or liquid cooling may be used for the stator conductors. Hydrogen is the coolant in the former case, and transil oil or water is commonly

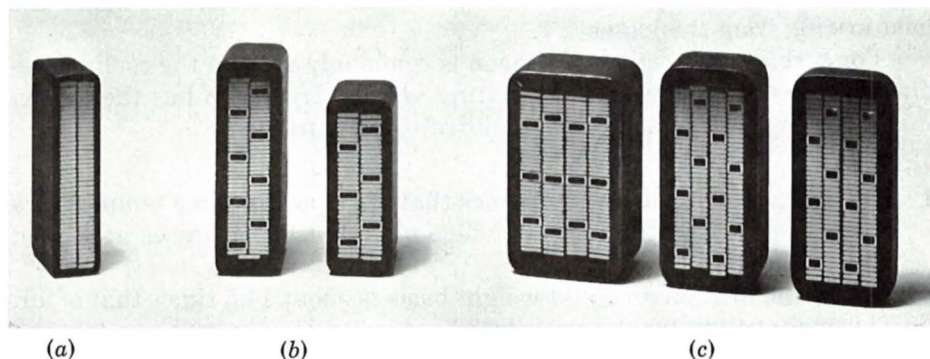


Fig. C-1. Cross sections of bars for two-layer stator windings of turbine-generators. Insulation system consists of synthetic resin with vacuum impregnation. (a) Indirectly cooled bar with tubular strands; (b) water-cooled bars, two-wire-wide mixed strands; (c) water-cooled bars, four-wire-wide mixed strands. (Brown Boveri Corporation.)

used in the latter. A sectional view of a conductor-cooled turbine generator is given in Fig. C-2. A large hydroelectric generator in which both stator and rotor are water-cooled is shown in Figs. 4-2 and 4-9.

C-4 EXCITATION SOURCES

The resultant flux in the magnetic circuit of a machine is established by the combined mmf of all the windings on the machine. For the conventional dc machine, the bulk of the effective mmf is furnished by the field windings. For the transformer, the net excitation may be furnished by either the primary or the secondary winding, or a portion may be furnished by each. A similar situation exists in ac machines. Furnishing excitation to ac machines has two different operational aspects which are of economic importance in the application of the machines.

a. Power Factor in AC Machines

The power factor at which ac machines operate is an economically important feature because of the cost of reactive kilovoltamperes. Low power factor adversely affects system operation in three principal ways. (1) Generators, transformers, and transmission equipment are rated in terms of kilovolt-amperes rather than kilowatts because their losses and heating are very nearly determined by voltage and current regardless of power factor. The physical size and cost of ac apparatus are roughly proportional to its kVA rating. The investment in generators, transformers, and transmission equipment for supplying a given useful amount of active power therefore is roughly inversely proportional to the power factor. (2) Low power factor means more current and greater I^2R losses in the generating and transmitting equipment. (3) A further disadvantage is poor voltage regulation.

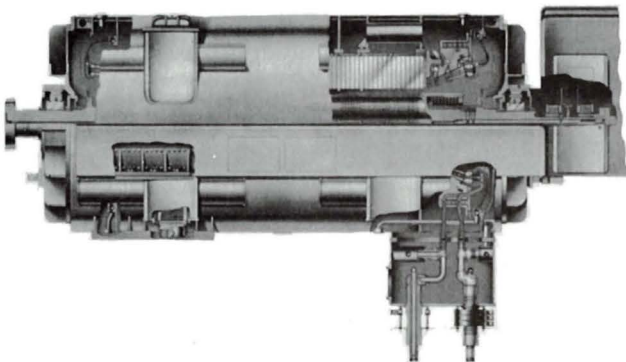


Fig. C-2. Cutaway view of a two-pole 3600 r/min turbine rated at 500 MVA, 0.90 power factor, 22 kV, 60 Hz, 45 lb/in² gage H₂ pressure. Stator winding is water-cooled; rotor winding is hydrogen-cooled. (General Electric Company.)

Factors influencing reactive-kVA requirements in motors can be visualized readily in terms of the relationship of these requirements to the establishment of magnetic flux. As in any electromagnetic device, the resultant flux necessary for motor operation must be established by a magnetizing component of current. It makes no difference either in the magnetic circuit or in the fundamental energy conversion process whether this magnetizing current be carried by the rotor or stator winding, just as it makes no basic difference in a transformer which winding carries the exciting current. In some cases, part of it is supplied from each winding. If all or part of the magnetizing current is supplied by an ac winding, the input to that winding must include lagging reactive kilovoltamperes, because magnetizing current lags voltage drop by 90° . In effect, the lagging reactive kilovoltamperes set up flux in the motor.

The only possible source of excitation in an induction motor is the stator input. The induction motor therefore must operate at a lagging power factor. This power factor is very low at no load and increases to about 85 to 90 percent at full load, the improvement being caused by the increased real-power requirements with increasing load.

With a synchronous motor, there are two possible sources of excitation: alternating current in the armature or direct current in the field winding. If the field current is just sufficient to supply the necessary mmf, no magnetizing-current component or reactive kilovoltamperes are needed in the armature and the motor operates at unity power factor. If the field current is less, i.e., the motor is *underexcited*, the deficit in mmf must be made up by the armature and the motor operates at a lagging power factor. If the field current is greater, i.e., the motor is *overexcited*, the excess mmf must be counterbalanced in the armature and a leading component of current is present; the motor then operates at a leading power factor.

Because magnetizing current must be supplied to inductive loads such as transformers and induction motors, the ability of overexcited synchronous motors to supply lagging current is a highly desirable feature which may have considerable economic importance. In effect, overexcited synchronous motors act as generators of lagging reactive kilovoltamperes and thereby relieve the power source of the necessity for supplying this component. They thus may perform the same function as a local capacitor installation. Sometimes unloaded synchronous machines are installed in power systems solely for power-factor correction or for control of reactive-kVA flow. Such machines, called *synchronous condensers*, may be more economical in the larger sizes than static capacitors.

Both synchronous and induction machines may become self-excited when a sufficiently heavy capacitive load is present in their stator circuits. The capacitive current then furnishes the excitation and may cause serious overvoltage or excessive transient torques. Because of the inherent capacitance of transmission lines, the problem may arise when synchronous generators are energizing long unloaded or lightly loaded lines. The use of

shunt reactors at the sending end of the line to compensate the capacitive current is sometimes necessary. For induction motors, it is normal practice to avoid self-excitation by limiting the size of any parallel capacitor when the motor and capacitor are switched as a unit.

b. Turbine-Generator Excitation Systems

As the available ratings of turbine-generators have increased, the problems of supplying the dc field excitation (amounting to 4000 A or more in the larger units) have grown progressively more difficult. The conventional excitation source is a dc generator whose output is supplied to the alternator field through brushes and slip rings. Cooling and maintenance problems are inevitably associated with slip rings, commutators, and brushes. Many modern excitation systems have minimized these problems by minimizing the use of sliding contacts and brushes.

A schematic diagram of one such system is given in Fig. C-3. At the heart of the system are silicon diode rectifiers, which are mounted on the same shaft as the generator field and which furnish dc excitation directly to the field. An ac exciter with a rotating armature feeds power along the shaft to the revolving rectifiers. The stationary field of the ac exciter is fed through a magnetic amplifier which controls and regulates the output voltage of the main generator. To make the system self-contained and free of sliding contacts, the excitation power for the magnetic amplifier is obtained from the stationary armature of a small permanent-magnet alternator also driven from the main shaft. The voltage and frequency of the ac exciter are chosen so as to optimize the performance and design of the overall system. Time delays in the response to a controlling signal are all short compared with the time constant of the main generator field. The system may have the additional advantage of doing away with need for spare exciters, generator-field circuit breakers, and field rheostats.

Another excitation system uses a shaft-driven alternator of conventional design as the main exciter. This alternator has a stationary armature and a rotating-field winding. Its frequency may be 180 or 240 Hz. Its output is fed to a stationary solid-state rectifier, which in turn supplies the turbine-generator field through slip rings.

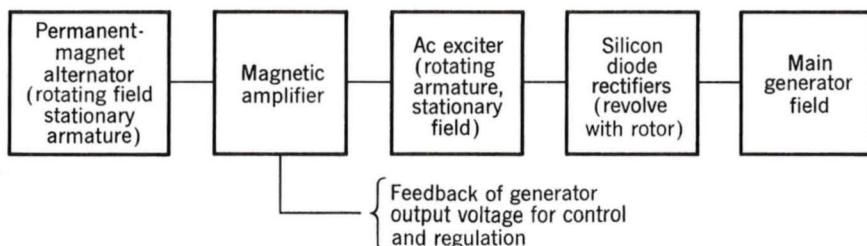


Fig. C-3. Diagrammatic representation of a brushless excitation system.

Excitation systems of the latest design are being built without any sort of rotating exciter-alternator. In these systems, the excitation power is obtained from a special auxiliary transformer fed from the local power system. Alternatively it may be obtained directly from the main generator terminals; in one system a special armature winding is included in the main generator to supply the excitation power. In each of these systems the power is rectified using phase-controlled silicon controlled rectifiers (SCRs). SCRs are similar to diode rectifiers, but they can be triggered by an external trigger signal so that the dc output voltage can be varied. These types of excitation system, which have been made possible by the development of reliable, high-power SCRs, are relatively simple in design and provide the fast response characteristics required in many modern applications.

C-5 ENERGY EFFICIENCY OF ELECTRIC MACHINERY

With increasing concern for both the supply and cost of energy comes a corresponding concern for efficiency in its use. Although electric energy can be converted to mechanical energy with great efficiency, achieving maximum efficiency requires both careful design of the electric machinery and proper matching of machine and intended application.

Clearly, one means to maximize the efficiency of an electric machine is to minimize its internal losses, such as those described in Art. C-1. For example, the winding I^2R losses can be reduced by increasing the slot area so that more copper can be used, thus increasing the cross-sectional area of the windings and reducing the resistance.

Core loss can be reduced by decreasing the magnetic flux density in the iron of the machine. This can be done by increasing the volume of iron, but although the loss goes down in terms of watts per pound, the total volume of material (and hence the mass) is increased; depending on how the machine design is changed, there may be a point beyond which the losses actually begin to increase. Similarly, for a given flux density, eddy-current losses can be reduced by using thinner iron laminations.

One can see that there are trade-offs involved here; machines of more efficient design generally require more material and thus are bigger and more costly. Users will generally choose the "lowest-cost" solution to a particular requirement; if the increased capital cost of a high-efficiency motor can be expected to be offset by energy savings over the expected lifetime of the machine, they will probably select the high-efficiency machine. If not, users are very unlikely to select this option in spite of the increased efficiency.

Similarly, some types of electric machines are inherently more efficient than others. For example, single-phase capacitor-start induction motors (Art. 11-1) are relatively inexpensive and highly reliable, finding use

in all sorts of small appliances, e.g., refrigerators, air conditioners, and fans. Yet they are inherently less efficient than their three-phase counterparts. Modifications such as a capacitor-run feature can lead to greater efficiency in the single-phase induction motor, but they are expensive and often not economically justifiable.

To optimize the efficiency of use of electric machinery the machine must be properly matched to the application, both in terms of size and performance. Since typical induction motors tend to draw nearly constant reactive power, independent of load, and since this causes resistive losses in the supply lines, it is wise to pick the smallest-rating induction motor which can properly satisfy the requirements of a specific application. Alternatively, capacitive power-factor corrections may be used. Proper application of modern solid-state control technology can also play an important role in optimizing both performance and efficiency.

There are, of course, practical limitations which affect the selection of the motor for any particular application. Chief among them is that motors are generally available only in certain standard sizes. For example, a typical manufacturer might make fractional-horsepower ac motors rated at $\frac{1}{8}$, $\frac{1}{4}$, $\frac{1}{2}$, $\frac{3}{4}$, and 1 hp (NEMA standard ratings). This discrete selection thus limits our ability to fine-tune our particular application; if our need is $\frac{7}{8}$ hp, we shall undoubtedly end up buying a 1-hp device and settling for a somewhat lower than optimum efficiency. A custom-designed and manufactured $\frac{7}{8}$ -hp motor can be economically justified only if it is needed in large quantities.

It should be pointed out that an extremely common source of inefficiency in electric motor applications is the mismatch of the motor to its application. Even the most efficient 50-hp motors will be somewhat inefficient when driving a 20-hp load. Yet mismatches of this type often occur in practice, due in great extent to the difficulty in characterizing operating loads and a tendency on the part of application engineers to be conservative to make sure that the system in question is guaranteed to operate in the face of design uncertainties. More careful attention to this issue can go a long way toward increasing the efficiency of energy use in electric machine applications.



Table of Constants and Conversion Factors for SI Units

CONSTANTS

Permeability of free space	$\mu_0 = 4\pi \times 10^{-7} \text{ H/m}$
Permittivity of free space	$\epsilon_0 = 8.854 \times 10^{-12} \text{ F/m}$
Acceleration of gravity	$g = 9.807 \text{ m/s}^2$

CONVERSION FACTORS

Length	1 m = 3.281 ft = 39.37 in
Mass	1 kg = 0.0685 slug = 2.205 lb (mass)
Force	1 N = 0.225 lb = 7.23 poundals
Torque	1 N·m = 0.738 lb·ft
Energy	1 J (W·s) = 0.738 ft·lb
Power	1 W = 1.341 × 10 ⁻³ hp
Moment of inertia	1 kg·m ² = 0.738 slug·ft ² = 23.7 lb·ft ²
Magnetic flux	1 Wb = 10 ⁸ maxwells (lines)
Magnetic flux density	1 Wb/m ² = 1 T = 10,000 gauss = 64.5 kilolines/in ²
Magnetizing force	1 A·turn/m = 0.0254 A·turn/in = 0.0126 oersted

- Ac machines
 - air-gap flux per pole, 182
 - electromotive force (emf), 182
 - introduction to, 150–159
 - laminations in, 148
 - mmf waves in, 173–181
 - power factor in, 579–581
 - rotating mmf waves in (see Magnetomotive force: rotating mmf waves in ac machines)
 - speed voltage, 182
 - rms value of:
 - concentrated windings, 183
 - distributed windings, 184
 - (See also Dc machines: Induction machines; Synchronous machines:)
- Ac windings, distributed:
 - air-gap inductances, 564–568
 - breadth factor, 559
 - chorded, 556
 - double-layer, 555
 - fractional-pitch, 556
 - full-pitch, 556
 - generated voltage per phase, 554–555
 - inductances of, 564–568
 - mmf of (see Magnetomotive force (mmf), of distributed windings)
 - phase belt, 556
 - pitch factor, 556
 - winding factor, 165, 557, 561
- Adjustable-speed solid-state ac motor drive systems, 374–380
- Air-gap inductances, of distributed windings, 564–568
- Air-gap line, 201
- Alternator (see Synchronous machines:)
- Amortisseur winding, 290, 324–325
- Amplidyne, 432
 - compensating winding of, 432
- Armature:
 - of ac machines, 148
 - of dc machines, 148
- Armature leakage reactance, 224, 344
- Armature mmf:
 - of ac machines, 561–564
 - of dc machines, 400–403, 410
- Armature mmf waves:
 - of concentrated full-pitch windings, 562
 - of distributed fractional-pitch windings, 562–564
- Armature reaction:
 - in dc machines, 401–403, 410
 - cross magnetizing, 401–403
 - in synchronous machines, 224
- Armature windings, 148
 - of ac machines, 150, 157
 - of dc machines, 159
- Asynchronous torque, 323
- Audio-frequency transformers, 67
- Autotransformers, 75–77
- Balanced three-phase systems, 176–177
- Base values for per unit systems, 82–83, 85
- Blocked-rotor test, 343–345
- Blondel two-reaction method, 270
- Breadth factor, 559

- Breakdown torque, 324, 339
- Brush-contact loss, 572
- Brushes, 150, 160, 356
- Brushless motors, 528
- Capability curve, 241–242
- Capacitor-type motors:
 - capacitor-start motor, 493–495
 - capacitor-start, capacitor-run, 495–496
 - permanent-split-capacitor motor, 495
- Coenergy:
 - density in magnetic fields, 109
 - determination of
 - force from, 108
 - determination of
 - torque from, 109, 113, 117, 189, 194
 - in electric field systems, 139–140
 - in linear systems, 111, 117
 - in magnetic field systems:
 - multiply excited, 117
 - torque from, 117
 - singly excited, 108
 - force from, 107
 - torque from, 109, 113
 - in nonlinear systems, 109
 - graphical interpretation of, 111
 - in rotating machines, 189, 194
 - in systems with permanent magnets, 118–124
 - in variable reluctance machines, 449
- Collector rings, 150
- Commutating poles, 423
- Commutation in dc machines (*see* Dc machines: commutation in)
- Commutator, 160
 - flashover of, 424
- Compensating winding:
 - of dc machines, 423–425
 - of amplidyne, 432
- Compound generator (*see* Dc generators: compound)
- Compound motor (*see* Dc motors: compound)
- Compounding curve, 240, 243
- Concentrated windings, 153, 163, 183
- Conductor cooling, 578
- Coercivity of permanent magnet materials, 26, 29
- Conservation of energy, 99
 - in lossless magnetic energy storage systems, 102
- Conservative system, 104
- Constant flux linkage, principal of, 279, 290
- Constant-horsepower drive, 427
- Constant-torque drive, 427
- Constants, table of, 584
- Continuous rating, 575
- Conversion factors, table of, 584
- Cooling of electric machines, 577–579
 - conductor, 578–579
 - hydrogen, 577–578
- Core loss:
 - in transformers, 51, 55
 - open-circuit, 73
 - in synchronous machines, open-circuit, 226
- Critical field resistance, 412
- Cumulative compounding, 397
- Cylindrical rotor, 153
- Damper windings, 267, 290
- Damping power, 302–303
- Dc generators:
 - compound, 395–396, 412
 - series winding of, 396
 - shunt winding of, 396
 - long-shunt connection, 406
 - short-shunt connection, 406
 - self-excited, 411–412
 - buildup of voltage, 411–412
 - critical field resistance, 412
 - dynamics of, 411–412
 - field-resistance line, 411
 - residual magnetism in, 395–396
 - separately excited, 395–396
 - series, 395
 - series-field diverter, 413
 - shunt, 412, 411–413
 - flat-compounded, 413
 - steady-state analysis, 411–414 (*See also* Dc machines;)
- Dc machines:
 - amplidyne, 432
 - compensating winding of, 432
 - analytical fundamentals:
 - electric circuit aspects, 404–407
 - magnetic circuit aspects:
 - armature reaction neglected, 407–409
 - effect of armature mmf, 410
 - applications, 433–435
 - armature mmf effect, 400–403, 410
 - armature reaction, 401–403, 410
 - cross-magnetizing, 401–403
 - demagnetizing effect of, 403

Dc machines (*Cont.*)

- limiting effects of, 403
- armature winding of, 159
- brush-contact voltage drop, 405
- brushes, 160, 421–422
- commutator of, 160
- commutating poles, 423
- commutation in, 161, 421–425
 - delayed commutation, 422
 - interpoles, effects of, 421–423
 - linear, 422
 - resistance commutation, 422
 - undercommutation, 422
 - voltage commutation, 422–423
- commutator action, 391, 398–400
- compensating windings, 423–425
- compound:
 - long-shunt connection, 406
 - flat-compounded, 413
 - short-shunt connection, 406
- direct axis of, 391
- direct-axis air-gap permeance, 394
- electromagnetic power in, 404
 - relationship to torque, 404
- elementary, 159–161
- essential features of, 391
- field-circuit connections, 394–395, 397, 406
- field winding of, 159, 161, 391
- flashover of, 424
- generated voltage, 392–393
- interpoles, 421–423
- magnetization curve, 393–394, 407–409
 - air-gap line, 394
- metadyne, 430–431
- mmf wave, 167–170
 - peak value of, 170
- pole-face winding, 423–425
- quadrature axis of, 391
- self-excited, 394
- separately excited, 394
- speed voltage, 393
- stator of, 391
- steady-state analysis, 410–421
- torque in, 392
- (*See also* Dc generators: Dc motors:)

Dc magnetizing curve, 18

Dc motors:

- compound, 396–397
- cumulative connection, 397
- differential connection, 397
- constant-horsepower drive, 427
- constant-torque drive, 427
- separately excited, 397

Dc motors (*Cont.*)

- series, 396–397
- shunt, 396–397
- speed control methods for, 425–430
 - armature-circuit-resistance control, 427
 - armature-terminal-voltage control, 428
 - field-current control, 426
 - shunt-field-rheostat control, 426–427
 - shunted armature method, 427–428
- Ward Leonard system, 428–430
- speed-torque characteristics, 396
- stabilizing winding, 426
- starting of, 416–421
- steady-state analysis, 414–421
- (*See also* Dc machines:)
- Deep-bar rotor, 359–362
 - effective resistance of, 360–361
 - leakage inductance of, 360–361
- Δ connection, 544–550
- Δ -Y equivalence, 79–80
- Differential compounding, 397
- Diode, flyback, 470
- Direct axis, 246
- Direct-axis air-gap permeance, 394
- Direct-axis quantity, 248
- Direct-axis time constants (*see* Synchronous machines: time constants in, direct-axis)
- Distributed windings (*see* Magnetomotive force, ac windings)
- Double-layer winding, 555
- Double-squirrel-cage rotor, 359–361
- dq0 transformation, 269–272
 - basic machine relations in, 272–276
 - introduction to, 246–252, 268–269
 - inverse transformation, 271
 - power-invariant form, 270
- Duty-cycle operation, 576
- Dynamic equations, 124–128

Eddy current loss, 22

Effective resistance:

- armature, 232
- deep-bar rotor, 360–361

Efficiency:

- defined, 74, 570
- energy, of electric machinery, 582–583

Electric field intensity, 10

Electric field systems, 96, 139–140

- Electrical angle, 152
- Electrical degrees, 152
- Electrical radians, 152
- Electromagnetic torque (*see* Coenergy: Energy: Dc machines: Synchronous machines: Induction machines:)
- Electromechanical energy-conservation principles, 95–124
- Electromotive force (emf), 10
 - in ac machines, 182
 - rms value of:
 - concentrated windings, 183
 - distributed windings, 184
- emf (*see* Electromotive force)
- Energy:
 - balance, 101
 - density in magnetic fields, 105
 - conservation of, 99
 - in lossless magnetic energy storage systems, 102
 - in electric field systems, 139–140
 - in linear systems, 105, 111, 116
 - in magnetic field systems:
 - multiply excited, 115–116
 - torque from, 115
 - singly excited, 105
 - force from, 107
 - torque from, 109
 - method, 99, 102
 - in nonlinear systems, 105
 - graphical interpretation of, 111
 - in systems with permanent magnets, 118–124
- Energy efficiency of electric machinery, 582–583
- Energy method, 99
- Equal-area methods, 305–308
- Excitation sources, 579–581
- Excitation systems, 579–581
- Excitation voltage, 223
- Exciting current, 20, 52

- Faradays' law, 9
- Ferromagnetic materials, 16–25
 - ac excitation characteristics, 19–25
 - axes of easy magnetization, 16
 - B-H curve, 17
 - core loss, 23
 - dc magnetization curve, 18
 - effective permeability, 16
 - exciting current, 20
 - rms value, 21
 - exciting voltamperes, 21
- Ferromagnetic materials (*Cont.*)
 - grain-oriented steel, 23
 - hysteresis in, 17, 22–23
 - loss mechanisms in:
 - eddy current, 22
 - hysteresis, 22–23
 - I^2R , 22
 - nonlinear properties, 20
 - nonoriented steel, 24
 - permeability of, 5, 16
 - relative, 5
 - rms voltamperes, 21
 - saturation in, 16, 18
 - silicon steel, 51
- Field axis, 391
- Field-resistance line, 411
- Field windings, 149
 - of dc machines, 159, 161, 391
 - of synchronous machines, 150, 217
- Finite element method, 109
- Flashover of commutator, 424
- Flux(es):
 - air-gap, per pole, 182
 - leakage (*see* Leakage flux)
 - linkage, 10
 - magnetic (*see* Magnetic flux)
 - mutual (*see* Mutual flux)
 - resultant core, 13
- Flux linkage, 10
 - constant, principal of, 279, 290
- Flyback diode, 470
- Force:
 - density, 97
 - in electric field systems, 96, 139–140
 - Lorentz force law, 96
 - right-hand rule for, 96
 - in singly excited magnetic field systems:
 - from coenergy, 108
 - from energy, 107
 - in systems with permanent magnets, 118–124
- Four-phase system, 552–553
- Fractional-horsepower motors, 488–530
- Fractional-pitch windings, 556, 562–568
- Frequency, of generated voltage 152–153
- Frequency response of transformers, 68–71
- Frequency-response testing of synchronous machines, 298–300
- standstill, 299–300

Fringing fields in air gaps, 6
 Full-pitch coil, 162, 561–562
 Full-pitch winding, 562, 564–568

General-purpose motor, 575
 Generated voltage(s):
 in ac machines, 181–185, 554–561
 rms value of:
 concentrated windings, 183
 distributed windings, 184,
 555–561

 in dc machines, 185–186
 frequency of, 152–153

Generators (*see* Dc generators: Hydroelectric generators, Synchronous machines: Turbine generators)

Heating in electric machines, 573–577

High-slip motor, 363–364

Hunting in synchronous machines, 219

Hydroelectric generators, 153

Hydrogen cooling, 577–578

Hysteresis loop, 17
 minor, 34

Hysteresis loss, 22–23

Hysteresis motors, 499–500

Ideal transformer, 57–60
 impedance transformation by, 59–60

Induced voltage, 10
 in ac machines, 182
 rms value of:
 concentrated windings, 183
 distributed windings, 184
 in dc machines, 393, 525
 in electromechanical systems, 125
 in rotating machines, 88

Inductance, 11
 air-gap, of distributed windings, 564–568
 leakage, 61, 193
 in rotating machines, 193, 204–205
 in transformers, 61
 of deep-bar rotor, 360–361
 of double-squirrel-cage rotor, 360–361
 mutual, 13
 self, 13

Inductance (*Cont.*)

 in synchronous machines (*see* Synchronous machines: inductances in)

Induction machines:
 air-gap flux per pole, 182
 elementary, 158–159
 excitation of, 580
 fluxes in, 325–328
 generator operation, 338–339
 introduction to, 321–325
 mmfs in, 325–328
 rotor winding in, 158
 self-excitation of, 580–581
 short circuit of, 371–374
 slip, 322
 at starting, 322
 per unit, 322
 slip frequency, 323
 squirrel-cage rotor, 322
 stator winding in, 158
 torque, 323
 asynchronous, 323
 breakdown, 324, 339
 from Thevenin's theorem, 336–342
 torque-speed curve, 338–342
 transformer action in, 158
 wound rotor, 322
 (*See also* Induction motors:)

Induction motors:
 polyphase:
 adjustable-speed solid-state ac motor drives, 374–380
 application considerations, 361–364
 blocked-rotor reactance, 344
 blocked-rotor test, 343–344
 equivalent circuit for, 343–344
 frequency for, 344
 breakdown torque, 339
 braking of, 338
 brushes in, 356
 deep-bar rotor, 359–361
 effective resistance of, 360–361
 leakage inductance of, 360–361
 design classes of, 361–364
 torque-speed curves for, 362
 double-squirrel-cage rotor, 359–361
 effective resistance of, 360–361
 leakage inductance of, 360–361
 dynamics of, 364–367

Induction motors (*Cont.*)

- efficiency of, 333
- equivalent circuits, 328–332
 - alternative forms, 333, 334
 - analysis of, 332–336
 - for blocked rotor conditions, 343–344
 - for transient analysis, 373
 - parameter determination for, 342–347
 - rotor, 331
 - stator, 328–329
- exciting current, 342
- flux waves, 325–328
- leakage impedances, 330, 343–344
 - slip frequency, 330
- linear (*see* Linear machines)
- mmf waves, 325–328
- no-load impedance, 343
- no-load losses, 342
- no-load test, 342–343
- plugging, 338
- power in:
 - air-gap, 333
 - from Thevenin's theorem, 336–342
 - internal mechanical, 333
 - no-load, 343
- reactances of:
 - leakage, distribution of, 344
 - magnetizing, 345
 - no-load, 343
 - transient, 372
- reduced voltage starting of, 362
- starting compensator for, 362
- resistances of:
 - blocked-rotor, 345
 - no-load, 343
 - rotor, 345
 - stator, 345
- referring of rotor quantities, 331
- rotational loss, 342–343
- rotor resistance, effects of varying, 356–359
- slip rings in, 356
- solid-state drive systems:
 - amplitude control, 379–380
 - constants volts per hertz control, 377
 - inverters, 375–378
 - typical waveforms, 377
 - pulse-width control, 380
- speed control of, 367–371
 - auxiliary devices, 370–371

Induction motors (*Cont.*)

- line-frequency control, 369
- line-voltage control, 369
- pole changing, 367–369
- rotor-resistance control, 369–370
 - adjustable-speed solid-state ac motor drive systems, 374–380
- speed-torque characteristic, 159
- squirrel-cage rotor, 322
 - mmf of, 326–328
- starting of, 364–367
 - reduced voltage, 362
- starting compensator, 362
- stator resistance, 345
- stray load losses, 342
- symmetrical three-phase short-circuit, 371–374
- testing of, 342–347
 - blocked-rotor, 343–345
 - no-load, 342–343
- Thevenin equivalent circuit, 336–337
- time constants:
 - open-circuit transient, 372
 - short-circuit transient, 372
- torque angle of, 326
- torque:
 - breakdown, 339
 - slip at, 339
 - from Thevenin's theorem, 336–342
- torque-slip characteristics, 324, 338–342
 - effect of rotor resistance on, 341–342
- torque-speed curve, 324, 338–342
 - effect of rotor resistance on, 341–342
 - under adjustable-frequency control, 379
- transient analysis, 371–374
 - equivalent circuit for, 373
- transient reactance, 372
- wound-rotor motors, 356–359
 - brushes in, 356
 - slip rings in, 356
- single-phase:
 - capacitor-start, 493–495
 - capacitor-start, capacitor-run, 495–496
 - double-revolving-field analysis, 490–492, 500–507
 - elementary, 489–492
 - equivalent circuits, 501–507

Induction motors (*Cont.*)

- mmf waves in:
 - backward-traveling, 490
 - effects of rotor motion on, 490–492
 - forward-traveling, 490
 - permanent-split-capacitor, 495
 - power in, 503–504
 - qualitative examination, 489–492
 - revolving-field theory, 500–507
 - running performance, 490–499
 - shaded-pole, 497
 - split-phase, 492–493
 - starting methods, 492–497
 - capacitor-type, 493–497
 - shaded pole, 497
 - split-phase, 492–493
 - torque:
 - backward component, 490–492, 503
 - pulsations, double-stator-frequency, 492
 - forward component, 490–492, 503
 - running, 503
 - starting, 489
 - torque-speed characteristic, 491
 - two-phase:
 - general theory, 507–512
 - symmetrical-component analysis, 507–512
 - unbalanced operation of, 507–512
- Infinite bus, 217
- Inner cooling, 578–579
- Insulation:
 - classes of, 575
 - life of, 573–574
- Interconnected synchronous generators, 256–258
- Interpoles, 421–423
- Inverters:
 - induction motor applications, 375–378
 - variable reluctance machine applications, 475–478
- Leakage fields, 8
- Leakage flux, 203
 - in rotating machines, 192, 203
 - components of, 204–205
 - in transformers, 51
- Leakage inductance (*see* Inductance, leakage)

Leakage reactances:

- in induction machines, 344, 360–361
 - in synchronous machines, 224
 - in transformers, 61, 63
- Life of insulation, 573–574
- Line current, 540–542
- Line-to-line voltage, 540
- Line-to-neutral voltage, 540
- Linear induction motors, (*see* Linear machines)
- Linear machines, 197–200
 - end effects in, 200
- Linearization of nonlinear equations, 130–131
- Long-shunt connection, 406
- Lorentz force law, 96
 - right-hand rule for, 96
- Loss of synchronism, 219
- Losses in electric machines, 569–573
 - brush-contact, 572
 - I^2R , 570–571
 - mechanical, 571
 - no-load rotational, 571
 - in induction machines, 342–343
 - open-circuit (no-load) core, 571–572
 - stray load, 572

Magnetic circuit model, 8

- Magnetic circuits, 3–9
 - analogy with electric circuits, 7
 - exciting current in, 20
 - fringing fields in, 3
 - leakage fields in, 8
 - permanent magnets in, 28–31
 - permeance of, 8
 - reluctance of, 7
 - resultant core flux in, 13
- Magnetic field intensity, 2
- Magnetic field systems:
 - multiply excited:
 - coenergy in, 117
 - energy in, 115–116
 - torque in, 117
 - singly excited:
 - coenergy in, 108
 - energy in, 105
 - force in, 107, 108
 - torque in, 109, 113
- Magnetic fields:
 - coenergy density in, 109
 - energy density in, 105

Magnetic fields (*Cont.*)

- fringing fields in air gaps, 6
- in rotating machinery:
 - with nonuniform air gaps, 171–173
 - with uniform air gaps, 173
- right-hand rule for, 4
- rotating, 176–179

Magnetic flux, 4

- air-gap space-harmonic fluxes, 204
- end-turn flux, 204
- leakage flux, 193, 203–205
- in multiwinding systems, 203–205
- mutual flux, 192
- per pole, 182, 196
- rotor leakage flux, 193
- slot-leakage flux, 204
- stator leakage flux, 193

Magnetic flux density, 2

- uniform across core cross-section in a magnetic circuit, 4

Magnetic hysteresis, 17

Magnetic materials (*see* Ferromagnetic materials, Permanent magnetic materials)

Magnetic saturation:

- in electric machinery, 200–203
- in ferromagnetic materials, 16
- magnetization curve, 201
 - air-gap line, 201
 - dc, 18
 - of dc machines, 393–394, 407–409
 - normal, 18
- open-circuit characteristic, 201
 - air-gap line, 201
 - for synchronous machines, 225–226
- saturation curve, 201
 - air-gap line, 201
- in synchronous machines, 225–226, 229–230

Magnetic stored energy, 14

Magnetization curve, 201

- air-gap line, 201
- dc, 18
- of dc machines, 393–394, 407–409
- normal, 18

Magnetizing current, of transformers, 18

Magnetizing reactance:

- in induction motors, 345
- in synchronous machines, 249
- in transformers, 63

Magnetomotive force (mmf), 3, 162–163

- of distributed windings, 162–170
 - in ac machines, 163–166
 - in dc machines, 167–170
 - peak value of, 170
- full-pitch coil, 162
- fundamental component of:
 - of concentrated, full-pitch coil, 163
 - of distributed winding, 165
- space harmonics, effects on, 165
- winding factor, 165
- in induction machines, 325–328
- rotating mmf waves in ac machines:
 - polyphase, 176–179
 - graphical analysis, 179–181
 - angular velocity of, 179
 - single phase, 174–176
 - resolved into rotating traveling waves, 176

Maxwell's equations, magneto-quasi-static form of, 2

Metadyne, 430–431

mmf (*see* Magnetomotive force)

mmf waves:

- of concentrated full-pitch windings, 562
- of distributed fractional-pitch windings, 562–564

Multicircuit transformers, 77–78

Mutual flux, 203

- in rotating machines, 192
- in transformers, 51

Mutual inductance, 13

Negative sequence, 508

Neutral current, 547

No-load rotational loss, 571

- in induction machines, 342–343
- in synchronous machines, 226

Normal magnetization curve, 18

Open-circuit characteristic, 201

- air-gap line, 201
- for synchronous machines, 225–226

Open-circuit core loss:

- in synchronous machines, 226
- in transformers, 73

Open-circuit test:

- for synchronous machines, 225–226

- Open-circuit test (*Cont.*)
 - for transformers, 72–73
- Open-circuit time constants, 284
- Open-delta connection, 79
- Output transformer, 68
- Overexcitation, 580
- Parallel operation of synchronous generators, 256–258
- Park's transformation (*see* dq0 transformation)
- Per unit systems, 82–87
 - base values for, 82–83, 85
- Permanent-split-capacitor motor, 495
- Permanent magnet materials, 26–38
 - ceramic magnets, 33
 - coercivity of, 26, 29
 - common materials, properties of, 32
 - demagnetization in 34–35, 38
 - ferrite magnets, 33
 - maximum energy product, 29, 30
 - minor hysteresis loops in, 34
 - rare-earth magnets, 33
 - recoil permeability, 34
 - recoil line, 34
 - residual flux density in, 26
 - stabilization of, 35–38
- Permanent magnet motors:
 - ac, 527–528
 - dc, 520–526
 - benefits of, 520
 - brushless, 528
 - disc construction, 523
 - speed voltage, 525
 - torque, 525
 - torque constant of, 525
 - stepping, 516–518
 - hybrid, 518–520
- Permeability, 5
 - of ferromagnetic material, 5, 16
 - of free space, 5
 - recoil, 34
 - relative, 5
- Permeance, 8
- Phase, 537
- Phase belt, 556
- Phase current, 540–542
- Phase order, 539
- Phase sequence, 539
- Phase voltage, 540
- Pitch factor, 556
- Plugging, 338
- Pole-changing motors, 367–369
- Pole-face winding, 423–425
- Polyphase induction motors (*see* Induction motors: polyphase)
- Positive sequence, 508
- Polyphase systems, 536, 552–553
- Power:
 - in dc machines, 404
 - in induction machines, 333, 336–342, 343
 - single-phase, 503–504
 - in synchronous machines, 276
 - damping, 302–303
 - synchronous, 302
 - in three-phase systems:
 - average per phase, 543
 - instantaneous, 542
 - reactive, 543
 - real, 543
 - at winding terminals, 14
- Power angle, 235
- Power-angle characteristics of synchronous machines:
 - steady state: 233–240
 - non-salient pole, 235
 - including the effects of external reactance, 235
 - salient-pole, 252–256
 - reluctance torque component, 253–254
- transient, 285–289
 - constant-voltage-behind-transient-reactance representation, 289
- Power factor:
 - in ac machines, 579–581
 - in three-phase system, 543–544
- Principal of constant flux linkages, 279, 290
- Pull-out torque, 219
- Quadrature axis, 246
- Quadrature-axis quantity, 248
- Quadrature-axis time constants, 294
- Rating of electric machines, 573–577
 - continuous, 575
 - operating temperature, 573
 - short-time, 575–576
 - temperature rise, 575
- Reactive capability curves, 241–242
- Reactive power in three-phase system, 543

- Reference directions:
 - generator, 224
 - motor, 224
- Reluctance, 7
- Reluctance motor, 497–498
- Reluctance torque, 254
- Remanent magnetization, 26
- Residual flux density, 26
- Resultant flux, 13
- Revolving-field theory, 500–507
- Right-hand rule, 4
- Root-mean-square (rms) horsepower, 576
- Rotating magnetic fields, 173–181, 500–507
- Rotational loss, no-load (*see* No-load rotational loss)
- Rotor, 148
 - cylindrical, 153
 - deep-bar, 359–362
 - double-squirrel-cage, 359–361
 - salient-pole, 153
 - squirrel-cage, 322
 - wound, 356–359
- Salient-pole effects (*see* Synchronous machines: salient-pole effects)
- Salient-pole rotor (*see* Synchronous machines: salient-pole rotor)
- Saturated synchronous reactance, 229
- Saturation (*see* Magnetic saturation:)
- Saturation curve (*see* Magnetization curve)
- Saturation effects (*see* Magnetic saturation:)
- SCR (short-circuit ratio), 229
- SCR (silicon controlled rectifier), 375
- Self-excited dc generators (*see* Dc generators: self-excited)
- Self-inductance, 13
- Separately excited dc generators, 395–396
- Series-field diverter, 413
- Series motors:
 - ac, 512–514
 - dc, 396–397
- Series universal motor, 512–514
- Service factor, 575
- Shaded-pole motor, 497
- Short circuit:
 - of induction machines, 371–374
 - of synchronous machines (*see* Synchronous machines: short circuit of)
- Short-circuit characteristic, 227
- Short-circuit load loss, 231–232
- Short-circuit ratio (SCR), 229
- Short-circuit test:
 - for synchronous machines, 227–233
 - for transformers, 71–72
- Short-shunt connection, 406
- Short-time rating, 575–576
- Silicon controlled rectifier (SCR), 375
- Single-line diagrams, 550–552
- Single-phase induction motors (*see* Induction motors: single-phase)
- Single-phase system, 536–537
- Slip, 322
- Slip frequency, 323
- Slip rings, 150, 217, 356
- Solid-state motor-drive systems (*see* Induction motors: polyphase: solid-state drive systems)
- Special-purpose motor, 575
- Speed control:
 - of ac series motor, 513
 - in adjustable-frequency systems, 374–380
 - of dc motors (*see* Dc motors: speed control methods for)
 - of induction motors (*see* Induction motors: polyphase: speed control of)
 - of synchronous motors, 374–380
- Speed voltage:
 - in ac machines, 182
 - rms value of:
 - concentrated windings, 183
 - distributed windings, 184
 - in dc machines, 393, 525
 - in electromechanical systems, 125
 - in rotating machines, 88
- Split-phase motor, 492–493
- Squirrel-cage rotor, 322, 359–361
 - mmf of, 326–328
- Stabilizing winding, 426
- Starting of single-phase motors, 492–497
- Starting compensator, 362
- Stator, 148
- Stepper motors (*see* Stepping motors)
- Stepping motors, 514–520
 - hybrid, 518–520
 - multistack variable-reluctance, 515
 - permanent-magnet, 516–518
 - single-stack variable-reluctance, 515
- Stray load loss, 342, 572
- Subtransient period, 292
- Subtransient reactances, 291

- Subtransient time constants, 293, 294
- Swing equation, 302
- Symmetrical components:
 - analysis of unbalanced operation of two-phase machines, 507–512
 - negative sequence, 508
 - positive sequence, 508
- Synchronous condenser, 580
- Synchronous inductance, 274
- Synchronous machines:
 - additional rotor circuits:
 - amortisseur circuits, 290
 - dampers circuits, 267, 290
 - effects of, 289–295
 - models for, 298–300
 - air-gap flux per pole, 182
 - armature-reaction mmf, 227
 - armature resistance:
 - effective value of, 232
 - typical value of, 227
 - armature winding of, 150, 217
 - brushes in, 150
 - capability curve, 241
 - derivation of, 241–242
 - collector rings, 150
 - compounding curve, 240
 - concentrated windings in, 153
 - cylindrical rotor, 153
 - magnetic fields, 171–173
 - dampers bars, 267
 - dampers currents, 267, 290
 - dampers windings, 267, 290
 - dampers power, 302–303
 - direct axis of, 246
 - distributed windings in, 153
 - dq0 transformation (*see* dq0 transformation)
 - dynamics of, 300–308
 - basic equations for, 301–303
 - swing equation, 302
 - linearized analysis, 303–305
 - non-linear analysis, 305–308
 - electromotive force (emf), 182
 - elementary, 150–158
 - equal-area method, 305–308
 - equivalent circuits:
 - steady-state, 224
 - transient:
 - constant-voltage-behind-transient-reactance, 289
 - including the effects of damper and rotor-body currents, 298–299
 - excitation systems, 217, 581–582
 - excitation voltage, 223
 - rms value of, 223
- Synchronous machines (*Cont.*)
 - field winding of, 150, 217
 - flux-linkage current relationships, 220, 273–274
 - in terms of dq0 variables, 274
 - flux waves in, salient pole effects
 - on, 246–248
 - harmonic effects, 246–247
 - frequency-response testing of, 299–300
 - standstill, 299–300
 - hunting in, 219
 - hydroelectric generators, 153
 - inductances of:
 - direct-axis:
 - synchronous, 274
 - transient, 280
 - quadrature-axis:
 - synchronous, 274
 - rotor self-inductance, 220–221
 - space-fundamental component of, 221
 - stator phase-to-phase mutual inductance, 222
 - stator self-inductance, 221–222
 - space-fundamental component of, 222
 - stator-to-rotor mutual, 221
 - synchronous, 222–223
 - direct-axis, 274
 - space-fundamental component of, 221
 - quadrature-axis, 274
 - transient:
 - direct-axis, 280
 - zero-sequence, 274
 - introduction to, 217–219
 - loss of synchronism, 219
 - losses in, 243
 - mmf waves in, salient pole effects
 - on, 246–248
 - harmonic effects, 246–247
 - no-load rotational loss in, 226
 - open-circuit characteristic, 225–226
 - open-circuit core loss, 226
 - open-circuit test, 225–226
 - overexcited operation of, 580
 - parallel operation of, 256–258
 - phasor diagrams, 234, 238
 - for salient-pole machines, 248–252
 - for short-circuit conditions, 228
 - for transient conditions, 287
 - poles, 152
 - power angle, 235

Synchronous machines (*Cont.*)

- power-angle characteristics (*see* Power-angle characteristics of synchronous machines)
- power output, 276
 - in terms of $dq0$ variables, 276
 - power-invariant form, 270
- production of three-phase voltages in, 155–156
- quadrature axis of, 246
- reactances of:
 - armature leakage, 224
 - typical value of, 227
 - armature reaction, 224
- direct axis:
 - magnetizing, 249
 - subtransient, 291
 - synchronous, 249
 - transient, 282
- quadrature-axis:
 - magnetizing, 249
 - subtransient, 291
 - synchronous, 249
 - transient, 294
- synchronous, 224
 - saturated, 229
 - determined from the short-circuit-ratio, 230
 - unsaturated, 228
- reactive capability of, 241
- reference directions for:
 - generator, 224
 - motor, 224
- reluctance torque in, 253–254
- rotor body currents, 267, 290
- salient-pole effects, 246–252
 - phasor diagrams, 248–252
 - under transient conditions, 282
- salient-pole rotor, 153
 - magnetic fields, 173
- salient-pole theory, 246–252
- saturation effects, 225–226, 229–230
- self-excitation of, 580–581
- short circuit of:
 - steady state, 227–233
 - sudden three-phase short circuit of, 276–285
 - analysis of:
 - armature and field resistance neglected, 278–283
 - field resistances included and transformer voltages neglected, 283–285
 - including subtransient effects, 291–294

Synchronous machines (*Cont.*)

- resistances and transformer voltages neglected, 283
- physical description, 276–278
- short-circuit characteristic, 227
- short-circuit load loss, 231–232
- short-circuit ratio (SCR), 229
- short-circuit test, 227–233
- single-phase:
 - hysteresis, 499–500
 - self-starting reluctance, 497–499
- slip rings in, 150, 217
- speed voltage, 182
 - $dq0$ components of, 275
 - rms value of:
 - concentrated windings, 183
 - distributed windings, 184
- stability of, 307
- steady-state analysis, 216–259
- steady-state operating characteristics, 240–245
- stray load loss, 232
- swing equation for, 302
- synchronous power, 302–303
- synchronous speed of, 151
 - relationship to electrical frequency, 152
- time constants in:
 - direct-axis:
 - open-circuit transient, 284
 - short-circuit subtransient, 293
 - short-circuit transient, 284
 - effects of external reactance on, 285
 - quadrature-axis:
 - short-circuit subtransient, 294
 - short-circuit transient, 294
- torque-angle curve, 218 (*see also* Power-angle characteristics of synchronous machines:)
- torque in, 156, 218, 276
 - in non-salient-pole machines, 186–196
 - in terms of $dq0$ variables, 276
 - power-invariant form, 270
 - pull-out, 219
- transformer voltage terms, 282
 - effects of neglecting, 283
- transient analysis:
 - introduction to, 267–269
 - models for:
 - constant-voltage-behind-transient-reactance, 288–289
 - equivalent-circuits including the effects of damper and rotor-body currents, 298–299

Synchronous machines (*Cont.*)
 (See also dq0 transformation)
 (See also Synchronous machines:
 sudden three-phase short circuit of)
 transient saliency in, 282
 turbine generators, 153
 underexcited operation, 580
 V curves, 243
 voltage:
 air-gap, 224
 excitation, 223
 rms value, 223
 behind leakage reactance, 224
 behind transient reactance, 288–289
 voltage equations, 274–275
 in terms of dq0 variables, 275
 Synchronous motors, 157
 amortisseur winding in, 324–325
 compounding curve, 243
 damper winding in, 324–325
 electromagnetic torque in, 157
 elementary, 157
 equivalent circuit for, 224
 overexcited operation, 580
 power factor, 243
 reluctance-type, 497–499
 reference directions for, 224
 speed control, 374–380
 speed of, 157
 starting of, 324–325
 torque in, 157
 underexcited operation, 580
 V curves, 243
 (See also Synchronous machines)
 Synchronous power, 302–303
 Synchronous reactance, 224, 228–230
 Synchroscope, 257
 Temperature limits, 573–575
 Tertiary winding, 78
 Thevenin's theorem, 336–337
 Three-phase circuits, 536–552
 balanced, 539
 currents in, balanced, 540–542
 Δ connection in, 538, 544–550
 Δ -Y equivalence, 79–80, 549–550
 four-wire three-phase, 538
 neutral conductor in, 539
 phase sequence in, 539
 power factor angle in, 543–544
 power in:
 average per phase, 543
 instantaneous, 542
 reactive, 543

Three-phase circuits (*Cont.*)
 real, 543
 reactive power in, 543
 single-line diagrams, 550–552
 three-wire three-phase, 538
 transformers in, 78–82
 unbalanced, 539
 voltamperes in, 543
 voltages in:
 balanced, 539–540, 542
 generation of, 537–539
 line-to-line, 540
 line-to-neutral, 540
 unbalanced, 539
 Y connection in, 538, 544–550
 Y- Δ equivalence, 79–80, 549–550
 Three-phase system (*see* Three-phase circuits)
 Three-phase transformer connections, 78–82
 Three-phase transformers, 78–82
 Thyristor, 375
 Time constants:
 in induction motors (*see* Induction motors: polyphase: time constants:)
 in synchronous machines (*see* Synchronous machines: time constants in)
 Torque:
 asynchronous, 323
 breakdown, 324, 339
 in dc machines, 392
 determination of:
 from coenergy, 113, 117, 189, 194
 from energy, 109, 115
 in induction machines, 336–342
 in multiply excited magnetic field systems, 115, 117
 in non-salient-pole machines, 186–196
 in permanent magnet dc machines, 525
 pull-out, 219
 reluctance, 118
 in single-phase induction motors, 489–492
 in singly excited magnetic field systems, 109, 113
 in synchronous machines, 156, 186–196, 218, 276
 in systems with permanent magnets, 118–124
 Torque-angle characteristics
 (*see* Power-angle characteristics of synchronous machines:)

Transducers, 95

Transformers:

- audio-frequency, 67
 - frequency characteristic of, 68–71
- autotransformers, 75–77
- cantilever equivalent circuits, 65–66
 - component currents in, 55, 61–62
 - component fluxes in, 60–61
- core loss in, 51, 55
 - open circuit, 73
- core-type, 51
- Δ - Δ connection, 79
- Δ -Y connection, 79
- distribution, 52
- efficiency of, 74
- equivalent circuits for:
 - cantilever circuits, 65–66
 - core-loss conductance of, 63
 - leakage reactances of:
 - primary, 61
 - secondary, 63
 - magnetizing susceptance of, 63
 - T circuit, 63
- equivalent impedance, 66
- equivalent reactance, 66
- equivalent resistance, 66
- exciting current, 51
 - core-loss component, 55
 - equivalent sine wave, 56
 - magnetizing component, 55
- frequency response of, 68–71
- ideal, 57–60
 - impedance transformation in, 59–60
- induced voltage (emf) in, 55
 - rms value, 55
- introduction to, 51–52
- iron-core, 51
- laminations in, 51
- leakage flux in, 51, 60, 63
- leakage inductance in, 61
- leakage reactances in:
 - primary, 61
 - secondary, 63
- magnetizing current of, 52
- multicircuit, 77–78
- mutual flux, 51
- no-load conditions in, 52–57
- open-circuit test, 72–73
- open-delta connection, 79
- output, 68
- per unit system for, 82–87
- polarity of, 58–59

Transformers (*Cont.*)

- power in, 58
 - core-loss, 56
- primary current:
 - exciting component of, 62
 - load component of, 61
- primary winding, 51
- ratio of transformation, 51
- referring factors, 60
- resultant mutual flux, 60
- secondary current in, 57
- secondary winding, 51
- shell-type, 51
- short-circuit test, 71–72
- T equivalent circuit, 63
- tertiary winding, 78
- tests, 71–75
 - in three-phase circuits, 78–82
- V connection, 79
- voltage regulation in, 74
- Y- Δ connection, 78
- Y-Y connection, 79
- Transient period, 292
- Transient reactance:
 - in induction machines, 372
 - in synchronous machines, 282, 294
- Transient saliency, 282
- Transient time constants:
 - in induction motors (*see* Induction motors: polyphase: time constants:)
 - in synchronous machines (*see* Synchronous machines: time constants in)
- Turbine generators, 153
 - excitation systems, 581–582
 - (*See also* Synchronous machines)
- Two-phase induction motors (*see* Induction motors, two-phase)
- Two-phase system, 552–553
- Two-value-capacitor motor, 495–496
- Underexcitation, 580
- Universal motor, 512–514
- V connection, 79
- V curves, 243
- Variable reluctance machines:
 - basics of analysis, 447–455
 - bifilar winding in, 457–458
 - castleated, 460
 - speed of, 461

Variable reluctance machines (*Cont.*)

- coenergy in, 449
- configurations, 447–448, 455
- current waveforms, 461–468, 470–475
- doubly salient, 447, 455–456
 - advantages of, 456
- drives, 468–478
 - components of, 470
 - controller, 470
 - current waveforms, 461–468, 470–475
 - chopping, 472–475
- inverters:
 - configurations, 475–478
 - rating, effects of saturation on, 480–483
- rotor position sensor, 470
- flux-current relationship, 447–449
 - mutual inductance effects, 450
- inductance, phase:
 - maximum, 455–456
 - minimum, 455–456
 - ratio, effect on torque, 455–456
- inverters for, 475–478
 - rating, effects of saturation on, 480–483
- nonlinear analysis, 478–483
- operating criteria, 455
- pole ratio, 450
 - relationship to speed, 458–461
- reliability of, 483–484
- saturation, effects of, 450, 454, 478–483
- singly salient, 447, 455–456

Variable reluctance machines (*Cont.*)

- stepping motors:
 - hybrid, 518–520
 - multistack variable-reluctance, 515
 - single-stack variable-reluctance, 515
 - torque, 449–450, 455, 461
 - current waveforms for, 461–468
 - ripple, 468
 - zeros of:
 - effects of, 454
 - elimination of, 456–457
 - test for, 456
 - winding configurations, 457
 - bifilar winding, 457–458, 477–478
 - Volt-amperes in three-phase system, 543
- Ward Leonard system, 428–430
- Winding configurations (*see* Ac windings, distributed:)
- Winding factor, 165, 557, 561
- Wound rotor, 322
- Wound-rotor motors, 356–359

Y connection, 544–550

Y- Δ equivalence, 79–80, 549–550

Zero-sequence component, 271

1293
W W COLLEGE STORE
527-2442
J 6035

ISBN 0-07-021134-5



90000

9 780070 211346